

Neanderthal stone-tipped spear technology: an experimental and archaeological investigation.

(Volume 1 of 2)

Submitted by Alice Oriana La Porta to the University of Exeter

as a thesis for the degree of

Doctor of Philosophy in Archaeology

In February 2019

This thesis is available for Library use on the understanding that it is copyright material and that no quotation from the thesis may be published without proper acknowledgement.

I certify that all material in this thesis which is not my own work has been identified and that no material has previously been submitted and approved for the award of a degree by this or any other University.

Signature:

**On se demande si vraiment on emmancherait l'outil au bout d'un bâton
pour aller chasser l'ours. Si oui, c'est indiscutablement une pointe !**

(Bordes, 1961, p. 37)

ACKNOWLEDGEMENTS

Academic research is above all encouragement, perseverance, and sense of community and, to this community of friends, colleagues, and researchers who have accompanied me along the way, I am very grateful.

I would like to begin by acknowledging Professor Cristina Lemorini and Dr Alex Pryor who accepted their invitation to be examiners of this research. I am very much honoured by their consideration.

This research couldn't have taken place without the financial help of the *Arts and Humanities Research Council* and the *South West and Wales Doctoral Partnership* which have funded not only my life in England but also my travels, study visits, equipment costs, and most importantly (through the *Student Development Funding* grant) the performance of the entire experimental programme of this thesis, without which this research would have been incredibly different. I am also indebted to the *OpenArch* project who generously covered some travel costs and consumable materials during the first-year experiments of this research.

I am, and I will always be incredibly grateful to Werner Pfeifer, Morten Kutschera, and Ingolf Pfeifer who literally fired their best shots into this work. I have learnt so much by watching and replicating the gestures of these fantastic craftsmen, and I am obliged they accepted to take part in this thesis's experimental programme and shared with me their knowledge and *savoir-faire* on prehistoric weaponry and ancient skills (Grazie Maestri!).

In academic terms, I would like to thank my supervisor Professor Rob Hosfield who, since our first interview at Reading University, has enthusiastically supported this research and guided me with positive advice without which this thesis would never have been possible (you are an incredible example to follow, thanks Rob!). I must also thank my supervisor Professor Linda Hurcombe for teaching me to look beyond the surface and to have an experimental approach to trials (not to mention her advice and the good prehistoric times, thanks Linda!). Dr Hajnalka Herold was also my mentor, and her advice was very

welcome during the more trying times (thanks for your upright support Hajnalka!).

I would also like to thank my former teacher, Professor Marie H el ene Moncel, for pushing me to submit a funding application for this research back in 2013, for allowing the investigation of the Abri du Maras' collection, for funding part of the lab expenses of this research, and for having shown an incredible support since my master years (merci beaucoup, Marie-H el ene!). I am also grateful to Professor Fabio Negrino e Marco Peresani who offered and allowed the study of Arma Delle Manie's collection, to the *Soprintendenza Archeologica della Liguria* for the authorization to conduct the analysis of the Arma Delle Manie artefacts, and to the *Museo Archeologico del Finale* (Italy) and its director Dr Daniele Arobba for their hospitality during my study visit in Liguria.

Of course, I am indebted to the *Steinzeitpark Dithmarschen* (Germany) Museum, its amazing director Dr Rudiger Kelm, and the *Friends of the Museum-F rderverein A za* association for having warmly welcomed the experiments of this thesis, for making available the spaces and the staff of the Museum, for the acquisition and disposal of the animal carcasses, and for always making me feel at home (vielen dank Albersdorf!). Similarly, I am also thankful to *Sagnlandet Lejre* (Denmark) Museum and Dr Laurent Mazet for hosting pre-experiments and public engagement activities related to this thesis's research. The high-speed videos were recorded thanks to the collaboration with filmmaker Dr Tom Boehme to whom I am obliged.

I would also like to thank Professor Andreu Oll e who kindly welcomed me into his microscopy modules and provided precious suggestions, and to the *Mus eum National d'Histoire Naturelle* (France) and the *Institut de Pal eontologie Humaine, the Institut Catal  de Paleoecologia Humana i Evoluci  Social* (Spain), and the entire staff for their hospitality during the different study visits and for having welcomed me into their laboratories (Paris and Tarragona are always a second home for me, thanks!). I am also indebted to Dr Marisa Lazzari and Dr Alex Pryor for their advice and for giving me the opportunity to teach during the last academic year.

This research led me to undertake first-hand experimental research to learn how to manufacture prehistoric weapons, cordages, and adhesives as Neanderthals would have possibly done so many times. During this time, I was blessed to have had incredible companions and now it is time to thank my entire “stone-age tribe”: Werner, Ingolf, Urda, Morten, Uli, Erika, Klaus, Markus, Jake, Lisa, Miika, Obbo, Solveig, Rainer, Lena, Emily, Miri, Uri, Kaciaryna, Lilith and her amazing kids, Maks, Stein and his family, and the flintknapper community at Lejre. Similarly, I am incredibly glad to have had the possibility to travel to Namibia and spent four weeks and Christmas Eve alongside with the Ju|'hoansi bushmen group of the Nyae Nyae Conservancy in Tsumkwe (Namibia), I will always remember their peacefulness, their ancient wisdom, their respect for nature and surrounding environment, their morning laugh, the giraffe Christmas dance, and the smoke of their pipe (Žàn!).

I would also like to acknowledge other researchers with whom I had great discussions during conferences or emails, and which have in a way or another participated in the content of this manuscript: Dr Antony Borel, Dr AnneMieke Milks, Justine Coppe, Dr AnneMieke Verbaas, Professor Manuel Vaquero, Dr Amelia Bargallo, Dr Josep Maria Vergès, Dr Veerle Rots (and the entire *Traceolab* research group), Dr Radu Iovita, Dr Katsuhiko Sano, Dr Joseba Rios Garaizar, Professor Richard Fullagar, Dr Javier Baena Preysler, Professor Sho Yamada, Dr Ignacio Martin-Lerma, Professor Estrella Mansur, Dr Jaoa Marreiros, Professor Nacho Clemente, Professor Laura Longo, Dr Roeland Paardekooper, Dr Andy Sorensen, Dr Gema Chacòn Navarro, Dr Camille Daujeard and Dr Hermine Xhaufalir. I especially want to thank Dr Erick Burgos Parra who have aided with the analysis of acceleration records and offered multiple reviews of theoretical physics (muchas gracias Erick!). Similarly, I am grateful to Dr Julian Donald and Dr Sheahan Bestel who read over a few sections of this thesis and offered a spelling review. Of course, all work remains my own.

One of the benefits of the peripatetic lifestyle are the friends we meet on the journey, to whom I am glad. I would like to start with my “Latino Lovers” who made my time in Exeter unforgettable, Adrian, Felipe, Francesco, Carlotta, Dori,

and David. To continue with my colleagues and friends in Exeter, Regina (my PhD buddy), Sinibaldo, Roberta, Giselle, Malavika, Emily, Belinda, Sabine (and her mum), Brice, Tine, Matt S, Leo, Giovanni, Federica, Matteo, Matt K, Raffa, Joao, Liliana, Lukas, Oscar (and the Tarragona folks), my flatmate Kate (and Leon), and many others. A special memory and thanks to my “French musketeers”, Cidalina, Julian, Pedro and Marco. I am also blessed to have had the support of many long-term friends who I met back in the day and with whom I share laughter and moaning, thanks to Maria Santa (thanks for sharing twenty years of our life), Annina, Elisa, Alessandro, Fabio, Gabriele, Ramon, Gilda, Sem and Anna, and Sergio.

There are not enough words to thank my family who has always believed and supported me, and also took advantage of my travels to visit me! Thanks to my sister Federica (may you have all the luck in your future), my father Primo, Nonna Lia, Nonno Tano, Zia Elvi, Zia Orny, Zia Mary, Francy, Ludo, Giulia, Mauro, Peppino, Zio Cesare, Zia Ina, Martina, Gaetano, Adriana, and all the other aunts and cousins.

Last, but not least, I should thank the most important person in my life who has supported me with her contagious enthusiasm during all these years, listened to all my moaning and tiredness, and accepted my prolonged absences from home... Grazie Mamma, questa tesi è anche la tua!

My last thought goes to the *Erasmus* and *Erasmus Mundus* projects which have funded part of my previous studies and allowed me to visit many different countries, through which I have learnt that equality lies in the value of preserving diversity and today with great humility I can say that I feel a citizen of Europe and of this world.

I have certainly omitted to mention the contributions of some. I apologise for this omission and sincerely thank them all.

Alice La Porta

7th February 2019

ABSTRACT

The appearance of stone-tipped spear technology is a crucial milestone in human evolution. Stone-tipped spears are potentially one of the earliest composite hunting weapons to be manufactured and used by humans, involving enhancement of technological, cognitive and social skills. However, due to poor preservation conditions and a deficiency of experimental data the detection of stone-tipped spears in the archaeological record and the identification of their delivery systems are still difficult to achieve. The use of stone-tipped spears as distance throwing weapons, or conversely as close-range thrusting weapons is, therefore, an outstanding debate in Palaeolithic archaeology. Accordingly, this thesis presents an integrated experimental and archaeological investigation to distinguish hand-delivered throwing from hand-delivered thrusting stone-tipped spears, to investigate the development of stone-tipped spear technology among Neanderthal populations in the European Middle Palaeolithic. Systematic experiments extensively tested and compared (i) the performance of hand-delivered throwing and thrusting stone-tipped spears, using Levallois point replicas; and (ii) the resulting microscopic use-wear traces and breakage patterns formed on the throwing and thrusting spear projectiles. Trained and skilled human participants threw and thrust experimental stone-tipped spears into animal carcass targets. For each throw and thrust, several variables along with acceleration profiles and slow-motion video footage were recorded. Integrated results between ballistic parameters and use-wear analysis showed (i) that hand-delivered stone-tipped spears were effective hunting weapons not only as close-range thrusting weapons but also as distance throwing weapons; and (ii) that microscopic use-wear traces and patterns provide useful markers for distinguishing hand-delivered throwing from hand-delivered thrusting stone-tipped spear projectiles. The cross-comparison of the experimental dataset of this thesis with two Middle Palaeolithic stone assemblages from Abris du Maras (France) and Arma Delle Manie (Italy) assisted in establishing that Neanderthals were employing hand-delivered stone-tipped spears at least from MIS 4/beginning of MIS 3, and that throwing distance weapons and selective hunting strategies were likely widespread in the European Middle Palaeolithic.

LIST OF CONTENTS (VOLUME 1)

Acknowledgements.....	4
Abstract	8
List of Contents (Volume 1).....	9
List of Contents (Volume 2).....	22
List of Figures (Volume 1)	24
List of Tables (Volume 1).....	47
List of Accompanying Material (USB stick).....	53
Abbreviations	55
INTRODUCTION.....	57
<i>The importance of studying stone-tipped spear technology in the Neanderthal world</i>	57
CHAPTER 1	66
<i>Middle Palaeolithic weaponry technology and hunting behaviour: state of the debate</i>	66
1.1 Weaponry terminology	66
1.1.1 Outline of hunting techniques conceivably used in Palaeolithic times	68
1.2 How to recognise hunting weapons in the archaeological records?	70
1.2.1 Morphometric studies for the recognition of projectile tools	70
1.2.2 Use-wear and experimental studies for the recognition of projectile tools	72
1.3 The anatomical capability of Neanderthals to throw and thrust spears	74
1.4 “Neanderthal the hunter”: hunting behaviour and weapon evidence in the late Early and Middle Palaeolithic	77
1.4.1 The first evidence of weaponry technology: single-unit untipped wooden spears	81
1.4.2 Untipped wooden spears vs stone-tipped spears	84
1.4.2.1 The demand for hafting.....	84
1.4.2.2 Untipped wooden spears vs stone-tipped spears: definition and cognitive implications.....	85

1.4.2.3	Usage of untipped vs stone-tipped spears: evidence from ethnography and experimental studies	91
1.4.3	Composite stone-tipped spear technology: indirect evidence	95
1.4.3.1	The role of convergent tools	95
1.4.3.2	Evidence of stone projectiles in Middle Paleolithic	97
1.4.3.2.1	The African record	98
1.4.3.2.2	The Eurasian record	99
1.5	<i>Outcomes: the contribution of this research</i>	102
CHAPTER 2	105
	<i>Use-wear analysis methodology</i>	105
2.1	<i>Definition and background</i>	105
2.2	<i>Technical equipment</i>	108
2.2.1	Stereomicroscopes	108
2.2.2	Optical Light Microscopes with incident light (OLMil)	109
2.2.3	Digital microscopes (DM)	110
2.2.4	Scanning Electron Microscope (SEM).....	111
2.2.5	Microscopes employed for this thesis.....	111
2.2.5.1	At the Department of Archaeology, University of Exeter	111
2.2.5.2	At the Natural History Museum (MNHN) of Paris	112
2.2.5.3	At the Archaeological Museum of Finale (Italy)	113
2.2.6	Comparison of images.....	117
2.3	<i>Terminology and use-wear recording location system</i>	127
2.4	<i>Macroscopic Traces: Types and Attributes</i>	130
2.4.1	Fractures.....	132
2.4.1.1	Background.....	132
2.4.1.1.1	Diagnostic Impact Fractures (DIFs).....	132

2.4.1.2	Classification of fractures.....	139
2.4.1.3	Classification of fractures adopted in this thesis.....	145
2.4.1.4	Fracture attributes.....	147
2.4.2	Edge-damage and its attributes.....	148
2.4.2.1	Background.....	148
2.4.2.2	Edge-damage attributes.....	149
2.5	<i>Microscopic Traces: Types and Attributes.....</i>	152
2.5.1	Edge-rounding (ER).....	152
2.5.1.1	Background.....	152
2.5.1.2	Edge-rounding attributes.....	153
2.5.2	Polish.....	154
2.5.2.1	Background.....	154
2.5.2.2	Polish Attributes.....	156
2.5.3	Linear traces, striations, and microscopic impact linear traces (MLITs).....	162
2.5.3.1	Background.....	162
2.5.3.2	Striations and MLITs attributes.....	166
2.5.4	Quantification.....	168
2.5.5	Residues.....	169
2.6	<i>Wear arising from other taphonomy processes.....</i>	170
CHAPTER 3	174
	<i>Protocol of analysis.....</i>	174
3.1	<i>Experimental stone tools: protocol of analysis.....</i>	174
3.2	<i>Archaeological stone tools protocol of analysis.....</i>	177
3.3	<i>Techno-morphological attributes.....</i>	179
3.4	<i>Comprehensive cleaning procedure for experimental tools.....</i>	183

3.4.1	Background.....	183
3.4.2	Cleaning protocol for the experimental Levallois points	184
3.4.2.1	Revision of the cleaning protocol.....	187
3.4.2.2	Usage of chemical acids	192
CHAPTER 4		196
<i>Experimental Programme: hand-delivered stone-tipped spear experiments and butchering knife experiments.....</i>		196
4.1	<i>Experimental purposes and rationale.....</i>	196
4.2	<i>Experimental sets.....</i>	201
4.2.1	Experimental dataset.....	207
4.3	<i>First set of experiments: hand-delivered throwing and hand-delivered thrusting stone-tipped spears.....</i>	210
4.3.1	Experimental variable: Levallois points flint replicas	216
4.3.1.1	Pre-experiment statistical analysis of experimental Levallois points	222
4.3.2	Experimental variable: spear system.....	224
4.3.2.1	Spear shaft replicas	225
4.3.2.2	Hafting arrangements: fore-shafts	231
4.3.2.3	Hafting arrangements: adhesives	237
4.3.2.4	Final hafting arrangements	238
4.3.3	Experimental variable: animal targets	240
4.3.4	Experimental variable: trained human participants	242
4.3.5	Brief outcomes of the first set of experiments.	244
4.4	<i>Second set of experiments: hand-delivered throwing and thrusting stone-tipped spears.....</i>	246
4.4.1	Experimental variable: Levallois points	258
4.4.2	Experimental variable: spear system.....	258

4.4.2.1	Spear shaft replicas	258
4.4.2.2	Hafting arrangements: fore-shafts and adhesives	263
4.4.3	Experimental variable: animal targets	264
4.4.4	Experimental variable: trained human participants	264
4.5	<i>Third set of experiments: butchering knife</i>	265
4.6	<i>Outcomes</i>	271
CHAPTER 5	273
	<i>Kinematics and effectiveness of throwing and thrusting hand-delivered stone-tipped spears in human performed experiments.</i>	273
5.1	<i>Introduction</i>	273
5.2	<i>Spear data acquisition and data processing</i>	280
5.2.1	Data acquisition	280
5.2.2	Data processing.....	285
5.2.2.1	Acceleration profiles construction	285
5.2.2.1.1	Throwing motions	285
5.2.2.1.2	Thrusting motions	288
5.2.2.2	Impact Velocities calculation.....	290
5.2.2.2.1	Throwing velocities	290
5.2.2.2.2	Thrusting velocities.....	292
5.2.2.3	Calculation of the kinetic energy (<i>KE</i>), momentum (<i>p</i>), maximum deceleration, and trajectory	294
5.2.2.3.1	Kinetic energy (<i>KE</i>) at the impact.....	294
5.2.2.3.2	Momentum (<i>p</i>) at the impact.....	297
5.2.2.3.3	Maximum deceleration	298
5.2.2.3.4	Trajectory of the hand-delivered throwing spears	298

5.3 Results of ballistic parameters of throwing and thrusting hand-delivered stone-tipped spears.....	304
5.3.1 Impact velocities	309
5.3.2 Kinetic energy (<i>KE</i>), momentum (<i>p</i>), maximum deceleration, and trajectory.....	309
5.3.2.1 <i>KE</i> at the impact.....	309
5.3.2.2 Momentum at the impact	311
5.3.2.3 Maximum Deceleration	312
5.3.3 Maximum penetration depth	313
5.3.4 Acceleration profiles	315
5.3.4.1 Throwing acceleration profiles	315
5.3.4.2 Thrusting acceleration profiles.....	320
5.3.5 Qualitative observations about the hand-delivered stone-tipped spear experiments.	324
5.4 Correlations between ballistic parameters and spear performance.....	331
5.4.1 Correlation between deceleration values and penetration depth	331
5.4.2 Correlation between penetration depth, TCSA, impact velocities, and impact location	333
5.5 Discussions and conclusions on the recorded ballistic parameters	338
5.5.1 Hand-delivered throwing spears - Impact velocities.....	338
5.5.2 Hand-delivered thrusting spears – Impact velocities.....	340
5.6 Discussions on the lethality of the hand-delivered spears	341
5.7 Outcomes.....	345
CHAPTER 6	352
<i>The macroscopic and microscopic use-wear traces of experimental Levallois points used as throwing and thrusting hand-delivered stone-tipped spears and butchering knives</i>	352
6.1 Introduction.....	352

6.2 Comparing throwing and thrusting experimental Levallois points used as hand-delivered spear projectiles: macroscopic trace results (see also Appendix A, Volume 2) 353

6.2.1	General results on fracture analysis	353
6.2.2	Fracture analysis results	355
6.2.3	Edge-damage analysis results	370
6.2.4	Exploring throwing and thrusting hand-delivered stone-tipped spear experiments: correlation between delivery systems (i.e. throwing vs thrusting) and fracture location ..	374
6.2.5	Exploring throwing and thrusting hand-delivered stone-tipped spear experiments: correlation between impact materials (i.e. hard vs soft tissues) and number of fractures	376
6.2.6	Outcomes: can macroscopic trace types, frequencies and patterns be used to distinguish between throwing and thrusting hand-delivered stone-tipped spear projectiles?	378

6.3 Comparing throwing and thrusting experimental Levallois points used as hand-delivered spear projectiles: microscopic use-wear results (see also Appendix A, Volume 2)..... 381

6.3.1	Overview	381
6.3.2	General results on microscopic use-wear traces	382
6.3.3	Microscopic use-wear traces observed on experimental Levallois points used in throwing hand-delivered stone-tipped spear experiments.....	385
6.3.3.1	Microscopic linear impact traces (MLITs) and striations.....	385
6.3.3.2	Striations in throwing points	392
6.3.3.3	Polish traces.....	393
6.3.3.3.1	Impact polish in throwing points	394
6.3.3.3.2	Other polish traces in throwing points	407
6.3.4	Microscopic use-wear traces observed on experimental Levallois points used in thrusting hand-delivered stone-tipped spear experiments	411
6.3.5	Microscopic use-wear location in throwing and thrusting hand-delivered stone-tipped spear experiments: correlation between delivery systems (i.e. throwing vs thrusting) and use-wear location.....	416

6.3.6 Outcomes: can microscopic use-wear types and frequencies be used to distinguish between throwing and thrusting hand-delivered stone-tipped spear projectiles?

418

6.4 Use-wear traces experimental Levallois points used as butchering knives (see also Appendix A, Volume 2)..... 421

CHAPTER 7 431

Hafting traces of experimental Levallois points used in throwing and thrusting hand-delivered stone-tipped spear experiments..... 431

7.1 Introduction and aims 431

7.2 Experimental sample 432

7.3 Hafting traces: definition and background..... 435

7.3.1 Features of prehension traces 436

7.3.2 Features of hafting traces 437

7.3.2.1 Haft limit or boundary 437

7.3.2.2 Macroscopic hafting traces 437

7.3.2.3 Microscopic hafting traces 439

7.3.2.4 Hafting Polishes 439

7.3.2.4.1.1 Polish distribution for different hafting arrangements 440

7.3.2.4.2 Hafting bright spots..... 441

7.3.2.5 Binding traces 441

7.3.3 Final remarks on hafting traces 442

7.4 Results of hafting traces (see also Appendix A, Volume 2) 443

7.4.1 Presence of haft boundary 444

7.4.2 Presence of proximal edge-damage..... 448

7.4.3 Presence of adhesive polishes (or polished layers) and adhesive residues..... 457

7.4.3.1 Polishes (or polished layers) as attributes with which to distinguish hafting arrangements 470

7.4.4	Presence of hafting bright spots	472
7.5	Overview.....	474
CHAPTER 8	477
	<i>Archaeological sample tools: selection of and introduction to the archaeological sites</i>	
	477	
8.1	<i>Archaeological sites: selection and rationale</i>.....	477
8.1.1	Objectives	479
8.2	<i>Arma Delle Manie (Italy)</i>.....	482
8.2.1	Introduction to the site	482
8.2.2	Stratigraphy and Chronology	485
8.2.2.1	Stratigraphy.....	485
8.2.2.2	Chronology.....	487
8.2.3	Landscape occupation and geological context.....	489
8.2.4	Paleo-environmental data: palynological, sedimentological, and micro-faunal analyses.....	491
8.2.5	Faunal assemblage and Taphonomy	492
8.2.6	Human remains	493
8.2.7	Raw material and Lithic assemblage.....	494
8.2.8	Lithic reduction sequences	495
8.2.8.1	Levallois points production at Arma Delle Manie.....	496
8.2.8.2	TCSA, TCSP, and tip angle values.....	500
8.2.9	Type of site and mobility.....	501
8.3	<i>Abri du Maras (Ardèche, France)</i>.....	503
8.3.1	Stratigraphy	505
8.3.2	Chronology	507
8.3.3	Landscape setting & raw material sources.....	508

8.3.4	Paleo-environmental data: faunal, charcoal and isotopic analyses.	509
8.3.5	Faunal assemblage at Abri du Maras.....	511
8.3.5.1	Faunal analysis of Level 4	512
8.3.6	Raw material and lithic assemblage.....	513
8.3.7	Lithic reduction sequences	514
8.3.7.1	Levallois points at Abri du Maras Level 4 (sublevels 4.1 and 4.2).....	516
8.3.7.1.1	TCSA, TCSP, and tip angle values	520
8.3.7.1.2	In situ or extra situ production	521
8.3.8	Type of site and mobility strategies	523
CHAPTER 9	525
	<i>Arma Delle Manie (Liguria, Italy): use-wear results of Levallois points and convergent tools.....</i>	525
9.1	<i>Archaeological dataset.....</i>	525
9.1.1	Sampling and procedure of analysis	526
9.1.2	State of preservation of the selected convergent stone tools	531
9.1.2.1	Chemical alterations	531
9.1.2.2	Mechanical alterations	535
9.1.2.3	Curation traces.....	536
9.1.2.4	Final considerations	537
9.1.3	Final sample	538
9.2	<i>Functional results</i>	540
9.2.1	Macroscopic analysis.....	540
9.2.1.1	Type and frequencies of fractures	540
9.2.1.1.1	Location of macroscopic traces	545
9.2.1.1.2	Macroscopic hafting traces.....	546
9.2.2	Microscopic analysis.....	548

9.2.2.1	Projectile tools: use-wear evidence	548
9.2.2.2	Tools used in longitudinal motions: use-wear	568
9.2.2.3	Tools used in transversal motions: use-wear evidence	572
9.2.2.4	Tools used in multiple motions: use-wear evidence	580
9.3	<i>Outcomes: functional interpretations</i>	581
CHAPTER 10	584
	<i>Abri du Maras (Ardèche, France): use-wear results of Levallois points and convergent tools</i>	584
10.1	<i>Archaeological dataset</i>	586
10.1.1	Sampling and procedure of analysis	586
10.1.2	State of preservation of the selected tools	590
10.1.2.1	Chemical alterations	591
10.1.2.2	Mechanical alterations	593
10.1.2.3	Final considerations	594
10.1.3	Final sample	596
10.2	<i>Functional results</i>	597
10.2.1.1	Projectile tools: use-wear evidence	597
10.2.1.2	Tools used in longitudinal motions: use-wear evidence	620
10.2.1.3	Tools used in transversal motions: use-wear evidence	624
10.2.1.4	Tools used in multiple motions: use-wear evidence	626
10.2.1.5	Used tools but unknown function: use-wear evidence	630
10.3	<i>Outcomes: functional interpretations</i>	634
CHAPTER 11	638
	<i>DISCUSSION</i>	638
11.1	<i>Research approaches</i>	638
11.1.1	Experimental approach	638

11.1.2	Ballistic approach	641
11.1.3	Use-wear approach	641
11.1.4	Archaeological approach.....	642
11.2 Assessing the performance and effectiveness of Middle Palaeolithic hand-delivered stone tipped spear replicas.....		643
11.3 Assessing diagnostic use-wear traces of experimental hand-delivered throwing and thrusting spear projectiles		647
11.3.1	Macroscopic diagnostic traces	647
11.3.2	Discussion on microscopic diagnostic traces.....	655
11.3.2.1	Presence and frequencies of microscopic linear impact traces (MLITs)	656
11.3.2.2	Presence and frequencies of “impact polish”.....	659
11.3.2.3	A hint on hafting traces	663
11.3.2.4	Overview	664
11.4 Assessing the presence of projectile tools within archaeological assemblages: implication for Neanderthals’ hunting behaviour.....		665
11.4.1	Comparison of archaeological results	665
11.4.2	Diagnostic impact fractures (DIFs) observed on the archaeological tools.....	667
11.4.3	Differences between the two assemblages: the support of microscopic use-wear analysis	671
11.4.3.1	Occupation at Arma Delle Manie	672
11.4.3.2	Occupation at Abri du Maras	674
11.5 Revisiting Neanderthal hunting strategies		676
CHAPTER 12.....		684
Conclusions.....		684
12.1 Research outcomes: experimental data		684
12.2 Research outcomes: archaeological data		688
12.3 Future directions		690

Bibliography..... 693

LIST OF CONTENTS (VOLUME 2)

APPENDIX A.....	809
<i>The register of use-wear traces of the experimental Levallois points series.....</i>	809
A.1 Introduction.....	810
A.2 Register of use-wear of experimental Levallois points used as throwing hand-delivered stone-tipped-spears (data from the first set of experiments, see Chapter 4).....	813
A.3 Register of use-wear traces of experimental Levallois points used as thrusting hand-delivered stone-tipped-spear (data from the first set of experiments, see Chapter 4).....	826
A.4 Register of use-wear traces of experimental Levallois points used as throwing hand-delivered stone-tipped-spears (data from the second set of experiments, see Chapter 4).....	839
A.5 Register of use-wear traces of experimental Levallois points used as thrusting hand-delivered stone-tipped-spears (data from the second set of experiments, see Chapter 4).....	886
A.6 Register of use-wear traces of experimental Levallois points used as butchering knives (data from the third set of experiments, see Chapter 4).....	923
APPENDIX B.....	940
<i>Levallois points and Levallois technology: definition and technological introduction.....</i>	940
B.1 Levallois methods and variability.....	941
B.1.1 Levallois points and convergent tools: definition.....	943
APPENDIX C.....	946
<i>Experiments and experimental data.....</i>	946
APPENDIX D.....	950
<i>Techno-morphometric data of the experimental Levallois points.....</i>	950
APPENDIX E.....	955
<i>Recorded ballistic parameters.....</i>	955
APPENDIX F.....	959
<i>Techno-morphometric data of the convergent tools of Arma Delle Manie (Italy).....</i>	959

APPENDIX G.....	964
<i>Techno-morphometric data of the analysed convergent tools of Abri du Maras (France).....</i>	<i>964</i>

LIST OF FIGURES (VOLUME 1)

Figure 1.1. Operational schemes of production and use of a stone-tipped spear and the single-unit simple wooden spear from Lombard and Haidle (2012, figure 2).	90
Figure 2.1. Left: The stereomicroscope Olympus SZ61 (located at the Department of Archaeology, University of Exeter). Right: Multiple-fractures observed with the stereomicroscope (OM 25x).....	109
Figure 2.2. Right: an example of a microscope showing the light pathway in a reflected and transmitted light microscope (image from https://www.olympus-lifescience.com/en/microscope-resource/primer/anatomy/reflected/ , last accessed 14-05-2015). Left: polish trace observed with an OLMil (OM 200x).....	110
Figure 2.3. The stereomicroscope and the OLMil microscopes located at the Department of Archaeology, University of Exeter. (Image La Porta).	112
Figure 2.4. The Hirox KH-8700 DM located at the Natural History Museum, Paris. (Image La Porta, with permission of MNHN, Paris).....	113
Figure 2.5. The Dino-lite Edge AM7915MZT DM employed at the Archaeological Museum of Finale (Liguria, Italy; Image La Porta).	114
Figure 2.6. Left: animal hair residue. Picture was taken with the OLMil (Olympus BX60) image with manual focus (Z-stack) based on 12 pictures at 100x (2 minutes realisation time). Right: animal flesh residue. Picture was taken with an Hirox- 8700 DM image with an automatically extended focus (Z-stack) based on 27 pictures, at 100x (Low-range objective lens, 20 seconds realisation time). (Image La Porta).	119
Figure 2.7. Snap fracture on a Levallois point used as a throwing spear-head. Left: picture was taken with an OLMil at 50x (scale=200µm). The fracture is not clear (no Z-stack used). Right: Dino-Lite Edge AM7915MZT picture at 50x (scale=1000µm). Fracture is clear (no Z-stack used). (Image La Porta).....	120
Figure 2.8. Well-developed polish on a retouched flake used as a scraper on commercial leather with the addition of ochre (use time 45 minutes). Pictures were taken after cleaning the tool. A) OLMil picture at 50x (scale=200µm); B) Dino-Lite Edge AM7915MZT picture at 50x (scale=1000µm); C) OLMil picture at 100x (scale=100µm); D) Dino-Lite Edge AM7915MZT picture at 100x (scale=500µm); E) OLMil picture at 200x (scale=50µm); F) Dino-Lite Edge AM7915MZT picture at 200x (scale=200µm); G) OLMil picture at 500x (scale=20µm); H) Dino-Lite Edge AM7915MZT picture at 220x (maximum magnification), (scale=200µm). Dino-lite pictures were all taken using the polariser filter. (Image La Porta).	121

Figure 2.9. Microscopic Linear Impact Traces (MLITs) on the distal ventral tip (Locus D1v) of an experimental Levallois point used as a throwing spear-head. Pictures were taken after cleaning the tool. A) OLMIL picture at 50x (scale=200µm); B) Dino-Lite Edge AM7915MZT picture at 50x (scale=1000µm); C) OLMIL picture at 100x (scale=100µm); D) Dino-Lite Edge AM7915MZT picture at 100x (scale=500µm); E) OLMIL picture at 200x (scale=50µm); F) Dino-Lite Edge AM7915MZT picture at 200x (scale=200µm); G) OLMIL picture at 500x (scale=20µm); H) Dino-Lite Edge AM7915MZT picture at 220x (maximum magnification), (scale=200µm). (Image La Porta)..... 124

Figure 2.10. Polish located on the ventral distal tip (locus D1v): (A) An archaeological Levallois point, (B) an experimental Levallois point. A) Hirox KH-8700 picture at 140x middle-range objective lens (Middle-low-range, MRO); B) OLMil picture at 100x (scale=100µm); C) Hirox KH-8700 picture at 200x MRO; D) OLMil picture at 200x (scale=50µm); E) Hirox KH-8700 picture at 400x MRO; E) OLMil picture at 500x (scale=20µm). (Image La Porta). 125

Figure 2.11. Recording location system of use-wear observations. The point has been divided into 14 independent loci: distal ventral portion (D1v, D2v, D3v); distal dorsal portion (D1d, D2d, D3d); mesial ventral portion (M1v, M2v); mesial dorsal portion (M1d, M2d); proximal ventral portion (P1v, P2v); proximal dorsal portion (P1d, P2d). (Image La Porta)..... 129

Figure 2.12. A fracture (with a bending initiation and a hinge termination; bottom picture, DM OM 40x) and a scar (with bending initiation and a step and a hinge termination, bottom picture, DM OM 30x). (Image La Porta). 131

Figure 2.13. Fracture classification proposed by the Ho Ho Committee, 1979 (Image from Hayden, 1979, figure 1)..... 134

Figure 2.14. Initiations and terminations of fractures. 1. Cone fracture, 2. Bending fracture, 2a. Feather-terminating bending fracture, 2b. Hinge-terminating bending fracture, 2c. Step-terminating bending fracture, 2d. Snap termination, 2e. Embryonic fracture, 2f. Spin-off fracture. (Image from Fisher et al., 1984, figure 23)..... 135

Figure 2.15. Cone scar with an indication of the point of impact (red circle), DM OM 40x. 139

Figure 2.16. Bending fracture (in blue a bending initiation fracture terminating in a double feather; in red a burination fracture with a bending initiation), DM OM 20x..... 140

Figure 2.17. Cone fracture profile (left). Bending fracture profile (right. Modified from Ho Ho Committee 1979). 141

Figure 2.18. Edge-damage and scar schematic representation (Image adapted from Claud, 2015, p. 133). 149

Figure 2.19. Scar morphology (Image adapted from Rots, 2010, p. 30)..... 150

Figure 2.20. Edge-damage distribution (Image adapted from Rots, 2010, p. 31).....	151
Figure 2.21. Kinematic representation of a tool during utilisation and its components (Image from Unrath et al., 1986).	153
Figure 2.22. Delineation of the locus in plan view. (Image La Porta).....	156
Figure 2.23. Polish distribution along the edge of the tool. (Image La Porta).....	157
Figure 2.24. Polish texture: smooth polish (left), rough polish (right). (Image La Porta)	158
Figure 2.25. Degree of Polish Linkage. The polish is represented in white (Image adapted from Jensen, 1994, figure 24).....	158
Figure 2.26. Polish topography: faint polish (top left), domed polish (top right), flat polish (bottom left), linear polish (bottom right). (Image La Porta).....	159
Figure 2.27. Polish extension (Image from Jensen 1994, p. 25, figure 9)	160
Figure 2.28. Polish directionality. The polish is shown represented in grey (Image La Porta).	161
Figure 2.29. A. Linear striations; B. MLITs. (Image La Porta).....	165
Figure 2.30. Directionality of striations and MLITs. (Image La Porta).....	167
Figure 2.31. Types of post-depositional alterations. A. White patina; B. Coloured patina; C. Glossy patina; D. Lacquer, numbering, nail polish and stickers (Image La Porta).	173
Figure 3.1. Cleaning of the archaeological stone tools of Abri du Maras, at the Natural History Museum (Paris). Tools were soaked in demineralised water and <i>Derquim</i> detergent for a 15-minute ultrasonic bath. (Image La Porta).	178
Figure 3.2. D corresponds to the technological axis of the tool, M to the morphological axis of the tool. L corresponds to the maximum length of the tool (Inizan et al., 1999, figure 41).	182
Figure 3.3. Morphometric attributes: maximum length, maximum width, and tip angle. (Image La Porta).....	182
Figure 3.4. Cleaning system of the experimental Levallois points (ELPs). From left to right: 1. Dirty tools; 2. ELPs left overnight immersed in H ₂ O with <i>Derquim</i> ; 3. ELPs after de-hafting; 4. ELPs in an ultrasonic tank, (Image La Porta).....	190
Figure 3.5. Documentation of the mould/casting technique of the experimental Levallois points (ELPs). 1. ELPs freshly knapped; 2. ELPs in an ultrasonic tank of pure acetone for 5 minutes; 3. Mould production of the distal tips of the ELPs, with the Provil Novo Light; 4. The moulds fixed	

in a horizontal position; 5. Preparation and measurement of the polyurethane resin, Feropur PR55; 6. Cast making. (Image La Porta).	191
Figure 3.6. Bright and greasy polished layer located on the ventral-mesial part of the tool, in close proximity to the haft-limit (features explained in CHAPTER 7). Pictures: OLMil, OM 100x (above) and 200x (below), (Tool ID TH-78).	193
Figure 3.7. Black and white picture (above) and coloured picture (below). The picture shows a brown tar deposit (bottom line) and a shiny and greasy polished layer which was a residue of the tar-adhesive (upper line). Pictures: OLMil, OM 100x, (Tool ID TH-66).	194
Figure 3.8. Bright and greasy spots of the adhesive (tar-based) used for the hafting. These were located on the ventral-mesial part of the tool, in close proximity to the haft-limit (features explained in CHAPTER 7). Picture: OLMil, OM 200x, (Tool ID TH-20).	195
Figure 4.1. First set of experiments: a sample of throwing experiment.	212
Figure 4.2. First set of experiments: a sample of the thrusting experiments.	212
Figure 4.3. Spear penetration after a throwing experiment (experiment code: TH-32).	214
Figure 4.4. Field-form used for the recording of each hand-delivered throwing or thrusting spear experiment, first set of experiments (experiment code: TH-32).	215
Figure 4.5. MK and the author during the knapping process for the reproduction of the experimental Levallois points.	216
Figure 4.6. Knapping process and hammerstone used.	217
Figure 4.7. Sample of the experimental Levallois points after knapping.	218
Figure 4.8. Flint Levallois point – raw material subtype 1. Picture OLMil at 100x.	221
Figure 4.9. Flint Levallois point – raw material subtype 2. Picture OLMil at 100x.	221
Figure 4.10. Boxplots of the maximum technological length (left) and the maximum technological width (right) values for TH and TR experimental Levallois points.	224
Figure 4.11. Boxplots of TCSA (left) and TCSP (right) values for TH and TR experimental Levallois points.	224
Figure 4.12. Experimental stone-tipped spear setup.	225
Figure 4.13. Shaft manufacturing process, first set of experiments.	228
Figure 4.14. The reinforcement system for the spear shafts' distal ends. Commercial sinew was bound around the spear's distal end and fixed with commercial tar.	229

Figure 4.15. Wooden spear shaft replicas produced for the first set of experiments.....	230
Figure 4.16. The wooden fore-shaft used in the first, second, and third sets of experiments. (Image La Porta and Tonelli).....	232
Figure 4.17. Left: Experimental Levallois point mounted in a female fore-shaft slot type and fixed with tar. Right: Technical drawing of a fore-shaft with a female haft slot type (lateral view, Image La Porta and Tonelli).....	234
Figure 4.18. Left: Experimental Levallois point mounted in a juxtaposed fore-shaft type and fixed with tar. Right: Technical drawing of a fore-shaft with a juxtaposed haft slot type (lateral view, Image La Porta and Tonelli).....	235
Figure 4.19. Left: Experimental Levallois point mounted in a flat fore-shaft type and fixed with tar. Right: Technical drawing of a fore-shaft with a flat haft type (lateral view, Image La Porta and Tonelli).....	236
Figure 4.20. Left: Production of the resinous adhesive recipe. Right: An experimental Levallois point hafted with the resin recipe glue (dorsal and ventral views).	237
Figure 4.21. Left: A lump of tar. Right: An experimental Levallois point hafted with the commercial tar (dorsal and ventral views).....	238
Figure 4.22. The three fore-shaft hafting arrangements tested in the first set of experiments. A. Juxtaposed slot hafting type; B. Flat slot hafting type; C. Female slot hafting type.....	239
Figure 4.23. Animal target positioned into the frame in a “running position”. The red circle indicates the aiming area.	242
Figure 4.24. Above: Camera setup. Cam1: Sony FS5 XDCAM High-speed Camera; Cam2: Canon Shot SX270 HS; Accelerometer setup. Below: IP and TB mounting the equipment and setting the cameras.	249
Figure 4.25. Accelerometer mounted in a custom-made slot on the spear shaft.	250
Figure 4.26. Picture archive system for the second set of experiments. 1: Experimenter is holding the spear and the tablet. 2: Tablet displaying information. 3: Target before the shot. 4: Spear inside the animal, frontal view. 5: Spear inside the animal, from the opposite side of the target. 6: Spear inside the animal, lateral view.	252
Figure 4.27. The author and WP during the recording process (after execution).	253
Figure 4.28. Picture archive system for the second set of experiments. 1: Wound with spear, frontal view. 2: Wound with spear, from the opposite site of the target. 3: Wound without a spear, frontal view. 4: Wound without a spear, from the opposite site of the target.	253

Figure 4.29. Second set of experiments: a sample of the throwing experiments.	256
Figure 4.30. Second set of experiments: a sample of the thrusting experiments.	257
Figure 4.31. Shaft manufacturing process (de-barking and first planning), second set of experiments.	260
Figure 4.32. Experimental spear shaft, second set of experiments.	262
Figure 4.33. Experimental fore-shafts manufacturing process (de-barking and first planning), second set of experiments.	264
Figure 4.34. Picture of the third set of experiments. 1: Deskinning, 2: Contact angle, 3: Filletting, 4: Sinew removal.	269
Figure 4.35. Field-form used for the recording of the “Comparative experiments”.	270
Figure 5.1. Acceleration on the X , Y and Z axes and the acceleration module (i.e. the relationship between acceleration variation and time) of a hand-delivered throwing spear experiment (experiment code: TH-81). Graph: La Porta and Burgos.	282
Figure 5.2. Example of a throwing (A) and a thrusting (b) acceleration profile with the indication of the impact events (in red circles). Graph: La Porta and Burgos.	284
Figure 5.3. Example of a data-file from the accelerometer X200-4. The spreadsheet shows the raw acceleration in the X , Y , and Z axes. The picture shows the first few entries (i.e. time intervals) of the spreadsheet. However, each spread-sheet counted between 30,000 and 60,000 entries (see accompanying material, acceleration spreadsheets on the USB stick).	284
Figure 5.4. Acceleration profile of a throwing spear in a hand-delivered experiment (experiment code: TH-62). Graph: La Porta and Burgos.	287
Figure 5.5. Acceleration profile of a thrusting spear in a hand-delivered experiment (experiment code: TR-55). Graph: La Porta and Burgos.	289
Figure 5.6. The 2D parabolic trajectory (X - Z axes) of the centre of mass of the spear during its flying time. Axes (X and Z) are in metres, (experiment code: TH-81). Graph: E. Burgos-Parra.	300
Figure 5.7. The graph shows the 3D trajectory of the centre of mass of the spear after leaving the hand of the thrower and just before impacting the animal (i.e. the flying time). Axes (X , Y , and Z) are in metres (experiment code: TH-81). Graph: E. Burgos-Parra.	301
Figure 5.8. X , Y , and Z components and module of the acceleration (experiment code: Th-81).	302

Figure 5.9. The gyration movement of the accelerometer (in red) on the symmetry axis of the spear. Top picture: experiment code TH-82, bottom picture: experiment code TH-62.....	303
Figure 5.10. Histograms of distributions of impact velocity frequencies of throwing (left) and thrusting (right) experiments.....	309
Figure 5.11. Histograms of distributions of the kinetic energy (<i>KE</i>) frequencies of throwing (left) and thrusting (right) experiments.....	310
Figure 5.12. Histograms of the distributions of momentum frequencies of throwing (left) and thrusting (right) experiments.....	312
Figure 5.13. Histograms of the distributions of maximum deceleration frequencies of throwing (left) and thrusting (right) experiments.	313
Figure 5.14. Histograms of skewed distributions of penetration depth frequencies of throwing (left) and thrusting (right) experiments.	314
Figure 5.15. “Full penetration” profiles. The spear hit and penetrated the target as shown by the fluctuating acceleration during the penetration time (in red; experiment code: TH-62).	318
Figure 5.16. “Bounced” acceleration profiles. The spears hit the target and bounced back, as shown by the second peak of acceleration (red circle; experiment code: TH-58 up picture)....	318
Figure 5.17. “Missed” acceleration profiles. The spear missed the target and went straight into the ground, as shown by the very short penetration time (red line; experiment code: TH-84).	319
Figure 5.18. “One-push” profile. The thruster pushed the spear inside the animal target only once as shown by the single acceleration peak (in red; experiment code: TR-89).	322
Figure 5.19. “Two-pushes” profile. The thruster double pushed the spear inside the animal target as shown by the two consecutive acceleration peaks (in red; experiment code: TR-83).	322
Figure 5.20. “Soft-tissue penetration” profile. The acceleration after impact shows a low value (around -6 m/s ² see red circle; experiment code: TR-57).	323
Figure 5.21. “Hard-tissue penetration” profile. The acceleration after impact shows a high value (around -25 m/s ² see red circle; experiment code: TR-90).	323
Figure 5.22. An example of a deeper penetration caused by a hand-delivered stone-tipped throwing spear (experiment code: TH-62).....	325
Figure 5.23. An example of a deeper penetration caused by a hand-delivered stone-tipped throwing spear (experiment code: TH-62).....	326

Figure 5.24. An example of a deeper penetration caused by a hand-delivered throwing stone-tipped spear (experiment code: TH-77).	327
Figure 5.25. Damage of the spinal ligaments caused by a hand-delivered throwing spear that bounced off (experiment code: TH-66).	329
Figure 5.26. Example of wounds and bone breakages caused by hand-delivered throwing spears.....	330
Figure 5.28. Correlation between the maximum deceleration after the impact (blue spots) and the penetration depth (red dots) for each shot (missed shots were not included).	332
Figure 5.29. Penetration depth (cm) of this thesis' hand-delivered throwing and thrusting spears.	343
Figure 5.30. Cumulative distributions of throwing and thrusting hand-delivered spear experiments divided per categories of impacts.	345
Figure 5.31. High-speed video-frames of a throwing motion. The position of the accelerometer is marked with a red circle (experiment code: TH-77), (Image La Porta).	349
Figure 5.32. High-speed video-frames of a thrusting motion. The position of the accelerometer is marked with a red circle (experiment code: TH-77), (Image La Porta).	350
Figure 5.33. Position of the X200-4 accelerometer on the experimental spear shaft. (Image La Porta).	351
Figure 5.34. J Pargeter throwing a hand-delivered stone-tipped spears into an unrealistic animal target from a very close distance on a plastic tarp (from Pargeter et al. 2016, 151, figure 5). .	351
Figure 6.1. Distribution of fracture types (in percentages %) in the experimental Levallois points according to their delivery systems (throwing in blue vs thrusting in red).	357
Figure 6.2. Bending fracture terminating in a double feather (in blue), plus a primary burination fracture (in red). DM OM 50x (experiment code: TH-85).	361
Figure 6.3. Bending fracture with a double step termination (in blue and red), DM OM 35x (experiment code: TR-93).	361
Figure 6.4. Multiple fractures. Bending fracture terminating into a hinge (in orange); bending fracture (with a missing initiation) with a hinge termination (in blue); small bending scars with feather termination (in red). DM OM 30x (experiment code: TH-79).	362
Figure 6.5. Bending fracture (with missing initiation) terminating in a double step (in red) plus a snap fracture, (in blue), DM OM 32x (experiment code: TR-74).	362

Figure 6.6. Multiple fractures. Two bending hinge fractures (with missing initiation; in red) plus bending scars (in blue), and cone scars (in orange), DM OM 80x (experiment code: TR-83).	363
Figure 6.7. Multiple fractures. A feather-terminating bending fracture (in blue); a bending fracture with a double step and feather termination (in red); a bending fracture with a step termination (in orange); a small hinge-terminating bending fractures (in light blue); a bending fracture with a feather termination (in green). DM OM 20x (experiment code: TR-89).....	363
Figure 6.8. Primary burination fracture, DM OM 35x (experiment code: TH-92).	365
Figure 6.9. Unifacial spin-off fracture (in red) departing from a snap fracture (in blue), DM OM 50x (experiment code: TH-34).....	366
Figure 6.10. Several unifacial spin-off fractures (in blue) departing from a snap fracture (in red) observed above the haft-limit (presence of tar), DM OM 17x (experiment code: TH-78).	367
Figure 6.11. Several unifacial spin-off fractures (in blue) departing from an 'S' shaped snap fracture (in red) observed above the haft-limit, DM OM 17x (experiment code: TH-78).....	367
Figure 6.12. Unifacial spin-off fracture (in blue) departing from a bending feather-terminating fracture (in red), plus a bending fracture (with a missing initiation) with a hinge termination (in orange), DM OM 25x (experiment code: TR-35).....	368
Figure 6.13. A small spin-off fracture (in orange on the left) plus a spin-off burination fracture (in red on the right; plus a step-terminating fracture with an indeterminate initiation in green) departing from a snap fracture (in blue), DM OM 50x (experiment code: TH-77).....	368
Figure 6.14. Edge-damage. Cone scars with scalar (in red) and half-moon (in blue) morphologies, DM OM 41x (experiment code: TR-80).	372
Figure 6.15. Edge-damage. Bending (in blue) and cone (in red) scars with half-moon/scalar morphology, DM OM 55x (experiment code: TR-55).	372
Figure 6.16. Edge-damage. Overlying of cone (in red) and bending (in blue) scars with elongated morphology, DM OM 55x (experiment code: TR-36).	373
Figure 6.17. Intense edge-damage, i.e. tip-crushing. The tip is completely crushed after impact creating multiple cone scars, DM OM 50x (experiment code: TR-86).	373
Figure 6.18. Distribution of distal (in blue), mesial (in red) <i>and</i> proximal (in green) fractures according to the delivery system (i.e. throwing vs thrusting).	375
Figure 6.19. Distribution of bending fractures (Bending), spin-off fractures (Spin-off) and primary burination fractures (PrimBur) according to the impact materials, i.e. hard tissues (in blue) vs soft tissues (in red).	377

Figure 6.20. Distribution of microscopic wear traces (in percentages %) in the experimental Levallois points, according to their delivery system (throwing in blue vs thrusting in red). 384

Figure 6.21. MLITs located on the ventral distal tip (Locus D1v). Picture: OLMil, OM 100x (above) and 200x (below), (experiment code: TH-78). The red arrow indicates the location or direction of the distal tip..... 388

Figure 6.22. MLITs located on the ventral distal tip (Locus D1v). Picture: OLMil, OM 50x (above) and 500x (below), (experiment code: TH-31). The red arrow indicates the location or direction of the distal tip. 389

Figure 6.23. MLIT located on the ventral distal tip (Locus D1v). Picture: OLMil, OM 100x, (experiment code: TH-82). The red arrow indicates the location or direction of the distal tip... 390

Figure 6.24. MLITs located on the ventral distal tip (Locus D1v). Picture: OLMil, OM 100x, (experiment code: TH-84). The red arrow indicates the location or direction of the distal tip... 390

Figure 6.25. MLITs resulting from impact against the ground. They are located on the ventral mesial face (Locus M2v). Picture: OLMil, OM 100x (experiment code: TH-71). The red arrow indicates the location or direction of the distal tip..... 391

Figure 6.26. MLITs resulting from impact against the ground. They are located on the ventral mesial face (Locus M2v). Picture: OLMil, OM 100x (experiment code: TH-81). The red arrow indicates the location or direction of the distal tip..... 392

Figure 6.27. MLITs observed with the ESEM, OM 1250x. Plastic deformation of the flint surface in form of channels. The red arrow indicates the location or direction of the distal tip (experiment code: TH-31)..... 392

Figure 6.28. Impact polish type A located on the distal tip (Locus D1v). The polish displays a bright and smooth appearance at 100x (above) and a domed-into-flat topography with deep striations at 200x (below). Picture: OLMil, OM 100x (above) and 200x (below), (experiment code: TH-20). The red arrow indicates the location or direction of the distal tip. 398

Figure 6.29. Impact polish type A located on the distal tip (Locus D1v). The polish shows a bright aspect at 200x (above) and multiple striations at 500x (below). Picture: OLMil, OM 200x (above) and 500x (below), (experiment code: TH-23). The red arrow indicates the location or direction of the distal tip..... 399

Figure 6.30. Impact polish type A located on the distal tip (Locus D1v). The polish shows a rough texture, a less bright aspect due to the coarse raw material, and small striations. The striations run slightly oblique to the axis of the tool. Picture: OLMil, OM 100x (above) and 200x (below), (experiment code: TH-32). The red arrow indicates the location or direction of the distal tip..... 400

Figure 6.31. Impact polish type A located on the distal tip (Locus D1v). The polish shows a moderately bright aspect at 200x (above) and multiple crossed striations at 500x (below). Picture: OLMil, OM 200x (above) and 500x (below), (experiment code: TH-92). The red arrow indicates the location or direction of the distal tip..... 401

Figure 6.32. Impact polish type A located on the distal lateral edges (Locus D3v). The polish shows a moderately bright aspect at 200x (above) with a flat topography and multiple oblique striations at 500x (below). Picture: OLMil, OM 200x (above) and 500x (below), (experiment code: TH-92). The red arrow indicates the location or direction of the distal tip. 402

Figure 6.33. Impact polish type A located on the distal tip (Locus D1v). The polish shows a moderately bright aspect at 100x (above) with a domed-into-flat topography and mineral appearance at 200x (below). The roundness of the edge is due to retouch. Picture: OLMil, OM 100x (above) and 200x (below), (experiment code: TH-82). The red arrow indicates the location or direction of the distal tip. 403

Figure 6.34. Impact polish type B located on the distal lateral edges (Locus D2v). The polish shows a smooth texture, domed topography, and reflective aspect. Only a few striations are present. Picture: OLMil, OM 100x (above) and 200x (below), (experiment code: TH-58). The red arrow indicates the location or direction of the distal tip. 404

Figure 6.35. Impact polish type B located on the distal lateral edges (Locus D3v). The polish shows a smooth texture, domed topography, and a reflective aspect. Only a few striations are present. Picture: OLMil, OM 100x (above) and 200x (below), (experiment code: TH-68). The red arrow indicates the location or direction of the distal tip. 405

Figure 6.36. Impact polish type B located on the distal lateral edges (Locus D2v). Very reflective polish with domed-into-flat topography and very little striations. Picture: OLMil, OM 100x (above) and 200x (below), (experiment code: TH-68). The red arrow indicates the location or direction of the distal tip. 406

Figure 6.37. Polish located on the distal tip (Locus D1v). The polish shows a poor development and a dull to medium-bright aspect. No striations were observed. Picture: OLMil, OM 100x (experiment code: TH-62). The red arrow indicates the location or direction of the distal tip... 408

Figure 6.38. Polish located on the distal tip (Locus D1v). The polish shows a poor development and a dull to medium-bright aspect. Few striations were observed. Picture: OLMil, OM 100x (above), 500x (below), (experiment code: TH-76). The red arrow indicates the location or direction of the distal tip..... 409

Figure 6.39. Well-developed polish located on the ventral distal tip (Locus D1v) of a thrusting experimental Levallois point. It shows a flat topography and bright aspect, OLMil OM 200x (experiment code: TR-83). The red arrow indicates the location or direction of the distal tip... 413

Figure 6.40. Generic and not very well developed polish located on the ventral distal tip (Locus D1v), OLMil OM 100x (experiment code: TR-69). The red arrow indicates the location or direction of the distal tip.....	414
Figure 6.41. Isolated spots of polish located on the ventral mesial part of the tool (Locus M1v), OLMil OM 100x (experiment code: TR-89).	414
Figure 6.42. Isolated spots of polish located on the ventral mesial part of the tool (Locus M1v), OLMil OM 200x (experiment code: TR-83).	415
Figure 6.43. MLITs located on the ventral distal tip (Locus D1v). Picture: OLMil, OM 100x, (experiment code: TR-89). The red arrow indicates the location or direction of the distal tip... ..	415
Figure 6.44. MLITs located on the ventral distal tip (Locus D2v inner surface). Picture: OLMil, OM 100x, (experiment code: TR-90). The red arrow indicates the location or direction of the distal tip.	416
Figure 6.45. Bending fracture with a step-feather termination (in red) plus two cone scars (in blue; experiment code BK-99), DM OM 56x.	424
Figure 6.46. Example of edge-damage observed on the experimental Levallois points used as butchering knives. Top picture: medium half-moon scars (DM OM 40x, experiment code BK-96); Bottom picture: large scalar and rectangular scars (DM OM 40x, experiment code BK-99). ...	425
Figure 6.47. Greasy and faint polish observed on the experimental Levallois points used as butchering knives. Top picture: experiment code BK-102, OLMil/OM 100x; Bottom picture experiment code BK-87, OLMil/OM 100x.....	426
Figure 6.48. Spots of polish due to bone contact. The polish shows flat topography with striations. Picture: OLMil/OM 100x (above) and 200x (below; experiment code BK-59).....	427
Figure 6.49. Fresh hide-like polish. The polish shows a large band of polish disturbed longitudinally along the edge, At 100x, the polish, already well-developed, presented a rough and greasy appearance (top picture). At 200x, the polish shows characteristic “craters” or large micro-pits traces Picture: OLMil/OM 100x (above) and 200x (below; experiment code BK-97).	428
Figure 6.50. Greasy and rough polish due to contact with fresh-hide of the wild boar. Top picture: experiment code BK-101, OLMil/OM 100x; Bottom picture: experiment code BK-100, OLMil/OM 200x.....	429
Figure 6.51. Comparison between the streaks of polish observed on the butchering fish knife (top picture, experiment code BK-102, OLMil/OM 100x) and the MLITs formed in a throwing	

experimental point due to impact against the ground (bottom picture, experiment code TH-71, OLMil/OM 100x).	430
Figure 7.1. Schematic drawing to show possible hafting arrangements and consequent trace distribution. A. Representation of the hafting limit; B. The tool is firmly fixed inside the shaft (e.g. tight hafting), edge-damage starts above the haft limit; C. The tool is loose inside the shaft (e.g. loose hafting), edge-damage starts below the haft limit; D. The tool is not inserted into the shaft, but it lays on top of it (e.g. flat hafting type; or sporadically in female hafting type), the edge-damage starts on the haft limit (Image La Porta).	439
Figure 7.2. Edge-damage due to projectile impact starting above the haft limit (red line). Trapezoidal and triangular scars (in red). A: ventral left side of the tool; B: dorsal left side of the tool. DM OM DM 51x (experiment code: TH-32).....	446
Figure 7.3. Edge-damage due to projectile impact starting above the haft limit (red line). Scalar and half-moon scars (in red). DM OM DM 67x (experiment code: TR-36).	447
Figure 7.4. Edge-damage due to projectile impact starting above the haft limit (red line). Half-moon scars (in red). OM DM 40x (experiment code: TH-39).....	447
Figure 7.5. An example of hafted Levallois points for hand-delivered stone-tipped spear experiments. The red line represents the line of separation between the area covered by the hafting system and the area not covered by the hafting system (i.e. haft limit). The blue line represents the limit of a fore-shaft slot under the tar adhesive (e.g. in a female slot). The orange area represents the area of contact between the proximal part of tool and the fore-shaft, with the adhesive as a medium, while the green line represents the area of contact between the striking platform of the tool and the fore-shaft, with the adhesive as a medium.	449
Figure 7.6. Distribution of macroscopic hafting traces according to their location on the selected experimental Levallois points (according to the recording location system, Section 2.3).....	451
Figure 7.7. Edge-damage due to the presence of a hafting system. Scalar and triangular scars. A: dorsal right proximal side of the tool; B: ventral right proximal side of the tool. DM OM 40x (experiment code: TR-87).	452
Figure 7.8. Edge-damage due to the presence of a hafting system. Scalar cone scar (with feather termination). DM OM 40x (experiment code: TR-22).....	453
Figure 7.9. Edge-damage due to the presence of a hafting system. Trapezoidal scar (in red). DM OM 60x (experiment code: TR-33).	453
Figure 7.10. Edge-damage (i.e. edge-crushing) due to the presence of a hafting system. DM OM 60x (experiment code: TH-23).....	454

Figure 7.11. Edge-damage due to the presence of a hafting system. DM OM 55x (experiment code: TH-92).....	454
Figure 7.12. Edge-damage due to the presence of a hafting system. Scalar plus small half-moon scars (in red). DM OM DM 80x (experiment code: TH-79).	455
Figure 7.13. Edge-damage due to the presence of a hafting system. DM OM DM 65x (experiment code: TR-34).	455
Figure 7.14. Edge-damage due to the presence of a hafting system. A: ventral left proximal side of the tool (trapezoidal plus small half-moon scars, in red); B: ventral right proximal side of the tool (small half-moon scars). DM OM 65x (experiment code: TR-36).....	456
Figure 7.15. Polish located on the proximal basal edge (Locus P1v). The polish shows a poor development with a dull-to-medium-bright aspect. Picture: OLMil 100x (experiment code: TH-24).	459
Figure 7.16. Polish located on the proximal basal edges (Locus P1v). The polish shows a poor development with a dull-to-medium-bright aspect. Picture: OLMil 100x (experiment code: TR-39).	459
Figure 7.17. Tar residue located on the proximal basal edges (Locus P1v). The residue has a granular and sticky texture. Picture: DM OM 50x (experiment code: TR-87).	461
Figure 7.18. Tar residue located on the mesial part of the tool (Locus M2v), clearly indicates the haft boundary. Picture: DM OM 30x (experiment code: TR-83).....	461
Figure 7.19. An example of adhesive residues and adhesive polish (or polished layer), located on the proximal ventral face (Locus P1v). At 100x, the adhesive polish (or polished layer) looks oily and greasy. Picture: OLMil 100x (experiment code: TH-66).	463
Figure 7.20. Adhesive polish (or polished layer), located on the proximal ventral face (Locus P2v). At 100x, the adhesive polish (or polished layer) looks oily and greasy, at 200x it shows numerous pits and a possible deposition above the surface. Picture: OLMil 100x (above), 200x (below) (experiment code: TH-20).....	464
Figure 7.21. Adhesive polish (or polished layer), located on the proximal ventral edge (Locus P2v). At 100x, the adhesive polish (or polished layer) looks oily and greasy, at 200x it shows numerous pits and a covering aspect. Picture: OLMil 100x (above), 200x (below) (experiment code: TR-34).....	465
Figure 7.22. Adhesive polish (or polished layer) at 500x. The polish shows an oily aspect and numerous pits, resembling micro-bubbles (red arrows). Picture: OLMil 500x (experiment code: TR-34).	466

Figure 7.23. Adhesive polish (or polished layer). Rough and very brilliant polish located on the bulbar area of the tool (Locus P1v). Picture: OLMil 100x (experiment code: TH-23).	468
Figure 7.24. Adhesive polish (or polished layer). Rough and very brilliant polish located on the bulbar area of the tool (Locus P1v). Picture: OLMil 100x (left), 200x (right), (experiment code: TH-20).	468
Figure 7.25. Adhesive polish (or polished layer). Rough and very brilliant polish located on the inner proximal ventral face (Locus P2v). It clearly indicates the haft boundary (below the red line). Picture: OLMil 100x (experiment code: TH-32).	469
Figure 7.26. Adhesive polish (or polished layer). Rough and very brilliant polish located on the inner proximal ventral face (Locus P1v). It clearly indicates the haft boundary (below the red line). Picture: OLMil 100x (experiment code: TR-93).	470
Figure 7.27. Distribution of microscopic hafting traces according to their location in the selected experimental Levallois points (according to the recording location system, Section 2.3).	471
Figure 7.28. Very bright, almost metallic, spots of polish, i.e. bright spots. They were located on the bulbar area of the tool (Locus P1v). Picture: OLMil 100x (above), 200x (below), (experiment code: TR-33).....	473
Figure 8.1. Geographic localisation of the selected Middle Palaeolithic archaeological sites. Map: La Porta and Oyaneder-Rodriguez.	480
Figure 8.2. Location of Arma Delle Manie site (Italy).	482
Figure 8.3. The setting of the Arma Delle Manie cave (the location of the waterways is indicated with light blue lines).	483
Figure 8.4. Arma Delle Manie cave, front-on view from the plateau (Picture La Porta).....	484
Figure 8.5. Arma Delle Manie stratigraphic profile (adapted from Cauche, 2007, figure 10). ..	486
Figure 8.6. Hearth at Arma Delle Manie (Level VII; image reproduced with permission of the Museo Archeologico del Finale).	486
Figure 8.7. The location of Arma Delle Manie and other key Middle Palaeolithic sites in Liguria (Italy).....	490
Figure 8.8. Raw material provenances in the Middle Palaeolithic region of Liguria (from Negrino and Porraz, 2008, figure 1).....	495
Figure 8.9. Example of Levallois points selected at Arma Delle Manie (Image La Porta with permission of Museo Archeologico del Finale).	499

Figure 8.10. Length/width ratio of the selected Levallois points (excluding fragments; n=27) at Abri du Maras.	500
Figure 8.11. The location of the Maras rock-shelter in the valley. The arrows indicate the directions from the site to the Ardèche River and to the plateau.	503
Figure 8.12. The location of Abri du Maras site and the main Middle Palaeolithic sites along the Middle Rhône Valley (south-eastern France). The extension of the Massif Central and Alps areas are shown in grey (from Daujeard et al., 2012, figure 1).....	504
Figure 8.13. Extension and progression of the Abri du Maras' excavation from 2006 to 2016 (from Moncel et al., 2017, figure 7).	505
Figure 8.14. The stratigraphic sequences of Maras shelter (modified from Richard et al. 2015, figure 2; and Moncel et al., 2012, figure 5).....	507
Figure 8.15. Primary herbivores taxa present in Level 4 and 5 of Abri du Maras (pictures from reindeer https://www.pbs.org/newshour/science/7-things-didnt-know-reindeer [last accessed 08-10-2018]; horse https://en.wikipedia.org/wiki/Horse [last accessed 08-10-2018]; bison http://www.ambisonsociety.org/ [last accessed 08-10-2018]; roe deer https://www.woodlandtrust.org.uk/visiting-woods/trees-woods-and-wildlife/animals/mammals/roe-deer/ [last accessed 08-10-2018]; wild boar https://blogs.fco.gov.uk/leightturner/2017/05/15/an-encounter-with-a-viennese-wild-boar-wildschwein/ [last accessed 08-10-2018]; red deer http://www.yorkshirecoastnature.co.uk/blog/290/a-royal-occasion [last accessed 08-10-2018]).	510
Figure 8.16. The localisation of the different flint types found at Abri du Maras within the local and regional context (from Moncel et al., 2014, figure 21).....	514
Figure 8.17. Levallois points and Levallois preferential flakes (from Moncel et al., 2017, figure 29).	516
Figure 8.18. The eleven techno-morphological types of Levallois points recognised at Abri du Maras (from La Porta, 2013, figure 11).	518
Figure 8.19. Overlaps of the silhouettes of two dimensional groups of Levallois points (from La Porta, 2013, figure 15).....	519
Figure 8.20. Length/width ratio (mm) of the Levallois points at Abri du Maras.	520
Figure 8.21. Tip angle measurement of the selected convergent stone tools.	521
Figure 9.1. Example of the selected convergent tools. A: Levallois point. B: proximal fragment of Levallois points. C: Mousterian point (see Annex B for definitions).	528

Figure 9.2. Degree of preservation of the selected convergent tools of Arma Delle Manie (n=47).	533
Figure 9.3. White patina and abrasion of the edges. Example of “mostly patinated” tool, DM OM 25x (Tool ID #I2 A 23-1967).	533
Figure 9.4. The granular and coarse aspect of the white patina at 100x, DM OM 100x (Tool ID #I2 A 23-1967).	534
Figure 9.5. Acid hole created by the corrosion of the stone surface, DM OM 135x (Tool ID #VII 1880).	534
Figure 9.6. Encrustations, edge abrasions, and patination phenomena, DM OM 95x (Tool ID #I2 A 23-1967).	536
Figure 9.7. Traces of lacquer and sticker, DM OM 13x (Tool ID #rem C 51-70).	537
Figure 9.8. Frequencies of traces (in blue) and no. of convergent tools (in red) with fracture (Arma Delle Manie, n=30).	543
Figure 9.9. Example of DIFs observed on the selected convergent tools of Arma Delle Manie. A: Spin-off burination fractures (indicated by the red line); B: Step-terminating bending fractures (in red); C: unifacial spin-off fractures (in red line).	544
Figure 9.10. Example of possible hafting traces observed on the selected convergent tools of Arma Delle Manie. A: black-brown residues (indicated by the red square), DM OM 180x (left) and 220x (right); B: (left) edge-damage, in form of a large sliced scar located on the mesial part of the tool, DM OM 50x; (right) bending scars located on the proximal part of the tool, DM OM 35x.	547
Figure 9.11. Projectile motion: Specimen #IV O5 416 with indications of trace locations (red x indicates the location of individual traces and letters show the location in which microscopic pictures where taken: Figure 9.12).....	550
Figure 9.12. Specimen #IV O5 416. Location A: Spin-off burination fracture (>5mm), DM OM 35x. Location B: MLIT departing from a previous fracture, DM OM 200x. Location C: double spin-off fractures (ventral face view), DM OM 30x. Location D: proximal notches (dorsal face view), DM OM 38x. Location E: proximal notches, DM OM 38x.	551
Figure 9.13. Projectile motion: Specimen #rem Ind 77/3 with indications of trace locations (red x indicates the location of individual traces and letters show the location in which microscopic pictures where taken: Figure 9.14).....	554
Figure 9.14. Specimen #rem Ind 77/3. Location A: (left) unifacial spin-off (0.5 mm) and spin-off burination fracture (1.55mm), DM OM 50x; (right) MLIT departing from the spin-off burination	

fracture, DM OM 200x. Location B: (left) edge-damage departing only from mesial part of the tool, DM OM 50x; (right) perpendicular and oblique striations located on the proximal part of the tool, DM OM 150x.	554
Figure 9.15. Projectile motion: specimen #rem L1 68mi with indications of trace locations (red x indicates the location of individual traces, letters the location where microscopic pictures were taken; Figure 9.16).	556
Figure 9.16. Specimen #rem L1 68mi. Location A: unifacial spin-off fractures DM OM 35x. Location B: spin-off burination fractures starting from a snap fracture, DM OM 35x.	556
Figure 9.17. Projectile motion: Specimen #rem L51 1 with indications of trace locations (red x indicates the location of individual traces and letters show the location in which microscopic pictures were taken: Figure 9.18).	559
Figure 9.18. Specimen #rem L51 1. Location A: multiple bending fractures, DM OM 55x. Location B: a possible MLIT (not-well-preserved), DM OM 110x. Location C: edge-damage, DM OM 50x. Location D: black-brown residues, DM OM 180x (left) and 220x (right).	560
Figure 9.19. Projectile motion: Specimen #III P6 92 with indications of trace locations (red x indicates the location of individual traces and letters show the location in which microscopic pictures were taken: Figure 9.20).	562
Figure 9.20. Specimen #III P6 92. Location A: multiple pattern of DIFs, bending step (in red), spin-off (in blue), fractures with bending-missing initiation and step termination (in green), DM OM 35x.	562
Figure 9.21. Projectile motion: Specimen #VII M1 897 with indications of trace locations (red x indicates the location of individual traces and letters show the location in which microscopic pictures were taken: Figure 9.22).	565
Figure 9.22. Specimen #VII M1 897. Location A: multiple patterns of DIF, bending step (in red), spin-off (in blue-red), burination fractures (in orange), DM OM 30x. Location B: faint and linear polish with longitudinal striations, DM OM 220x. Location C: bending scars (step in green and red, feather in blue) on the proximal part of the tool, DM OM 35x.	565
Figure 9.23. Possible projectile motion: Specimen #VII G 2014 VII M1 897 with indications of trace locations (red x indicates the location of individual traces and letters show the location in which microscopic pictures were taken: Figure 9.24).	567
Figure 9.24. Specimen #VII G 2014. Location A: large (<5mm) spin-off fracture (in red), DM OM 32x. Location B: spin-off burination fracture, DM OM 32x.	567

Figure 9.25. Longitudinal motion: Specimen #VII G 2067 with indications of trace locations (red x indicates the location of individual traces and letters show the location in which microscopic pictures where taken: Figure 9.26)..... 570

Figure 9.26. Specimen #VII G 2067. Location A: Faint polish located on the distal tip, DM OM 155x. Location B: Edge-damage, DM OM 40x. Location C: striations parallel to the edge, DM OM 180x (left) 200x (right). 571

Figure 9.27. Transversal motion: Specimen #VII 1880 G with indications of trace locations (red x indicates the location of individual traces and letters show the location in which microscopic pictures where taken: Figure 9.28)..... 575

Figure 9.28. Specimen #VII 1880 G. Location A: (left) polish with a transversal development, DM OM 41x, (right) polish with oblique striations, DM OM 150x. Location B: polish with oblique striations, DM OM 150x (left) 180x (right). 575

Figure 9.29. Transversal motion: specimen #rem 600r with indications of trace locations (red x indicates the location of individual traces and letters show the locations in which microscopic pictures where taken: Figure 9.30)..... 576

Figure 9.30. Specimen #rem 600r. Location A: (left) polish with oblique striations, DM OM 195x, (right) edge-damage, DM OM 115x. Location B: well-developed polish and edge-rounding, DM OM 45x (left), 220x (right). Location C: polish with oblique striations, DM OM 220x..... 577

Figure 9.31. Specimen #rem 600r. Location D: extensive edge-rounding, with striations and polish on the dorsal central ridge (interpreted as resultant of a hafting system), DM OM 50x (left), 150x (right). 577

Figure 9.32. Transversal motion: Specimen #VII G 2067 with indications of trace locations (red x indicates the location of individual traces and letters show the location in which microscopic pictures where taken: Figure 9.33)..... 579

Figure 9.33. Specimen #VII G 2067. Location A1: faint polish and edge-rounding on the dorsal tip, DM OM 26x (left), DM OM 60x (right). Location A2: polish with oblique striations, DM OM 150x (left), DM OM 200x (right)..... 579

Figure 10.1. Example of the selected convergent tools. A: unretouched Levallois point. B: Triangular Levallois flake. C: convergent déjeté scraper. D: cortical point (see Annex B for definitions). 589

Figure 10.2. The granular and shiny aspect of the patination phenomena. Example of “lightly patinated tool”, DM OM 600x. (Tool ID #J6 4.1 45). 592

Figure 10.3. Percentages of post-depositional alterations affecting the selected tools (n=70) for functional analysis at Abri du Maras Level 4.....	593
Figure 10.4. Modern trampling (i.e. crushed edge) visible due to the lack of patination, DM OM 35x (Tool ID #J6 4.1 45).....	594
Figure 10.5. Example of degree of post-depositional alterations affecting the convergent tools of Abri du Maras Level 4. A: Mostly-preserved tool. B: low-altered tool. C: Mostly-altered tool. ..	596
Figure 10.6. Projectile motion: Specimen #J7 111 4.1 with indications of trace locations (red x indicates the location of individual traces and letters show the location in which microscopic pictures where taken [Figure 10.7], the red line indicates the possible haft limit).....	601
Figure 10.7. Specimen #IJ7 111 4.1. Location A: primary burination fracture (in blue), bending fracture terminating in a feather/step (in red) and abundant edge-damage on the left ventral tip (in green), DM OM 12x. Location B: poorly preserved MLIT departing from the previous burination fracture, DM OM 600x. Location C: proximal edge-damage (with possible indication of the haft limit), SM OM 50x;.....	601
Figure 10.8. Projectile motion: Specimen #M6 894 4.2 with indications of trace locations (red x indicates the location of individual traces and letters show the location in which microscopic pictures where taken [Figure 10.9]).....	604
Figure 10.9. Specimen #M6 894 4.2. Location A: mesial snap fracture from which departed a large spin-off fracture (>5mm), SM OM 10x. Location B: the mesial snap fracture (in red) plus a step-terminating fracture (in blue) on the dorsal face, SM OM 10x. Location C: the mesial snap fracture cut the retouch on the dorsal distal face, SM OM 30x. Location D: polish located right on the fracture line. It shows a bright aspect with a domed-into flat topography and few longitudinal striations within it (showing analogues attributes to the observed experimental “impact polish”, see Section 6.3.3.3.1), DM OM 400x.....	605
Figure 10.10. Projectile motion: Specimen #M6 1033 4.2 with indications of trace locations (red x indicates the location of individual traces and letters show the location in which microscopic pictures where taken [Figure 10.11]).....	607
Figure 10.11. Specimen #M6 894 4.2. Location A: (left) snap fracture of the distal tip, SM OM25x; (right) polish located on the fracture line of the snap fracture. It shows a flat topography with longitudinal striations, DM OM 400x. Location B: snap fracture (in red) plus edge-damage (crushing of right lateral edge, in green), SM OM. Location C: sliced notch on the right dorsal edge, SM OM 25x. Location D: rough and dull polish located on the right dorsal notch, DM OM 600x.....	608

Figure 10.12. Projectile motion: specimen #I6 336 4.1 with indications of trace locations (red x indicates the location of individual traces and letters show the location in which microscopic pictures where taken [Figure 10.13], the red line indicates the possible haft limit)..... 610

Figure 10.13. Specimen # I6 336 4.1. Location A: primary burination fracture starting on the distal tip, associated with edge-damage on the lateral dorsal edges, SM OM 45x. 610

Figure 10.14. Projectile motion: specimen #M8 54 4.1 with indications of trace locations (red x indicates the location of individual traces and letters show the location in which microscopic pictures where taken [Figure 10.15]). 612

Figure 10.15. Specimen # M8 54 4.1. Location A: bending fracture terminating in a step-hinge on the dorsal distal tip and distal edge-damage (D1d), SM OM 15x, and DM OM 6x. Location B: abrasion of the dorsal central ridge, DM OM 600x (left picture) and 1000x (right picture). 612

Figure 10.16. Projectile motion: specimen # J7 35 4.1. with indications of trace locations (red x indicates the location of individual traces and letters show the location in which microscopic pictures where taken [Figure 10.17]). 614

Figure 10.17. Specimen #J7 35 4.1. Location A: bending fracture terminating in a step/hinge on the dorsal tip (in red), plus distal edge-damage (in green), SM OM 25x. 614

Figure 10.18. Projectile motion: specimen #M7 192 4.2 with indications of trace locations (red x indicates the location of individual traces and letters show the location in which microscopic pictures where taken [Figure 10.19], the blue line indicates the retouch, and red line the possible haft limit)..... 616

Figure 10.19. Specimen # M7 192 4.2. Location A: bending fracture terminating in a hinge on the distal ventral tip (in red) plus small cone scars (in blue), DM OM 6x. Location B: notch characterises by sliced scars (in red) on the dorsal right edge, SM OM 25x..... 617

Figure 10.20. Projectile motion: specimen # F6 39 4. with indications of trace locations (red x indicates the location of individual traces and letters show the location in which microscopic pictures where taken [Figure 10.21], and red line the possible haft limit). 619

Figure 10.21. Specimen #F6 39 4.2. Location A: bending fracture with undetermined termination on the distal tip (in red), and modern trampling, DM OM 35x. Location B: edge-damage, on the left dorsal edges, SM OM 35x. 619

Figure 10.22. Longitudinal motion: specimen #K6 379 4.1 1 with indications of trace locations (red x indicates the location of individual traces and letters show the location in which microscopic pictures where taken [Figure 10.23], the red line indicates the possible haft limit). 622

Figure 10.23. Specimen # K6 379 4.1. Location A: polish located on the distal ventral tip. At 140x (A1) it shows a very bright aspect (DM OM 140x); at 400x (A2), the polish shows a linked degree and a domed-flat topography (DM OM 4000x); at 600x (A3) the polish shows edge-rounding and longitudinal striations embedded in the polish (DM OM 600x). Location B: edge-damage and bending-step fractures on the proximal right edge (interpreted as a result of insertion in the haft) the red circle indicates the position of the black globular residue, SM OM 50x. Location C: black strip of globular residue (similar to the experimental tar adhesives, see Figure 7.17) DM OM 100x and 400x. 623

Figure 10.24. Transversal motion: specimen #H6 26 4.1 with indications of trace locations (red x indicates the location of individual traces and letters show the location in which microscopic pictures where taken [Figure 10.25]). 625

Figure 10.25. Specimen #H6 26 4.1. Location A: edge-damage (triangular and scalar scars) on the distal ventral end of tool, SM OM 10x. Location B: edge-damage (scalar scars) on the lateral dorsal edge, SM OM 20x. Location C: edge-rounding and polish located on the ventral distal edge (left) DM OM 140x, (right) the polish presents a pitted aspect and an intrusive distribution (the shiny lustre is possibly due to post-depositional alteration), DM OM 400x. 625

Figure 10.26. Multiple motions: specimen # K6 371 4.1 with indications of trace locations (red x indicates the location of individual traces and letters show the location in which microscopic pictures where taken [Figure 10.27]). 628

Figure 10.27. Specimen #K6 371 4.1. Location A: intense edge-rounding on the distal dorsal tip, DM OM at 12x and 24 x. Location B1: three bending fractures with step and hinge terminations (in red), on the distal ventral tip, DM OM 18x. Location B2: (left) polish located on the distal tip (D1v). It shows an invasive distribution along the edge, DM OM 400x; (right) the same polish presents a fluid aspect, a smooth texture, and a flat topography, DM OM 600x. Location C: edge-damage on the lateral edge that present large scalar scars, SM OM 10x. 629

Figure 10.28. Unknown motion: specimen #N6 186 4.1 with indications of trace locations (red x indicates the location of individual traces, letters the location where microscopic pictures where taken [Figure 10.29]). 631

Figure 10.29. Specimen #N6 186 4.1. Location A: edge-damage (scalar and half-moon scars) located on the distal portion of the tool, SM OM 35x; Location B: edge-damage (sliced and half-moon scars) located on the mesial portion of the tool, SM OM 50x. 631

Figure 10.30. Unknown use: specimen # M6 368 4.1 with indications of trace locations (red x indicates the location of individual traces, letters the location where microscopic pictures where taken [Figure 10.31]). 633

Figure 10.31. Specimen # M6 368 4. 1. Location A: Edge-damage (rectangular and trapezoidal scars) on the left ventral edge of the tool, SM OM 30x. 633

Figure 11.1. Types and frequencies of fractures according to the recorded impact velocities of the same projectiles (DIFs and MLITs are within black squares). 653

Figure 11.2. Number of recorded MLITs according to the impact velocities of the same projectiles. 658

Figure 11.3. Example of impact polish observed on experimental Levallois points used in throwing motions (left picture: OLMil/OM 50x; right picture: OLMil/OM 200x, experiment code TH-23). 659

Figure 11.4. Comparison between the “flat and reflective” polish described by Lammers-Keijers (et al., 2015, Figure 3.d; above) located on the distal tip of experimental arrowheads, and the “impact polish” described in this thesis, located on a throwing spearheads (below, TH-20). ... 663

LIST OF TABLES (VOLUME 1)

Table 1.1. Archaeological evidence of wooden spears (from Thieme, 1997; Oakley et al., 1977; Serangeli et al., 2012; Schoch et al., 2015). NP: not preserved.	82
Table 2.1. Technical specifications of the three different microscopes used during this thesis.	115
Table 2.2. Magnification range of the three different microscopes used in this thesis.	118
Table 2.3. Type of diagnostic impact fractures by previous publications.	137
Table 2.4. Classification of the different type of fractures. Primary Fractures: bending-fractures (step terminating bending fractures, feather and hinge terminating bending fractures, and snap fractures), and primary burination-fractures. Secondary Fractures: unifacial spin-off fractures, bifacial spin-off fractures, and spin-off burination fractures. The DIF proposed are: step terminating bending fractures, unifacial spin-off fractures, bifacial spin-off fractures, primary burination fractures, and spin-off burination fractures (as proposed by Lombard, 2005a).	143
Table 3.1. Cleaning protocol: a comparison between the two cleaning systems.	189
Table 4.1. Overview of the three sets of experiments with the specification of the dataset for each set (LPs: experimental Levallois points).	204
Table 4.2. Overview of the experimental tool datasets.	209
Table 4.3. Morphometric attributes of experimental Levallois points used in throwing and thrusting experiments, and the results of the Student's t-test results (T-test).....	223
Table 4.4. Measurements for the realistic spear shaft replicas of the first set of experiments in comparison to the published measurements of Schöningen spears I-III from Thieme (1977). All measurements were taken from the front (distal end) with a digital calibre.	227
Table 4.5. First set of experiments: hafting arrangements.	240
Table 4.6. Faunal list of Abris du Maras and Arma Delle Manie sites. Percentage of Individual Specimens per Taxon, from Daujeard and Moncel (2010, p. 375), and Valensi and Psathi (2004, p. 259).	241
Table 4.7. Penetration depth of hand-delivered throwing and thrusting spears of the first set of experiments.	244
Table 4.8. The contingency table shows the frequencies of Levallois points that remained hafted or de-hafted during the experiments, in relation to the experimental hafting variables employed in the first set of experiments.	244

Table 4.9. Measurements for the standardised spear shafts of the second set of experiments compared with the published measurements of Schöningen spear II from Schoch et al. (2015). All measurements were taken from the front (distal end) with a digital calibre.	261
Table 4.10. Third set of experiments. Butchering experiment summary.....	268
Table 5.1. A comparison of the throwing spear's impact velocities estimated or recorded in previous experiments and the results reported in this thesis (in green).	277
Table 5.2. A comparison of the thrusting spear's impact velocities estimated or recorded in previous experiments and the results reported in this thesis (in green).	278
Table 5.3. A comparison of the impact velocities estimated or recorded in previous ethnographic sources or sports science experiments and the results reported in this thesis (in green).	279
Table 5.4. An example of the spreadsheet of linear acceleration (experiment code: TH-81) where the impact event is highlighted in green as it is the biggest change between two adjacent time intervals, in a specific phase of the experiment. The negative value of the impact event corresponds to a change in the acceleration vector, which becomes negative as the impact event corresponds to a deceleration.	283
Table 5.5. An example of the spreadsheet of linear acceleration (experiment code: TH-62) where the beginning of the flying time is highlighted in green as it is the biggest change between two adjacent time intervals, in that phase of the experiment. The negative value of the flying time event corresponds to a change in the acceleration vector, which becomes negative as it corresponds to a deceleration (i.e. when the spear leaves the hand there is no more force applied to it).	291
Table 5.6. An example of the spreadsheet of linear acceleration (Experiment code: TH-62) where the impact event is highlighted in green as it is the biggest change between two adjacent time intervals, in that phase of the experiment. The impact shows a negative vector as it corresponds to a deceleration.	292
Table 5.7. An example of the spreadsheet of linear acceleration (Experiment code: TR-69) where the beginning of the thrusting time is highlighted in green as it is the biggest change between two adjacent time intervals, in that phase of the experiment. The thrusting time shows a positive vector as it corresponds to a full acceleration (i.e. when the human thruster started the action and applied the full force to the spear).	293
Table 5.8. An example of the spreadsheet of linear acceleration (Experiment code: TR-69) where the impact event is highlighted in green as it is the biggest change between two adjacent time intervals, in that phase of the experiment. The impact time shows a negative vector as it corresponds to a deceleration.	293

Table 5.9. Force values (in N) recorded in previously published thrusting spear experiments. Data from Milks et al. (2016, table 8) and Gaudzinski-Windheuser et al. (2018, p. 40).	296
Table 5.10. The ballistic parameters of hand-delivered throwing (TH) and thrusting (TR) stone-tipped spears when used by trained human participants on realistic targets.	305
Table 5.11. Descriptive statistics of ballistic parameters of hand-delivered throwing (TH) and thrusting (TR) stone-tipped spears.....	308
Table 5.12. The maximum penetration depth of this thesis' hand-delivered throwing and thrusting stone-tipped spears (in green) compared with previously published results of untipped hand-delivered thrusting spears (Milks et al. 2016) and untipped and stone-tipped throwing spears fired using a crossbow (Wilkins et al. 2014).	314
Table 5.13. Shea' (2006) TCSA values.....	334
Table 5.14. Tip-cross section area (TCSA) and Tip-cross sectional perimeter (TCSP) values of this thesis's experimental Levallois points used in throwing and thrusting experiments, plus, the results of the Shapiro-Wilks and Pearson's R tests.	335
Table 5.15. Results of Spearman's Rho correlation test.....	337
Table 5.16. Frequencies and percentages of the penetration depth for each set of experiments (TH and TR), classified by lethal (>20 cm), partial (5-20 cm), and failed (<5 cm).	344
Table 6.1. Number of experimental Levallois points with fractures, according to the delivery system (i.e. throwing and thrusting). Note: frequencies refer to the number of tools with fractures or diagnostic impact fractures (DIFs). LP stands for experimental Levallois points.	354
Table 6.2. Fracture types and frequencies observed on the experimental Levallois points, according to delivery system, i.e. throwing and thrusting. Note: the fracture number and frequencies refer to fracture counts, not tools with fractures (more than one fracture can occur on a tool).....	356
Table 6.3. Number of experimental Levallois with edge-damage, according to the delivery system (i.e. throwing and thrusting). Note: frequencies refer to the number of tools with traces. LP stands for experimental Levallois points.	371
Table 6.4. Location of fractures (i.e. distal, mesial, and proximal) according to the delivery system of the experiments (i.e. throwing vs thrusting). Note: the fracture number and frequencies refer to fracture counts, not tools with fractures (more than one fracture can occur on a tool).....	375
Table 6.5. Distribution of fractures according the impact materials (i.e. hard vs soft tissues) ..	376

Table 6.6. Polish, striations, and microscopic linear impact traces (MLITs) recorded on the experimental Levallois points, according to the delivery system (i.e. throwing and thrusting). Note: trace frequencies refer to the number of tools with a specific trace (more than one trace type can occur on a tool). LP stands for experimental Levallois points.	384
Table 6.7. Localisation of microscopic use-wear traces (i.e. MLITs, polish, and striation traces) on the experimental Levallois points (LP), according to the delivery system (i.e. throwing and thrusting). Note: distal loci include traces recorded in D1v, D2v, D3v, D1d, D2d, D3d loci; mesial loci include traces recorded in M1v, M2v, M1d, M2d loci; proximal loci include traces recorded in P1v, P2v, P1d, P2v loci (see Section 2.3).....	417
Table 6.8. Trace types and frequencies observed on the experimental Levallois points, used as butchering knives. Note: the number and frequencies refer to the number of tools with traces (more than one fracture can occur on a tool).	423
Table 7.1. Selected sample of experimental Levallois points (and their experimental variables) for the use-wear analysis of hafting traces.....	434
Table 7.2. Hafting traces recorded on the selected sample of experimental Levallois points, according to the delivery systems and hafting arrangements. Note: trace number refers to the number of tools with the observed trace (more than one trace can occur on a tool). LP stands for experimental Levallois points.	444
Table 7.3. A summary of the observed hafting traces according to the hafting arrangements used in this thesis's experiments.....	476
Table 8.1. Selected archaeological assemblages with the number of Levallois Points (LP) and Convergent Tools (CT) selected for use-wear analysis in this thesis.	479
Table 8.2. European Middle Palaeolithic assemblages with significant number of Levallois points (LP), including the archaeological sites selected in this study (in green).	481
Table 8.3. Results of the radiometric and paleo-environmental dating of Arma Delle Manie' archaeological levels (data from Arobba et al., 1976; Abassi, 1999; Karatsori, 2003; Mehidi, 2005).	488
Table 8.4. The main faunal and vegetation taxa in the Arma Delle Manie' archaeological levels.	492
Table 8.5. Tools selected for functional analysis according to techno-morphological categories and archaeological level (the frequencies of tool for each level were calculated from the tool totals presented in Leger [2012] and Santaniello [2011]).	497

Table 8.6. TCSA and TCSP values of the Levallois points from Arma Delle Manie (excluding fragments) compared with TCSA values of ethnographic and experimental projectiles (data from Shea (2006, table 1).....	501
Table 8.7. Results of the radiometric dating of Level 4 and Level 5 of Abri du Maras site (data from Richard et al., 2015; Moncel and Michel, 2000).....	508
Table 8.8. The main herbivores and vegetation species presented at Abri du Maras Level 4 and 5.....	510
Table 8.9. TCSA values of the Levallois points from Abri du Maras (excluding fragments) compared with TCSA values of ethnographic and experimental projectiles (data from Shea, 2006, table 1).....	521
Table 9.1. Types and frequencies of convergent tools selected at Arma Delle Manie for techno-functional analyses. The tools were divided by their archaeological levels (stone tools' number per level were calculated from Cauche, 2007, table 4).	529
Table 9.2. Degree of post-depositional alterations affecting the convergent tools of Arma Delle Manie (n=47).	538
Table 9.3. The total number of selected convergent tools examined divided by the analytical approaches used.	539
Table 9.4. Type and frequencies of fractures observed on the selected convergent tools of Arma Delle Manie (n=30). Note: the fracture numbers and frequencies refer to fracture counts, not tools with fractures (more than one fracture can occur on a tool).	541
Table 9.5. Frequencies of traces according to their location on the tools (F: fractures; DIFs: diagnostic impact fractures; MLITs: microscopic linear impact traces; ED: edge-damage).	545
Table 9.6. Functional interpretation of the selected convergent tools (n=30).	581
Table 9.7. Functional interpretations of the convergent tools (n=30) according to the types of motion.	583
Table 10.1. Distribution of the stone tools of Abri du Maras (until 2016) divided by technological categories (data from Moncel et al., 2017; Moncel et al., 2014; La Porta, 2013).	585
Table 10.2. Tools selected for functional analysis according to techno-morphological categories.	588
Table 10.3. Degree of post-depositional alterations affecting the convergent tools of Abri du Maras Level 4 (n=70).	595

Table 10.4. The total number of selected convergent tools examined per analytical approaches used.....	596
Table 10.5. Type and frequencies of fractures observed on the convergent tools of Abri du Maras (n=32). Note: the fracture numbers and frequencies refer to fracture counts, not tools with fractures (more than one fracture can occur on a tool).	599
Table 10.6. Functional interpretation of the analysed convergent tools (n=32).	634
Table 10.7. Functional interpretations of the convergent tools (n=30) of Abri du Maras, according to their techno-morphological class.	637
Table 11.1. DIF frequencies recorded in this study (in green) and DIF frequencies recorded in previous projectile experiments.....	654
Table 11.2. Frequencies of DIFs recorded at Arma Delle Manie and Abris du Maras (in green) compared with experimental frequencies of DIFs.	669
Table 11.3. Frequencies of DIFs recorded at Arma Delle Manie and Abris du Maras (in green) compared with Middle Palaeolithic, MSA, Upper Palaeolithic, Palaeoindian and Bronze Age sites.	669
Table 11.4. European Middle Paleolithic site with presence of Levallois points and/or convergent tools analysed for use-wear analysis.	672

LIST OF ACCOMPANYING MATERIAL (USB STICK)

Folder 1: accelerometer data.

Folder 2: comments and video.

Folder 3: slow-motion videos (high-speed camera records).

ABBREVIATIONS

AMH: anatomical modern human

DIF(s): diagnostic impact fracture(s)

DM(s): digital microscope(s)

ESEM: environmental scanning electron microscope

ESR: electron spin resonance

LP(s): Levallois point(s)

MLIT(s): microscopic linear impact trace(s)

MRO: middle range objective lens

MSA: Middle Stone Age

OLM(s): optical light microscope(s)

OLMil: optical light microscope with incident lights

OM: original magnification

SEM: scanning electron microscope

TCSA: tip cross-sectional area

TCSP: tip cross-sectional perimeter

TH: throwing

TR: thrusting

U-series: uranium series dating

GLOSSARY

Stone-tipped spear technology refers to composite weapon systems that combine a spear shaft with a stone tool.

Hand-delivered weapon(s) refers to weapons that are delivered by hands.

Mechanically delivered weapon(s) refers to weapons delivered with a medium, such as a spear-thrower or a bow.

Projectile(s) and/or projectile tool(s) refers to all artefacts such as organic or inorganic tips, points, flakes, armatures, heads, or barbs mounted in a shaft, regardless of the type of weapon and their delivery system (thrusting spear-points are therefore included).

Projectile weapon(s) refers herein to all, untipped and tipped, weapons that present a shaft system, regardless of the type of weapon and their delivery system (therefore including, hand-delivered spears, spear-thrower darts, and bow-arrows).

INTRODUCTION

THE IMPORTANCE OF STUDYING STONE-TIPPED SPEAR TECHNOLOGY IN THE NEANDERTHAL WORLD

This research commenced when, as an Erasmus Mundus MA student of Quaternary and Prehistory at the Muséum National d'Histoire Naturelle (MMHN, Paris), I was offered the fantastic opportunity to study an entire Middle Palaeolithic assemblage of Levallois points from an ongoing archaeological excavation. The archaeological level of Abri du Maras (Ardèche, France), later called Abri du Maras Level 4, yielded the presence of $n=51$ Levallois points (corresponding to around 2% of the entire level production). The main research question at this point concerned the reconstruction of the operational sequences employed by Neanderthals to produce these Levallois points (La Porta, 2013). As the technological results showed that the deliberate operational sequences used to produce the Levallois points at Abri du Maras Level 4 were mainly Levallois unidirectional convergent schemes (La Porta et al., 2015; Moncel et al., 2014; La Porta, 2013), the next step was to understand the aim of that specific production. Why did Neanderthals at Abri du Maras Level 4 deliberately decide to produce $n=51$ Levallois points (and extra convergent tools) within the chronological span of that archaeological level? Were the Levallois points fulfilling specific functional tasks or, conversely, were they used as multipurpose tools due to the morphological characteristic of their shape (i.e. two sharp convergent edges and a tip)? The techno-morphometric analyses, combined with a preliminary sample analysis ($n=8$ tools) of the macroscopic damage on the tools, suggested that a part of the Levallois points at Abri du Maras Level 4 could have been used as projectile tools, possibly mounted on spear-shafts (La Porta, 2013; Moncel et al., 2014; La Porta et al., 2015). However, a further archaeological and experimental investigation was necessary to corroborate the “projectile hypothesis” for the Levallois points of Abri du Maras Level 4, and the main aim became to further understand how Neanderthals could possibly have used their hunting weapons. It was in the context of this research that the understanding of hand-delivered stone-tipped

spear technology among European Neanderthals became my main scope of research, ultimately culminating in this thesis.

In evolutionary terms, the adoption of stone-tipped hunting weapons was a “key moment” in human prehistory as it encapsulated fundamental changes in the technological and cognitive skills of human species (MacDonald, 2007; Haidle, 2010; Wadley et al., 2009; Villa and Soriano, 2010; Lombard and Haidle, 2012; Villa and Roebroeks, 2014; Lombard and Wadley, 2016). It has been proposed that hunting weaponry technology could represent one of the main cultural markers of an enhanced and sophisticated behaviour associated with the radical cognitive and physiological changes between the earlier species of *Homo* and the Anatomically Modern Humans (AMH) (Mellars, 1995; Stringer and Gamble, 1993; Bar-Yosef, 1998; McBreaty and Brooks, 2000; Brooks et al., 2006; Shea, 2006; Churchill and Rhodes, 2009; Rhodes and Churchill, 2009; Shea and Sisk, 2010; Sisk and Shea, 2011; Brown et al., 2012). However, the timing and geographical distribution of this cognitive and physiological change are widely debated in Palaeolithic archaeology (Mellars, 1973, 1995, 1999, 2005; Stringer and Gamble, 1993; Bar-Yosef, 1998, 2002; McBreaty and Brooks, 2000; Henshilwood et al., 2003; Stringer, 2002; d’Errico et al., 1998, 2003, 2005; d’Errico, 2003; Wadley, 2003; Brooks et al., 2006; Shea, 2006, 2009; Shea and Sisk, 2010; Lombard and Parsons, 2011; d’Errico and Stringer, 2011; Zilhão, 2011; Villa and Roebroeks, 2014). Some authors suggest that a radical change in behavioural patterns (i.e. “modern human behaviour”; Mellars, 1989) occurred in Eurasia around 40-50 Ka, coinciding with the dispersal of the AMH from the Levant corridor (Mellars, 1973, 1995, 1999; Stringer and Gamble, 1993; Bar-Yosef, 1998; Stringer, 2002; Shea, 2006; Shea and Sisk, 2010). Others have alternatively suggested that this change was not an abrupt phenomenon, but rather a gradual acquisition of sophisticated behaviours, developing in Africa during the late Middle Stone Age (MSA) from around 100-200 Ka (McBreaty and Brooks, 2000; Barham, 1998, 2002; Wadley, 2003; Henshilwood et al., 2001, 2003; Brooks et al., 2006; Marean et al., 2007; Lombard and Parsons, 2011). Other researchers have argued that cognitive

and behavioural innovations were not uniquely restricted to AMH, but were adopted and replaced both by African and Eurasian human species from around 200 Ka to 40 Ka (d'Errico, 2003; d'Errico et al., 1998, 2003; d'Errico and Stringer, 2011; Zilhão, 2011; Villa and Roebroeks, 2014). Consequently, the emergence of hunting weaponry technology is a crucial part of this research field, allowing for inferences to be made regarding behavioural complexity in at least two human species (Neanderthals and AMH).

Over the last two decades, models for the evolution of hunting weaponry technology have been affected by broader scientific models which have pervaded Palaeolithic archaeological research (Shea, 2006; Churchill and Rhodes, 2009; Shea and Sisk, 2010; Sisk and Shea, 2011). Until a decade ago, the most accepted hypothesis was that mechanically-delivered hunting weaponry technology, i.e. bow and arrow weapons (defined as “complex stone projectile technology”, Shea, 2006; see Section 1.1), spread into Europe around 50-40 Ka, from the Levantine corridor, carried by AMH (Shea, 1997, 2006; Mellars, 2006). The reception of these theories resulted in the formulation of unilinear evolutionary models for the development of weapons (Churchill, 1993; Shea, 1997, 2006; Rhodes and Churchill, 2009; Shea and Sisk, 2010; Sisk and Shea, 2011). These models theorised that heavy, close-range thrusting spears were the first weapons employed by human species (such as *Homo heidelbergensis*, *Homo neanderthalensis*, and possibly *Homo erectus*), although the time in which thrusting spears appeared was and still is poorly clarified (Milo, 1998; Shea, 2006; Wilkins et al., 2012; Sahle et al., 2012; Rots, 2013; Rots and Plisson, 2014; see also Section 1.4.3). Throwing spears, on the other hand, have been proposed to be adopted following the instance of the development of the human capability to throw, which remains largely debated (Churchill and Rhodes, 2009; Rhodes and Churchill, 2009; Shaw et al., 2012; Berger and Trinkaus, 1995, but see Trinkaus, 2012; Roach et al., 2013; Roach and Richmond, 2015; see also Section 1.3). The invention of mechanically-delivered weapons (such as spear-thrower javelins and bow-arrows) was, finally, adopted only by *Homo sapiens*. The leading hypothesis argued that long-distance throwing weapons, mainly throwing spears, were not

in use among pre-AMH species (Shea, 2006; Churchill and Rhodes, 2008; Shea and Sisk, 2010; Sisk and Shea, 2011) primarily due to an anatomical incapability to throw in Neanderthal and pre-Neanderthal populations (Schmitt et al., 2003; Rhodes and Churchill, 2009; but see Roach et al., 2013). It was thus concluded that Neanderthals relied on close-range hunting techniques involving heavy close-distance thrusting spears only (Schmitt et al., 2003; Shea, 2006; Churchill and Rhodes, 2009; Shea and Sisk, 2010; Sisk and Shea, 2011).

These hypotheses presented several methodological and theoretical constraints, which new archaeological discoveries and recent investigations into human biomechanics have proven inaccurate (see Section 1.4.3 and 1.3). As expressed in Section 1.3, recent experimental research in the field of biomechanics (Roach et al., 2012, 2013; Maki, 2013; Roach and Richmond, 2015a, 2015b) has proven that throwing mechanisms are much more complex than they were previously thought to be (Churchill, 1993; Churchill et al., 1996; Schmitt et al., 2003; Churchill and Schmitt, 2003; Rhodes and Churchill, 2009), and that the anatomical capability to throw was acquired by pre-AMH species possibly around 2 Ma (Roach et al., 2013). New archaeological discoveries have shown that mechanically-delivered hunting weaponry technology (i.e. bow and arrows) emerged in the African late Middle Stone Age around 100-70 Ka (see also Lombard, 2015), if not earlier (300 Ka, in Zambia; Taylor, 2011; Barham, 2002), as evidence from Pinnacle Point 5-6 site, Sibudu cave, and Umhlatuzana may suggest the presence of stone arrow points (Backwell et al., 2008; Wadley and Mohapi, 2008; Lombard and Phillipson, 2010; Lombard, 2011; Bradfield and Lombard, 2011; Brown et al., 2012). However, it is important to note that stone and bone-tipped hand-delivered spears may have still been in use (Lombard, 2005b; Villa et al., 2009b; Henshilwood et al., 2001; Backwell et al., 2008). Therefore, Shea's (2006) hypotheses which posit (i) an indigenous origin of the mechanically-delivered hunting weaponry technology, dated around 45-40 Ka and linked to Europe and the Levant; (ii) the occurrence of heavy and close-range distance thrusting weapons only, no longer seem valid, as partly reviewed by the same author (Shea and Sisk, 2010).

However, there is still an outstanding knowledge gap concerning the timing of the first appearance of both throwing and thrusting stone-tipped spears (i.e. the possible first composite weapons) in the archaeological records, both in the European Middle Palaeolithic and African Middle Stone Age (see Section 1.4.3). If on one hand, the Neanderthals' ability to produce spears *sensu lato*¹ is widely accepted (Knecht, 1997; Shea, 1997; Shea, 2006; Iovita and Sano, 2016) due to multiple discoveries of wooden spears associated with both Neanderthal and pre-Neanderthal hominins (Movius, 1950; Thieme, 1997; Oakley et al., 1977; Thieme and Veil, 1985; Wagner, 1995; Schoch et al., 2015; Gaudzinski-Windheuser et al., 2018; see Section 1.4.1). On the other hand, the adoption of stone-tipped spears in the Early and Middle Palaeolithic is still poorly understood and hardly debated (Villa and Soriano, 2010; Rots and Plisson, 2014, contra Wilkins et al., 2012; Rots and Plisson, 2014, contra Lazuén, 2012, but see Lazuén 2014; Gaudzinski-Windheuser et al., 2018). Although several Middle Palaeolithic stone tool assemblages have demonstrated the presence of stone projectile tips, through the analysis of diagnostic impact fractures and projectile wears (Villa and Lenoir, 2006, 2009; Villa et al., 2009a; Villa and Soriano, 2010; Rots, 2013; Hardy et al., 2013; see also Section 1.4.3.2.2), the ways in which these possible projectiles were employed (i.e. delivery systems) remain unidentified. Therefore, if it is accepted, as a result of archaeological evidence (see Section 1.4.3), that Neanderthals produced and employed stone-tipped spears, it is still necessary to investigate and clarify how these weapons were used, i.e. as hand-delivered thrusting spears only, or as hand-delivered throwing spears as well. Understanding the differences between thrusting and throwing spear delivery systems can, in fact, contribute to determining whether and when changes in hunting techniques and cognitive behaviours occurred (Wadley et al., 2009; Wadley, 2010; Lombard and Haidle, 2012; Williams et al., 2014; see Section 1.4.2.2).

¹ *Sensu lato* refers here to all spear weapons either single unit spears, i.e. untipped spears, or composite spears, i.e. tipped-spears.

Previous weaponry experiments have investigated the mechanical principles of fracturing (Cotterell and Kamminga, 1977, 1985, 1987; Ho Ho Committee, 1979; Cotterell et al., 1985; Odell, 1988; Odell and Cowan, 1986) and established parameters to differentiate fractures that originated from a knapping technique (Knudson, 1979; Shea and Klenck, 1993; Sano, 2009, 2012a; Pargeter, 2011) from those use-fractures resulting from projectile impacts (Barton and Bergman, 1982; Bergman and Newcomer, 1983; Fischer et al., 1984; Odell and Cowan, 1986; Odell, 1988; Geneste and Plisson, 1989; Geneste and Plisson, 1990; Geneste and Plisson, 1993; Dockall, 1997; Lombard, 2005a; Lombard and Pargeter, 2008). Although four types of fractures have been identified as diagnostic of projectile activities (i.e. step-terminating bending fracture, primary burination fracture, and bifacial and unifacial spin-off fractures, see Lombard, 2005a; Ho Ho Committee, 1979), the discrimination between different weapon delivery systems (e.g. thrusting spear, throwing spear, spear-thrower javelin, or bow and arrow, see Section 1.1) remains an arduous task for the use-wear analyst (see Rots and Plisson, 2014). Therefore, it is crucial to investigate new methodological approaches that may allow the distinction between mechanically propelled projectiles (i.e. bow/arrows and spear-thrower darts) and hand-thrown and hand-thrust spears to be drawn with greater confidence.

New experimental approaches, based primarily on ballistic and use-wear analyses, have been adopted in an attempt to distinguish mechanically-delivered projectiles from hand-delivered projectiles (Hutchings and Bröchert, 1997; Hutchings, 1999, 2011; Iovita et al., 2014; Sano et al., 2016; Coppe and Rots, 2017), and hand-thrown spear projectiles from hand-thrust spear projectiles (Hutchings, 2011; Iovita et al., 2016; Rots, 2016; Milks et al., 2016). The physical-mechanical use-wear approach allows for the investigation of the formation of different types of use-traces, focusing on impact velocities of the weapons (Hutchings, 2011; Iovita et al., 2014, 2016; Sano et al., 2016; Pargeter et al., 2016). These new methods have the potential to quantify impact velocities in brittle-solids and correlate them with resulting use-wear traces. However, the preliminary application of some of these methods (e.g. Wallner lines analysis, see Hutchings, 2011) has shown that their applicability in an

archaeological context is limited, as some traces (e.g. Wallner lines) form only in very fine-grained brittle solids (e.g. obsidian tools). Moreover, experimental studies investigating the distinctions between spear throwing and spear thrusting trace patterns exclusively through the analysis of fracture velocity ranges and loading rates have failed to discriminate between the two systems, as both throwing and thrusting systems fell into the same “semi-static” loading rate (Iovita et al., 2016). Therefore, further and more-comprehensive research focusing on macroscopic and microscopic use-wear is required to investigate the different use-wear patterns between throwing and thrusting hand-delivered stone-tipped spear projectiles.

Accordingly, this thesis was motivated by this gap in archaeological research and seeks to investigate the macroscopic and microscopic use-wear traces and ballistic parameters of hand-delivered throwing and thrusting stone-tipped spear projectiles. To do so, the following rationale and procedure were employed.

- To investigate the ongoing debate on Middle Palaeolithic stone-tipped spear technology and Neanderthal’s hunting behaviour, a thorough examination of the historical background, theories and applied methodologies was undertaken (presented in CHAPTER 1).
- Levallois points were chosen as a unique techno-morphological tool type for the analyses of this thesis. This is because, for a long time, Levallois points and/or Mousterian points were debated to be used as possible spear tips (Bordes, 1961; Dibble, 1987; Holdaway, 1989; Shea, 1987, 1988, 1997). However, a comprehensive investigation, combining experimental and archaeological analyses, to assess the aptitude of this specific tool type to be effective throwing and thrusting spear tips was required (see also Section 1.4.3).
- Based on this discussion, a combined methodology, integrating experimental archaeology with use-wear analysis, was selected for the analysis of experimental and archaeological of Levallois points series.

The use-wear methodology and protocol of analysis are presented in CHAPTER 2 and CHAPTER 3.

- Subsequently, the first step was the creation of an extensive and comprehensive experimental reference collection for use-wear analysis, including throwing and thrusting hand-delivered spear Levallois point projectiles and Levallois points used in functional tasks other than weaponry. The experimental program assessed the viability of experimental stone-tipped spears mounted with Levallois point flint replicas, and it provided comparative use-wear data to aid in the interpretation of the archaeological evidence (presented in CHAPTER 4).
- The creation of this robust experimental dataset, in which the use-wear traces were documented, also included the kinematic analysis and the recording of experimental ballistic parameters resulting from the examination of the throwing and thrusting movements of hand-delivered stone-tipped spears (presented in CHAPTER 5).
- The next step was the investigation of microscopic and macroscopic use-wear traces generated by throwing and thrusting hand-delivered spear motions on experimental Levallois points, to identify and quantify diagnostic patterns and frequencies of traces (presented in CHAPTER 6). Hafting traces were also analysed for a limited sample (presented in CHAPTER 7)
- The trace resulting from the use-wear analysis formed also a catalogue of macroscopic and microscopic traces diagnostic of projectile utilisation (presented in Appendix A, Volume 2).
- The last step was the comparison of the experimental stone tools with archaeological Middle Palaeolithic stone tools (i.e. Levallois points and convergent tools), to assist in establishing whether or not Neanderthals were producing and employing stone-tipped spear technology. Abri du Maras (France) and Arma Delle Manie (Italy) archaeological sites were selected as samples of European Middle Palaeolithic sites. They were

selected because the assemblages were available to the author, they were well-excavated, and they presented relatively high frequencies of Levallois points when compared to other Middle Palaeolithic sites (data presented in CHAPTER 8).

- The use-wear results from the selected archaeological Levallois points and convergent tools of Arma Delle Manie (Italy) indicated a high presence of projectile elements, besides showing also other functional utilisations (data presented in CHAPTER 9).
- The use-wear results from the selected archaeological Levallois points and convergent tools of Abri du Maras (France) indicated that, besides being multifunctional tools (Plisson and Beyries, 1998), a portion of the selected Levallois points was also used as projectile tools (data presented in CHAPTER 10).
- The different results achieved by this research, and the comparison between experimental and archaeological use-wear traces is discussed in CHAPTER 11.
- The conclusions of this study (presented in CHAPTER 12) suggested that Neanderthals were employing hand-delivered stone-tipped spears, possibly also in throwing motions, at least from MIS 4 (as documented at Abri du Maras Level 4) to MIS 3 (as documented at Arma Delle Manie). The correlations between the use-wear results, the faunal assemblages, and the zooarchaeological records of both Arma Delle Manie and Abri du Maras also suggested fascinating outcomes regarding possible monospecific exploitive hunting of faunal taxa (i.e. reindeer at Abri du Maras and red deer at Arma Delle Manie). Monospecific hunting is discussed within the broader context of advanced strategic hunting techniques and greater forecasting and planning activities suggesting Neanderthals may have possessed enhanced cognitive skills (see CHAPTER 11 and CHAPTER 12).

CHAPTER 1

MIDDLE PALAEO-LITHIC WEAPONRY TECHNOLOGY AND HUNTING

BEHAVIOUR: STATE OF THE DEBATE

1.1 Weaponry terminology

“Prehistoric hunting weaponry” is herein defined as the ensemble of weapons primarily used in hunting activities. The prehistoric innovation of hunting weapons shows a progressive effort to enhance the user’s ability to cause lethal and/or disabling wounds to animals. Among prehistoric hunting weapons, projectile weapons are the most widely studied. “Prehistoric projectile weapons” are herein considered to be the ensemble of launched weapons (i.e. when the weapons leave the user’s hands) mostly used in hunting activities, although warfare activities are also conceivable (Knecht, 1997, p. 11). Projectile weapons can be seen to increasingly strive to increment the protection of the user, as they can inflict lethal or disabling wounds from a distance (Shea, 2006, p. 1).

Previous research has distinguished the main types of prehistoric weapons as follows (Knecht, 1997; Iovita and Sano, 2016):

- Hand-delivered thrusting spears: such as tipped and untipped spears thrust into the animal by hand. They are not considered projectile weapons as they do not leave the hands of the user.
- Hand-delivered throwing spears: such as tipped and un-tipped spears propelled by hand. They are commonly defined as long and robust projectile spears (Knecht, 1997; Hughes, 1998).
- Spear-thrower darts (herein used interchangeably with javelins): such as tipped and untipped darts propelled with a spear-thrower or atlatl. They are commonly thought to be lighter and thinner than hand-delivered spears (Hughes, 1998),
- Bow and arrows: such as tipped and untipped arrows propelled with a bow.

All of the above weapon types (i.e. spears, darts, and arrows) can be manufactured as single-unit weapons or as composite weapons. “Single-unit weapons” are here defined as untipped weapons which are manufactured from a single material and do not involve the connection of a tool and/or fore-shaft, e.g. untipped organic spears, darts, and arrows. “Composite weapons” are here defined as tipped weapons which are manufactured using a combination of different materials and involve a connection with a tool and/or fore-shaft through the process of hafting, e.g. tipped spears, darts, and arrows hafted to a tool and/or fore-shaft.

Seeing as projectile weapons can be delivered either by hand or through the use of a device (such as a spear-thrower or bow), it is necessary to clarify the choice of terminology. Some researchers in the past have employed the term “projectile technology” to refer to all weapons that, during utilisation, leave the hands of the user (Knecht, 1997; Lombard and Pargeter, 2008). However, others have employed the term exclusively for spear-thrower darts and bows and arrows, which are weapons mechanically propelled with a device (Shea, 2006; Brooks et al., 2006; Shea and Sisk, 2010; Lombard and Phillipson, 2010). Others have even used the term to refer to all weapons, regardless of whether or not they leave the hand of the user (hence the inclusion of thrusting spears; Rots and Plisson, 2014). Thus, in order to avoid confusion and mystification, this thesis has adopted a clearer terminology, as proposed by Lombard and Haidle (2012, p. 23):

- Hand-delivered weaponry herein refers to weapons thrust or thrown by hands (i.e. without the aid of a device), whether they leave the hands of the user (i.e. untipped and tipped throwing spears) or not (i.e. untipped and tipped thrusting spears).
- Mechanically delivered weaponry herein refers to weapons propelled with a device, such as bows and arrows and/or spear-thrower darts.

The “mechanically-delivered weaponry” concept (Lombard and Haidle, 2012) is equivalent to Shea (2006) and Shea and Sisk’s (2010) concept of “complex projectile technology”. However, “mechanically-delivered weaponry” is

preferable as it is an unequivocal concept which rejects cognitive bias concerning the human species that made and employed the weapons. Likewise, the oppositional term “early projectile technology”, which has ambiguously referred to both hand-delivered spears and early evidence of bows and arrows (Erlandson et al., 2011; Wilkins et al., 2012; Iovita, 2012), is here not used.

Moreover, hand-delivered and mechanically-delivered weapons have also been discussed in the context of delivery-ranges to the animal target (Churchill, 1993; Ellis, 1997; Hughes, 1998), such as:

- Short-range or close quarter weapons (<10 m) are generally associated with hand-delivered systems, such as throwing or thrusting spears (Churchill, 1993).
- Long-range or middle quarter weapons (between 10 m and 30 m) are generally associated with mechanically delivered systems, such as spear-thrower darts and bow-arrows (Churchill, 1993; Hughes, 1998).

Lastly, due to the complexity of recognising the different weapon types and delivery systems in the archaeological record, the term “projectile weapon” refers herein to all untipped and tipped weapons that present (or may have presented) a shaft system, regardless of the type of weapon and their delivery system (therefore including, hand-delivered spears both throwing and thrusting, spear-thrower darts, and bow-arrows). Whereas, the terms “projectile tool(s)” or “projectile(s)” herein are referred to all artefacts such as tips, points, or barbs mounted in a shaft, regardless of the type of weapon and their delivery system. Thrusting spear-points are therefore included (see also Glossary).

1.1.1 Outline of hunting techniques conceivably used in Palaeolithic times

Palaeolithic techniques used in the hunting of large mammals (hunting or trapping techniques used on fish, birds, and small mammals are not included here) have been the focus of ethnographic and archaeological synthesis

(Churchill, 1993; Ellis, 1997; Frison, 2004; White et al., 2016). They can be summarised as follows:

- Disadvantage hunting refers to the techniques in which the hunter limits the escape of the prey and drives it into a disadvantaged position in which the hunt can be finished, usually using close-range weapons (Churchill, 1993, p. 16). In disadvantage hunting, the hunter can take advantage of topographic landmarks and natural traps (such as swamps, cliffs, sinkholes, or bottlenecks) to drive the prey into a disadvantageous position (see White et al., 2016, table 4).
- Ambush hunting refers to the technique in which the hunter (sometimes in a hidden position) waits until the prey is within close range to surprise and attack it, generally with close-range weapons (Churchill, 1993, p. 16; Frison, 2004, p. 190). Approaching, camouflage, and luring techniques can also be considered components of ambush hunting as these still involve a final surprise attack on the prey, although Churchill (1993, p. 16) considered these to be separate hunting techniques.
- Direct attack is when the hunter directly aims for or attacks the prey with a weapon, mainly employing long-range weapons (Frison, 2004, p. 196).
- Persistence hunting refers to the techniques in which the hunter chases the prey (wounded or unwounded) until the prey succumbs to exhaustion and/or is put in a disadvantageous position (see also Lieberman and Bramble, 2007). The hunter may finish the prey with a coup de grâce, typically employing close-range weapons (Churchill, 1993; Ellis, 1997). Tracking animal prints can be part of this technique.

In ethnographic cases, it has been observed that these techniques are generally not utilised exclusively, but they can be applied together to first disadvantage the prey before finally pursuing and finishing it (Churchill, 1993, p. 16).

1.2 How to recognise hunting weapons in the archaeological records?

Prehistoric hunting weapons can be easily identified when they are still preserved in the archaeological record. The presence of a shaft provides a host of useful information: the size of the weapon, type of hafting, the diameter of the hafting system, the centre weight of the weapon, and the overall morphology (Thomas, 1978; Hughes, 1988). Moreover, preserved shafts or fore shafts also provide a technical understanding of the manufacturing process (i.e. chaîne opératoire) of the weapon. Unfortunately, prehistoric weapons were made of perishable organic materials, and are not easily preserved in the archaeological record. Nevertheless, a few preserved weapons have been found in anaerobic environments such as water-logged sediments (Becker, 1945; Movius, 1950; Malmer, 1966; Oakley et al., 1977; Thieme, 1997; Larsson and Sjöström, 2011; Schoch et al., 2015), providing insight into the technical choices of prehistoric populations (see Section 1.4.1).

However, excluding these rare cases of preservation, the archaeological record is comprised exclusively of the remains of artefacts (either stone, bone, antler) that could have been used as projectiles. It is from these surviving artefacts that archaeologists are able to identify and investigate weaponry technology. To do this, several methodological approaches have been developed, such as morphometric attributes, use-wear analysis, and experimental studies.

1.2.1 Morphometric studies for the recognition of projectile tools

Numerous studies have investigated potential projectiles through an examination of the overall morphology of the artefacts and their morphometric attributes.

The presence/absence of a neck, shoulder, tangs, notches, lanceolate shapes, triangular cross-section, and other such attributes have often been proposed as morphometric indicators of projectile utilisation (Tixier, 1967; Heizer and Hester, 1978; Thomas, 1981; Hughes, 1998; Shea, 2006; Sisk and Shea, 2009, 2011). In the last few decades, tip cross-sectional area and perimeter (TCSA and TCSP) values have been considered to be good ballistic proxies though which

to assess projectile points and distinguish between different weapon systems (Hughes, 1998; Shea, 2006; Sisk and Shea, 2009, 2011). However, the majority of these morphological attributes are often linked to the tool's ability to be hafted, regardless of whether or not the tool was then used as a projectile (Flenniken and Wilke, 1989; Flenniken and Raymond, 1986). Besides, morphological examination of specific morphometric attributes of possible projectiles (such as tip cross-section, edges, and tip angles) are often based on assumed correlations between ethnographic and/or experimental projectiles and archaeological artefacts (Thomas, 1978; Dibble, 1984, 1987; Holdaway, 1989; Shott, 1997; Shea, 2006; Shea and Sisk, 2010), underpinned by the notion that intraspecific factors could have been shared across time, space, and different human groups. However, the widely employed morphometric attributes that have purported to be good proxies in distinguishing projectile tools (i.e. tip cross-sectional area and perimeter - TCSA and TCSP; Shea, 2006; Sisk and Shea, 2009) have been recently challenged and have been proven misleading by several experimental and use-wear studies (Newman and Moore, 2013; Clarkson, 2016). As a result, these techniques are increasingly being neglected in the archaeological examination of projectile tools (Rots and Plisson, 2014; Clarkson, 2016; Hutchings, 2016; Rots, 2016;). In conclusion, morphometric attributes may be suitable to assist in the identification of archaeological artefacts that share the same morphometric (and aerodynamic) attributes of ethnographic or experimental projectiles, but they cannot alone prove that the archaeological tools were used as projectile weapons (Rots and Plisson, 2014; Hutchings, 2016).

As a result, this study has included the analysis of selected morphometric attributes (measured according to the main techno-morphometry of the Levallois point type, see Section 3.3) to verify their potential viability in assessing and distinguishing different projectile tools (see CHAPTER 5); however, considering the above observations, the morphometric analysis was not the chosen methodology of this research.

1.2.2 Use-wear and experimental studies for the recognition of projectile tools

Use-wear analysis has proven to be an effective methodology through which to identify projectile tools in archaeological assemblages (Barton and Bergman, 1982; Moss, 1983a, 1983b; Fischer et al., 1984; Odell and Cowan, 1986; Shea, 1988; Geneste and Plisson, 1989, 1990, 1993; Dockall, 1997; Lombard et al., 2004; Lombard, 2005a, 2005b; Villa and Lenoir, 2006; Pargeter, 2007, 2013; Lombard and Pargeter, 2008; Villa et al., 2006, 2009a; Rots, 2009, 2013; Villa and Soriano, 2010; Lombard and Phillipson, 2010; Yaroshevich et al., 2010; Hutchings, 2011; Hardy et al., 2001, 2013; Lemorini and Cocca, 2013; Tomasso et al., 2015, 2018; Iovita and Sano, 2016; Pargeter et al., 2016; Coppe and Rots, 2017; Rots et al., 2017).

Comparisons made between impact wear traces occurring in experimental projectiles and analogous traces observed on archaeological tools demonstrate that it is indeed possible to identify archaeological projectiles (Moss, 1983a, 1983b; Fischer et al., 1984; Odell and Cowan, 1986; Caspar and De Bie, 1996; Geneste and Plisson, 1989, 1990, 1993; Soriano, 1998; Crombé et al., 2001; Lombard, 2005a; Pargeter, 2007; Lombard and Pargeter, 2008; Sano and Oba, 2015; Rots et al., 2017). Use-wear studies have also investigated incidences of fractures occurring during knapping activities (Keeley, 1980, p. 25-28; Moss, 1983c; Vaughan, 1985; Geneste and Plisson, 1993; Sano, 2009) and/or the post-depositional process (Shea and Klenck, 1993; McBrearty et al., 1998; Sano, 2009, 2012, Pargeter, 2011; Pargeter and Bradfield, 2012a), as opposed to fractures occurring during projectile utilisation. They found that tools used in activities other than projectile utilisation showed significantly lower frequencies of fractures than projectile tools (3% vs >30% fracture frequencies, Pargeter, 2011, 2013; Pargeter and Bradfield, 2012a). As projectiles cannot be used without hafting, hafting traces have been the focus of more and more recent investigations (Beyries, 1987b; Odell, 1996; Rots, 2003, 2004, 2009, 2010, 2016; Lombard 2005b, 2006a, 2006b, 2007; Pawlik, 2011), although it is useful to highlight that hafting traces alone are not necessarily indicative of projectile utilisation. Residue analysis has also focused on the identification of organic

and mineral residues left on the surface of stone tools, which could possibly indicate hafting or projectile use (Hardy et al., 2001, 2013; Lombard, 2004, 2008; Lombard et al., 2004; Wadley et al., 2004; Gibson et al., 2004; Lombard and Wadley, 2007; Fullagar et al., 2009; Fullagar, 2016).

However, because the direction of the impact and the contact material between the weapon and the target can be identical for spears, darts, or arrows, use-wear methodology is still investigating the possibility of distinguishing between specific weapon systems. Nevertheless, the establishment of precise use-wear patterns and experimental criteria to allow for the distinguishing of different weapon and delivery systems is the direction in which recent use-wear and experimental investigations are moving towards (Hutching, 1999, 2011, 2015; lovita et al., 2014; Sano et al., 2016; Milks et al., 2016; lovita et al., 2016; Pargeter et al., 2016; Coppe and Rots, 2017; Gaudzinski-Windheuser et al., 2018).

Therefore, this study has chosen the use-wear analysis as the main methodology of research in the attempt to verify the viability of use-wear analysis in assessing and distinguishing between hand-delivered throwing and hand-delivered thrusting spear projectiles (see CHAPTER 2).

1.3 The anatomical capability of Neanderthals to throw and thrust spears

The ability to throw (*sensu lato*) has been observed in different species of primates (Goodhall, 1964, 1986; Chevalier-Skolnikoff et al., 1982; Hopkins et al., 1993, 2012). However, while primates can throw sticks, stones, and other objects, humans are the only ones that can throw with accuracy and high velocities (Roach et al., 2013, p. 483). Nevertheless, due to the difficulty of reconstructing the muscular and skeletal morphology of extinct hominin species, the ability of genus *Homo neanderthalensis* to throw/launch is still under debate (Churchill and Rhodes, 2008; Rhodes and Churchill, 2009; Shaw et al., 2012; Roach et al., 2013; Roach and Richmond, 2015).

In 1995, Berger and Trinkaus proposed that the patterns of bone trauma in Neanderthal fossil records, which presented a high level of upper body trauma (head and neck breakages) similar to the bone breakage distribution of North American rodeo riders, could suggest that Neanderthals practised close-quarters ambush hunting in Middle Palaeolithic times.

Drawing on this idea, Churchill and colleagues (Churchill et al., 1996; Schmitt et al., 2003; Churchill and Rhodes, 2009) proposed the well-received hypothesis that Neanderthals were only capable of using thrusting spears as confrontational weapons in close-range hunting events (Churchill, 1993). The main arguments in support of this hypothesis were built on the knowledge that Neanderthals showed higher levels of bilateral humeral asymmetry than modern humans (Holocene *Homo sapiens*) (Trinkaus et al., 1994), and this was interpreted as the result of repetitive bimanual close-range hunting activities with thrusting spears only (Churchill et al., 1999; Schmitt et al., 2003). The fact that Neanderthals were characterized by higher levels of humeral retroversion angles (Rhodes and Churchill, 2009) and narrower glenoid fossa (Churchill and Rhodes, 2009) than Upper Palaeolithic modern human populations, in the researchers' opinions, was only related to thrusting activities that would have resulted in mechanical loading and bending movement responses in the observed anatomical adaptations in the dominant-limb of Neanderthals (Churchill et al., 1996, p. 36; Schmitt et al., 2003, p. 112). Therefore, Churchill

and colleagues (Churchill et al., 1996; Schmitt et al., 2003; Rhodes and Churchill, 2009; Churchill and Rhodes, 2009) proposed the hypothesis that thrusting motions were one of the main activities, if not the only one, to create humeral bilateral diversity in Neanderthals, implying that throwing was not in use among the Neanderthal population but, instead, became common in the late Upper Palaeolithic humans (Schmitt et al., 2003; Rhodes and Churchill, 2009; Churchill and Rhodes, 2009).

Although there were no clear muscular-skeletal indications that Neanderthals could not throw objects from relatively short-distances (as also stated by Shea, 1997, p. 83), the “thrusting hypothesis of Neanderthals” became broadly adopted by different authors (Shea, 2006; Shipman, 2008; Sisk and Shea, 2009, 2011; Shea and Sisk, 2010), and it created the paradigm that throwing was not in use among Neanderthal populations (Schmitt et al., 2003; Rhodes and Churchill, 2009; Churchill and Rhodes, 2009; Shea, 2006; Sisk and Shea, 2009, 2011). This paradigm was also reinforced by the fact that, at the time of the research, there was very little evidence supporting the use of projectiles among Neanderthals (but see Shea, 1988), a piece of evidence that has been challenged in recent years (see section 1.4.3.2.1 and 1.4.3.2.2).

However, the hypothesis that humeral bilateral diversity in Neanderthals is caused only by thrusting activities has been challenged by several authors (Shaw et al., 2012; Roach et al., 2012, 2013; Roach and Richmond, 2015a, 2015b). Shaw et al. (2012) demonstrated, through a set of experiments, that other activities such as animal-hide preparation (which is a highly time-consuming activity) can cause a bilateral humeral strength asymmetry as well. Moreover, the recent works of Roach and colleagues (Roach et al., 2013), published in *Nature-International Journal of Science*, stated that throwing capabilities rely on a package of different anatomical adaptations, and that shoulder morphology alone cannot explain how humans generated the abilities necessary for precise and powerful throwing motions (Roach et al., 2013, p. 2). By analysing high-speed 3D kinematics and kinetic movements of the shoulder during the performance of baseball throwing motions, they observed that low humeral torsion and laterally oriented glenohumeral joints were the main

anatomical morphological features that allowed for high-speed throwing movements (Roach et al., 2013, p. 3). Cross comparing these results with the archaeological fossil records, they found that low values of humeral torsion were already present in the australopithecine species, while a fully, laterally oriented glenoid position was definitely present in *Homo erectus*. The adaptation of these anatomical parts, although probably selected for functional tasks other than throwing, would have permitted the storage of elastic energy in the shoulder, and facilitated high-speed throwing movements in the early members of the genus *Homo* (Roach et al., 2013, p.4), dating the origins of throwing capabilities back to at least 2 Ma (Roach and Richmond, 2015a). Moreover, a recent discovery on Neanderthal bone remains at the Tourville-la-Rivière site suggests the presence of skeletal trauma due to repeated throwing activities, dated to MIS 7 (Faivre et al., 2014).

In conclusion, the recent improvement of biomechanics studies and the re-analysis of shoulder morphologies (Shaw et al., 2012; Roach et al., 2012, 2013; Maki, 2013; Roach and Richmond, 2015a, 2015b) show that the complexity of throwing mechanics and human shoulder evolution cannot be connected to a single morphological adaptation or functional task (for instance thrusting activities). These are instead linked to a more complex mosaic of physiological changes and cognitive behaviours (Isaac, 1987; Young, 2003; Roach et al., 2013), which are now being observed two million years ago (Roach and Richmond, 2015a). Therefore, the ability to throw was already acquired before the separation between Neanderthals and Sapiens (either if this happened around 440-410 Ka, Endicott et al., 2010; or 550-750 Ma, Meyer et al., 2016) suggesting that Neanderthals were capable of throwing movements, even if these were somehow different than AMH throwing movements.

1.4 “Neanderthal the hunter”: hunting behaviour and weapon evidence in the late Early and Middle Palaeolithic

Human hunting behaviour is quite unique compared to nonhuman primates. This is because humans generally approach prey that exceeds their body size and they cooperate in the acquisition, processing, and transportation of the prey (Stiner, 2002, p. 5).

Referring to Early Pleistocene hominins diet, it is generally accepted that the meat consumption of large mammals increased around 2 Ma (Dominguez-Rodrigo, 2002; Dominguez-Rodrigo and Barba, 2007; Dominguez-Rodrigo et al., 2014), either through scavenging (Binford, 1981, 1987; Shipman, 1983; Stiner, 1991, 1994) or prime acquisition behaviour (Isaac, 1978; Bunn, 1981, 1986; Pott, 1984; Blumenschine et al., 1994; Dominguez-Rodrigo, 1999; Dominguez-Rodrigo and Barba, 2007; Dominguez-Rodrigo et al., 2014).

Among Neanderthals, the idea that their consumption of meat was mainly based on scavenging, as suggested by Binford (1981, 1985, 1987, 1988) and Stiner (1994), is no longer accepted (Gaudzinski, 1996, 1999; 2006; Gaudzinski and Roebroeks, 2000; Patou-Mathis, 2000; Valensi and Psathi, 2004; Bocherens et al., 2005; Bocherens, 2009; Rendu et al., 2012; Daujeard et al., 2017). Stiner's (1994) hypothesis, which argued that scavenging was still visible among Neanderthals around 55 Ka (due to faunal assemblages which were primarily dominated by cranial bones, like those at the Grotta Guattari and Grotta dei Moscerini sites), has been proven unreliable (Marean, 1998; Marean and Kim, 1998; Marean and Assefa, 1999; Mussi, 1999). Recent research has shown that Neanderthals' subsistence strategies and hunting behaviours were well planned and adapted to different environments, showing that Neanderthals (and possibly earlier hominins) were capable hunters (McBrearty and Brooks, 2000; Gaudzinski and Roebroeks, 2000; Roebroeks, 2001; Richards and Trinkaus, 2009; Villa and Roebroeks, 2014; White et al., 2016).

Archaeozoological studies have documented that Neanderthal predation of medium and large ungulates was specialised and intercepted specific animal species and/or target ages, whether this occurred through selective hunting

activities (Gaudzinski and Roebroeks, 2000; Gaudzinski, 2006; Gaudzinski-Windheuser and Kindler, 2012) or selection during butchering processes (White et al., 2016). However, the faunal assemblages from several Middle Palaeolithic sites testify to the exploitation of single animal taxa (mainly ungulates) in large numbers or in mass killings, suggesting that specialised and cooperative hunting strategies among Neanderthals were aimed towards monospecific exploitations, according to the surrounding environment and the season of the year (Gaudzinski, 1996, 1999, 2006; Gaudzinski and Roebroeks, 2000; Conard and Prindiville, 2000; Burke, 2000; Patou-Mathis, 2004; Rodríguez-Hidalgo et al., 2016). Monospecific exploitation of single taxa is attested from MIS 9-7 (Rodríguez-Hidalgo et al., 2016) among pre-Neanderthal populations, but it becomes prevalent among Neanderthals from MIS 6 onwards (Gaudzinski, 1996, 1999; Gaudzinski and Roebroeks, 2000; Gaudzinski-Windheuser et al., 2006; Patou-Mathis, 2000; Valensi and Psathi, 2004; Fiore et al., 2004; Daujeard et al., 2017;), without any specific change during the early Upper Palaeolithic (Grayson and Delpech, 2002, but see Mellars, 1973, 1995). Discrete episodes of mass killing of large mammals are testified in several open-air Middle Palaeolithic sites, such as:

- Reindeer at Salzgitter-Lebenstedt, Les Pradelles, Jonzac, Combe-Grenal, and Abri du Maras (Airvaux, 1999; Gaudzinski and Roebroeks, 2000; Discamps and Faivre, 2017; Daujeard et al., 2017).
- Bovids at La Borde, Mauran, Coudoulous, and Wallertheim (Jaubert et al., 1990; Farizy et al., 1994; Gaudzinski, 1996).
- Horses at Starosele, Orgnac 3, Zwolen, and the Rhineland region (Patou-Mathis, 1999; Burke, 2000; Moncel et al., 2012; Conard and Prindiville, 2000).
- Red deer in the South of France and North-west of Italy (Conard and Prindiville, 2000; Valensi and Psathi, 2004; Fiore et al., 2004).
- Sporadically, hibernating bears in caves (Romandini et al., 2018).

Middle Palaeolithic monospecific faunal assemblages share several common features, such as: the accumulation of faunal assemblages during short but repeated hunting episodes; the association of animal bones that present evident human modifications (such as cutmarks and bone breakages) with stone tools; mortality profiles that show catastrophic or mass killing profiles of the same species; and selective transportation of the carcasses before or after the butchering (Gaudzinski-Windheuser, 2006; White et al., 2016; Daujeard et al., 2017). The exploitation of a single mammal taxa should have involved an extensive knowledge of the ethological behaviour of the single animal species and the surrounding landscape. This is also suggested by the presence of natural barriers (karstic depression, ravines, cliffs) in several open-air killing sites that could have been used to drive the animals into a disadvantageous position (see also White et al., 2016). Moreover, the species of hunted animals suggests that Neanderthals were not constrained by the size of the animal. Instead, they often preferred larger prey (Patou-Mathis, 2000, p. 399). In several Middle Palaeolithic sites, it has also been observed that prime-adult individuals were often the most abundant (Patou-Mathis, 2000; Gaudzinski and Roebroeks, 2000; Hoffecker and Cleghorn, 2000), indicating that Neanderthals possibly selected specific ages as their prey and targeted them during the hunting (Gaudzinski and Roebroeks, 2000) or the butchering process (White et al., 2016).

Although Neanderthals were strategic and cooperative hunters that could rely on a high protein regime (Richards et al., 2000, but see Hardy et al., 2012; Bocherens et al., 2005), isotopic and residues analyses have shown that Neanderthals also integrated their diet with marine resources (Stringer et al., 2008; Bicho and Haws, 2008; Cortés-Sánchez et al., 2011; Brown et al., 2011; Hardy and Moncel, 2011), plants (Henry et al., 2011; Hardy et al., 2012; Hardy and Moncel, 2011; Weyrich et al., 2017), and small mammals (Brown, 2009; Blasco et al., 2012), showing that Neanderthals diversified their diet depending on the geographic setting and seasonal fluctuations in resources. While the sporadic capture of birds, for the exploitation of non-utilitarian supplies such as feathers, has been linked to enhanced symbolic behaviours and to the possible

occurrence of traps (Peresani et al., 2011; Hardy and Moncel, 2011; Finlayson et al., 2012; Romandini et al., 2014; Gómez-Olivencia et al., 2018). Recent discoveries also indicate that Neanderthals around 50 Ka were exploiting large mammals not only for protein resources (in the form of meat, marrow, and fat) but also for producing secondary goods, such as bone tools and clothing (Auguste, 2003; Valensi and Psathi, 2004; Soressi et al., 2013; Daujeard et al., 2014). The manufacture of bone tools by Neanderthals possibly pre-dated the arrival of the Anatomic Modern Human (AMH) in Eurasia (Soressi et al., 2013), suggesting that Neanderthals were capable of shaping animal bones to produce standardised and specific-task objects, providing more evidence concerning the cognitive and figurative capabilities of this species (d'Errico et al., 2003; Zilhão, 2012). Recent discoveries have, in fact, further revealed Neanderthal's abilities to manufacture decorative objects, such as shells and ornaments (Zilhão et al., 2010; Soressi and d'Errico, 2007; Radovčić et al., 2015; Hoffmann et al., 2018a), symbolic images (Rodríguez-Vidal et al., 2014; Hoffmann et al., 2018b, but see Pearce and Bonneau, 2018, and Hoffmann et al., 2018c), emblematic constructions (Jaubert et al., 2016), and/or to bury their peers (Pettitt, 2011).

Therefore, emerging from the mosaic of evidence presented above is a picture of a human species, i.e. *Homo neanderthalensis*, which was capable of cooperative and planned strategies of selective and systematic hunting, and was flexible to the environmental limits of the geographic availability and seasonality of the animal taxa. Neanderthals were also capable of adapting their ecological and alimentary niche for the consumption of marine, plant, small animal resources, and sporadic scavenged prey. Furthermore, the discovery of figurative objects and images suggests that the cognitive ability to hold abstract thoughts and non-utilitarian behaviours were already developed among Neanderthal populations (Hoffmann et al., 2018a; Jaubert et al., 2016; d'Errico et al., 2003; Zilhão, 2012), at least from the second part of the Middle Palaeolithic (around 150 Ka).

Although we now have a better appreciation of the complex and sophisticated hunting and behavioural strategies used by Neanderthals, the hunting weapons

employed for a long phase of the late Early and Middle Palaeolithic remain still largely unidentified and poorly understood.

1.4.1 The first evidence of weaponry technology: single-unit untipped wooden spears

It is only with the discovery of the Middle and Late Pleistocene wooden spears (Table 1-1) that the first identification of weaponry technology in the Palaeolithic becomes possible.

The earliest evidence of wooden spears came from the interglacial Schöningen site in Germany (Thieme, 1997; Schoch et al., 2015; see Table 1-1). Here, nine wooden spears were found in association with stone tools and the butchered remains of horses (Thieme, 1997; Schoch et al., 2015). New U-Th and thermoluminescence dating attributed the position of the stratigraphic layer Schöningen-13 to MIS 9 (Richter and Krbetschek, 2015; Sierralta et al., 2012; Urban and Sierralta, 2012; Geyh and Müller, 2005), although the correlation between the Holsteinian layers and MIS 9 is controversial (see Scourse, 2006; Ashton et al., 2008). The collection counts ten wooden untipped spears plus some wooden implements mainly made of spruce (*Picea sp.*) except for one made of pine (*Pinus sylvestris*) (Thieme, 1997; Schoch et al., 2015). Another possible wooden spear was discovered at Clacton-on-Sea (England) in 1911 (Oakley et al., 1977; see Table 1-1). The implement, a broken wooden tip, made from yew (*Taxus sp.*), was described as “coming from an undisturbed part of the freshwater” from the interglacial Hoxnian layer (Cf. Warren, 1922, p. 323; Oakley et al., 1977), which assigns the possible spear to MIS 11 (Bridgland et al., 1999; Ashton, 2017, p. 144). A third completed but fragmented un-tipped wooden spear was found at Lehringen (Germany). It dates back to the Eemian stage, corresponding to MIS 5e (Movius, 1950; Thieme and Veil, 1985; Table 1-1). The wooden spear, also manufactured from yew (*Taxus sp.*), was found near the skeleton of an elephant, or possibly inside it (Thieme and Veil, 1985). Other not-well preserved wooden sticks or broken pieces have been reported at the Cannstatt I-Stuttgart site (Germany) and are likely to date back to MIS 7 (Wagner, 1995); at Bilzingsleben (Germany) which

has been correlated either to the Holsteinian interglacial period MIS 9 (Serangeli et al., 2012) or to MIS 11 (Mania and Mania, 2005, p. 98), (Table 1-1); and at Ljubljana (Slovenia), dated at around 37 Ka (MIS 4) (Gaspari et al., 2011).

Other wooden objects, interpreted as digging sticks or shovels, have been recently found in Aranbaltza III (Spain; dated between 137–50 Ka, Rios-Garaizar et al., 2018), at Poggetti Vecchi (Italy; dated to MIS7-6, Aranguren et al., 2018), and at Abric Romaní (Spain; dated at around 50 Ka, Carbonell and Castro-Curel, 1992; Allué et al., 2012).

Table 1-1. Archaeological evidence of wooden spears (from Thieme, 1997; Oakley et al., 1977; Serangeli et al., 2012; Schoch et al., 2015). NP: not preserved.

Archaeological site	N. of implements	Type of implements	Wood species	Year of discovery	Dating
Clacton-on-Sea	1	n=1 broken wooden spear tip	Yew (<i>Taxus sp.</i>)	1911	MIS 11 (around 400 Ka)
Bilzingsleben	NP	NP	NP	1998	MIS 11 or MIS 9 (around 300 Ka)
Schöningen	12	n= 10 wooden spears n=1 burnt wooden artefact n=1 throwing stick	n= 11 Spruce (<i>Picea sp.</i>) (n=1 Pine (<i>Pinus sylvestris</i>))	1994-199	MIS 9 (around 300 Ka)
Cannstatt I	1	n=1 wooden stick	Acer (<i>Acer campestre</i>)	1995	MIS 7 (around 200 Ka)
Lehringen	1	n=1 wooden spear	Yew (<i>Taxus sp.</i>)	1948	MIS 5e (around 120 Ka)
Ljubljana	1	n=1 wooden spear	NP	2011	MIS 4 (around 37 Ka)

The functionality of Middle and Late Pleistocene wooden spears has been long debated. They have been interpreted as hand-thrown spears (Thieme, 1997;

Oakley et al., 1977; Villa and Soriano, 2009), hand-thrust spears (Schmitt et al., 2003; Milks, 2016; Gaudzinski-Windheuser et al., 2018), and multipurpose wooden tools (Gamble, 1987). However, a recent experimental study has shown that modern replicas of Schöningen spears, replicating the measurements and raw materials, performed well in hand-delivered thrusting experiments (Milks et al., 2016). Furthermore, Gaudzinski-Windheuser et al. (2018) reported two possible hunting wounds, recorded on the pelvis and a cervical vertebra of two fallow deer skeletons, from the site of Neumark-Nord (Germany), dated at 120 Ka. These hunting lesions have been linked to the use of a thrusting untipped wooden spear used in a close-range hunting episode (Gaudzinski-Windheuser et al., 2018). This interpretation was also proposed for another possible hunting lesion, reported from the site of Boxgrove (UK), dated at 500 Ka. Here, a left scapula of a horse showed semi-circular damage which was deemed to be resultant of the impact of a wooden spear (Roberts and Parfitt, 1999), although this interpretation is not fully accepted (Gaudzinski-Windheuser, 2016, p. 92).

In conclusion, archaeological discoveries and recent experimental studies suggest that wooden spear technology was present in the European Middle Pleistocene era, possibly from MIS 13 (if Boxgrove evidence is accepted, Roberts and Parfitt, 1999), MIS 11 (Oakley et al., 1977), or MIS 9 (Thieme, 1997; Richter and Krbetschek, 2015; Sierralta et al., 2012; Urban and Sierralta, 2012) onwards, with the last surviving evidence dated during MIS 5e (Movius, 1950; Thieme and Veil, 1985) or MIS 4 (Gaspari et al., 2011). Based on the dating of the archaeological levels where the wooden spears were found, the hominins species that may have produced and used the earliest wooden spears could be *Homo heidelbergensis*, and/or, depending on the accepted dating of the emergence of early Neanderthal features (see Stringer, 2012 for the Sima de los Huesos fossils now dated to >530 Kya), Neanderthals might have also been the creators of the first wooden spears (Bischoff et al., 2007; Schoch et al., 2015).

Concerning the utilisation of the untipped wooden spears, the latest archaeological discovery at the Neumark-Nord site (Gaudzinski-Windheuser et

al., 2018) and the experimental study of hand-delivered spear mechanics (Milks, 2016; Schmitt et al., 2003) suggest that Middle and Late Pleistocene untipped wooden spears were used for close-range hunting, possibly in thrusting motions (Gaudzinski-Windheuser et al., 2018; Shea, 2006; Schmitt et al., 2003).

Notwithstanding these discoveries' support of the appearance of untipped wooden spear technology in the Early and Middle Pleistocene of Europe, they reveal very little about the emergence and adoption of another type of weaponry technology - stone-tipped spear technology, for which other types of evidence are necessary.

1.4.2 Untipped wooden spears vs stone-tipped spears

A stone-tipped spear compared to an untipped wooden spear is a step forward in the evolution of the human mind. To produce a stone-tipped weapon that is composed of multiple elements, i.e. the shaft and the tool, there is a new concept that must be involved first - the concept of hafting.

1.4.2.1 The demand for hafting

Hafting is a process by which a tool (stone, bone, antler, metal, or wood) is inserted into a handle. In evolutionary terms, hafting allowed for better protection of the user's hands, diminishing the possibility of infection; increased the effectiveness of the tool during the process of utilisation acting like a lever (Barham, 2013).

The invention of hafting has been linked to various technological and cognitive changes (Ambrose, 2001, 2010; Wynn, 2009; Wadley et al., 2009; Wadley, 2009, 2010; Haidle, 2009, 2010; Lombard and Haidle, 2012; Barham, 2013). The technical innovations involved:

- The ability to produce adhesives (i.e. glues) to attach the tool onto the handle, by chemical and mechanical production methods.
- The ability to create binding materials to consolidate the attachment between the tool and the handle.

The cognitive innovations involved:

- The ability to abstract, as the maker would need to conceptualise the sticking of two different parts together before the final production of the hafted tool.
- The ability to plan and execute different operational tasks in a continuum (also defined as working memory, see Section 1.4.2.2).
- The ability to anticipate future needs as hafting involves the anticipated preparation of multiple elements, such as the adhesive and the binding materials which are prepared in advance for later use.

Therefore, the understanding of hafting and composite technologies must have been a critical requirement for the production of stone-tipped spears (Rots and Van Peer, 2006; Rots, 2004, 2016).

1.4.2.2 Untipped wooden spears vs stone-tipped spears: definition and cognitive implications

Stone-tipped spears are composite weapons (Ambrose, 2010) meaning that they result from the combination of multiple elements, i.e. the spear shaft, the stone tool, and the hafting materials. Whereas, untipped wooden spears are single-unit weapons meaning that they consist of a single element (Haidle, 2009), i.e. a spear shaft with a carved, pointed end.

The manufacture of stone-tipped spears, when compared to the manufacture of untipped wooden spears, required a much more complex mindset with enhanced cognitive skills. The comparison between wooden spears and stone-tipped spears' operational sequences (i.e. chaînes opératoires; Figure 1.1), as expressed by Lombard and Haidle (2012), reveals that stone-tipped spears represent essential innovation in technological, behavioural, and cognitive capabilities (Haidle, 2009; Lombard and Haidle, 2012; Waidley, 2009). The experimental manufacture of a wooden spear (as presented by Lombard and Haidle, 2012, figure 2) includes five sequential levels of action (Figure 1.1):

-
1. The collection of raw materials such as a hammerstone and chert for the stone scraper, a tree trunk/branch for the shaft, spark materials for the fire required for the manufacture of the shaft.
 2. The conceivable creation of the fire for scraping the wooden shaft and consolidating the tip.
 3. The production of the stone scraper for working the wooden shaft.
 4. The production of the wooden spear.
 5. The final utilisation of the wooden spear against the prey.

In contrast, the experimental manufacture of a stone-tipped spear (very similar to the one presented in this thesis, see CHAPTER 4) includes nine sequential levels of action (Figure 1.1):

1. The collection of numerous raw materials, such as a hammerstone and chert for the stone scraper and stone point; a tree trunk/branch for the shaft; spark materials for the fire; collection of bark, resin and/or hematite for the production of adhesives; collection of a grinding stone and/or an organic recipient; collection of a stirring tool; and collection of vegetal binding materials or animal sinew.
2. The creation of the fire for producing the adhesives and possibly for scraping the wooden shaft.
3. The manufacture of the wooden shaft.
4. The production of the adhesives, either by compound methods (i.e. adhesives that combine resin-based materials with the addition of ochre, beeswax, or other softening agents) or distillation methods (i.e. tar-based adhesives that involve the process of distillation from a tree's bark). Both methods include the making of a fire and the transformation of several raw materials.
5. The production of the stone point.

-
6. The manufacture of binding materials.
 7. The mental template for the composition of the wooden shaft, the stone point, the adhesive, and the binding.
 8. The final manufacture of the stone-tipped spear.
 9. The final utilisation of the stone-tipped spear against the prey.

Therefore, the production of stone-tipped spears introduces more complex operational sequences (see Figure 1.1), which correspond to innovative cognitive concepts. This is because the human maker of a stone-tipped spear would need to remember the first accomplished task in order to continue to the next working task, in a sequence of operational levels that would result in the final manufacture of the composite weapon (similarly to propositions concerning the production of compound adhesives, Lombard and Haidle, 2012; and hafting tools Barham, 2013; Wynn, 2009). Moreover, the maker of a stone-tipped spear would need to produce materials (such as the shaft, stone point, adhesives, and bindings) that do not serve an immediate need, but would instead be used at a later time (e.g. adhesives can be prepared in advance and stored for months, Wadley et al., 2015), enhancing the ability to forecast needs and to plan for enduring activities. The ability to remember and store practical information for short periods of time for the competition of sequential tasks is considered to be 'working memory' (Coolidge and Wynn, 2005; Wynn and Coolidge, 2004), while the ability to plan different tasks for future and anticipated needs is referred to as 'constructive memory' (Ambrose, 2010). In order to finalise the execution of a stone-tipped spear, the prehistoric maker would have had to possess both categories of memory (i.e. working and constructive memory). Ambrose (2010) states that composite tools demand enhanced working and constructive memories. These types of cognitive memories are also associated with the frontal lobe of Broca's area, which is the part of the brain responsible for language and grammatical construction (Aboitiz and Garcia, 1997). Therefore, the first prehistoric makers of composite stone-tipped spears would have had the ability to process long-term planning, forecasting, the anticipation of needs, abstractive, cooperative, and recursive language capabilities, which are

monitored both by the working and constructive memory (Ambrose, 2010; Coolidge and Wynn, 2005; Wynn and Coolidge, 2004).

Equally, experimental studies show that the intentional manufacture of adhesives (both compound and distilled methods) involves the understanding of chemical changes and the mechanical properties of the materials (Wadley, 2010; Groom et al., 2015; Kozowyk et al., 2017a), as well as requiring enhanced cognitive processes of prediction, planning, and abstraction (Wadley, 2001, 2010; Haidle, 2010). It has been argued that compound adhesives indicate complex cognitions and enhanced working memory (Wadley et al., 2019; Haidle, 2010; Wynn and Coolidge, 2004). However, recent experimental works have also shown that the production of distilled adhesives, such as tar-based adhesive, shares numerous similarities to compound adhesives and are equal in the complexity of cognition (Kozowyk et al., 2017a; Groom et al., 2015; see also Section 1.4.3.2.2).

Moreover, the appearance of prepared core technologies such as Levallois, Discoid, or Kombewa methods (or Mode 3; Clark, 1969) around 300-250 Ka represents one of the major technological and cognitive innovations of the Middle Pleistocene (White et al., 2011; Foley and Lahr, 1997; Otte, 1995; Bordes, 1971). These technologies require indeed two technological expedients that reflect cognitive development. Levallois methods, as well as other prepared core technologies, necessitate a clear conceptual separation of two distinctive and hierarchical surfaces and a preparation phase of the core that allows the extraction of flakes with a controlled and anticipated morphology (Boëda, 1986, 1995; see also Volume 2, Appendix B, Figure 145 and Figure 146). These technologies' core preparation phase and predetermination of the end-products indicates that motorial control and complex manipulation (Karakostis et al., 2018), planning and anticipation of future needs, as well as “visual imaging” and a “visual template” (Gowlett, 1984), and decision-making were cognitive capabilities present in the mind of later Middle Pleistocene flintknappers, both Neanderthals and early *Homo sapiens*. Knappers had a clear idea of the morphology of the stone tools they needed, and applied concepts such as Levallois in a flexible rather than rigid manner (e.g. Schlanger, 1996).

Therefore, the evidence of adhesive production, hafting processes, and predetermined reduction sequences in the Middle Palaeolithic of Europe, from around 300 Ka (see 1.4.3.2.2), might indicate that the technical and cognitive capabilities of Neanderthal populations in Europe were just as developed as those of African AMH populations during the African late MSA (from around 300 ka) (Kozowyk et al., 2017a, b; Wadley, 2005, 2010; Wadley et al., 2009).

**This image has been removed by the author of
this thesis/dissertation for copyright reasons.**

Figure 1.1. Operational schemes of production and use of a stone-tipped spear and the single-unit simple wooden spear from Lombard and Haidle (2012, figure 2).

1.4.2.3 Usage of untipped vs stone-tipped spears: evidence from ethnography and experimental studies

As demonstrated above, stone-tipped spears require more significant effort and skills to be produced than untipped wooden spears (see Figure 1.1). The brittleness of the stone tool on tipped weapons and the possible breakages (or loss) of the point has been highlighted as further complicating factors that add risk to hunting activities (Waguespack et al., 2009; Bleed, 1986; but see below discussion). Stone-tipped weapons would have also required longer maintenance times than untipped spears, involving continuing adjustments of the hafting system and maintaining the sharpness of the stone tool (i.e. re-sharpening or changing the tool). Therefore, the extra production and maintenance costs of stone-tipped spears would have needed to have been outweighed by economic returns in food procurement, functional reliability of the weapon, and/or social benefits (Ellis, 1997).

Ethnographic literature can assist in the understanding of the possible uses and benefits of stone-tipped spears as opposed to untipped wooden spears (Ellis, 1997; Henry, 1997; Churchill, 1993). However, it must be stressed that ethnographic parallels between Palaeolithic spears' usage and modern ethnographic examples can be misleading. The danger of imposing a uniform vision of ethnographic societies onto much earlier periods that might have been ruled by different environmental, cultural, and physical conditions is an ever-present risk. Nevertheless, ethnographic sources are here employed to merely explore similarities or differences between untipped and stone-tipped spear systems and they are presented in collaboration with experimental studies.

Ellis (1997), in his overview on the factors influencing the use of stone projectiles in ethnographic societies, produced a comprehensive synthesis of the possible advantages and disadvantages that stone-tipped weapons may have had in comparison with untipped weapons. These are as follows:

- Stone-tipped weapons have commonly been regarded in ethnographic studies as more effective than untipped weapons for the capacity of their sharp edges to penetrate more deeply into the prey and cause major

damage (Arndt and Newcomer, 1986; Christenson, et al., 1986; Ellis, 1997; Churchill, 1993). However, recent experiments using tipped and untipped spears have demonstrated that the difference in penetration depth between the two weapon types was not statistically significant, rejecting the hypothesis that stone-tipped spears penetrated deeper than untipped spears (Wilkins et al., 2014, but see Waguespack et al., 2009). However, these recent studies have also demonstrated that stone-tipped spears caused larger wound channels than untipped spears, which would result in more severe bleeding and tissue damage for the prey, confirming the assumption that stone-points increase the “killing power” and, therefore, the effectiveness of the weapons (Wilkins et al., 2014).

- Ethnographic sources also revealed that stone-tipped spears were used almost exclusively on “large animals” (Ellis, 1997, p. 40; Churchill, 1993, table 1.2). This has been linked to the fact that smaller game is easier to catch/hunt with traps or slings, and that stone-tipped spears would have damaged the skin, tissue, and meat of small prey more than untipped weapons. However, to the best of the author's knowledge, no experiments have been performed to test this assumption.
- Another suggested an advantage of stone-tipped spears is the additional weight of the weapon, which can increase its effectiveness (Ellis, 1997, p. 52). The physics and ballistic explanations behind this assumption are correct. A higher weapon mass results in higher levels of kinetic energy, and more force is transferred from the weapon into the prey, resulting in deeper penetration depth and larger wounds (as suggested by Hughes, 1998, p. 349; Churchill et al., 2009, p. 167).

With regards to the performance of stone-tipped weapons in comparison with untipped weapons, ethnographic and experimental research are somewhat contradictory.

- Archaeological experiments have obtained conflicting results in terms of the penetration depth of tipped vs untipped weapons. The experiments of Wilkins et al. (2014) demonstrated an insignificant difference in

penetration depth between stone-tipped spears and untipped spears. Whereas Waguespack et al. (2009) proved that stone-tipped arrows penetrated 10 cm deeper than untipped arrows, and this difference was statistically significant. The different experimental results could be related to the type of target employed and to the different weapon systems. Therefore, future experiments using comparative experimental protocols are required in order to further investigate the difference in effectiveness between tipped and untipped hand-delivered spears.

In terms of the brittleness of the stone points and the risk of breakage or loss of the point, i.e. the reliability, ethnography seems to support the hypothesis that the brittleness of the stone tool in stone-tipped spears could instead be an advantage (Ellis, 1997, p. 56). This assumption seems logical for two reasons:

- If a stone-point breaks, or it becomes loose inside the prey, it generally causes more substantial haemorrhage and slows down the animal, facilitating possible tracking (as also reported by a *Ju/'hoansi* member of the *Tsumkwe* Bushmen group at *Naye Naye Concession Area*, personal communication, Namibia 2016).
- If the stone-point detaches from the shaft, it helps in the recovery of the larger part of the weapon, which is an advantage because the shaft is the part of the weapon that takes longer to manufacture.

Therefore, the ethnographic and experimental evidence presented above indicates that, although the production and maintenance costs associated with stone-tipped spears were higher, the economic returns (enhanced by factors such as greater effectiveness, lethality, and reliability of the weapon) associated with the use of stone-tipped spears in the hunting of large animals could justify the effort.

However, no stone-tipped spears or composite weapons have ever been discovered for the Middle Palaeolithic archaeological record, although Levallois and Mousterian points have often been discussed in this context.

The first discoveries of composite weapons are dated only to the Upper Palaeolithic. A composite barbed point has been recently found in the Gravettian levels of Le Prés de Laure (France; Tomasso et al., 2018); at Combe Saunière cave (France) the first spear-thrower antler hook appeared from the Solutrean levels of the (around 17.500 BP; Cattelain, 1989); whereas the first bow and arrows appeared at the sites of Stellmoor (Rust, 1943) dated around 12 Ka during the Younger Dryas (Weber et al., 2011). Thus, as expressed in Section 1.4.3, only indirect evidence can shed light on the adoption and emergence of stone-tipped spear technology.

1.4.3 Composite stone-tipped spear technology: indirect evidence

No spears with attached stone or organic tips (or other composite weapons) have ever been discovered in Middle Palaeolithic archaeological sites, therefore, the evidence of the possible usage of stone-tipped spears can only be inferred by indirect evidence, i.e. by the analysis of the stone tools.

1.4.3.1 The role of convergent tools

Convergent stone tools (such as Levallois points, Mousterian points, and/or convergent scrapers) have been considered for a long time as a fundamental element of the Neanderthal toolkit (Bordes, 1953, 1954, 1961). Convergent tools were produced by employing different knapping methods (e.g. Levallois, Discoid, opportunistic, Laminar; see Inizian et al., 1999) and reduction sequences (for instance, unidirectional and centripetal to name few; Boëda, 1982, 1994, 1995; Boëda et al., 1990; Van Peer, 1992; Dibble and Bar-Yosef, 1995; see also Appendix B, Volume 2), resulting in tools with different morphologies. The production of these tools and their proportions in the archaeological records vary according to the site, in relation to cultural elements (Bordes, 1953, 1961), functional elements (Binford, 1983), and across time and space (White and Ashton, 2003; Adler et al., 2014).

In the past, most studies have focused on the convergent tools from the Near East and South Africa, where unifacial or bifacial points were dated back to the pre-Middle Stone Age, appearing around 500 Ka (Wilkins et al., 2012) and 300 Ka (Adler et al., 2014) in Africa; and from around 270-180 Ka in the Near East (e.g. at Tabun cave, Mercier and Valladas, 2003; and Kebara cave, Shea, 1988, 1997). In these geographical areas, research has indicated that convergent tools, as well as having multiple utilisations (Plisson and Beyries, 1998), were largely employed as projectile points, most probably as spear-heads (Shea, 1988, 2006; Marks, 1998; Shea et al., 2001, 2002; Lombard, 2005b; Villa and Lenoir, 2006; Brooks et al., 2006; Lombard and Pargeter, 2008; Sisk and Shea, 2009; Bonilauri, 2010; Villa and Soriano, 2010; Wilkins et al., 2012; Sahle et al., 2013).

Contrarily, in Europe, between MIS 9 to MIS 3, various convergent tools have been produced and, some of them, testify a standardised and predetermined (or voluntary) production, as such for example the Levallois points (Boëda, 1982; see also Appendix B, Volume 2). Levallois and Mousterian points in Europe are documented from around MIS 7 (e.g. at the Vaufrey Layer VIII site, Villa et al., 2009a) or early MIS 6 (e.g. at Biache-Saint-Vaast, Rots, 2013; La Cotte de St. Brelade, Callow, 1986; and Bouheben, Villa and Lenoir, 2006). However, before 2014 (the year when this research began), the study of convergent tools in the European Middle Palaeolithic was still underrepresented (as suggested also by Villa et al., 2009, p. 2), with only a few researches that had broadly focused on the functional implications of the convergent tools production (Villa and Lenoir, 2006, 2009; Villa et al., 2009; Lazuén, 2012; Rots, 2013). Consequently, the role and function of convergent tools in the European Middle Palaeolithic remained open to research, and the question of their usage as spear projectiles needed to be addressed.

However, it is also acknowledged that this thesis does not exclude the possibility that stone projectiles in the Middle Palaeolithic could have also been employed as tips for projectile techniques other than hand-delivered throwing or thrusting spears (e.g. as spear-thrower darts and/or arrow-heads). However, considering (i) the current lack of direct evidence of use of spear-thrower and/or bow and arrow technologies in European Middle Palaeolithic sites (see Section 1.4.2.3), in possible contrast to the African MSA (e.g. Lombard and Phillipson, 2010; Shea, 2009; Brooks et al., 2006); (ii) the limited morphological standardisation of European Middle Palaeolithic convergent tools (Dibble, 1987, 1995; Rolland and Dibble, 199); and (iii) the results of previous experiments that indicate scarce effectiveness of Middle Paleolithic convergent tools used as arrow-heads (Sisk and Shea, 2009), this thesis chose not to test the possibility of the use of Middle Palaeolithic convergent tools as dart-heads or arrow-heads by Neanderthals. These topics of research could, however, be fascinating and they would deserve future investigation and appropriate experimental protocols (which were not possible to develop within the timeframe of this research),

particularly if new convergent tool assemblages with different morphological and/or standardisation characteristics are identified in the future.

But why choose the Levallois point as a unique techno-morphological type for the experimental and archaeological analyses?

First, because for a long time Levallois points were considered effective spearheads (Bourlon, 1906, p. 313; Bordes, 1961, p. 21). However, this evidence was mostly based on speculative typological attributes of this tool type, and no data coming from replicative experiments testing the effectiveness of this techno-morphological tool type were available. Secondly, because Levallois points in the different Middle Paleolithic archaeological sites have frequently shown impact fractures (Shea, 1988, but see Plisson and Beyries, 1998; Villa and Lenoir, 2006, 2009; Villa et al., 2009; Wilkins, 2012; Sahle, 2012; Rots, 2009, 2013; Hardy et al., 2013; Lazuén, 2012; La Porta et al., 2015; Yaroshevich et al., 2016) that could indicate a specific function of this specific tool type as a projectile implement. However, a comprehensive experimental investigation assessing the multiple utilisations of this specific techno-morphological tool type was still warranted. Third, because previous experiments that have tested the effectiveness of Middle Palaeolithic stone-tipped spears, have also employed replicas of Levallois points (Shea et al., 2001; Sisk and Shea, 2009; Iovita et al., 2014), and it was this author's intention to produce data comparable with previous experiments. Lastly, because Levallois point (see also Appendix B, Volume 2 for definition) is a tool easily distinguishable in any archaeological assemblage, and this is not always the case with other Middle Palaeolithic convergent tools (Goval et al., 2015).

Below evidence concerns the presence of projectile stone tools in the Middle Palaeolithic archaeological record are presented.

1.4.3.2 Evidence of stone projectiles in Middle Paleolithic

The evidence for the early stone-projectiles in the European Middle Palaeolithic and African MSA is still highly debated, as the recognition criteria (i.e. use-wear traces) have been challenged (e.g. Rots and Plisson, 2014, contra Wilkins et

al., 2012, and Lazuén, 2012; Plisson and Beyries, 1998, contra Shea, 1988). Furthermore, if stone-tipped spear technology was in use in the European Middle Palaeolithic, it is still discussed how stone-tipped spears could have been used, i.e. as throwing or thrusting spears (Schmitt et al., 2003; Churchill and Rhodes, 2008; Rhodes and Churchill, 2009; Shaw et al., 2012; Roach et al., 2013; Roach and Richmond, 2015). Therefore, below is reported a review of the evidence for the use of Middle Palaeolithic and MSA convergent tools as possible projectiles, with a critique of the debate concerning the criteria for the recognition of projectiles and the identification of the ways in which Neanderthals may have used stone-tipped spears.

1.4.3.2.1 The African record

Recently, stone points from the Kathu Pan site (South Africa) dated at 500 Ka have been interpreted as the earliest stone tools to be hafted in shafts and used as hand-delivered spears (Wilkins et al., 2012, but see Rots and Plisson, 2014, and Wilkins et al., 2015), although this interpretation is not widely accepted (Rots and Plisson, 2014). A second possible piece of evidence for the existence of early projectile utilisation comes from the MSA site of Gademotta (Ethiopia), dated at 279 Ka. Here obsidian stone tools with possible impact traces (and Wallner Lines) have been associated with the use of stone-tipped hunting weapons (Sahle et al., 2013), although the interpretation of these projectiles, as hand-delivered throwing stone-tipped spears or spear-thrower darts, is somewhat vague (Douze and Delagnes, 2016). From the same period, the distal fragment of a stone point embedded in a cervical vertebra of the extinct giant buffalo (*Pelorovis antiquus*) at the Klasies River Mouth site (South Africa) has been interpreted as the result of a hunting episode which probably involved stone-tipped spears (Milo, 1998).

However, what emerges from the African early MSA is a geographically and chronologically fragmentary archaeological record. The additional evidence from Eurasia is therefore crucial.

1.4.3.2.2 The Eurasian record

In Western Europe, the earliest evidence of stone projectiles, dated at around 250 Ka (MIS 6), comes from the French Middle Palaeolithic site of Biache-Saint-Vaast (Rot, 2013). Here, use-wear analyses have revealed the presence of 16 convergent tools, interpreted as stone projectiles from spear weapons (Rot, 2013, p. 498). From MIS 6, Mousterian points with possible impact fractures were identified at La Cotte de St. Brelade site in the Channel Islands (Villa et al., 2009a); at the La Verde site (Spain), which has produced one stone projectile evidence (Lazuén, 2012); and at the Bouheben site (France), where six Mousterian points were identified as stone projectiles (Villa and Lenoir, 2006, 2009). However, the above evidence is not devoid of uncertainty.

During MIS 5 in Western Europe, evidence of stone projectiles have been reported at the Middle Palaeolithic site of Fresnoy-au-Val (France), dated at MIS 5a, with one Levallois point showing impact traces (Goval et al., 2015, p. 13); at the Sesselfelsgrötte site (Germany), dated between MIS 5a and MIS 4, with 13 tools showing impact traces (Rots, 2009, figure 8); at the Lezetxiki site (Spain), with two tools showing macroscopic impact features (Lazuén, 2012); and at Cova Eirós (Spain), with four conceivable stone projectiles (Lazuén, 2012). However, most of these assemblages have been analysed only through low power use-wear analysis, and the functional interpretation of the weapon type has been inferred without the provision of supporting experimental evidence.

From MIS 4 onwards, evidence of stone projectiles in Western and Eastern Europe and the Levant areas increases. At the Abris du Maras site (France), combined residue analysis (Hardy et al., 2013), along with use-wear and morphometric analysis (La Porta, 2013; La Porta et al., 2015), highlighted the presence of between four and six convergent tools used as projectiles for hand-delivered stone-tipped spears (Moncel et al., 2014). Similarly, at the Bettencourt-Saint-Ouen site (France), dated as late MIS 5a/early MIS 4, six Levallois points have been interpreted as spear-heads (Rots, 2016, p. 183). At Cueva Morín (Spain), dated at MIS 4, five stone tools were interpreted as

projectiles for possible spears following macroscopic analysis (Lazuén, 2012). At Abric del Pastor (Spain), dated at MIS 3, four Mousterian tools were interpreted as projectile tips for spears due to their frequencies of impact fractures (Villa and Soriano, 2010; Villa and Lenoir, 2006, 2009). At the Oscurusciuto site (Italy), the correlation between impact traces and morphometric values suggested that six Mousterian points dated to MIS 3 could have been used as projectiles for hand-delivered stone-tipped spears (Villa et al., 2009a). In Crimea at Inden-Altendorf (Pawlik and Thissen, 2011), Starosele (with five Micoquian points), and the Buran Kaya III sites (with six Foliolate points) (Hardy et al., 2001), from MIS 5 to MIS 2, stone projectiles have been identified through residues and use-wear analysis among the Micoquian tools. In the Levant area, Levallois points with impact fractures have been reported at Misliya Cave (Yaroshevich et al., 2016) and Kebara Cave (Shea, 1988, 1997). However, at Kebara Cave, a second microscopic use-wear analysis suggested a different utilisation (plant use) for the same tools (Plisson and Beyries, 1998).

Complementing the use-wear evidence, possible hunting lesions have been reported from several Middle Paleolithic sites, suggesting that stone-tipped weaponry technology could have been present in the European Middle Palaeolithic from MIS 6-5 onwards. For example, the discovery of a fragment of a Levallois point found embedded in the third cervical vertebra of a wild ass from the site of Umm-el-Tlel in Syria Level VI, dated at 70 Ka (Boëda et al., 1999), has been interpreted, considering the angle of contact with the bone, as a possible penetration event during a hunting scenario (Boëda et al., 1999). At the La Quina site a reindeer ulna and vertebra were found embedded with flint tools (Gaudzinski-Windheuser, 2016, p. 92); at Lynford site (UK) a trauma resulting from a possible inflicted spear wound has been suggested for a mammoth (*Mammuthus primigenius*) rib bone dated at MIS 4 (Schreve et al., 2006). Whereas, at Shanidar 3 (Iraq) a lesion on the left ninth rib of a Neandertal individual has been interpreted as the wound possibly caused by a low kinetic energy weapon (Stewart, 1977; Trinkaus and Zimmerman, 1982, but see Churchill et al., 2009), generating a debate about intra-specific (among Neanderthals) or extra-specific (Neanderthals vs AMH) competition.

Finally, archaeological evidence of adhesive production in the Middle Palaeolithic era suggests that the “know-how knowledge” of producing glues and attaching stone tools into shafts or handles was already present from MIS 6. The earliest evidence of tar-based adhesives was found at the Middle Pleistocene site at Campitello Quarry (Italy), dated around 250 Ka (end of MIS 8 beginning of MIS 7). Here, two flakes were discovered partially covered in birch-bark-tar possibly to protect the hands of the users (Mazza et al., 2006). Two lumps of birch tar were also found at the Middle Palaeolithic site of Konigsau (Germany) dated to MIS 5e (Grünberg, 2002). One fragment presented a human fingerprint while the other showed the negative impression of a wooden shaft (Grünberg, 2002). Traces of bitumen used as hafting adhesives were found on Levallois and Mousterian points from the Middle Palaeolithic site Umm el Tiel (Syria), dated between 71 Ka and 40 Ka (Boëda et al., 1996, 2008). Various other European sites, such as Pech de l’Azé (Soressi and d’Errico, 2007), Cueva Antón and Cueva de Los Aviones (Zilhão et al., 2010; Hoffmann et al., 2018a) have also yielded the presence of minerals such as ochre. This can be linked to the production of adhesives (as an additive agent see Lombard, 2007), although given its various other uses (Roebroeks et al., 2012, p. 1889), including representations for symbolic purposes (Zilhão et al., 2010), this is less certain evidence of hafting. Nonetheless, recent archaeological experiments have proved that Neanderthal populations had the right set of technological and cognitive skills to produce a significant amount of tar-based adhesive (Groom et al., 2015; Kozowyk et al., 2017a, 2017b). Other recent studies, using use-wear analyses, have also suggested that Neanderthals were regular and systematic fire makers who owned specialist tool-kits to produce and control fire (Sorensen et al., 2018, but see also Sandgathe et al., 2011).

In conclusion, archaeological evidence from the Eurasian Middle Palaeolithic has shown that (i) stone projectiles were present from around MIS 6 - MIS 5; (ii) Neanderthals were capable hunters and possessed the technical and cognitive skills to produce composite tools; (iii) the capability of throwing was already acquired before the separation between Neanderthals and Sapiens (Roach et al., 2013; see Section 1.3). However, there is still a further big question that

needs answering: how did Neanderthals accomplish their hunting? Did Neanderthals employ close-range thrusting stone-tipped spears only, or did they also employ stone-tipped spears that could cover a longer distance when used as a projectile, i.e. hand-delivered throwing spears?

Functional interpretations of archaeological stone tool projectiles are hampered by a critical methodological limitation: Middle Palaeolithic stone projectiles have all been interpreted as stone-tipped spear projectiles in absence of comparisons with experimental stone projectiles used in throwing and/or thrusting hand-delivered spear motions (Villa and Lenoir, 2006, 2009; Villa et al., 2009; Villa and Soriano, 2010; Rots, 2009, 2013; Lazuén, 2012; Yaroshevich et al., 2016). Therefore, the identification of the delivery system of these Middle Paleolithic stone projectiles still remains debated.

1.5 Outcomes: the contribution of this research

Following the state of art concerning stone-tipped spear technology in Middle Palaeolithic and the difficulty in recognising different spear projectiles, this thesis aims to specifically test the following hypotheses:

- I. That Middle Palaeolithic stone-tipped spear replicas (mounted with experimental Levallois points) were effective hunting weapons (effectiveness expressed by penetration depth, in cm) when used in hand-delivered throwing and thrusting spear motions.
- II. That the stone tips of experimental spears delivered in a hand-throwing motion develop different wear traces to those delivered in a hand-thrusting motion, when using the same techno-morphological stone tool type (i.e. a Levallois point). This is because projectile use-wear traces form under different ballistic parameters, such as different values of impact velocities, kinetic energy (KE), momentum (p), and deceleration (which are investigated through a ballistic examination).
- III. That the wear traces formed on stone tools used as spear tips, i.e. tools hafted and used as thrown and thrust spear-heads, were different than the wear traces formed on equivalent stone tools that were deployed

differently in other experimental activities, i.e. as handheld or hafted butchering tools.

If the hypothesis (i, ii) and/or (iii, iv) are confirmed through experimental data, the next step in this work will be to test another hypothesis in the archaeological record:

- IV. That the use-wear differences demonstrated in hypothesis (i) and/or (ii) are still visible and preserved in artefacts from the archaeological record, in order to test the presence/absence of archaeological projectiles tools.

Therefore, the corroboration or rejection of the hypothesis (iii) will thus underpin the testing of the final hypothesis of this thesis:

- V. That Neanderthals produced and employed stone-tipped spears, and that these spears were used either in thrusting or throwing activities respectively or in both activities.

To test the above hypotheses, an interdisciplinary methodology is presented below. This methodology was based on several stages of investigation:

- I. The performance of controlled archaeological experiments, including the use of hand-delivered stone-tipped spears (both throwing and thrusting) and butchering knives (both handheld and hafted) (see CHAPTER 4).
- II. The ballistic examination of hand-delivered stone-tipped spears' parameters (see CHAPTER 5).
- III. The techno-morphological and use-wear examination of the experimental artefacts (see CHAPTER 6 and CHAPTER 7).
- IV. The techno-morphological and use-wear examination of archaeological stone tools following the methods outlined in point III above (see CHAPTER 10 and CHAPTER 9).

In the next chapter, the use-wear methodology employed in this study is presented.

CHAPTER 2

USE-WEAR ANALYSIS METHODOLOGY

2.1 Definition and background

The use-wear analysis is a specific methodology in archaeology that aims to identify how stone tools were used in their lifetime in an attempt to infer their function.

This method is based on the observation of wear traces on the edges and/or surfaces of stone tools, formed during utilisation. The observation of these diagnostic traces allows for a functional interpretation. This methodology has been proven to be effective in identifying the types of movements carried out by the tool and materials upon which the stone tool was used (Semenov, 1964; Tringham et al., 1974; Hayden, 1979; Keeley, 1980; Moss, 1983a; Odell, 1981; Anderson-Gerfaud, 1981; Vaughan, 1985; Plisson, 1985; Van Gijn, 1989; Beyries, 1987; Anderson et al., 1993; Hurcombe, 1992; Lemorini et al., 2003; Longo and Skakun, 2008; Bicho et al., 2015).

The systematic methodological development of use-wear analysis was achieved by the Russian archaeologist S Semenov (Semenov, 1964). Focusing on the alteration of the active edges of archaeological and experimental stone-tools, he observed a relationship between the degree of wear traces and the function of the artefacts. Semenov's observations on different raw materials (lithic and bone tools), focused mainly on the attributes of edge-damage at low magnifications (low power approach, magnifications <100x; see also Tringham et al., 1974). The translation of his PhD thesis into English (Semenov, 1964) contributed to the spread of the use-wear discipline into Western Europe and to the consolidation of its applications.

During this phase, use-wear investigations were characterised mainly by a low-power approach (from 5x to 70x magnification), although some studies also introduced high-power investigation (magnification >100x; Keeley and Newcomer, 1977; Hayden, 1979). The low-power approach focused mainly on

macro traces (i.e. edge-damage, fractures and to a certain extent striations) resulting from the use of experimental stone tools against different worked material (e.g. bone, wood, antler, meat, shin, fresh hide) (Tringham et al., 1974; Odell, 1975, 1981; Kamminga, 1982). However, with this approach, it is possible to identify mainly the hardness of the worked material (e.g. bone, wood and antler materials were referred as hard materials, while meat and fresh hide were referred as soft materials; Tringham et al., 1974; Odell, 1981; Kamminga, 1982). Therefore, the identification of the specific worked materials associated with corresponding wear traces was nonetheless challenging to achieve with low magnification analysis.

It is for this reason that the second substantial contributions to the use-wear field came with the introduction of the high-power approach (magnification >100x, using reflected light microscopes) made by L Keeley (1980). High-power analysis contributed not only to distinguish the degree of wear damage of the edges of prehistoric stone tools but, according to Keeley (1974, 1980), it allowed the recognition of the different types of worked material (e.g. wood, bone, antler, hide, meat, plant). This was achieved mainly through the identification and distribution of microscopic wear traces, among which polish formation was the most important (Vaughan, 1985). The high-power approach contributed to promoting the use-wear discipline. However, it also presented a few limitations associated with the fact that distinct worked materials can produce similar polishes (e.g. overlapping features between bone and antler polishes) and that polish traces were difficult to quantify.

The methodological constraints of both the low-power and high-power approaches generated a lengthy debate on the advantages and limitations of the two different methodologies, and on the evaluation of these approaches through the introduction of blind tests (Keeley and Newcomer, 1977; Odell and Odell-Vereecken, 1980; Shea, 1987; Rots et al., 2006; Hamon and Plisson, 2008; Evans, 2014). The debate contributed to the development of new analytic methods, improving the accuracy of the description of traces' attributes, and emphasised the necessity of developing quantitative methods of analysis. The Uppsala conference in 1989 (Graslund et al., 1990) gradually condensed the

division between the “low-power” and “high-power” approaches, showing the complementary between low-power and high-power use-wear methodologies (Odell, 2001; Van Gijn, 1989).

During the 1980s and 1990s, a flourishing period for use-wear analysis began. The research focused on the development of identification criteria for polish traces (Anderson-Gerfaud, 1981; Moss, 1983a; Mansur-Franschomme, 1983, 1986; Vaughan, 1985; Plisson, 1985; Beyries, 1987; Van Gijn, 1989; Jensen, 1994). Studies investigated the effect of post-depositional modifications on use-wear traces (Plisson, 1983a; Levi Sala, 1986; Plisson and Mauger, 1988), and research attempted to standardised criteria for the quantification of wear traces and polish attributes (Dumont, 1982; Grace et al., 1985; Beyries et al., 1988).

It is indeed the identification of polish types (e.g. wood, bone, antler, meat, plants) and the quantification of these traces that became even more debated during the 1980s and 1990s (Newcomer et al., 1986; Moss, 1987; Bamforth, 1988; Hurcombe, 1988; Grace, 1989). As a result, the latest research has made an effort to minimize the subjectivity of the observations and to identify new methods for quantifying wear traces and their attributes (Grace et al., 1985; Beyries et al., 1988; Estévez and Urquijo, 1996; González-Urquijo and Ibáñez-Estévez, 2003; Dumont, 1982; Anderson et al., 2006).

New comparative quantification methods have been proposed, such as image processing techniques (Grace et al., 1985; Estévez and Urquijo, 1996; González-Urquijo and Ibáñez-Estévez, 2003), interferometry (Dumont, 1982), tribology analysis (Anderson et al., 2006), and quantification of polish by calculating luminance or roughness means (Beyries et al., 1988). At this moment, recent advances in microscopy equipment appear to be very promising for advancing the measurements of wear attributes. The use of the laser scanning confocal microscope (Evans and Donahue, 2008; Ibáñez et al., 2014), laser profilometry (Stemp and Stemp, 2001), and focus variation microscopy (Macdonald, 2014; Evans and Macdonald, 2011) have been tested with promising results for the measurement of microscopic traces' parameters. These methods alongside with the classic techniques used in use-wear and

residue analysis (e.g. optical microscopes, that includes low power and high power magnifications, and scanning electron microscope - SEM) are the current basis of the use-wear methodology.

2.2 Technical equipment

Use-wear analysts usually utilise different types of microscopes depending on the research topic and questions (Borel et al., 2014; Ollé and Vergès, 2008, 2014; Evans and Macdonald, 2011; Evans and Donahue, 2008; Stemp and Stemp, 2003; Rots, 2003).

The main research questions have rigidly defined the selection of technical equipment for this study: (a) the identification of projectile wear on experimental Levallois points, (b) the distinction between throwing vs thrusting spear wears, (c) the comparison of these identified wear patterns with wear on archaeological samples. As a result, the following microscopes were used (Table 2-1):

1. stereomicroscopes for the observation, identification and interpretation of macroscopic wear traces (see Section 2.2.1),
2. optical microscopes with reflected lights (i.e. metallurgical microscopes) for the observation, identification and interpretation of microscopic wear traces (see Section 2.2.2),
3. digital microscopes (e.g. the Hirox KH-8700 and the Dino-lite edge AM7915MT microscopes) instead of metallurgic microscopes, when these were inaccessible (see Section 2.2.3).

Each piece of equipment is described below.

2.2.1 Stereomicroscopes

Stereomicroscopes provide a continuous focus, a good perception of field depth (e.g. high depth of field), and a long working distance (Pawlik, 2001). The magnification ranges from 10x to 100x or more, depends on the model. They allow a three-dimensional image (e.g. a stereoscopic vision) which is created through the combination of two independent ocular systems. This makes the

stereomicroscope the most suitable equipment for the identification of edge-damage, macro fractures (Figure 2.1), and for the identification of wear location during the first step of the use-wear analysis (Van Gijn, 2014).



Figure 2.1. Left: The stereomicroscope Olympus SZ61 (located at the Department of Archaeology, University of Exeter). Right: Multiple-fractures observed with the stereomicroscope (OM 25x).

2.2.2 Optical Light Microscopes with incident light (OLMil)

Optical Light Microscopes using incident light (e.g. metallographic microscopes) are designed for the study of opaque samples (as opposed to transmitted light microscopes which are designed for the study of translucent sections). They are mostly used in use-wear analysis to identify polish, striations, and any microscopic wear at high magnification (from 50x to 500x; Table 2-1).

The main components of a metallographic microscope are the objective lens and the eyepiece (Figure 2.2). Using the incident light microscope, a light beam is reflected through the objective lens onto the sample. When the light beam is reflected, it goes back inside the objective lens, and through a set of convergent lens, before, reaching a second lens system located in the eyepiece (Figure 2.2). This captures the image and sends it to the eye (Figure 2.2). As a result, the overall magnification of an image obtained with an OLMil (100x, 200x, 500x) is a combination of the magnifications of both the eyepiece (10x) and the objective lens (numerical aperture 10x/0.30, 20x/0.46, 50x/0.80).

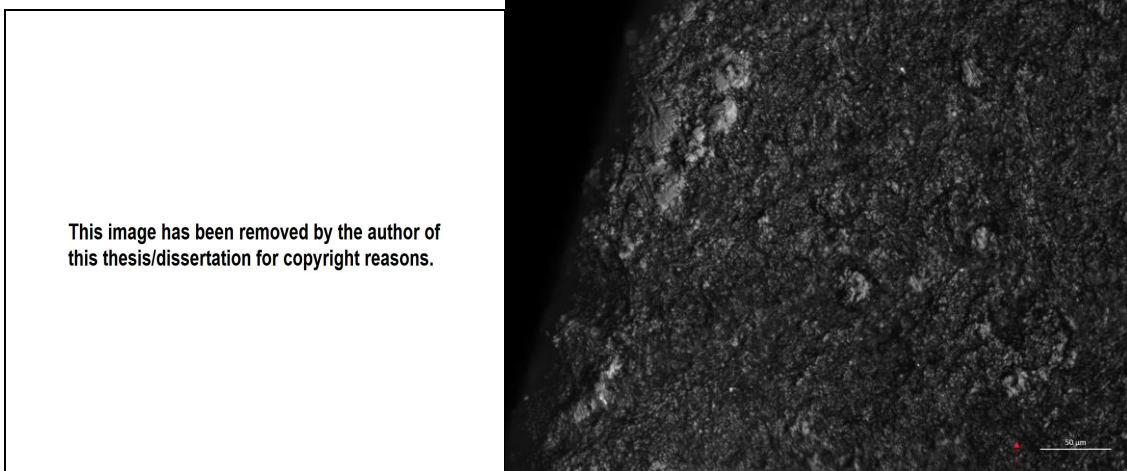


Figure 2.2. Right: an example of a microscope showing the light pathway in a reflected and transmitted light microscope (image from <https://www.olympus-lifescience.com/en/microscope-resource/primer/anatomy/reflected/>, last accessed 14-05-2015). Left: polish trace observed with an OLMil (OM 200x).

A difficulty is that regular lenses have an objective distance of 3.0 mm at 20x magnification (=200x with 10x eyepieces) and 0.6 mm at 50x magnification (=500x with 10x eyepieces) (Pawlik, 2001). At these magnifications, OLMil has a very shallow depth of focus ($1.30\ \mu\text{m}=0.0013\ \text{mm}$) and a very small working distance (at 50x the working distance is 0.66 mm). Despite the shallow depth of focus and the small working distance (which may be problematic for the analysis of big size samples), the OLMil is the most suitable machine for the analysis of microscopic wear traces (e.g. polish, striations, MLITs, edge rounding; see Section 2.5).

2.2.3 Digital microscopes (DM)

The first digital microscope, manufactured by the Hirox Co Ltd, entered the market in the late 80s. However, its adoption by use-wear analysts has been comparatively recent. Its usage is mainly linked to the possibilities of image processing, quantification of use-wear, and 3-D modelling applied to use-wear analysis (Plisson, 2014; Borel et al., 2014).

These systems use LED lighting. They do not have eyepieces and objective lenses as the image are produced and enhanced digitally. The DMs have either their own screen or can be connected via USB to a separate PC. Thus, a digital

microscope does not use optical magnification, but relies solely on digital magnification, with the limits of the magnification being defined by the extent to which the image can be enlarged on a screen (Plisson, 2014, p. 113).

2.2.4 Scanning Electron Microscope (SEM)

Scanning electron microscopes (SEM) or environmental scanning electron microscopes (ESEM) were not employed in this study as they were not available facilities at the University of Exeter - Department of Archaeology.

However, free access of an ESEM (FEI Quanta 600) became available to the author, during a study visit at the “Institut Català de Paleoecologia Humana i Evolució Social” (IPHES; Tarragona, Spain). On this occasion, the author had the possibility of free access the ESEM and observe one selected experimental tool (i.e. tool TH-31) that presented a specific pattern of use-wear trace (i.e. microscopic impact linear traces MLITs, see Section 2.5.3).

In future, the use of SEM or ESEM microscopes will be incorporated in order to investigate the formation processes of projectile diagnostic use-wear traces.

2.2.5 Microscopes employed for this thesis

During this thesis, a range of different microscopes was used in different locations, as listed below.

2.2.5.1 At the Department of Archaeology, University of Exeter

The experimental Levallois point collection was analysed at the Department of Archaeology, University of Exeter, with a stereomicroscope and an OLMil with incident light.

A binocular stereomicroscope Olympus SZ61 (6.7x to 45x) was used for the identification of edge-damage and impact fractures (Figure 2.3).

An OLMil Olympus BX60 MS (manual stage, 50x to 500x), with incident light and bright field illumination, was used to observe polish surfaces, striations, edge-rounding, and possible adhesive residues. For both microscopes, images

were taken with an Axiocam 503Color camera, using Zen2 Blue Edition Software (Figure 2.3, Table 2-1).



Figure 2.3. The stereomicroscope and the OLMil microscopes located at the Department of Archaeology, University of Exeter. (Image La Porta).

2.2.5.2 At the Natural History Museum (MNHN) of Paris

The Abri du Maras (Ardèche, France) archaeological collection was located at the Institut de Paléontologie Humaine (IPH, Paris), a department of the Natural History Museum of Paris (MNHN). Here, the stone tools were examined with a binocular microscope to record macroscopic traces (such as edge-damage and fractures), and with a Hirox KH-8700 digital microscope to record microscopic traces (such as polish surfaces, striations, edge-rounding, and possible adhesive residues). The Hirox KH-8700 digital microscope was used because optical light microscopes with incident lights were unavailable at the MNHN.

The binocular microscope was a Leica S8APO (10x to 80x). Images were recorded with a Leica MC120HD camera, using LAS Software 4.8.0 Edition.

The Hirox KH-8700 DM (Figure 2.4, Table 2-1) ranges from 35x to 2500X and can be used with co-axial and bright field light. The mid-range objective lens (140x to 1000x) was the most utilised. Low-range (35x to 1000x) and high-range (1000x to 7000x) objective lenses were also available. A fibre-optic adapter provided a flexible lighting arrangement, including a polarised filter,

variable angle, and co-axial lighting. The Hirox KH-8700 software obtained In-focus and 3D images. This captured slices of the image at different heights using an automatic Z-axis control and focus.

Access to the archaeological collection and its facilities was organised through collaboration between the author and Professor MH Moncel² (MNHN).



Figure 2.4. The Hirox KH-8700 DM located at the Natural History Museum, Paris. (Image La Porta, with permission of MNHN, Paris).

2.2.5.3 At the Archaeological Museum of Finale (Italy)

The Arma Delle Manie (Savona, Italy) archaeological collection was located at the Archaeological Museum of Finale (Liguria, Italy). The Arma Delle Manie collection, located at the Archaeological Museum of Finale (Savona, Italy), could not be transported due to national legislation. Therefore, analysis had to be undertaken with a portable DM. This purchase was funded by the University of Exeter, Department of Archaeology.

² Professor MH Moncel kindly offered to take in charge the fees for the access to the microscope facilities at the MNHN.

Here, the stone tools were investigated macroscopically and microscopically with a Dino-Lite Edge AM7915MZT USB digital microscope (10x to 220x; Table 2-1) supported by a mechanical stage Dino-lite RK-10A (Figure 2.5).

Access to this collection was organised through collaboration between the author, the Director of the Archaeological Museum of Finale (Dr D Arobba), and Professors M Peresani (University of Ferrara) and F Negrino (University of Genoa).

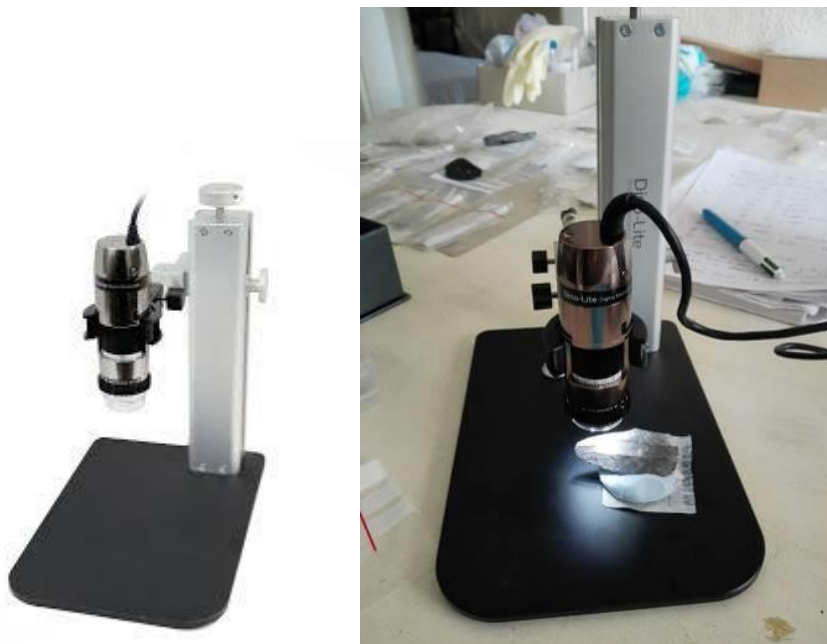


Figure 2.5. The Dino-lite Edge AM7915MZT DM employed at the Archaeological Museum of Finale (Liguria, Italy; Image La Porta).

Table 2-1. Technical specifications of the three different microscopes used during this thesis.

Optical Light Microscope (OLMil)	
Brand and model	Olympus BX60
Description	Olympus BX60 Microscope with Transmitted and Reflected Light 12V 100watt Transmitted and Reflected Light Sources Wide Trinocular Head Pair of 10x/26.5mm Eyepieces 4 Position Reflected Light Turret Bright field/Dark field/DIC for Reflected Light Analyser/Polarizer Cube for Reflected Polarized Light 2" x 3" Mechanical Stage
Objective lenses	5x/0.15 NA 12mm Working Distance (WD) Universal Plan for Bright field (UM PlanFL BD) Objective 10x/0.30 NA 6.5mm WD UM PlanFL BD Objective 20x/0.46 NA 3.0mm WD UM PlanFL BD Objective 50x/0.80 NA, 0.66mm WD UM PlanFL BD Objective
Camera	Axiocam 503Color camera 3 megapixels, Zen2 Blue Edition Software
Digital USB Microscope	
Brand and model	Dino-Lite Edge AM7915MZT
Description	Interface USB 2.0 Resolution 5M pixels (2592x1944) Magnification 10X~220X Frame Rate 10fps in 5MP/3MP/2MP, MJPEG; 25fps in 1.3MP, MJPEG; 30fps in VGA, MJPEG Lighting 8 white LEDs Extended Depth of field (EDOF) Extended Dynamic Range (EDR) Adjustable Polarizer

Digital Microscope	
Brand and model	Hirox KH-8700
Description	Monitor Display size Full HD LCD 21.5" Monitor Light source Lamp High Intensity LED Interface Lan 10BASE-T/100BASE-TX/1000BASE-T, USB2.0 6 Ports (2 x Side, 4 x Back) Motorized Z-axis Specifications: Stage Stroke Distance 30 mm (1.18") Motor / 85 mm (3.34") Manual, Multiple functions (see http://hirox-europe.com/products/microscope/index8700.html?PHPSESSID=q5snk93cf61o92gc9q66ahubk4 ; last accessed 05-05-2017)
Main Objective lenses used	Model MXG-2500 REZ Lighting Method Co-Axial, Dark Field and Mixed Low Range: 35-250x; Middle Range: 140-1000x; High Range: 350x-2500x WD 10mm
Camera	Image sensor 1/1.8-inch, 2.11 Mega-pixel CCD Sensor Scanning Mode Progressive Scan Total Pixels 2.11 Mega-pixels 1688 (H) x 1248 (V) Frame Rate 24 Frame at 1600 x 1200 Pixel Resolution

2.2.6 Comparison of images

This section compares the images produced by two different sets of microscopes used for analysis in this thesis: metallographic and digital microscopes.

A gallery of images taken at equivalent magnifications with both types of microscopes was produced as a result (Figure 2.8, Figure 2.9, Figure 2.10). This gallery shows the types of visual information each microscope is able to produce. As magnification varies with screen type and system, the magnification and the scale are both always specified.

The microscopes being compared are (Table 2-1):

- (i) the OLMil Olympus BX60 MS (mechanical stage; 50x to 500x), used with incident light and bright field illumination, (Figure 2.3, Table 2-1),
- (ii) the Hirox KH-8700 DM (35x to 2500x) (Figure 2.4, Table 2-1),
- (iii) the Dino-Lite Edge AM7915MZT DM (10x to 220x) (Figure 2.5, Table 2-1).

The OLMil with incident light has fixed objective lenses (numerical aperture 5x/0.15 10x/0.30, 20x/0.46, 50x/0.80; Table 2-1) and pictures were taken at fixed magnification: 50x, 100x, 200x, and 500x.

The Hirox KH-8700 digital microscope has low-range (35x to 250x), medium-range (140x to 1000x), and high-range (350x to 2500x) objective lenses (Table 2-1). Pictures were taken mainly (low-range lenses were sometimes used to document macro traces) using the medium-range objective lens at fixed magnification: 140x, 200x, 400x, 600x, 800x.

The Dino-Lite Edge AM7915MZT DM has continuous magnification (10x to 220x). Pictures were taken at different magnifications depending on the type of trace and the image quality reduction as a result of to digital zoom (Table 2-1).

Table 2-2. Magnification range of the three different microscopes used in this thesis.

Magnification	OLMil	Hirox KH-8700	Dino-lite AM7915MZT
35x - 50x		x	x
50x	x	x	x
100x	x	x	x
200x	x	x	x
400x		x	
500x	x	x	
600x -1000x		x	
Automatic Z-stack		x	

Micro-topography

Both the OLMils and DMs have a narrow depth of field (Table 2-1). To overcome this, an extended focusing system or focus stacking (Z-Stack) software is needed (Borel et al., 2014; Plisson, 2014). This software automatically stacks multiple images with different focal points. At higher magnification, large numbers of photographs are required to create a clear image. To enable this, the microscopes often use a motorised stage for rapid and accurate data acquisition. The result is a high magnification image with a wide depth of field (Figure 2.6).

The Olympus BX60 OLMil (at the Department of Archaeology, University of Exeter) had only a manual stage and, as such, the pictures required for Z-Stack could only be acquired manually. The extended focus was produced using Zen2 Blue Edition software. Therefore, the acquisition of extended focus images with the OLMil BX60 was a complex, time-consuming task.

The Hirox KH-8700 DM was utilised instead of an automatic stage and Z-stack programme. As a result, fewer, and less precise, extended focus images were acquired with the OLMil with incident light Olympus BX60 than with the Hirox KH-8700 DM (Figure 2.6).



Figure 2.6. Left: animal hair residue. Picture was taken with the OLMil (Olympus BX60) image with manual focus (Z-stack) based on 12 pictures at 100x (2 minutes realisation time). Right: animal flesh residue. Picture was taken with an Hirox- 8700 DM image with an automatically extended focus (Z-stack) based on 27 pictures, at 100x (Low-range objective lens, 20 seconds realisation time). (Image La Porta).

Trace identifications

Well-developed polish was easy to identify with the OLMil and Hirox KH-8700 DM (Figure 2.8). It was less clearly identified with the Dino-Lite Edge AM7915MZT (Figure 2.8). This was especially true at medium magnification (60x-100x). In this range, with the Dino-lite DM, the polish became less marked and more homogenous. Polarising filters, however, facilitated polish identification (Figure 2.8). When the polish was not well developed, it was generally more visible with the OLMil (Figure 2.9) and Hirox KH-8700 DM (Figure 2.10) than with the Dino-Lite Edge AM7915MZT DM (Figure 2.9). Striations and linear traces were generally more observable at high magnifications (200x-500x) with the OLMil. The Dino-Lite Edge AM7915MZT LED lights, however, created a flat, uniform image of the surface of the object (Figure 2.9). Striations and linear traces were therefore visible with the OLMil than with the Dino-Lite Edge AM7915MZT DM.

The Dino-Lite Edge AM7915MZT DM provides better imaging for fractures and edge-damage (Figure 2.7). Because the objective lens is incorporated into the camera system, the image is displayed directly on a computer screen (in live view). This allows a stereoscopic vision that facilitates the identification of fractures and scars. The OLMIL, instead, requires continuous refocusing to

allow for clear observation and evaluation of fracture depth (Borel et al., 2014), making the analysis of macro traces difficult (Figure 2.7).

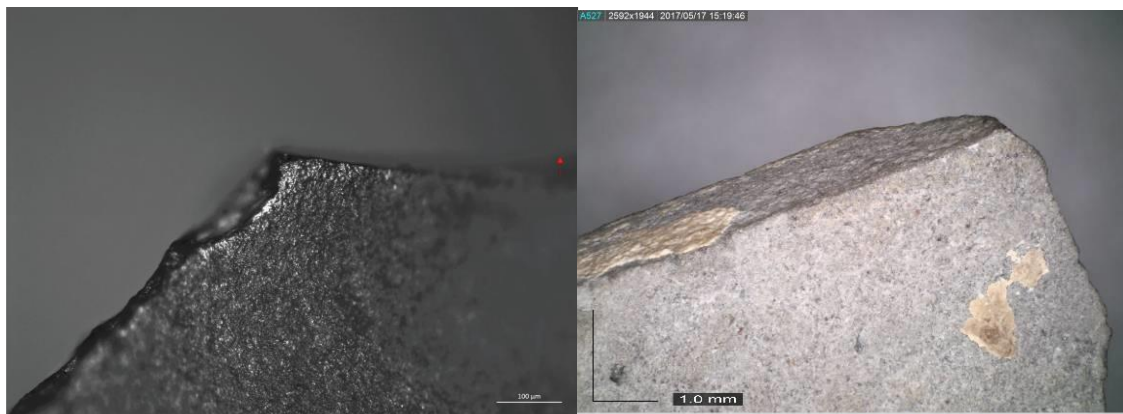


Figure 2.7. Snap fracture on a Levallois point used as a throwing spear-head. Left: picture was taken with an OLMil at 50x (scale=200µm). The fracture is not clear (no Z-stack used). Right: Dino-Lite Edge AM7915MZT picture at 50x (scale=1000µm). Fracture is clear (no Z-stack used). (Image La Porta).

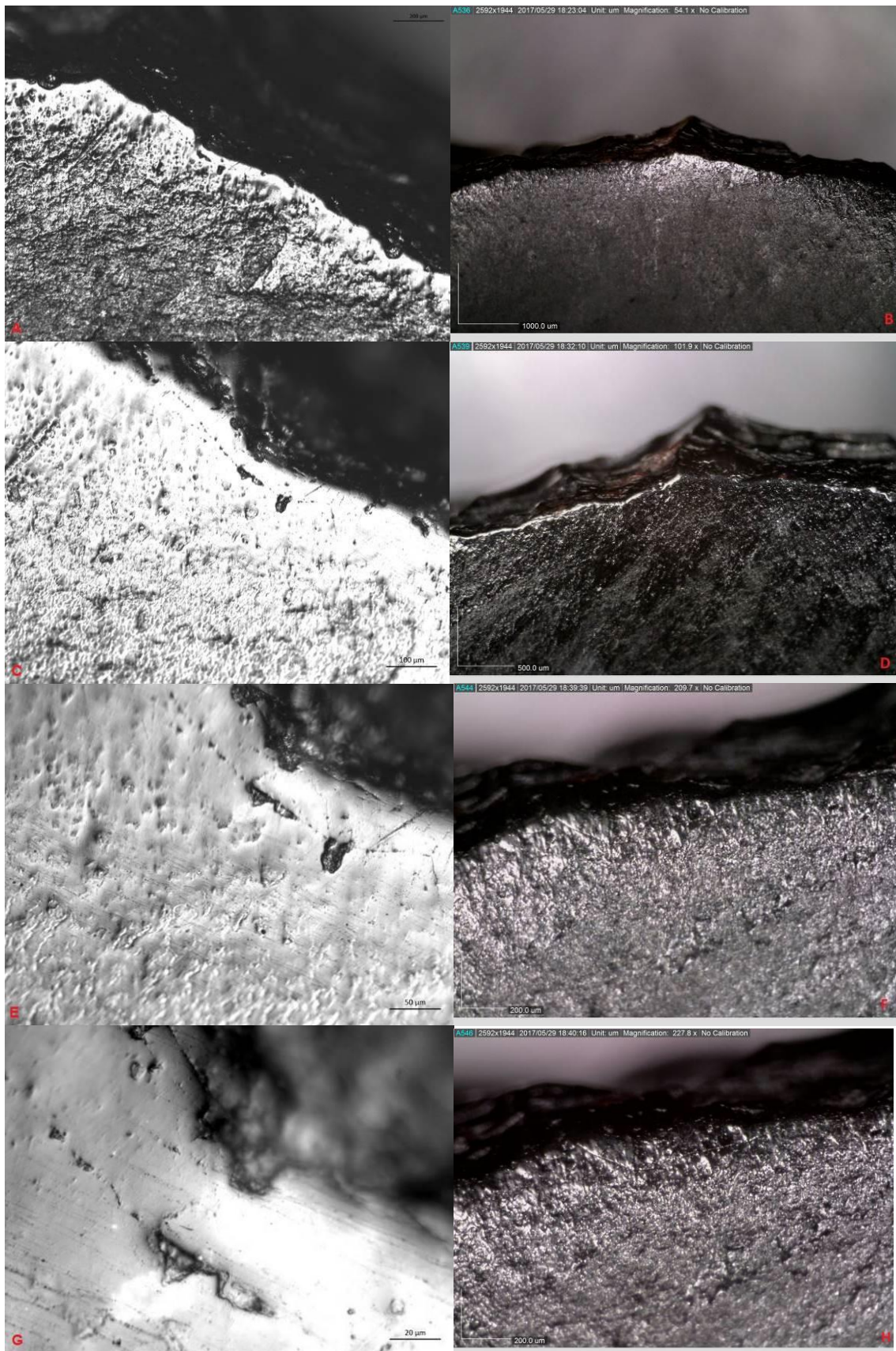


Figure 2.8. Well-developed polish on a retouched flake used as a scraper on commercial leather with the addition of ochre (use time 45 minutes). Pictures were taken after

cleaning the tool. A) OLMil picture at 50x (scale=200 μ m); B) Dino-Lite Edge AM7915MZT picture at 50x (scale=1000 μ m); C) OLMil picture at 100x (scale=100 μ m); D) Dino-Lite Edge AM7915MZT picture at 100x (scale=500 μ m); E) OLMil picture at 200x (scale=50 μ m); F) Dino-Lite Edge AM7915MZT picture at 200x (scale=200 μ m); G) OLMil picture at 500x (scale=20 μ m); H) Dino-Lite Edge AM7915MZT picture at 220x (maximum magnification), (scale=200 μ m). Dino-lite pictures were all taken using the polariser filter. (Image La Porta).

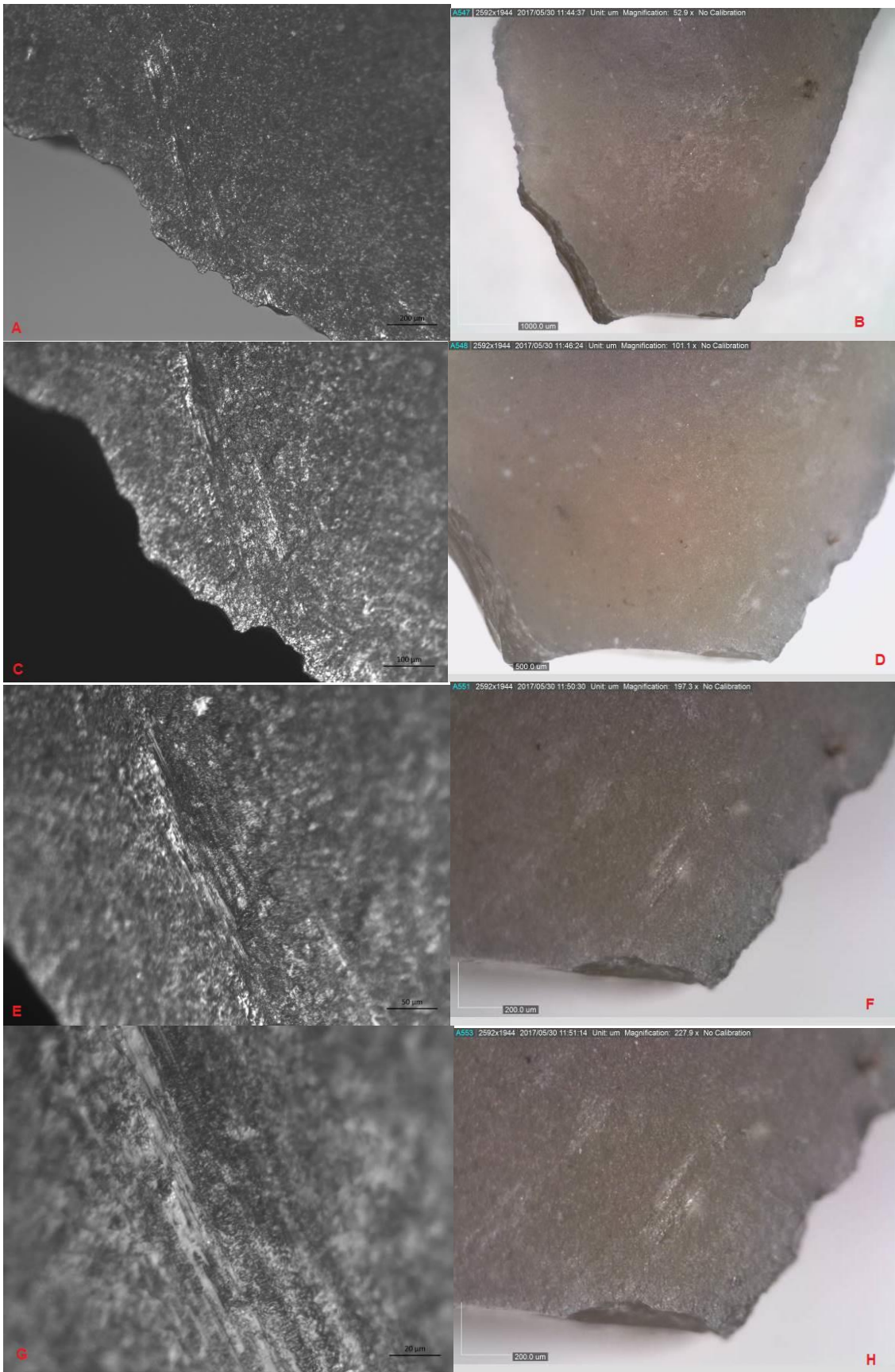


Figure 2.9. Microscopic Linear Impact Traces (MLITs) on the distal ventral tip (Locus D1v) of an experimental Levallois point used as a throwing spear-head. Pictures were taken after cleaning the tool. A) OLMIL picture at 50x (scale=200µm); B) Dino-Lite Edge AM7915MZT picture at 50x (scale=1000µm); C) OLMIL picture at 100x (scale=100µm); D) Dino-Lite Edge AM7915MZT picture at 100x (scale=500µm); E) OLMIL picture at 200x (scale=50µm); F) Dino-Lite Edge AM7915MZT picture at 200x (scale=200µm); G) OLMIL picture at 500x (scale=20µm); H) Dino-Lite Edge AM7915MZT picture at 220x (maximum magnification), (scale=200µm). (Image La Porta).

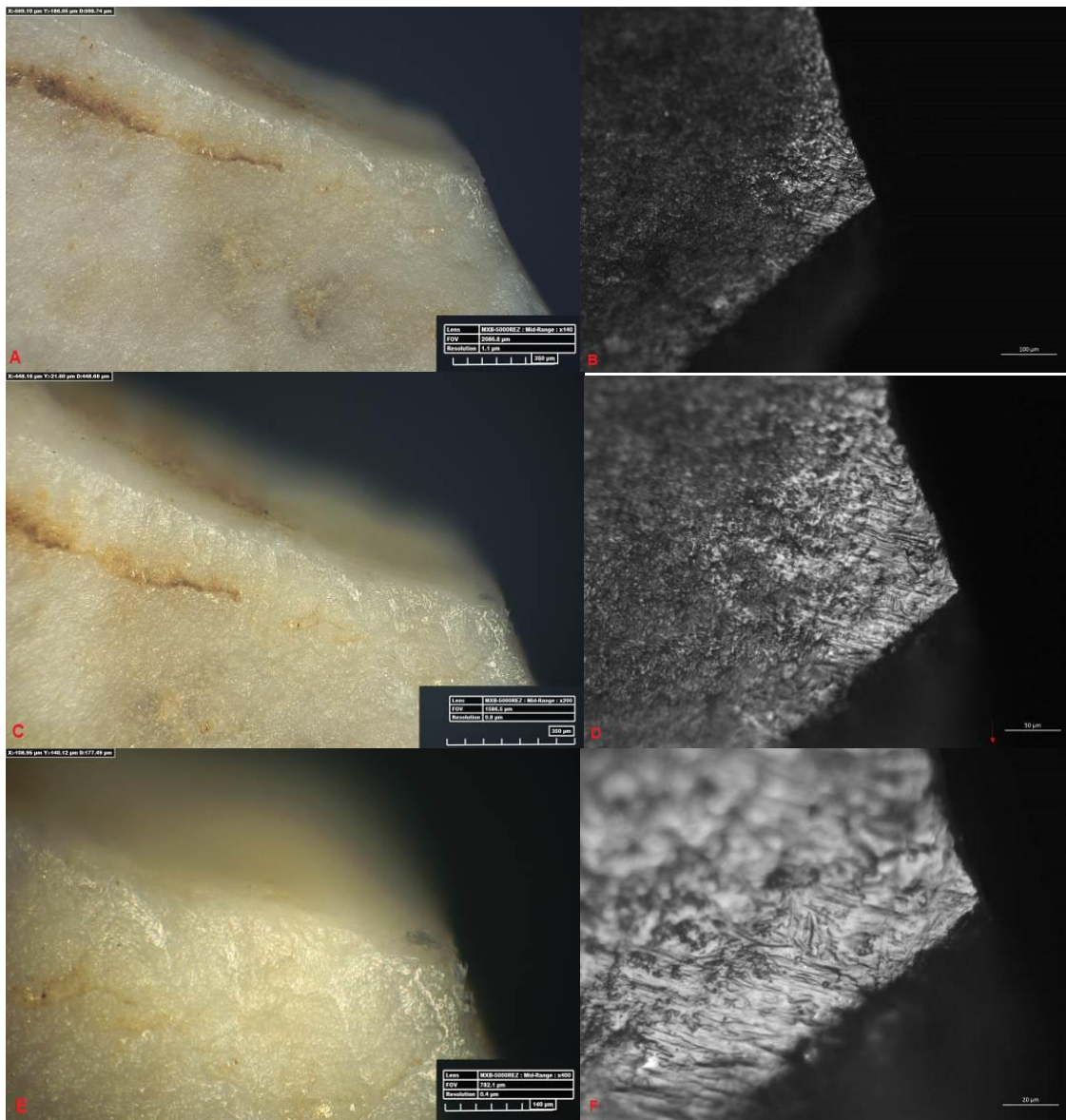


Figure 2.10. Polish located on the ventral distal tip (locus D1v): (A) An archaeological Levallois point, (B) an experimental Levallois point. A) Hirox KH-8700 picture at 140x middle-range objective lens (Middle-low-range, MRO); B) OLMil picture at 100x (scale=100 μ m); C) Hirox KH-8700 picture at 200x MRO; D) OLMil picture at 200x (scale=50 μ m); E) Hirox KH-8700 picture at 400x MRO; E) OLMil picture at 500x (scale=20 μ m). (Image La Porta).

Overview

Both the OLMIL and Hirox KH-8700 DM use a narrow, precisely focused light beam that is visible with the naked eye. This allows the observer to identify where on the object the microscope is focused, efficiently highlighting where is the location of the wear on the tool surface. With the Dino-Lite Edge

AM7915MZT, LED lights span all over the surface, and the observer is, therefore, unable to identify the precise observation point.

The use of OLMILs or DMs, however, is complementary in microscopy. Portable DMs do have noted limitations, however, they enable the study of museum collections that would otherwise be academically neglected, and allow for *in situ* analysis on archaeological excavations. They are also the most economically viable solution outside of established labs. High-resolution DMs (i.e. Hirox KH-8700, Hirox RH-2000, Keyence VHX-6000s), on the other hand, are relatively new machines. They have better potential for image processing and 3D modelling but are still in their developmental stage. Few articles using this equipment have been published (Boschin and Crezzini, 2012; Mélard et al., 2016; Moretti et al., 2016; Crezzini and Boschin, 2016) and fewer still are related to use-wear analysis on stone-tools (Hardy et al., 2013; Aranguren et al., 2012). OLMILs with incident lights, instead, are featured in a much more significant amount of literature; mainly due to their widespread proliferation in labs. As a result, these machines have been used more than any other type over the last two decades by use-wear analysts and, because of this, they offer more opportunities for comparison and cross-analysis with other OLMIL-based studies.

2.3 Terminology and use-wear recording location system

The following is a precise description of the terminologies used.

- i. Face: the ventral or dorsal side of any stone tool,
- ii. Surface: a generic term indicating any zone between ridges (arêtes) and/or edges (Inizan et al. 1999; Rots, 2010, p. 11).
- iii. Left and Right Laterals: when the artefact is viewed ventral face up with the proximal end towards the observer³.
- iv. Locus (plural loci): an individual spatial unit of the tool. It also indicates the position of a specific trace.

A standardised location system (Vaughan and Plisson, 1986) was created to record the spatial location of macroscopic and microscopic traces on the tool surfaces.

The location system used in this thesis divides the tool into the following technologically defined sections: distal, mesial, and proximal (Figure 2.11), as defined along the morphological axis of the tool (Inizan et al., 1999). Every section was subdivided into different loci on the basis of a morphological axis. A total of 14 independent loci on ventral and dorsal faces were established (Figure 2.11).

The distal portion (or tip) is where most diagnostic projectile traces were found. In this thesis, it is measured as $\frac{1}{3}$ of the total length of the tool, starting from the distal end or tip (Figure 2.11). It was divided into six distinct loci (Figure 2.11):

- 1) Distal ventral tip locus (D1v),
- 2) Distal ventral left locus (D2v),

³ Normally in lithic technology, the identification of the left and right laterals is based on the artefact being orientated dorsal face up, with the proximal end nearest to the observer. However, during functional analysis, the artefacts were orientated ventral face up, with the ventral face being the first to be analysed.

-
- 3) Distal ventral right locus (D3v),
 - 4) Distal dorsal tip locus (D1d),
 - 5) Distal dorsal left locus (D3d),
 - 6) Distal dorsal right locus (D2d).

The Mesial section has four subdivisions (Figure 2.11):

- 1) Mesial ventral left locus (M1v)
- 2) Mesial ventral right locus (M2v)
- 3) Mesial dorsal left locus (M1d)
- 4) Mesial dorsal right locus (M2d).

The projection of the morphological axis displayed the separation between the left and right loci (Figure 2.11). This works much better than then using the technological axis as it gives priority to the tip. The entire mesial section is $\frac{1}{3}$ of the total length of the tool (Figure 2.11).

The Proximal section has four subdivisions (Figure 2.11):

- 1) Proximal ventral left locus (P1v)
- 2) Proximal ventral right locus (P2v)
- 3) Proximal dorsal left locus (P1d)
- 4) Proximal dorsal right locus (P2d).

The entire proximal section is $\frac{1}{3}$ of the total length of the tool (Figure 2.11).

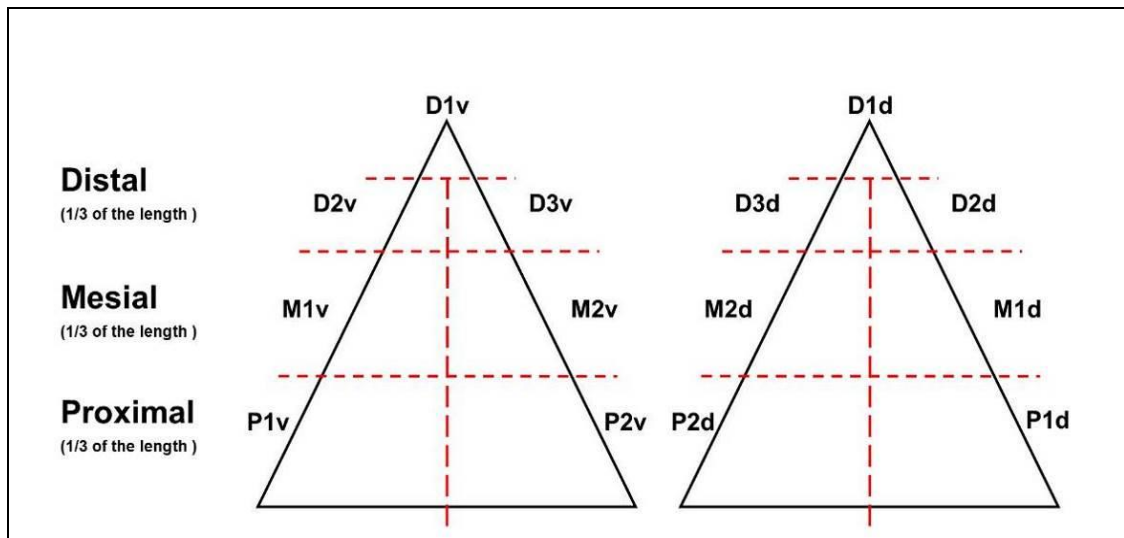


Figure 2.11. Recording location system of use-wear observations. The point has been divided into 14 independent loci: distal ventral portion (D1v, D2v, D3v); distal dorsal portion (D1d, D2d, D3d); mesial ventral portion (M1v, M2v); mesial dorsal portion (M1d, M2d); proximal ventral portion (P1v, P2v); proximal dorsal portion (P1d, P2d). (Image La Porta).

2.4 Macroscopic Traces: Types and Attributes

Macroscopic traces, such as edge-damage (i.e. scars, see Section 2.4.1) and fractures (i.e. breaks, see Section 2.4.1), are good indicators of the possible utilisation of stone tools. These traces are generally observed at low magnifications (10x-80x) and are described according to the morphology, distribution, initiation, and termination of the scars along the edges of the stone tools (Tringham et al., 1974; Odell, 1975, 1981; Hayden, 1979; Keeley, 1980; Kamminga, 1982; Odell and Cowan, 1986; González and Ibáñez, 1994).

However, as fractures and edge-damage are the main criteria for the identification of projectile tools (see Section 1.2.2, and they are often undefined categories) a definition to differentiate the two traces is provided, following Coppe and Rots (2017, p. 113). Fractures and edge-damage have been defined as follows:

- Fractures, herein, refers to fractures only. A fracture is a break that cuts off the entire edges, removing it from one edge to the other edge (see also Coppe and Rots, 2017, p. 113) (Figure 2.12).
- Edge-damage, herein, is defined as a single scar and/or an overlying of a group of scars. A scar is defined as the removal of a chip (or micro-flake) from an edge while it propagates further into the surface (Figure 2.12 and Figure 2.18). It forms when the propagation of the scar, after the initial strike, does not reach both lateral edges of a tool, causing only the removal of a micro-flake and not the complete break (Cotterell and Kamminga, 1987; Coppe and Rots, 2017, p. 113).

The distinction between a break and a scar, however, is not always clear as they are a continuation of the same category of traces.

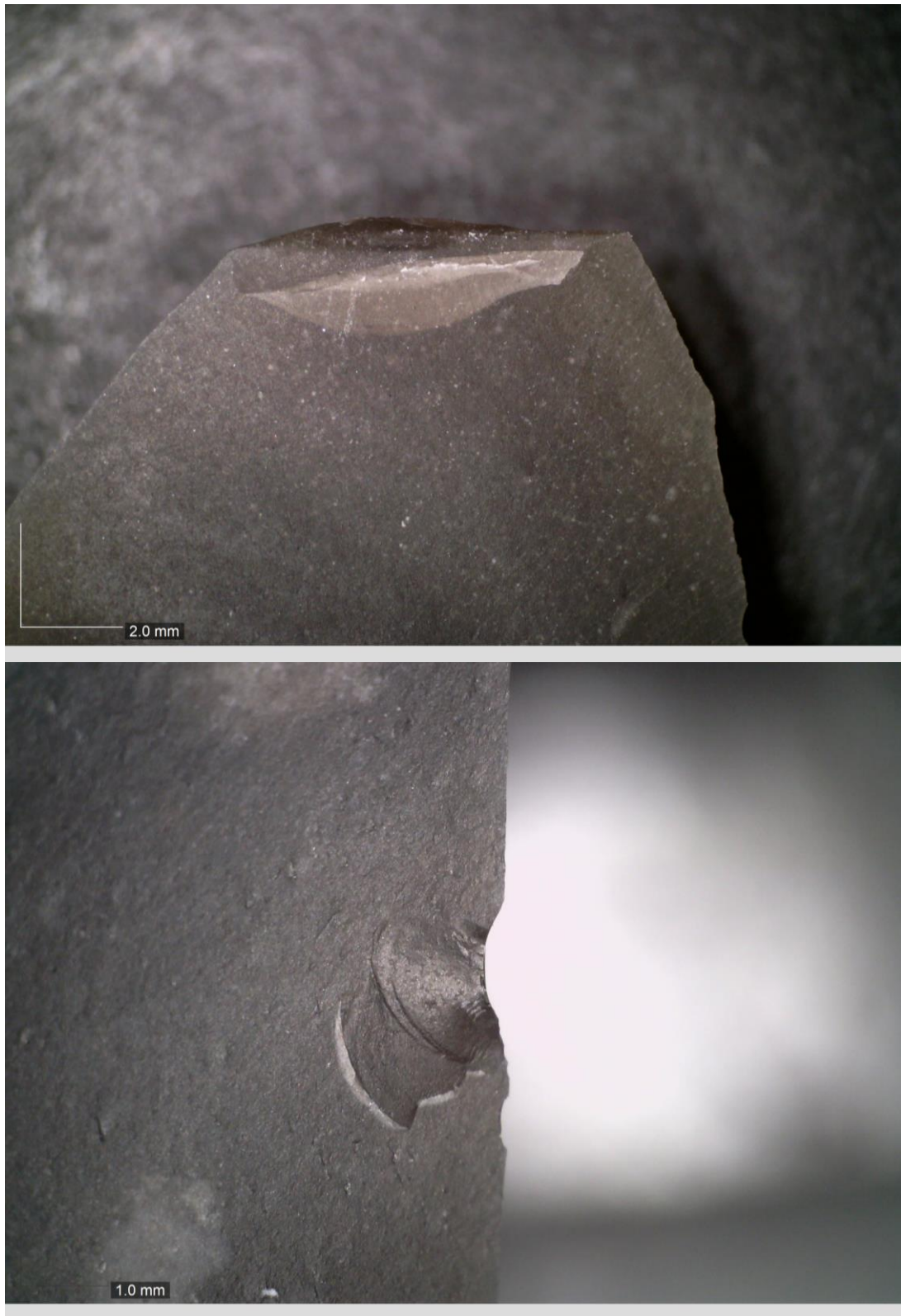


Figure 2.12. A fracture (with a bending initiation and a hinge termination; bottom picture, DM OM 40x) and a scar (with bending initiation and a step and a hinge termination, bottom picture, DM OM 30x). (Image La Porta).

2.4.1 Fractures

2.4.1.1 Background

Fractures can be the result of different voluntary and/or accidental activities such as knapping or flaking (Crabtree, 1972; Cotterell et al., 1985; Cotterell and Kamminga, 1777, 1986, 1987; Hayden, 1979), post-depositional processes (Shea and Klenck, 1993; McBrearty et al., 1998; Sano, 2009, 2012, Pargeter, 2011; Pargeter and Bradfield, 2012a), and utilisation activities (see below). However, when fractures are also the result of the utilisation of stone tools, the identification of the fracture type can be useful to assist in the establishing the possible function of stone tools, mainly when related to hunting activities (Hayden, 1979; Barton and Bergman, 1982; Bergman and Newcomer, 1983; Fisher et al., 1984; Odell and Cowan, 1986; Odell, 1988; Geneste and Plisson 1989, 1990, 1993). The analysis of specific fracture attributes can help to discriminate fractures resulting from hunting activities from fractures caused under other conditions (Fischer et al., 1984; Odell and Cowan, 1986; Geneste and Plisson, 1990).

2.4.1.1.1 Diagnostic Impact Fractures (DIFs)

Since the beginning of fracture analysis in use-wear methodology, numerous researchers have emphasised the importance of specific fracture types in the identification of projectiles tools (Witthoft, 1968; Frison, 1974, 1989; Ahler and McMillan, 1976; Bergman and Newcomer, 1983; Moss, 1983a, 1983b; Fischer et al., 1984; Odell and Cowan, 1986; Odell, 1988; Crombé et al., 2001; Shea, 1988; Dockall, 1997; Lombard, 2005a, 2005b; Lombard and Pargeter, 2008; Pargeter, 2007; Sano and Oba, 2015; Rots, 2016; Iovita et al., 2014; Pargeter et al., 2016; Coppe and Rots, 2017; Rots et al., 2017). Multiple studies have investigated the mechanisms of fracture formation in brittle solids (Hayden, 1979; Odell, 1981; Cotterell et al., 1985; Cotterell and Kamminga, 1977, 1987; Dockall, 1997), contributing to the differentiation between fractures resulting from compressive stress, e.g. cone fractures, and fractures resulting from bending forces, e.g. bending fractures (Ho Ho Committee, 1979; Cotterell and Kamminga, 1987). Bending fractures were the first fracture types to be referred

to as potential diagnostic fractures for projectile utilisation (Bergman and Newcomer, 1983; Bergman et al., 1988). However, initial studies on diagnostic impact fractures provided unclear definitions for the different types of bending fractures, instigating general confusion with regards to fracture terminology (e.g. Bergman and Newcomer, 1983; Dockall, 1997). This confusion was partially overcome during the Lithic Use-Wear Conference at Columbia University (Hayden, 1979). The Ho Ho Committee (1979) proposed a clearer terminology and an explicit classification of fractures types. The morphology of a fracture's initiation and termination was also defined (Ho Ho Committee, 1979). Mechanical fractures were classified by (i) their initiations (either cone or bending fractures; Figure 2.13), and (ii) their termination profile (step, hinge, feather, snap fractures; Figure 2.13). As a result, the Ho Ho Committee (1979) classification still provides the foundations of fracture nomenclature and classification to this day (Figure 2.13)

This image has been removed by the author of this thesis/dissertation for copyright reasons.

Figure 2.13. Fracture classification proposed by the Ho Ho Committee, 1979 (Image from Hayden, 1979, figure 1).

Following the Ho Ho Committee's (1979) classification, Fischer et al. (1984) formulated the first comprehensive experimental study on projectile use-wear traces. Their experiments identified three types of fractures diagnostic of projectile impacts, such as step-terminating bending fractures, unifacial spin-off fractures, and bifacial spin-off fractures (Figure 2.14.2c, Figure 2.14.2f). They also emphasised, however, that diagnostic impact fractures (DIFs) can be created under specific loads, pressures, and forces unrelated to projectile actions, i.e. production processes (débitage) or post-depositional activities (for instance trampling), although in these cases they appear with low frequencies (<3%, Pargeter and Bradfield, 2012). Moreover, Fischer et al. (1984) identified, through high-power analysis (200x-400x magnification), the presence of microscopic linear impact traces (MLITs; see Section 2.5.3 for definition), which appeared to be diagnostic of projectile utilisation (Moss, 1983a; Fischer et al., 1984).

**This image has been removed by the author of
this thesis/dissertation for copyright reasons.**

Figure 2.14. Initiations and terminations of fractures. 1. Cone fracture, 2. Bending fracture, 2a. Feather-terminating bending fracture, 2b. Hinge-terminating bending fracture, 2c. Step-terminating bending fracture, 2d. Snap termination, 2e. Embryonic fracture, 2f. Spin-off fracture. (Image from Fisher et al., 1984, figure 23).

Odell and Cowan (1986) obtained similar results to Fischer et al. (1984). They found that bending fractures and secondary fractures (e.g. spin-off fractures) occurred frequently on projectile tools (both retouched and unretouched tools), with different patterns and locations to those produced in knapping activities. However, they employed a more ambiguous fracture classification than Fischer et al. 1984, and they included hinge-terminating bending fractures into the DIF category (Table 2-3).

Geneste and Plisson (1989, 1990, 1993), in their techno-functional study of French Solutrean shouldered points (or *pointes à cran*), identified several causes of mechanical fractures (e.g. débitage and retouch activities, trampling, voluntary breakage, and utilisation). They found, however, that bending fractures, spin-off fractures, and burination fractures occurred with significantly

higher percentages (40% vs 3%) in projectile tools than in tools employed in other activities (e.g. knapping or trampling, <3%).

Following these results, several authors have combined different approaches for describing fractures diagnostic of projectile activities, as well as adding additional categories of DIFs. This has added ambiguity to terminology and subsequent confusion in terms of the categories of fractures which are considered diagnostic of projectile use (see also Coppe and Rots, 2017). For instance, hinge-terminating bending fractures have, on occasion been considered DIFs (Caspar and De Bie, 1996; O'Farrell, 2004; Sano, 2009; Lazuén, 2012), as were feather-terminating bending fractures (Caspar and De Bie, 1996; O'Farrell, 2004; Villa and Lenoir, 2009; Sano, 2012) (Table 2-3).

To reduce this inconsistency, an attempt to homologate fracture types diagnostic of projectile activities has been proposed by Lombard (2005a; Lombard and Pargeter, 2008). This research suggests that four types of fractures should be considered diagnostic of impact, when, within the assemblage, they occur with percentages equal or superior to 20-30%. These are (i) step termination bending fractures, (ii) unifacial spin-off fractures >6mm, (iii) bifacial spin-off fractures, and (iv) burination impact fractures. This because the other fractures types (i.e. cone fractures and bending fractures terminating in a hinge or feather) can also occur in activities different than projectiles. Therefore, this study followed Lombard (2005a) methodology for the analysis of DIFs (see Section 2.4.1.2).

Table 2-3. Type of diagnostic impact fractures by previous publications.

Reference	Diagnostic Impact Fractures									
	Step-terminating bending Fracture	Hinge-terminating bending Fracture	Feather-terminating bending Fracture	Snap bending Fracture	Burination-like Fracture	Flute-like Fracture	Spin-off Fracture	Bifacial Spin-off Fracture	MLITs	Crushing
Bergman and Barton, 1982 Bergman and Newcomer, 1983					X	X				
Moss, 1983									X	
Fischer et al., 1984	X						X	X	X	
Odell and Cowan, 1986	X	X			X	X			X	
Geneste and Plisson, 1989	X	X	X		X		X			X
Caspar and De Bie, 1996	X	X	X		X		X			
Dockall, 1997	X	X	X		X		X		X	X
Villa and Lenoir, 2006	X				X		X	X		
Villa and Lenoir, 2009	X		X		X	X	X	X		
Lombard, 2005a Lombard and Pargeter, 2008	X				X		X	X	X	
Wilkins et al., 2012	X				X		X			X
Sano, 2012 Sano and Oba, 2015	X	X	X	X (with S-shape only)	X	X	X	X	X	X
Rots, 2013	X	X	X		X		X	X	X	X
Iovita et al. 2014					X	X	X	X		X

The identification of the delivery system (i.e. i.e. how stone points were propelled, such as arrows, javelins [spear-thrower darts], or hand-delivered spears) has also been seen to be essential in the identification of fractures related to hunting activities (Knecht, 1997; Iovita and Sano, 2016).

Assuming that diagnostic impact fractures are equal, regardless of the morphology of the stone tool tips, the size, and the way in which the weapon has been delivered (Fischer et al., 1984; Geneste and Plisson, 1990; Lombard, 2005a; Dockall, 1997; Lombard and Pargeter, 2008; Pargeter, 2013), new approaches attempt to identify the delivery systems of projectile implements (Hutchings, 1999, 2011, 2015; Shea, 2006; Iovita et al., 2014, 2016). Controlled experiments with projectile stone tools have recently explored the formation of different types of fractures and wear traces (e.g. Wallner Lines and fracture wings; Kerkhof and Müller, 1969; Hutchings, 2011), focusing on specific physical and mechanical variables, such as impact velocity and kinetic energy (Hutchings, 2011; Iovita et al., 2016; Sano et al., 2016; Pargeter et al., 2016). These experiments seek to understand how velocity and, subsequently, kinetic energy during impact influence the formation and size of impact fractures in brittle solids (Hutchings, 1999, 2011; Iovita et al., 2016). Perhaps these analyses will offer better ways for future researchers to distinguish between projection modes on very fine-grained materials (e.g. obsidian tools). For the moment, more data and larger experimental collections are needed to understand impact fracture velocities and kinetic energy at impact.

2.4.1.2 Classification of fractures

In this thesis, fractures were divided and described accordingly to their initiations and terminations (Table 2-4). Considering the initiation, fractures were categorised in:

1. Cone initiating fractures

A cone fracture and/or scar, created by compressive stress (Kamminga et al., 1985), is a scar where the initiation starts from a small area (Figure 2.15) with a visible point of impact. The crack starts from the precise point of impact, i.e. the “Hertzian cone”, which is clearly visible (Figure 2.15). This point of impact represents the initiation of the fracture, and it generally shows a narrow and concave profile (Fischer et al., 1984; Cotterell and Kamminga, 1987) (Figure 2.15 and Figure 2.17).

These can originate from multiple activities, such as knapping and retouch, post-depositional processes (i.e. trampling), and utilisation.



Figure 2.15. Cone scar with an indication of the point of impact (red circle), DM OM 40x.

2. Bending initiating fractures

These are fractures or scars that result from the application of force distributed over a large surface (Figure 2.16). The fracture occurs far from the impact location (Fischer et al., 1984; Cotterell and Kamminga, 1987), generating a wide point of contact and an initiation with a convex profile (Figure 2.16 and Figure 2.17). As the propagation of the scar, after the initial strike, reaches both lateral faces of the tool (Cotterell and Kamminga, 1987; Coppe and Rots, 2017, p. 113), it causes the complete fracture (or removal) of the edge.

Bending fractures generally initiate from one face of the stone tool (either dorsal or ventral) and terminate on the opposite face.

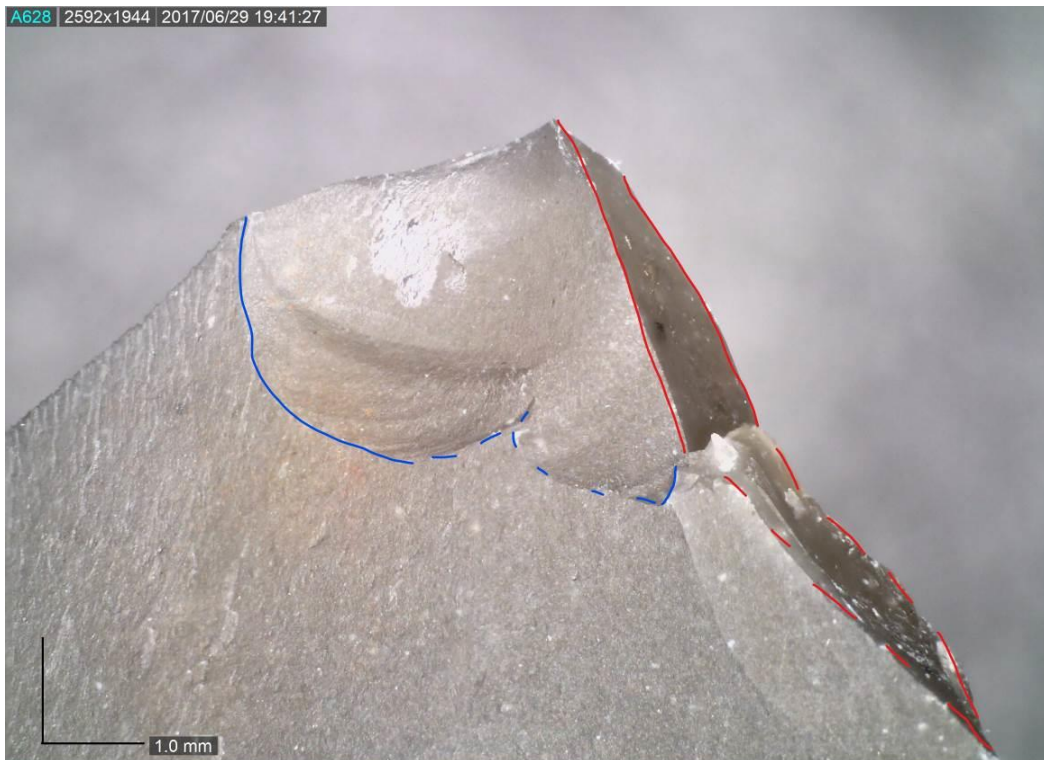


Figure 2.16. Bending fracture (in blue a bending initiation fracture terminating in a double feather; in red a burination fracture with a bending initiation), DM OM 20x.



This image has been removed by the author of this thesis/dissertation for copyright reasons.

Figure 2.17. Cone fracture profile (left). Bending fracture profile (right. Modified from Ho Ho Committee 1979, figure 1).

Considering the terminations, fractures were categorised in (Table 2-4):

1. Step-terminating fractures

A step termination fracture and/or scar terminates at 90° on the opposite surface (Table 2-4). It is formed by the arresting of the force during the crack propagation (Fischer et al.,1984; Cotterell and Kamminga, 1987).

2. Hinge-terminating fractures

A hinge termination fracture and/or scar results in a bending fracture which meets the opposite surface with a curved or reflected profile (Table 2-4). It is formed by a decrease in velocity during the crack propagation (Cotterell and Kamminga, 1987).

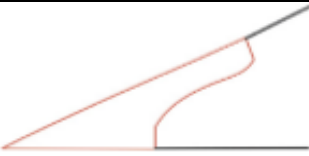
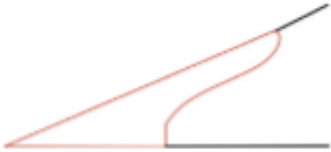


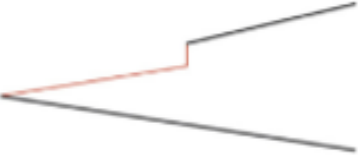
3. Feather-terminating fractures

A feather termination fracture and/or scar occurs when the break continues through to the opposite surface (Cotterell and Kamminga, 1987). The crack propagates through the solid material without change of force or velocity (Table 2-4).

4. Snap fractures

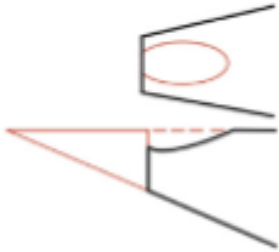
A snap fracture continues perpendicular to the opposite surface (Ho Ho Committee, 1979) (Table 2-4). This type of fracture occurs both under compressive and bending stresses.

Table 2-4. Classification of the different type of fractures. Primary Fractures: bending-fractures (step terminating bending fractures, feather and hinge terminating bending fractures, and snap fractures), and primary burination-fractures. Secondary Fractures: unifacial spin-off fractures, bifacial spin-off fractures, and spin-off burination fractures. The DIF proposed are: step terminating bending fractures, unifacial spin-off fractures, bifacial spin-off fractures, primary burination fractures, and spin-off burination fractures (as proposed by Lombard, 2005a).

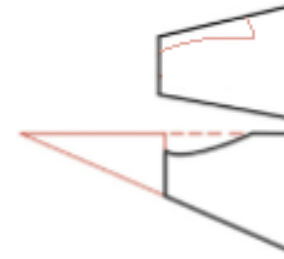
Primary Fractures			
Bending Fracture			
Step-terminating (Diagnostic)	Hinge-terminating (Not Diagnostic)	Feather-terminating (Not Diagnostic)	Transversal Snap-terminating (Not Diagnostic)
			
Primary Burination (Diagnostic)			
			

Secondary Fractures

Spin-off (Diagnostic) Unifacial/Bifacial



Spin-off Burination (Diagnostic)



2.4.1.3 Classification of fractures adopted in this thesis

In this thesis, the above categories of fractures, i.e. cone and bending fractures, were further categorised as primary and secondary fractures, as follows (Table 2-4):

A. Primary fractures

Primary fractures are fractures (i.e. cone or bending) that initiate directly from an edge or a surface, as follow (Table 2-4):

- Cone fractures (see above for definition) terminating in a step, hinge or feather.
- Bending fractures (see above for definition) terminating in a step, hinge, feather, or snap
- Primary Burination fractures are fractures that run parallel or slightly oblique to the main axis of the tool (Table 2-4). They can initiate from a surface or an edge and they always terminate on an edge (see also Coppe and Rots, 2017). Primary burination fractures can present cone or bending initiations. However, to be considered diagnostic of impact, they must show a bending initiation. If a cone initiation is present, they are most likely connected to the knapping activities (débitage process), and are thus not considered diagnostic of impact (Sano, 2009; Pargeter, 2011; Pargeter and Bradfield, 2012). They can have different terminations, such as step, hinge, and feather (although a feather termination is the most common).

B. Secondary fractures

Secondary fractures are any types of fractures that initiate from an earlier fracture (Table 2-4). The type of fractures that depart from an earlier fracture, in previous literature have been called spin-off fractures (Fischer et al., 1984; Lombard, 2005). Spin-off fractures in this thesis have been categorised in unifacial/bifacial spin-off and spin-off burination fractures.

-
- Unifacial or bifacial Spin-off fractures. Unifacial or bifacial spin-off fractures are breaks that originate from previous fractures and terminate on a surface (Table 2-4) (Fischer et al., 1984; Coppe and Rots, 2017). They are possibly caused by the compression forces that occur when two fragments of the same tool break off (Fischer et al., 1984). They present a cone initiation with possible different terminations: step, hinge, and feather. Unifacial spin-offs fractures occur on only one face (either dorsal or ventral) of the tool, whereas bifacial spin-off fractures occur on both faces of the tool (i.e. both dorsal and ventral faces).
 - Spin-off burination fractures or secondary burination fractures. Spin-off burination fractures are breaks that initiate from a previous fracture, but they run parallel or oblique to the main axis of the tool and always terminate on an edge (Table 2-4) (Coppe and Rots, 2017). They can have a bending or cone initiation and step, hinge, or feather terminations. However, only bending initiation spin-off burination fractures are diagnostic of projectile impact activities.

In this thesis, all fracture types (i.e. cone, bending, primary and secondary fractures) were identified, described, and recorded into the database to complete a comprehensive interpretation. However, only the following fractures were considered diagnostic of projectile impact activities (i.e. diagnostic impact fractures, DIFs) as proposed by Lombard (2005a) (see Table 2-4):

- I. Step-terminating bending fractures,
- II. Primary burination fractures,
- III. Unifacial and bifacial spin-off fractures,
- IV. Spin-off burination fractures.

2.4.1.4 Fracture attributes

In this thesis fractures were recorded based on the following attributes:

- **Location of the fracture initiation:** the locus/loci where the fracture initiation is observed. Proximal (e.g. loci D1v, D2v, D3v, D1d, D2d, D3d), mesial (e.g. loci M1v, M2v, M1d, M2d), and distal parts (e.g. loci P1v, P2v, P1d, P2d) (see Section 2.3).
- **Type of initiation:** 1. Cone, 2. Bending, 3. Indeterminate initiation (when the type of initiation is not clearly recognizable or is missing [i.e. the termination is not present on the tool because snapped off, Coppe and Rots, 2013]) (Ho Ho Committee, 1979; Cotterell and Kamminga, 1987), (Figure 2.17). The initiation of a fracture is the surface where the break originates.
- **Type of termination:** 1. Step, 2. Hinge, 3. Feather, 4. Snap, 5. Multiple, 6. Indeterminate (Ho Ho Committee, 1979; Fischer et al., 1984; Cotterell and Kamminga, 1987), (Table 2-4).

A fracture can present 1. Single termination, 2. Double termination, 3. When a scar presented double or multiple terminations, all terminations were recorded and counted.

- **Location of the fracture termination:** the locus/loci where the fracture termination is observed. Proximal (e.g. loci D1v, D2v, D3v, D1d, D2d, D3d), mesial (e.g. loci M1v, M2v, M1d, M2d), and distal parts (e.g. loci P1v, P2v, P1d, P2d) (see Section 2.3).

2.4.2 Edge-damage and its attributes

2.4.2.1 Background

Previous experimental research has shown that the morphology and distribution of edge-damage or scars are likely related to the type of movement and the resistance (or hardness) of the worked material (Tringham et al., 1974; Odell, 1981). For example, it is generally observed that soft worked materials (e.g. meat, fresh hide, or vegetal materials) generate limited semi-circular scars, while hard worked materials (e.g. wood, bone, antler, or dry hide) produce large numbers of triangular and/or trapezoidal scars (Tringham et al., 1974; Odell, 1981). It has also been experimentally observed that transverse actions (e.g. scraping or planing) create edge-damage on the non-contact surface (Figure 2.21; Tringham et al., 1974; Odell, 1981), while longitudinal actions (e.g. sawing or cutting) cause edge-damage on both surfaces of the tool (Tringham et al., 1974). However, other researchers have observed that the duration of the work, rather than the worked material, led to major or minor degrees of edge-damage with scars of different morphologies (Akoshima, 1987; Van Gijn, 1989), demonstrating that edge-damage morphology and distribution are highly variable. Edge-damage alone, therefore, cannot be indicative of the action or contact material alone (Vaughan, 1985). The formation of the scars along the edges can, in fact, be influenced by a multitude of other criteria, including the contact angle force, the duration of utilisation, and other activities other than utilisation, such as production (e.g. débitage, or retouch) and post-depositional processes (e.g. trampling, dropping, or incidental contact).

That said, scar morphology and location can provide additional information about the kinematics of the utilisation process (Borel, 2010).

**This image has been removed by the author of
this thesis/dissertation for copyright reasons.**

Figure 2.18. Edge-damage and scar schematic representation (Image adapted from Claud, 2015, p. 133).

2.4.2.2 Edge-damage attributes

Edge-damage (ED) in this thesis has been recorded based on the following attributes:

- **Location:** the locus/loci where the ED is observed, for instance, proximal (e.g. loci D1v, D2v, D3v, D1d, D2d, D3d), mesial (e.g. loci M1v, M2v, M1d, M2d), and distal parts (e.g. loci P1v, P2v, P1d, P2d) (see Section 2.3).
- **Morphology:** the shape of the scar, for instance, 1. Scalar, 2. Trapezoidal, 3. Triangular, 4. Rectangular, 5. Half-moon (or sliced), 6. Narrow into wide, 7. Indeterminate (Figure 2.19). If multiple morphologies were observed, the most recurrent was recorded.

**This image has been removed by the author of
this thesis/dissertation for copyright reasons.**

Figure 2.19. Scar morphology (Image adapted from Rots, 2010, p. 30).

- **Size:** the maximum depth of the scar (Figure 2.18). 1. Small (<0.5mm), 2. Medium (0.5-1mm), 3. Large (1-2mm), 4. Very Large (2mm).
- **Scar initiation:** type of initiation (see Section 2.4.1.2). 1. Cone, 2. Bending, 3. Indeterminate initiation (when the type of initiation is not clearly recognisable, Figure 2.17).
- **Scar termination:** type of termination (see Section 2.4.1.2). 1. Step, 2. Hinge, 3. Feather, 4. Snap, 5. Indeterminate termination (when the type of termination is not clearly recognisable). A scar can present 1. Single termination, 2. Double termination, 3. Multiple terminations (Table 2-4). When a scar presents double or multiple terminations, all were recorded.
- **Distribution:** the distribution of the scars along the edge, for instance, 1. One, 2. Continuous, 3. Discontinuous, 4. Overlapping (Figure 2.20).

This image has been removed by the author of this thesis/dissertation for copyright reasons.

Figure 2.20. Edge-damage distribution (Image adapted from Rots, 2010, p. 31).

- **Degree of edge-damage:** 1. Low, 2. Medium, 3. Intense (although this is a subjective assessment, it is valid to state the relative development of the edge-damage, on the same raw material and studied by the same analyst).
- **Association:** with other traces.

2.5 Microscopic Traces: Types and Attributes

Microscopic wear analysis (also defined as High Power analysis) requires an optical microscope with incident lights (100x to 500x), digital microscopes over 100x, and/or SEM for clear identification. The main types of microscopic wears (e.g. edge-rounding, polish, and microscopic linear traces) identify in use-wear analysis are described below.

2.5.1 Edge-rounding (ER)

2.5.1.1 Background

Edge-rounding is the blunting of the cutting edge. When this is due to utilisation, edge-damage occurs as a result of mechanical abrasion between the edge and the worked material (Figure 2.21; Keeley, 1980; Vaughan, 1981; Mansur-Franchomme, 1983).

The degree and localisation of the edge-rounding depend on:

- (i) Duration of utilisation: A longer utilisation of the stone tool creates more edge-rounding than shorter utilisation (Mansur-Franchomme, 1983);
- (ii) Raw material grain size: To develop equivalent edge-rounding coarse-grained raw materials require a more prolonged contact duration than fine-grained raw materials (Borel, 2010);
- (iii) Hardness of the worked material: Harder materials produce a higher degree of edge-rounding than softer materials (Vaughan, 1981);
- (iv) Movement and contact angle: Transversal movements produce more edge-damage than longitudinal movements (Mansur-Franchomme, 1983; Borel, 2010), such as sickle-edges or hide-scrapers;
- (v) Presence of abrasive agents: The inclusion of abrasive agents (sand, straw, etc.) increases edge-damage (Mansur-Franchomme, 1983; Vaughan, 1985).

This image has been removed by the author of this thesis/dissertation for copyright reasons.

Figure 2.21. Kinematic representation of a tool during utilisation and its components (Image from Unrath et al., 1986).

2.5.1.2 Edge-rounding attributes

Edge-rounding (ER) has been recorded in this thesis based on the following attributes:

- **Location:** the locus/loci where the ER is observed. Proximal (loci D1v, D2v, D3v, D1d, D2d, D3d), mesial (loci M1v, M2v, M1d, M2d), and distal parts (loci P1v, P2v, P1d, P2d) (see Section 2.3).
- **Development:** the degree of edge-rounding observed. 1. None, 2. Poor, 3. Moderate, 4. Extensive (although this is a subjective assessment, it is valid to state the relative development of the edge-damage, on the same raw material and studied by the same analyst).
- **Association with other traces.**

2.5.2 Polish

2.5.2.1 Background

The definition, formation, and description of polish traces have been one of the most debated topics in use-wear studies (Grace et al., 1985; Vaughan, 1985; Plisson and Mauger, 1988; Van Gijn 1989). The definition of polish or a polished surface has been difficult to establish. The word “polish” has been described as an altered surface that reflects lighter than its surrounding area and cannot be removed by (weak, Van Gjin, 1989, p. 17) chemical acids or solvents (Vaughan 1981, p. 132). However, this definition has not been fully accepted as polish can be altered by chemical agents (Plisson and Mauger, 1988). At present, there is thus not a comprehensive definition of ‘polish’ as its origin and formation are both rather vague.

To this end, below is presented a synthesis of the principal theories of polish formation, although these are still under debate (Witthoft, 1967; Del Bene, 1979; Kamminga, 1979; Anderson 1980; Anderson-Gerfaud, 1982, 1983; Mansur-Franchomme, 1983; Unger-HaMLITon, 1984; Fullagar, 1991).

- I. **Abrasion Model:** The utilisation of a stone tool against a contact material under high but localised forces generates mechanical abrasion on specific spots of the stone’s surface (generally on the highest micro-topographic areas). During abrasion, these areas lose material. Polish is then formed by the gradual loss of superficial material, and by the flattening of these surfaces (Del Bene, 1979). Abrasive and intrusive agents (like sands and dust) may also boost the abrasion process (Semenov, 1964; Kamminga, 1979; Fullagar, 1991).
- II. **Friction-fusion Model:** (Witthoft, 1967). During the utilisation process, the friction of the stone tool against a contact material generates heat (Witthoft, 1967). This frictional heat causes fusion of the silica on a microscopic scale. In Witthoft’s (1967) proposition, this polish formation process is characteristic of plant contact materials (e.g. in sickle tools)

because the opal contained in plants, in the form of phytoliths, generates significant friction.

- III. **Depositional Polish Model:** (Del Bene, 1979). This model suggests that, if heated, the phytoliths contained in plant worked materials melt, forming an additive siliceous layer on the surface of the stone tools (Del Bene, 1979). This additive layer is what we define as polish. However, the mechanics of this adhesion are not clear (see also Mansur-Francomme, 1983; 1986).
- IV. **Amorphous Silica-Gel Model:** (Anderson 1980; Anderson-Gerfaud, 1981). This model is based on the hypothesis that the silica (SiO_2), having reached its melting point, does not return to a crystalline state. Instead, it becomes a colloidal gel (Witthoft, 1967). This occurs during the utilisation of stone tools on siliceous materials (i.e. plant, wood, antler, or bone materials).

Anderson-Gerfaud (1981; Anderson, 1980) proposes that the silica presented, both on the surface of the tool and in the worked material (e.g. only plants, bone, antler or wood), changes state during utilisation from solid to gel-colloidal, forming an amorphous-gel. This silica-gel, once solidified, produces amorphous silica which forms the polish (Anderson-Gerfaud, 1981; Mansur-Francomme, 1983; Unger-Hamilton, 1983; 1984). Following Anderson-Gerfaud (1981), the silica-gel change of state is driven by several factors, including temperature, pressure, friction, abrasion by intrusive particles, hardness of the tool's raw material, presence of water, acids contained in plants, and the presence of non-siliceous crystalline substances such as calcium oxalate (found in certain plants) (Anderson-Gerfaud, 1981). Furthermore, this amorphous silica-gel may help to embed particles or residue from the worked material (i.e. phytoliths).

The friction-fusion and abrasion models are not very plausible (Kamminga, 1979; Anderson-Gerfaud, 1981; Mansur-Francomme, 1983; Fullagar, 1991; Unger-Hamilton, 1983; Ollé and Vergés, 2008, 2014). They do not explain the

extra and intra-specific variability of the polish types. The silica-gel model is currently the prevalent model, although there are still many aspects (intra-specific polish variability, chemical bond; see also Ollé and Vergés, 2008) of it that are still critical.

2.5.2.2 Polish Attributes

In this thesis, the following attributes were described for the precise and correct identification of polishes and projectile traces.

- **Polish Location:** the locus/loci where the polish is observed. Proximal (loci D1v, D2v, D3v, D1d, D2d, D3d), mesial (loci M1v, M2v, M1d, M2d), and distal parts (loci P1v, P2v, P1d, P2d) (see Section 2.3).
- **Locus Delineation:** the shape of the locus (edge delineation) where the polish is located. 1. Straight, 2. Concave, 3. Convex, 4. Pointed (Figure 2.22).

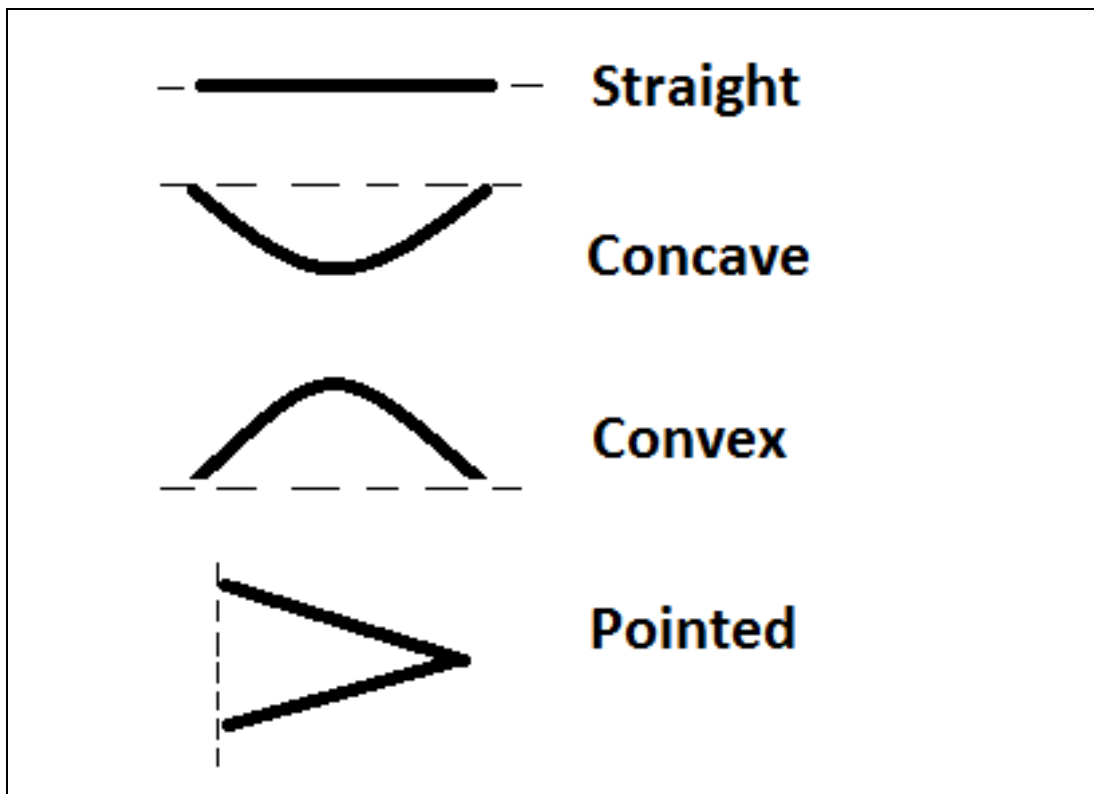


Figure 2.22. Delineation of the locus in plan view. (Image La Porta).

- **Polish Brightness:** the brilliance of the polish when observed at 200x. 1. Dull, 2. Intermediate, 3. Bright. Although this is a subjective assessment, other attempts to measure brightness on an absolute scale have not been effective in the past (Dumont, 1982). It is thus more valid to state the relative brightness of the polish created by different worked materials (on the same raw material) when they are studied by the same analyst.
- **Polish Distribution:** the distribution of the polish along the edge or on a surface when observed at 100x. 1. Linear, 2. Isolated spotted/scattered, 3. Immediate edge, 4. Areas cover (Figure 2.23).

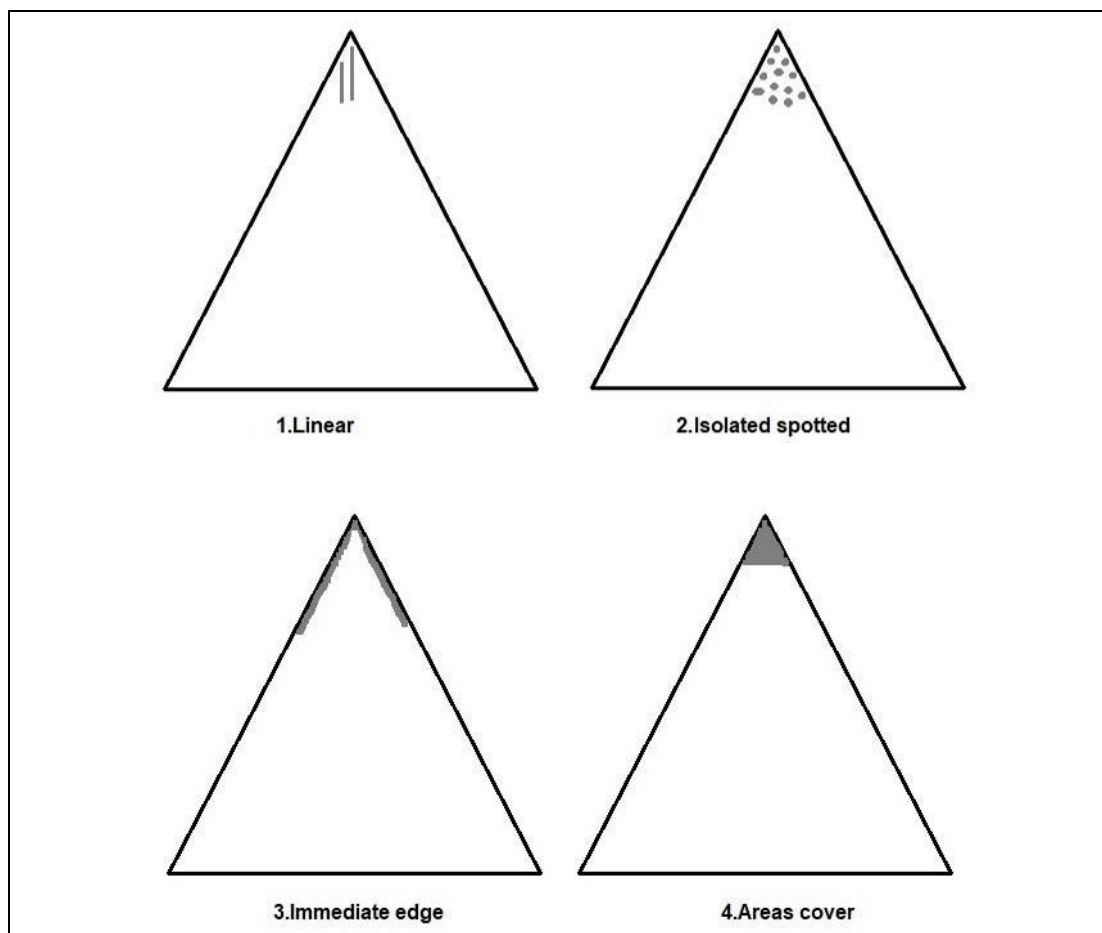


Figure 2.23. Polish distribution along the edge of the tool. (Image La Porta).

-
- **Polish Texture:** the texture refers to the micro-unevenness of the polish when observed at 200x. Rough polish has an uneven appearance and smooth polish seems more fluid. 1. Smooth, 2. Rough (Figure 2.24).

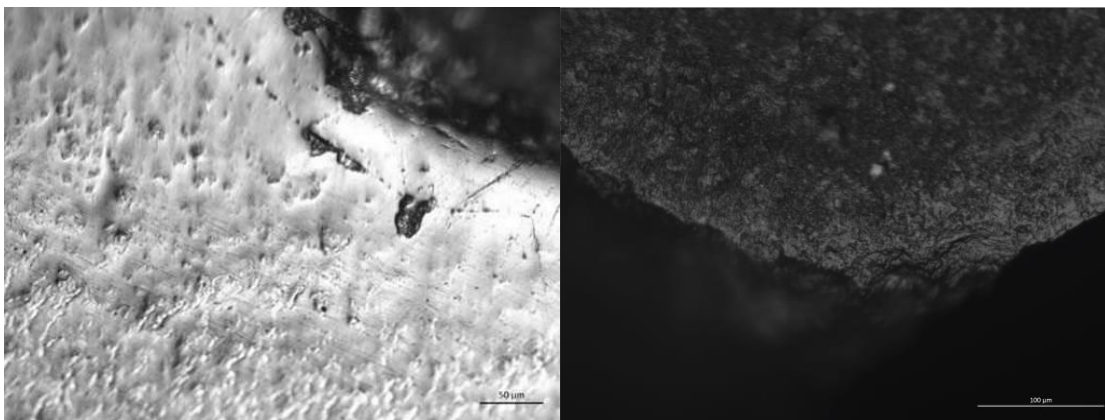


Figure 2.24. Polish texture: smooth polish (left), rough polish (right). (Image La Porta)

- **Degree of polish linkage:** The degree of polish when observed at 200x.
 1. Scattered (presence of unlinked areas of polish distributed over an edge or surface),
 2. Linked (the polished areas are joined together),
 3. Covering (when polished areas are entirely linked up, forming a uniform layer of polish) (Figure 2.25).

This image has been removed by the author of this thesis/dissertation for copyright reasons.

Figure 2.25. Degree of Polish Linkage. The polish is represented in white (Image adapted from Jensen, 1994, figure 24).

-
- **Polish Topography:** the micro-topography of the polish observed at 200x. 1. Not well-developed polish, 2. Domed polish, 3. Flat polish, 4. Linear filled polish (Van Gijn, 1989, p. 31), (Figure 2.26).

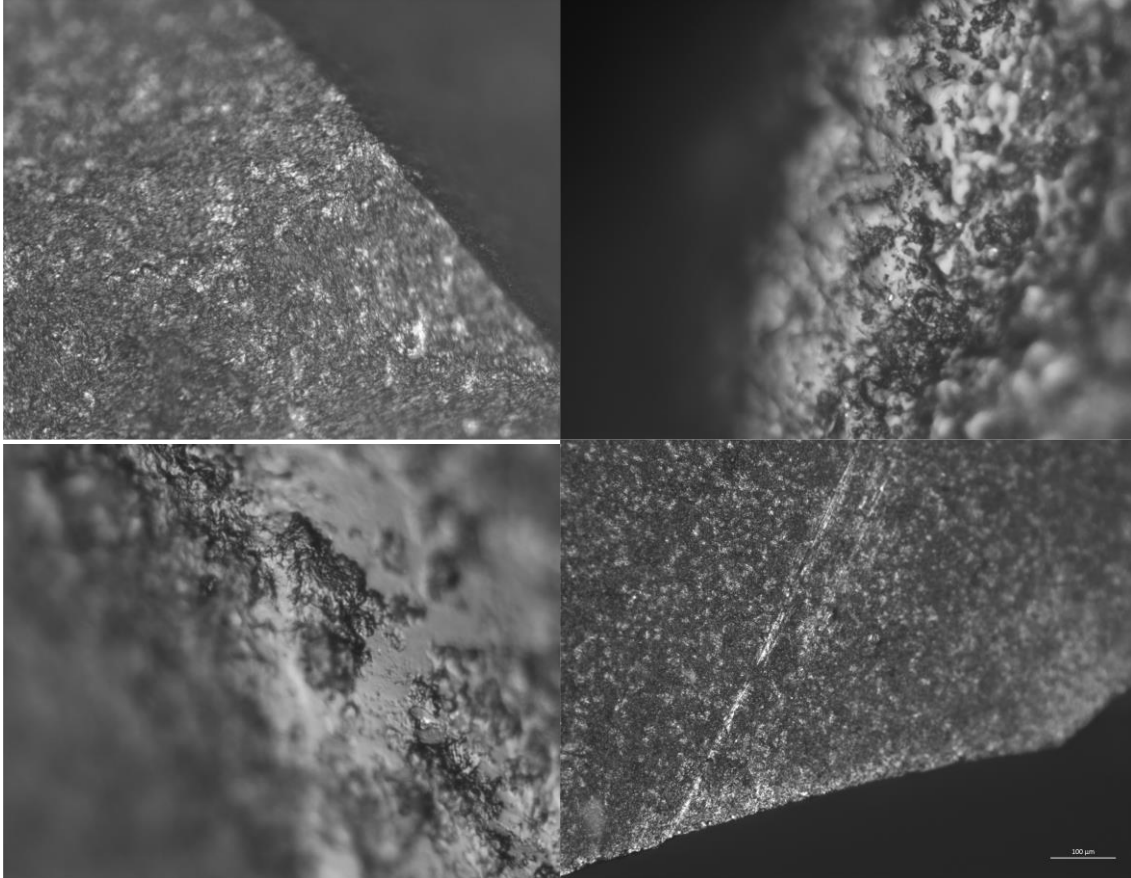


Figure 2.26. Polish topography: faint polish (top left), domed polish (top right), flat polish (bottom left), linear polish (bottom right). (Image La Porta).

- **Polish Development:** the development of a polished area is evaluated on a relative scale from one to four when observed at 200x. 1. Poor, 2. Medium, 3. Well developed, 4. Extensive (Rots, 2010, p. 33).

Although this is a subjective assessment, it is valid to state the relative development of the polish created by different worked materials (on the same raw material) and studied by the same analyst.

-
- **Polish Extension:** the extent to which the polish covers the edge or surface 1. Marginal (1-100 μ m), 2. Medium (100-500 μ m), 3, Invasive (>500 μ m), (Jensen, 1994, p. 25) (Figure 2.27);

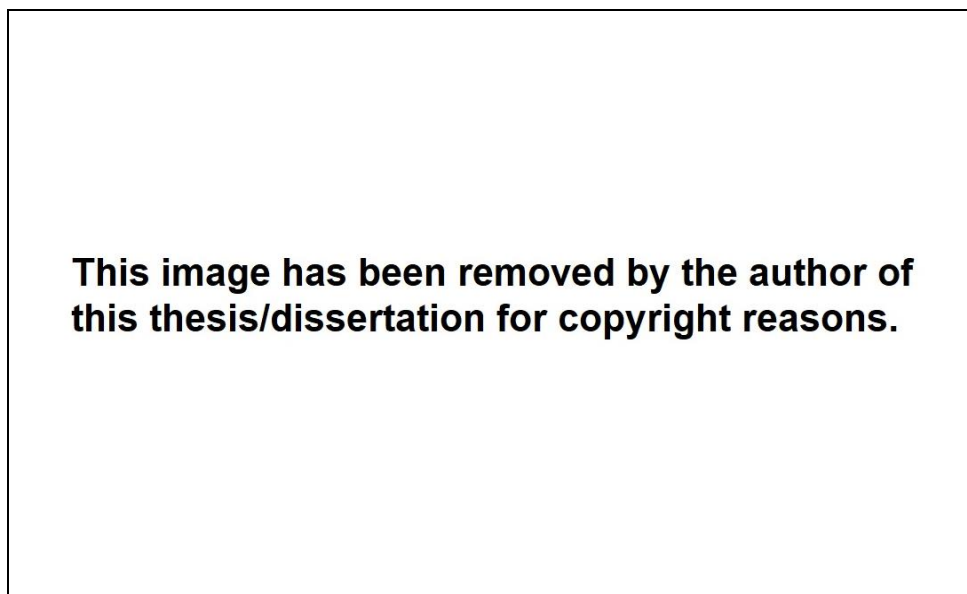


Figure 2.27. Polish extension (Image from Jensen 1994, p. 25, figure 9)

- **Direction of the polish:** considering the morphological axis of the tool. 1. Parallel, 2. Perpendicular, 3. Oblique (Figure 2.28).

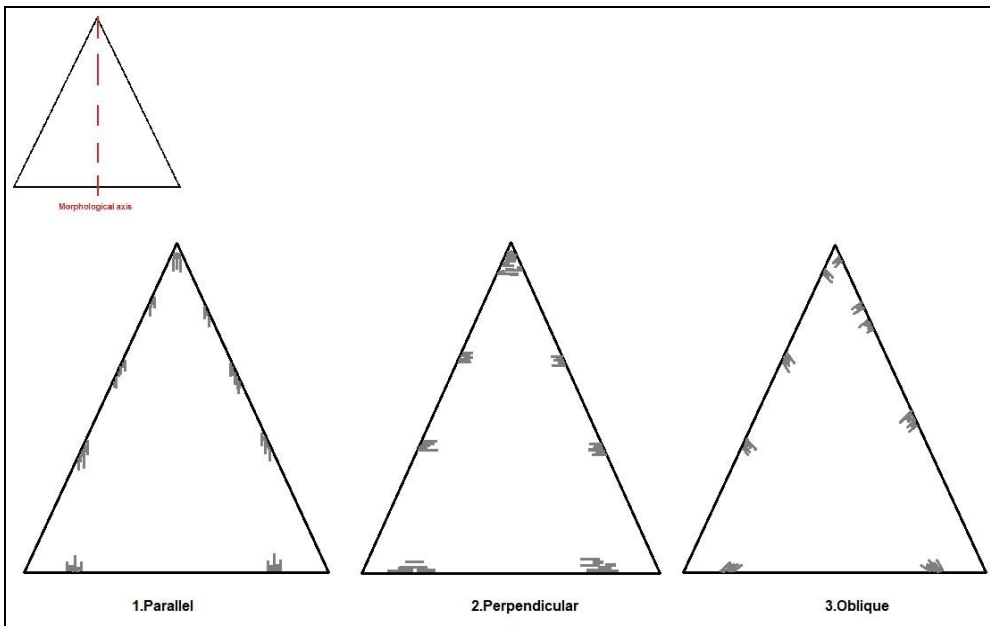


Figure 2.28. Polish directionality. The polish is shown represented in grey (Image La Porta).

- Association with other traces.

2.5.3 Linear traces, striations, and microscopic impact linear traces (MLITs)

2.5.3.1 Background

The term “striations” has been used in the past to define different types of linear traces indicating the directionality of the tool’s movement during its use (Semenov, 1964; Del Bene, 1979; Keeley, 1980, p. 23; Keeley and Newcomer, 1977; Mansur-Francomme, 1983, 1986, p. 93-99). However, striations can also form during alteration processes (Levi-Sala, 1986), but in this case, they show a more random distribution, lacking patterns of directionality, and are rarely associated with other use traces (Keeley and Newcomer, 1977; Mansur-Francomme, 1986, p. 97).

The definitions of the appearance and formation of the striation or linear wear vary broadly between the different analysts. Broadly, the formation of striations depends on the condition of the surface of the stone tool during utilisation (Mansur-Francomme, 1983, 1986).

Semenov (1964, p. 88) proposed that striations result from “scratching agents” acting against the surface of stone tools. These agents are particles of hard material (e.g. sand grains, small chips of bone, or flint). During utilisation, these particles scratch the surface of the tool (Keeley, 1980, p. 23-24).

According to Del Bene (1979), adhesive mechanisms, like the deformation and translocation of particles from the surface of the worked material into the surface of the stone tool or vice versa, could also explain the formation of striations (Del Bene, 1979, p. 169).

Kamminga (1979, p. 148) adopted a classification based on the morphology of the striations. Linear striations were called “sleeks”, and irregular striations were called “furrows” (or fern-like). Furrow-like striations are formed by hard particles (sand or mineral grains) that detach material from the surface, forming an irregular channel. The morphology of the channel (e.g. the furrow-striations) depends on the degree of hardness of the raw material, the morphology of the scratching particles, the pressure applied during the movement, and the

chemical bond of the siliceous surface. The sleek-like striations are instead the result of a plastic deformation, which is defined as “hydrolysed silica displacement” (Kamminga, 1979). The particles scratch the surface while forming a silica gel (hydrolysis process) and a channel. The gel is then translocated along the striation (Kamminga, 1979).

Keeley (1980, p. 23) did not try to explain the mechanism of formation and classified striations accordingly to their dimensions (e.g. deep vs shallow striations).

Mansur-Franchomme (1986) attempted to clarify the mechanisms of formation of striations based on the SEM observation of experimental tools. She recognised four types (Mansur-Franchomme, 1986, p. 97-98):

- a) striations “à fond rugueux”, defined as irregular striations, with a U-shape channel and dull appearance (Mansur-Franchomme, 1986, p. 97).
- b) striations with “à fond lisse”, defined as bright and shallow striations, which may show polish within the striations. They were divided into fern-like or “fougère” and ribbon-like or “ruban” striations (Mansur-Franchomme, 1986, p. 98).
- c) additive striations, defined as showing an additive and bright appearance (Mansur-Franchomme, 1986, p. 98).
- d) filled striations, characteristic of plant polish (Mansur-Franchomme 1986, 98).

However, Mansur-Franchomme’s (1986) classification has proved difficult to replicate, based on the rather qualitative description of the different types of striations (see also Van Gijn, 1989, p. 32), and the amorphous silica-gel theory that it assumes (Section 2.5.2), which is not widely accepted at the moment (Ollé and Vergès, 2008). Further research is therefore needed to clarify the formation processes of striations and polish wear (see also Borel et al., 2014).

With regards to this, and regarding this thesis, another category of linear traces has been recognised as diagnostic of projectile impact activities, i.e.

microscopic linear impact traces (MLITs) (Moss, 1983a; Fischer et al., 1984). MLITs are defined as linear bands or stripes of polish with striations around or within the polish. As MLITs indicate the directionality of the tool (e.g. the directionality of the projectile impact), in this thesis they contribute towards the linear traces or striations category.

In this thesis striations and MLTs are thus classified as the following, based on optical incident light microscope observation only (100x-400x magnification) (Figure 2.9):

- regular-edge(s) or irregular-edge(s) striations,
- MLITs, linear band of polish surrounded by striations or including striations.

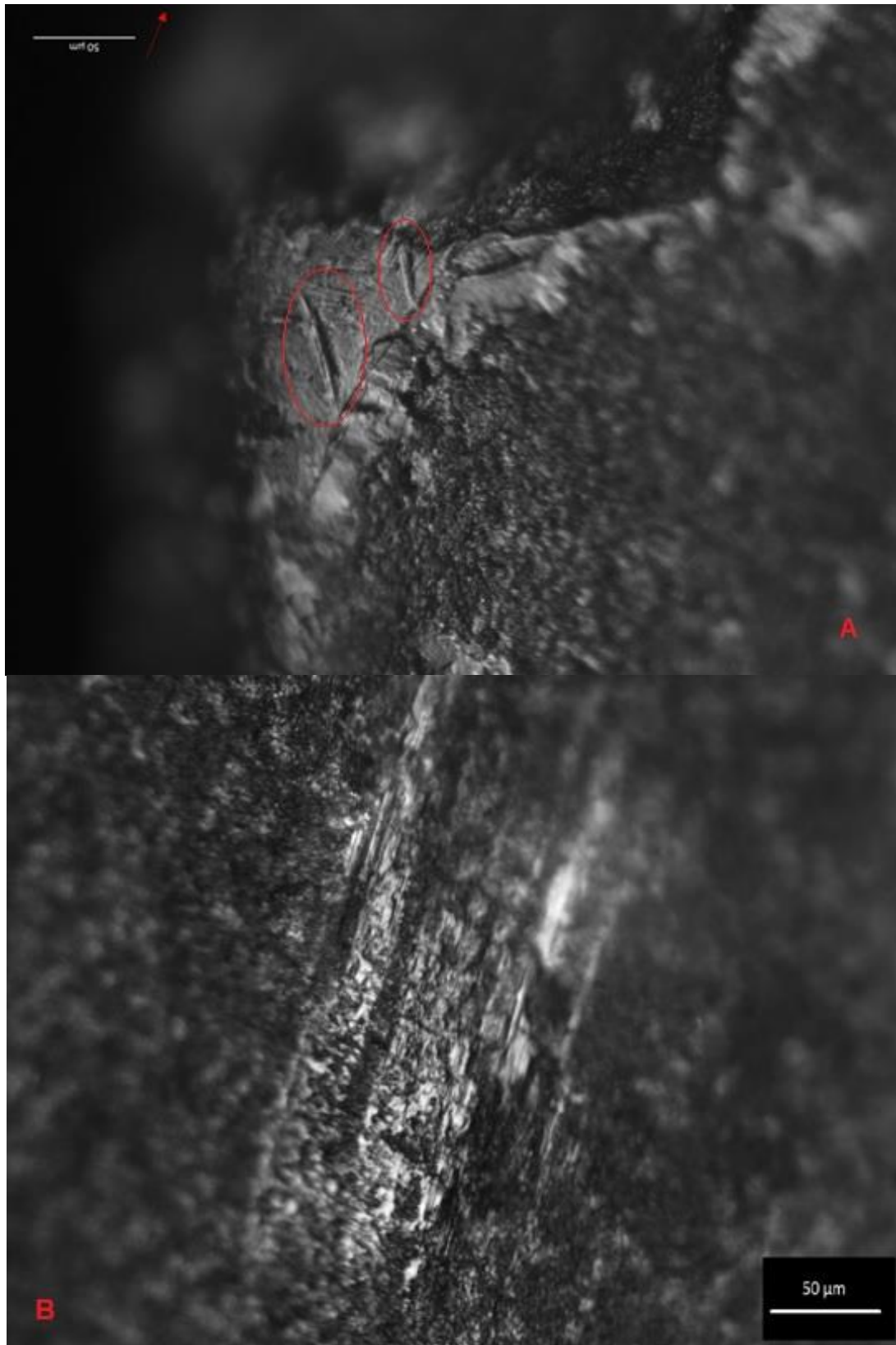


Figure 2.29. A. Linear striations; B. MLITs. (Image La Porta).

2.5.3.2 Striations and MLITs attributes

Following previous studies (Keeley, 1980; Kamminga, 1979; Plisson, 1985; Vaughan, 1985; Mansur-Francomme, 1983; Van Gijn, 1989; Gonzalez and Ibañez, 1994; Borel, 2010), several attributes are described in this thesis:

- **Location:** the locus/loci in which the polish is observed. Proximal (loci D1v, D2v, D3v, D1d, D2d, D3d), mesial (loci M1v, M2v, M1d, M2d), and distal parts (loci P1v, P2v, P1d, P2d) (see Section 2.3).
- **Locus Delineation:** (see Section 2.5.2.2.) 1. Straight, 2. Concave, 3. Convex, 4. Pointed (Figure 2.22).
- **Amount:** the number of striations observed in the same locus. 1. None, 2. One, 3. Double, 4. Multiple, 5. Striation(s) within polish.
- **Morphology of the Striation:** morphology of striations when observed at 200x. 1. Regular and Irregular striations, 2. MLITs (Figure 2.9).
- **Direction to the Tip:** considering the morphological axis of the tool. 1. Parallel, 2. Oblique, 3. Perpendicular, 4. Crossed/Random (Figure 2.30).

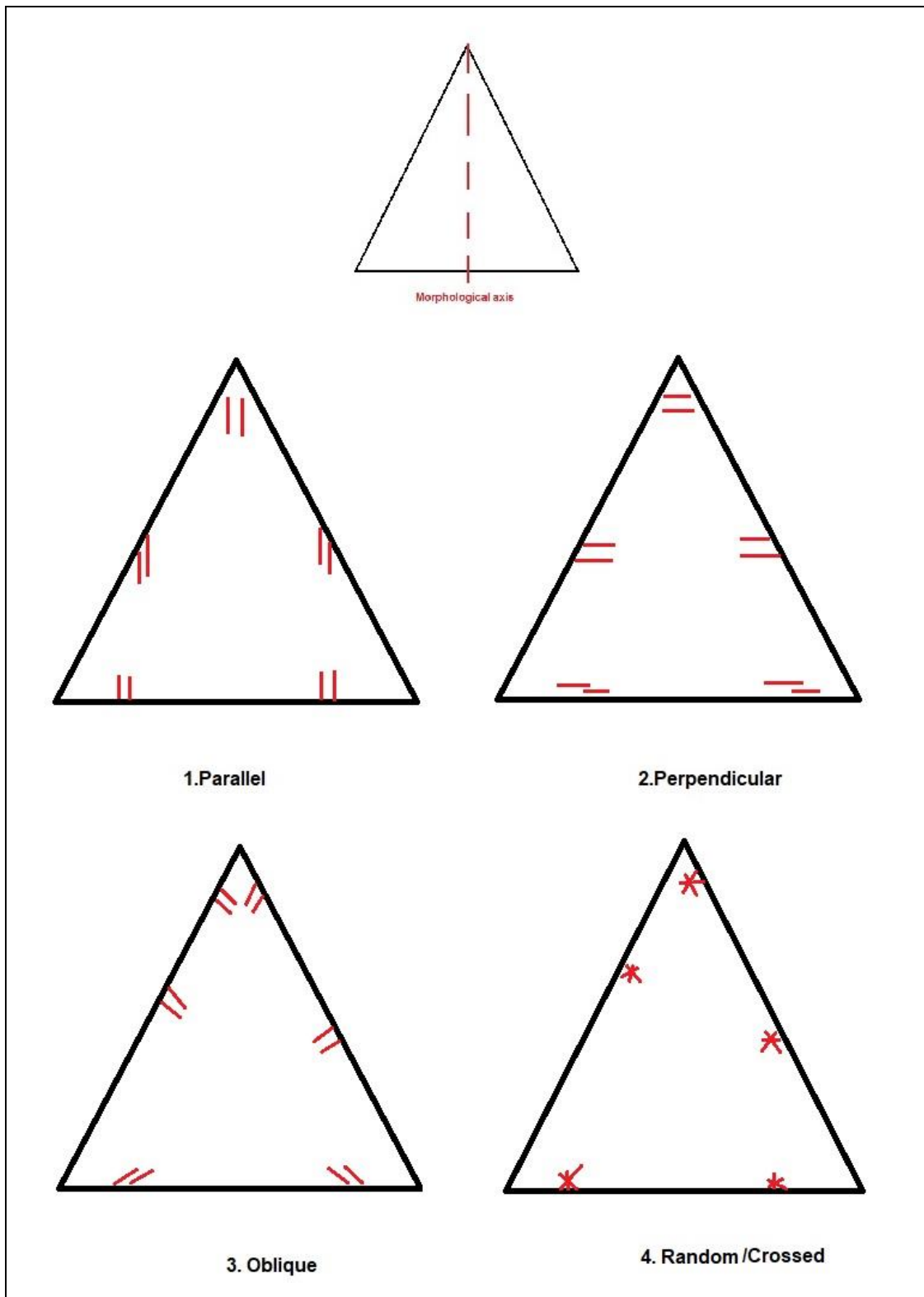


Figure 2.30. Directionality of striations and MLITs. (Image La Porta).

- Association with other traces.

2.5.4 Quantification

Edge-rounding, polish, MLITs, and striations were counted considered the number of tools in which these traces were observed and recorded. The frequencies of use-wear traces were then referred to the number of tools that presented the specific trace type. Therefore, more than one trace type could occur on a tool, and a trace type could be presented in multiple locations (or loci, see Section 2.3) of the tool.

2.5.5 Residues

Use-associated residues are portions of the worked material that remain on the surface of the tool (Fullagar, 2006). They can assist in the identification of the worked material (Fullagar et al., 1996; Hardy and Garufi, 1998; Langejans, 2010; Wadley et al., 2004; Lombard, 2008; Hardy et al., 2013) and in the identification of hafting traces (Rots and Williamson, 2004; Pawlik, 2004; Lombard and Wadley, 2007). Their various aspects and their morphology can be observed at different magnification ranges (100x-500x or over), and chemical analysis can also be used to identify their origins (Lemorini et al., 2014; Prinsloo et al., 2014; Croft et al., 2018).

Residue and use-wear analysis are two complementary methods that, when combined, permit superior interpretation of the tool's use and allow for speculation on the way in which it was manufactured. However, some difficulties remain present in residue analysis, including contamination from ancient or modern residues, the construction of a reference collection, and specialist chemical laboratory access and skills. As a result of these limitations, residue analysis was not conducted for the purpose of this thesis. Nevertheless, when adhesive residues were observed (e.g. resin-based or tar-based adhesive residues), both in experimental and archaeological stone tools, they were recorded according to their location on the tool and their qualities, such as colour (e.g. brown-reddish) and texture (e.g. smooth or rough).

2.6 Wear arising from other taphonomy processes

Mechanical or chemical alterations can affect stone tools after they have been discarded, lost, or deposited into the archaeological context (Van Gijn, 1989, 2010).

Mechanical alterations

Abrasion (through transport or small-scale sediment movements), trampling, excavation methods or post-excavation practices can all generate mechanical alterations that can affect the stone tool after deposition. Traces of metal from trowels or sieving are easily recognisable under the microscope. They exhibit a metallic appearance and have a highly reflective metallic polish. Abrasion from the sediment surrounding the stone tool can also be identified, regardless of whether its location on the cutting edge is isolated or randomly distributed. It appears as a very bright polished surface. It generally affects the highest topographic spot of the artefact which has been most exposed to the sediment.

Edge-damage and mechanical fractures, due to post-depositional processes have been investigated (Levi-Sala, 1986; Shea and Klench, 1993; Sano, 2009, 2012; Pargeter, 2011; Pargeter and Bradfield, 2012). Modern experiments have asserted that feather, hinge and snap terminations can originate from trampling processes, excavation, or post-excavation activities. However, they show different localisation (generally randomly distributed) and frequencies (generally < 3% of the tools of the total assemblage) than scars and fractures due to utilisation.

Chemical alterations

Chemical alterations form various types of patina and are developed while the tool is in the ground. White, gloss, and coloured patina are the most common post-depositional chemical alterations (Rottländer, 1975; Van Gijn, 1989; Levi-Sala, 1986; Plisson and Mauger, 1988; Howard, 2002).

White patina has been described as a thin white layer that covers the artefact. Under the microscope, it shows a granular texture and dispersed glare (Van

Gijn, 1989, p. 51-58), (Figure 2.31). Experiments have demonstrated that white patina forms quickly in alkaline (PH >7) environments (Plisson and Mauger, 1988). White patina development can also be associated with a decrease in tool weight (Van Gijn, 1989). In siliceous rocks (mainly flint), this is caused by water loss between the quartz crystals of the cryptocrystalline structure of the chert (dehydration).

Gloss patina results in a smooth, almost polished appearance (Van Gijn, 1989, p. 54). Experiments have shown that this is likely to affect stone tools deposited in an acidic environment (PH <4), such as peat (Rottländer, 1975; Howard, 2002). Gloss patina is microscopically very similar to utilisation polish when analysed with OLMILs (Figure 2.31), however, this can be differentiated by an SEM (Rottländer, 1975).

Museum collections

Museum's stone tool collections commonly display traces of graphite, ink, lacquer, nail polish, and stickers (Figure 2.31). Artefacts may have also been treated with acids, acetones, or chemical reagents (Van Gijn, 1989, p. 57).

Attributes

Post-depositional alterations are critical variables in use-wear studies, as they can distort the analysis and thus compromise the reliability of the analyst's interpretation. Therefore, during use-wear examination, mechanical and chemical post-depositional alterations were recorded and inserted into the database system, as follows:

- **Presence/absence of Patina:** 1. Present, 2. Absent
- **Type of Patina:** 1. White patina, 2. Gloss Patina, 3. Coloured 4. Combination of previous.
- **Distribution of the patina on the stone tool surface:** the locus/loci where the patina was observed. Proximal (loci D1v, D2v, D3v, D1d, D2d, D3d), mesial (loci M1v, M2v, M1d, M2d) and distal parts (loci P1v, P2v, P1d, P2d) (see Section 2.3).

-
- **Amount of Patina:** <25%, 50%, >75%, 100% of the tool surface.
 - **Encrustation Presence:** 1. Present, 2. Absent
 - **Distribution of the encrustations on the stone tool surface:** the locus/loci where the encrustations were observed. Proximal (loci D1v, D2v, D3v, D1d, D2d, D3d), mesial (loci M1v, M2v, M1d, M2d) and distal parts (loci P1v, P2v, P1d, P2d) (see Section 2.3).
 - **Number of encrustations:** <25%, 50%, >75%, 100% of the tool surface

Moreover, when archaeological tools presented a high degree of chemical or mechanical post-depositional alterations, they were not included in the use-wear examination (see CHAPTER 9 and CHAPTER 10 for details).

In the next chapter the protocol of analysis of experimental and archaeological tools is presented.

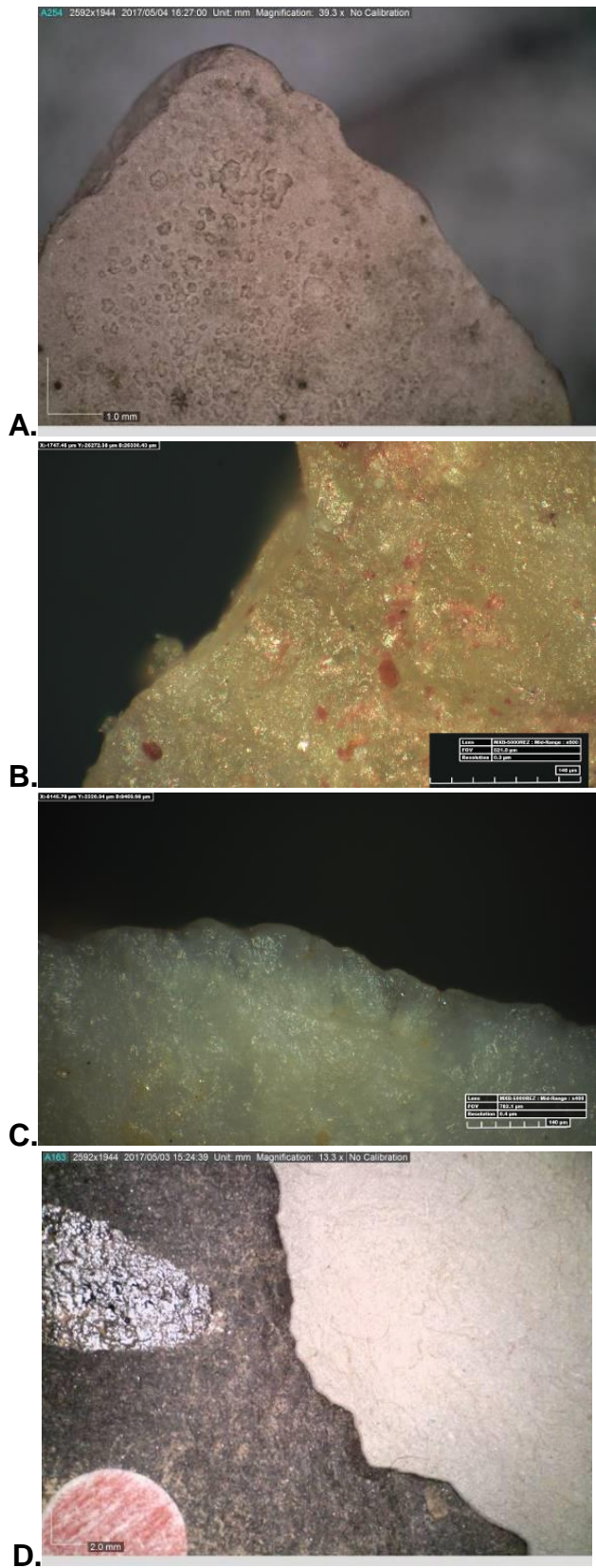


Figure 2.31. Types of post-depositional alterations. A. White patina; B. Coloured patina; C. Glossy patina; D. Lacquer, numbering, nail polish and stickers (Image La Porta).

CHAPTER 3

PROTOCOL OF ANALYSIS

A protocol of analysis for experimental and archaeological stone tools, allowing for replicability, was developed for this thesis.

3.1 Experimental stone tools: protocol of analysis

The following steps were applied to each of the experimental Levallois points analysed as part of this thesis:

1. Experimental Levallois points (n=80) flint replica were knapped (see Section 4.3.1) and bagged into individual zip-lock bags.
2. Techno-morphological features and attributes (see Section 3.3) of the experimental tools were observed and recorded into a database (see Appendix D, Volume 2).
3. Experimental tools were cleaned before proceeding with the casting procedure. The tools were put into individual plastic bags (Figure 3.5). These were filled with pure acetone and put into an ultrasonic tank (at a temperature of 0°) for 5 minutes. They were subsequently rinsed with fresh water and placed on tissue paper (starch free) to air dry (Figure 3.5).
4. Before performing the experiments, the experimental tools were cast (Figure 3.5). This created high-resolution dental casts of the edges and distal tips of the experimental Levallois points, allowing for comparison before and after the experiments, and assisting in understanding the development of use-wear (Ollé, 2003). Moulds (negative impressions) of the distal tip and the two lateral edges of the experimental Levallois points were made. A silicone-based, high-resolution dental impression material, called Provil Novo Light (Provil ® Novo Light) was applied with a plastic spatula to create the moulds (Ollé and Verges, 2008, p. 40) (Figure 3.5). The casts (positive impressions) were formed by pouring a

-
- rigid bi-component polyurethane resin, Feropur PR55, into the Provil Novo moulds (Ollé and Verges, 2014, p. 62). The casts, once dried, were left inside the mould and were placed inside individual plastic bags before being stored in boxes.
5. The experimental tools (distal tip and lateral edges) were observed at low magnification (6.7x to 45x) with a stereomicroscope (Olympus SZ61, see Section 2.2.5) in order to document débitage or production wear traces (Newcomer, 1976; Keeley, 1980, p. 25-28).
 6. The experimental tools were cleaned again, as per the process outlined in Step 3, to remove traces of the casting materials.
 7. A total of n=60 archaeological experiments using the experimental Levallois points were performed (i.e. n=28 throwing, n=24 thrusting, and n=8 knife experiments, see CHAPTER 4).
 8. After the experiments, the Levallois points were individually bagged into plastic bags and wrapped in bubble wrap. This was to prevent further shock damage during transportation and storage.
 9. Upon arrival in the lab, the tools were left overnight in a bath of H₂O with *Derquim* detergent (without phosphates), (Ollé and Verges, 2008, p. 40). This moistened any organic residues left behind from the experiments and helped with the de-hafting process.
 10. The experimental Levallois points that had been hafted during the experiments (see CHAPTER 4) were removed from their fore-shafts/handle with manual pressure (as indicated in Section 3.3).
 11. The experimental tools were chemically cleaned before the use-wear examination, as indicated in Section 3.4.
 12. The experimental tools were observed at low magnification with a stereomicroscope Olympus SZ61 (6.7x to 45x magnification, see Section 2.2.5) in order to identify and describe impact fractures, edge-damage, hafting traces, and adhesive residues.

-
13. The tools were observed under high magnification (50x to 500x) with an Olympus BX60 (metallographic microscope, see Section 2.2) in order to identify and describe polishes, striations, microscopic linear impact traces (MLITs), hafting traces, and edge-rounding.
 14. All traces were recorded photographically. The stereomicroscope took photographs with 10x to 80x magnification. The metallographic microscope took photographs at fixed magnifications (e.g. 100x, 200x, and 500x). All attributes were entered into a bespoke digital database system on a trace-by-trace basis. A paper form was used to conduct a systematic observation of use-wear traces (free descriptions were also noted, allowing for the inclusion of additional information and the recording of unexpected wear traces).

3.2 Archaeological stone tools protocol of analysis

The following steps were applied to each of the archaeological Levallois points and convergent tools analysed as part of this thesis:

1. Levallois points within each archaeological assemblage were sorted and selected (as described in CHAPTER 9 and CHAPTER 10).
2. Techno-morphological features and attributes (see Section 3.3) of the archaeological Levallois points and convergent tools were observed, analysed, and recorded into a database (see Appendix F and G, Volume 2).
3. Before the use-wear analysis, all archaeological tools were cleaned in an ultrasonic tank (at a temperature of 0°) with demineralised water and *Derquim* detergent (phosphates free) for 15 minutes (Figure 3.1). They were subsequently rinsed with fresh water and placed on tissue paper to air dry (Figure 3.1). Acetone was used to remove traces of marking or deposits that could scatter the light of the microscope. Cleaning (such as that involving HCl or NaOH) was not undertaken (see Section 3.4).
4. The archaeological tools were first observed at low magnification (from 10x up to 80x) in order to document the location of traces and to record fractures, edge-damage, and possible hafting traces.
5. Only selected archaeological tools were observed under high magnifications (either with a Dino-lite Edge AM7915MZT with 10x-220x magnifications or with an Hirox KH-8700 with 35x to 1000x magnifications; see Section 2.2) to identify polishes, striations, MLITs, hafting traces and edge-rounding.
6. All traces were recorded photographically. For low power analysis, pictures were taken at 10x to 80x magnification, whereas for high power analysis, pictures were taken at fixed magnifications (i.e. 50x, 75x, 100x, 150x, 200x, and 220x with the Dino-lite Edge AM7915MZT; and 50x, 100x, 200x, 400x, 600x, and 800x with the Hirox KH-8700). Results were

entered into a bespoke digital database system on a trace-by-trace basis. A paper form was used to record a systematic observation of use-wear traces (free descriptions were also noted, allowing for the inclusion of additional information and the recording of unexpected wear traces).

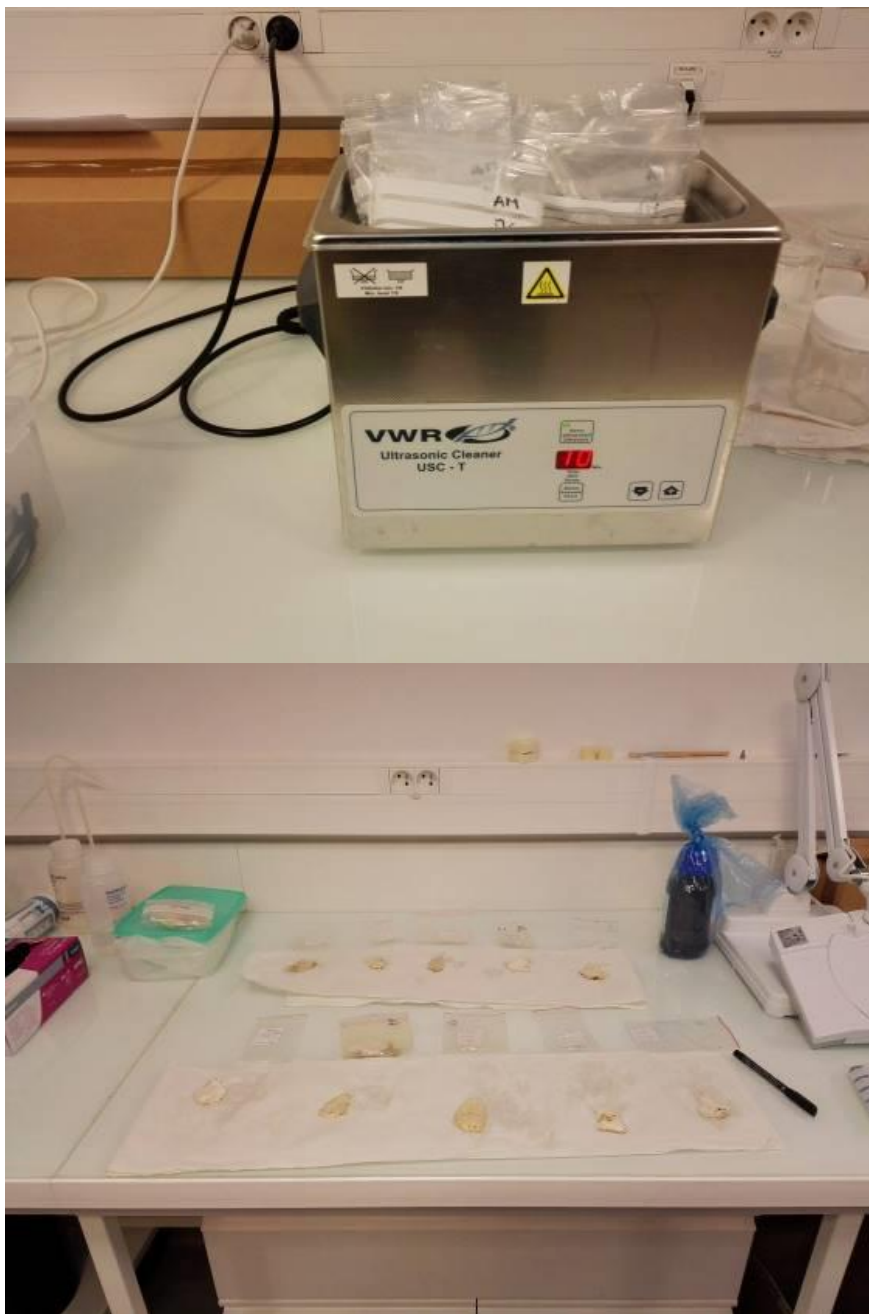


Figure 3.1. Cleaning of the archaeological stone tools of Abri du Maras, at the Natural History Museum (Paris). Tools were soaked in demineralised water and *Derquim* detergent for a 15-minute ultrasonic bath. (Image La Porta).

3.3 Techno-morphological attributes

The following technological and morphological attributes were recorded for both experimental and archaeological stone tools (a few modifications were made for the archaeological tools, when necessary). These attributes were logged in the database system as follows (see Appendix D, F and G, Volume 2):

- **Tool Identification Number (ID, CODE):** Tool ID with an indication of the archaeological level and a square number for the archaeological tools, or an experimental code for the experimental tools (i.e. experiment type plus tool number).
- **Raw Material Type:** 1. Flint, 2. Quartz, 3. Quartzite, 4. Limestone, 5 Dolomite. It is worth noting that experimental tools were made of flint, and the archaeological tools selected were mostly flint raw materials.
- **Raw Material Grain Size:** 1. Coarse, 2. Medium, 3. Fine.
- **Maximum Length (mm):** This was recorded from the striking platform to the distal end, following the technological axis (Inizan et al., 1999, p. 107; Figure 3.3). When the Levallois points (or convergent tools) were déjeté tools (e.g. tools where the technological axis is different from the morphological axis, Inizan et al., 1999, p. 107), they were oriented and measured following the morphological axis (i.e. the axis of the maximum symmetry of an object; Inizan et al., 1999, p. 145) (Figure 3.2). All measurements were recorded with a digital calliper.
- **Maximum Width (mm):** This was recorded as perpendicular to the main axis of the tool (Figure 3.3). All measurements were recorded with a digital calliper.
- **Maximum Thickness (mm):** This was recorded as the maximum depth of a tool's profile. All measurements were recorded with a digital calliper.
- **Tip Angle (°):** This was measured with a protractor, and was considered to be the intersection between the two edges (Figure 3.3). Each

measurement was repeated three times to ascertain an accurate measurement.

- **Right Edge-Angle/Left Edge-Angle (°):** The Edge-Angle measurement was taken at the mid-point of each lateral edge with a protractor. Each measurement (right and left) was repeated three times to ascertain an accurate measurement.
- **Flaking Angle (°):** The Flaking Angle is the intersecting angle between the striking platform and ventral face (Inizan et al., 1999, p. 142). It provides the angle of detachment of the stone tool.
- **Cortex Percentage and Localization:** 1. Present (percentage of cortex <25%, 50%, >75%, 100%), 2. Absent.
- **Striking Platform Type:** 1. Cortical, 2. Flat, 3. Dihedral, 4. Facetted, 5. “En Chapeau”, 6. Linear, 7. Winged, 8. Punctiform, 9. Missing (after Inizan et al., 1999).
- **Techno-morphological Type:** 1. Levallois point, 2. Triangular Levallois flake, 3. Retouched convergent tool (see APPENDIX B, Volume 2 for details).
- **Direction of the Negative Removals:** 1. Unidirectional Longitudinal, 2. Unidirectional Convergent, 3. Bidirectional Longitudinal, 4. Bidirectional Convergent, 5. Centripetal, 6. Peripheral, 7. Indeterminate (see Section 8.3.7.1 for details).
- **Retouch:** 1. Present, 2. Absent. If present:
 - **Retouch Localisation and Type:** 1. Parallel, 2. Sub-parallel, 3. Scaled, 4. Stepped (after Inizan et al., 1999).
- **Typological Type:** when retouch was present, Bordes (1961) was used as a typological reference list.

-
- **TCSA Index (mm):** Calculated with the formula (Shea, 2006, p. 824):

$$(0.5 \times \text{maximum width in mm}) \times \text{maximum thickness in mm}$$

- **TCSP index (mm):** Calculated with the formula (Sisk and Shea, 2009, p. 2044):

$$1/2 \text{ maximum width} \times \text{maximum thickness}$$

This image has been removed by the author of this thesis/dissertation for copyright reasons.

Figure 3.2. D corresponds to the technological axis of the tool, M to the morphological axis of the tool. L corresponds to the maximum length of the tool (Inizan et al., 1999, figure 41).

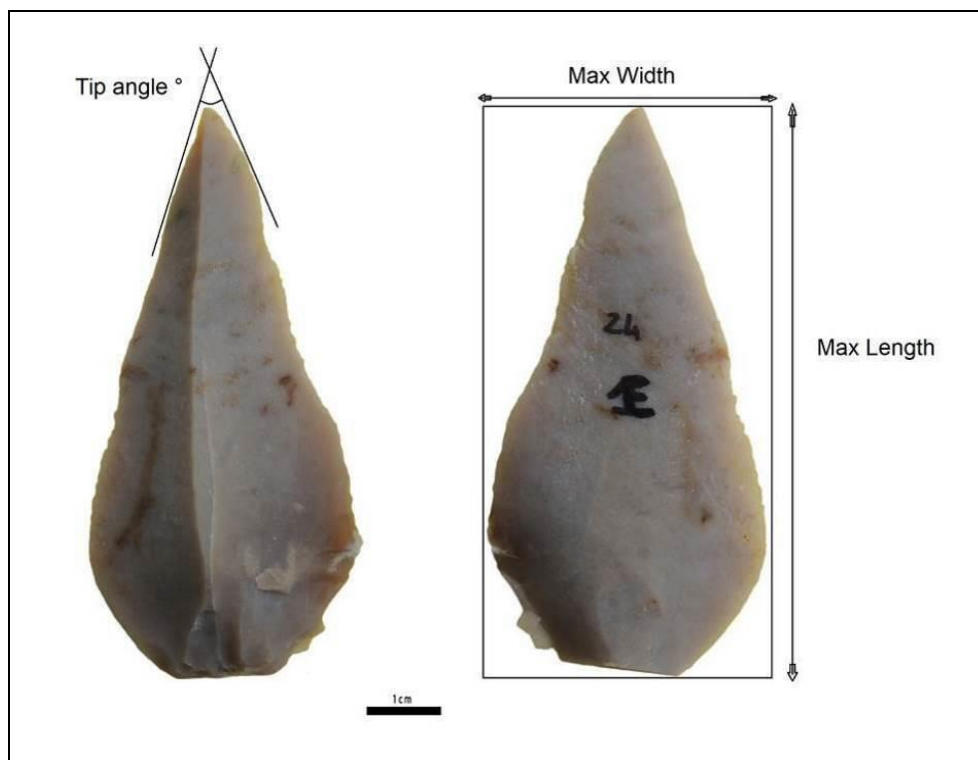


Figure 3.3. Morphometric attributes: maximum length, maximum width, and tip angle. (Image La Porta).

3.4 Comprehensive cleaning procedure for experimental tools

3.4.1 Background

The cleaning of stone tools is a necessary procedure prior to use-wear examination (Keeley, 1980), however cleaning protocol tends to be dictated by the research questions of the project, the type of artefact, and the microscopic analysis that the analyst decides to carry out. For instance, the preparation of a stone tool sample for SEM or confocal microscopic analysis would require a more intense cleaning protocol (see Macdonald, 2014; Ollé and Vergès, 2014, 2008; Evans and Donahue, 2008) than the preparation of a sample for metallurgic microscopic analyses (see Borel et al., 2014). This is because SEM analysis necessitates the removal of all possible dust particles and residues before the coating of the tools. Likewise, the cleaning protocol for residue analysis (e.g. water pipette extraction or water filtering and drying) is different from that of other types of microscopic analysis (see Fullagar, 2006). In short, there is no singular cleaning protocol “recipe” as the cleaning procedure should be adapted to suit the aims of the research and the type of analysis to be performed.

For use-wear analysis utilising optical microscopes with incident lights (i.e. metallographic microscope), Keeley (1980) proposed a protocol that involved a strict chemical cleaning, in which experimental tools would be immersed in 10% HCl acid (hydrochloric acid) and 30% of NaOH (sodium hydroxide), for at least 20 minutes (Keeley, 1980, p. 11). This protocol was formulated with the intention of removing deposits that could cover the stone tool surface and obscure use-wear, thus achieving a more comprehensive and valid comparison between experimental and archaeological tools (Keeley, 1980, p. 11). However, Plisson and Mauger (1988) and Plisson (1983) observed that prolonged exposure to heated chemical solutions (e.g. NaOH or CaO acids) could alter the microstructure and chemical bond of the polish, resulting in the loss or modification of the polish (Plisson and Mauger, 1988, p. 9, but see Coffey, 1994).

As a result, different cleaning protocols for experimental stone tools were tested in order to establish the most appropriate method of chemical cleaning. Some researchers proposed the use of only HCl acid in immersion (Anderson-Gerfaud, 1981, 1982), while others stopped using HCl acid altogether (Moss, 1983a), instead opting for a weaker immersion in NaOH (Moss, 1986). More recently, use-wear analysts proposed the use of gentler cleaning protocols, based on ultrasonic immersions in 3-5% HCl acid (to remove mineral deposits that may obliterate use-wear) and 5% NaOH (to remove organic residues) (Van Gijn, 1989). However, recent studies on use-wear analysis have favoured chemical acid-free cleaning protocols (Borel et al., 2014; Ollé and Vergès, 2014, 2008; Vergès and Ollé, 2011). This cleaning tends to centre around repeated ultrasonic baths in demineralised water with neutral soap, followed by several ultrasonic immersions in acetone to remove mineral deposits (Borel et al., 2014, p. 47; Vergès and Ollé, 2011, p. 1017; Ollé and Vergès, 2008, p. 40), and the use of H₂O₂ (hydrogen peroxide) to remove organic deposits (Ollé and Vergès, 2014, p. 62; Xhaufclair et al., 2016, p. 102).

3.4.2 Cleaning protocol for the experimental Levallois points

An initial cleaning protocol was set up to clean the first n=20 experimental Levallois points used as throwing and thrusting spear points.

Upon arrival in the lab, the experimental Levallois points were still attached into their fore-shafts (Figure 3.4). They were fixed using commercial tar and beeswax-resin adhesives (see Section 4.4.2.2) and, as such, the first point of enquiry was how to remove the Levallois points from the hafting arrangements without heating the tools, which might have caused alterations to the use-traces (Plisson and Mauger, 1988, p. 7). In an initial attempt, the tools were left for 24 hours in a bath of H₂O with *Derquim* detergent (Figure 3.4) (Ollé, 2003; Ollé and Vergès, 2008). This moisturised the glue on the hafting arrangements and allowed for the detachment of the stone points from the wooden fore-shafts. The wood of the fore-shaft absorbed the water of the solution, and eventually fissured. The solution also helped with the removal of intense animal grease, guts, hair, and organic residue left over from the experiments. Every 6 to 12

hours the soapy water solution was replaced. After 24 hours, the Levallois points could be removed from their fore-shafts by hand through the application of light friction between the points and the fore-shafts.

When the experimental Levallois points were removed from their fore-shafts, it became apparent that the amount of adhesive (commercial tar and resin) attached to the tools was still abundant. Previous publications have shown that acetone is particularly efficient in removing adhesive residues (Rots, 2010, p. 36; Rots, 2004, p. 12). The experimental tools (n=12) were therefore further cleaned using the following procedure (Figure 3.4):

- i. Submersion in a 20-minute ultrasonic bath in H₂O with *Derquim* detergent to remove organic particles and to help with the detachment of the adhesive deposits.
- ii. Submersion in a 20-minute ultrasonic bath in hydrogen peroxide H₂O₂ (7%) to remove organic residues (as suggested by Plisson and Mauger, 1988, p. 7; Ollé and Vergès, 2014, p. 62; Xhaufclair et al., 2016, p. 102).
- iii. Submersion in a 10-minute ultrasonic bath in pure acetone to remove adhesive deposits.
- iv. Submersion in a 5-minute ultrasonic bath in H₂O with *Derquim* detergent to remove the acetone's print.

This cleaning protocol has been previously tested and employed by numerous researchers and with different raw materials (Ollé et al., 2016; Borel et al., 2014; Ollé and Vergès, 2014; Asryan et al., 2014; Vergès and Ollé, 2011). However, the protocol was adapted for this study by including a longer immersion time in acetone to better remove the deposits of adhesives (from two to ten minutes, Table 3-1) and a longer ultrasonic bath in H₂O₂ to allow for the removal of organic residue (Table 3-1).

However, when these experimental tools, once cleaned, were examined under the metallographic microscope (an OLM with incident lights) an bright and greasy “polished layer” became visible since lower magnifications (Figure 3.6,

Figure 3.7, Figure 3.8). This layer appeared to be very oily and greasy, and it covered part of the proximal areas of the experimental tools (Figure 3.8). It was clear from the microscopic analysis of the location of this layer on the tools that these traces were the deposits of the adhesives (tar and resin based), still present on the surface of the experimental projectiles (Figure 3.6, Figure 3.7). However, as these deposits could compromise other wear traces identification (i.e. hafting traces), the experimental tools were cleaned again.

The additional cleaning, undertaken to remove the adhesive deposits, was tested at the IPHES in Tarragona, in collaboration with Professor A Ollé. White spirit was used to remove the deposits of tar and resin. White spirit is a petroleum liquid, primarily used as an organic solvent for removing adhesive and paint residue. It was first used in the field of use-wear analysis by Mansur-Francomme (1983). It was tested on two unused flakes which were plunged in tar and air-dried (these were not part of this thesis' experimental use-wear register or collection). The tools were soaked in white spirit inside a glass beaker overnight. They were then washed, immersed in acetone for 30 minutes in an ultrasonic tank and, finally, were rinsed with plenty of demineralised water. The white spirit removed all traces of adhesive, and no residues were observed during a subsequent microscopic examination (10-500x). Therefore, the n=20 experimental tools were additionally cleaned as follows (Figure 3.4, Table 3-1):

- v. The tools were soaked for 10 minutes in white spirit.
- vi. The tools were submerged for 5-minutes in an ultrasonic bath of pure acetone to remove the oily appearance of the white spirit.
- vii. The tools were submerged for 5-minutes in an ultrasonic bath of H₂O with *Derquim* detergent to remove previous solvent halos.
- viii. Finally, the tools were rinsed with fresh water and placed on tissue paper to air-dry.

If adhesive deposits were still present (on a microscopic base of 100x-500x), and were still compromising possible wear traces, this procedure (i.e. steps v to viii) was repeated for a maximum of two times (i.e. three times in total; this limit

was posed to prevent the deterioration of polish traces as a result of intense cleaning). If after the repetition of the cleaning protocol, for a maximum of three times, the microscopic adhesives traces were still present onto the tool surface, they were recorded and documented (see CHAPTER 7 and Appendix A, Volume 2).

This protocol demonstrated that the use of tar and resin adhesives and the removal of these adhesives must be carefully evaluated by use-wear analysts. Employing petroleum and resin-based adhesives in high quantities must be thoughtfully planned before an experiment and taken into consideration during the cleaning phase. If experimental tools have been hafted with a high amount of tar and/or resin-based adhesives, a short bath in white spirit is recommended. This will ensure the elimination of adhesive deposits, and will reduce the risk of confusion when differentiating between hafting traces and use-wear traces (see also CHAPTER 7).

3.4.2.1 Revision of the cleaning protocol

The above cleaning protocol was employed for the first n=20 experimental tools. However, a faster and localised cleaning system needed to be implemented for the remaining experimental stone tools (n=40; Table 3-1). It counted the following steps (Table 3-1):

- i. The tools were bathed overnight in H₂O with *Derquim* detergent before proceeding with de-hafting.
- ii. The tools were submerged for 20-minute in an ultrasonic bath of H₂O with *Derquim* detergent to remove organic particles and to assist in the detachment of the adhesive deposits.
- iii. The tools were submerged for 20-minute in an ultrasonic bath of H₂O₂ (7%) to remove organic residues (Ollé and Vergès, 2008),
- iv. Each tool was placed upside down into a glass beaker of acetone for 20-minute. The acetone level covered only the distal and mesial areas, without interfering with the proximal area where the adhesive was

located. The acetone was used to remove mineral deposits and adhesive deposits that may have adhered on the mesial and distal area of the tools during the hafting process.

- v. After the acetone bath, each tool was immersed, as outlined above, in another beaker, in preparation for a subsequent 5-minute immersion in white spirit to ensure that no adhesive deposits would remain.
- vi. Each tool was immersed again, as outlined above, in another beaker for a subsequent 2-minute bath in clean acetone, to remove the oily residue of the white spirit and ensure the removal of mineral deposits.
- vii. Each tool was subject to a supplementary 5-minute ultrasonic bath in H₂O with *Derquim* detergent to remove the acetone's halo.
- viii. Finally, tools were rinsed with fresh water and placed on tissue paper to air-dry.

This adaptation of the cleaning procedure was preferable as it reduced the time needed to complete the cleaning protocol and cut lab-related costs. At this stage, this revised cleaning system assured that the distal and mesial parts (the zones where diagnostic projectiles traces are more likely to be observed) of the n=40 experimental tools were chemically and locally cleaned in a shorter period. However, the same tools presented the remains of adhesive deposits on the proximal part of the tools, which prevented a detailed analysis of hafting traces. Therefore, the use-wear analysis for hafting traces was instead performed only the first n=20 experimental tools that were previously cleaned, following the complete cleaning protocol as expressed in Section 3.4.2 (see CHAPTER 7).

In conclusion, while the first cleaning protocol would have ensured a chemical cleaning of the entire tool (e.g. distal, mesial, and proximal parts) it also required a longer and not feasible amount of time, for which the second cleaning protocol was employed (Table 3-1).

Table 3-1. Cleaning protocol: a comparison between the two cleaning systems.

Experimental Levallois points	Cleaning protocol												
	Overnight bath in H ₂ O with <i>Derquim</i>	Manually de-hafting	A 20-minute ultrasonic bath in H ₂ O with <i>Derquim</i>	A 20-minute ultrasonic bath in hydrogen peroxide	A 10-minute ultrasonic bath in pure acetone (x3)	A 5-minute immersion in white spirit (x3)	5-minute ultrasonic bath in pure acetone	20-minutes immersion in pure acetone	5-minute immersion in white spirit	2- minute ultrasonic bath in pure acetone	5-minute ultrasonic bath in H ₂ O	Rinsed and dried	
N=20	x	x	x	x	x	x	x					x	x
N=40	x	x	x	x				x	x	x	x		x

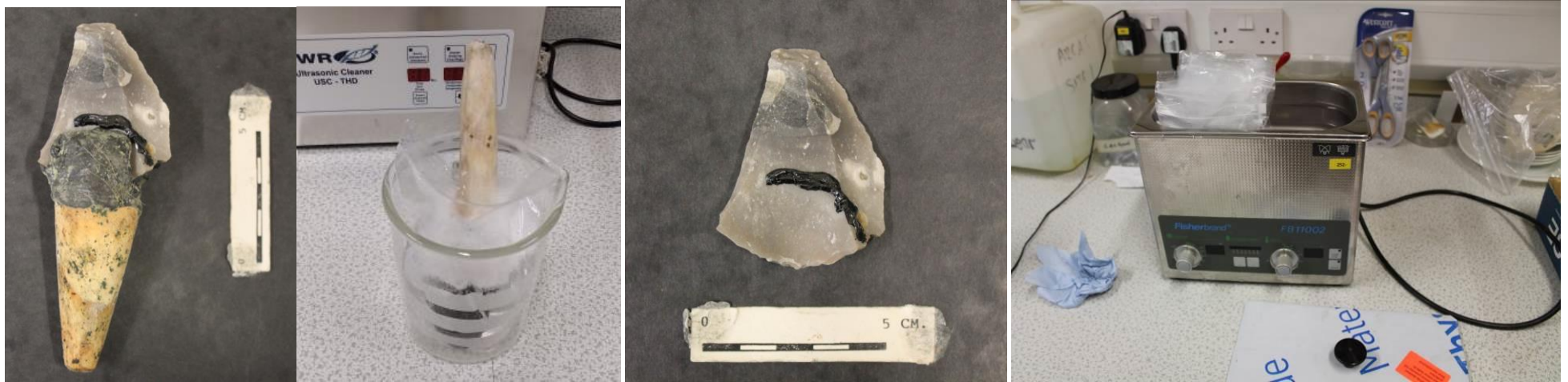


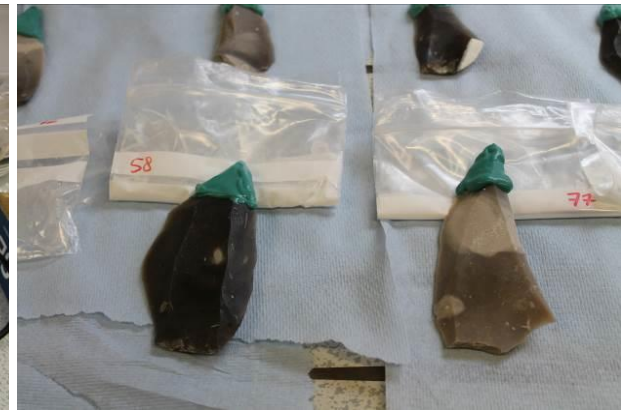
Figure 3.4. Cleaning system of the experimental Levallois points (ELPs). From left to right: 1. Dirty tools; 2. ELPs left overnight immersed in H₂O with *Derquim*; 3. ELPs after de-hafting; 4. ELPs in an ultrasonic tank, (Image La Porta).



1



2



3



4



5



6

Figure 3.5. Documentation of the mould/casting technique of the experimental Levallois points (ELPs). 1. ELPs freshly knapped; 2. ELPs in an ultrasonic tank of pure acetone for 5 minutes; 3. Mould production of the distal tips of the ELPs, with the Provil Novo Light; 4. The moulds fixed in a horizontal position; 5. Preparation and measurement of the polyurethane resin, Feropur PR55; 6. Cast making. (Image La Porta).

3.4.2.2 Usage of chemical acids

The use of chemical acids, such as 3-5% HCl (hydrochloric acid) and/or 3-5% NaOH (sodium hydroxide), was not undertaken, as exposing the experimental tools to further chemical cleaning could have altered the siliceous surfaces of the tools and/or polishes.

The HCl was replaced with long ultrasonic baths of H₂O₂ (hydrogen peroxide, 7%) and pure acetone. Hydrogen peroxide removes any organic deposits that could adhere onto the tool and/or polish surface, but has no effect on the siliceous surface of the tool (Plisson and Mauger, 1988, p. 7; Mansur-Francomme, 1986, p. 54); whereas pure acetone eliminates inorganic deposits, such as calcareous residues and minerals (Borel et al., 2014; Ollé and Vergès, 2008).

However, when experimental tools were observed to have large, brighter areas (which reflected the light of the microscope with the appearance of well-developed polish), it became unclear whether or not these spots were actual polish, or rather some reluctant animal flesh residue still present on the experimental projectiles. Therefore, in select cases (i.e. tools TH-20, TH-23, TH-32, TH-52, TH-68, TH-77, TH-92, TR-83), a solution of HCl (3.5%) was applied locally, by dropping a few drops directly on the tool surface with a pipette, and was then rinsed off with plenty of fresh water after few minutes.

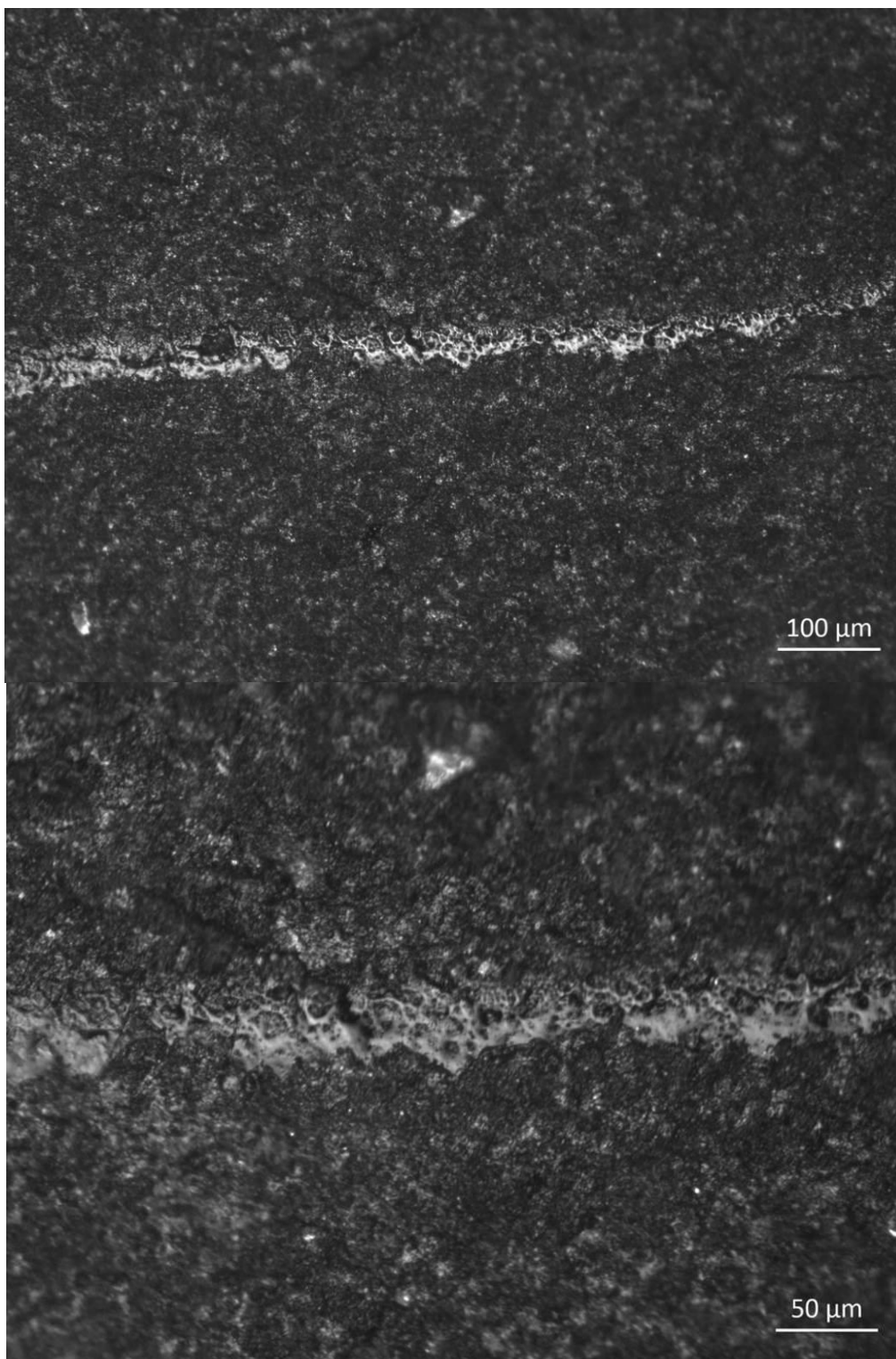


Figure 3.6. Bright and greasy polished layer located on the ventral-mesial part of the tool, in close proximity to the haft-limit (features explained in CHAPTER 7). Pictures: OLMil, OM 100x (above) and 200x (below), (Tool ID TH-78).

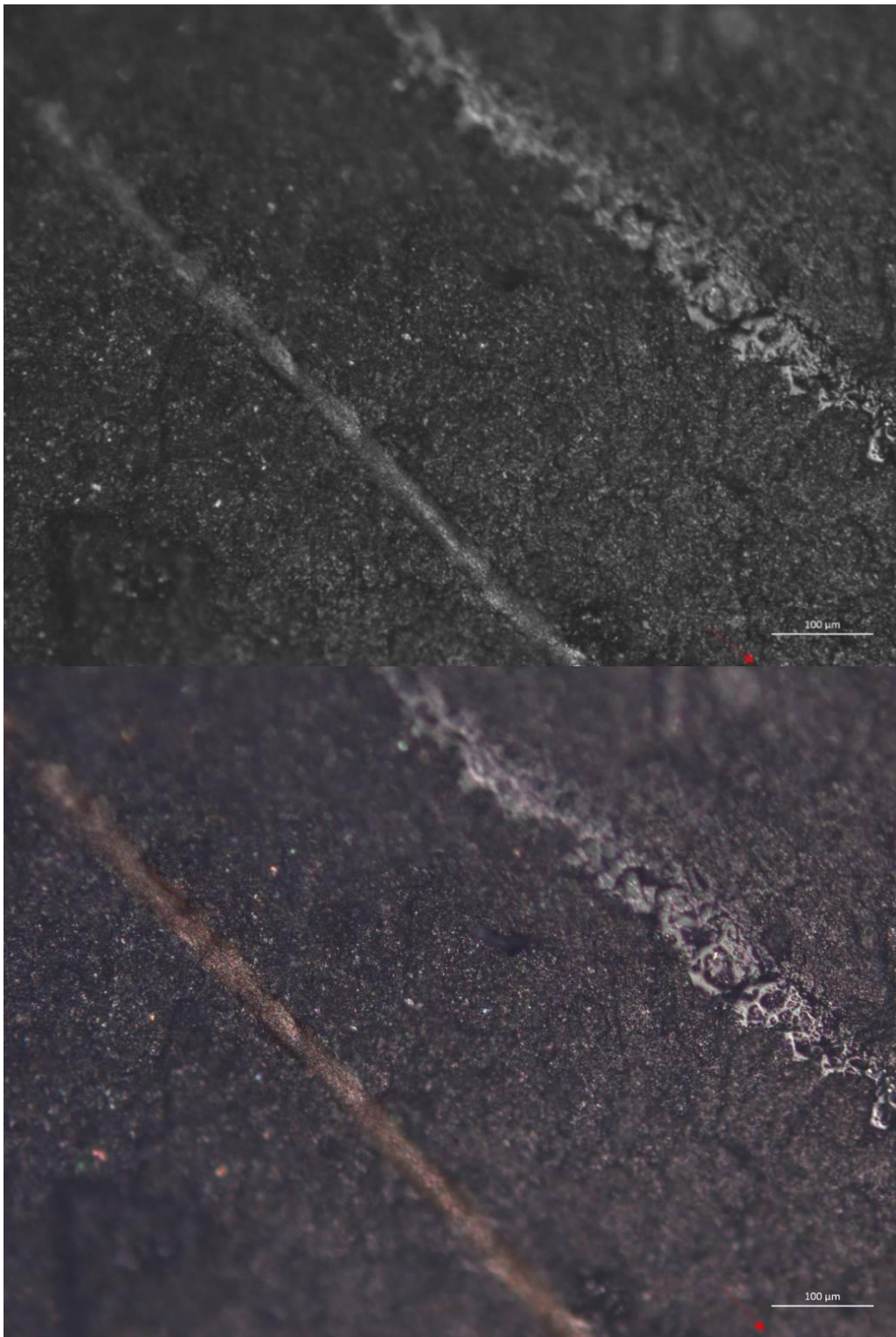


Figure 3.7. Black and white picture (above) and coloured picture (below). The picture shows a brown tar deposit (bottom line) and a shiny and greasy polished layer which was a residue of the tar-adhesive (upper line). Pictures: OLMil, OM 100x, (Tool ID TH-66).

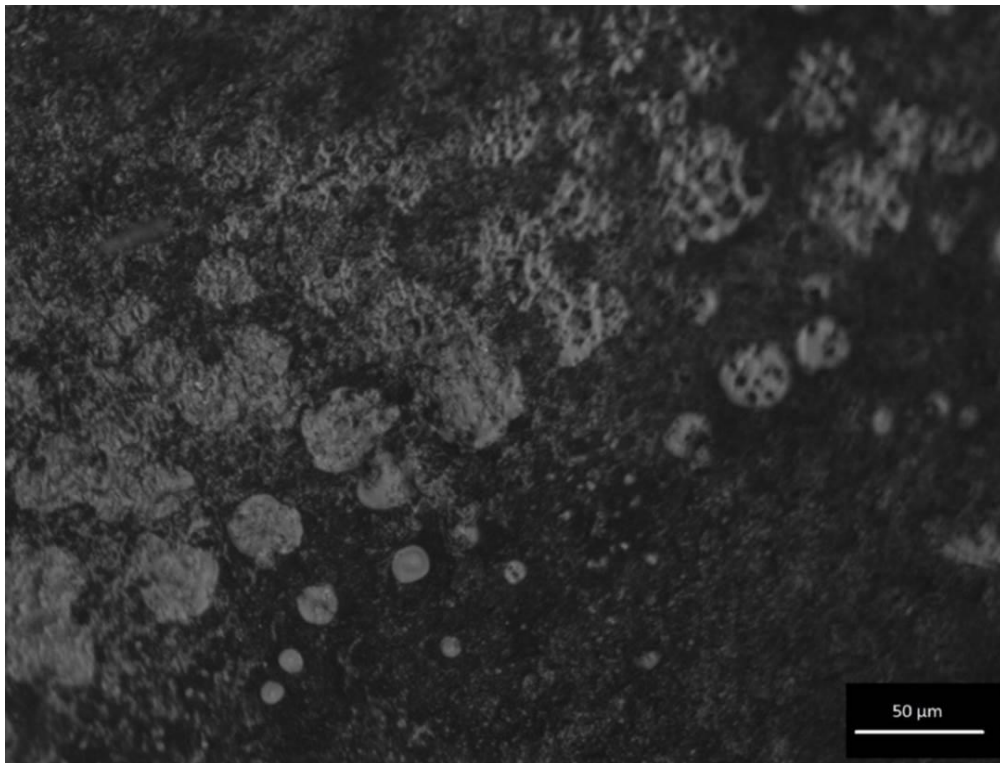


Figure 3.8. Bright and greasy spots of the adhesive (tar-based) used for the hafting. These were located on the ventral-mesial part of the tool, in close proximity to the haft-limit (features explained in CHAPTER 7). Picture: OLMil, OM 200x, (Tool ID TH-20).

The next chapter described the experimental programme of this thesis and the variables designated for each experiment.

CHAPTER 4

EXPERIMENTAL PROGRAMME: HAND-DELIVERED STONE-TIPPED SPEAR EXPERIMENTS AND BUTCHERING KNIFE EXPERIMENTS

4.1 Experimental purposes and rationale

The main purpose of this thesis's experimental programme was to create an extensive and systematic use-wear reference collection to identify and distinguish, if possible, between hand-delivered stone-tipped spear throwing and hand-delivered stone-tipped spear thrusting diagnostic use-wear traces, when using Levallois point flint replicas as stone tool morpho-type. Alongside this, butchering experiments, also using Levallois point flint replicas, were performed to give a sample control of the use-wear traces that can form in experimental Levallois points when used in activities other than projectile utilisation. Ballistic parameters of hand-delivered throwing and thrusting spear motions were recorded (see CHAPTER 5) in order to evaluate the effectiveness of Middle Palaeolithic stone-tipped spear replicas when used in hand-delivered throwing and thrusting motions, and investigate the formation of projectile use-wear traces.

In order to do this, the theoretical framework at the base of this thesis's archaeological experiments has been carefully considered, as follows.

Experimental archaeology is a scientific method based on a hypothetical-deductive process (Outram, 2008). The experimentation process is constituted by the formulation of a clear hypothesis and the choice of an accurate methodology that can test specific research questions (Coles, 1973; Reynolds, 1999; Outram, 2008). The formulation of clear hypotheses is the first step in the implementation of a "good" experiment (Franklin, 1981). If the hypothesis is well fashioned, it can be tested through the experiment, and it can be accepted as valid or rejected as false (Popper, 1959). The desire to answer a research question by testing a hypothesis, against a strict methodology, is what separates an archaeological experiment from a re-enactment activity, as

emphasised by previous researchers (Coles, 1973; Reynolds, 1999; Outram, 2008). However, there are some constraints on the process of archaeological experimentation (Tringham, 1978; Reynold, 1999; Outram, 2008; Van Gijn, 2010):

- a) The “authenticity” of the methods and materials used in an archaeological experiment (Outram, 2008).
- b) The degree of expertise of the experimenters (Tringham, 1978; Outram, 2008; Van Gijn, 2010).

These are particularly evident when the researcher is carrying out archaeological experiments under the framework of use-wear analysis as the range of activities and tasks performed with experimental stone tools have to be similar to what happened in the past. This is because the replication of specific activities and tasks carried out with stone tools is the only way to understand the wear formation process and undertake macroscopic and microscopic use-wear comparisons between experimental and archaeological tools (Van Gijn, 2010; Rots, 2010).

To overcome these constraints, two types of archaeological experiments can be undertaken: actualistic or replicative experiments (Outram, 2008), and laboratory experiments (Skibo, 1992).

Laboratory experiments (Skibo, 1992) address a specific research question by controlling all the parameters and allowing only a small number of variables. They are performed in a laboratory environment and often use machines or devices to allow replication. Although in laboratory experiments parameters and variables are mostly kept under control, there are “inevitable internal experimental assumptions” (cf. Eren et al., 2016, p. 106) that affect the choice of the specific variables employed in the experiments (see also Eren et al., 2016). It has, therefore, been questioned as to what extent laboratory experiments are relevant when evaluating archaeological records (Outram, 2008) and addressing behavioural processes (Keeley, 1974b; Van Gijn, 2014; Eren et al., 2016). Moreover, in the context of use-wear analysis, it has been

observed that laboratory experiments using machines or robots replicate unrealistic activities and tasks, producing standardised use-wear traces which are barely comparable with the archaeological traces observed on stone tools used by real people (Bamforth, 2010; Van Gijn, 2010, 2014; Rots and Plisson, 2014).

Actualistic or replicative experiments (Outram, 2008; Bamforth, 2010), on the other hand, can address problems of authenticity and savoir-faire (Bamforth, 2010; Van Gijn, 2014). They attempt to reconstruct “natural” conditions by employing raw materials that are known to have been available during the period under research, and then replicate similar archaeological scenarios. However, actualistic or replicative experiments have also been considered to add extra internal variability to the experiments, and this internal variability may contribute to a “deficiency of control” in the experimental process (Iovita et al., 2016, p. 74; Noak and Gaudzinski-Windheuser, 2018).

However, it is this author’s opinion (as well as others, see Eren et al., 2016; Milks et al., 2016; Clarkson, 2016; Clarkson et al., 2015; Rots and Plisson, 2014) that, seeing as the “archaeological records” cannot be truly replicated, laboratory experiments and replicative experiments are not in opposition, but are rather a continuum of the same analytical spectrum. Moreover, it is possible, and it was the main experimental approach of this research, to combine the replicability of controlled experiments with the adoption of realistic experimental variables.

However, considering the research framework of this thesis, some constraints had to be considered when choosing the experimental variables:

- (i) European Middle Palaeolithic stone-tipped spears, if their evidence is confirmed (Villa and Lenoir, 2006, 2009; Villa and Soriano, 2010), would have been used mainly, and possibly exclusively, by *Homo neanderthalensis*. However, as *Homo neanderthalensis* became extinct somewhere between 40 Ka (Higham et al., 2014; Moroni et al., 2013; Benazzi et al., 2011; Pinhasi et al., 2011) or 28,000 years ago (Zilhão,

2013; Finlayson et al., 2006; Ovchinnikov et al., 2000), modern experiments cannot engage with “Neanderthal participants”.

- (ii) Equally, experiments testing Middle Palaeolithic hand-delivered throwing and thrusting stone-tipped spears cannot rely on the same Middle and Late Pleistocene fauna. The fossil evidence from Pleistocene megafauna confirms that the Late Quaternary extinction event began around 50 Ka and peaked between 14 Ka and 11 Ka. 35% of Eurasian animal species became endangered or extinct (Kosh and Barnosky, 2006). Thus, modern experiments cannot test the Palaeolithic weapons against mammoths, steppe bison, or other Pleistocene mammals simply because these species are not alive today. Besides, larger living faunal taxa (such as horses or cows) are often of limited availability and budget.

That said, the specificity of this thesis, i.e. the comparison between the archaeological Levallois points and the experimental Levallois points used in throwing and thrusting spear motions to infer a Neanderthal’s capability of using throwing and/or thrusting stone-tipped spears, required replication processes that incorporated controlled but realistic experimental variables. For example, previous experiments investigating use-wear and fracture patterns in projectile tools have employed firing-machines (such as calibrated cross-bows or airguns) to modulate the kinetic energy (*KE*) and impact velocities of experimental stone projectiles (Shea et al., 2001; Pargeter, 2007; Schoville, 2010; Hutchings, 2011; Iovita et al., 2014; Wilkins et al., 2014). Others have instead contemplated the use of standardised isotropic materials (such as lime-glass, porcelain, or foam) as a substitute for raw flint materials for the production of experimental stone tools (e.g. in projectile experiments, Iovita et al., 2014), while others have opted for the use of ballistic gel targets (Iovita et al., 2014; Wilkins et al., 2014; Sano and Oba, 2015; Milks et al., 2016; Coppe and Rots, 2017).

However, it has recently been shown that human hand-delivery spear mechanics, both throwing and thrusting motions, are difficult to mimic (Roach and Richmond, 2015; Maki, 2013) and that *KE* and impact velocities alone cannot truly replicate hand-delivered spear mechanics (Milks et al., 2016; and

see also CHAPTER 5). Consequently, in projectile experiments, the use of firing-machines (such as calibrated cross-bows and air-guns) can only replicate impact velocities (if set with correct parameters, see CHAPTER 5), but cannot replicate the entire kinematic mechanism, such as the torque and spin (for throwing projectiles), the change in momentum, and the energy transferred into the target (for thrusting projectiles) (as demonstrated in CHAPTER 5 of this thesis, and expressed by others such as Milks et al., 2016; Rots and Plisson, 2014; Iovita et al., 2014). The differences, caused by the adoption of firing-machines, may result in the formation of experimental use-wear traces that are hardly comparable with archaeological use-wear traces. Furthermore, as expressed in CHAPTER 5, a review of previous literature showed a lack of recorded ballistic parameters (i.e. impact velocities and *KE* values) in the calibration of possible fire-machines used in both throwing and thrusting spear experiments, for which a correct calibration at the time of this thesis' experiments would have been difficult to estimate. Therefore, in order to allow for comparability between the experimental results and the archaeological artefacts, this research has opted to use trained and skilled human participants as the experimental variable for the delivery of experimental throwing and thrusting stone-tipped spears (see Section 4.3.4).

With regards to the use of ballistic gel targets in projectile experiments, as proposed by others (Iovita et al., 2014; Wilkins et al., 2014; Sano and Oba, 2015; Milks et al., 2016; Iovita et al., 2016; Coppe and Rots, 2017) a primary concern prevented its use. Ballistic gel has primarily been tested in projectile experiments investigating only macroscopic traces, such as diagnostic impact fractures (DIFs) and edge-damage (Coppe and Rots, 2017; Iovita et al., 2014; Wilkins et al., 2014), and/or human biomechanisms (Milks et al., 2016). However, the ballistic gel has never been employed in use-wear experiments seeking to investigate the formation of microscopic use-wear traces such as polish, striations, or other microscopic wear. This is because the formation process of polish, striations, and other microscopic use-wear traces depends entirely on the characteristics of the contact material used (such as meat, bone, skin, plants) (Hayden, 1979; Del Bene, 1979; Anderson, 1980; Anderson-

Gerfaud, 1981; Levi-Sala, 1988; Fullagar, 1991; Ollé and Vergès, 2008). Furthermore, it has been noted that certain ballistic gel recipes create homogenous and unrealistic targets that do not entirely mimic the mechanics of the projectile impact, creating instead unrealistic use-wear traces (as expressed by Rots and Plisson, 2014, p. 160). Therefore, as this thesis aimed to investigate the formation of macroscopic as well as microscopic projectile use-wear traces and compare them with archaeological use-wear traces, the use of ballistic gel targets was considered unsuitable. Instead, fresh animal targets (i.e. carcasses, see Section 4.3.3) were believed to be a much more appropriate experimental variable for this thesis's experimental purposes.

Regarding the use of Levallois point flint replicas, previous projectile controlled experiments using isotropic raw materials for the reproduction of experimental tools (such as lime-glass Levallois point replicas, Lovita et al., 2014, 2016), have not compared their experimental results (i.e. experimental use-wear traces) with archaeological artefacts (i.e. archaeological use-wear traces). Accordingly, as one of the leading research objectives of this thesis was the comparison of experimental use-wear traces observed in experimental Levallois points with archaeological use-wear traces observed in archaeological Levallois flint points, flint was considered to be the most appropriate raw material to use as an experimental variable.

4.2 Experimental sets

The experimental programme of this thesis counted three different set of experiments (Table 4-1).

The first two sets of experiments (1st and 2nd sets) aimed to evaluate the effects of different experimental variables on the formation of diagnostic use-wear associated with hand-throwing and hand-thrusting spear motions on experimental Levallois points. These sets of experiments employed different experimental variables and utilised alternate recording procedures and equipment (Table 4-1).

The first set of experiments were designed to (i) document macroscopic and microscopic diagnostic use-wear types and patterns in relation to throwing and thrusting spear motions, (ii) assess three specific hafting types (female, juxtaposed, flat) and their reliability, and (iii) test the effectiveness of throwing and thrusting stone-tipped spears when hand-delivered by human participants in relation to penetration depth (Table 4-1). This is because, at the time of experimentation (July 2015), no experiments had ever tested the effectiveness of Middle Palaeolithic stone-tipped spear replicas when delivered by hand (but see Frison, 1989 for Clovis point spear experiments). The efficiency of Middle Palaeolithic stone-tipped spears mounted with Levallois points and delivered by hand was therefore unknown. In order to test the efficiency of these weapon types, controlled yet realistic variables (e.g. realistic replicas of archaeological artefacts) were chosen for the performance of the spear experiments (as indicated in Section 4.2.1 and Table 4-1). Representative wooden spear shafts replicating Schöningen spears (Thieme, 1997) were mounted (using three different hafting systems, see Section 4.3.2.2) with Levallois points flint replicas, and were hand-thrown or hand-thrust into animal targets by trained human participants until damage was visible (see Section 4.2.1).

The second set of experiments (July 2016) was fashioned based on the results of the first set of experiments.

After having verified the effectiveness of stone-tipped Levallois spears in hand-delivered throwing and thrusting activities (see Section 4.3.5 and CHAPTER 5), the second set of experiments, as well as investigating the formation of diagnostic use-wear traces associated with hand-throwing and hand-thrusting spear motions, aimed to investigate the kinematics of hand-delivered spear mechanics and test the influence that ballistic parameters (such as impact velocities, *KE*, impact location) can have on the formation of projectile use-wear traces (Table 4-1). Therefore, controlled variables (i.e. standard replicas of archaeological artefacts) were chosen for the performance of the spear experiments (as indicated in Section 4.3.5 and Table 4-1). Standardised wooden spear shafts replicating Schöningen spears II (Schoch et al., 2015; see Section 4.3.2.1) were produced and mounted (using a single hafting system,

see Section 4.3.2.1) with Levallois points flint replicas (see Section 4.4.1). Each spear was hand-thrown or hand-thrust only once into animal targets by trained human participants (see Section 4.3.5). High-speed videos and spear accelerations were recorded (with accelerometer and high-speed camera devices), with penetration depth, to analyse the human performance and to record the ballistic parameters (see Section 4.3.5).

The third set of experiments was designed as a control sample, to observe macroscopic and microscopic use-wear traces on hafted and hand-held Levallois points used to complete non-weaponry tasks, e.g. butchering activities (Table 4-1). The primary purpose was to differentiate wear traces produced during projectile activities from other use-wear traces produced in non-weaponry activities (see Section 4.5).

All three sets of experiments were realised at the Steinzeitpark Dithmarschen Open-air Museum (Albersdorf, Germany). Partnership with the Steinzeitpark museum facilitated collaboration with highly skilled craft people, with a wealth of experience in manipulating prehistoric raw materials and a high level of expertise and “know-how” in the production and utilisation of stone tools and ancient weapons.

Table 4-1. Overview of the three sets of experiments with the specification of the dataset for each set (LPs: experimental Levallois points).

Experimental set	Experiment type	Number of experiments	Purpose of the experiments	Recorded variables	Recording system
First set of experiments	Hand-delivered throwing stone-tipped spears	6	<ol style="list-style-type: none"> Formation of diagnostic use-wear Effectiveness of hand-delivered stone-tipped spears 	<p>Raw material artefacts and morphometric artefacts: Levallois point flint replicas (4.3.1), statistically tested (4.3.1)</p> <p>Shaft type and shaft dimension: realistic replicas of Schöningen spears I-III (Thieme, 1997; 4.3.2.1)</p> <p>Hafting system: 3 types of fore-shafts (4.3.2.2), 2 types of adhesives (4.3.2.3)</p> <p>Delivery system: hand-delivered by trained human participants (4.3.4)</p> <p>Distance range: 5 m</p> <p>Target: freshly killed animal carcasses (4.3.3)</p> <p>Number of shots: maximum of 5</p>	<p>Field forms</p> <p>Penetration depth (in cm)</p> <p>Impact location</p> <p>Pictures and standard videos</p>
	Hand-delivered thrusting stone-tipped spears	6	<ol style="list-style-type: none"> Formation of diagnostic use-wear Effectiveness of hand-delivered stone-tipped spears 	<p>Raw material artefacts and morphometric artefacts: Levallois point flint replicas (4.3.1), statistically tested (4.3.1)</p> <p>Shaft type and shaft dimension: realistic replicas of Schöningen spears I-III (Thieme, 1997; 4.3.2.1)</p> <p>Hafting system: 3 types of fore-shafts (4.3.2.2), 2 types of adhesives (4.3.2.3)</p> <p>Delivery system: hand-delivered by trained human participants (4.3.4)</p> <p>Distance range: 2 m</p> <p>Target: freshly killed animal carcasses (4.3.3)</p> <p>Number of shots: maximum of 5</p>	<p>Field forms</p> <p>Penetration depth (in cm)</p> <p>Impact location</p> <p>Pictures and standard videos</p>

Second set of experiments	Hand-delivered throwing stone-tipped spears	22	<ol style="list-style-type: none"> 1. Formation of diagnostic use-wear 2. Recording of ballistic parameters (i.e. acceleration, impact velocities, <i>KE</i>, and momentum) 	<p>Raw material artefacts and morphometric artefacts: Levallois point flint replicas (4.3.1), statistically tested (4.3.1)</p> <p>Shaft type and shaft dimension: standard replicas of Schöningen spears II (Schoch et al., 2015; 4.4.2.1)</p> <p>Hafting system: 1 type of fore-shaft and 1 type of adhesives (4.4.2.2)</p> <p>Delivery system: hand-delivered by trained human participants (4.4.4)</p> <p>Distance range: 5 m</p> <p>Target: freshly killed animal carcasses (4.4.3)</p> <p>Number of shots: 1</p>	<p>Field forms</p> <p>Accelerometer (acceleration)</p> <p>High-speed videos (n=10)</p> <p>Penetration depth (cm)</p> <p>Impact location</p> <p>Pictures and standard videos</p>
	Hand-delivered thrusting stone-tipped spears	18	<ol style="list-style-type: none"> 1. Formation of diagnostic use-wear 2. Recording of ballistic parameters (i.e. acceleration, impact velocities, <i>KE</i>, and momentum) 	<p>Raw material artefacts and morphometric artefacts: Levallois point flint replicas (4.3.1), statistically tested (4.3.1)</p> <p>Shaft type and shaft dimension: standard replicas of Schöningen spears II (Schoch et al., 2015; 4.4.2.1)</p> <p>Hafting system: 1 type of fore-shaft and 1 type of adhesives (4.4.2.2)</p> <p>Delivery system: hand-delivered by trained human participants (4.4.4)</p> <p>Distance range: 2 m</p> <p>Target: freshly killed animal carcasses (4.4.3)</p> <p>Number of shots: 1</p>	<p>Field forms</p> <p>Accelerometer (acceleration)</p> <p>High-speed videos (n=10)</p> <p>Penetration depth (cm)</p> <p>Impact location</p> <p>Pictures and standard videos</p>
Third set of experiments	Butchering knife	8	<ol style="list-style-type: none"> 1. Formation of diagnostic use-wear 	<p>Raw material artefacts and morphometric artefacts: Levallois point flint replicas (4.3.1)</p> <p>Hafting presence: 1. Hafted, 2. Hand-held</p> <p>Hafting type: (if hafted) 1 type of fore-shaft (female) and 1 type of adhesive (commercial tar)</p>	<p>Field forms</p> <p>Pictures and standard videos</p>

			<p>Time of utilisation: in minutes</p> <p>Contact material: 1. Roe deer, 2. Salmon, 3. Wild boar</p> <p>Contact material specification: (the material that the tool came into contact with during the experiment) 1. Skin, 2. Hair, 3. Flesh (any meat material), 4. Bone</p> <p>Contact material freshness: 1. Fresh (12 hours after culling)</p> <p>Motion: 1. Cutting, 2. Sawing, 3. Scraping, 4. Shaving, 5. Multiple (with indication)</p> <p>Direction of the motion to the active edge: 1. Longitudinal 2. Transversal 3. Crosswise 4. Multiple (with indication); The direction of the motion: 1. Unidirectional, 2. Bidirectional 3. Multiple (with indication)</p> <p>Contact angle: (the angle formed by the tool and the contact material) 1. 0-30°, 2. 31-60°, 3. 61-90°, 4. 90°, 5. Multiple (indication)</p> <p>Prehensive part of the tool: indication of the part of the tool which was hand-held or hafted (using the Loci/Locus identification system, see Section 2.3).</p> <p>Active part of the tool: indication of the part of the tool which in contact with the contact material (using the Loci/Locus identification system, see Section 2.3).</p>	
Total		60		

4.2.1 Experimental dataset

The realisation of the three sets of experiments (presented above) generated a large experimental dataset, composed as follows (Table 4-2):

- A large and systematic use-wear reference collection designed for the investigation of projectile use-wear traces. It counted n=60 experimental flint Levallois points used in hand-delivered stone-tipped spear experiments (n=52) and butchering experiments (n=8). It also included the high-resolution dental casts of the experimental Levallois points realised before utilisation (see Section 3.1 and Table 4-2).
- A spear shafts collection, resulting from the manufacture of the experimental spear shafts used during the first and second sets of experiments, which counted n=12 experimental wooden spear shafts (Table 4-2).
- A database of acceleration records, high-speed videos, and penetration measurements recorded during the performance of hand-delivered stone-tipped spears (Table 4-2). This counted n=40 acceleration records (n=22 throwing acceleration and n=18 thrusting acceleration, Table 4-2; see also accompanying files, accelerometer data on the USB stick), and n=20 slow-motion videos (n=10 for throwing experiments and n=10 for thrusting, Table 4-2; see also Section 4.3.5 and accompanying files, slow-motion videos on the USB stick).

The n=60 Levallois point flint replicas, forming part of the use-wear reference collection, were used for the following experiments (Table 4-2):

- N=28 hand-delivered throwing stone-tipped spear experiments (accomplished during the performance of two different sets of experiments, see Section 4.2).
- N=24 hand-delivered thrusting stone-tipped spear experiments (accomplished during the performance of two different sets of experiments, see Section 4.2). The slight difference in the number of

throwing and thrusting experiments is due to the missing shots of the throwing experiments.

- N=8 butchering knife experiments (accomplished during the performance of the third set of experiments, see Section 4.2).

Additionally, before the utilisation process (i.e. the experiments), three high-resolution, silicone-based, and polyurethane-based dental casts were manufactured for each experimental Levallois point, replicating a negative and positive impression of the distal tip and left and right edges (see Section 3.1 for details). As a result of this protocol of analysis, the high-resolution dental casts tripled the number of experimental observations, as each tool was represented by the flint tool itself and three high-resolution dental casts (Table 4-2). Therefore, the final use-wear collection counted n=60 experimental Levallois points and n=180 high-resolution dental casts (Table 4-2), which were all microscopically examined.

Table 4-2. Overview of the experimental tool datasets.

Experiment type	Experimental Levallois points	High-resolution resin casts (before utilisation)	Acceleration records	Videos		Spear shaft
				Slow motion	Standard	
Hand-delivered stone-tipped throwing spear experiments	28	84 (3 casts per tool)	20	10	28	4
Hand-delivered stone-tipped thrusting spear experiments	24	72 (3 casts per tool)	20	10	24	8
Butchering knife experiments	8	24 (3 casts per tool)	-	-	8	-
Total	60	180	40	20	60	12

4.3 First set of experiments: hand-delivered throwing and hand-delivered thrusting stone-tipped spears

The first set of experiments occurred in July 2015, with twelve replicas of Levallois points mounted as stone-tipped spears (n=6 used in throwing experiments and n=6 used in thrusting experiments). The experiments' purpose was to assess a preliminary set of research questions:

1. Can macroscopic trace types (such as diagnostic impact fractures and edge-damage), frequencies, and patterns be used to distinguish between hand-delivered throwing and thrusting spear motions (using Levallois points as a tool morpho-type)?
2. Can microscopic trace types (such as polish, microscopic linear impact traces [MLITs], and striations), frequencies, and patterns be used to distinguish between hand-delivered throwing and thrusting spear motions (using Levallois points as a tool morpho-type)?
3. Were Middle Palaeolithic stone-tipped spear replicas effective hunting weapons when used for hand-delivered throwing and thrusting spear motions?
4. Can macroscopic and microscopic use-wear traces distinguish between specific and different hafting arrangements (i.e. female, juxtaposed, and flat hafting slot types)?

Specifically:

5. Were flint Levallois points effective projectiles (effectiveness expressed by penetration depth, in cm) for hand-delivered throwing and thrusting stone-tipped spears?

Accordingly, in order to verify use-wear formation and the effectiveness of Middle Palaeolithic hand-delivered throwing and thrusting spears, controlled yet realistic sets of variables were tested for each group of experiments (see Table 4-1). Penetration depth (in cm) and impact location were recorded for each shot in order to assess the efficiency of the spear systems.

Performance of the experiments

Flint replicas of Levallois points modelled after the ones found in selected archaeological sites were manufactured (see Section 4.3.1). Among these, twelve were chosen for the first set of experiments and were statistically tested (see Section 4.3.1.1 for details). Four realistic shaft replicas of selected Schöningen spears (Thieme, 1997) were manufactured (see Section 4.3.2.1). From these, one shaft replica was used to execute hand-delivered throwing spear experiments and one to execute hand-delivered thrusting spear experiments, the other shafts were produced and kept as reserve shafts in case of breakage or internal damage of the first shaft (see Section 4.3.2.1). To maintain the spear shaft as an experimental constant (e.g. standard weight, dimensions, and shape) and to easily switch the projectiles during the experiments, the 12 Levallois points replicas were hafted longitudinally onto shaft connectors, i.e. wooden fore-shafts (see Section 4.3.2.2 and Figure 4.12). Finally, the n=12 experimental Levallois points (inserted into the fore-shafts) were connected into the main spear shafts during the experiments. The experimental Levallois points were randomly assigned to two experimental sub-populations (Table 4-1):

- N=6 hand-thrown stone-tipped spear experiments.
- N=6 hand-thrust stone-tipped spear experiments.

All the spears were hand-thrown and hand-thrust by trained human participants (see Section 4.3.4 and Figure 4.1, Figure 4.2). Before each set of experiments, the participants were verbally briefed, and they were allowed to have two practice shots (with a spear that was not included in the final dataset). Both participants were right-handed and executed the experiments barefooted (Figure 4.1 and Figure 4.2).



Figure 4.1. First set of experiments: a sample of throwing experiment.



Figure 4.2. First set of experiments: a sample of the thrusting experiments.

The first experiments to be performed were the hand-delivered throwing experiments (11th July 2015). They were all performed by WP a trained participant (see Section 4.3.4).

The stone-tipped spears were thrown until visible damage (discernible by the naked eye) was observed on the experimental Levallois points (up to a maximum of 5 shots). The participant (WP) performed the first three throwing experiments (4 shots in total during a 20-minute trial) before having a break (20 minutes to minimize fatigue issues), and the last three throwing experiments (10 shots in total during 45 minutes in total) after the break. WP performed the experiments mimicking the gestures he would have completed in a real hunting scenario. His hypothetical purpose was to “kill and knock down the animal” (WP personal communication, 11 July 2015), replicating as closely as possible the hunting gestures he perpetuated during his experience in real hunting alongside

with the Namibian bushmen (see Section 4.3.4). For the throwing experiments, a freshly killed roe deer carcass was used as a target (see Section 4.3.3).

Two days after (13th July 2015), the hand-delivered thrusting experiments were performed. All thrusting experiments were executed with two-hands standing movements, by IP a trained participant (see Section 4.3.4).

The stone-tipped spears were thrust until visible damage (discernible by the naked eye) was observed on the experimental Levallois points (up to a maximum of 5 shots). The participant performed the first three thrusting experiments (4 shots in total during a 15-minute trial) before having a break (15 minutes to minimize fatigue issues), and the last three thrusting experiments (3 shots in total during 10-minute trial) after the break. For the thrusting experiments, a second freshly killed roe deer carcass was used as a target (see Section 4.3.3).

The throwing stone-tipped spears were all shot into the fresh animal carcasses from a 5 m distance (Figure 4.1). The thrusting stone-tipped spears were stabbed from a 2 m distance (Figure 4.2). Both distance ranges complied with the suggested distance for hand-delivered ethnographic spears (Churchill, 1993; Hughes, 1998) and previous projectile spear experiments (Schmitt et al., 2003; Shea et al., 2001; Sisk and Shea, 2009; Iovita et al., 2016; Sano et al., 2016; Pargeter et al., 2016). Penetration depth (in cm), from the entrance hole until the distal end of the spear, were recorded for each shot (Figure 4.3), excluding the instances in which the spear missed the target.

The weather conditions during the performance of the experiments (11th-13th July 2015) were dry and mild, with a fair amount of clouds, low-wind, and a maximum temperature of between 12-14 °C.



Figure 4.3. Spear penetration after a throwing experiment (experiment code: TH-32).

Video and slow-motion pictures (at 1/200s) recorded the execution of each throwing and thrusting experiment, along with human movements.

Field-forms were used to record each experiment and individual shot (Figure 4.4). The forms recorded the following fields: experiment type, date, experiment ID, individual shot number, tool ID, shaft code, hafting code (slot hafting type plus adhesive type), impact location, penetration (in cm), wound dimension (length*width in cm), notes, and any occurrences of de-hafting (Figure 4.4). The forms also supported the use-wear analyst during the microscopic observation phase in the lab. After the experiments, all forms were digitised.

Experiment type: Throwing						Date: 12-07-2015			
Experiment Code: TH-32						Experimenter: WP			
Shot	Exp ID	Tool ID	Shaft Code	Hafting Code	Impact location	Penetration (cm)	Wound (cm)	Note	De-hafting
1	TH-32	32	1	Flat+R	Stomach	49	4.5*1	The spear hit and penetrated the animal's guts	No
2	TH-32	32	1	Flat+R	Spine	7	3*0.8	The spear hit and penetrated the spine before bouncing off	Yes
3	TH-32	32	1	Flat+R	Rib cage	25	4*1.2	The spear hit and penetrated the rib cage, breaking two rib bones (6th and 7th ribs)	No
4	TH-32	32	1	Flat+R	Spine	2	2*0.9	The spear hit and penetrated the spine before bouncing off	Yes
—	—	—	—	—	—	—	—	—	—

Figure 4.4. Field-form used for the recording of each hand-delivered throwing or thrusting spear experiment, first set of experiments (experiment code: TH-32).

Below each experimental variable employed in the first set of experiments is described.

4.3.1 Experimental variable: Levallois points flint replicas

The production of experimental Levallois points was the first step of the experimental programme. The experimentation for the reproduction of Levallois point flint replicas took place at the Department of Archaeology, University of Exeter, during November 2014 in collaboration with MK⁴, a skilled flintknapper from Norway (Figure 4.5).



Figure 4.5. MK and the author during the knapping process for the reproduction of the experimental Levallois points.

As realistically as possible, the Levallois points were manufactured using the same technological reduction sequences employed by Neanderthals at Abris du Maras (La Porta, 2013; Moncel et al., 2014) and Arma Delle Manie (Cauche, 2002,2012; Santaniello, 2011; Leger, 2012) archaeological sites (see also Sections 8.3.7.1 and 8.2.8.1) (Figure 4.7).

A total of 80 Levallois points (for the performance of the first, second, and third sets of experiments) were freshly knapped (Figure 4.5) and immediately inserted into separate plastic bags to avoid friction and formation of possible wear. They were produced by direct percussion with hard-stone hammers (Figure 4.6). They were mostly un-retouched (only 12 points out of 80 were retouched to adjust the lateral convergences of the point), (Figure 4.7). The retouch type, if applied, was direct, marginal, short, and semi-abrupt (Inizan et al., 1999, p. 87). After knapping, all experimental points were moulded and cast, photographed, measured for the recording of techno-morphological attributes

⁴ Morten Kutschera's Prehistoric Arts and Crafts.

(see CHAPTER 2), and then cleaned and observed with a stereomicroscope to check possible production wear (see CHAPTER).



Figure 4.6. Knapping process and hammerstone used.



Figure 4.7. Sample of the experimental Levallois points after knapping.

Choice of raw materials

The experimental Levallois points were all made of flint. This because flint is a good isotropic material and it presents similar mechanical properties (such as elasticity, conchoidal fracturing and compressive strength) to many other siliceous rocks such as silcrete, quartz and quartzite. Therefore, the selection of flint as the experimental raw material permitted general comparisons to other siliceous rock types. Flint was also selected for the experimental artefacts because the archaeological Levallois point assemblages selected for this research were mostly made on local flint (from regional outcrops in the Ardèche [France] and Liguria [Italy], see CHAPTER 8). However, in order to reduce transport costs and keep the transportation of the raw material (100 kg) practical and affordable, the flint used for the experimental replications was purchased from a single outcrop in the UK (i.e. Upper Cretaceous flint, see below). Therefore, the Cretaceous English flint used for the replication of the experimental Levallois points was a different type of flint than the one employed by Neanderthals to make the archaeological tools of Abri du Maras (i.e. flint from the Ardèche region, see CHAPTER 8), and a different type of siliceous rock than the ones employed by Neanderthals at the Arma Delle Manie site (i.e. siliceous limestone rocks, see CHAPTER 8). Although it is acknowledged that certain specific differences exist among different types of flint (such as grain-size or degree of wear), these are not of a high order of magnitude and did not significantly impact on the thesis results. As demonstrated in CHAPTER 6 and 7, the experimental flint Levallois points showed comparable mechanical and abrasive traces both to the traces observed on the archaeological tools at both sites (e.g. mechanical fractures, polishes, and linear traces; see CHAPTER 8 and 9), and to traces reported by previous experiments using flint and other siliceous rocks (De la Peña et al., 2018; Taipale and Rots, 2018; Pargeter et al., 2016; Sano and Oba, 2015; Pargeter, 2013; Fischer et al., 1984).

Provenance of the raw materials

The flint used for the experimental Levallois points came from the outcrop exploited by Somborne Chalk Quarry (NGR: SU341286, Hampshire, UK). The

flint nodules originated from the Upper Cretaceous white chalk layers exposed at the quarry. The nodules' cortex was entirely covered with chalk (2-5 mm thick, Figure 4.6), while the internal texture presented a fine-grained size (to the naked eye). The flint presented good knapping properties (tested by the author prior to the purchase). During experimentation, however, two sub-types of flint were depicted. Subtype 1 was black in colour, with a microscopic fine-grain size and a dull appearance (observed at 100x with an optical light microscope with incident light [OLMil]), without impurities (fossils or flaws) (Figure 4.8). Subtype 2 was light grey in colour, with a microscopic medium-grain size and bright appearance (observed at 100x with OLMil), with sporadic microfossils and flaws (Figure 4.9).

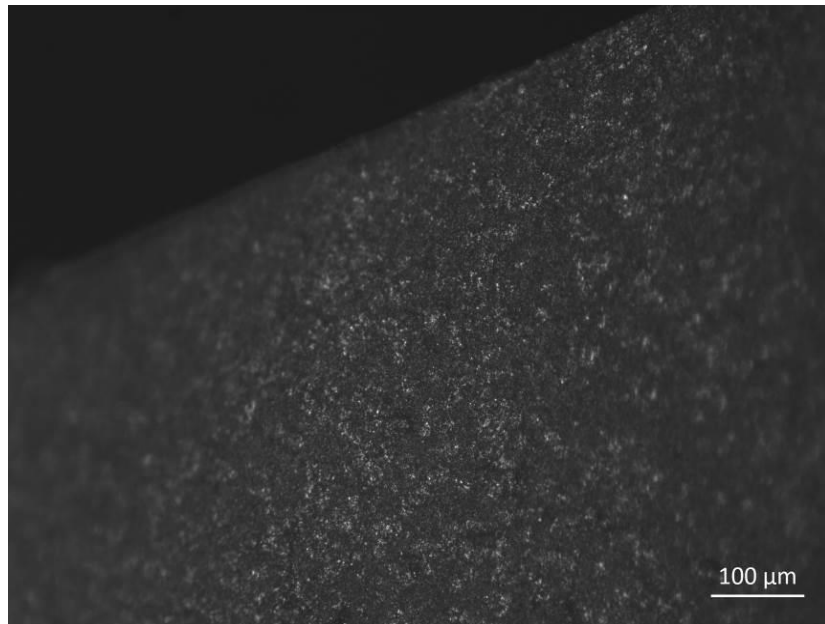


Figure 4.8. Flint Levallois point – raw material subtype 1. Picture OLMil at 100x.

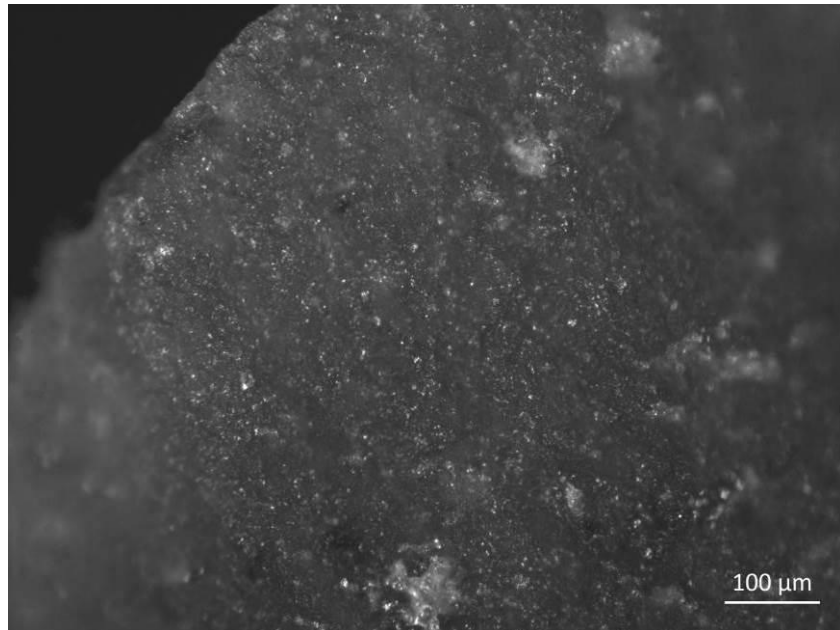


Figure 4.9. Flint Levallois point – raw material subtype 2. Picture OLMil at 100x.

However, the raw material provenance was sourced from the same geological outcrop and level in order to maintain the internal consistency of the flint, the nodules showed some variances (such as colour and the presence of microfossils), which are characteristic of the internal and individual variability of each raw material core.

4.3.1.1 Pre-experiment statistical analysis of experimental Levallois points

After the production, the experimental Levallois points were randomly assigned to three different experimental sub-populations: (i) Levallois points for throwing experiments (n=28); (ii) Levallois points for thrusting experiments (n=26); and (iii) Levallois points for butchering experiments (n=8), (the remaining ones [n=20] were kept as substitutes in case of breakage during the laboratory or transport activities and/or for possible future experiments). The three groups were kept constant throughout the entire experimental programme.

As it has been argued that the morphological variability of experimental stone tools can influence the formation of use-wear traces and the performance of projectile experiments (Odell and Cowan, 1986; Rots and Plisson, 2014; Sano and Oba, 2015), the two sub-populations of Levallois points (i.e. throwing and thrusting experiments) were statistically tested to verify whether or not they showed significant differences in the morphometric attribute values. Six morphometric attributes were selected: maximum technological length, maximum technological width, maximum technological thickness, TCSA and TCSP values, and weight (Table 4-3). They were carefully chosen according to the internal morphological variability of the experimental Levallois points, and considering previous publications (Inizan et al., 1999, Shea, 2006; Sisk and Shea, 2009).

The SPSS statistical package (IBM SPSS Statistic 24 Software) was used for all statistical analysis. Parametric statistical tests were utilised to determine the statistical significance of normally distributed data whereas when the data were not normally distributed or showed different variances, analysis engaged with non-parametric tests. In this case, the statistical significance of the difference among the morphological attributes for the experimental Levallois points used in throwing, thrusting, and butchering experiments was assessed by using the independent Student's t-test (as the data were normally distributed and the homogeneity of variance was not statistically significant).

Table 4-3. Morphometric attributes of experimental Levallois points used in throwing and thrusting experiments, and the results of the Student's t-test results (T-test).

Morphometric values	Throwing (n=28)	Thrusting (n=24)	T-test results
Length			
Mean	76.10714	72.58333	t= 1.107,
Max	104	100	p 0.274
Min	60	50	
SD	10.44328	12.51752	
Width			
Mean	44	39.95833	t= 1.741,
Max	62	53	p 0.088
Min	30	22	
SD	8.632411	7.997169	
Thickness			
Mean	10.96429	11.0625	t= -0.090,
Max	19	18	p 0.928
Min	4	4.5	
SD	3.834368	4.000849	
P Weight			
Mean	34.92857	31.70833	
Max	73	63	
Min	15	12	
SD	14.87212	13.04	
TCSA			
Mean	251.3929	227.6042	t=0.738,
Max	558	423	p 0.464
Min	60	58.5	
SD	124.7274	104.5709	
TCSP			
Mean	132.7257	120.7086	t=1.715,
Max	187.2996	159.1697	p 0.093
Min	90.13319	66.72136	
SD	26.07952	24.11227	

Overall (Table 4-3), the statistical results showed that the morphology of the experimental throwing and thrusting Levallois points were not statistically different. There was no statistically significant difference in length (t=1.107, p-value= 0.274; Table 4-3 and Figure 4.10), width (t=1.741, p-value= 0.088; Table 4-3 and Figure 4.10), thickness (t=-0.090, p-value=0.928; Table 4-3), TCSA (t=0.738, p-value= 0.464; Table 4-3 and Figure 4.11), and TCSP (t=1.715, p-value=0.093; Table 4-3 and Figure 4.11) mean values between throwing and thrusting Levallois points sub-populations. As a result, it was possible to conclude that the morphological variability was not sufficiently significant to

influence the formation of use-wear traces or the performance of the experiments.

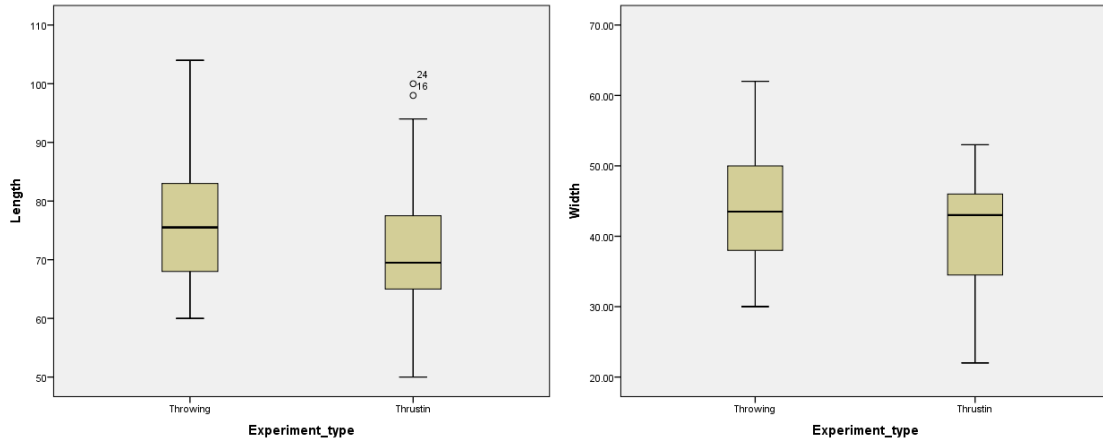


Figure 4.10. Boxplots of the maximum technological length (left) and the maximum technological width (right) values for TH and TR experimental Levallois points.

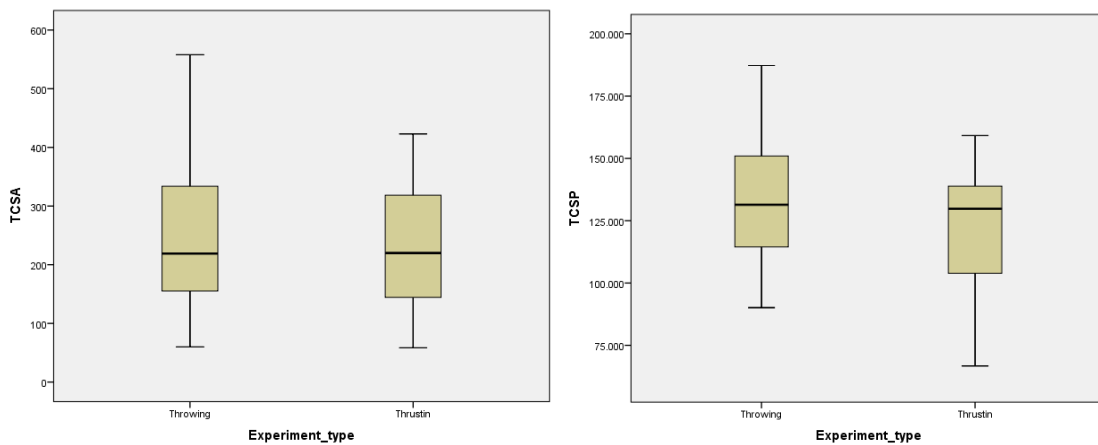


Figure 4.11. Boxplots of TCSA (left) and TCSP (right) values for TH and TR experimental Levallois points.

4.3.2 Experimental variable: spear system

After the production and statistical tests, the experimental Levallois points were used to manufacture the stone-tipped spears. Each experimental stone-tipped spear used in the first set of experiments was composed by the following parts (Figure 4.12):

- a) The main wooden spear shaft,

- b) The fore-shaft connecting the spear shaft and the experimental Levallois point,
- c) The experimental Levallois point as a spear-head.



Figure 4.12. Experimental stone-tipped spear setup.

Below each experimental variable is explained and discussed.

4.3.2.1 Spear shaft replicas

For the first set of experiments, four experimental wooden spear shafts were manufactured (Figure 4.13 and Figure 4.15).

Spear shaft replicas were, in this thesis, designed to match published data concerning the wooden spear shafts from the Schöningen site (Thieme, 1997). Although it is acknowledged that Schöningen spears were untipped wooden shafts (Schoch et al., 2015; Thieme, 1997) and that the addition of a stone projectile point required a necessary adaptation of the distal end of the shaft, in the absence of direct evidence of stone-tipped spears in the Middle Palaeolithic record (see CHAPTER 1), the Schöningen's evidence was the highest in terms of the number of wooden spears that were complete, well-preserved, and well-published (Schoch et al., 2015; Thieme, 1997). Moreover, one of the main purposes of this thesis was to test the effectiveness of Middle Palaeolithic stone-tipped spears. Such spears have previously been considered not to be effective due to their heavy mass and thick shafts (see Table 4-5; Churchill, 1993; Churchill et al., 1996; Shea, 2006; Churchill and Rhodes, 2009).

Therefore, the choice and use of Schöningen-type wooden shafts, rather than other models (e.g. ethnographic examples), ensured that the thesis experiments could test the main aerodynamic characteristics of Middle Palaeolithic-type spears. While the Schöningen spears (MIS 9) are untipped, it is important to note that the Schöningen spear shafts are comparable to the length and diameter values of ethnographic throwing and/or thrusting spears (Table 4-4; Milks et al., 2016; Churchill, 1993; Oakley et al., 1977). The use of the Schöningen spears as a shaft model was therefore felt to provide a robust basis for experimentally assessing the relationships between kinetic energy, weight and general performance.

Table 4-4. Measurements of Schöningen spears shafts and other ethnographic spears (data from ¹Thieme, 2007; ²Oakley et al., 1997; ³Hughes, 1998).

Spear type	Length (m)	Maximum diameter (mm)	Mass (g)
Schöningen spears ¹	1.82-2.30	30-36	ND
Ethnographic thrusting spears ²	1.84-2.71	24-30	283-1358
Ethnographic throwing spears ²	1.58-2.61	12-23	113-453
Ethnographic thrusting spears ³	1.67-2.25	21-23	1019
Ethnographic throwing spears ³	2.66-4.00	13-23	614

Accordingly, four realistic shaft replicas of Schöningen spears I-III were manufactured (Table 4-5 and Figure 4.15). The spear shafts' dimensions replicated published measurements from Schöningen spears I-III in Thieme (1997), which were the only data available at the time of the first set of experiments (July 2015⁵). The spear shafts had a length of 210 cm and a maximum diameter of approximately 30-32 mm nearby the point of balance (see Table 4-5). They weighed between 512 g and 1010 g ($M=833$, $SD=184$;

⁵ Schoch et al., 2015 was published only a few weeks after the execution of the experiments.

Table 4-5). The different values (diameter and weight) between the shafts (Table 4-5) were due to the internal variation of the wood and morphological differences.

Table 4-5. Measurements for the realistic spear shaft replicas of the first set of experiments in comparison to the published measurements of Schöningen spears I-III from Thieme (1977). All measurements were taken from the front (distal end) with a digital calibre.

Shaft ID	Length (m)	Dia. at distal end / front (cm)	Dia. at 50 cm (cm)	Dia. at 90 cm (cm)	Dia. at 1200 cm (cm)	Dia. at 1500 cm (cm)	Dia. at 2000 cm (cm)	Mass (g)	Point of balance (cm from distal end)
Schöningen spears I-III (data available at the time of the experiments)	1.82-2.30		30-36	29-47					
E1-TH (employed)	2.1	22	32	30	29	25	20	512	112
C1-TR (employed)	2.1	24	36	31	29	28	23	1010	121
R1 (back-up)	2.1	24	36	32	31	28	20	862	99
D1 (back-up)	2.1	24	32	33	30	26	20	702	95

These replicas were manufactured with the intent of recreating realistic shaft replicas by following the natural anatomical curve of the trunk (i.e. without removing the characteristic bends of the spruce). The shafts were thus handmade using hand-tools, and no planning or smoothing of the wooden shaft surface was done (Figure 4.13).

The spear shafts were all made of German spruce (*Picea abies*). The wood was offered by the ownership management of Albersdorf forest (Germany). The trees grew in a natural forest environment in mild, wintery conditions. The freshly cut trunks (n=4) were de-barked (bark stripped off) by hand and then carved against the fibres (with metal hand-tools), following the natural anatomical curve of the trunk to reach the required diameter (Figure 4.13). They were then bent on an open low-fire of softwood logs (fire temperature not

recorded) to reduce the natural curvatures of the wood. Each wooden shaft was held to the fire at the exact point of curvature and left to warm up for around 5-8 minutes. Immediately afterwards, the curved part was bent between two wooden poles to straighten the shaft. The heat of the fire allowed the wood to bend without provoking internal breakages. This process was repeated for all curved parts of the four shafts (for a total of approximately 2 hours of work).



Figure 4.13. Shaft manufacturing process, first set of experiments.

After the manufacturing process, a 2.5 cm hole was carved into the distal end of each shaft, in order to create a slot through in which the fore-shafts could be inserted (Figure 4.14). The distal end of each shaft was then reinforced and

wrapped with a commercial sinew⁶ (75 cm length) coated with commercial tar (5 g), to reinforce the shaft and prevent breakages during the execution of the experiments (as suggested by several craft people; Figure 4.14).

Once manufactured, the four shafts were randomly divided between hand-throwing and hand-thrusting spear experiments. Shaft E1 was randomly selected for the performance of the throwing experiments (Table 4-5). The second shaft (R1) was kept as a reserve shaft in case of breakage or internal damage of the first shaft (Table 4-5). Shaft C1 was randomly selected for the performance of the thrusting experiments (Table 4-5). The fourth shaft (D1) was kept as a reserve (Table 4-5). The use of a single shaft allowed the shaft dimension variables to be controlled during the experiments.



Figure 4.14. The reinforcement system for the spear shafts' distal ends. Commercial sinew was bound around the spear's distal end and fixed with commercial tar.

⁶ Plant binding materials (e.g. nettle cordages) might have been also been employed. However, commercial sinew was preferred as it was a homogeneous material.



Figure 4.15. Wooden spear shaft replicas produced for the first set of experiments.

4.3.2.2 Hafting arrangements: fore-shafts

As expressed in Section 4.2, the n=12 experimental Levallois points employed in the first set of experiments were inserted into the main spear shaft using wooden fore-shaft connectors.

Although wooden fore-shafts are not testified in the Middle Palaeolithic records, and currently there is no evidence of the use of fore-shaft elements among Neanderthal populations, fore-shafts were employed here to easily connect a single spear shaft with multiple experimental projectiles (see Figure 4.12) and to allow for swift changing of the stone tools during the experiments. Otherwise, each experimental point would have been mounted in a separate single shaft, significantly increasing the number of shafts to be produced, the time and costs of manufacturing and the experimental variability (as also endorsed by others who have previously employed fore-shafts in projectile spear experiments, see Pargeter et al., 2016; Iovita et al., 2014; Shea et al., 2001; Frison, 1989). Alternatively, each experimental point could have been hafted into the shaft during the experiments' performance, but this would have compromised the experimental performance and the freshness of the animal carcass.

However, seeing as the use of a fore-shaft could have affected the results of the throwing and thrusting experiments, a corroborative test was completed. Two extra spear shafts (not included in the dataset) were manufactured, as described in Section 4.3.2.1

- The first shaft was directly hafted with an experimental Levallois point (not included in the dataset), without the use of a fore-shaft.
- The second shaft was connected to an experimental Levallois point (not included in the dataset) through a wooden fore-shaft.

Both experimental spears were then thrown (from 5 m) and thrust (from 2 m) into a hay bale (2.5 m diameter) 5 times, respectively. Both spears hit and penetrated the hay bale each time. None of the experimental Levallois points (with or without the fore-shafts) de-hafted during the test and, therefore, fore-shafts were manufactured and used.

Fore-shafts

Each fore-shaft was made of spruce, and had a cylindrical-conical shape (Figure 4.16). They measured 75 mm in length, had a maximum diameter of 25 mm, and each weighed approximately 10 g (Figure 4.16). The fore-shafts were inserted into the spear shaft using a male-female interlocking system and were fixed with commercial tar (Figure 4.12 and Figure 4.16).

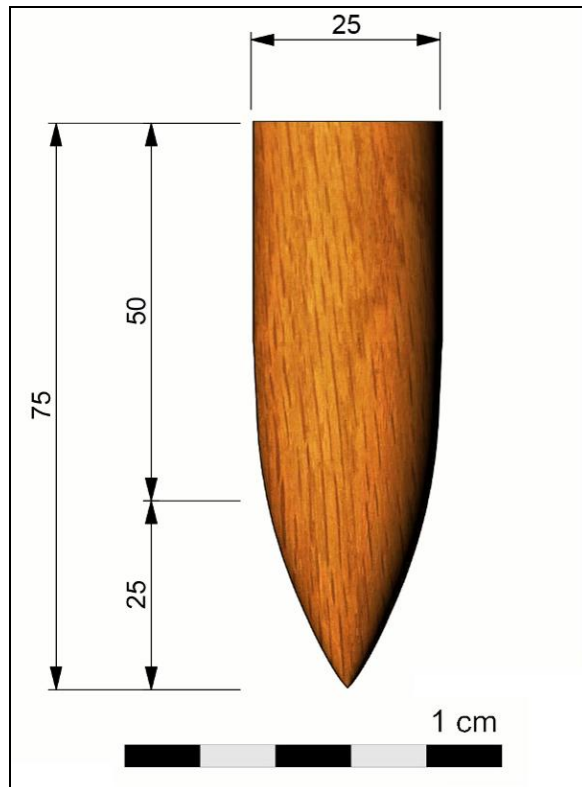


Figure 4.16. The wooden fore-shaft used in the first, second, and third sets of experiments. (Image La Porta and Tonelli).

The choice of the hafting slots (i.e. the shape of the distal termination of the fore-shaft arrangement that the stone tool must be inserted into, Figure 4.22), was carefully considered, bearing in mind three main constraints:

1. No Middle Palaeolithic examples of handle or shaft arrangements are known or well-published.⁷

⁷ Schoch et al. (2015, p. 217) stated that wooden objects, possibly used as hafting elements, were found at the Schöningen site, however, these are not illustrated or described in any published work.

-
2. The experimental Levallois point had to be firmly fixed into the fore-shaft to ensure maximum stability and penetration, but the fixation had to be also adapted to the morphology of the stone tool.
 3. It was difficult to experimentally haft these thick and often curved Levallois points in such a way that the directional stability of the points was optimal.

Therefore, during the first experimental set, three different types of hafting slots were tested to verify which hafting arrangements were the most effective in relation to the morphology of the Levallois points (Table 4-6).

1. Fore-shaft with a female haft slot type. The female haft type consists of a groove at the distal end of the shaft where the stone tool is inserted (Figure 4.17). This haft type requires the use of adhesives to fix the stone tool in the haft, and/or bindings. Ligature is not essential if an adhesive is used. It is one of the simplest hafting types, allowing a stable and straight fixation of the tool into the main shaft/fore-shaft axis. Female haft types are documented in the archaeological record (Bar-Yosef, 1987; Anderson-Gerfaud, 1983; but not in the Middle Palaeolithic), and they have been previously employed in projectile experiments (Fisher et al., 1984; Geneste and Plisson, 1990; Shea et al., 2001; Pargeter, 2007; Rots, 2010; Pargeter et al., 2016; Lombard and Pargeter, 2008).

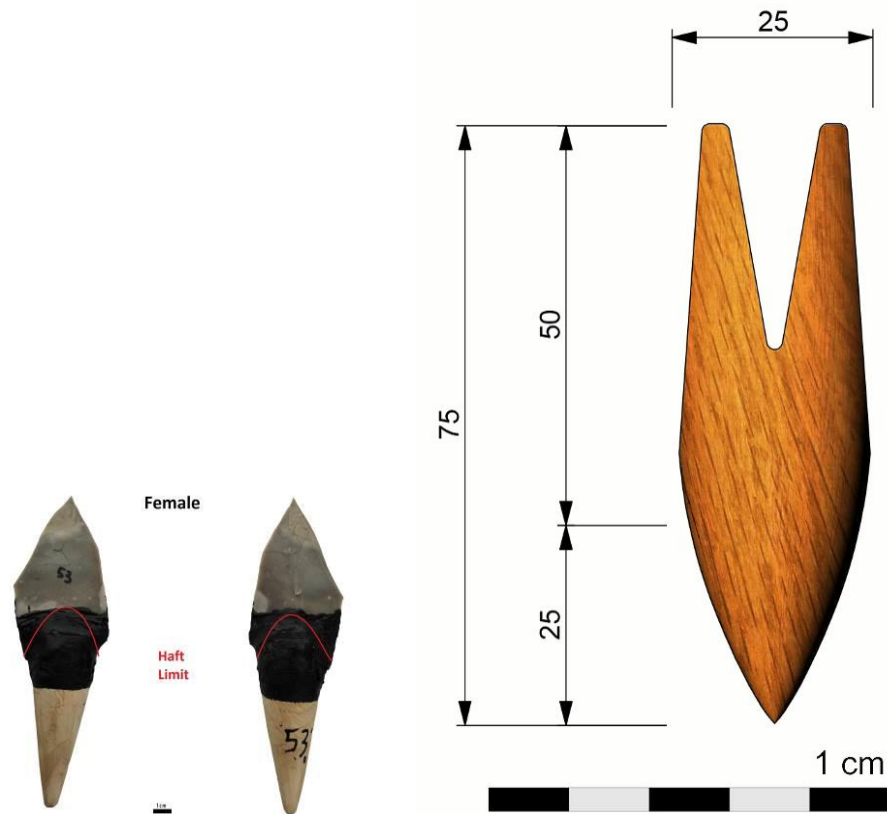


Figure 4.17. Left: Experimental Levallois point mounted in a female fore-shaft slot type and fixed with tar. Right: Technical drawing of a fore-shaft with a female haft slot type (lateral view, Image La Porta and Tonelli).

2. A fore-shaft with a juxtaposed haft slot type. The juxtaposed haft type consists of a shaft with an L shape at the distal end. The stone tool is located on the shaft and is fixed with adhesive and/or binding (Figure 4.18). This system permits thick and curved points to comfortably fit into a hafting slot. However, a stable fixation with a significant amount of adhesive (e.g. 20-40 g of commercial tar) and/or bindings is essential. Juxtaposed hafts are very rare in archaeological records (Rots, 2010, p. 10), but they have been employed in previous experiments (Fisher et al., 1984; Shea et al., 2001; Rots, 2010) and are documented in ethnographic examples of axes and adzes (Rots, 2010, p.10).

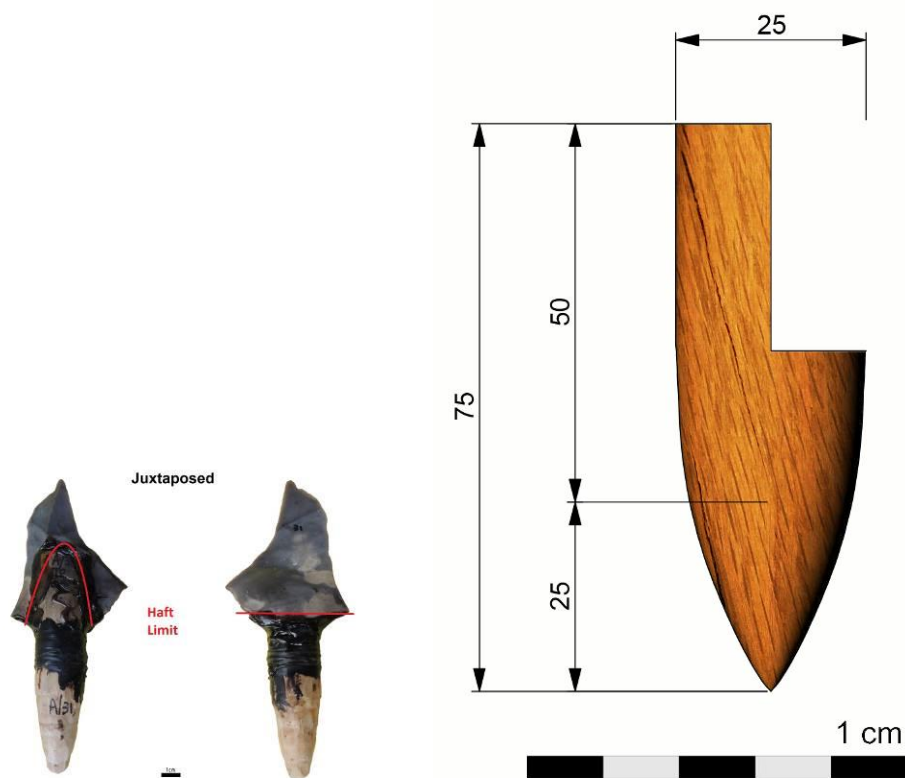


Figure 4.18. Left: Experimental Levallois point mounted in a juxtaposed fore-shaft type and fixed with tar. Right: Technical drawing of a fore-shaft with a juxtaposed haft slot type (lateral view, Image La Porta and Tonelli).

3. A fore-shaft with a flat haft type. The flat haft type consists of a flat distal end to the shaft, where the stone tool is attached only by a lump of adhesive over the head of the haft, which has neither a groove nor hole (Figure 4.19). The use of adhesive is compulsory in this hafting type, while the use of binding is optional. Flat haft types are suitable for the fixation of transversal or geometric microliths into arrow shafts, few of which have been preserved in archaeological records (Larsson and Sjöström, 2011).

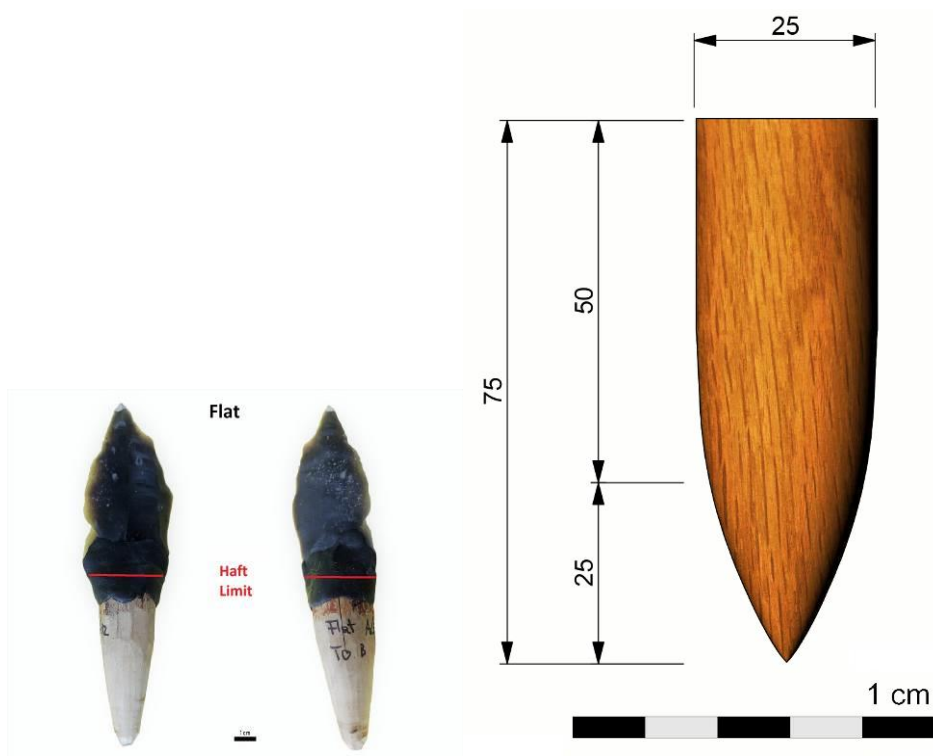


Figure 4.19. Left: Experimental Levallois point mounted in a flat fore-shaft type and fixed with tar. Right: Technical drawing of a fore-shaft with a flat haft type (lateral view, Image La Porta and Tonelli).

No binding (to bind the Levallois point into the fore-shaft) was adopted in the hafting system so as not to add another variable to the experiments.

4.3.2.3 Hafting arrangements: adhesives

During the first set of experiments, two types of adhesives were tested to haft the Levallois points into the fore-shafts:

- Resinous adhesives, produced (by WP and the author) with a recipe of 75% commercial spruce melted bain-marie (or heated water bath) in an aluminium pot and mixed with 25% of commercial beeswax, were tested (Figure 4.20). The percentage and combination of the two different ingredients were suggested by craft people working at the Steinzeitpark Museum (following decades of experience), but the percentage was also in agreement with previous experimental works (Coppe and Rots, 2017, p. 114). Here, resinous adhesives were tested, bearing in mind their regular utilisation as experimental variables in previous experiments testing projectile performance and use-wear traces.



Figure 4.20. Left: Production of the resinous adhesive recipe. Right: An experimental Levallois point hafted with the resin recipe glue (dorsal and ventral views).

-
- Tar adhesives, i.e. a commercial tar⁸ (Figure 4.21) was purchased and tested accordingly to Middle Palaeolithic evidence of the use of bitumen and tar adhesives among Neanderthal populations (Mazza et al., 2006; Koller et al., 2001; Grünberg, 2002; Boëda et al., 1996, 2002; Kozowyk et al., 2017; see also CHAPTER 1).



Figure 4.21. Left: A lump of tar. Right: An experimental Levallois point hafted with the commercial tar (dorsal and ventral views).

4.3.2.4 Final hafting arrangements

Finally, the 12 experimental Levallois points were first dipped into the selected adhesive (i.e. either tar or resin) up to their proximal part and then inserted into the selected fore-shaft applying a light pressure by hands, as follows (Table 4-6):

- N=4 Levallois Points were hafted into four fore-shafts with a female slot (Figure 4.22.c). Two Levallois Points were fixed with tar and two with resin.
- N=4 Levallois Points were hafted into four fore-shafts with a juxtaposed slot (Figure 4.22.a). Two Levallois Points were fixed with tar and two with resin.

⁸ The commercial tar was purchased from a German bush-crafter, who reported that the tar was composed by 80% birch-tar and 20% bitumen (Pallasch pers. communication, 2015).

- N=4 Levallois Points were hafted into four fore-shafts with a flat slot (Figure 4.22.b). Two Levallois Points were fixed with tar and two with resin.

These were then assigned to throwing and thrusting experiments respectively, as described in Table 4-6. The insertion of the fore-shafts into the main spear shafts required only a couple of seconds, and was done before the execution of each experiment.

The hafting process of the n=12 experimental Levallois points was supervised by WP and MC, two experts craft people, in collaboration with the author (see Section 4.3.4).

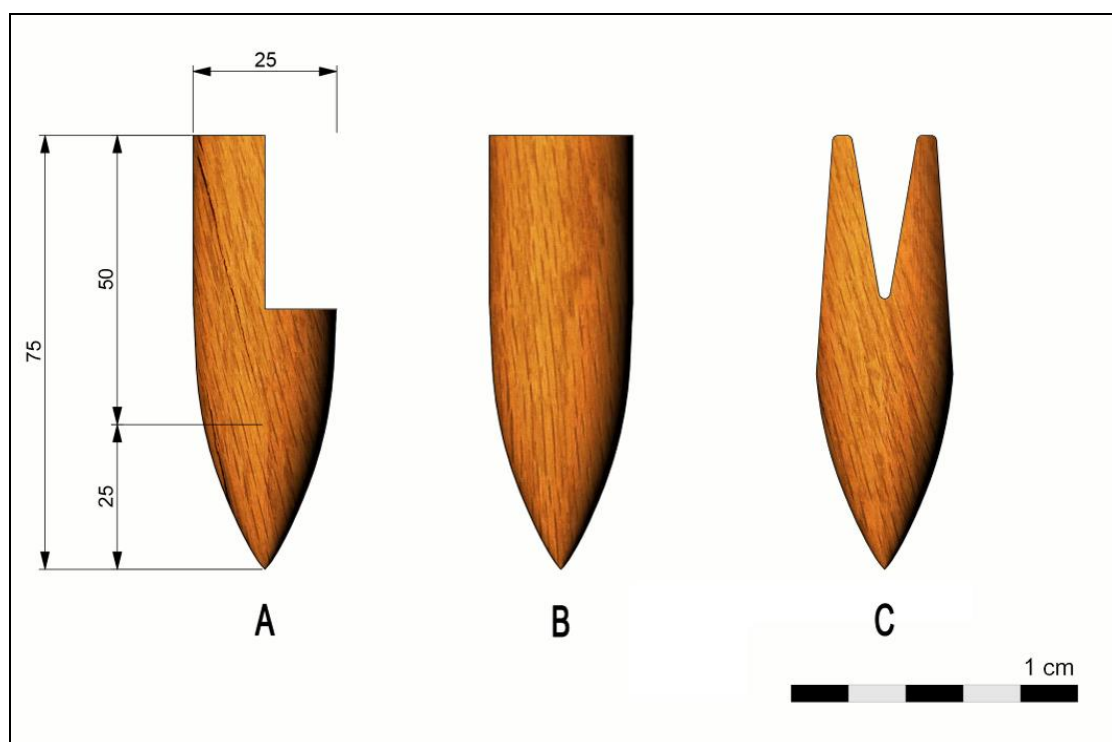


Figure 4.22. The three fore-shaft hafting arrangements tested in the first set of experiments. A. Juxtaposed slot hafting type; B. Flat slot hafting type; C. Female slot hafting type (Image La Porta and Tonelli).

Table 4-6. First set of experiments: hafting arrangements.

Experiment type	Hafting type						Total
	Female slot plus resin	Female slot plus tar	Flat slot plus resin	Flat slot plus tar	Juxtaposed slot plus resin	Juxtaposed slot plus tar	
Hand-delivered throwing stone-tipped experiments	1	1	1	1	1	1	6
Hand-delivered thrusting stone-tipped experiments	1	1	1	1	1	1	6
Total	2	2	2	2	2	2	12

4.3.3 Experimental variable: animal targets

As expressed in Section 4.1, animal targets (i.e. roe deer carcasses) were used both in the first and second sets of the experiments. Roe deer (*Capreolus capreolus*) species were selected because:

- (i) *Cervidae* species were well represented in each archaeological site selected for this thesis (Daujeard and Moncel, 2010; Valenci and Psathi, 2004; see also Table 4-7),
- (ii) Within the family of *Cervidae*, the roe deer (*Capreolus capreolus*) species were the most cost-effective. Other animals, such as horses and reindeer, well represented in the faunal assemblages of the two archaeological sites (Daujeard and Moncel, 2010; Valenci and Psathi, 2004), would have incurred high costs and involved complicated disposal issues.

Table 4-7. Faunal list of Abris du Maras and Arma Delle Manie sites. Percentage of Individual Specimens per Taxon, from Daujeard and Moncel (2010, p. 375), and Valensi and Psathi (2004, p. 259).

Archaeological sites	<i>Equus caballus Germanicus</i>	<i>Cervus elaphus</i>	<i>Capreolus capreolus</i>	<i>Rangifer tarandus</i>	<i>Dama dama</i>	<i>Capra ibex</i>	<i>Sus scrofa</i>	<i>Megaloceros sp.</i>	<i>Bison sp.</i>	<i>Bos p.</i>	<i>Carnivores sp.</i>
Abris du Maras (Levels 4-6)	22%	64%	3%	9%			2%				
Arma delle Manie (Level I-VII)	0.5%	65%	19.5%		1%	4%	4%			4%	2%

The animal carcasses were provided directly by the Steinzeitpark Dithmarschen Open-air Museum (Germany), in agreement with their ethical approval requirements. The carcasses were provided without heads and organs, in agreement with the German national regulations. They weighed between 45 and 50 kg each, and they were all young adult males (2-4 years old).

During the hand-delivered stone-tipped spear experiments, the roe deer targets were positioned in a wooden frame (driven into the ground for 50 cm) mimicking a “running position”. The running position assumed the posture of the animal during a run, with the anterior legs projected forward and firmly fixed into the frame in stepping forward pose (Figure 4.23). Although, it is acknowledged that is not possible to reproduce the natural muscular tension of an alive animal, the stretching of the anterior and posterior legs allowed the pulling of the muscles and contributed to the tension of the animal carcass during the impact.

The lack of internal organs in the animal targets may have affected the formation of use-wear traces. However, as demonstrated in CHAPTER 5 and CHAPTER 6, in this thesis most use-wear traces (both mechanical fractures

and microscopic traces) formed primarily by impacts against hard tissues (such as bones and, to certain extent, muscle tissues) which were all well represented by the animal carcasses. Therefore, it is likely that the absence of internal organs has had a small effect on the use-wear formations during these experiments. Moreover, some of the previous projectile experiments have used “meat sandwiches” (i.e. a combination of meat interlayered with bones; Shea et al., 2001, 2002), portions of the carcass (i.e. only the rib cage; Sano and Oba, 2015), or carcasses without organs (Pargeter, 2007). No previous references were found for the utilisation of entire animal targets with organs (indicating the difficulty of finding entire animal carcasses for experimental purposes).



Figure 4.23. Animal target positioned into the frame in a “running position”. The red circle indicates the aiming area.

4.3.4 Experimental variable: trained human participants

It has been emphasised that the involvement of trained participants is an improvement for spear throwing and thrusting studies (Gaudzinski-Windheuser et al., 2018; Milks et al., 2016; Schmitt et al., 2003). Moreover, it has been shown that cooperating with skilled craftspeople has an impact on the development of use-wear, as their familiarity with gestures and the accuracy of

their movements produces more comparable use traces for the archaeological record (Beyries, 1993, 1997; Van Gijn, 2010, p. 30-31; Milks et al., 2016).

Accordingly, two trained male participants, WP and IP, were recruited and they volunteered to take part in all sets of experiments (first, second, and third sets of experiments). Ethical approval was obtained from the Steinzeitpark museum. The mass of the two participants was 80 kg and 98 kg respectively, and their heights were 1.81 m and 1.92 m (values that fall within the highest mean body mass and stature estimated for *Homo neanderthalensis*, i.e. 173.3 and 179.5 cm stature and 93.1–95.4 kg mass; Arsuaga et al., 1999).

WP performed all of the throwing experiments (first and second sets) and the butchering experiments (third set). WP has collaborated with the Steinzeitpark open-air museum (Germany) over the last ten years. He is a craft expert specialising in the reproduction and use of experimental replicas of prehistoric artefacts, with a focus on skill acquisition from ethnographic sources. He grew up in Namibia, where he spent twenty years living and working alongside with the Ju/'hoansi bushmen group (at the Nyae Nyae Conservancy, Namibia). His experience in the Namibian Kalahari Desert has enabled him to practice traditional prehistoric hunting techniques and to learn real hunting strategies. He is an excellent weapon-maker, flint-knapper, and stone-tool user. He has more than thirty years' experience with hand-delivered spears and atlatl-spear throwing.

IP performed all the thrusting experiments (first and second sets of experiments). IP is WP's oldest son. He is studying for a bachelor's degree in Experimental Archaeology at the University of Kiel (Germany), and he is an expert hand-delivered spear and atlatl-spear user.

MC another expert craft person working at the Steinzeitpark museum supervised the hafting process of the experimental Levallois points hafted for the execution of the hand-delivered stone-tipped spear experiments.

4.3.5 Brief outcomes of the first set of experiments.

Hand-delivered throwing spears recorded a penetration depth mean of 43.33 cm, while hand-delivered thrusting spears recorded a penetration depth mean of 22.43 cm (Table 4-8), which were both above the endorsed lethal threshold (20 cm) for killing large mammals (Hughes, 1989; Frisson, 1989; Friis-Hansen, 1990) (but see CHAPTER 5 for detailed results and statistical analysis). Therefore, despite the small sample size (n=12 experiments), the first set of experiments showed that stone-tipped spears mounted with Levallois points were effective spears when hand-thrown or hand-thrust by trained human participants (but see CHAPTER 5).

Table 4-8. Penetration depth of hand-delivered throwing and thrusting spears of the first set of experiments.

First set of experiments	Hand-delivered throwing spears (n=6)	Hand-delivered thrusting spears (n=6)
Penetration depth (cm)	M 43.33 Max 120 Min 5 SD 35.87	M 22.43 Max 40 Min 2 SD 15.15

Despite the small sample size (n=12 experiments), the first set of experiments also indicated that the most effective hafting arrangement was the female hafting slot type used in combination with commercial tar adhesives (Table 4-9). Female hafting slot types had the lowest de-hafting percentage, followed by juxtaposed and flat hafting slots (Table 4-9). Tar-based adhesives were more effective than resin-based adhesives (Table 4-9) as 66.6% of Levallois points hafted with commercial tar remained hafted into the fore-shafts, while only 33.3% of Levallois points hafted with commercial resin (mixed with beeswax) remained hafted into the fore-shafts (Table 4-9). Considering the small sample size, no statistical tests were run.

Table 4-9. The contingency table shows the frequencies of Levallois points that remained hafted or de-hafted during the experiments, in relation to the experimental hafting variables employed in the first set of experiments.

Hafting slot type	Stay hafted	De-hafted
Female	75% (n=1 tools)	25% (n=3 tools)
Juxtaposed	50% (n=2 tools)	50% (n=2 tools)
Flat	-	100% (n=4 tools)
Adhesive type	Stay Hafted	De-hafted
Commercial tar	66.6% (n=4 tools)	33.3% (n=2 tools)
Commercial resin (plus beeswax)	33.3% (n=2 tools)	66.6% (n=4 tools)

4.4 Second set of experiments: hand-delivered throwing and thrusting stone-tipped spears

The second set of experiments occurred in July 2016, with forty replicas of hand-delivered stone-tipped spears (n=22 in throwing experiments, and n=18 in thrusting experiments). The second set of experiments aimed to assess additional research questions, such as:

1. Can macroscopic trace types (such as diagnostic impact fractures and edge-damage), frequencies, and patterns be used to distinguish between hand-delivered throwing and thrusting spear motions (using Levallois points as a tool morpho-type)?
2. Can microscopic trace types (such as polish, MLITs, and striations), frequencies, and patterns be used to distinguish between hand-delivered throwing and thrusting spear motions (using Levallois points as a tool morpho-type)?
3. Could a relationship be established between the energy yielded by the spear (i.e. impact velocity and KE) and the attributes of macroscopic and microscopic use-wear, both in hand-throwing and hand-thrusting activities?

Moreover:

4. If the impact velocities of the hand-delivered stone-tipped spears influenced the type and frequencies of diagnostic impact fractures, both in hand-throwing and hand-thrusting activities.
5. If the impact velocities of the hand-delivered stone-tipped spears influenced the presence/absence, extension, distribution, texture, or brightness of diagnostic microscopic use-wear traces, both in hand-throwing and hand-thrusting activities.

Specifically, to verify:

-
6. If there was a correlation between the penetration depth of the weapons and their impact location.
 7. If there was a correlation between the morphometric values of the experimental Levallois points (i.e. TCSA and TCSP) used as projectiles and the penetration depth of the experimental hand-delivered throwing and thrusting spears.

Accordingly, in order to verify the use-wear formation in throwing and thrusting spear projectiles under certain kinematic conditions, controlled sets of variables were tested for each group of experiments (see Table 4-1). Acceleration (with an accelerometer machine), slow-motion videos (with high-speed camera), penetration depth (in cm) and the impact location of each spear experiment were recorded.

Performance of the experiments

Following their manufacture, n=40 experimental Levallois points were selected for the second set of experiments and these were statistically tested (see Section 4.3.1). Eight experimental spear shafts replicating newly published measurements of selected Schöningen spears (Schoch et al., 2015) were manufactured. Contrary to the first set of experiments, the experimental spear shafts had a uniform shape, standard morphology, and a smoothed surface (see Section 4.4.2.1). From these, one experimental shaft was used for the execution of the hand-delivered throwing spear experiments and one for the thrusting experiments, the other shafts were produced and kept as reserve shafts in case of breakage or internal damage of the first shaft (see Section 4.4.2.1). As previously discussed in Section 4.3.2.2, in order to maintain the experimental variable constant of the spear shaft and to easily switch projectiles during the experiments, the n=40 Levallois points flint replicas were hafted longitudinally onto fore-shafts. However, during the second set of experiments, only one fore-shaft type and adhesive type was tested (see Section 4.4.2.2) to allow the hafting system variable to be controlled. Finally, the n=40 experimental Levallois points (inserted into the fore-shafts) were connected into the main spear shafts during the experiments (as shown in Figure 4.12). The

experimental Levallois points were randomly assigned to two experimental sub-populations (Table 4-1):

- N=22 hand-thrown stone-tipped spear experiments.
- N=18 hand-thrust stone-tipped spear experiments (the difference in the number of experiments between the throwing and thrusting sets balanced the throwing shots that missed the target).

For both throwing and thrusting experiments, acceleration and high-speed videos were recorded. Spear acceleration was measured using an Impact Accelerometer x200-4 (Gulf Coast Data Concepts; see Figure 4.25 and CHAPTER 5). The accelerometer measured 12 mm in length and 25.4 gr. It was mounted directly onto the shaft in a custom-made slot located 35 cm right of the point of balance of the shaft (Figure 4.25). It was manually activated before the start of each throwing or thrusting experiment and deactivated at the end of it (when the spear was motionless). Moreover, a sample of 10 individual throwing and 10 individual thrusting experiments were instead recorded using a Sony PXW-FS5 XD High-Speed Camera (200 fps), in collaboration with filmmaker TB⁹ (Figure 4.24). Standard motion videos were recorded with a Canon camera (Power Shot SX270 HS mounted in a tripod) for each throwing and thrusting experiment, from the preparation of the launch (starting point) until 30 secs after the impact with the target (ending point), (Figure 4.24 and accompanying files, slow-motion videos on the USB stick).

⁹ The collaboration between the filmmaker Dr TB and the author was the result of a scientific project, which resulted in the creation of a documentary focused on the framework of this experimental research programme, broadcasted for the German Ndr Channel. In return, Dr TB assisted and furnished the equipment for the video recording of the 2nd set of experiments.



Figure 4.24. Above: Camera setup. Cam1: Sony FS5 XDCAM High-speed Camera; Cam2: Canon Shot SX270 HS; Accelerometer setup. Below: IP and TB mounting the equipment and setting the cameras.

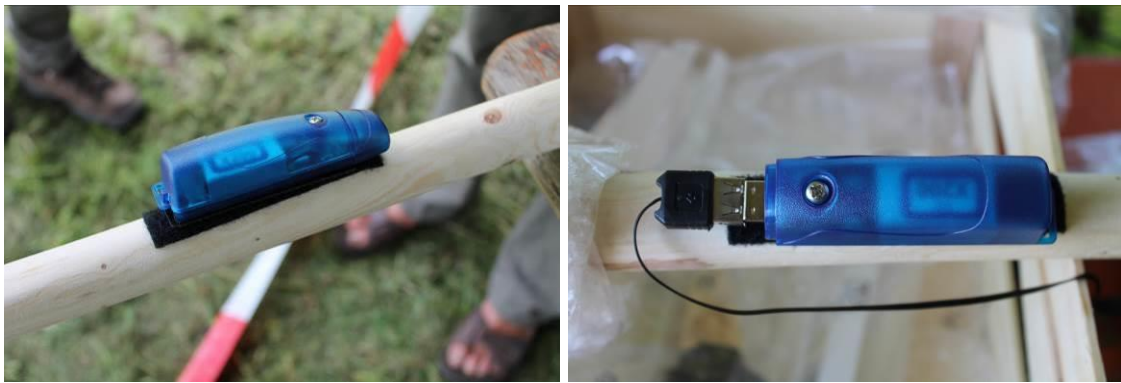


Figure 4.25. Accelerometer mounted in a custom-made slot on the spear shaft.

Such a comprehensive recording system required a precise setup prior to the execution of the experiments.

Before the start of each throwing/thrusting experiment, a picture was taken with a hand-held camera (Canon EOS 400D) of the experimenter holding the experimental stone-tipped spear and a tablet (Figure 4.26). The tablet displayed the experiment code, the individual number of shots, the experiment type, the tool ID, the shaft code, the name of the experimenter, and the date (Figure 4.26). The same variables were also recorded into a field form (as described in Section 4.2.1 and Figure 4.4). After this first documentation, the accelerometer was switched on and the high-speed camera and standard video camera were activated. The participant was then free to start the throwing/thrusting experiment when ready. During the execution of the throwing/thrusting experiment, a Canon camera (EOS 1100D, 18-55 mm, mounted on a tripod) took pictures at 1/200s to shoot slow-motion sequence images of the human movements (as Figure 4.29 and Figure 4.30). Immediately after the impact, the high-speed camera and the accelerometer were switched off and the data were recorded automatically by the devices. The impact location, penetration, wound dimensions (when applicable), and a full description of the experiment was recorded after each experiment (Figure 4.27). Penetration was registered in cm from the entrance hole to the distal end of the spear (Figure 4.3). The length and width (mm) of the wound was recorded for each shot (Figure 4.28). Next, pictures of the experiment were taken with a portable camera (Canon EOS 400D): eight pictures of the spear inside the target (two frontal, four laterals, and two rear view); four pictures of the wound with the spear still inside (two frontal,

and two rear view); and four pictures of the wound once the spear had been removed (two frontal, and two rear view). If the spear bounced off or missed the target, pictures were taken to indicate the position of the spear on the ground (two frontal, four lateral, and two rear views). Other pictures were taken whenever it was deemed appropriate. Periodically, standard videos were recorded along with an explanation of the impact location and the damage made to the animal target.



Figure 4.26. Picture archive system for the second set of experiments. 1: Experimenter is holding the spear and the tablet. 2: Tablet displaying information. 3: Target before the shot. 4: Spear inside the animal, frontal view. 5: Spear inside the animal, from the opposite side of the target. 6: Spear inside the animal, lateral view.



Figure 4.27. The author and WP during the recording process (after execution).



Figure 4.28. Picture archive system for the second set of experiments. 1: Wound with spear, frontal view. 2: Wound with spear, from the opposite site of the target. 3: Wound without a spear, frontal view. 4: Wound without a spear, from the opposite site of the target.

The spears were hand-thrown and hand-trusted by WP and IP respectively, both trained in traditional hunting and ancient weapon utilisation (see Section 4.3.4). The participants were allowed two practice shots before the beginning of each experimental set (with a spear that was not included in the final dataset). Both participants were right-handed. WP executed the experiments with shoes, IP executed the experiments barefoot.

The first experiments (n=22) to be performed were the hand-delivered throwing experiments (14th July 2016), performed by WP (see Section 4.3.4). Unlike the first set of experiments, the stone-tipped spears were thrown only once in order to make a direct association between the type of use-wear traces and the impact location and contact material. The participant (WP) performed the first half of the throwing experiments (12 shots in total during a 60 min trial) before having a break (30 mins to minimize fatigue issues), and the second half of the throwing experiments (10 shots in total during a 50 min trial) after the break. For the execution of the throwing experiments, a freshly killed roe deer carcass was used as a target (see Section 4.4.3 and 4.3.3). Throwing stone-tipped spears were all shot into the fresh animal carcasses from a 5 m distance (Figure 4.29), a distance range that follows well within the distance suggested for hand-delivered ethnographic spears (Churchill, 1993; Hughes, 1998) and used in previous spear experiments (Shea et al., 2001; Iovita et al., 2014; Sano and Oba, 2016).

On the 16th July 2016, the hand-delivered thrusting experiments were performed by IP (see Section 4.3.4). All thrusting experiments were executed with two-hands standing movements. The participant (IP) performed the first half of the thrusting experiments (10 shots in total during a 40 min trial) before having a break (30 mins to minimize fatigue issues), and the second half of the thrusting experiments (8 shots in total during a 35 min trial) after the break. For the execution of the thrusting experiments, a second freshly killed roe deer carcass was used as a target (see Section 4.4.3 and 4.3.3). Thrusting stone-tipped spears were stabbed from a 2 m distance (Figure 4.30), a distance range that follows well within the distance suggested for hand-delivered ethnographic

spears (Churchill, 1993; Hughes, 1998) and used in previous spear experiments (Schmitt et al., 2003; Shea et al., 2001; Milks et al., 2016).

The weather conditions during the performance of the experiments (14th and 16th July 2016) were dry and mild, with a fair amount of clouds, low-wind, and a maximum temperature of between 10-12°C.

Each experimental variable employed in the second set of experiments is described below.



Figure 4.29. Second set of experiments: a sample of the throwing experiments.



Figure 4.30. Second set of experiments: a sample of the thrusting experiments.

4.4.1 Experimental variable: Levallois points

The experimental Levallois points employed in the second set of experiments were manufactured and statistically analysed, as described in Section 4.3.1.

4.4.2 Experimental variable: spear system

Each experimental stone-tipped spear used in the second set of experiments was composed of: a standardised spear shaft, a wooden fore-shaft connecting the spear shaft, and the experimental Levallois point (as in Figure 4.12). Each experimental variable is explained and discussed below.

4.4.2.1 Spear shaft replicas

Spear shaft replicas used in this thesis were designed to match the published data concerning wooden spear shafts from the Schöningen site (Schoch et al., 2015; Thieme, 1997) for the motivations explained in Section 4.3.2.1.

However, for the second set of experiments, the main purpose was to manufacture experimental spear shafts that had a uniform shape and a standard morphology. This purpose allowed the shaft variables to be controlled, by reducing the internal variation of the spear morphology variables, so that this variable could not affect the ballistic results during the hand-throwing and hand-thrusting spear experiments.

Accordingly, eight standardised spear shafts were produced, matching the newly published measurements of Schöningen spear II (Schoch et al., 2015; Figure 4.31). The standardised spear shafts were all made of spruce, as described in Section 4.3.2.1 (Figure 4.32). In contrast to the first set of experiments, the trunks (n=8) were cut, de-barked (the bark stripped off), and worked with an electric planer and sander to eliminate the natural bends of the wood and obtain a standard shape with a smooth surface (Figure 4.31). The diameter and length were verified throughout the manufacturing process (with a digital calibre), to meet the required values. The spear shafts had a length of 210 cm and a maximum diameter of 37 mm (Table 4-10 and Figure 4.32). The shaft length was adapted to 210 cm (Table 4-10), because the hafting system

(stone tool plus the fore-shaft) added a further 20 cm to the shaft length, for a total spear length of 230 cm, analogous to Schöningen spear II (see Table 4-10). They weighed between 665 g and 975 g ($M=842$, $SD=111$; Table 4-10). The different values (diameter and weight) between the shaft replicas were resultant of the internal variation of the wood and subtle morphological differences (Table 4-10).

After the manufacturing process, the distal end of each shaft was carved with an electric drill to create a 2.5 cm hole, in order to create a slot into which the fore-shafts could be inserted. The distal end of each shaft was then reinforced and wrapped with commercial sinew and coated in tar (as described in Section 4.3.2.1, Figure 4.14, and Figure 4.32) to reinforce the shaft and secure it from breakages.



Figure 4.31. Shaft manufacturing process (de-barking and first planning), second set of experiments.

Table 4-10. Measurements for the standardised spear shafts of the second set of experiments compared with the published measurements of Schöningen spear II from Schoch et al. (2015). All measurements were taken from the front (distal end) with a digital calibre.

Shaft ID	Length (m)	Dia. at distal end (cm)	Dia. at 50 cm (cm)	Dia. at 80 cm (cm)	Dia. at 1200 cm (cm)	Dia. at 1500 cm (cm)	Dia. at 2000 cm (cm)	Weight (gr)	Weight + Acc.	Point of balance (cm from distal end)
Schöningen spear II	2.3			37						
SP-TH1	2.1	25	33	37	32	28	20	665	690	95
SP-TR1	2.1	25	33	37	31	27	20	965	990	88
SP2	2.1	25	32	36	32	28	20	789		95
SP3	2.1	25	33	37	32	28	20	721		93
SP4	2.1	25	32	36	31	28	20	841		94
SP5	2.1	25	32	36	31	27	20	810		92
SP6	2.1	25	32	37	30	27	20	973		90
SP7	2.1	25	32	37	31	27	20	975		90



Figure 4.32. Experimental spear shaft, second set of experiments.

Once manufactured, the eight shafts were randomly divided between hand-throwing and hand-thrusting spear experiments. Shaft SP-TH1 was randomly selected and used for the throwing experiments (Table 4-10) and Shaft SP-TR1 was randomly selected and used for the thrusting experiments (Table 4-10). All other shafts were produced and kept as reserve shafts in case of breakage or internal damage of the first shaft (Table 4-10). The use of a single shaft allowed the shaft dimension variables to be controlled.

4.4.2.2 Hafting arrangements: fore-shafts and adhesives

As explained in Section 4.3.2.2, each experimental Levallois point was hafted into cylindrical-conical fore-shafts (75 mm length and 25 cm diameter, Figure 4.16), made of spruce, and then mounted onto the main spear shaft during the experiments.

However, for the second set of experiments, in order to allow the hafting system variable to be controlled, only one hafting arrangement was utilised. All Levallois points were hafted into fore-shafts with female haft slot types only (see Section 4.3.2.2 and Figure 4.17) and fixed with commercial tar only (see Section 4.3.2.3 and Figure 4.17). Also, the fore-shafts were worked with an electric planer and sander to obtain a standard shape with a smooth surface (Figure 4.33). The 40 experimental Levallois points were first dipped into the tar adhesive up to their proximal part and then inserted into the fore-shaft applying a light pressure by hands. No binding was adopted in the hafting system so as not to add another variable to the experiments. The experimental Levallois points and relative standard fore-shafts were then linked into the standardised shaft replica (as in Figure 4.12) during the experiments. The hafting process of the n=40 experimental Levallois points was supervised by WP and MC, two experts craft people, in collaboration with the author (see Section 4.3.4).



Figure 4.33. Experimental fore-shafts manufacturing process (de-barking and first planning), second set of experiments.

4.4.3 Experimental variable: animal targets

For the performance of the second set of experiments, the stone-tipped spears were hand-thrown and hand-thrust into fresh carcasses of roe deer (*Capreolus capreolus*), as described in Section 4.3.3 (see also Section 4.3.3 for validation). One fresh carcass was used for the throwing experiments (14th July 2016) and a second one was used for the thrusting experiments (16th July 2016). These two carcasses of roe deer were then used for the execution of the butchering experiments (third set of experiments, see Section 4.5), to achieve the maximal utilisation of each single animal body.

4.4.4 Experimental variable: trained human participants

Hand-delivered throwing experiments (n=22) were performed by WP, whereas hand-delivered thrusting experiments (n=18) were performed by IP, for the reasons described in Section 4.3.4 (see also Section 4.1 for validation).

4.5 Third set of experiments: butchering knife

The third set of experiments aimed to create a control sample of experimental data, documenting the use-wear traces produced on Levallois points used in non-weaponry tasks, i.e. butchering activities. These data could then be compared with the use-wear traces formed during hand-delivered spear activities (i.e. first and second sets of experiments; see also Table 4-1).

The third set of experiments aimed to assess:

- The observation of types and frequencies of macroscopic and microscopic traces could Levallois points develop if used as tools in animal butchering activities.

and to answer the following question:

- Can macroscopic and microscopic use-trace types, frequencies, and patterns be used to distinguish between spear projectile activities and butchering activities (using Levallois points as a tool morpho-type)?

The primary objective was to understand the extent to which macroscopic and microscopic projectile impact traces differ from use-wear traces produced during other tasks that involve contact with animal tissues. The processing of animal carcasses (such as butchering activities or filleting strips of meat for storage reasons) can create a distinctively faint, greasy, and slightly scattered “meat polish” which can be similarly observed on projectile tools (Moss, 1983a; Fischer et al., 1984). Similarly, using stone tools for activities that involve the butchering of fish can produce microscopic striations similar to the MLITs observed on projectile tools, but perhaps with different texture, locations, distribution, patterns, and/or frequencies (Van Gijn, 1989, p. 44).

While several experiments have tested the formation of macro-fractures arising from other activities (such as trampling) and compared them with projectile DIFs (Shea and Klenck, 1993; Sano, 2009; Pargeter and Bradfield, 2012; Schoville, 2014) few experiments have directly compared butchering tools’ and projectile tools’ macro-traces (but see Van Gijn, 1989; Moss, 1983a). Thus, the third set

of experiments consisted of a comparative use-wear referential base which could provide better data for a comparison between macroscopic and microscopic projectiles' traces and butchering tools' traces, specifically on Levallois points.

Accordingly, n=8 experimental Levallois points (n=4 hafted and n=4 hand-held) were used as butchering knives to butcher entire animal or fish carcasses. Although the scale of the experiments might appear limited (eights experiments in total), each experimental tool was used for the butchering of the entire animal or fish carcass. Some experiments lasted for over two hours. Moreover, all of the butchering experiments were performed by WP - a skilled craft person with strong technical and practical knowledge of prehistoric butchering (see Section 4.3.4). Each experiment was thus a unique event for the acquisition of information concerning use-wear formation and stone tool utilisation during traditional butchering activities.

Performance of the experiments

Following manufacturing and random selection (see Section 4.3.1), four hafted and four hand-held Levallois points were used as butchering tools to butcher entire animal carcasses.

Four Levallois points (n=4) were hafted into a wooden handle with female haft slot type (as described in Section 4.3.2.2) and fixed using commercial tar (see Section 4.3.2.3). No bindings were employed. The handles replicated the shape and dimensions of the wooden fore-shafts used in the hand-delivered spear experiments simply because it was an ergonomic handle shape and there were few fore-shafts left from the second set of experiments. They measured 75 cm in length with a maximum width of 25 mm (Figure 4.16). The other Levallois points (n=4) were instead used with bare hands.

The experimental Levallois points were used in the following experiments (Table 4-11):

-
- Roe deer butchering¹⁰: 2 hafted Levallois points and 2 hand-held Levallois points were used for the butchering of two roe deer carcasses, as in Table 4-11.
 - Salmon butchering¹¹: 1 hafted Levallois point and 1 hand-held Levallois point were used for the butchering of two salmon fishes, as in Table 4-11.
 - Wild boar butchering: 1 hafted Levallois point and 1 hand-held Levallois point were employed for the butchering of one wild boar, as in Table 4-11.

The animal species employed for the third set of experiments were selected (i) according to their presence in the archaeological record (e.g. roe deer, see Section 4.3.3), (ii) the cost of the animal carcasses (e.g. Steinzeitpark's offer a wild boar carcass), (iii) and the verification of the formation of some specific use-wear traces (e.g. analogies between MLITs and fish striations).

Field-forms were employed to record each experiment and the experimental variables (Figure 4.35). The form recorded the following fields: experiment type, date, experiment ID, experimenter, tool ID, hafting presence, hafting code (slot type plus adhesive type), the purpose of the experiment, type of action, type of movement, contact material, contact material specification, contact material freshness, time of utilisation, description, and a visual record of the active tool zones during the experiment (Figure 4.35 and Table 4-1). The forms also supported the use-wear analyst during the microscopic observation phase in the lab. After the experiments, all forms were digitalised.

¹⁰ The carcasses of roe deer were butchered after the execution of the second set of experiments, to achieve the maximal utilisation of each single animal body.

¹¹ The salmon and wild boar meat, after the experiments, were consumed. The Steinzeitpark open-air museum (Germany) provided the animal carcasses in agreement with their ethical approval requirements.

Pictures were taken to record the angle of contact between the stone tool and the contact material, the position of the experimenter's hands, the action carried out, and the progression of the experiment (Figure 4.34).

Table 4-11. Third set of experiments. Butchering experiment summary.

Butchering experiments	Roe deer	Salmon	Wild boar
Hafted Levallois points	2	1	1
Hand-held Levallois points	2	1	1
Total	4	2	2

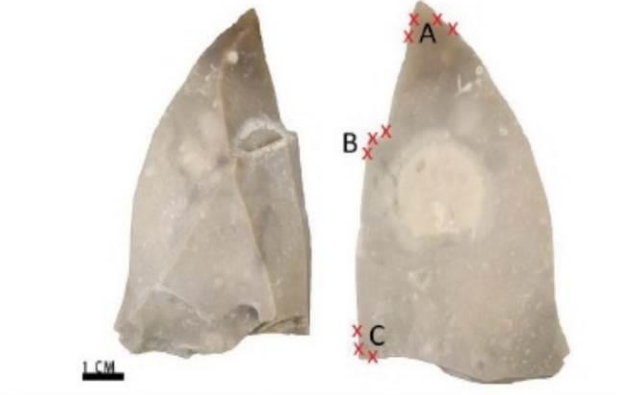


Figure 4.34. Picture of the third set of experiments. 1: Deskinning, 2: Contact angle, 3: Filleting, 4: Sinew removal.

Experiment type: Butchering Knife	Date: 15-07-2017
Experiment ID: BK-100	Experimenter: WP

Tool ID: 100	Hafting: Y N (hand-held)	Type: Fe Ju Fl	Adhesive: Res Tar	
Purpose: Butchering	Action: Skinning, dismembering, fileting	Motion: Cutting, sawing, shaving		
Contact Mat: Wild boar	Specification: Skin, flesh, meat,	State: Fresh	Time (min): 100	
Description:	The experimental Levallois point was held with bare hands. It was used as a knife to butcher an entire wild boar carcass. It was utilised in multiple motions (cutting, sawing, shaving) and actions (skinning, dismembering, and filleting) for 100 minutes. The tool was efficient.			

Drawing:



- A: active zone during the experiment
- B: active zone during the experiment
- C: active zone during the experiment

Figure 4.35. Field-form used for the recording of the “Comparative experiments”.

4.6 Outcomes

The conceptualisation and performance of the experimental programme presented above, and especially the selection of the experimental variables used for the hand-delivered throwing and thrusting of stone-tipped spears, were mainly driven by the deficiency of experimental data on hand-delivered throwing and, to a certain extent, hand-delivered thrusting (see Milks et al., 2016; Gaudzinski-Windheuser et al., 2018) spear mechanisms, and resultant use-wear traces.

Previous experiments that have replicated spear mechanisms using fire-machines (Shea et al., 2002; Pargeter, 2007; Iovita et al., 2014, 2016; Sano and Oba, 2015), have claimed to ensure the maximum experimental control during the performance of the experiments. This, however, has resulted in a deficiency of comparable use-wear traces and reliable datasets of human performance and ballistic data for hand-delivered spear mechanisms (as shown in CHAPTER 5). It is the opinion of the author, as well as others (Rots and Plisson, 2014; Van Gijn, 2014), that experiments that aim to compare experimental data (e.g. use-wear traces) with archaeological records (e.g. use-wear traces) should guarantee a comparability of intentions (expressed through the choice of representative experimental variables) in order to produce comparable results. The replication of spear activities with mechanical devices and ballistic gel targets can possibly mimic motion, but clearly do not replicate the ways in which prehistoric spears were used. Spear mechanisms are far more complex than the simple replication of their impact velocities and possibly *KE* on ballistic gel targets (as demonstrated in the next chapter).

By selecting controlled but realistic variables, this experimental programme aimed to replicate use-wear traces and measure realistic ballistic measurements of hand-delivered throwing and thrusting stone-tipped spears, reaching a statistically effective sample. Although this experimental approach can be enhanced in future investigations, it is also key to re-evaluate experimental protocols when investigating spear technologies. The sacrifice of some control (i.e. fire-machines and, to a certain extent, ballistic gel targets) can

be overturned by the adoption of single human trained participant and specific recording systems that ensure the compatibility of the data provided.

The following chapter reports the data on kinematic and ballistic parameters recorded during the second set (2nd) of experiments.

CHAPTER 5

KINEMATICS AND EFFECTIVENESS OF THROWING AND THRUSTING HAND-DELIVERED STONE-TIPPED SPEARS IN HUMAN PERFORMED EXPERIMENTS.

This chapter describes the kinematics of the Middle Palaeolithic stone-tipped spear replicas used in throwing and thrusting experiments with trained participants and realistic animal targets. All the data have been recorded during the second set of experiments (see Section 4.4). These experiments were designed to reproduce the use-wear traces created by manually-delivered throwing and thrusting spear movements. However, during the experiments, ballistic parameters, such as acceleration, impact velocities, kinetic energy (KE), momentum (p), acceleration profiles, and penetration depth were also recorded. The results of these experiments have provided, for the first time in an archaeological context, a comprehensive data-set of the realistic ballistic parameters of both throwing and thrusting hand-delivered spear motions. Moreover, for the first time, realistic ballistic results were integrated and compared with a detailed register of projectile use-wear traces, both for throwing and thrusting motions (see CHAPTER 6), contributing to the creation of an extensive experimental data-set that could be employed in future research.

5.1 Introduction

Projectile weapons vary in their dynamic and ballistic parameters in relation to their delivery systems (i.e. the mode of propulsion of the weapon) and morphometric characteristics (e.g. the mass of the projectiles, the tip cross-sectional area, the edge angles, and the shaft morphometry). Therefore, if the morphometric characteristics of projectiles are kept under control during experiments, different delivery systems could lead to different impact velocities, KE , momentum, penetration depth values and, finally, differences in the perceived lethality of the weapon. However, as the kinematics of hand-

delivered spear systems, especially throwing motions, have not been largely tested, the ballistic parameters of hand-delivered spears are also not well-known (but see Milks et al., 2016 and Gaudzinski-Windheuser et al., 2018 for hand/delivered thrusting spear experiments).

Previous experiments testing the performance and use-wear results of Early and Middle Palaeolithic spears (either tipped or untipped) have primarily employed firing-machines, such as calibrated cross-bows (Carrère and Lepetz, 1988; Shea et al., 2001; Wilkins et al., 2014; Sano and Oba, 2015), and air-guns (Iovita et al., 2014, 2016) with estimated ballistic measurements (Table 5-1 and Table 5-2). Only a few later experiments (Schmitt et al., 2003; Milks et al., 2014; Gaudzinski-Windheuser et al., 2018) have contemplated the use of trained (Milk et al., 2016) or less-trained (Schmitt et al., 2003) human participants through which to record ballistic parameters (Table 5-2). However, these approaches were exclusively associated with thrusting experiments with untipped spears and small sample sizes (Schmitt et al., 2003; Milks et al., 2016; Gaudzinski-Windheuser et al., 2018). A recent piece of research (Pargeter et al., 2016) presented the use-wear results of hand-delivered stone-tipped spear projectiles and recorded the impact velocities of throwing spears. However, these experiments were performed by a non-trained participant (the author) from a very close distance (not stated in the paper but estimated to be <2 m when considering the scale of the picture, as shown in Figure 5.34).

In sports science, there have been a small number of experiments that have registered the velocities of stabbing knives (Chadwick et al., 1999; Horsfall et al., 1999; Miller and Jones, 1996), thrown baseballs (Roach et al., 2013), and thrown sports-javelins throwing (Maki, 2013; Liu et al., 2010; Morriss et al., 1996; Best et al., 1993; Miller and Munro, 1983; Terauds, 1975) (Table 5-3). However, these experiments differ entirely from Palaeolithic spear experiments as a result of the different mass and shapes of the objects/weapons, the type of movements, and the purposes of the actions (Roach et al., 2013; Maki, 2013). For these reasons, the ballistic parameters recorded in sports science

experiments are difficult to compare with archaeological spear throwing experiments.

The only available ballistic parameters for throwing stone-tipped spears were thought to come from ethnographic data (Cotterell and Kamminga, 1990, p. 166; Hughes, 1998, p. 352) (Table 5-3). However, further investigation of the sources cited by Hughes (1998, p. 352) for throwing spear velocities showed that these parameters referred only to arrowheads' velocities (Van Buren, 1974), and, sports-javelin velocities (Miller and Munro, 1983), and that the velocities indicated for throwing spears were only an estimation of the velocity of the arm alone, without the atlatl (Butler, 1975, p. 107). Cotterell and Kamminga (1990, p. 166) reported a speculative estimation of throwing spear velocity (at 20 m/s), however, this was only for a spear thrown from a 50 m distance. As such, ethnographic data demonstrate a lack of recorded ballistic parameters for hand-delivered throwing spears.

It is, therefore, possible to report a deficit of extensive experimentations pertaining to hand-delivered spear systems and ballistic parameters. This deficit has resulted in (i) a limited understanding of throwing and thrusting spear mechanics and biomechanics (but see Mills et al. .2016); (ii) a complete lack of representative ballistic parameters for throwing spear motions; and (iii) only approximations of the experimental variables employed in spear experiments (Shea et al., 2001, 2002; Iovita et al., 2014, 2016; Sano and Oba, 2015; Sano et al., 2016; Wilkins et al., 2014; Hutching, 2011). Previous experiments have therefore only estimated the impact velocities of experimental stone-tipped spears, building upon insufficient data with broad ranges of variation (e.g. between 7 m/s and 30 m/s for throwing (Table 5-1), and between 1 m/s and 13.4 m/s for thrusting motions) (Table 5-2), with results that are difficult to compare.

Therefore, part of the experiments proposed in this thesis (second set of experiments, see Section 4.4) seeks to provide representative ballistic parameters of throwing and thrusting stone-tipped spears when hand-delivered

by trained human participants to realistic animal targets. The outcomes of the second set of experiments provided data for the following purposes:

- To compare the ballistic parameters of throwing and thrusting spear-motions to the resultant use-wear traces in order to establish the processes for the formation of impact fractures and microscopic impact traces.
- To provide comparative ranges and means for impact velocities, mass, *KE*, and momentum when throwing and thrusting hand-delivered spears, which could then be used in future experiments in the field of spear projectile technology.
- To investigate hand-delivered spear mechanics.

In order to achieve these objectives, the following ballistic parameters of both throwing and thrusting hand-delivered spear motions were recorded:

- Acceleration and, subsequently, impact velocities.
- The profile of acceleration of the throwing and thrusting motions.
- Maximum depth of penetration.

The above parameters lead to the calculation of the following values:

- Kinetic energy (*KE*).
- Momentum (*p*).
- Maximum deceleration at the impact.

These ballistic parameters are presented in this chapter given their stand-alone significance and are then cross-compared with the projectile use-wear traces in CHAPTER 6 and CHAPTER 11.

Table 5-1. A comparison of the throwing spear's impact velocities estimated or recorded in previous experiments and the results reported in this thesis (in green).

Throwing spear experiments				
Type of delivery	Velocity range (m/s)	Velocity mean (m/s)	Recording system for velocity	Source
Hand-delivered (trained)	8.45 - 13.40	11.76	Accelerometer	Experiments conducted for this thesis
Mechanically (cross-bow)		13	Not stated	Pargeter, 2007
Mechanically (cross-bow)		25.1	Chronometer	Hutchings, 2011
Mechanically (cross-bow)	8.9 - 9.4	8.9 (untipped spears) 9.4 (tipped spears)	Radar gun	Wilkins et al., 2014
Mechanically (air gun)	7 - 30	9.5 (Low-velocity weapons) 15 (Middle-velocity weapons) 30 (High-velocity weapons)	Light recorder	Iovita et al., 2014
Mechanically (cross-bow)	17.8	17.8	Not stated	Sano et al., 2016; Sano and Oba, 2015
Manually (not-trained)	Not stated	9	Chronometer	Pargeter et al., 2016

Table 5-2. A comparison of the thrusting spear's impact velocities estimated or recorded in previous experiments and the results reported in this thesis (in green).

Thrusting spear experiments				
Type of delivery	Velocity range (m/s)	Velocity mean(m/s)	Recording system for velocity	Source
Hand-delivered (trained)	3.01 - 6.92	5.02	Accelerometer	Experiments conducted for this thesis
Mechanically (cross-bow)	1.0 - 1.5	Not recorded	Estimated	Shea et al., 2001, 2002
Manually (not-trained)	1.7 - 4.5	Not stated	Standard videos	Schmitt et al., 2003
Mechanically (cross-bow)	8.9 - 9.4	8.9 (untipped spears) 9.4 (tipped spears)	Radar gun	Wilkins et al., 2014
Mechanically (thrusting pendulum)	2.7	Not stated	Light recorder	Iovita et al., 2016
Manually (trained)	2.8 - 6.2	4.6	High speed cameras	Milks et al., 2016
Manually (trained)	2.2 - 6.8	4.2 (median)	Accelerometer	Gaudzinski-Windheuser et al., 2018

Table 5-3. A comparison of the impact velocities estimated or recorded in previous ethnographic sources or sports science experiments and the results reported in this thesis (in green).

Ethnographic data and sports science experiments				
Type of delivery	Velocity range (m/s)	Velocity mean (m/s)	Recording system for velocity	Source
Hand-delivered throwing spears	8.45 - 13.40	11.76	Accelerometer	Experiments conducted for this thesis
Ethnographic spear-throwing		20	Estimation (50 m distance)	Cotterell and Kamminga, 1990
Ethnographic spear-throwing (*spear-thrower darts after verification)	13.9 - 25.5	17.8	Estimation from ethnographic data	Hughes, 1998
Sport's javelin		30.17 (distance 88 m)	Accelerometer	Terauds, 1975
Sport's javelin	25 - 30			Miller and Munro, 1983
Sport's javelin		32.3	Not stated	Petranoff's release velocity reported by Gregor and Pink, 1985
Sport's javelin	24.1 - 30.3		High-speed camera	Best et al., 1993
Sport's javelin	25.33 - 1.67 (distance 51 m)	20.73	Radar speed gun	Baugh, 2003
Hand-delivered thrusting spears	3.01 - 6.92	5.02	Accelerometer	Experiments conducted for this thesis
Knife stabbing (one-hand)	2.6 - 9.2	5.8	Motion camera	Chadwick et al., 1999
Knife stabbing (one-hand)	6 - 10	5.8	High speed cameras	Horsfall et al., 1999
Spear thrusting (one-hand, trained)	3.3 - 6.7	4.7	Accelerometer	Connolly et al., 2001

5.2 Spear data acquisition and data processing

In order to preserve the replicability of the experiments, variables were controlled and recorded during experiments for both throwing and thrusting hand-delivered stone-tipped spears. These experimental variables are presented in Section 4.4. The procedure followed for the acquisition and processing of the ballistic parameters of the experimental spears is outlined below.

Data were analysed and processed in collaboration with Dr E Burgos Parra from the College of Engineering, Mathematics, and Physical Sciences at the University of Exeter, and was computed using Microsoft Excel 2016 (by the author) and MATLAB R2017a (by Dr Burgos Parra). The statistical analyses were computed (by the author) using IBM SPSS Statistics 24.

5.2.1 Data acquisition

A total of $n=22$ throwing and $n=18$ thrusting hand-delivered stone-tipped spear experiments (data coming from the second set of experiments, see Section 4.4). were recorded capturing the acceleration (m/s^2) with an X200-4 accelerometer data logger (Gulf Coast Data Concepts)¹². $N=10$ throwing and $n=10$ thrusting experiments respectively were also recorded with a Sony FS5 high-speed camera (200 fps; see Section 4.4). Slow-motion videos allowed for the visual recording of throwing and thrusting hand-delivered spear experiments at a low frame-rate for this sub-sample ($n=20$) and recorded the backup control of the impact velocity measurements.

¹² The accelerometer Gulf Coast Data Concepts X200-4 was purchased through the Student Development Funding (SDF) allowance (£4100) granted to the author in 2016, through the Arts and Humanities Research Council (AHRC), for the realisation of the entire experimental programme. Therefore, the choice of the accelerometer was driven by criteria of feasibility and costs.

The X200-4 accelerometer recorded the linear acceleration in the three Cartesian axes (X, Y, and Z; Figure 5.1) at a sampling rate of 200 Hz. The accelerometer was mounted directly onto the spear shaft in a forward-facing position (Figure 5.33), on the point which corresponded to its centre of gravity of the spear (which had been previously calculated, see Table 4-10). While assuming the vector motion of the rigid bodies, the root square of the sum of the three squared values of acceleration on the X, Y, and Z axes provided the acceleration module¹³ of the spear (Figure 5.1).

¹³ The acceleration module is defined as:

$$a_{\text{mod}} = \sqrt{a_x^2 + a_y^2 + a_z^2}$$

where sqrt is the square root. The module of a vector is defined as the square root of the sum of the values of each component of the vector squared. So, in this case, the acceleration module is the square root of the sum of each acceleration component, squared.

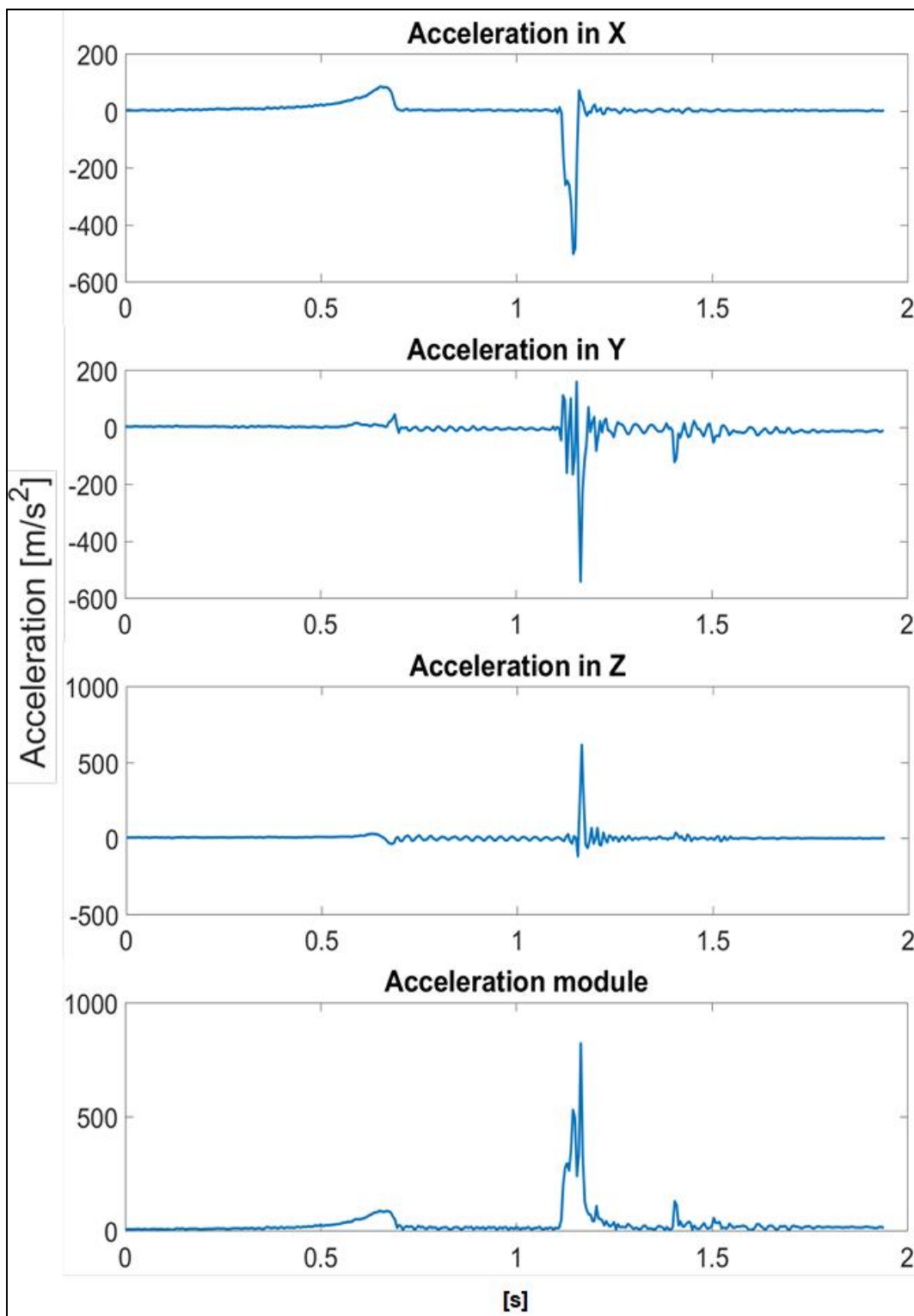


Figure 5.1. Acceleration on the X, Y and Z axes and the acceleration module (i.e. the relationship between acceleration variation and time) of a hand-delivered throwing spear experiment (experiment code: TH-81). Graph: La Porta and Burgos.

The X200-4 accelerometer automatically created a data-file (i.e. a spreadsheet) for each shot/experiment. The spreadsheet provided the raw acceleration of the X, Y, and Z axes, recorded in a time series at a rate of 0.005 seconds (Figure 5.3). The measurement, by default, included a constant offset caused by the Earth's gravitational constant and the accelerometer counting system. Therefore, to determine the acceleration in the International System of Units (m/s^2), the raw data were first divided by a calibration constant (163.8 counts/g) and then multiplied by the standard gravity constant (9.807 m/s^2). This allowed the final acceleration (m/s^2) in the X, Y, and Z axes to be obtained. Once the final acceleration series were computed, the spear impact on the target appeared as pronounced peaks in the time series associated with the X axis, which were significantly larger than other peaks (Figure 5.2). Impact events were defined as the biggest single change in the acceleration (i.e. when the acceleration exceeded a previous threshold) between two adjacent time intervals, in a specific phase of the experiment (e.g. passing from 20.4163 m/s^2 to -162.0729 m/s^2 in a single interval of 0.005 seconds, Table 5-4).

Table 5-4. An example of the spreadsheet of linear acceleration (experiment code: TH-81) where the impact event is highlighted in green as it is the biggest change between two adjacent time intervals, in a specific phase of the experiment. The negative value of the impact event corresponds to a change in the acceleration vector, which becomes negative as the impact event corresponds to a deceleration.

Time [s]	Acceleration (m/s^2)
47.367	0.53885
47.372	1.07769
47.377	1.616538
47.383	1.317179
47.387	3.053462
47.392	1.79615
47.397	5.26872
47.402	13.83038
47.407	20.4163
47.412	-162.0729
47.417	-91.4841

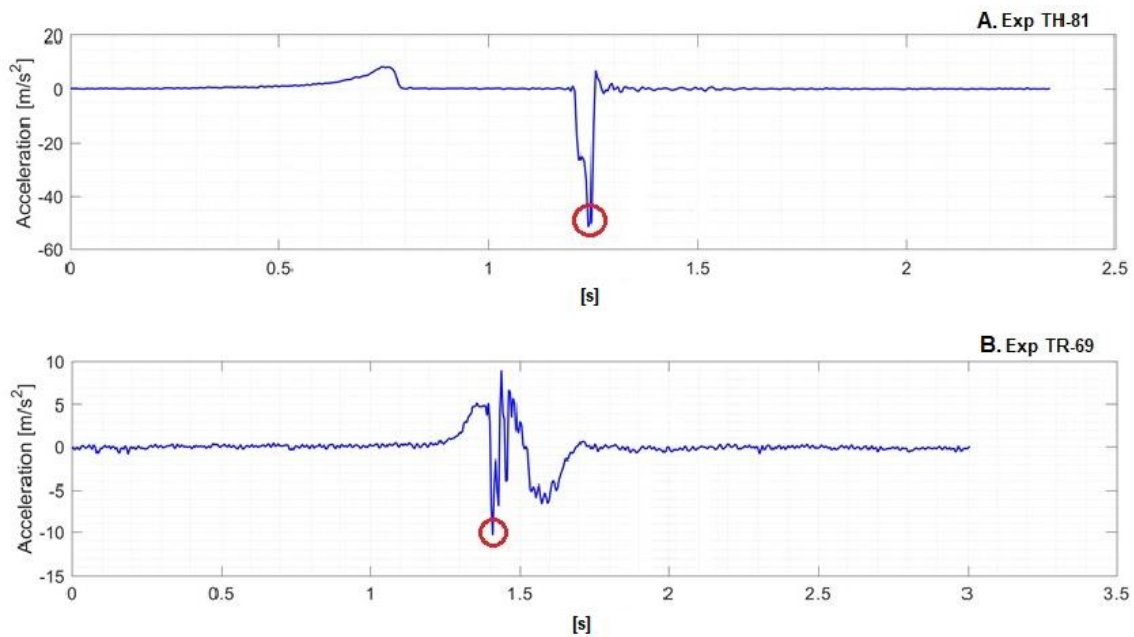


Figure 5.2. Example of a throwing (A) and a thrusting (b) acceleration profile with the indication of the impact events (in red circles). Graph: La Porta and Burgos.

;Title	http://wv X200-4			Analog Dev ADXL375	
;Version	1110	Build date	Dec 30 20	SN:CCDC120026A3640	
;Start_tim	2016-07-1 06:05:50.410				
;Temperat	-999	deg C	Vbat	3830 mv	
;SampleR	200 Hz				
;Deadban	0 counts				
;Deadban	0 sec				
;Headers	time	Ax	Ay	Az	
	0.077911	-68	-127	-181	
	0.082947	-88	-161	-183	
	0.087951	-102	-113	-222	
	0.092956	-95	-113	-186	
	0.097961	-100	-174	-150	
	0.102966	-113	-167	-213	
	0.108002	-109	-122	-209	
	0.113006	-90	-117	-136	
	0.118011	-99	-106	-143	
	0.123016	-100	-113	-149	
	0.128021	-84	-149	-115	
	0.133056	-72	-133	-143	
	0.138061	-74	-102	-193	
	0.143066	-93	-109	-195	
				

Figure 5.3. Example of a data-file from the accelerometer X200-4. The spreadsheet shows the raw acceleration in the X, Y, and Z axes. The picture shows the first few entries (i.e. time intervals) of the spreadsheet. However, each spread-sheet counted between 30,000

and 60,000 entries (see accompanying material, acceleration spreadsheets on the USB stick).

5.2.2 Data processing

From the processed acceleration data-sets, the following ballistic parameters were computed: acceleration profiles, calculation of impact velocities, calculation of KE, calculation of the momentum (p), and calculation of the maximum deceleration at the impact. The maximum penetration depth was also measured by the author on the animal carcass (see Section 4.4 and Figure 4.3).

5.2.2.1 Acceleration profiles construction

Acceleration profiles of throwing and thrusting spear motions were computed plotting the X -axis' acceleration over time (Figure 5.4 and Figure 5.5).

5.2.2.1.1 Throwing motions

For the throwing of hand-delivered spears, each acceleration profile showed relevant features which were defined as: throwing time, flying time, impact event, and penetration event (Figure 5.4).

“Throwing time” represents the launch phase of the spear (Figure 5.4). The throwing time is defined as the time span between the commencement of the throwing movement, as marked by a monotonical increment of acceleration in time, to the point where the spear leaves the hand of the human thrower, as marked by a sudden decrease in acceleration (meaning that there was no more force applied to the spear as the spear had left the hand of the thrower) (Figure 5.4).

Immediately following the throwing time, the acceleration profile depicts the flight phase of the throwing spear, also called “flying time” (Figure 5.4). Flying time is defined as the time span between the spear leaving the hand of the human thrower and the point when the spear hits the target (Figure 5.4). Flying time is characterised by steady acceleration (since the short distance from the

target did not allow a deceleration over time), appearing as a steady line on the time series (Figure 5.4).

The impact event (i.e. the moment when the spear hits the target, or the ground in the case of a missed shot) was marked by an abrupt change of acceleration (i.e. a deceleration), appearing as a pronounced peak in the time series (Figure 5.4). This deceleration corresponded to a change in the vector velocity of the spear, and therefore a change in the spear momentum (see Section 5.2.2.3.2 for definitions).

Immediately after the impact event, the acceleration profile shows the “penetration event”. The penetration event is considered to be the time span between the spear penetrating the target and the instant at which acceleration reaches zero or, in the case of a missed shot, the time from the first contact with a target to zero acceleration.

After the penetration event, the acceleration profile shows a “tail”, during which the spear is held in position in order to switch off the accelerometer and record the penetration depth, causing slight oscillation (Figure 5.4).

Selected throwing acceleration profiles are presented in Section 5.3.4.

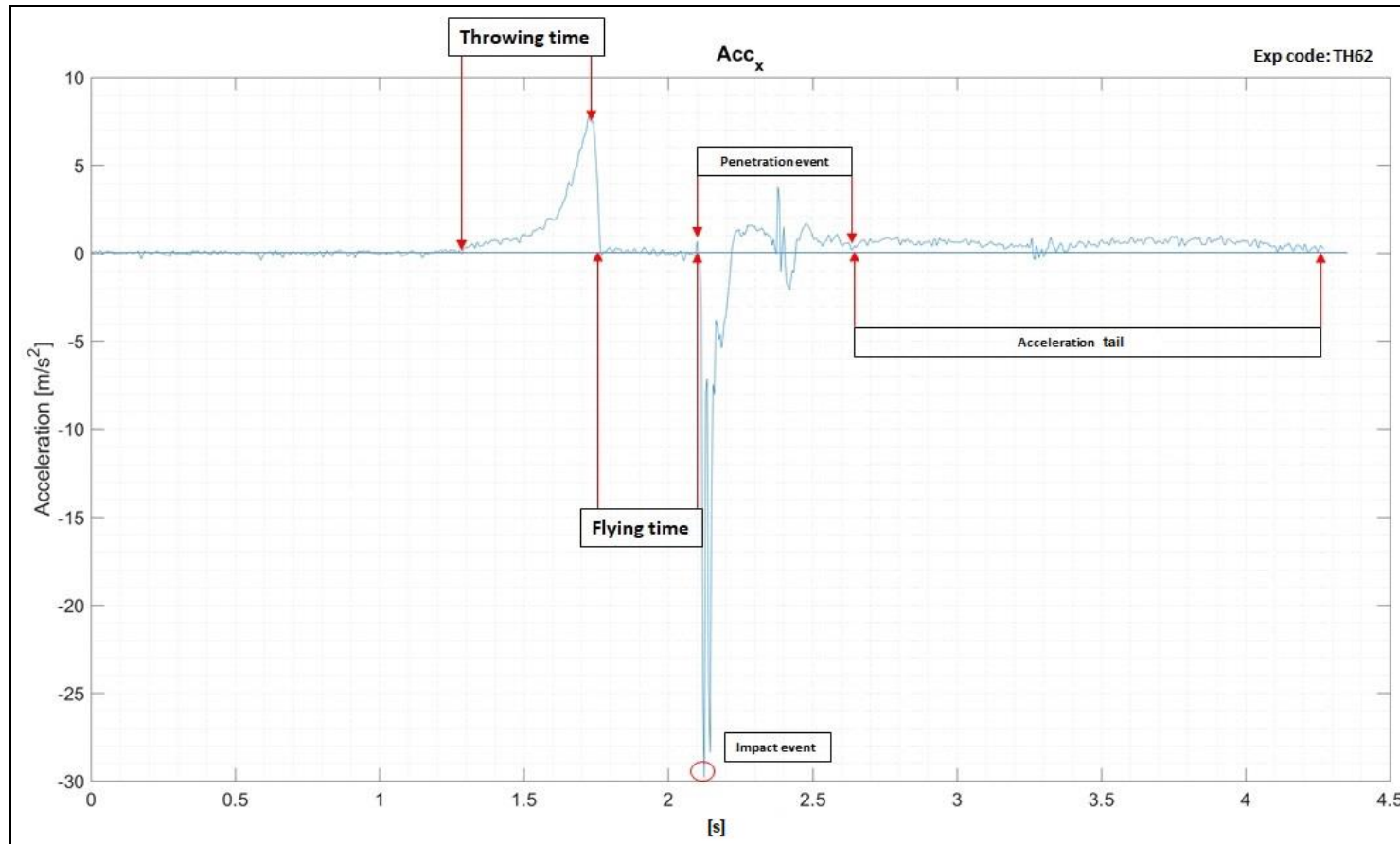


Figure 5.4. Acceleration profile of a throwing spear in a hand-delivered experiment (experiment code: TH-62). Graph: La Porta and Burgos.

5.2.2.1.2 Thrusting motions

During the thrusting motion, the spear does not leave the hand of the human-thruster. As such, thrusting acceleration profiles show different features than those demonstrated in throwing profiles. The relevant features were identified as: thrusting time, impact event, and stabbing time (Figure 5.5).

The “thrusting time” is the launch phase of the spear (Figure 5.5) and is defined as the time span between the commencement of the thrusting movement, which is marked by a monotonical increase of acceleration, and the moment the spear hits the target, as marked by an abrupt deceleration during a short interval of time (0.005 seconds). The impact event appeared in the time series as a pronounced peak (Figure 5.5), corresponding to the maximum deceleration of the projectile (described in Section 5.2.2.3.3).

Immediately after the thrusting time, the acceleration profile shows the “stabbing time” (i.e. penetration phase). The stabbing time is the time span between the spear penetrating the target and the moment at which acceleration is zero (Figure 5.5) or, in the case of a missed shot, the time between the first contact with a target and zero acceleration (Figure 5.5). It is followed by a tail, as described in the throwing acceleration profiles.

Selected thrusting acceleration profiles are presented in Section 5.3.4.

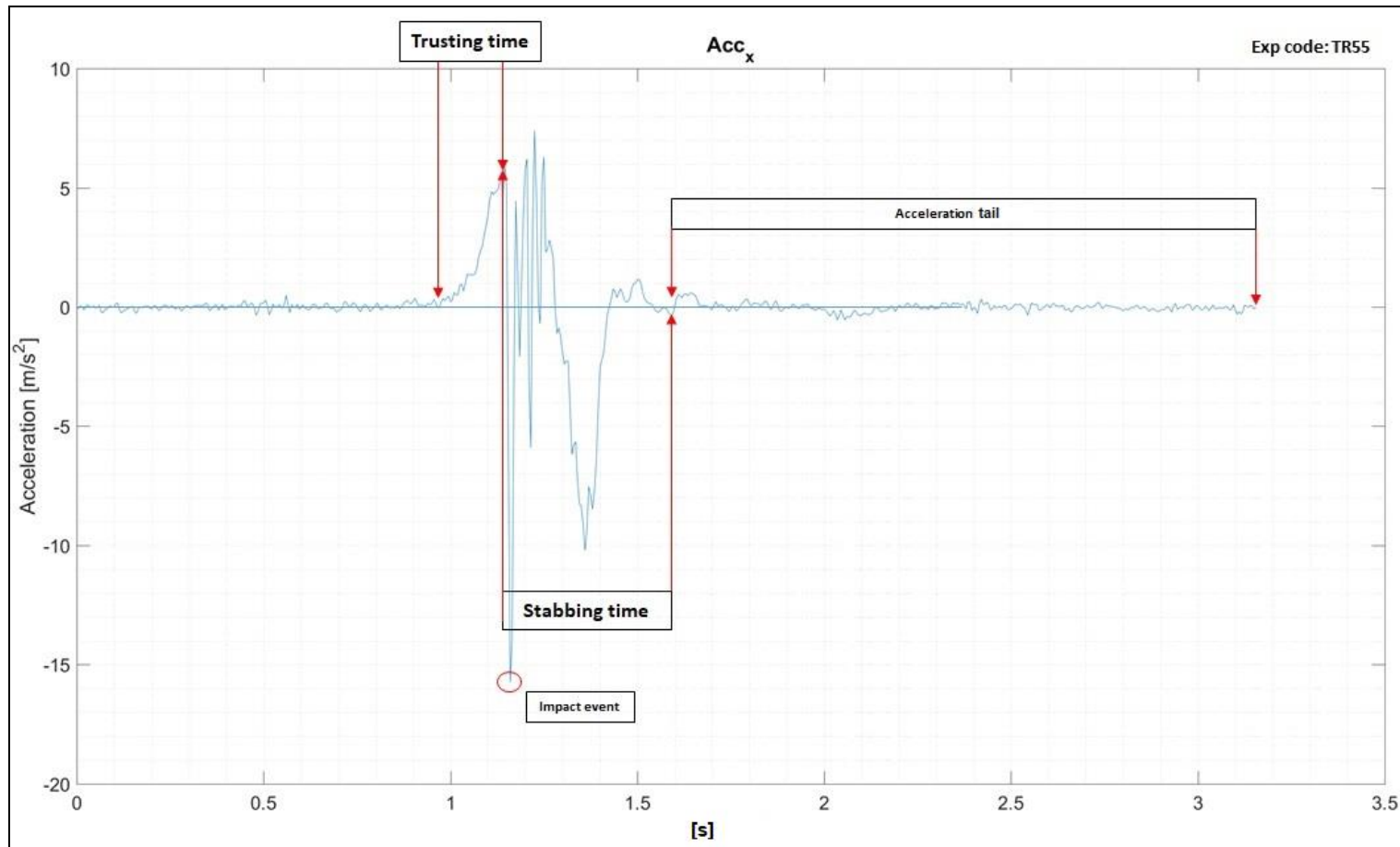


Figure 5.5. Acceleration profile of a thrusting spear in a hand-delivered experiment (experiment code: TR-55). Graph: La Porta and Burgos.

5.2.2.2 Impact Velocities calculation

5.2.2.2.1 Throwing velocities

Impact velocities (m/s) for throwing hand-delivered spear experiments were calculated with the following formula:

$$V = D/T$$

D is the distance between the spear position at the starting point (recorded at the point where the accelerometer was located on the shaft) and the spear position at the impact point (recorded at the point where the accelerometer was located on the shaft); and T is the time between the release of the spear and the spear hitting the impact point (Figure 5.31).

The D (distance) was calculated based on the position of the accelerometer at the beginning of the motion (i.e. when the spear first left the hand of the human thrower, considered as D_1), and at the end of it (i.e. when the spear hit the target or the ground, considered as D_0). The final distance (D) was defined as the distance between D_1 and D_0 . These distances (D_1 and D_0) were calculated from the sample of high-speed video-frames provided with measuring tape (see Figure 5.31, Figure 5.32, and accompanying material, folder – slow motion videos on the USB stick). The mean of the distance (D) for the throwing experiments was 3.8 m (recorded on $n=10$ experiments, SD 0.12 m).

The T (time) of a throwing spear (also called “flying time”) was considered to be the time span between the spear leaving the hand of the human thrower (T_1), and the spear hitting the target or the ground (T_0). On the acceleration profile, T_1 was marked by a sudden deceleration at the end of the “throwing time” (Figure 5.4). This deceleration meant that there was no more force applied to the spear as the spear had left the hand of the thrower (Figure 5.4). On the acceleration spread-sheet, this change in acceleration was marked as the biggest single change in the acceleration (i.e. when the acceleration exceeded a previous threshold) between two adjacent time intervals, in a specific phase of

the experiment (e.g. passing from 4.25519m/s^2 to -0.38462 m/s^2 in a single interval of 0.005 seconds, Table 5-5). T_0 (i.e. final impact), appeared as a pronounced negative deceleration peak in the time series, which was significantly larger than other previous peaks (Figure 5.4). On the acceleration spread-sheet, T_0 was marked as another biggest single change in the acceleration (i.e. when the acceleration exceeded a previous threshold) between two adjacent time intervals, in a specific phase of the experiment (e.g. passing from 0.335775 m/s^2 to -24.35897 m/s^2 in a single interval of 0.005 seconds, Table 5-6). The total time (T) was calculated as the difference between T_1 and T_0 , and it was calculated from the acceleration spread-sheet of each throwing experiment (see accompanying material, folder 1 - accelerometer data, on the USB stick).

Table 5-5. An example of the spreadsheet of linear acceleration (experiment code: TH-62) where the beginning of the flying time is highlighted in green as it is the biggest change between two adjacent time intervals, in that phase of the experiment. The negative value of the flying time event corresponds to a change in the acceleration vector, which becomes negative as it corresponds to a deceleration (i.e. when the spear leaves the hand there is no more force applied to it).

Time [s]	Acceleration (m/s^2)
34.459	7.86325
34.464	7.82662
34.469	7.88156
34.474	7.04518
34.479	5.71429
34.484	4.25519
34.489	-0.38462

Table 5-6. An example of the spreadsheet of linear acceleration (Experiment code: TH-62) where the impact event is highlighted in green as it is the biggest change between two adjacent time intervals, in that phase of the experiment. The impact shows a negative vector as it corresponds to a deceleration.

Time [s]	Acceleration (m/s ²)
34.830	0.005006
34.835	0.140415
34.840	0.335775
34.845	-24.35897
34.855	7.619048
34.860	6.776557

5.2.2.2.2 Thrusting velocities

Impact velocities of thrusting hand-delivered spear experiments were calculated with the same formula as throwing experiments:

$$V = D/T$$

The distance (D) for thrusting experiments was calculated as explained in Section 5.2.2.2.1. The mean of the distance (D) for the thrusting experiments was 0.81 m (recorded on n=10 experiments, SD 0.13 m), from the sample of high-speed video-frames provided with measuring tape (Figure 5.32).

However, as the spear does not leave the hand of the human-thruster during the thrusting motion, the time (T) of a thrusting spear (also called “thrusting time”) was considered to be the time span between the commencement of the thrusting movement (T₁) and the spear hitting the target (T₀). The beginning of the thrusting movement (T₁) corresponded to a monotonical increase of the linear acceleration on the acceleration profile (Figure 5.5). On the acceleration spread-sheet, T₁ was marked as the point at which the acceleration first started to increase and it is marked as the biggest single change in the acceleration (i.e. when the acceleration exceeded a previous threshold) between two adjacent time intervals, in a specific phase of the experiment (corresponding to a positive acceleration, Table 5-7), while T₀ (i.e. the final impact) was marked as another biggest single change between two adjacent time intervals, in the

specific phase of the experiment (e.g. passing from 31.0136 m/s² to -66.45769 m/s² in the next 0.005 seconds, Table 5-8). It appeared as a pronounced deceleration peak in the time series, which was significantly larger than other peaks (Figure 5.5). The time (T) was then calculated as the difference between T₁ and T₀, and it was deduced from the acceleration spread-sheet of each thrusting experiment (see accompanying material, folder 1 - accelerometer data, on the USB stick).

Table 5-7. An example of the spreadsheet of linear acceleration (Experiment code: TR-69) where the beginning of the thrusting time is highlighted in green as it is the biggest change between two adjacent time intervals, in that phase of the experiment. The thrusting time shows a positive vector as it corresponds to a full acceleration (i.e. when the human thruster started the action and applied the full force to the spear).

Time [s]	Acceleration (m/s ²)
14.262	-4.90949
14.267	-0.11974
14.272	3.53243
14.277	4.69423
14.282	5.21526
14.287	5.65538
14.292	6.41910

Table 5-8. An example of the spreadsheet of linear acceleration (Experiment code: TR-69) where the impact event is highlighted in green as it is the biggest change between two adjacent time intervals, in that phase of the experiment. The impact time shows a negative vector as it corresponds to a deceleration.

Time [s]	Acceleration (m/s ²)
14.495	39.0364
14.500	52.2082
14.505	31.0136
14.510	-66.45769
14.515	-99.80628

5.2.2.3 Calculation of the kinetic energy (*KE*), momentum (*p*), maximum deceleration, and trajectory

5.2.2.3.1 Kinetic energy (*KE*) at the impact

The kinetic energy (i.e. the energy that an object has due to its motion) of the spears was calculated as follows:

$$KE = \frac{1}{2} m v^2$$

Here the *m* is the mass of the spear (in grams), and *v* is the velocity of the spear at impact (in m/s, calculated as explained in Section 5.2.2.2.1 and 5.2.2.2.2).

Throwing experiments behave as conservative systems after the spear leaves the hand of the thrower. This means that the total energy of the system is conserved and, in this scenario, it is possible to calculate the *KE* before and after the impact. The *KE* was deduced after having calculated the impact velocities of the throwing experiments, as expressed in Table 5-10.

For thrusting experiments, the calculation of the *KE* is more complicated as spear-thrusting is a non-conservative system in which there is always an external and non-uniform force and, therefore, additional mass applied to the system. This force corresponds to the mass of the human-thruster (body plus arm) transferred into the spear during the impact. Therefore, in order to calculate the mass and hence the *KE* of thrusting spears, it is essential to know the force applied by the human thruster into the spear.

A solution could be to calculate the force applied by the human thruster directly into the spear. However, this force has to be calculated for each single experiment, because the force applied into the spear is not a constant value since it is affected by external factors (i.e. human factors, see below). In previous experiments, this force has been calculated using loading gauges/cells that record the force directly on the spear shaft (Schmitt et al., 2003; Milks et al., 2016; Gaudzinski-Windheuser et al., 2018). However, the addition of loading

devices¹⁴ significantly increases the mass of the spear, which results in different *KE* and momentum (p) values in comparison to a spear without loading devices. The change in *KE* and momentum (p) values could, therefore, drastically affect the formation of use traces, both on the bones and on the projectiles. Moreover, the loading cell must be mounted on the distal tip of the experimental shaft, which has an influence on the penetration depth of the spears as the spear cannot completely penetrate the animal. Therefore, because the experiments proposed in this thesis were designed to reproduce use-wear traces and record representative ballistic parameters in controlled but realistic experiments, the use of loading cells was rejected.

Nonetheless, the *KE* of the thrusting experiments (i.e. the “total”¹⁵ mass of the thrusting spears, which is the sum of the mass of the spear plus the additional mass of the human thruster) was calculated by employing force values from previously published data, i.e. from Milks et al. (2016)¹⁶ using the method provided by Churchill et al., 2009 (p. 168; explained below).

Although Milks’ et al. (2016) experiments presented certain analogies with the experiments presented in this thesis, it is important to take into account different experimental variables (e.g. different spear systems and different human participants). Therefore, the results presented below for the *KE* of the thrusting experiments have a certain degree of approximation that derives from internal experimental variability and that needs to be considered when comparing these results with experiments that have recorded force values with loading devices.

¹⁴ For instance, loading cells alone can weight up to 500 g but matched with the loading poles they reach around 2 kg (depending on brands and models).

¹⁵ The total mass of the spear herein refers to the mass of the spear plus the additional mass of the human thruster, transferred into the spear.

¹⁶ Milks and colleagues’ (2016) force values were chosen because they employed similar experimental variables to this thesis’ experiments, i.e. hand-delivered motions and trained human participants (Milks et al., 2016, p. 198).

The variability in force values recorded from previous thrusting spear experiments (as shown by the SD and Max and Min values of the force values in Table 5-9, and also suggested by Milks et al., 2016, p. 198) is due to the fact that, in any experimental study and indeed in any real-world scenario, the total mass of a thrusting spear is going to vary due to external factors (such as the type of techniques, e.g. one hand as opposed of two hands thrusting moveemnt; e.g. the balance of the body weight, and the position of the legs; fitness of the users, e.g. body and or age differences; concentration and adrenaline of the human thruster). Therefore, the estimate of force values between two different sets of experiments (i.e. this thesis' experiments and Milks' [et al., 2016] experiments) may fall within the range of variability that exists in replication processes.

Table 5-9. Force values (in N) recorded in previously published thrusting spear experiments. Data from Milks et al. (2016, table 8) and Gaudzinski-Windheuser et al. (2018, p. 40).

Previous thrusting experiments	Force values (in N)	Number of experiments
Milks et al., 2016	Min= 362 Max= 1120 Mean= 661.0 SD= 186.2	N=39 experiments
Gaudzinski-Windheuser et al. 2018	Min= 634.6 Max= 1953.8 Median= 1034.2 SD= Not reported	N=39 experiments

The total mass of the thrusting experiments was calculated as follow. Given the mean of force of 661.0 N (as reported by Milks et al., 2016, table 8) (see also Table 5-9), the mean of impact velocity for thrusting spears recorded in this thesis (i.e. 4.86 m/s, see Section 5.3.1), and deceleration time registered in this thesis's thrusting experiments (i.e. 0.005s), the additional mass of the thrusting

spears could be estimated as a constant of 0.680 kg (i.e. F/\bar{a}). This constant (defined as active mass, m_{act}) added to the actual mass of each spear (defined as spear mass, m_{sp}), with the formula:

$$M = m_{act} + m_{sp}$$

gives the total mass (M) of the spear in a thrusting motion.

Therefore, the *KE* for thrusting spear experiments was calculated as follows:

$$KE = \frac{1}{2} m v^2$$

5.2.2.3.2 Momentum (p) at the impact

The momentum (p) is a vector quantity of a moving body often measured in the field of wound ballistics (Sellier and Kneubuehl, 1994). If the mass of the studied object does not change in time, Newton's First Law states that an object in motion continues its motion until a force acts upon it. The momentum (p) is, therefore, defined as the mass of the object multiplied by its velocity (Cotterell and Kamminga, 1992). The formula used to calculate the momentum of throwing and thrusting stone-tipped spears for this thesis's experiments was the following:

$$p = m\bar{v}$$

m is the mass of the spear (recorded for each spear in g) and \bar{v} is the velocity before the impact (i.e. impact velocity, calculated as in Section 5.2.2.2).

A change of momentum, Δp , occurs when a force (F) is applied during an interval of time (Δt), therefore:

$$\Delta p = F\Delta t$$

The conservation of the linear momentum occurs in systems where the net force from external sources is zero. Momentum is thus conserved in throwing experiments before and after the impact, but this is not the case for thrusting

experiments as there is always the presence of the force of the human thruster over the spear. Therefore, before to calculate the thrusting spear momentum, the total mass of the thrusting spears was estimated, as expressed in Section 5.2.2.3.1 (i.e. total mass, $M = m_{act} + m_{sp}$). Once, the total mass was estimated, the KE values of thrusting spear momentum were calculated with the following formula:

$$p = m\bar{v}$$

where m is the total mass of the spear (i.e. $m_{act} + m_{sp}$, see Section 5.2.2.3.1) and \bar{v} is the velocity before the impact (calculated as in Section 5.2.2.2).

5.2.2.3.3 Maximum deceleration

The maximum deceleration shows how quickly the spear decreased its acceleration (and thus its velocity) after impact. The maximum deceleration corresponds to the value of the acceleration at the impact (e.g. in experiment TH-62 the acceleration at the point of impact is equal to -24.35897 m/s^2 falling from 0.005006 m/s^2 , and returning to 7.619048 m/s^2 in a time interval of 0.05s see Table 5-6).

This proved to be a relevant ballistic parameter when compared with the maximum penetration depth of the spears (Session 5.4).

5.2.2.3.4 Trajectory of the hand-delivered throwing spears

The trajectories of the spears were calculated using the following equation of projectile motion:

$$\bar{X}(t) = \bar{x}_0 + \bar{v}_0 t + \bar{a} \frac{t^2}{2}$$

Where \bar{X} is the position of the centre of mass of the spear (accelerometer position) at a given time (t), \bar{x}_0 is the position at time (t_0), \bar{v}_0 is the velocity at time (t_0), and \bar{a} is the acceleration of the object.

The X-Z plane position of the accelerometer was plotted in a 2D graph to show the elevation and expected parabolic trajectory of the projectile during its flying time (i.e. after leaving the hand of the thrower and just before impacting the target) (Figure 5.6).

In addition, a 3D trajectory of a sample hand-thrown spear was plotted in a graph where a deviation from the $Y=0$ on the Y axis was observed (Figure 5.7). There was also a small perturbation which scarcely visible on the $Y-Z$ axes plane in the graph (Figure 5.8). This perturbation, during the flying time, might have been produced by the torque of the projectile caused by the air resistance (i.e. the drag; Cotterell and Kamminga, 1992; Hughes, 1998). This torque may have caused the precession of the spear, i.e the oscillation at the rear part of the spear (defined as the change of angular velocity and angular momentum produced by a torque).

The analysis of high-speed videos has also suggested that hand-delivered throwing spear (delivered at a distance of 5 m) were also affected by a spin phenomenon (spin defined as the gyration of a projectile on its symmetry axis, Cotterell and Kamminga, 1992). For instance, video #TH-62 (in accompanying material, folder – slow-motion videos on the USB stick) shows a rotation of the accelerometer on the symmetry axis of the spear during the flying time of the hand-delivered throwing spears (see also Figure 5.9, although the spin effect is more evident in the slow-motion videos). The spin effect has been observed also for all the other slow-motion videos of the hand-delivered throwing spears (see the accompanying material, folder – slow-motion videos on the USB). This observation corroborates the hypothesis the spin effects are active also on hand-delivered throwing spear weapons (contra Iovita et al. [2014] who claimed that hand-delivered throwing spear due to the short flying distances may have not been affected by spin phenomena), and they may have also played a role in the formation of the use-wear traces of projectile tools.

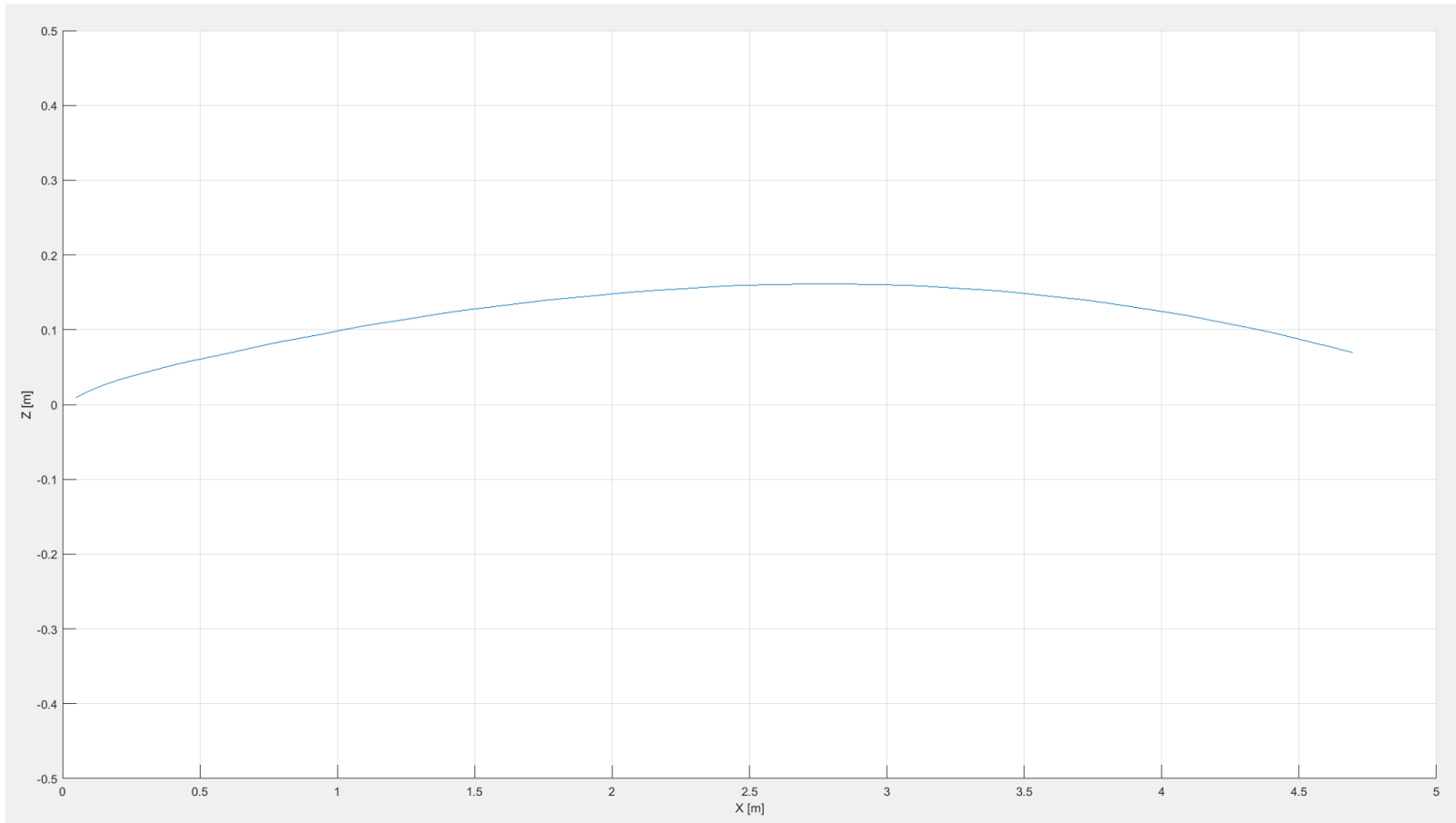


Figure 5.6. The 2D parabolic trajectory (X-Z axes) of the centre of mass of the spear during its flying time. Axes (X and Z) are in metres, (experiment code: TH-81). Graph: E. Burgos-Parra.

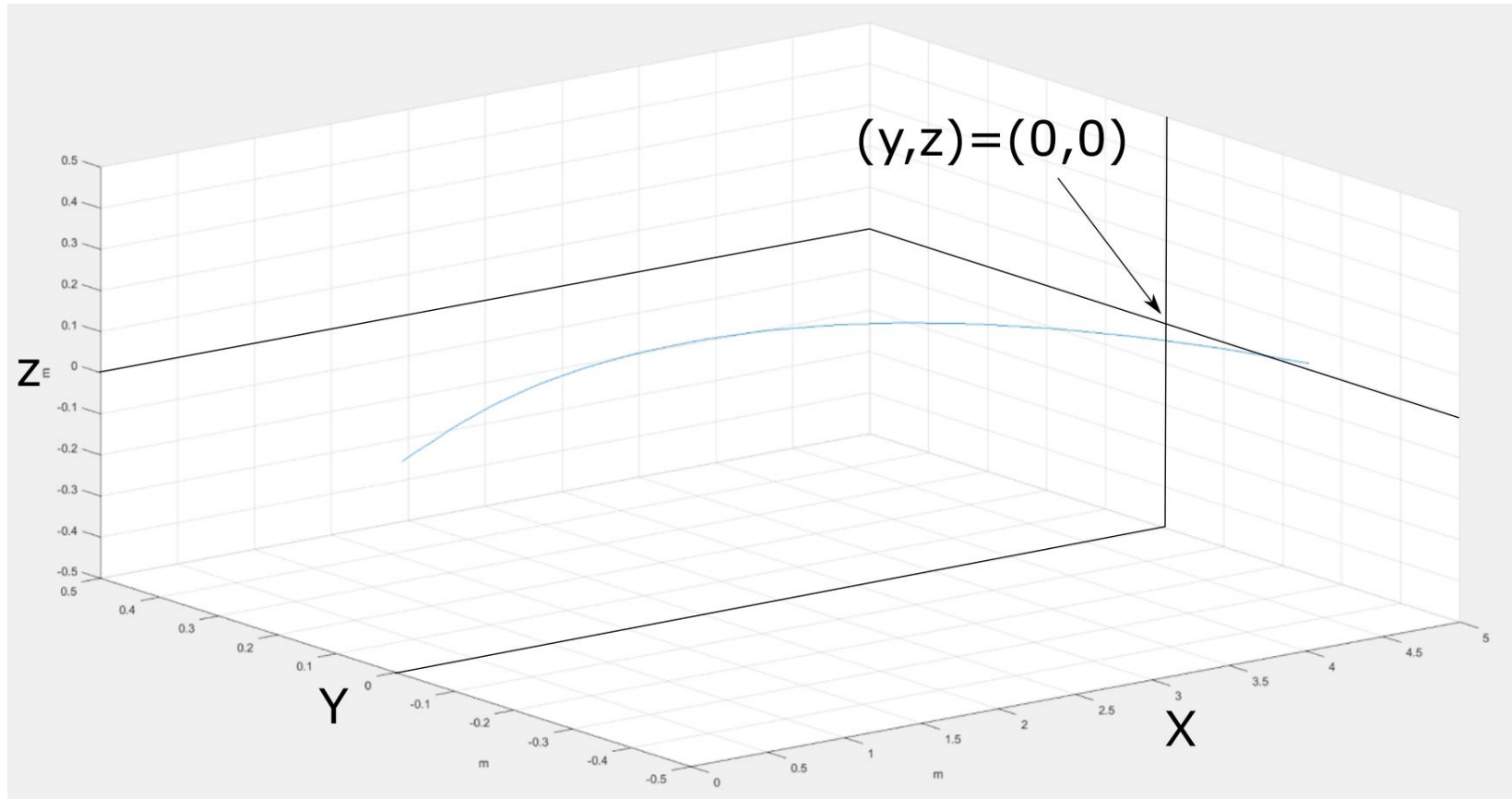


Figure 5.7. The graph shows the 3D trajectory of the centre of mass of the spear after leaving the hand of the thrower and just before impacting the animal (i.e. the flying time). Axes (X , Y , and Z) are in metres (experiment code: TH-81). Graph: E. Burgos-Parra.

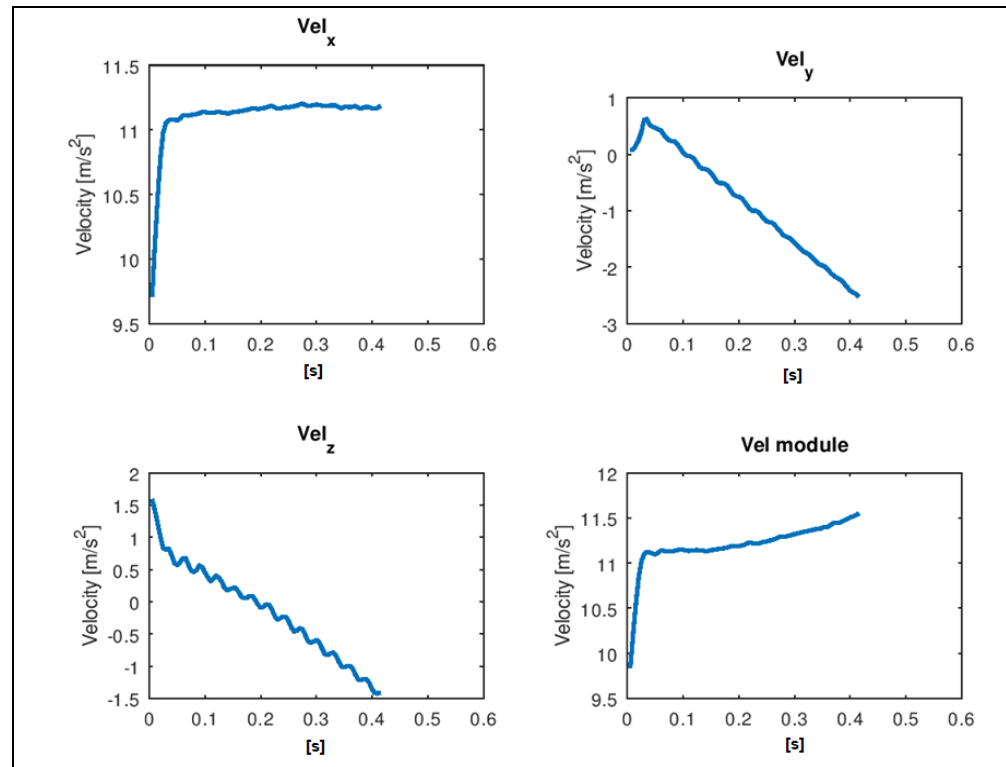


Figure 5.8. X, Y, and Z components and module of the acceleration (experiment code: Th-81).

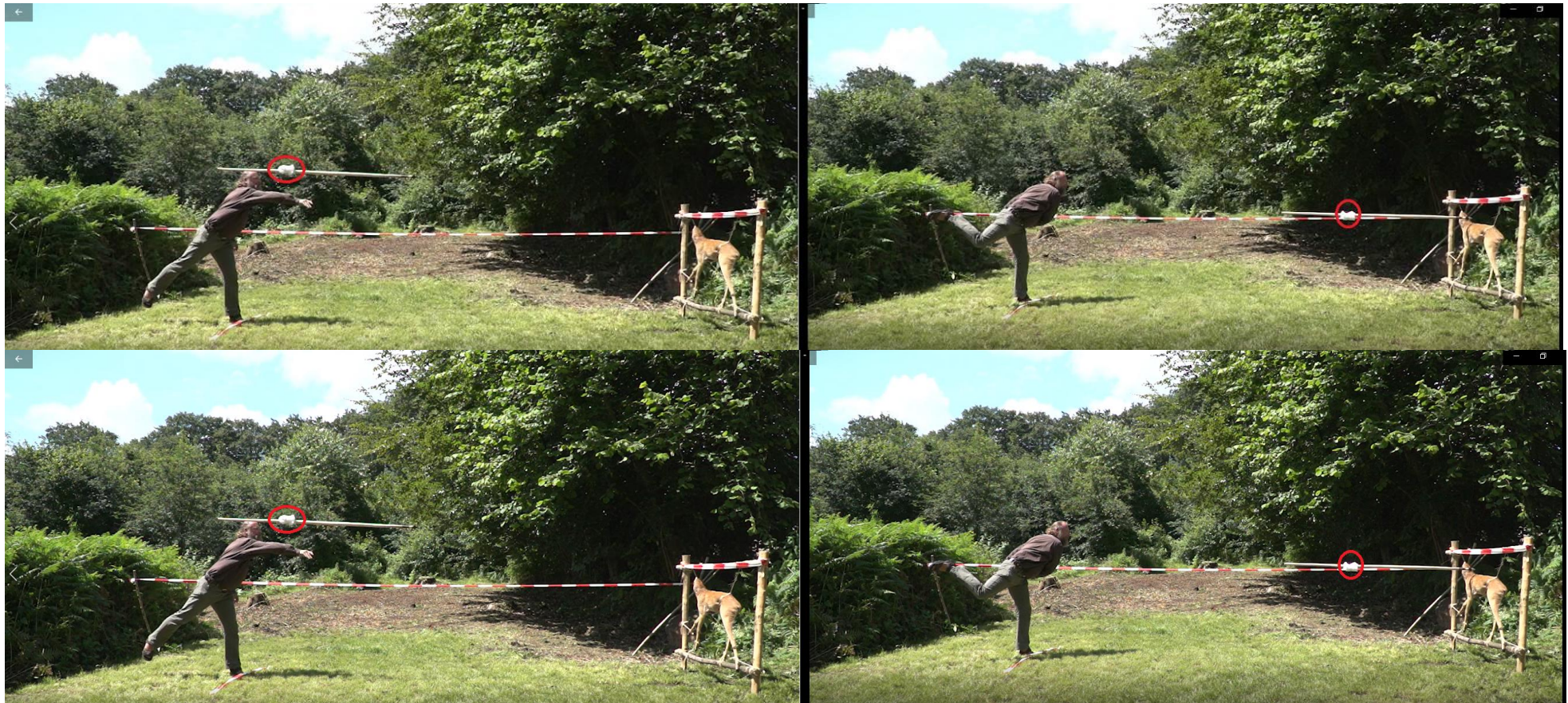


Figure 5.9. The gyration movement of the accelerometer (in red) on the symmetry axis of the spear. Top picture: experiment code TH-82, bottom picture: experiment code TH-62.

5.3 Results of ballistic parameters of throwing and thrusting hand-delivered stone-tipped spears

Table 5-10 shows the results of the realistic ballistic parameters of hand-delivered throwing and thrusting stone-tipped spear experiments (second set of experiments, see CHAPTER 2). The sample counted n=40 experiments recorded with the X200-4 accelerometer. However, because two recordings were not suitable for analysis due to a deactivation of the device during the trial, the final sample amounted to n=38 experiments (n=22 throwing and n=16 thrusting experiments). The results are presented below.

Table 5-10. The ballistic parameters of hand-delivered throwing (TH) and thrusting (TR) stone-tipped spears when used by trained human participants on realistic targets.

Exp. ID	Exp Type	Velocity (m/s)	KE (J)	P (kgm/s)	Max deceleration (m/s ²)	Penetration depth (cm)	Spear Mass (g)	Wound (mm) Length*width
52	TH	11.17	43.17	7.73	38.61	14	692	40*20
53	TH	11.91	47.92	8.03	29.52	43	675	50*32
56	TH	12	45.45	7.57	NA	NA	631	Missed
58	TH	11.3	42.09	7.44	46.92	5	659	40*20
60	TH	11.61	43.93	7.55	35.32	11	651	50*25
61	TH	11.76	44.33	7.52	34.5	45	640	45*30
62	TH	10.06	32.46	6.44	29.8	39	641	46*20
66	TH	11.71	43.84	7.48	31.08	4	639	30*38
67	TH	11.62	44.96	7.73	66.33	14	666	45*25
68	TH	12	48.3	8.04	21.19	42	670	60*10
71	TH	11.05	39.16	7.08	NA	NA	641	Missed
73	TH	11.69	44.36	7.58	64.14	2	649	05*10
76	TH	12.02	46.29	7.69	NA	NA	640	Bounced off

77	TH	11.7	44.57	7.61	28.42	51	651	30*35
78	TH	12.2	46.52	7.62	56.48	2	625	40*02
79	TH	12.76	51.02	7.98	105.09	4.5	626	50*13
81	TH	12.12	46.17	7.61	NA	NA	628	Missed
82	TH	9.59	29.04	6.05	NA	NA	631	Missed
84	TH	8.78	24.53	5.57	NA	NA	635	Missed
88	TH	8.45	22.61	5.34	NA	NA	632	Missed
91	TH	13.4	57.85	8.63	65	4	644	04*30
92	TH	11.61	44.48	7.65	57.82	2.8	659	15*33
Average	TH	11.59	42.21	7.36	45.68	18.88	646.59	27 cm²
54	TR	4.66	14.24	6.11	10.65	2	632	05*05
55	TR	3.01	6.11	4.06	15.63	74	670	
57	TR	5.13	17.36	6.77	6.71	45	640	20*40
63	TR	4.65	14.32	6.16	11.21	2	645	20*03
64	TR	3.38	7.72	4.57	11.18	74	673	60*15
65	TR	4.26	11.88	5.58	21.51	0	630	30*38
69	TR	6.78	30.10	8.88	10.38	102	630	50*25

70	TR	4.28	12.22	5.71	19.23	77	655	40*35
72	TR	5.85	22.56	7.71	21.28	1	639	05*05
74	TR	3.31	7.23	4.36	5.8	4	640	05*10
80	TR	4.5	13.40	5.95	NA	NA	644	Missed
83	TR	6.92	31.05	8.97	22.17	48	617	30*35
85	TR	5.82	22.16	7.61	26.35	5	629	04*30
86	TR	4.44	12.98	5.84	NA	NA	637	Missed
87	TR	4.5	13.33	5.92	NA	85	637	50*30
89	TR	6.42	27.20	8.47	31.88	2.5	640	60*20
90	TR	5.17	17.80	6.88	26.49	119	652	44*04
93	TR	5.82	22.49	7.72	17.01	6.5	648	10*20
Average	TR	4.86	16.90	6.52	16.44	40.43	642.11	30 cm²

Table 5-11. Descriptive statistics of ballistic parameters of hand-delivered throwing (TH) and thrusting (TR) stone-tipped spears.

	Impact Velocity TH (m/s ²)	Impact Velocity TR (m/s ²)	Kinetic energy TH (J)	Kinetic energy TR (J)	Momentum TH (kgm/s)	Momentum TR (kgm/s)	Max Deceleration TH (m/s ²)	Max Deceleration TR (m/s ²)
Mean	11.59	4.86	42.21	16.90	7.59	6.52	45.68	16.44
Max	12.76	6.92	51.06	31.05	8.04	8.97	105.09	31.88
Min	10.06	3.01	32.46	6.11	6.44	4.06	21.19	5.80
SD	0.62	1.41	4.70	7.54	0.44	1.47	24.03	7.53
Shapiro-Wilks test results	p=0.131	p=0.245	p=0.003	p=0.225	p=0.009	p=0.486	p=0.016	p=0.416

5.3.1 Impact velocities

The impact velocities recorded for throwing hand-delivered stone-tipped spears ranged from 12.76 m/s to 10.06 m/s (mean= 11.59 m/s, SD= 0.62 m/s) (Table 5-11), while the impact velocities recorded for thrusting hand-delivered stone-tipped spears ranged from 6.92 m/s to 3.01 m/s (mean= 4.86 m/s, SD= 1.41 m/s) (Table 5-11). Histograms of the data-sets showed a unimodal distribution both for throwing and thrusting series (Figure 5.10). The Shapiro-Wilks test (suitable for small sample sizes) demonstrated a normal distribution for throwing ($p=0.131$) and a normal distribution for thrusting ($p=0.245$). Thus, when these parameters were used in the statistical analysis, parametric tests were conducted accordingly.

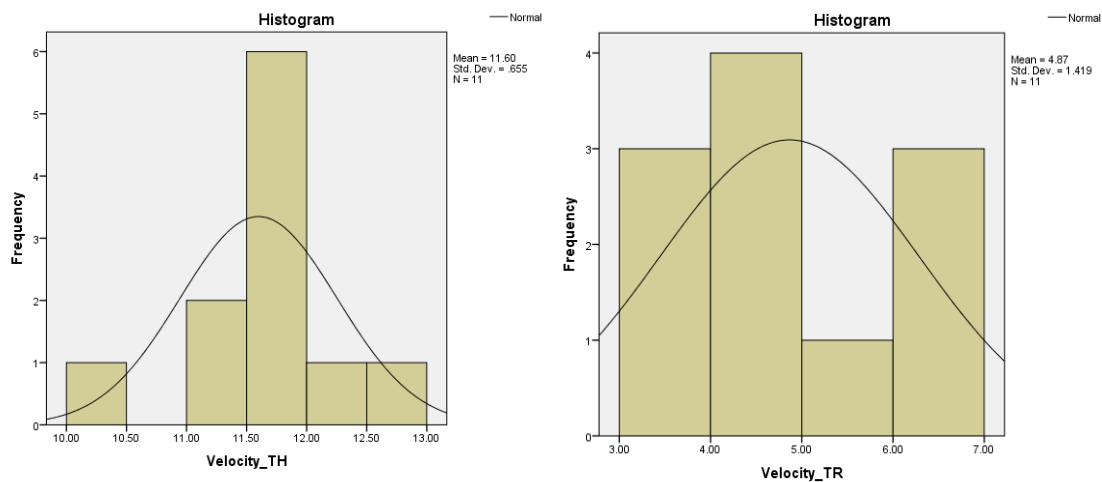


Figure 5.10. Histograms of distributions of impact velocity frequencies of throwing (left) and thrusting (right) experiments.

5.3.2 Kinetic energy (KE), momentum (p), maximum deceleration, and trajectory

5.3.2.1 KE at the impact

The KE at the moment of impact for throwing hand-delivered stone-tipped spears ranged from 51.06 J to 32.46 J (mean= 44.21 J, SD= 4.70 J) (Table 5-11), while the KE at the moment of impact for thrusting hand-delivered stone-tipped spears ranged from 31.054 J to 6.115 J (mean= 16.902 J, SD= 0.509 J)

(Table 5-11). The wide range of *KE* values is due to differences on impact velocities and mass of the spears. Histograms of the data-sets showed a slightly skewed distribution for throwing and a normal distribution for the thrusting series (Figure 5.11). The Shapiro-Wilks test (suitable for small sample sizes) confirmed a non-normal distribution for throwing ($p=0.003$), and a normal distribution for thrusting ($p=0.225$). Thus, when these parameters were used in the statistical analyses, parametric and non-parametric tests were conducted accordingly.

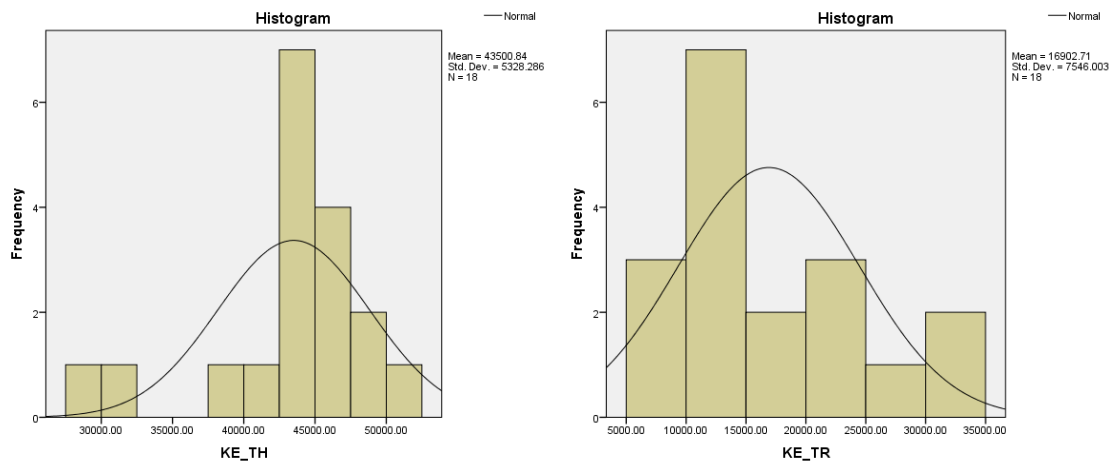


Figure 5.11. Histograms of distributions of the kinetic energy (*KE*) frequencies of throwing (left) and thrusting (right) experiments.

While the *KE* values for throwing can be used as references for further comparison with other experiments, special care must be taken when using the thrusting *KE* values as a result of the approximations made during their calculation (see Section 5.2.2.3). Nevertheless, both ranges of values are representative of human-performed stone-tipped spear experiments, and are the first reported data in the field (Table 5-11). Histograms of distributions of the kinetic energy (*KE*) frequencies of throwing (left) and thrusting (right) experiments.

5.3.2.2 Momentum at the impact

The momentum (p) at the moment of impact recorded for throwing hand-delivered stone-tipped spears ranged from 8.04 kg*m/s to 6.44 kg*m/s (mean= 7.59 kg*m/s, SD=0.44 kg*m/s) (Table 5-11), whereas the momentum (p) at impact recorded for thrusting hand-delivered stone-tipped spears ranged from 8.975 kg*m/s to 4.064 kg*m/s (mean= 6.520 kg*m/s, SD=1.477 kg*m/s) (Table 5-11). The wide range of momentum values is due to differences on impact velocities and mass of the spears. Histograms of the data-sets showed a slightly skewed distribution for throwing and a unimodal distribution for thrusting series (Figure 5.12). The Shapiro-Wilks test (suitable for small sample sizes) confirmed a non-normal distribution of the throwing momentum series ($p=0.009$) and a normal distribution for thrusting ($p=0.486$). Thus, when these parameters were used in the statistical analyses, parametric and non-parametric tests were conducted accordingly.

While the values for throwing can be used as references for further comparison with other experiments, special care must be taken when using the thrusting momentum values due to the approximations taken during calculation (see Section 5.2.2.3). However, both ranges of values are representative of human performed stone-tipped spear experiments and are the first reported data in the field.

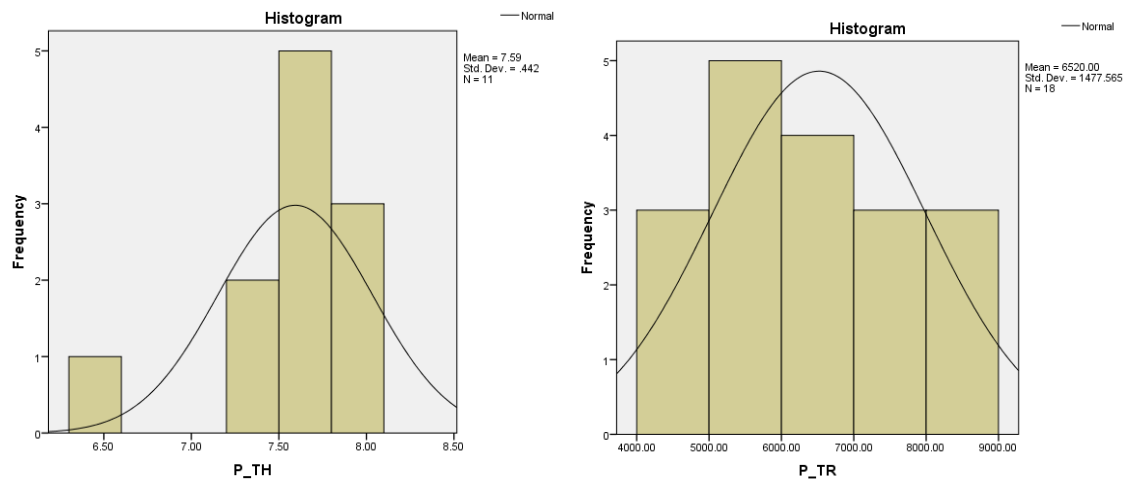


Figure 5.12. Histograms of the distributions of momentum frequencies of throwing (left) and thrusting (right) experiments.

5.3.2.3 Maximum Deceleration

The maximum deceleration (m/s^2) recorded for throwing hand-delivered stone-tipped spears ranged from 105 m/s^2 to 21 m/s^2 (mean= 45 m/s^2 , SD= 24 m/s^2) (Table 5-11), while the maximum deceleration (m/s^2) recorded for thrusting hand-delivered stone-tipped spears ranged from 31 m/s^2 to 5 m/s^2 (mean= 16 m/s^2 , SD= 7 m/s^2) (Table 5-11). The wide range of values is possibly due to differences in the impact locations (as expressed in Section 5.4). Histograms of the data-sets showed a skewed distribution for throwing and a unimodal distribution of thrusting series (Figure 5.13). The Shapiro-Wilks test (suitable for small sample sizes) confirmed a non-normal distribution for throwing ($p=0.016$) and a normal distribution for thrusting ($p=0.416$). Thus, when these parameters were used in the statistical analyses, parametric and non-parametric tests were conducted accordingly.

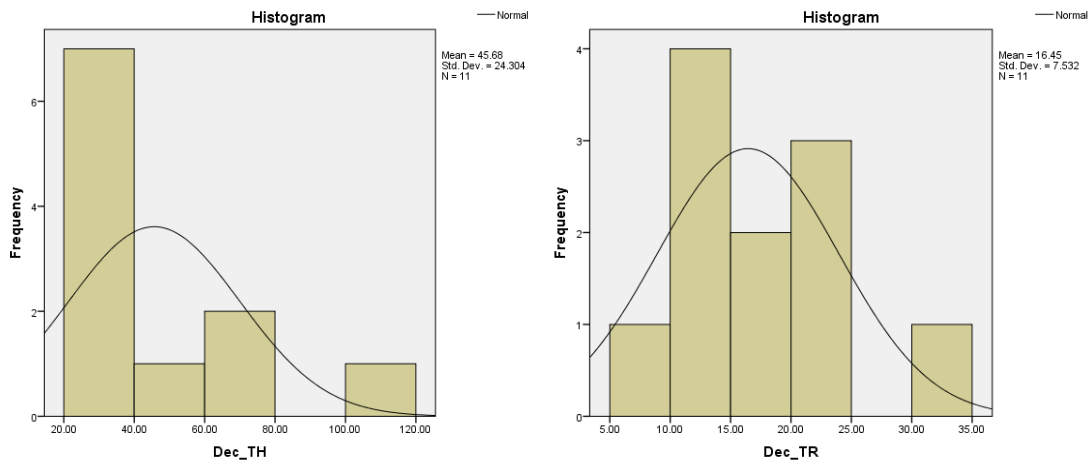


Figure 5.13. Histograms of the distributions of maximum deceleration frequencies of throwing (left) and thrusting (right) experiments.

5.3.3 Maximum penetration depth

The maximum penetration depth was calculated for all of the hand-delivered spear experiments (first and second set of experiments; see CHAPTER 2). Penetration depth (cm) was recorded from the entrance hole until the distal end of the spear. This was recorded for each launch, except when the spear missed the target. All missed shots were thus excluded from the analysis.

The mean of the penetration depth recorded for all throwing hand-delivered stone-tipped spears experiments was 30.96 cm, ranging from 95 cm to 2 cm (Table 5-12). The mean of the penetration depth recorded for all thrusting hand-delivered stone-tipped spears experiments was 37.92 cm, ranging from 122 cm to 0.5 cm (Table 5-12). The mean values both for throwing and thrusting spears are superior to the lethal threshold (20 cm) theorised to kill large mammals (Hughes, 1988). Histograms of the data-set showed a left-skewed distribution for both series (Figure 5.14). The Shapiro-Wilks test (suitable for small sample sizes) confirmed a non-normal distribution of both data-sets ($p=0.003$ for throwing and $p=0.005$ for thrusting, Table 5-12). Thus, when these parameters were used in the statistical analyses, non-parametric tests were conducted.

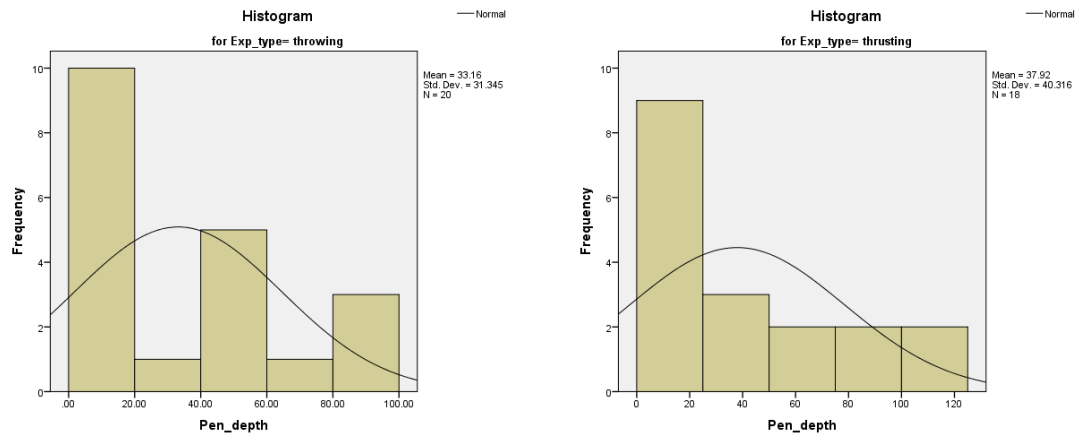


Figure 5.14. Histograms of skewed distributions of penetration depth frequencies of throwing (left) and thrusting (right) experiments.

Table 5-12. The maximum penetration depth of this thesis' hand-delivered throwing and thrusting stone-tipped spears (in green) compared with previously published results of untipped hand-delivered thrusting spears (Milks et al. 2016) and untipped and stone-tipped throwing spears fired using a crossbow (Wilkins et al. 2014).

Penetration depth (cm)	Mean (cm)	Median (cm)	Max (cm)	Min (cm)	SD (cm)	N. of shots	Source	Shapiro-Wilks test
Hand-delivered stone tipped spears TH	30.9	14	95	2	31.34	28	This thesis's experiments	p=0.003
Hand-delivered stone tipped TR	37.9	20	122	0.5	40.23	24	This thesis's experiments	p=0.005
Mechanically delivered stone-tipped spears TH	20.0	-	23.2	15	1.8	10	Wilkins et al., 2014	
Mechanically delivered untipped spears TH	22.2	-	25.5	19	1.9	10	Wilkins et al., 2014	
Hand-delivered untipped TR	11.9	-	14.5	9.3	1.3	39	Milks et al., 2014	

5.3.4 Acceleration profiles

The acceleration profiles (see also 5.2.2.1) provide a visualisation of the acceleration of the spear over the time span of the experiments (i.e. single shots). They act as a visual summary of the different phases of the experiment, from the point of view of the acceleration.

The acceleration profiles were computed individually and then clustered into categories of impact motions. Before the penetration event, the required parameters could be calculated in a quantitative manner. However, once the spear entered the target, the new system (spear plus animal) was too complex to quantify. Difficulties in terms of the analysis of the profiles arose from the fact that, after the spear hit the target, the new system (created by the spear, the animal target, and its constraints) behaved in an unpredictable manner and it was not possible to clearly elucidate the behaviour of the spear. In addition to this, the spear did not always hit and perforate the animal (sometimes they bounced back or missed the target). This complexity can be observed in the profile of the acceleration during the “penetration event”, which contains multiple peaks that were not possible to ascribe to a singular event.

5.3.4.1 Throwing acceleration profiles

For throwing hand-delivered spear motions (n=22 experiments recorded with the X200-4 accelerometer), three categories of acceleration profiles could be observed:

- “Full penetration” profiles: when the spears hit and fully penetrated the animal target (Figure 5.15). These profiles show a deceleration peak, i.e. the impact event, followed by a fluctuating acceleration during the penetration event (Figure 5.15). The degree of fluctuation is due to the change in the acceleration of the spears in relation to the impact materials. Impact with hard tissues, such as bone, created greater deceleration peaks than impact with soft tissues, such as meat (see also Section 5.4). Seven profiles for this category were observed (see

accompanying material, folder - slow-motion videos 52TH, 53TH, 61TH, 62TH, 67TH, 68TH, and 77TH on the USB stick).

- “Bounced or glanced” profiles: when the spears hit the animal target but they bounced back onto the ground (Figure 5.16), or they glanced over the wooden frame (Figure 5.16). These profiles show a deceleration peak, i.e. the impact event, followed by a second acceleration peak as a result of an increase in speed during the rebound or deflection of the spear (Figure 5.16). Twelve profiles for this category were observed (see accompanying material, folder - slow-motion videos 58TH, 60TH, 66TH, 73TH, 78TH, 79TH, 91TH, 92TH, 66TH, 71TH, 76TH, and 82TH on the USB stick).
- “Missed” profiles: when the spears missed the target and went straight into the ground (Figure 5.17). The profiles show a deceleration peak, i.e. the impact event, followed by a short and steady acceleration during their penetration into the ground (Figure 5.17). Four profiles were observed (see accompanying material, folder - slow-motion videos 56TH, 81TH, 84TH, and 88TH on the USB stick).

The acceleration profiles have also indicated the occurrence of a spin rotation effect when spears were hand-thrown over a short distance (5 m). In Figure 5.6, it is possible to observe the parabolic trajectory of the spear while it is flying towards the target. Whereas, Figure 5.9 shows the spinning effect of the hand-delivered throwing spears. The spin results are a combination of two forces: the force of the thrower, which is applied in the centre of mass of the spear and produces the forward linear movement; and a gravitational force which is exerted on the surface of the shaft. This spin rotation may have an influence on resultant microscopic impact wear traces (as suggested in CHAPTER 6).

In conclusion, the acceleration profiles showed that realistic hand-delivered throwing spear motions are characterised by a high degree of variation after impact due to the type of penetration (full penetration vs bouncing) and impact

location (hard or soft tissue impact). Moreover, they testified the presence of a spear spin rotation movement in throwing distances of 5 m and the presence of oscillation as a result of a torque force (see Section 5.2.2.3.4). However, it is possible, but it would need further verification, that spin rotations in distances shorter than 2m are not present (see Iovita et al., 2014). However, the large variability recorded for the acceleration profiles after the impacts warrants further investigation since the different profiles and, therefore, type of penetrations can be due to differences in the angle of impact between the spears and the target, in the level of *KE* of the spears at the moment of impact, or to differences in the locations of impact (e.g. soft tissues, hard tissues).

These outcomes generate several points of discussion when compared with previous experiments in the field of spear technology (see Section 5.5).

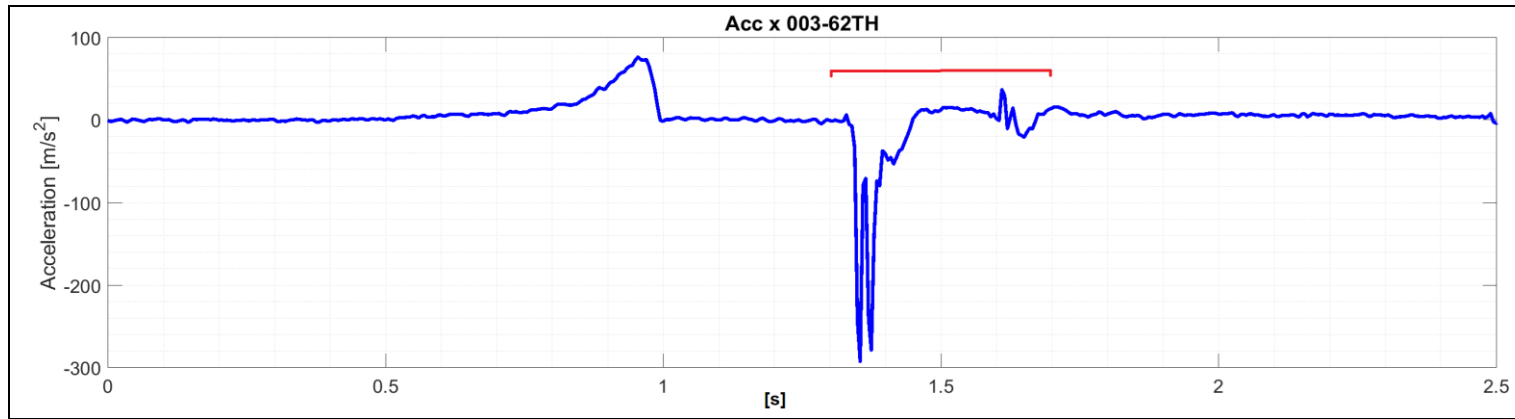


Figure 5.15. “Full penetration” profiles. The spear hit and penetrated the target as shown by the fluctuating acceleration during the penetration time (in red; experiment code: TH-62).

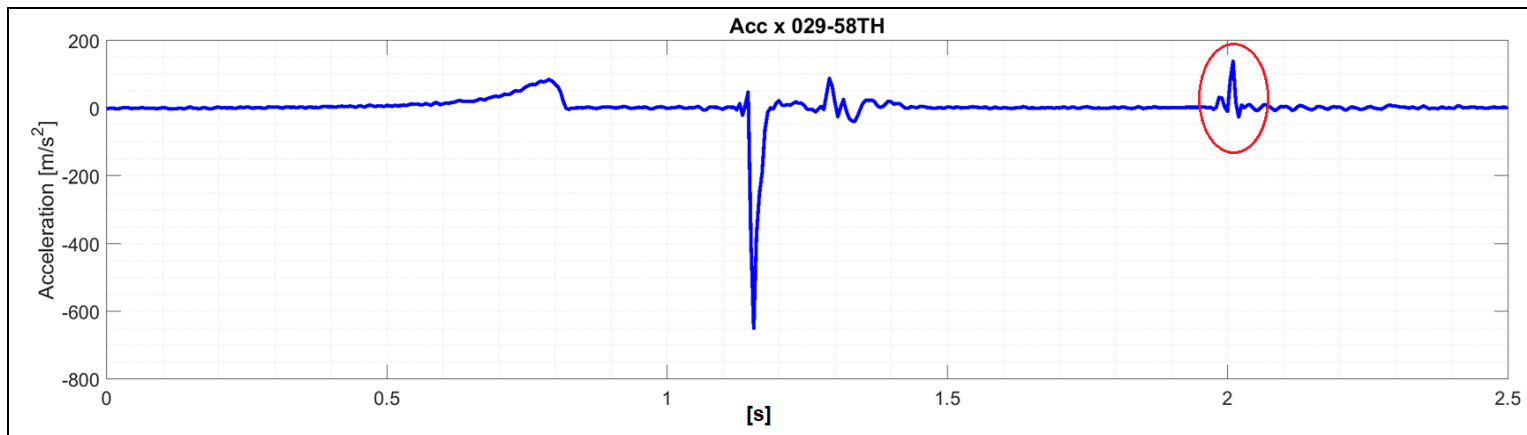


Figure 5.16. “Bounced” acceleration profiles. The spears hit the target and bounced back, as shown by the second peak of acceleration (red circle; experiment code: TH-58 up picture).

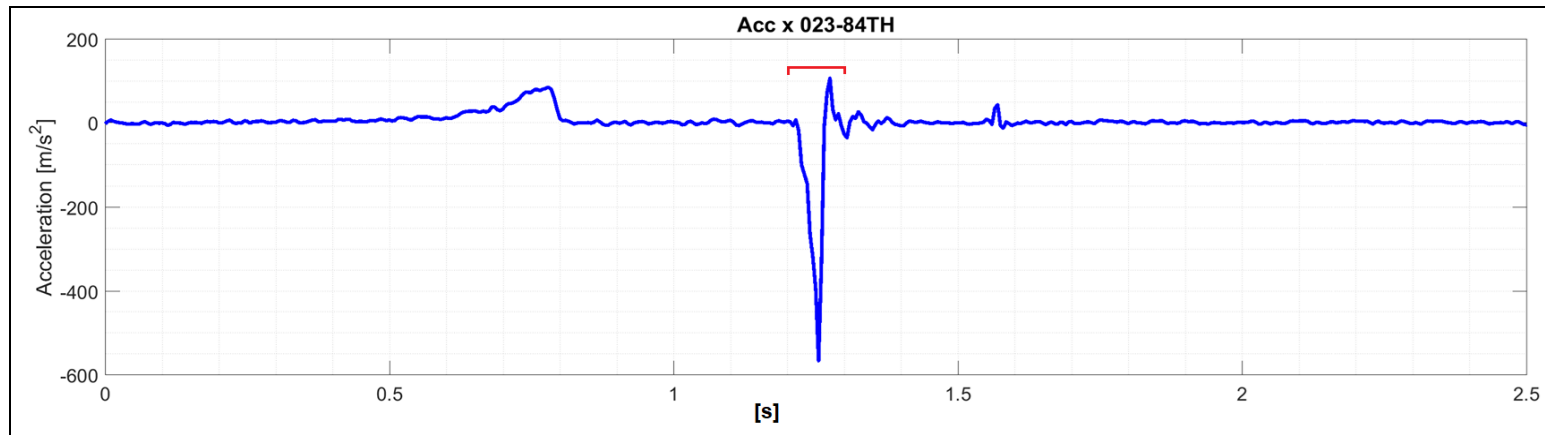


Figure 5.17. “Missed” acceleration profiles. The spear missed the target and went straight into the ground, as shown by the very short penetration time (red line; experiment code: TH-84).

5.3.4.2 Thrusting acceleration profiles

Thrusting hand-delivered spear motions (n=16 experiments recorded with the X200-4 accelerometer) showed a large variability of acceleration profiles. This is because thrusting motions are non-isolated systems, in which the human thruster holds the spear and applies force during the entire execution of the movement, generating a non-conservative system (meaning that there is always an external and non-uniform force applied to the system). Therefore, thrusting acceleration profiles were influenced by several factors, such as:

- The choice of the human thruster to block or continue the thrusting action (by applying more force to the spear), thus resulting in different acceleration profiles.
- The response of the target to the force applied against it, dependant on the constrains of the animal and Newton's third law (action and reaction).
- The human-behaviour factor, dependant on the: technique used by the human-thruster, the body mass, force, stature, fitness, adrenaline, and general skills of the person (as also suggested by Milks et al., 2016).
- The impact location of the spear. Impact with hard tissues, such as bone, created greater deceleration peaks and shortened penetration depths, in contrast with the data from impacts with soft tissues, such as meat (see Section 5.4)

Consequently, the thrusting acceleration profiles should be described on a case-by-case basis, although with reference to some broad categories, as follows:

- The profile on Figure 5.18 (accompanying file 89TR on the USB stick) shows an initial acceleration peak (corresponding to the thrusting time, see 5.2.2.1) followed by a short stabbing time (0.02"; see Section 5.2.2.1) and a tail. This means that the human-thruster stopped the thrusting action (without applying more force) after the first acceleration

peak. These types of profiles were deemed to be “one-push profiles” (in line with Milks et al., 2016, p. 196).

- Figure 5.19 (accompanying file 83TR on the USB stick) shows an initial acceleration peak (corresponding to the thrusting time, see 5.2.2.1) followed by a second acceleration peak (i.e re-acceleration). This means that, after the impact, the human thruster continued the thrusting action (by applying more force) with a second push into the target. These types of profiles were termed “two-pushes profiles” (in line with Milks et al., 2016, p. 196).

Also, thrusting profiles can denote the type of impact material. It has been observed that lesser deceleration (generally below -20 m/s^2 for thrusting) occurred only when the spears hit and penetrated soft tissues, while greater deceleration (generally above -20 m/s^2 for thrusting) occurred only when the spears hit hard tissues (see also Section 5.2.2.3). This was also observable on the acceleration profiles.

- The profile on Figure 5.20 (accompanying file 57TR on the USB stick) shows a “one-push profile”, and indicates an impact against soft tissue as the deceleration did not exceed -6 m/s^2 .
- The profile on Figure 5.21 shows a “one-push profile”, and indicates an impact against hard tissue as the deceleration exceeded -25 m/s^2 .

The acceleration profiles showed that the same participant (IP) was able to adapt his technique and modulate his force (expressed here in a change of acceleration) in each experiment in relation to the impact location and personal choices. This outcome generates several arguments for discussion when compared with previous experiments in the field of spear technology (see 5.5).

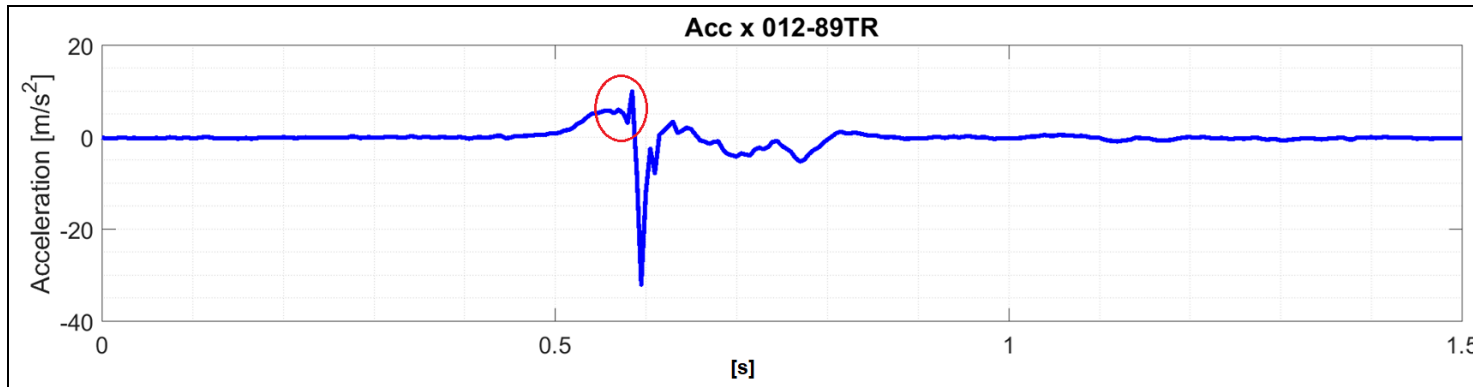


Figure 5.18. “One-push” profile. The thruster pushed the spear inside the animal target only once as shown by the single acceleration peak (in red; experiment code: TR-89).

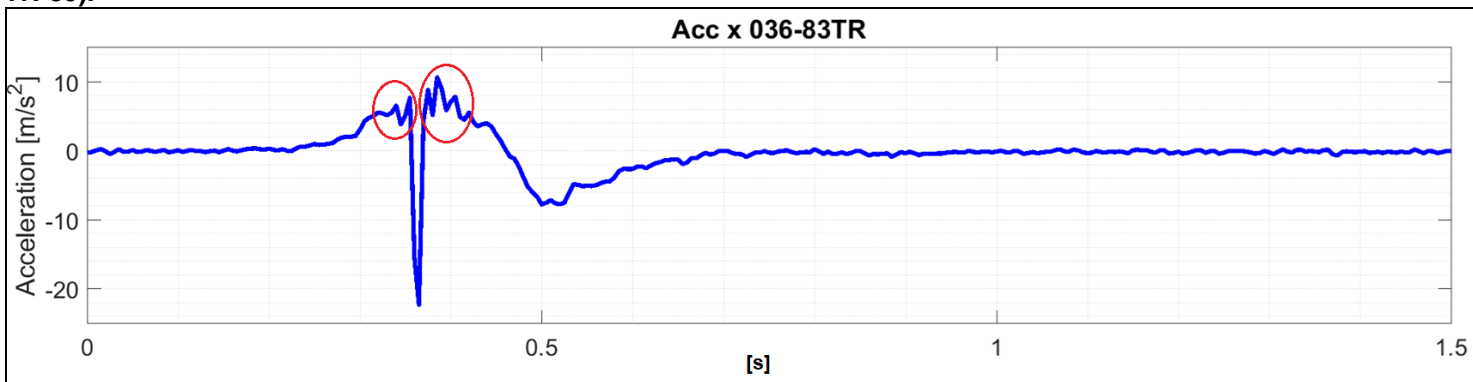


Figure 5.19. “Two-pushes” profile. The thruster double pushed the spear inside the animal target as shown by the two consecutive acceleration peaks (in red; experiment code: TR-83).

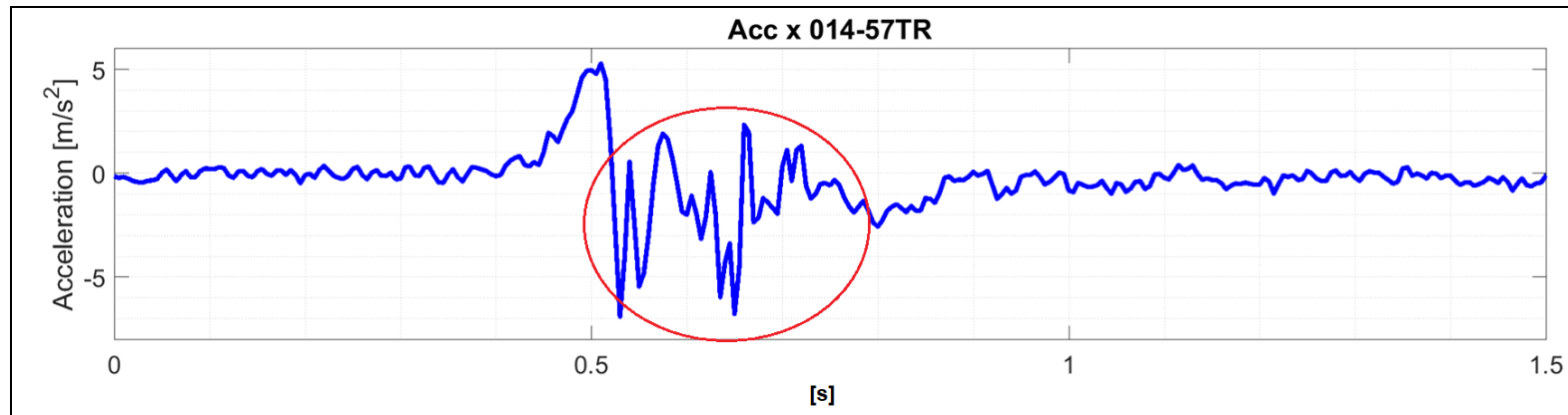


Figure 5.20. “Soft-tissue penetration” profile. The acceleration after impact shows a low value (around -6 m/s^2 see red circle; experiment code: TR-57).

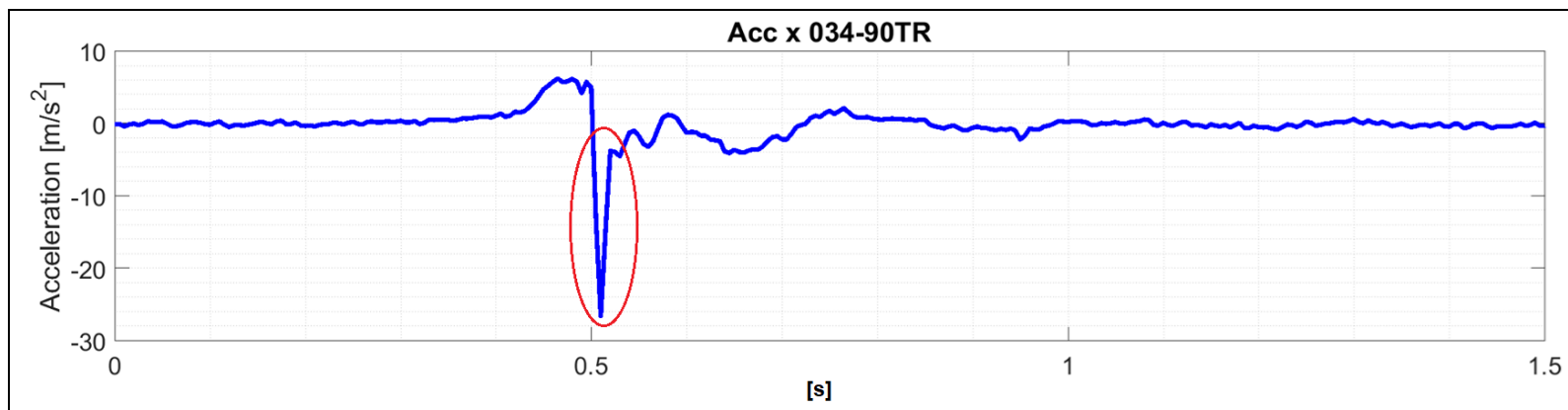


Figure 5.21. “Hard-tissue penetration” profile. The acceleration after impact shows a high value (around -25 m/s^2 see red circle; experiment code: TR-90).

5.3.5 Qualitative observations about the hand-delivered stone-tipped spear experiments.

The following section is a summary of the observations recorded by the author during the throwing and thrusting hand-delivered stone-tipped spear experiments.

Throwing spears (see accompanying material, folder - comments and videos on the USB stick).

Hand-delivered throwing spears that penetrated the animal target created large wound cavities (Figure 5.26). The recorded measurements of the wounds (Table 5-10) show that spears created wounds with a mean length of 366 mm and a mean width of 20 mm at the entrance hole (Table 5-11, Figure 5.26).

The spears that impacted soft (such as meat, flesh, skin) or medium-hard tissues (such as the rib cage) generally had a deeper penetration depth than spears that impacted hard tissues (such as scapula and vertebrae bones), as statistically demonstrated in Section 5.4. In real hunting, spears that had deeper penetration depths (>20 cm; Figure 5.22, Figure 5.23, and Figure 5.24) would have been lethal¹⁷ shots because they would either have hit and perforated vital organs severed the main blood arteries (e.g. the jugular vein), or caused the disarticulation of joints. In a real hunting scenario, if a stone-tipped spear (as the ones reproduced for this thesis's experiments) would be stuck into a prey (and the animal was still able to move) it is likely to image that the spear would have hindered the escape of the animal (see Figure 5.22, Figure 5.23 where the spears are deeply stuck into the target).

¹⁷ Lethality is here defined as the ability of a weapon to cause death instantly.



Figure 5.22. An example of a deeper penetration caused by a hand-delivered stone-tipped throwing spear (experiment code: TH-62).



Figure 5.23. An example of a deeper penetration caused by a hand-delivered stone-tipped throwing spear (experiment code: TH-62).



Figure 5.24. An example of a deeper penetration caused by a hand-delivered throwing stone-tipped spear (experiment code: TH-77).

The spears that instead partially penetrated and/or bounced off the animal target (penetration <20 cm), in a real hunting scenario, they would have suddenly impacted against the animal and possibly stopped its running. In fact, throwing spears arriving with a mean *KE* of 45 J (Table 5-11) would have had an enormous stopping power¹⁸ (as well as a great lethality).

Furthermore, the spears that penetrated the rib cage generally broke more than one rib bone during the same shot (a few spears broke three or sometimes four; Figure 5.26), (see accompanying material, folder - comments and videos [MV_3674] on the USB stick). It is theorised that, during the penetration phase, the throwing spears dissipated their *KE* by breaking the rib bones (which behave as obstacles on the spear's trajectory) and, depending on the angle of impact or the *KE* of the spear, they either became wedged inside the animal

¹⁸ Stopping power is defined as the ability of a weapon to traumatise a target and immediately incapacitate, and thus, halt its movement (Kneubuehl, 2011, p. 166).

because of the animal's skin (which behaves as an elastic material) or they completely perforated the rib cage from side to side (see accompanying comments videos on the USB stick). The spears that hit the spine or shoulder blade instead wounded the animal target, but they often bounced off due to the hardness of the impact tissues (see 5.4). However, although they bounced, during impact the spears caused severe cutting and wounds to the animal target (often cutting off the spinal ligaments and crushing small bone portions; Figure 5.25), (see accompanying comments and videos on the USB stick). In a real hunting scenario, it is likely to think that the impact of these spears, would have possibly shocked the animal and knocked it down for a couple of minutes (in which, hypothetically, the hunter could have killed the animal by stabbing it while it was on the ground).



Figure 5.25. Damage of the spinal ligaments caused by a hand-delivered throwing spear that bounced off (experiment code: TH-66).



Figure 5.26. Example of wounds and bone breakages caused by hand-delivered throwing spears.

5.4 Correlations between ballistic parameters and spear performance

Correlation and regression analyses were calculated to statistically interpret and compare the results of the ballistic parameters (data coming from the second set of experiments, see CHAPTER 2).

5.4.1 Correlation between deceleration values and penetration depth

It has been noticed that the acceleration profiles can denote the type of impact material. It has been observed that lesser deceleration, between 20 and 40 m/s² (in throwing experiments) and between 1 and 20 m/s² (in thrusting experiments), occurred only when the spears hit and penetrated soft tissues, while greater deceleration, between 40 and 110 m/s² (in throwing experiments) and between 20 and 40 m/s² (in thrusting experiments), occurred only when the spears hit hard tissues. This was also observable on the acceleration profiles. Therefore, the maximum deceleration (m/s²) of the spears, which indicates the rate at which the spear decreased its velocity as it hit the target (Section 5.2.2.3), was correlated with the impact locations (i.e. soft or hard tissues) to see whether or not a correlation existed between the maximum deceleration (i.e. change of velocity) and the impact against soft or hard tissues. The graph shown in Figure 5.27 shows that lower deceleration (e.g. for throwing experiments), between 0 m/s² and 40 m/s², occurred only when the spears hit the soft tissues of the animal target (e.g. meat, animal fur, and rib cage), while higher deceleration, between 40 m/s² and 110 m/s², occurred only when the spear hit the hard tissues of the animal target (e.g. the spine and shoulder blade) (Figure 5.27). An independent T-test for parametric data (since the maximum deceleration values were confirmed normally distributed by the Shapiro-Wilks tests both for throwing $p=0.258$ and thrusting $p=0.432$ experiments) was conducted to compare the maximum deceleration values of impacts against soft tissues versus impacts against hard tissues. The T-test results showed a statistical difference in the maximum deceleration values between soft tissues and hard tissues impact locations [$t(13)=-3.283$, $p=0.006$, with $F=3.068$, $p=0.103$] (see also Figure 5.27). These results suggest that soft tissues produce less resistance to penetration than hard tissues and therefore less energy is lost at

the moment of impact, resulting in deeper penetration depth, and thus a smaller change in momentum and a smaller change in velocity.

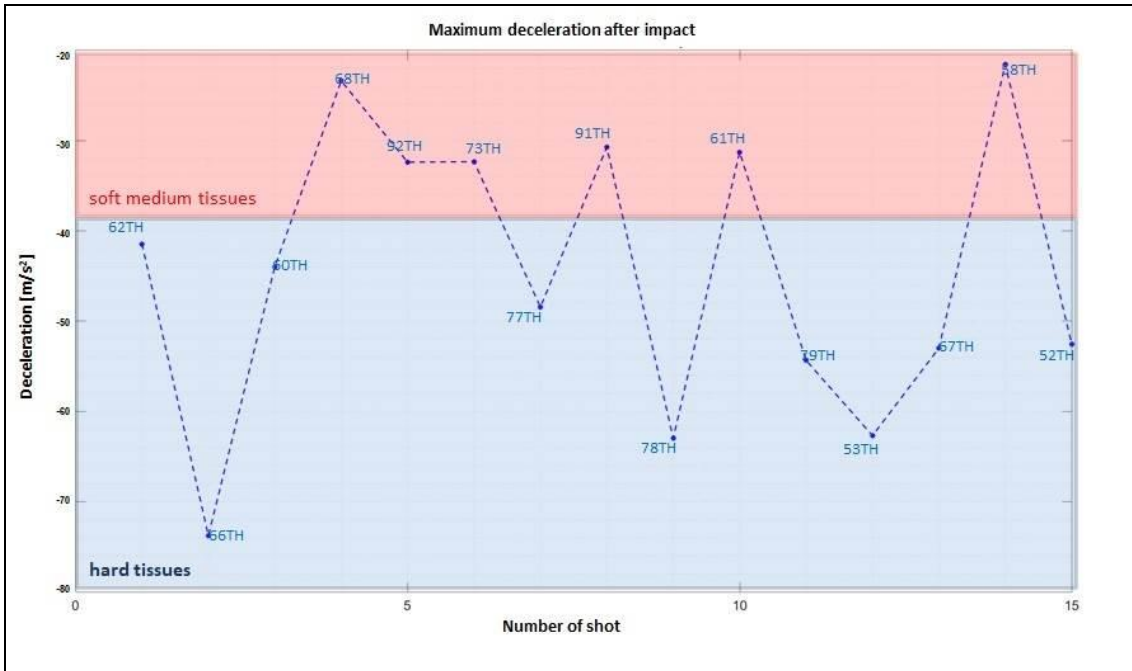


Figure 5.27. Maximum deceleration after the impact of each shot (missed shots were not included).

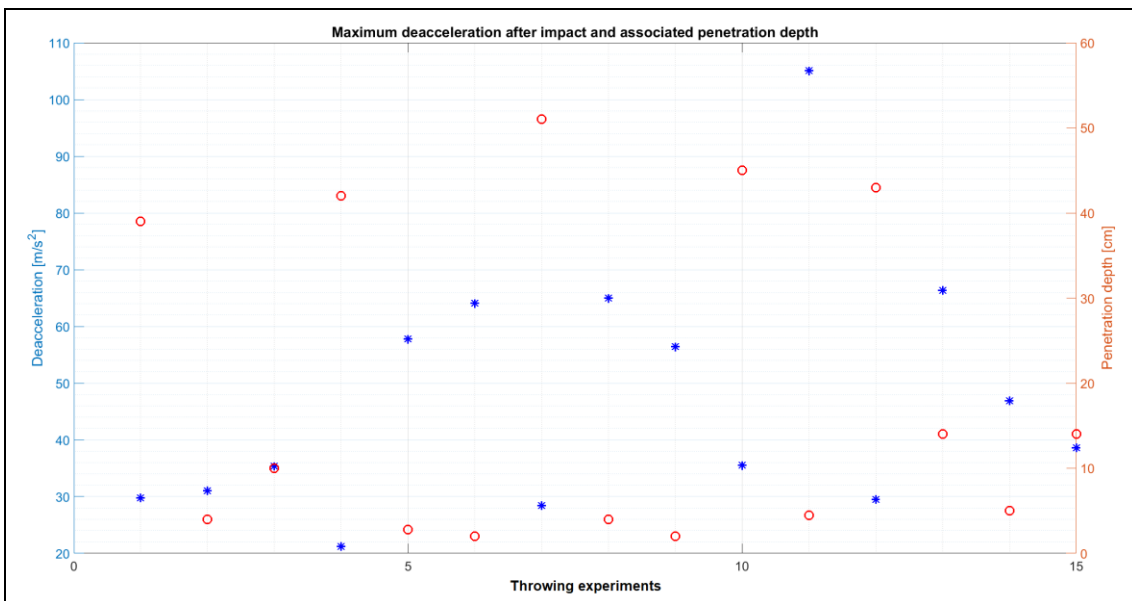


Figure 5.28. Correlation between the maximum deceleration after the impact (blue spots) and the penetration depth (red dots) for each shot (missed shots were not included).

Therefore, the penetration depth was included in the correlation analysis (excluding the missing shots; Figure 5.28). The graph in Figure 5.28 shows that whenever the maximum deceleration was in a low range (between 20 m/s² and 40 m/s², e.g. for throwing experiments), the penetration depth of the spear was consistently greater than 40 cm, meaning that the spear hit a soft tissue and deeply penetrated through the animal target (Figure 5.28). Whereas, when the deceleration was in a high range (between 40 m/s² and 110 m/s², e.g. for throwing experiments), the penetration depth was consistently less than 20 cm, meaning that the spear hit a hard tissue of the animal which halted its penetration (Figure 5.28). The same was observed for thrusting experiments. This negative correlation was also confirmed statistically significant by the Spearman's rho test for non-parametric data ($r_2=-.639$ $p=0.034$, significant correlation). This result clearly indicates an inverse relation between the impact location and the penetration depth, meaning that the penetration depth of spear is closely related to the impact location on the target, i.e. impact locations against soft tissues result in deeper penetration depths than impact locations against hard tissues.

These data are important since puts in doubts some morphometric values of stone points (such as TCSA or TCSP; Shea, 2006; Sisk and Shea, 2009) which have been previously emphasised in relation to the lethality (expressed in penetration depth) of Palaeolithic hunting weapons (see below).

5.4.2 Correlation between penetration depth, TCSA, impact velocities, and impact location

TCSA and TCSP values (Shea, 2006; Sisk and Shea, 2009; see Section 3.3) have been deemed to be critical morphometric values in terms of their ability to distinguish the delivery systems of Palaeolithic stone projectiles (whether arrows, spear thrower darts, or spear-heads; Shea, 2006). The underlying principle is that for deeper penetration of the stone projectile¹⁹, the TCSA value

¹⁹ In this thesis, the term projectile refers to all stone tools (or also organic tools) mounted in a shaft, regardless of the type of weapon and their delivery system (see also Glossary).

of the stone tool must be as small as possible. If the stone projectile is designed to open a hole large enough for the shaft to enter unimpeded, it is suggested that TCSA must fall within precise small range of values (Table 5-13), calculated through experiments and ethnographic samples (Shea, 2006; Table 5-13). Shea (2006, p. 3) suggests that stone points that have TCSA values of above 250 mm² are associated with spear weapon systems, while points with TCSA values of less than 100 mm² are associated with arrow or dart weapon systems. Therefore, to verify the association between TCSA values and maximum penetration of stone projectile weapons, the strength of the correlation between the penetration depth and TCSA and TCSP values of this thesis's hand-delivered stone-tipped spears was tested.

Table 5-13. Shea' (2006) TCSA values.

Samples	TCSA Mean	TCSA SD	TCSA Min	TCSA Max
Arrow tips	33	20	8	146
Spear-thrower dart tips	56	20	24	34
Thrusting spear tips	168	89	20	392

The experimental Levallois points employed in this thesis for the second set of experiments, showed TCSA values ranging between 96 mm² and 503 mm² (mean 236 mm²) for throwing, and between 58 mm² and 423 mm² (mean 221 mm²) for thrusting (Table 5-14). TCSP values, on the other hand, ranged between 84 mm² and 171 mm² (mean 131 mm²) for throwing experimental Levallois points, and between 78 mm² and 159 mm² (mean 123 mm²) for the thrusting ones (Table 5-14). TCSA and TCSP values for throwing and thrusting experimental Levallois points were proven not significantly different (see Section 4.3.1.1).

The strength of the correlation between TCSA and TCSP values, respectively, and maximum penetration depth was evaluated with a Pearson's R correlation test for parametric data (as both the TCSA and TCSP for throwing and thrusting

data were normally distributed, see Shapiro-Wilks test in Table 5-14). The results of the Pearson's R coefficient between TCSA and TCSP values respectively, and maximum penetration depth indicated a very weak and statistically not significant correlation between TCSA and penetration depth, both for throwing ($r=0.108$) and thrusting ($r=0.081$) (Table 5-14), and a weak correlation between TCSP values and penetration depth both for throwing ($r=0.395$) and thrusting ($r=0.269$) (Table 5-14). This suggests that TCSA and TCSP values are poor proxies for the ballistic interpretation of projectile weapons' penetration and lethality.

Table 5-14. Tip-cross section area (TCSA) and Tip-cross sectional perimeter (TCSP) values of this thesis's experimental Levallois points used in throwing and thrusting experiments, plus, the results of the Shapiro-Wilks and Pearson's R tests.

Type of experiment	TCSA mm ²	TCSP mm ²	Shapiro-Wilks (normality) test		Pearson's correlation	
			TCSA	TCSP	Correlating TCSA and penetration depth (cm)	Correlating TCSP and penetration depth (cm)
This thesis' experiments Throwing points (n=22)	M 236 SD 124 Min 96 Max 503	M 131 SD 28.33 Min 84 Max 171	p= 0.438	p= 0.854	($r= 0.108$, $p= 0.702$)	($r= 0.081$, $p= 0.774$)
This thesis' experiments Thrusting points (n=18)	M 221 SD 103 Min 58 Max 423	M 123 SD 21.41 Min 78 Max 159	p= 0.108	p= 0.410	($r= 0.395$, $p= 0.144$)	($r= 0.269$, $p= 0.333$)

However, one can argue that the correlation coefficients for each pair of variables (e.g. for penetration depth and TCSA or TCSP) do not only show the correlation between penetration depth and morphometric values, as they can be influenced by other variables, such as the impact velocity or impact location of the spear. Therefore, multiple correlations (also known as partial correlation)

were run using a partial Spearman's rho correlation test for non-parametric data (as impact velocities data were non-normally distributed, see Shapiro-Wilks test in Table 5-11). The correlation measured the effect of the relationships between individual pairs of variables (i.e. TCSA, impact velocities, and penetration depth) taken one at a time, while the other variables were held constant. The correlation between impact location and TCSA was instead tested with the Mann-Whitney ranking non-parametric test (because the impact location was an ordinal variable and the penetration depth followed a non-normal distribution).

The partial Spearman's Rho correlation test indicated a very weak and a statistically not significant correlation between the penetration depth and TCSA, whilst holding the velocity constant ($r=0.174$; Table 5-15). It also indicated a very weak and statistically not significant negative correlation between the impact velocity and TCSA whilst holding the penetration depth constant ($r=-0.021$; Table 5-15), and a weak but statistically not significant correlation between penetration depth and velocity while holding the TCSA constant ($r=0.3968$; Table 5-15). Therefore, no association could be found between penetration depth, TCSA and impact velocities. Conversely, the Mann-Whitney ranking test indicated a statically significant relationship between impact locations (soft vs hard tissues) and penetration depth ($U=9.500$ $p= 0.039$). Therefore, the results of partial correlation showed that TCSA and impact velocities were not significant predictors of penetration depth. Surprisingly, impact velocities were not significant predictors of penetration depth, whereas the impact location (soft vs hard tissues) was revealed to be a good predictor of penetration depth. Thus, it can be concluded that both TCSA and TCSP values alone are not adequate ballistic proxies for distinguishing projectile delivery systems (contra Shea, 2006 and Sisk and Shea, 2009). Likewise, impact velocities alone are not good proxies to infer about the lethality of hand-delivered stone-tipped spears (contra Wilkins et al., 2014).

Table 5-15. Results of Spearman's Rho correlation test.

Partial correlations (Spearman's rho)	Correlating penetration depth and TCSA , whilst holding the velocity constant	Correlating TCSA and velocity , whilst holding the penetration constant	Correlating penetration depth and velocity , whilst holding the TCSA constant
	(r(12) = 0.174 , p= 0.553)	(r(12) = - 0.021 p= 0.943)	(r(12) = - 0.368 p= 0.195)

5.5 Discussions and conclusions on the recorded ballistic parameters

The results of the analysis of the ballistic parameters of the experimental stone-tipped spears thrown and thrust by trained human participants have raised essential points of discussion. Below the results for each set of experiments are discussed.

5.5.1 Hand-delivered throwing spears - Impact velocities

There are no published studies of hand-delivered throwing spears (either wooden or stone-tipped) which have ever recorded ballistic parameters, such as impact velocities, *KE*, change of momentum, maximum deceleration of the spear during impact (together with penetration depth). Therefore, this study represents the first attempt in archaeology to experimentally measure the ballistic parameters of hand-delivered throwing spears, and it provides accurate and representative ballistic parameters for future experiments that aim to calibrate mechanical devices for spear experiments.

The values of throwing spears' impact velocities recorded in the experiments of this thesis (Table 5-11) demonstrated the extreme uniformity of the human participant's throwing abilities, as proved by the mean value of impact velocity (11.59 m/s^2) and its standard deviation (0.73 m/s^2) (Table 5-11). These data attest to the experience and skills of the human participant WP (see also Section 4.3.4). Moreover, it confirms the experimental assumption that using a single and trained human participant reduces the experimental variability in weapon trials.

The range of impact velocities recorded in of the experiments of this thesis was not comparable with the ethnographic spear-throwing velocities proposed by Hughes (1998) or by Cotterell and Kamminga (1990) (see Table 5-3). This is because, as expressed in Section 5.1, Hughes' (1998) data referred to spear-thrower darts velocities, whereas Cotterell and Kamminga's (1990) velocity was only a theoretical estimation for a spear thrown at a distance of 50 m. Hence, the range of impact velocities recorded in this thesis experiments tended to be lower than the

ethnographic data recorded for darts (Table 5-3), which is expected due to the different delivery systems.

The range and mean of this thesis hand-delivered throwing spear experiments (mean 11.59 m/s) were lower than those of all sport's javelin experiments (Table 5-3). Baugh (2002) and Miller and Munro (1983) reported a sports javelin velocity range between 25 m/s and 30 m/s, while Petranoff scored the highest velocity ever recorded for a sports javelin thrown at 32.3 m/s (Gregor and Pink, 1985). The different ranges and means of impact velocity between hand-delivered throwing spears and sports javelins confirm the diversity in techniques, and therefore the difference in ballistic parameters between the two systems, as already suggested by other research in sports science (Roach et al., 2012; Maki, 2013). Sports javelins' technique aims to cover a long distance²⁰ with a wide target area, whereas hand-delivered spears when used for hunting, need to balance much smaller distances with an emphasis on accuracy to hit the animal target. Moreover, the sports javelins technique starts with a "run up" phase, which hand-delivered throwing spears, when used for hunting purposes, would have possibly avoided it to do not advertise the presence of the hunter and do not scare the animal prey away. Therefore, the observed ballistic diversity between sports darts and Palaeolithic spears brought into question the results of previous experiments. These experiments had tested the use-wear of Palaeolithic spear projectiles by calibrating the firing-machines using estimated measurements from the field of sports science (Iovita et al., 2014, 2016; Shea et al., 2001, 2002), an approach which appears to be questionable in light of the results of this thesis.

Previous experiments employing firing-machines (such as calibrated cross-bows or air-guns) to replicate Palaeolithic spear throwing and use-wear traces have indeed

²⁰ The current Olympic record for javelin throw, men category, is of 94.58 m (see www.olympic.org/montreal-1976/athletics/javelin-throw-men; last accessed 03-11-2018)

estimated the impact velocities at either a low range, between 7 m/s and 9.4 m/s (Wilkins et al., 2014; Iovita et al., 2016), or a high range, between 13 m/s and 25 m/s (Sano et al., 2016; Sano and Oba, 2015; Pargeter, 2007; Hutchings, 2011). However, neither of these ranges are comparable to the hand-delivered throwing spear velocities recorded in this thesis (mean 11.76 m/s), although these can slightly change depending on the human thrower. Wilkins et al. (2014) estimated throwing impact velocities at 9 m/s (Table 5-1), while Sano and Oba (2015), Iovita et al. (2016), Pargeter (2007), and Hutchings (2011) estimated throwing impact velocities at 17.8 m/s, 15 m/s, and 13 m/s respectively, and none of these estimates are in agreement with the results of this thesis (Table 5-1). As loading rates such as velocity, force and *KE* are the principal agents of fracture formation (Cotterell and Kamminga, 1987), the use-wear results presented by these previous experiments can be questionable and barely comparable between them and with the current research. The results presented above stress the importance of correctly calibrated firing-machines in controlled lab experiments which aim to replicate use-wear trace formation and spear biomechanics. Moreover, they provide solid ballistic parameters for future experiments, both in the field of use-wear analysis and biomechanics.

5.5.2 Hand-delivered thrusting spears – Impact velocities

The impact velocities presented in this thesis, from thrusting experiments with a trained human participant, have scored higher impact velocities than previous experiments with untrained human participants (Schmitt et al., 2003) (3.01-6.92 m/s vs 1.7-4.5 m/s (Table 5-2), suggesting that a single and skilled human participant provides results of a higher impact velocity, reducing experimental variability.

The range and mean of thrusting impact velocities recorded in this thesis's experiments match those in studies conducted by Milks et al. (2016) and Gaudzinski-Windheuser et al. (2018) on hand-delivered spears thrust by human participants (Table 5-2). However, the heavier mass of the spears used by Milk et

al. (2016) and Gaudzinski-Windheuser et al. (2018) may have contributed to slightly lower velocity values (4.66 m/s in Milks et al., 2016; 4.2 m/s in Gaudzinski-Windheuser et al., 2018; 4.86 m/s in this thesis's experiments). These data suggest the importance of not overbalancing the mass of the experimental spears. For instance, in the experiments of Gaudzinski-Windheuser's et al. (2018), the total mass of the spear was 3.13 kg which was about two kilos heavier than any recorded ethnographic and experimental thrusting spear-shaft (Oakley et al., 1977; Hughes, 1998, table 3). The heavier spear may have influenced the final velocities of the spear (which were lower, as heavier spears tend to slow down the velocity) and, to a certain extent, the use traces recorded on the animal bones (seeing as a heavier mass causes higher levels of *KE* which may cause different crack and wound patterns on the bone in comparison to a lighter spear).

Furthermore, for the thrusting experiments, the results show that previous thrusting spear experiments that have used firing-machines (such as calibrated cross-bows or a thrusting pendulum) have underestimated the impact velocities. Iovita et al. (2016) estimated the velocity of the pendulum to 1.1-2.7 m/s, while Shea et al. (2001) estimated the velocity of the crossbow to 1.0-1.5 m/s (Table 5-2). Both of these ranges are much lower than the hand-delivered thrusting spears velocities recorded in this thesis (mean of 5.02 m/s, Table 5-2).

5.6 Discussions on the lethality of the hand-delivered spears

The analysis of the penetration depths (Section 5.3.3) shows that stone-tipped thrusting spears had a higher penetration mean (37.92 cm) than the stone-tipped throwing spears (30.96 cm) (Figure 5.29; Table 5-12). This result is expected considering that in a thrusting motion there is the additional force of the human thruster during the penetration. However, these results show that both throwing and thrusting stone-tipped spears had penetration depth means greater than 20 cm, which is considered to be the lethal threshold to kill a large mammal (Hughes, 1998; Frisson, 1989).

Moreover, the ranges and means of penetration depths recorded for stone-tipped hand-delivered spears in this thesis were much higher than in any previous experiments (Milks et al., 2016; Wilkins et al., 2014). The ranges and means of hand-delivered throwing spears presented in this thesis showed higher penetration depths than those shown by untipped and tipped spears when fired with calibrated cross-bows (Wilkins et al., 2014, table S4 in file S1; see Table 5-12). Likewise, the ranges and means of penetration depths recorded for stone-tipped thrusting spears in this thesis were considerably higher than untipped hand-delivered thrusting spears (as expressed in Milks et al., 2016, table 6; see Table 5-12). They were also higher than tipped mechanically-delivered spears (mean 37.9 cm vs 22.2 cm as expressed in Wilkins et al., 2014, table S4 in file S1; see Table 5-12). These results could suggest that stone-tipped spears, when hand-delivered by trained participants, penetrate deeper than untipped spears (contra Wilkins et al., 2014). However, it is worth noting that these comparisons are drawn from results emerging from different experiments which have employed different experimental variables. Therefore, future experimentation is required in order to further investigate the difference between tipped and untipped spear systems.

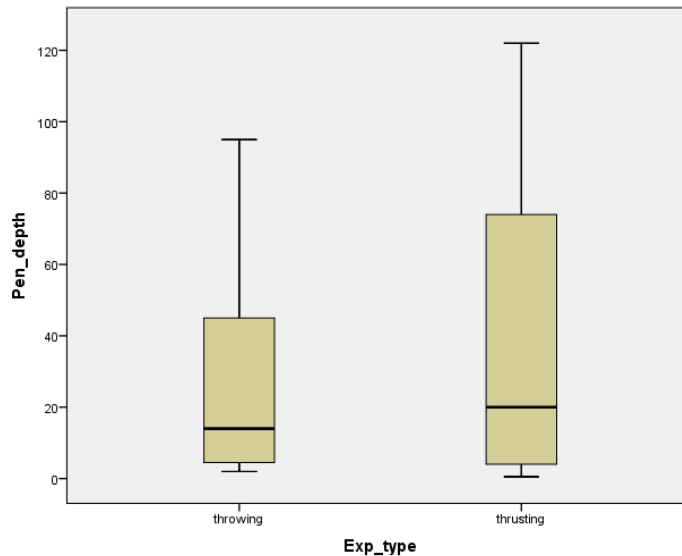


Figure 5.29. Penetration depth (cm) of this thesis' hand-delivered throwing and thrusting spears.

Furthermore, when the two different penetrations are compared (using a Man-Whitney-U test for non-normally distributed data), it appears that the thrusting spear penetration depth was not significantly different from the throwing penetration depth ($U= 107.500, p= .621$). Therefore, considering that both throwing and thrusting stone-tipped spears had penetration depth means higher than 20 cm, both systems can be considered powerfully lethal and well-performing weapons.

However, although the means of the two-penetration depths exceed the endorsed lethal threshold (20 cm), their standard deviations showed a high amount of variation (Table 5-12). In order to explore this variation, each experiment was classified according to three categories of penetration lethality: lethal wound (penetration > 20 cm), partial wound (penetration 5-20 cm), and failed (penetration < 5 cm), (Figure 5.17).

Table 5-16. Frequencies and percentages of the penetration depth for each set of experiments (TH and TR), classified by lethal (>20 cm), partial (5-20 cm), and failed (<5 cm).

Penetration lethality	Throwing n=28	Thrusting n=24
<5 cm (failed)	6	7
	21.5%	29.2%
5-20 cm (partial wound)	3	4
	10.7%	16.6%
>20 cm (lethal wound)	8	9
	28.5%	37.5%
Missed	6	1
	21.5%	3.5%
(NA, previous hole)	5	3
	17.3%	12.5%

Table 5-16 shows that thrusting experiments had a slightly higher percentage of failed shots (<5 cm penetration depth) than throwing experiments, yet they reported a slightly higher percentage of lethal wounds. The failed shots, however, were all related to impact against hard tissues (i.e. hard bone like scapula, or spine), whereas the higher percentage of lethal wounds for thrusting can be interpreted in the light of higher proportions of missed shots for throwing spears. Indeed, when the cumulative distribution of the two samples (TH and TR penetration depths; Figure 5.30) were tested using a Kolmogorov-Smirnov test (for non-normally distributed data), their difference was not statistically significant ($D= 0.641$, $p\text{-value}=0.806$). It is, therefore, possible to suggest that stone-tipped spears when hand-throwing from a distance of 5 m into animal carcasses were as effective as hand-delivered stone-tipped spears hand-thrust from a distance of 2 m into animal carcasses. However, it has to be acknowledged that the different

proportions of missed shot between the two series have also to be taken into account, and further investigation is warranting to test the difference in the performance of hand-delivered throwing spears when used in different distance ranges.

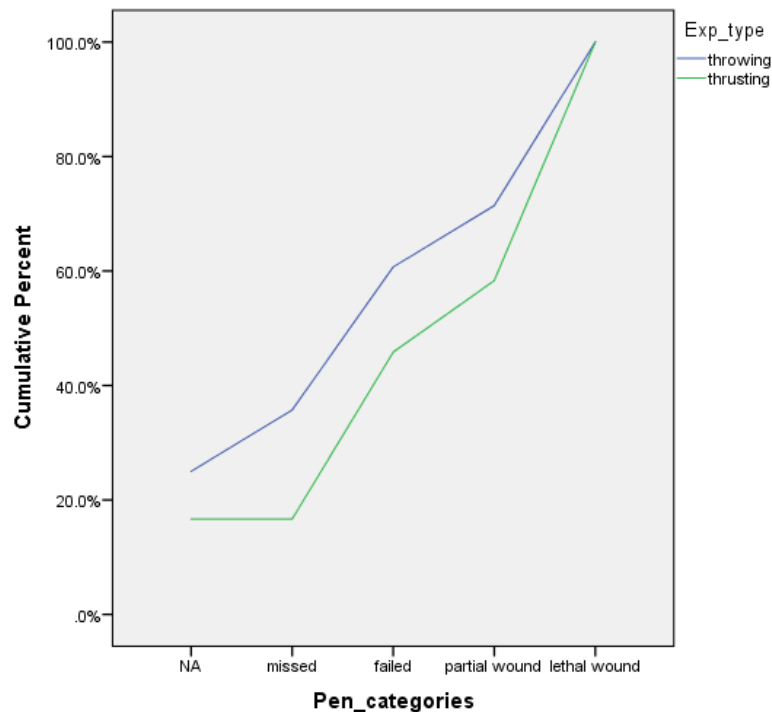


Figure 5.30. Cumulative distributions of throwing and thrusting hand-delivered spear experiments divided per categories of impacts.

Therefore, considering that both hand-delivered throwing and thrusting stone-tipped spears had penetration depth means higher than 20 cm, both systems can be considered powerfully lethal and well-performing weapons.

5.7 Outcomes

The results presented show that previous mechanically delivered throwing spear experiments have used estimated impact velocities from sports science (Shea et al., 2001, 2002; Wilkins et al., 2014; Sano and Oba, 2015; Iovita et al., 2016; Sano et al., 2016) and/or ethnographic data (Iovita et al., 2014; Hutchings, 2011) without contemplating the possibility of performing pilots or replicative tests to corroborate

the impact velocities' means. Unfortunately, this has meant that previous fire-delivered throwing and thrusting spear experiments testing Early, or Middle Palaeolithic weapons have employed estimates of impact velocities that do not match with the ballistic parameters presented in this thesis. The use of a wide range of impact velocities (see Table 5-1 and Table 5-2) may have created experimental data that do not allow for effective comparisons. A miscalculation of impact velocities (Shea et al., 2001, 2002; Iovita et al., 2014; 2016; Sano and Oba, 2015) may have well resulted in different use-wear traces and patterns. Similarly, different levels of velocities (during the calibration of firing machines) may also result in a change in *KE* and momentum, and therefore in possibly different penetration depth rates (as in Wilkins et al., 2014).

Moreover, analysis of the acceleration profiles for throwing has suggested the existence of a spin rotation motion in hand-delivered spears when thrown at short distance ranges (5 m) (see Section 5.2.2.3.4). This spin rotation can influence the depth of penetration into the animal and affect the formation of use-wear traces. Moreover, spin has not been observed in other throwing experiments when using firing-machines (Iovita et al., 2014, 2016; Wilkins et al., 2014; Sano and Oba, 2015), suggesting that throwing biomechanics are as difficult to mechanically replicate as well as thrusting biomechanics (as suggested by Rots and Plisson, 2014, but without ballistic evidence). Analysis of the acceleration profiles (see Section 5.3.4) for throwing experiments have also shown that, when the spears hit the target, they did not always necessarily penetrate the animal as sometimes they bounced. This fact can be linked to the different angles of contact between the weapon and the target, different levels of *KE*, and to the location of the impact of the weapon. As demonstrated by the correlation between penetration depth and impact location (see Section 5.4), soft tissues allow for deeper penetration than hard tissues. Therefore, when the throwing spears hit hard tissues, such as spine and shoulder plate bones, they often pierced the skin but immediately bounced back without reaching full penetration. Whereas, when the throwing spears hit soft tissues, they often fully penetrated the animal. These different behaviours cannot

be entirely replicated by ballistic gel targets, especially when the morphology of the target does not mimic the morphology of the animal and when ballistic gelatine targets do not include bone tissues (see also CHAPTER 11).

In terms of thrusting experiments, analysis of the acceleration profiles revealed that thrusting motions were also very variable actions (Section 5.3.3). The human thruster implements different choices and techniques in response to the target. He/she can decide to continue the thrusting motion by applying more force to the spear and therefore producing momentum, or he/she can choose to block the motion by stopping his/her force. However, these decisions cannot be simulated by firing-machines as they depend upon several physical and behavioural human variables (see Section 5.3.4). Therefore, firing-machines can only estimate impact velocities, but they cannot replicate the entire thrusting motion as they fail to reproduce the peaks of acceleration made in response to the target.

The above discussion brings into question the relevance of using firing-machines in replicating spear mechanisms, as others have already suggested (Hutchings, 2011; Rots and Plisson, 2014; Milks et al., 2016; Iovita et al., 2016; Sano et al., 2016; Coppe and Rots, 2017; Gaudzinski-Windheuser et al., 2018). The combination of data suggests that firing-machines can only replicate impact velocities (if set with correct parameters), but they cannot replicate other kinematics mechanisms such as the torque and spin (for the throwing spear projectiles), the change in momentum, and the energy transferred into the target (for thrusting spear projectiles, as also suggested by Milks et al., 2016). Whereas, as shown by the correlation between penetration depth and impact location (Section 5.4), ballistic gel targets alone cannot entirely recreate the behaviour of an animal target if bone tissues are not incorporated into it.

The results of hand-delivered stone-tipped spears from realistic but controlled experiments have provided new data which facilitate the understanding of the kinematics of hand-delivered spear systems. These results also offer representative and realistic ballistic parameters such as impact velocities,

acceleration profiles, KE values, change of momentum values, and maximum deceleration and maximum penetration depths both for throwing and thrusting spears. These parameters, especially for hand-delivered throwing spears, have been recorded for the first time in an experimental work. They thus provide accurate parameters for future experiments which aim to correctly calibrate mechanical devices. Moreover, they have corroborated the assumption that calibrated firing-machines do not replicate the complexity of human throwing and thrusting motions, inviting future research to carefully conceive experimental protocols for projectile spear experiments.

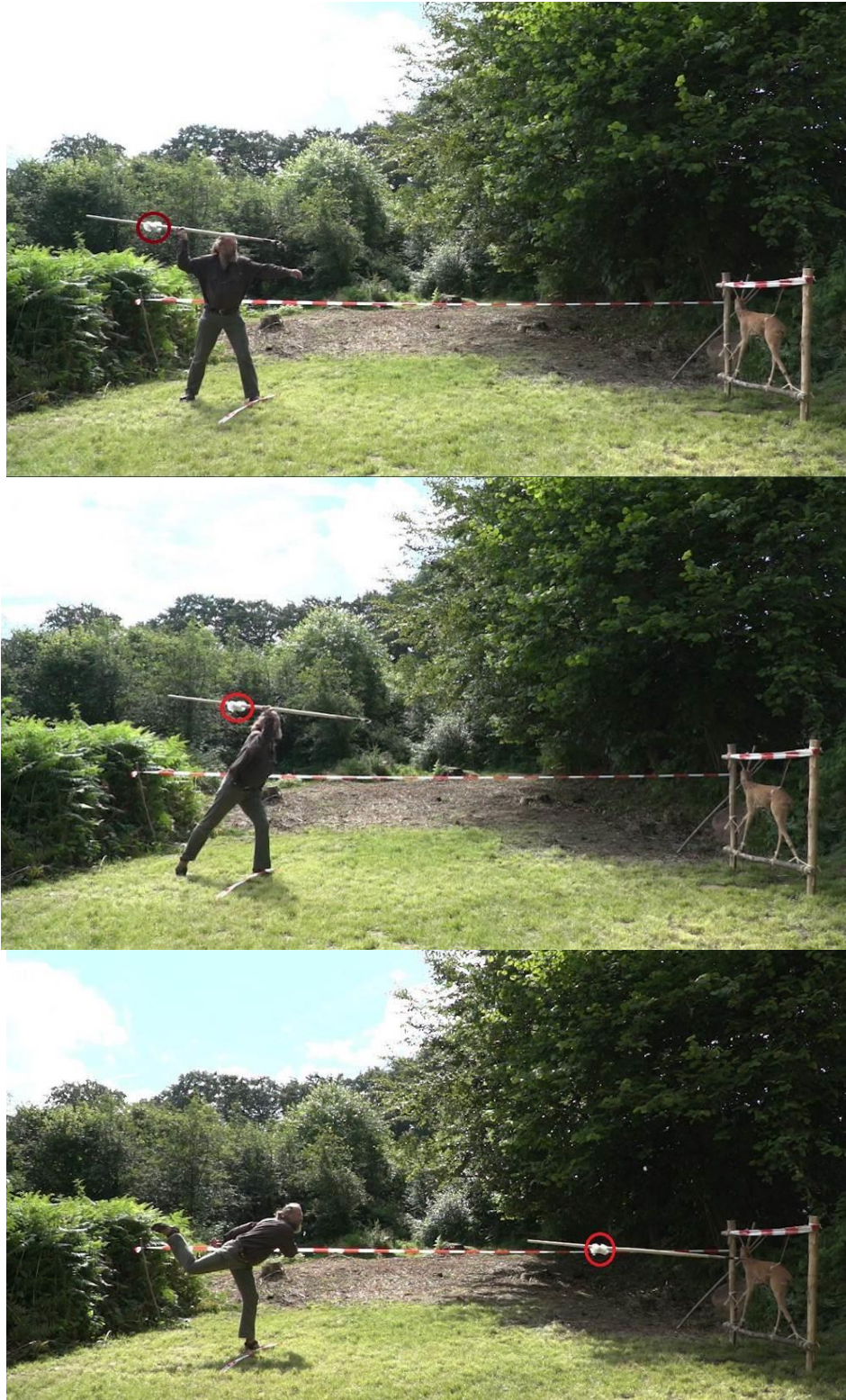


Figure 5.31. High-speed video-frames of a throwing motion. The position of the accelerometer is marked with a red circle (experiment code: TH-77), (Image La Porta).



Figure 5.32. High-speed video-frames of a thrusting motion. The position of the accelerometer is marked with a red circle (experiment code: TH-77), (Image La Porta).



Spear tip

Figure 5.33. Position of the X200-4 accelerometer on the experimental spear shaft. (Image La Porta).

This image has been removed by the author of this thesis/dissertation for copyright reasons.

Figure 5.34. J Pargeter throwing a hand-delivered stone-tipped spears into an unrealistic animal target from a very close distance on a plastic tarp (from Pargeter et al. 2016, 151, figure 5).

CHAPTER 6

THE MACROSCOPIC AND MICROSCOPIC USE-WEAR TRACES OF EXPERIMENTAL LEVALLOIS POINTS USED AS THROWING AND THRUSTING HAND-DELIVERED STONE-TIPPED SPEARS AND BUTCHERING KNIVES

6.1 Introduction

This chapter presents the results of the macroscopic and microscopic use-wear analysis of the experimental Levallois points used in the throwing and thrusting hand-delivered stone-tipped spear experiments (see CHAPTER 4). These experiments' main purpose was to test whether or not different use-wear traces, patterns, and frequencies could be used to distinguish between experimental projectiles²¹ used in throwing hand-delivered spear motions and those used in thrusting hand-delivered spear motions.

Macroscopic traces, i.e. fractures and edge-damage (see Section 2.4), were recorded in an attempt to identify and quantify diagnostic fractures, patterns, and/or frequencies that may occur on throwing and thrusting experimental Levallois points used as hand-delivered spear projectiles, in order to distinguish between the two different delivery systems. All fracture types (i.e. cone, bending, primary, and secondary fractures, see Section 2.4 for definition) were identified, described, and recorded. However, for the purpose of this thesis, only four types of fractures (i.e. step-terminating bending fractures, primary burination fractures with a bending initiation, secondary unifacial and bifacial spin-off fractures, secondary spin-off burination fractures; see Section 2.4.1 for definition) were recorded as diagnostic of projectile impact activities, following Lombard's (2005) method.

²¹ In this thesis, the term projectile and projectile tool refers to all tools mounted on a shaft, regardless of the type of weapon and delivery system (see also Glossary).

Microscopic traces, i.e. polish, microscopic linear impact traces (MLIT), striations, and edge rounding (see Section 2.5) were also identified, described, and recorded as an additional aid to discriminate between throwing and thrusting experimental Levallois points used as hand-delivered spear projectiles

The results presented below show that macroscopic traces (e.g. fractures) occurred with similar patterns and frequencies in both throwing and thrusting experimental Levallois points . Whereas, the identification of microscopic use-wear traces (e.g. polish and microscopic impact linear traces), and the quantification of their types and frequencies, were crucial in evaluating the occurrence of specific trace types (both in throwing and thrusting spear motions) and attempting a first experimental distinction between throwing and thrusting experimental Levallois points used as hand-delivered spear projectiles.

6.2 Comparing throwing and thrusting experimental Levallois points used as hand-delivered spear projectiles: macroscopic trace results (see also Appendix A, Volume 2)

6.2.1 General results on fracture analysis

Experimental Levallois points used as throwing and thrusting hand-delivered stone-tipped spears showed a high overall frequency of fractures (39.28% of throwing points and 50% of thrusting points had fractures, Table 6-1). However, Levallois points used in thrusting motions showed higher frequencies of fractures than Levallois points used in throwing motions (50% to 39.28%, Table 6-1).

Table 6-1. Number of experimental Levallois points with fractures, according to the delivery system (i.e. throwing and thrusting). Note: frequencies refer to the number of tools with fractures or diagnostic impact fractures (DIFs). LP stands for experimental Levallois points.

This thesis's experiments	Throwing (LP n=28)	%	Thrusting (LP n=24)	%
Total tools with Fractures	11	39.28	12	50
Total tools with DIFs	11	39.28	12	50

With regards to the presence of diagnostic impact fractures (DIFs, Table 6-1), the throwing and thrusting experimental Levallois points showed DIF frequencies above the recorded frequencies of experimental tools used in activities other than projectile (e.g. trampling and/or knapping activities). Previous experimental tools used in trampling and knapping activities have presented an overall frequency of DIFs ranging from 3% to 6% (Fischer et al., 1984; Shea and Klenck, 1993; Sano, 2009, 2012a; Pargeter and Bradfield, 2012; Pargeter, 2013), whereas the experimental Levallois points of this study reported DIF frequencies of 39.28% for throwing points and 50% for thrusting points (Table 6-1) (see also CHAPTER 11 for discussion).

6.2.2 Fracture analysis results

Throwing and thrusting experimental Levallois points used as hand-delivered spear projectiles showed similar fracture types but with different frequencies (Table 6-2). Table 6-2 shows that spin-off fractures were the most recurrent type of fractures, both in throwing and thrusting experimental Levallois points, followed by bending fractures with different terminations, and primary burination fractures (see also Figure 6.1). Amongst bending fractures, hinge and snap fractures were the most recurrent types (Table 6-2).

Each fracture type recorded in the experimental Levallois points used as hand-delivered spears is described below according to their frequencies in each delivery system (i.e. throwing vs thrusting experimental Levallois points).

Table 6-2. Fracture types and frequencies observed on the experimental Levallois points, according to delivery system, i.e. throwing and thrusting. Note: the fracture number and frequencies refer to fracture counts, not tools with fractures (more than one fracture can occur on a tool).

Type of fractures	Throwing (n=28 LP)	%	Thrusting (n=24 LP)	%	Chi ² results
<u>Bending</u>	12	34.2	19	46.3	$\chi^2=0.109$, df=4, p-value=0.741
Step-terminating	2	5.7	2	4.8	
Hinge-terminating	2	5.7	6	14.6	
Feather-terminating	1	2.8	3	7.3	
Snap	6	17.1	8	17	
'S' shaped snap	1	2.8	-	-	
<u>Primary burination bending</u>	1	5.7	1	2.4	$\chi^2=3.046$, df=1, p-value=0.081
<u>Spin-off</u>	22	62.8	21	51.2	$\chi^2=2.938$, df=1, p-value=0.085
Unifacial/Bifacial spin-off	19	54.2	18	43.9	
Burination spin-off	3	8.5	3	7.3	
Total Fractures	35	100	41	100	
Total DIFs (Step-terminating bending, unifacial/bifacial spin-off, burination spin-off, primary burination snap fractures)	25	71.4	24	58.5	$\chi^2=3.265$, df=7, p-value=0.352

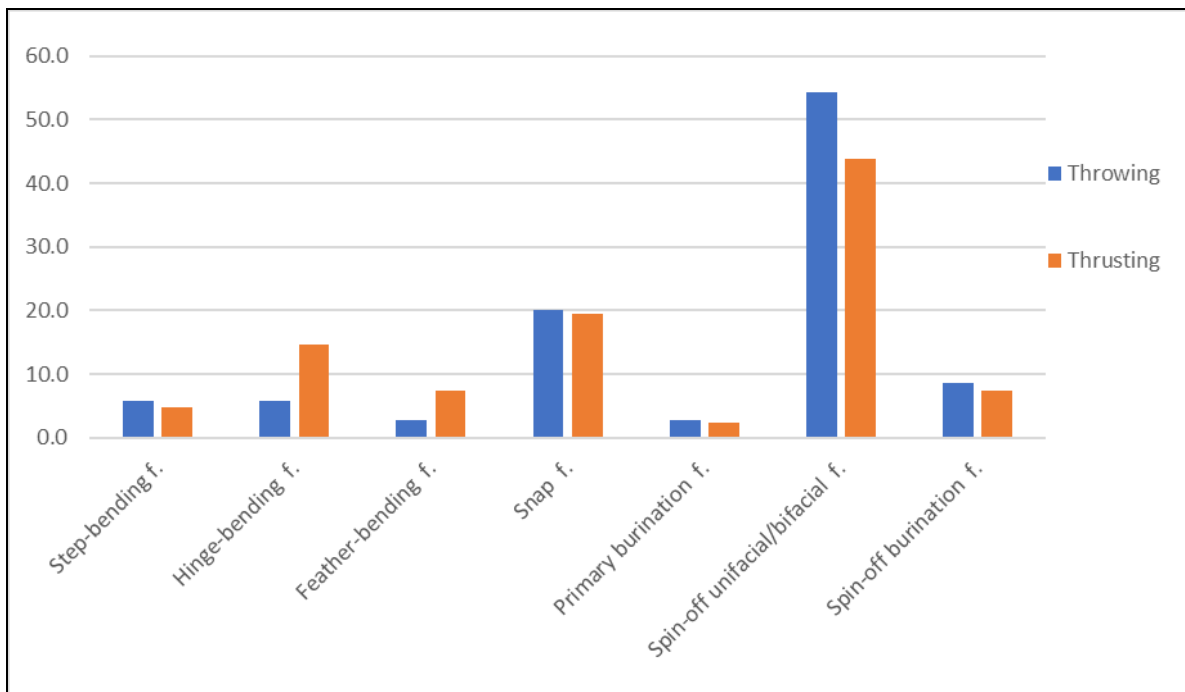


Figure 6.1. Distribution of fracture types (in percentages %) in the experimental Levallois points according to their delivery systems (throwing in blue vs thrusting in red).

Bending fractures

Bending fractures have been defined as primary fractures that initiate far from the impact location, generating an initiation with a convex profile (see also Section 2.4.1; Ho Ho Committee, 1979). They can present different terminations from which they are named, such as step-terminating bending fractures, hinge-terminating bending fractures, feather-terminating bending fractures, and snap fractures (see also Section 2.4.1; Ho Ho Committee, 1979).

Snap fractures (see Section 2.4.1 for definition) were the most common type of bending fractures occurring both in throwing and thrusting experimental Levallois points (Table 6-2 and Figure 6.1). They were more recurrent in throwing than in thrusting points (20% and 17% respectively, Table 6-2), but this was not a statistically different pattern between the two delivery systems (p -value=0.741, Table 6-2). Snap fractures were often located on the distal part of the experimental projectiles (initiating from Locus D1, see Section 2.3) and were associated with

unifacial or bifacial spin-off fractures (Figure 6.9, Figure 6.13). A few snap fractures (n=3) were instead observed on the mesial portion of the experimental projectiles (initiating from Locus M1 or M2, see Section 2.3), as a result of a clean breakage of the tool into two fragments (e.g. proximal and distal fragment) (Figure 6.10 and Figure 6.11). One experimental throwing point (tool TH-78) showed an 'S' shaped snap fracture on the mesial portion of the tool (Locus M2v, Figure 6.11; Sano, 2009). It has been experimentally observed that the 'S' shaped snap fracture forms when mechanical longitudinal stress propagates on the tool's surface, but finds resistance as a result of a well-fixed hafting system (Sano, 2009). As the hafting system stops the propagation of the longitudinal stress, the projectile point snaps into two fragments which may present an 'S' shaped profile (Figure 6.11). 'S' shaped snap fractures (Sano, 2009) or width-wide bending fractures (Rots and Plisson, 2014) are therefore diagnostic of projectile impact activities (Sano, 2009, 2012a) and, in this study, were included in the counting of diagnostic impact fractures (total DIFs; Table 6-2). The other snap fractures were instead not considered diagnostic of projectile activities as they can also occur in high percentages in trampling and knapping activities (Odell and Cowan, 1986; Geneste and Plisson, 1993; Dockall, 1997; Lombard, 2005; Sano, 2009, 2012a; Pargeter and Bradfield, 2012) and in this study they were thus not included in the counting of diagnostic impact fractures (total DIFs; Table 6-2).

Hinge-terminating bending fractures (see Section 2.4.1 for definition) were the second most recurrent type of bending fractures after snap fractures, both in throwing and thrusting experimental Levallois points (Table 6-2 and Figure 6.1). They were more recurrent in thrusting than in throwing points (14.6% to 5.7% respectively, Table 6-2), but this was not a statistically different pattern between the two delivery systems (p-value=0.741, Table 6-2). Bending fractures with a hinge termination often initiated on the distal part of the experimental projectiles (initiating from Locus D1, see Section 2.3) and often ended with a double termination (Figure 6.4 and Figure 6.6). Hinge-terminating bending fractures are defined ambiguously in existing literature as some authors have considered them

diagnostic of projectile activities (Odell and Cowan, 1986; Geneste and Plisson, 1989; Sano and Oba, 2015) and some others have not (Fischer et al., 1984; Villa et al., 2005; Lombard, 2005; Villa and Lenoir, 2006, 2009; Lombard and Pargeter, 2008; Iovita et al., 2014; Pargeter et al., 2016). However, following Lombard's (2005) method of analysis, in this study, bending fractures with a hinge termination were not included in the counting of diagnostic impact fractures (total DIFs; Table 6-2).

Feather-terminating bending fractures (see Section 2.4.1 for definition) occurred with low frequencies both in thrusting and in throwing experimental Levallois points (Table 6-2 and Figure 6.1). They were more recurrent in thrusting than in throwing points (7.3% and 2.8% respectively, Table 6-2), but this did not present a statistically significant difference between the two delivery systems (p -value=0.741, Table 6-2). Bending fractures with a feather termination often began on the distal part of the experimental projectiles (initiating from Locus D1, see Section 2.3; Figure 6.2 and Figure 6.7). As well as hinge-terminating bending fractures, also feather terminations in bending fractures have been considered diagnostic of projectile motions by few authors (Caspar and De Bie, 1996; O'Farrell, 2004; Sano, 2009; Lazuén, 2012). However, following Lombard's (2005) method of analysis, in this study, bending fractures with a feather termination were not included in the counting of diagnostic impact fractures (total DIFs; Table 6-2).

Step-terminating bending fractures (see Section 2.4.1 for definition) showed low frequencies, both in throwing and thrusting experimental Levallois points (Figure 6.1). They were more recurrent in throwing than in thrusting points (5.7% and 4.8% respectively, Table 6-2), but this was not a statistically different pattern between the two delivery systems (p -value=0.741, Table 6-2). They often began on the distal part of the experimental projectiles (Locus D1, see Section 2.3) and frequently ended with a double termination (Figure 6.3, Figure 6.5, and Figure 6.7).

In previous literature, bending fractures with a step termination have been considered to be one of the most diagnostic traces of projectile impact activities

normally occurring with high frequencies (Fischer et al., 1984; Odell and Cowan, 1986; Geneste and Plisson, 1989; Caspar and De Bie, 1996; O'Farrell, 2004; Lombard, 2005; Villa and Lenoir, 2006, 2009; Villa et al., 2009a; Lombard and Pargeter, 2008; Sano and Oba, 2015; Rots, 2016). Therefore, in this study, bending fractures with a step termination were included in the counting of diagnostic impact fractures (total DIFs; Table 6-2; but see also CHAPTER 11 for further discussions).

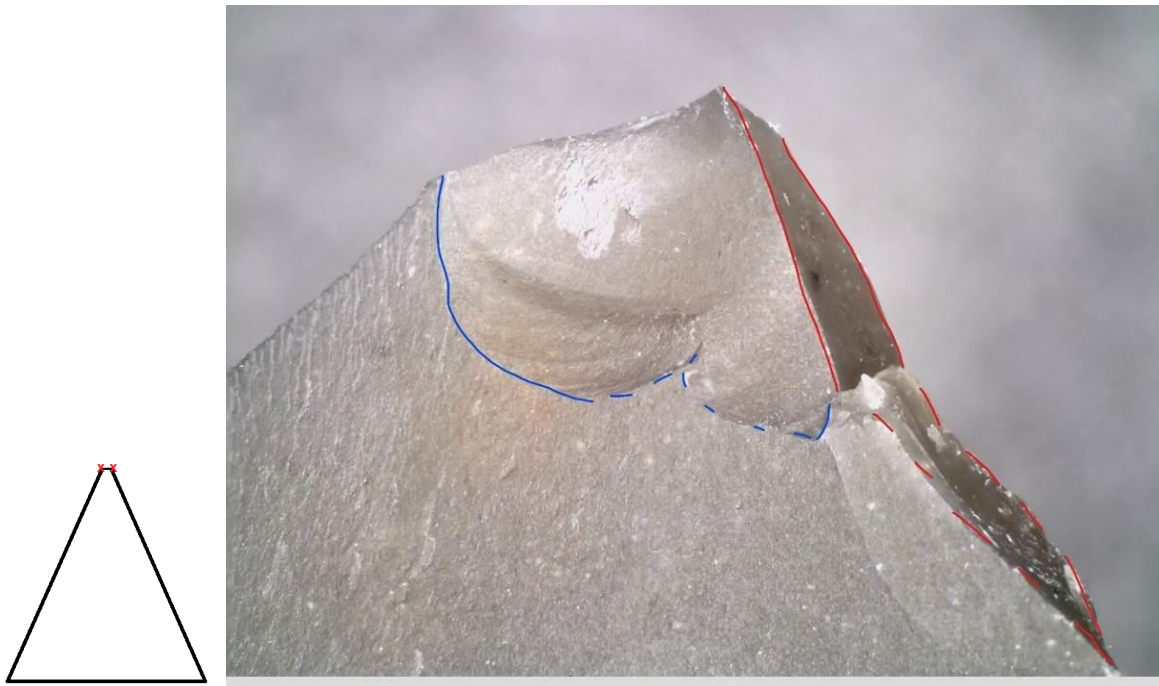


Figure 6.2. Bending fracture terminating in a double feather (in blue), plus a primary burination fracture (in red). DM OM 50x (experiment code: TH-85).

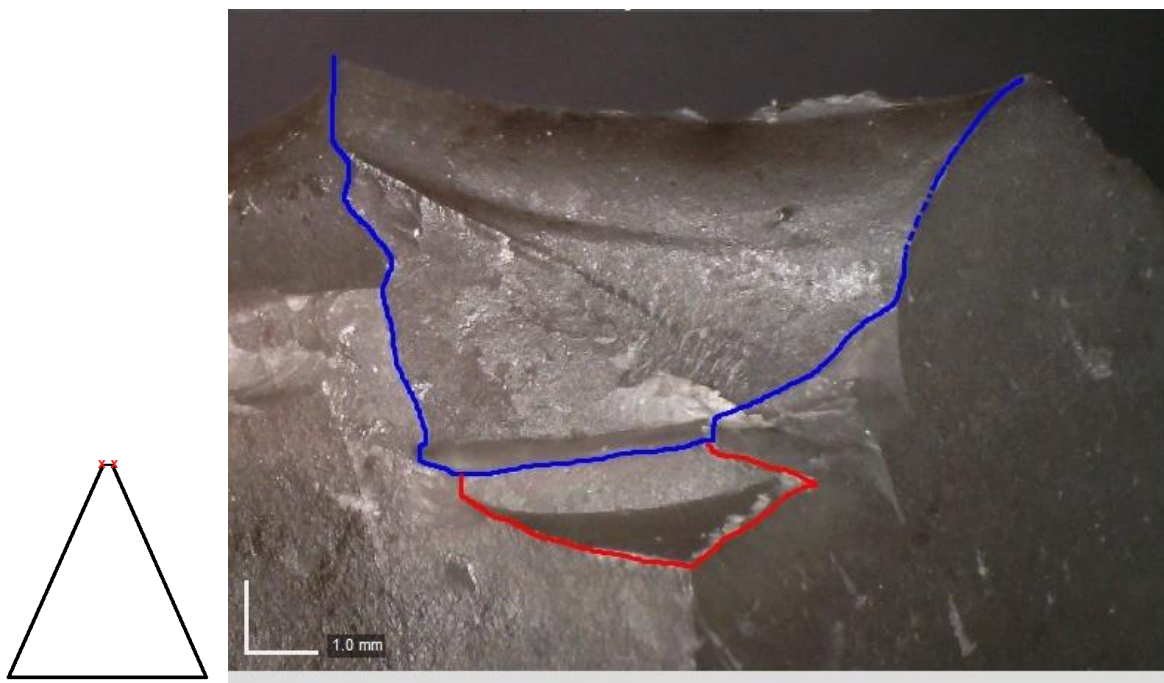


Figure 6.3. Bending fracture with a double step termination (in blue and red), DM OM 35x (experiment code: TR-93).

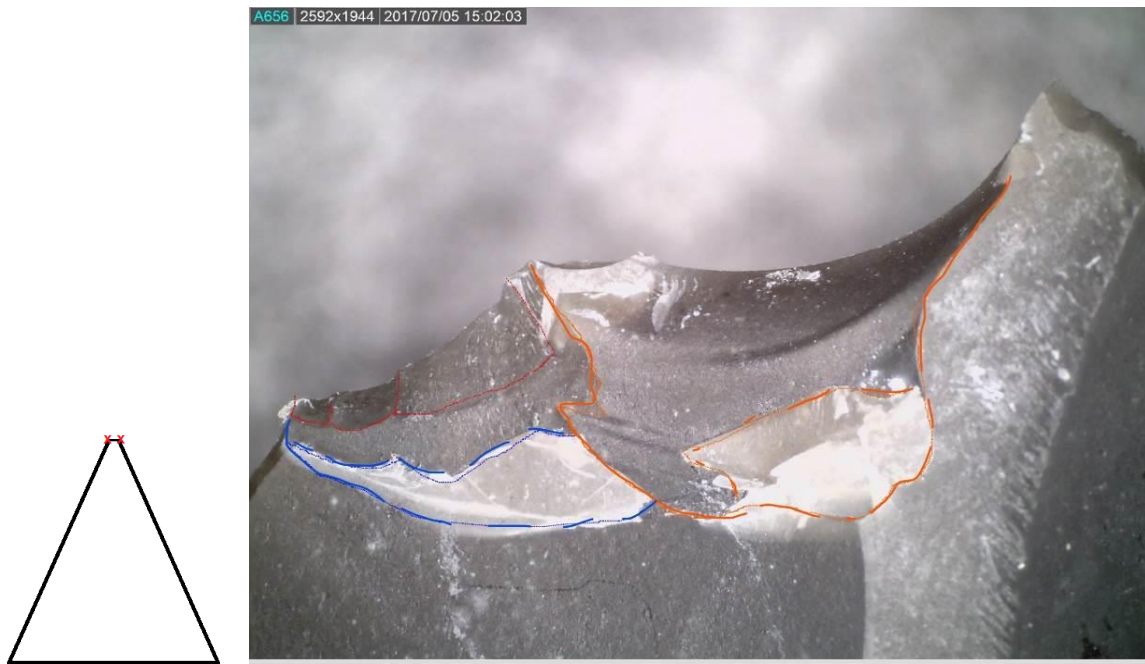


Figure 6.4. Multiple fractures. Bending fracture terminating into a hinge (in orange); bending fracture (with a missing initiation) with a hinge termination (in blue); small bending scars with feather termination (in red). DM OM 30x (experiment code: TH-79).

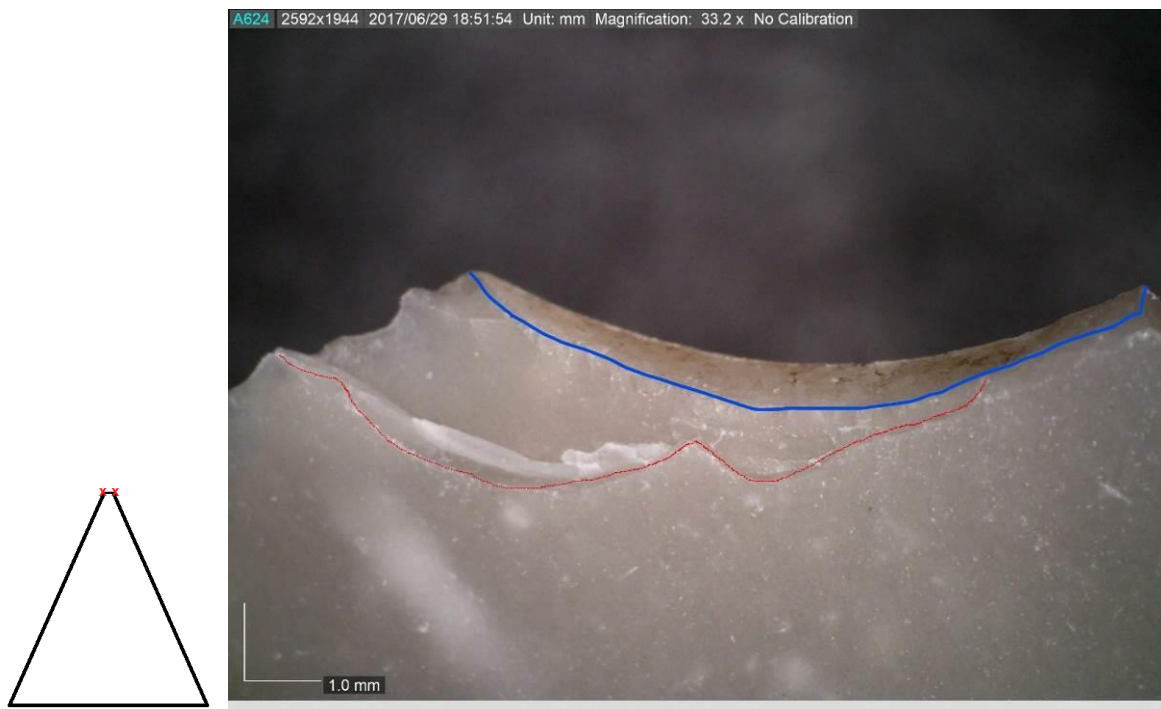


Figure 6.5. Bending fracture (with missing initiation) terminating in a double step (in red) plus a snap fracture, (in blue), DM OM 32x (experiment code: TR-74).

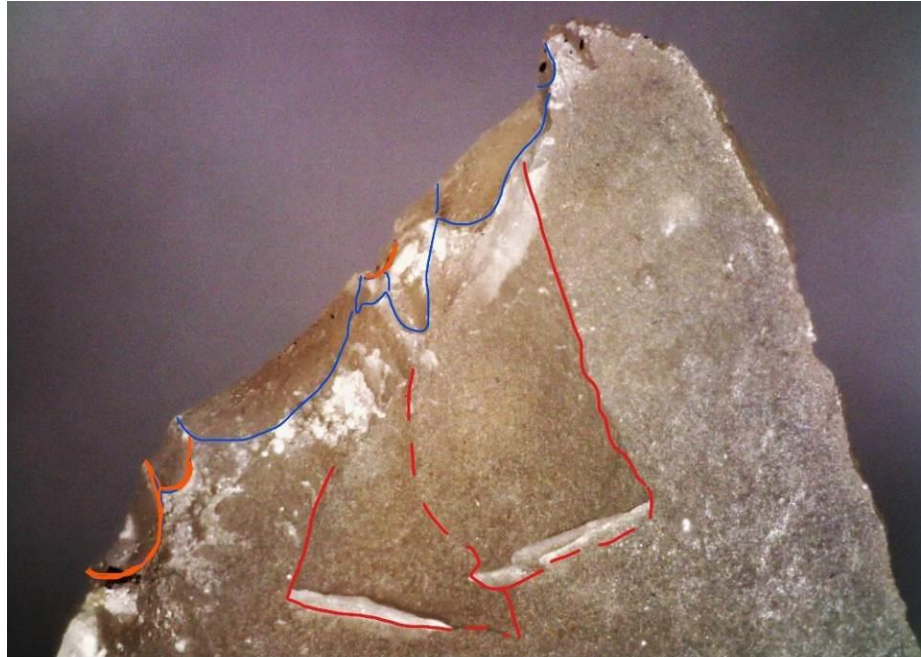
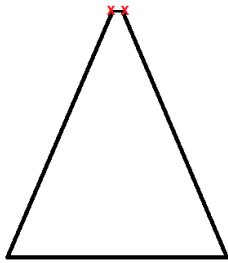


Figure 6.6. Multiple fractures. Two bending hinge fractures (with missing initiation; in red) plus bending scars (in blue), and cone scars (in orange), DM OM 80x (experiment code: TR-83).

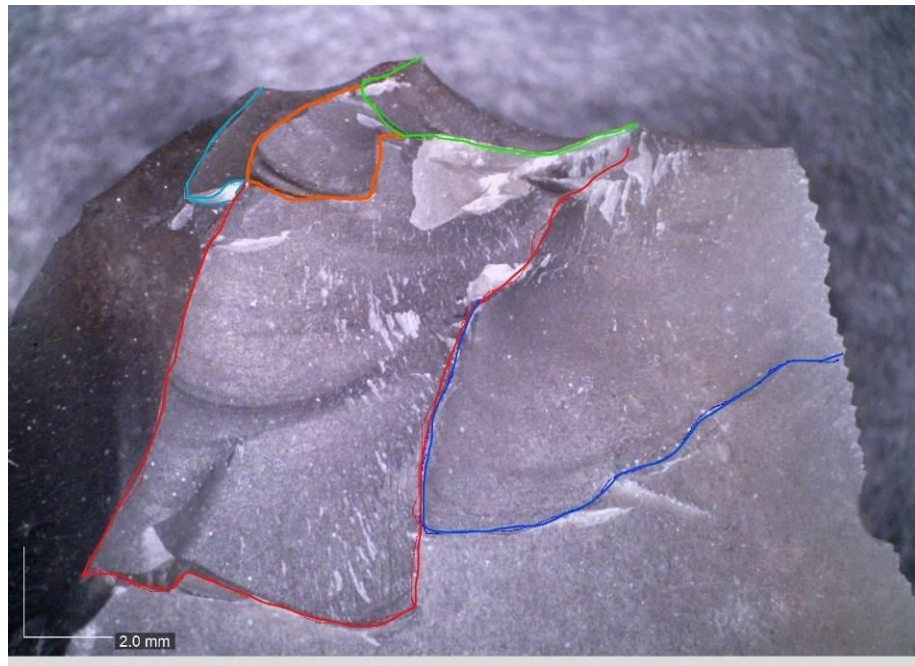
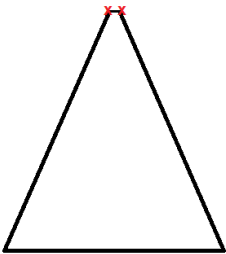


Figure 6.7. Multiple fractures. A feather-terminating bending fracture (in blue); a bending fracture with a double step and feather termination (in red); a bending fracture with a step

termination (in orange); a small hinge-terminating bending fractures (in light blue); a bending fracture with a feather termination (in green). DM OM 20x (experiment code: TR-89).

Primary burination bending fractures

Primary burination fractures (also called 'impact burination', 'burination fractures', or 'longitudinal breaks with bending initiations' in previous literature) were defined as fractures that can initiate from an edge or surface but always terminate on an edge (Coppe and Rots, 2017), running parallel or slightly oblique to the main axis of the tool (see also Section 2.4.1; Figure 6.2 and Figure 6.8). Only primary burination fractures with a bending initiation were, however, considered diagnostic of projectile impact activities, as primary burination fractures with a cone initiation can also occur during activities other than projectiles (Villa et al., 2005; Lombard, 2005; Villa and Lenoir, 2006, 2009; Lombard and Pargeter, 2008; Pargeter et al., 2016). Therefore, primary burination fractures with bending initiation were included in the counting of diagnostic impact fractures (total DIFs; Table 6-2).

Primary burination fractures occurred at very low frequencies, both in throwing and thrusting experimental Levallois points (Table 6-2 and Figure 6.1). They were slightly more recurrent in throwing than in thrusting points (2.9% and 2.4% respectively, Table 6-2), but this did not present a statistically significant difference between the two delivery systems (p -value=0.081, Table 6-2). Primary burination fractures propagated along the lateral edge of the distal tip and they presented a bending initiation, without a clear point of impact (Figure 6.2 and Figure 6.8).

The low frequencies of primary burination fractures recorded in this study are further discussed in CHAPTER 11.



Figure 6.8. Primary burination fracture, DM OM 35x (experiment code: TH-92).

Spin-off fractures

The spin-off fractures were defined as secondary fractures departing from an earlier surface (see Section 2.4.1 for definitions; Fischer et al., 1984; Lombard, 2005). They included unifacial and bifacial spin-off fractures (Figure 6.9, Figure 6.10, Figure 6.11, and Figure 6.12; Fischer et al., 1984; Lombard, 2005) and spin-off burination fractures (Figure 6.13; Coppe and Rots, 2013).

In this study, unifacial and bifacial spin-off fractures were the most common type of fractures, occurring both in throwing and thrusting experimental Levallois points (Table 6-2 and Figure 6.1). However, they were more recurrent in throwing than in thrusting points (54.2% to 43.9% respectively, Table 6-2), but this was not a statistically different pattern between the two delivery systems (p -value=0.085, Table 6-2). On the other hand, spin-off burination fractures showed a lower occurrence, both in throwing and thrusting points (8.5% to 7.3%, Table 6-2 and Figure 6.1). Throwing points showed slightly higher frequencies of spin-off

burination fractures than thrusting points, but this was not statistically significant (p -value=0.085, Table 6-2).

In previous literature, spin-off fractures have been considered to be one of the most diagnostic traces of projectile impact activities (Fischer et al., 1984; Lombard, 2005; Lombard and Pargeter, 2008; Villa and Lenoir, 2006, 2009; Sano and Oba, 2015). Therefore, the high frequencies of spin-off fractures recorded in this study confirm the importance of this category of fractures as diagnostic of projectile activities and, consequently, in this study, they have been included in the counting of diagnostic impact fractures (total DIFs; Table 6-2).

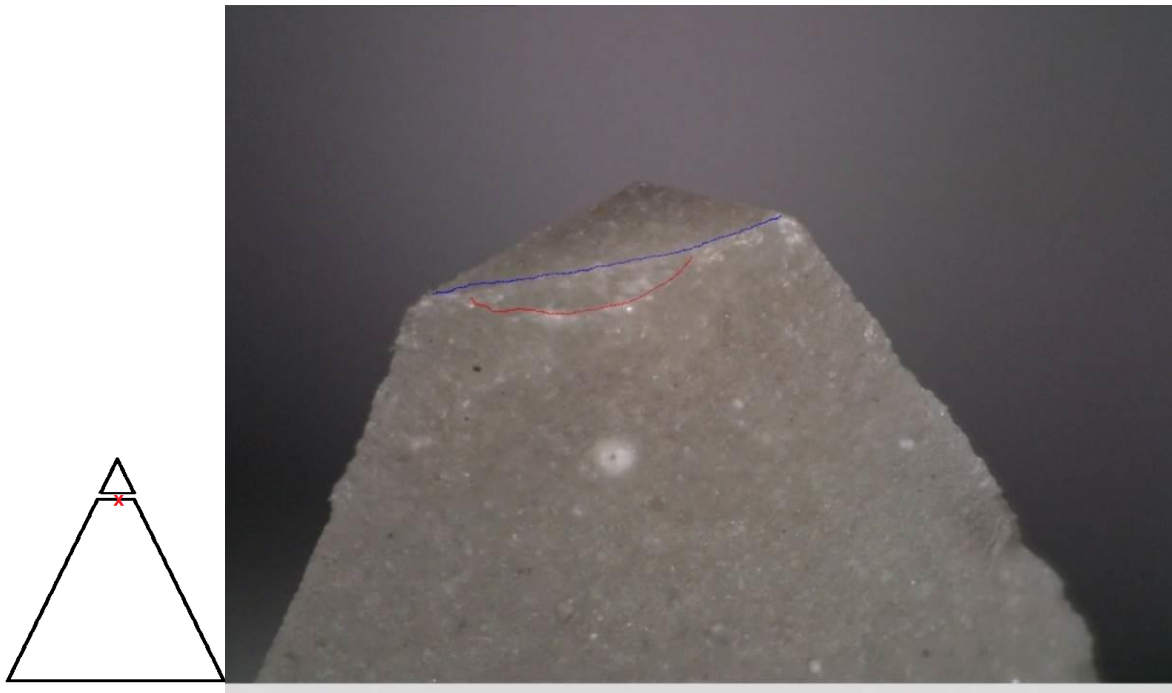


Figure 6.9. Unifacial spin-off fracture (in red) departing from a snap fracture (in blue), DM OM 50x (experiment code: TH-34).

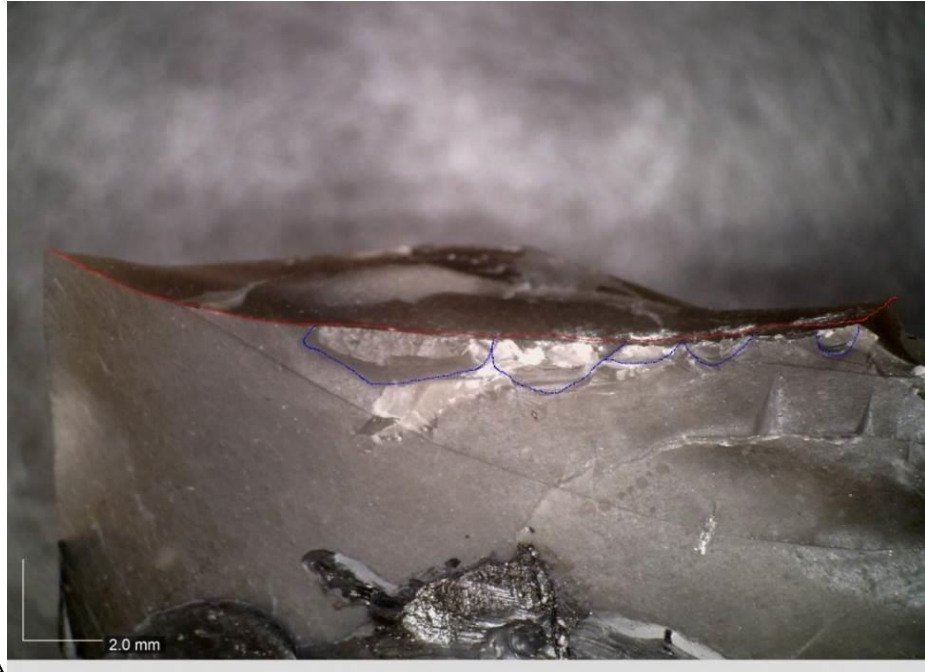
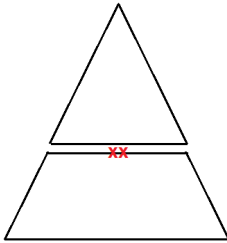


Figure 6.10. Several uniface spin-off fractures (in blue) departing from a snap fracture (in red) observed above the haft-limit (presence of tar), DM OM 17x (experiment code: TH-78).

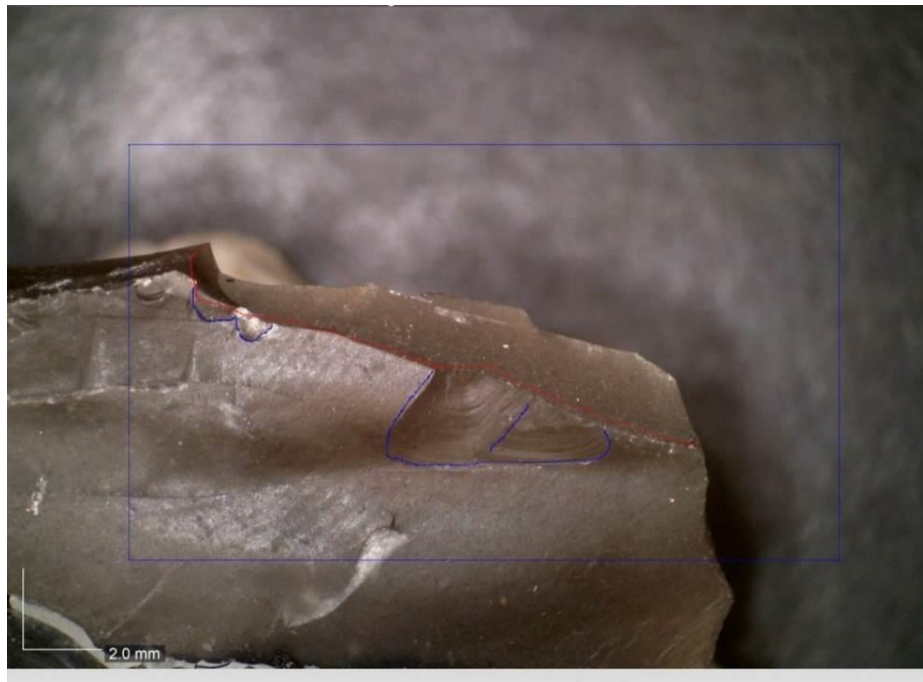
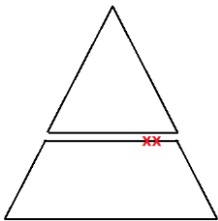


Figure 6.11. Several uniface spin-off fractures (in blue) departing from an 'S' shaped snap fracture (in red) observed above the haft-limit, DM OM 17x (experiment code: TH-78).

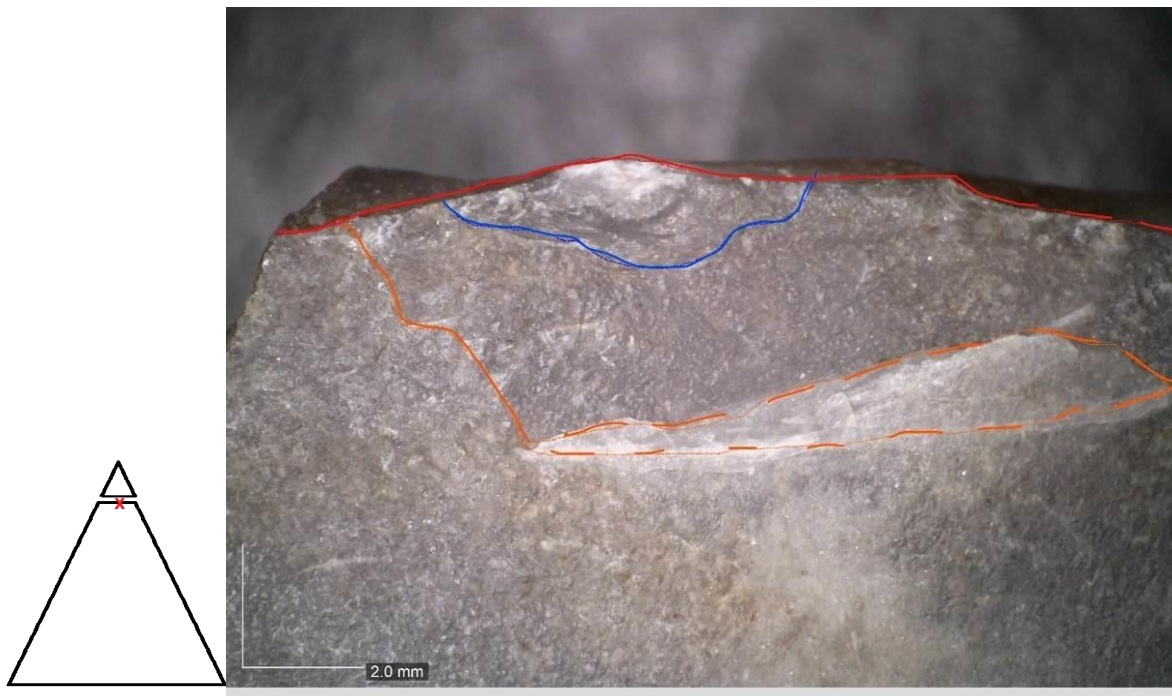


Figure 6.12. Unifacial spin-off fracture (in blue) departing from a bending feather-terminating fracture (in red), plus a bending fracture (with a missing initiation) with a hinge termination (in orange), DM OM 25x (experiment code: TR-35).



Figure 6.13. A small spin-off fracture (in orange on the left) plus a spin-off burination fracture

(in red on the right; plus a step-terminating fracture with an indeterminate initiation in green) departing from a snap fracture (in blue), DM OM 50x (experiment code: TH-77).

6.2.3 Edge-damage analysis results

Edge-damage is here defined as a trace pattern formed by single scars or the overlaying of a group of scars along the lateral edge of a tool (see also Section 2.4.2 for definition; Figure 6.14, Figure 6.15, and Figure 6.16). Occasionally, this appears as a complete crushing of the edges or distal tip (i.e. tip or edges crushing; Figure 6.17).

The scars which composed the edge-damage, observed on the experimental Levallois points used as throwing and thrusting hand-delivered spear projectiles, presented mostly cone initiations but different terminations (e.g. step, feather, or hinge). They generally showed an overlapping (Figure 6.16), discontinuous (Figure 6.14) or continuous (Figure 6.17) distribution, and diverse morphologies (e.g. scalar, elongated, half-moon, trapezoidal, triangular; Figure 6.17, Figure 6.14, and Figure 6.15; see Section 2.4.2.2). Scar size ranged from medium (0.5-1 mm) to very large dimensions (2 mm) (see Section 2.4.2.2).

In this study, thrusting experimental Levallois points showed higher frequencies of edge-damage than throwing points (41.6% to 14.28% respectively, Table 6-3), suggesting that thrusting motions create more severe damage than throwing motions possibly because of the greater dispersion of force involved in the thrusting actions.

Intense edge-damage or edge-crushing was mostly recorded in experimental Levallois points (more often in thrusting points) that hit against hard tissues (such as scapulae and vertebrae; Figure 6.14, Figure 6.15, and Figure 6.16). Impact against hard tissues may have, in fact, generated several longitudinal stresses that could not dissipate in a unique fracture, resulting instead in damage of the edges and/or a complete crushing of the edges or distal tip (correlating with what has been observed by Odell and Cowan, 1986, p. 204). As a result, edge-damage (i.e. scars) was mostly located on the distal tip (Locus D1, see Section 2.3) and/or on the lateral distal edges (Loci D2 and D3, see Section 2.3) of the experimental

Levallois points, which were the areas that first came into contact with the hard tissues. However, edge-damage alone cannot be used as a diagnostic trace of a specific delivery system or a specific activity, as it also occurs on scraping, boring tools, débitage, and activities other than projectiles (Tringham et al., 1974; Vaughan, 1985; Van Gijn, 1989; Dockall, 1997; Lemorini and Cocca, 2013). Nonetheless, if severe edge-damage is observed in association with diagnostic projectile impact traces, such as DIFs or microscopic linear impact traces (MLITs, later on this chapter), it might suggest that the stone tool impacted against hard tissues or it was subjected to higher values of force, as observed in the experimental Levallois points used in thrusting motions (see also CHAPTER 11 for further discussions).

Table 6-3. Number of experimental Levallois with edge-damage, according to the delivery system (i.e. throwing and thrusting). Note: frequencies refer to the number of tools with traces. LP stands for experimental Levallois points.

Type of traces	Throwing (LP n=28)	%	Thrusting (LP n=24)	%
Edge-damage	4	14.28	10	41.6

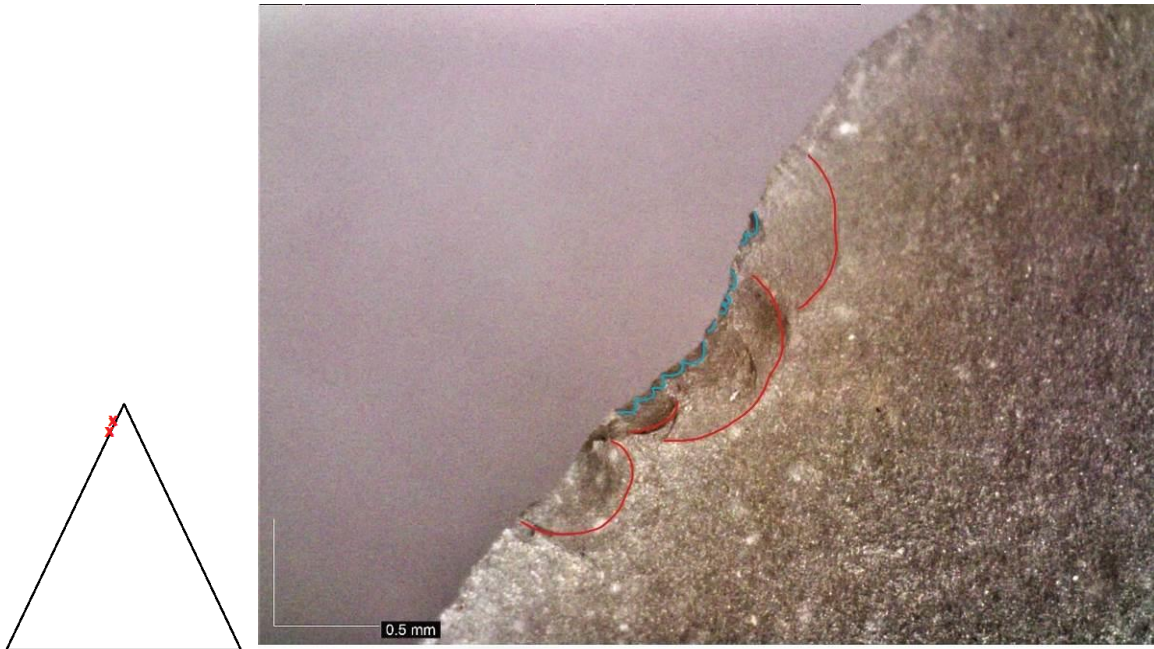


Figure 6.14. Edge-damage. Cone scars with scalar (in red) and half-moon (in blue) morphologies, DM OM 41x (experiment code: TR-80).

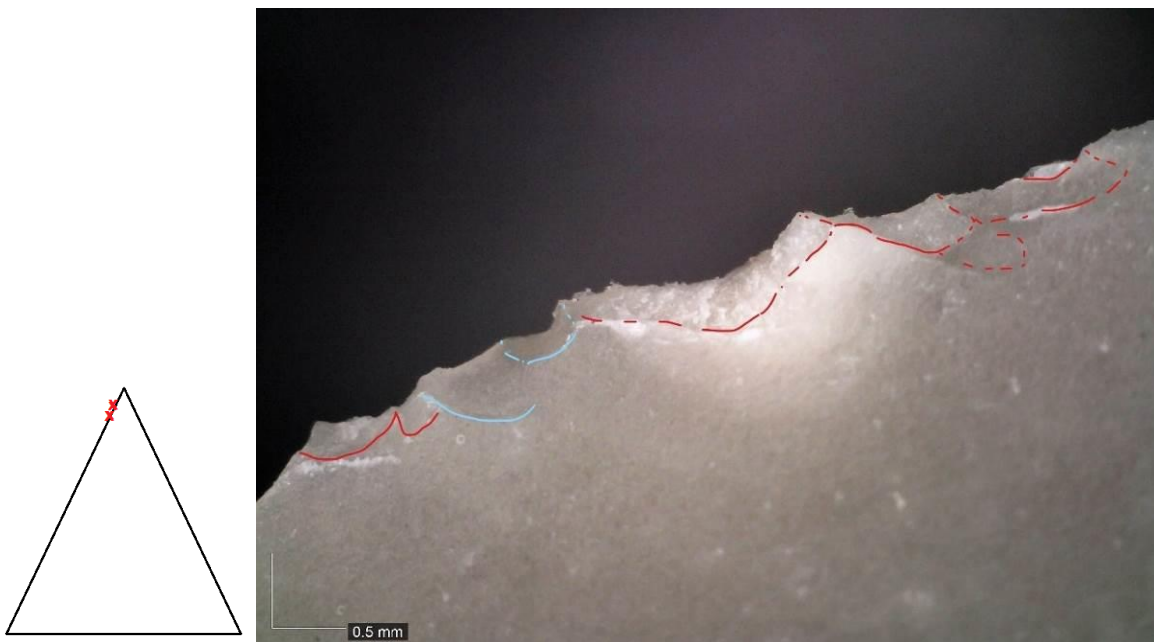


Figure 6.15. Edge-damage. Bending (in blue) and cone (in red) scars with half-moon/scalar morphology, DM OM 55x (experiment code: TR-55).

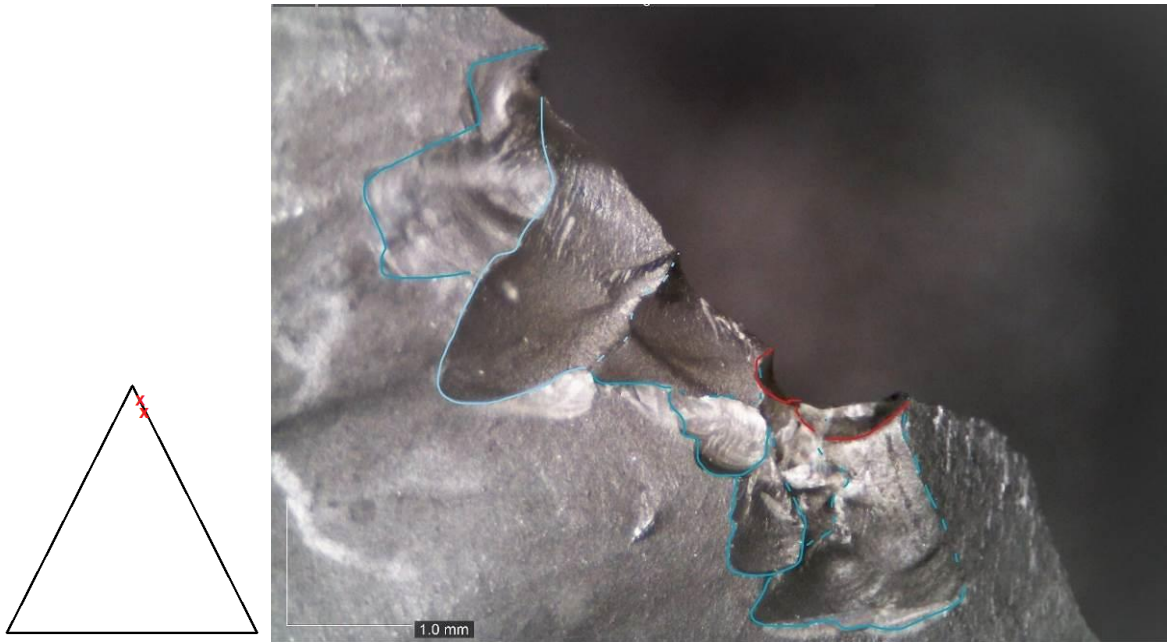


Figure 6.16. Edge-damage. Overlying of cone (in red) and bending (in blue) scars with elongated morphology, DM OM 55x (experiment code: TR-36).



Figure 6.17. Intense edge-damage, i.e. tip-crushing. The tip is completely crushed after impact creating multiple cone scars, DM OM 50x (experiment code: TR-86).

6.2.4 Exploring throwing and thrusting hand-delivered stone-tipped spear experiments: correlation between delivery systems (i.e. throwing vs thrusting) and fracture location

During experimentation and use-wear analysis, a clear difference emerged between the locations of fractures in the two different delivery systems. Two patterns were observed: thrusting experiment Levallois points correlated with higher frequencies of distal fractures (i.e. fractures initiating from the distal part of the tool), while throwing experiment Levallois points correlated with higher frequencies of mesial fractures (i.e. fractures initiating from the distal part of the tool, after that the point broke off in two fragments; Figure 6.18). Therefore, the strength of correlation between the location of fractures (in the distal, mesial, or proximal part of the tool) and the two different delivery systems was evaluated with a Chi² test. The correlation between the location of fractures and delivery system was proven statistically significant ($\chi^2=73.973$, $df=1$, $p\text{-value}=0.000$, Table 6-4), indicating that a correlation between the delivery system and the location of fractures existed. Throwing experimental Levallois points exhibited significantly higher frequencies of mesial fractures than thrusting experimental Levallois points.

These results are in agreement with those of Coppe and Rots (2017), who found that an increase in impact velocity corresponds to an intensification of mesial fractures. Coppe and Rots' (2017) experimental arrow-points (i.e. high-speed projectiles) showed higher frequencies of mesial fractures than spear-thrower spear-points (i.e. medium-speed projectiles). Therefore, the higher frequencies of mesial fractures recorded in this study can be correlated to the increase of impact velocities recorded in the throwing experimental Levallois points (11.59 m/s to 4.86 m/s velocity mean, see Table 5-10). However, it is important to note that the interpretation of the delivery system of a projectile tool cannot rely on the location of fractures only. The presence of mesial fractures alone cannot be considered diagnostic of a precise delivery system if not in association with other diagnostic projectile impact traces.

Table 6-4. Location of fractures (i.e. distal, mesial, and proximal) according to the delivery system of the experiments (i.e. throwing vs thrusting). Note: the fracture number and frequencies refer to fracture counts, not tools with fractures (more than one fracture can occur on a tool).

Fracture location	Throwing LP		Thrusting LP		Chi ² results
Distal fractures	20	57.2%	41	100%	χ ² =73.973, df=2, p-value=0.000
Mesial fractures	15	42.8%	-		
Proximal fractures	-		-		
Total fractures	35	100%	41	100%	

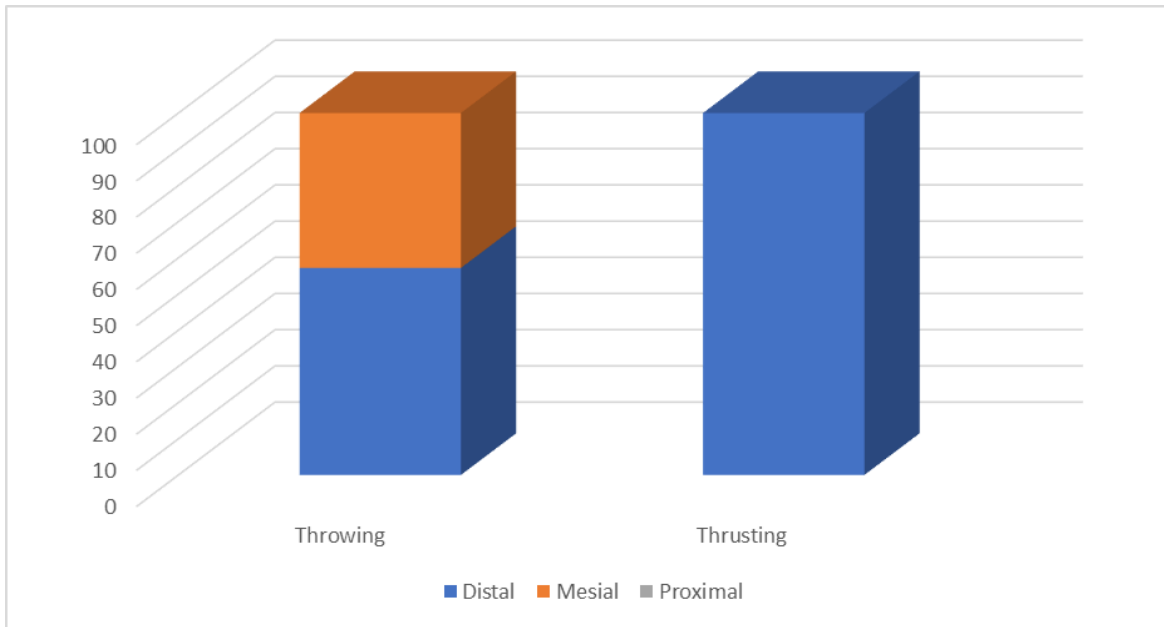


Figure 6.18. Distribution of distal (in blue), mesial (in red) and proximal (in green) fractures according to the delivery system (i.e. throwing vs thrusting).

6.2.5 Exploring throwing and thrusting hand-delivered stone-tipped spear experiments: correlation between impact materials (i.e. hard vs soft tissues) and number of fractures

During the experimentation and use-wear analysis, it was also observed that impact against hard tissues (i.e. bone contact materials) caused more fractures than impact against soft tissues (i.e. meat, flesh, and skin contact materials). Therefore, the strength of the correlation between impact materials (i.e. hard vs soft tissues) and number of fractures was evaluated with a Chi² test.

Figure 6.19 shows a clear correlation between the higher number of fractures and impact against hard tissues (i.e. bone contact materials). The majority of fractures formed when the hand-delivered stone-tipped spears (both in throwing and thrusting experiments) impacted against hard tissues (such as shoulder blade, spine, and rib cage; Table 6-5). While impact against soft tissues (such as skin, flesh, and meat) produced only sporadic fractures (Table 6-5). As a matter of fact, the results of the Chi² test indicated a statistically significant correlation between impact material and the number of fractures ($\chi^2= 176.720$, $df=2$, $p\text{-value}=0.000$, Table 6-5). These results show that impact against hard tissues (i.e. bone contact materials) caused a higher number of fractures than impact against soft tissues (i.e. skin, flesh, and meat contact materials), both in throwing and thrusting experimental Levallois points used in hand-delivered stone-tipped spear experiments.

Table 6-5. Distribution of fractures according the impact materials (i.e. hard vs soft tissues)

Impact materials	Bending fractures	Spin-off fractures	Primary Burination fractures	Chi ² results
Hard tissues	29	43	2	$\chi^2= 176.720$, $df=2$, $p\text{-value}=0.000$
Soft tissues	2			

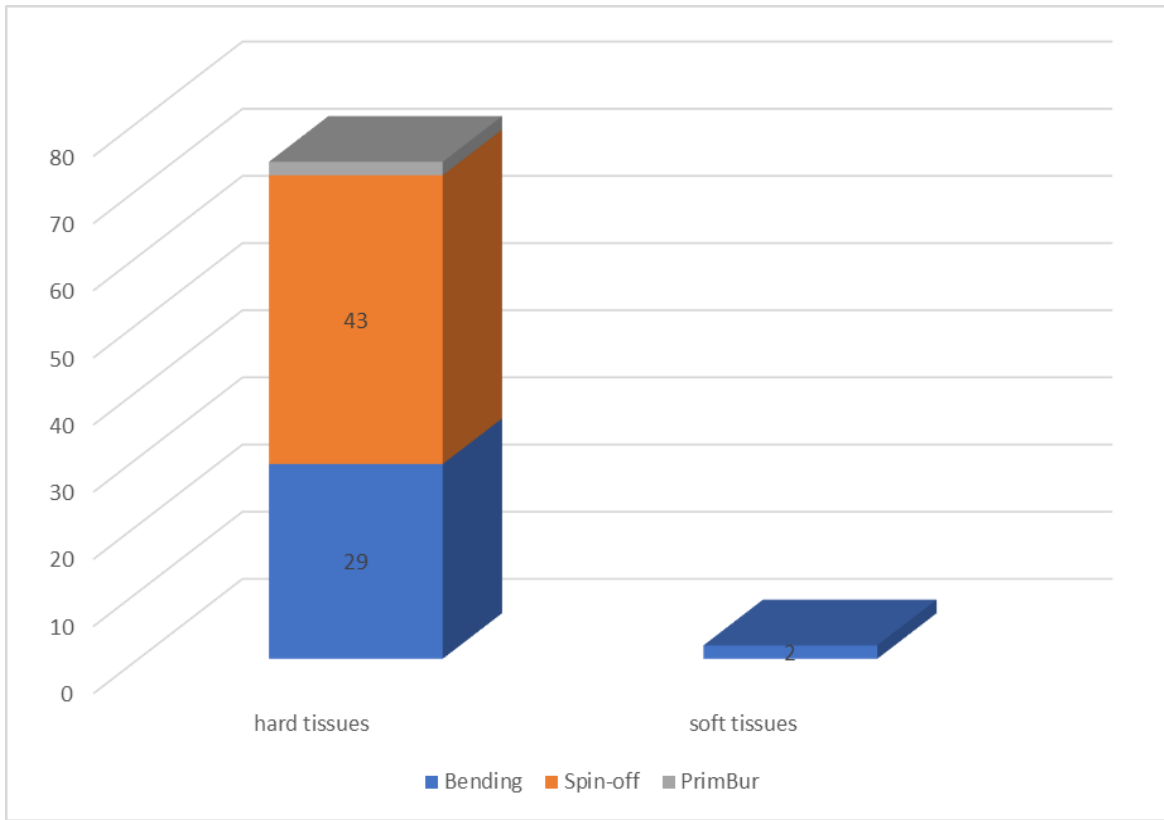


Figure 6.19. Distribution of bending fractures (Bending), spin-off fractures (Spin-off) and primary burination fractures (PrimBur) according to the impact materials, i.e. hard tissues (in blue) vs soft tissues (in red).

6.2.6 Outcomes: can macroscopic trace types, frequencies and patterns be used to distinguish between throwing and thrusting hand-delivered stone-tipped spear projectiles?

The results of hand-delivered throwing and thrusting stone-tipped spear experiments demonstrated that the relationship that exists between fracture type and delivery system is very complex. Fracture analysis provided relevant information concerning which types of fractures and frequencies could be observed, both in throwing and thrusting hand-delivered stone-tipped spear projectiles. However, no statistically significant difference between the two delivery systems can be found by analysing macroscopic traces alone (Table 6-2).

It has been noticed that experimental Levallois points used for thrusting broke more often than those that were thrown, showing an overall higher frequency of fractures (50% to 39.28%, Table 6-1). However, this criterion alone cannot be considered a diagnostic feature.

Likewise, it has been observed that spin-off fractures (unifacial/bifacial spin-off and spin-off burination fractures) occurred more often in throwing than in thrusting experimental Levallois points (54.2% to 43.9%, Table 6-2 and Figure 6.1). However, this difference was not statically significant ($\chi^2=2.938$ df=1 p-value=0.085) as spin-off fractures formed both in throwing and in thrusting experimental Levallois points. Therefore, this fracture type alone cannot be considered diagnostic of one or the other delivery system (see also CHAPTER 11 for discussions). The same observation is valid for primary burination fractures, which occurred more often in throwing than in thrusting experimental Levallois points (5.7% to 2.4%, Table 6-2 and Figure 6.1), but this difference was not statistically significant ($\chi^2=3.046$, df=1, p-value=0.081).

Similarly, it has been observed that bending fractures were more recurrent in thrusting than in throwing points (5.7% to 4.8%, Table 6-2 and Figure 6.1). Nevertheless, this difference was not statistically significant to infer a difference

between throwing and thrusting experimental Levallois points ($\chi^2=0.109$ df=1 p-value=0.741).

Intense edge-damage (often presenting an utter crushing of the edges or digital tip) was much more frequent in thrusting experimental Levallois points (41% to 14%, Table 6-3). However, this trace pattern alone cannot be used as an indicator of thrusting activities if not in association with other diagnostic projectile impact traces (e.g. DIFs and/or MLITs, see below in this chapter).

Relevant information has also been gathered on the correspondence between fracture type and velocity of the weapons. Step fractures and primary burination fractures appeared in very low frequencies, both in throwing and thrusting experiments, suggesting that these bending fracture categories are indicative of high-speed projectiles only (as also suggested by Iovita et al., 2014; but see CHAPTER 11 for further discussions).

It has also been demonstrated that throwing experimental Levallois showed higher frequencies of mesial fractures than thrusting experimental Levallois points but, although there is a significant difference between the two delivery systems ($\chi^2=73.973$, df=1, p-value=0.000, Table 6-4), the location of fractures alone cannot be considered diagnostic of one particular delivery system. Equally, it was noticed that most fractures were generated as a result of impact with hard tissues (i.e. bone contact materials), a fact that provides insight into the difficulty of correctly interpreting both experimental and archaeological projectile tools that did not impact against hard tissues, as these tools may not develop sufficient diagnostic traces to allow an interpretation as projectile elements.

In conclusion, the overall results indicated that observed types and frequencies of fractures do not provide clear trace patterns to allow for differentiation between throwing and thrusting hand-delivered stone-tipped spear projectiles. No statistically significant relationship can be proven between impact fracture types and delivery systems ($\chi^2=3.265$, df=7 p-value=0.352, Table 6-2). Therefore, the

analysis of fractures, although supporting the identification of projectile stone tools (through the identification and quantification of DIFs), alone (i.e. if not in combination with a high-power use-wear analysis) cannot be considered a reliable method to discriminate between throwing and thrusting hand-delivered stone-tipped spear projectiles (but see also CHAPTER 11 for further discussions).

6.3 Comparing throwing and thrusting experimental Levallois points used as hand-delivered spear projectiles: microscopic use-wear results (see also Appendix A, Volume 2)

6.3.1 Overview

Polish surfaces, striations, and microscopic linear impact traces (MLITs) resulting from throwing and thrusting hand-delivered stone-tipped spear experiments were examined with an Olympus BX60 optical microscope with incident lights, using a magnification range from 50x to 500x (see also Section 2.5). All of the experimental Levallois points were cleaned before the high-power microscopic examination, as described in Section 3.4.2. As such, the microscopic use-wear pictures and results presented below were recorded only following the cleaning procedure.

A detailed, high-power use-wear analysis of the experimental Levallois points used in hand-delivered stone-tipped spear experiments was considered to be a crucial step in order to enlarge the current knowledge on projectiles' diagnostic impact traces. In the past, use-wear studies of experimental and archaeological projectiles²² have primarily focused on low-power use-wear analysis (but see Moss, 1983a; Fischer et al., 1984; Rots, 2013; Tomasso et al., 2015; Rots et al., 2017), with special emphasis on fractures and DIF identification (Shea, 1998; Soriano, 1998; Geneste and Plisson, 1989, 1990, 1993; Shea et al., 2001; Lombard, et al., 2004; Lombard, 2005b, 2006b; O'Farrell, 2004; Pargeter, 2007, 2013; Lombard and Pargeter, 2008; Villa et al., 2009a, 2009b; Villa and Lenoir, 2006, 2009; Lombard and Phillipson, 2010; Villa and Soriano, 2010; Yaroshevich et al., 2010, 2016; Lazuén, 2012; Wilkins et al., 2012; Iovita et al., 2014). This is mostly because low-power use-wear analysis allows the researcher to examine a larger number of tools in a short period of time. However, as a result, experimental

²² In this thesis, the terms 'projectile' and 'projectile tool' refer to all stone tools mounted on a shaft, regardless of the type of weapon or delivery system (see Glossary).

projectiles have often been referred to as a category of tool that does not develop numerous microscopic use-wear traces, with the exception of microscopic linear impact traces (MLITs; Moss, 1983a; Fischer et al., 1984). This is because the time of contact between the worked material and the projectile tools has been considered too short for the polish and other microscopic use-wear traces to develop (Rots and Plisson, 2014, p. 156; Van Gijn, 1989; Fischer et al., 1986).

The results of the high-power use-wear analysis on n=28 throwing and n=24 thrusting experimental Levallois points used in hand-delivered spear experiments, however, suggest otherwise. The data presented below shows that throwing and thrusting experimental Levallois flint point replicas when carrying out hand-delivered spear motions allowed for the development of polish traces, striations, and microscopic linear impact traces (Table 6-6). Moreover, the frequencies of specific microscopic use-wear traces (e.g. MLITs and polish traces) have been proven statistically significant for hand-delivered throwing spears (see below), suggesting that microscopic use-wear traces form reliable evidence for distinguishing between throwing and thrusting hand-delivered spear projectiles, at least in an experimental dataset.

The results are presented below.

6.3.2 General results on microscopic use-wear traces

Microscopic use-wear traces and frequencies of the experimental Levallois points used as hand-delivered stone-tipped spears revealed interesting differences between throwing and thrusting experimental tools (Table 6-6).

The results indicated that throwing experimental Levallois points showed an overall higher frequency of microscopic use-wear traces than thrusting experimental Levallois points (Table 6-6 and Figure 6.20). Table 6-6 shows that throwing experimental Levallois points exhibited significantly higher frequencies of polish traces, striations, and microscopic linear impact traces (MLITs) than thrusting experimental Levallois points. It was found that MLITs were significantly more

common in throwing experimental Levallois points than thrusting experimental Levallois points (71.4% to 8.3% respectively, Table 6-6 and Figure 6.20), and this was proven to be a statistically different pattern between the two delivery systems (p-value=0.000, Table 6-6). Similarly, throwing experimental Levallois points showed a more frequent occurrence of polish traces than thrusting experimental Levallois points (64.2% to 20.8% respectively, Table 6-6 and Figure 6.20), and these trace patterns were proven to be statistically significant (p-value=0.000, Table 6-6). It was also observed that striations occurred more often in throwing than in thrusting experimental Levallois points (46.4% to 12.5%, Table 6-6 and Figure 6.20), and this was a statistically significant difference between the two delivery systems (p-value=0.000, Table 6-6). Moreover, among throwing experimental Levallois points, MLITs were the most recurrent type of microscopic use-wear trace (71.4%), followed by polish (64.2%) and striations (46.4%), (Table 6-6 and Figure 6.20). Whereas, among thrusting experimental Levallois points, low frequencies of polish (20.8%) and striations (12.5%) were recorded, followed by very low frequencies of MLITs (8.3%) (Table 6-6 and Figure 6.20).

Below, throwing and thrusting experimental Levallois points are divided into two different categories, and they are described in accordance with the types and frequencies of microscopic use-wear traces recorded.

Table 6-6. Polish, striations, and microscopic linear impact traces (MLITs) recorded on the experimental Levallois points, according to the delivery system (i.e. throwing and thrusting). Note: trace frequencies refer to the number of tools with a specific trace (more than one trace type can occur on a tool). LP stands for experimental Levallois points.

This thesis experiments	Throwing (LP n=28)	%	Thrusting (LP n=24)	%	Chi ² results
Total tools with polish	18	64.2	5	20.8	$\chi^2= 25.920$, df=1, p-value= 0.000
Specific polish	16	57.1	2	8.3	
Not-specific polish	2	8	3	12.5	
Total tools with striations	13	46.4	3	12.5	$\chi^2=81.920$, df=1, p-value= 0.000
Total tools with MLITs	20	71.4	2	8.3	$\chi^2= 169.280$, df=1, p-value= 0.000
Total tool with microscopic use-wear traces	22	78.5	5	20.8	

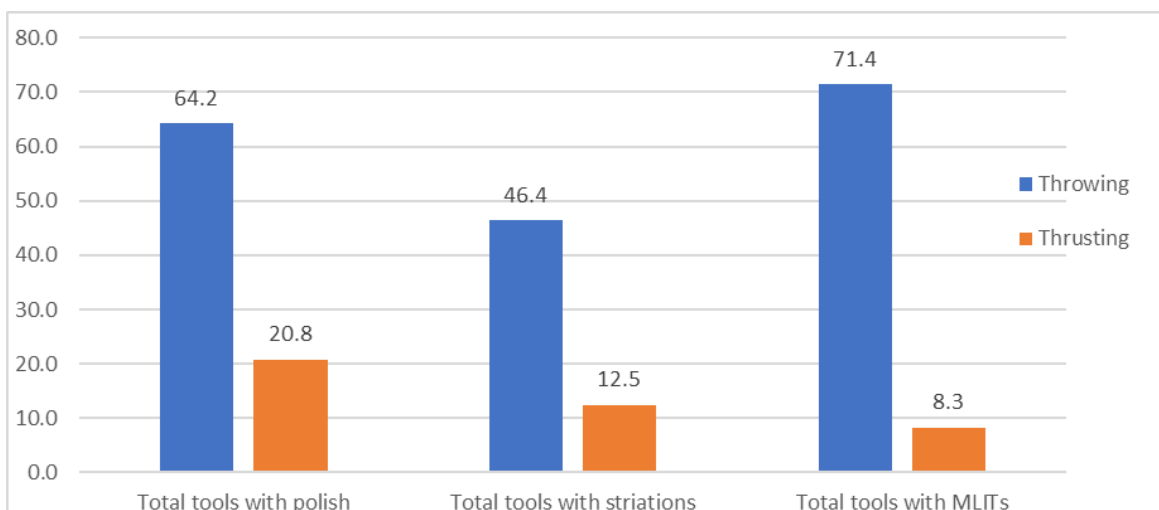


Figure 6.20. Distribution of microscopic wear traces (in percentages %) in the experimental Levallois points, according to their delivery system (throwing in blue vs thrusting in red).

6.3.3 Microscopic use-wear traces observed on experimental Levallois points used in throwing hand-delivered stone-tipped spear experiments

Among n=28 experimental Levallois points used as throwing hand-delivered stone-tipped spears, n=22 points in total developed microscopic use-wear traces such as MLITs, polish, and striations which could be associated with projectile impact activities (Table 6-6). No edge-rounding was observed in the throwing experimental Levallois points (Table 6-6). Microscopic use-wear traces (e.g. adhesive residues and polishes) related to the hafting process were identified, and these are described in CHAPTER 7.

6.3.3.1 Microscopic linear impact traces (MLITs) and striations

Microscopic linear impact traces (MLITs) are here defined as linear bands or stripes of polish with striations around or within the polish (Moss 1983a; Fischer et al., 1984) (Figure 6.21 - Figure 6.26).

In this study, MLITs were the most common type of microscopic traces observed in the throwing experimental Levallois points (Figure 6.20). They were more recurrent in throwing than in thrusting points (71.4% to 8.3% respectively, Table 6-6), and this was a statistically different pattern observed between the two delivery systems (p-value=0.000, Table 6-6).

MLITs recorded in throwing experimental Levallois points were very similar to those described by Fischer et al. (1984, p. 28) and Moss (1983a, p. 95). They appeared as long linear bands of polish in “long and shining stripes” (Fischer et al., 1984, p. 28) (Figure 6.21 - Figure 6.24). The polish that developed within the MLITs appeared as a very bright, almost metallic polish (already at 100x), with a smooth texture and abundant striations within it (from 200x, Figure 6.22). In the throwing experimental Levallois points, MLITs were visible from 50x (Figure 6.22), but they became clearly observable at 100x (Figure 6.21), and from 200x it was

possible to appreciate the texture of the polish and the internal striations (Figure 6.21).

In the throwing experimental Levallois points, MLITs were often long and exhibited clear features of directionality, running parallel to the direction of the impact (i.e. parallel to the morphological axis of the tools) (Figure 6.21 - Figure 6.26). Generally, they represented the best indicators for identifying the direction of the impact of the experimental projectiles analysed in this study.

In the throwing experimental Levallois points, MLITs developed mostly on the inner surface of the distal ventral face of the tools (i.e. Loci D2v, D3v; Figure 6.21 - Figure 6.24). Rarely, they were also observed on the mesial ventral surface (Loci M1v, M2v; Figure 6.25, Figure 6.26). They were never observed on the dorsal face of the experimental throwing points. When present, MLITs were often in groups of two (Figure 6.21, Figure 6.22) or occurring in their multitudes on a single tool (Figure 6.25, Figure 6.26).

In throwing experimental Levallois points, MLITs mostly developed on throwing points that impacted against hard tissues (i.e. bone materials; Figure 6.21 - Figure 6.24), but they were also observed on throwing points that missed the target and hit the ground (Figure 6.25, Figure 6.26). However, the MLITs resulting from impact against bone materials were located on the distal ventral tip (in Loci D1v, D2v or D3v). They were bright (almost metallic), long, and wide (up to 300 μ n-micron length) and presented abundant strips of polish all around or within them (Figure 6.22). Whereas, the MLITs resulting from impact against ground materials (i.e. mineral particles from the soil) were located on the mesial ventral face (in the inner surface of Loci M1v, M2v). They were rather dull, but long and thin, and did not show strips of polish all around (Figure 6.25, Figure 6.26).

When MLITs (tool TH-31) were observed with an ESEM microscope (FEI ESEM Quanta 600; at the IPHES Institute in Tarragona, Spain; see also Section 2.2.4), it was possible to observe that MLITs caused a plastic deformation of the flint

surface (as suggested by Fischer et al., 1984), resembling a central groove surrounded and filled up by stripes of polish (Figure 6.27). These observations were in agreement with Fischer's (et al., 1984) assumption that MLITs were the result of the plastic deformation of the stone tool surface, caused by scratching agents. Fischer et al. (1984) proposed that the "scratching agents" responsible for the formation of MLITs were flint micro-flakes that detached directly from the stone tool during the impact (Fischer et al., 1984,). However, seeing as, in this study, MLITs have also been observed in throwing experimental Levallois points that did not present fractures or edge-damage (and therefore no micro-flakes were removed from the tool surface), it seems plausible that the formation of MLITs is linked to the action of multiple and different scratching agents that hit the stone tool surface during the impact. Those particles could be flint micro-flakes that have detached from the stone tool (as originally suggested by Fischer et al., 1984), but they could also be dust and mineral particles present in the contact materials (e.g. bone or soil, as observed in the throwing experimental Levallois points of this study).

However, a further experimental investigation is essential in the future to better understand the formation process of MLITs and their relationship with the impact velocities of projectiles (see also discussions in CHAPTER 11).

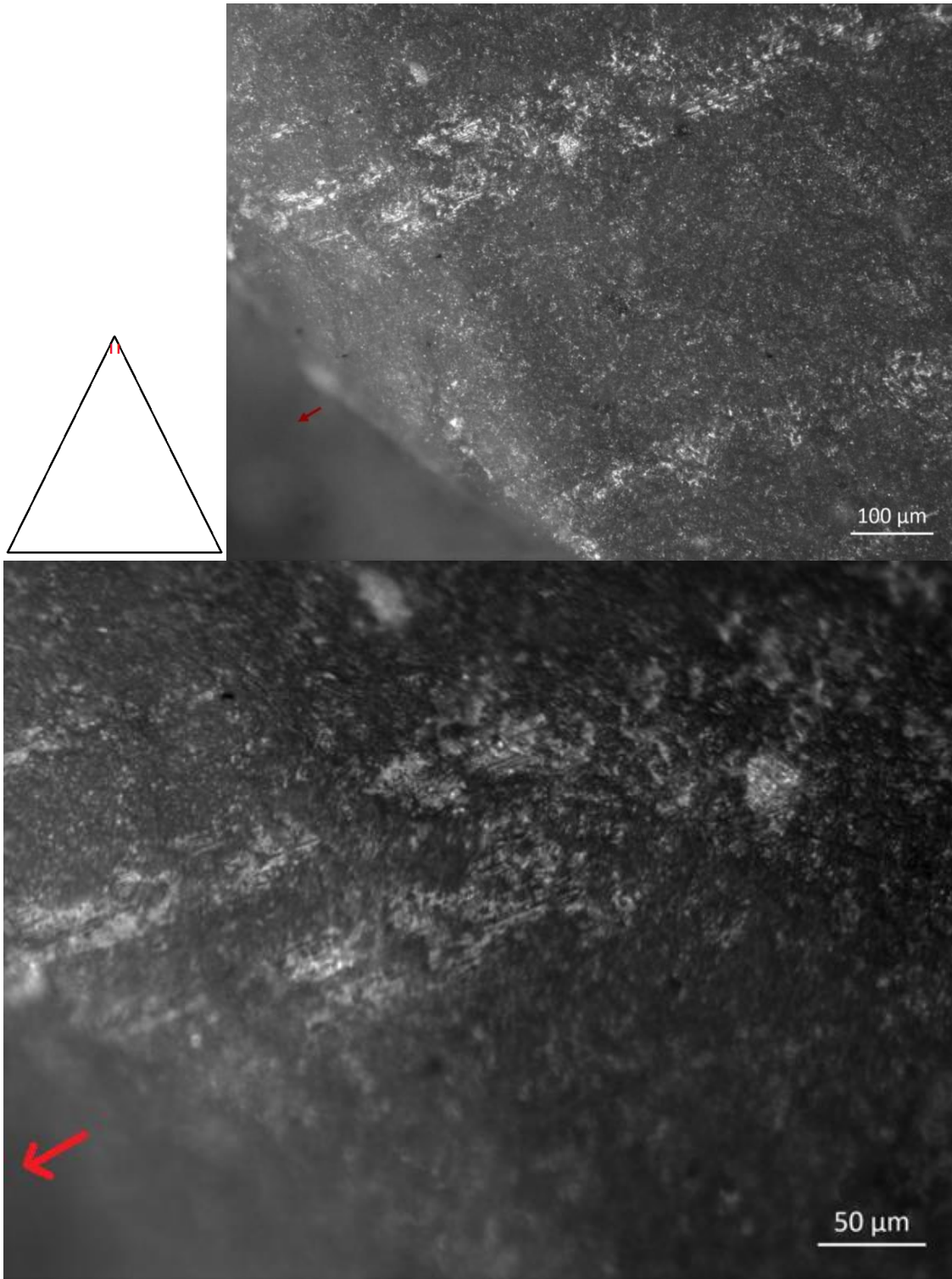


Figure 6.21. MLITs located on the ventral distal tip (Locus D1v). Picture: OLMil, OM 100x (above) and 200x (below), (experiment code: TH-78). The red arrow indicates the location or direction of the distal tip.

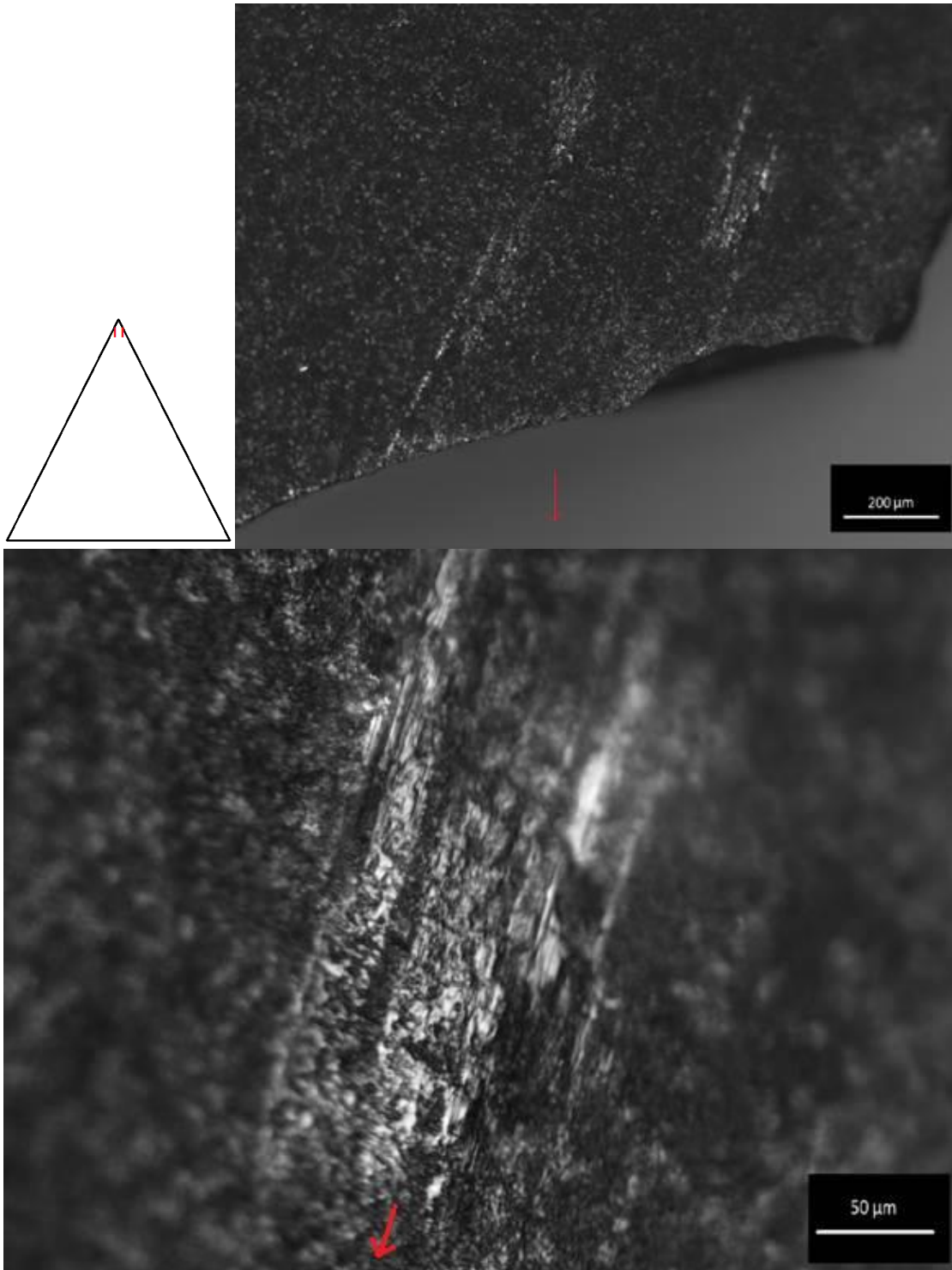


Figure 6.22. MLITs located on the ventral distal tip (Locus D1v). Picture: OLMil, OM 50x (above) and 500x (below), (experiment code: TH-31). The red arrow indicates the location or direction of the distal tip.

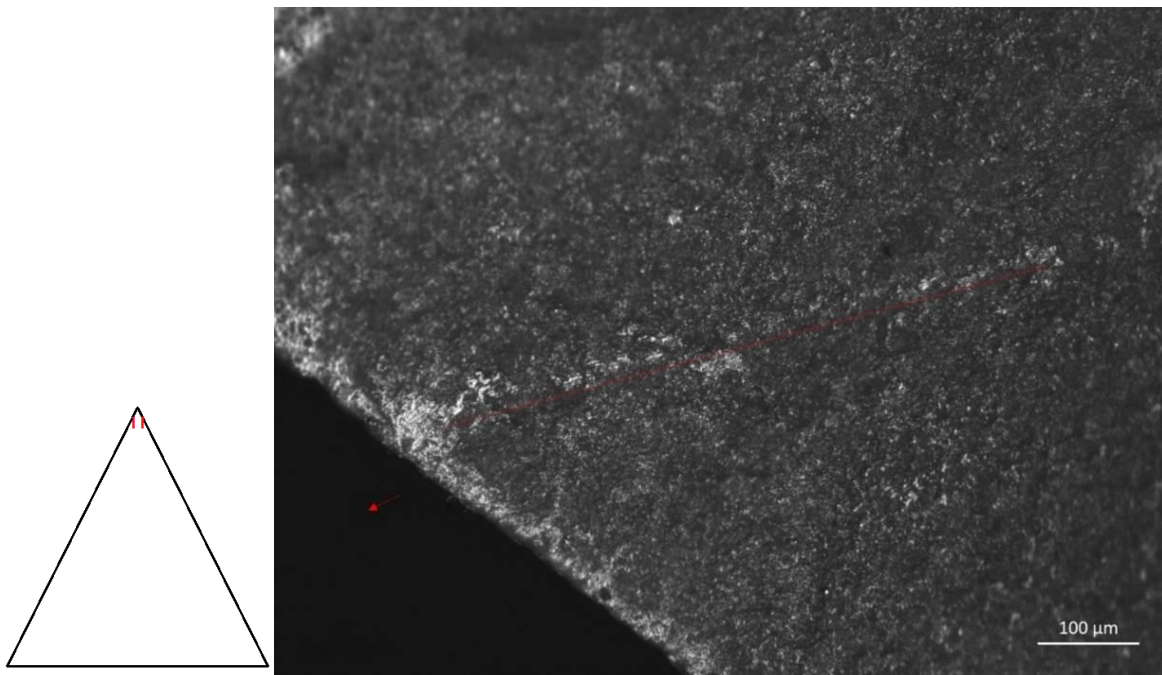


Figure 6.23. MLIT located on the ventral distal tip (Locus D1v). Picture: OLMil, OM 100x, (experiment code: TH-82). The red arrow indicates the location or direction of the distal tip.

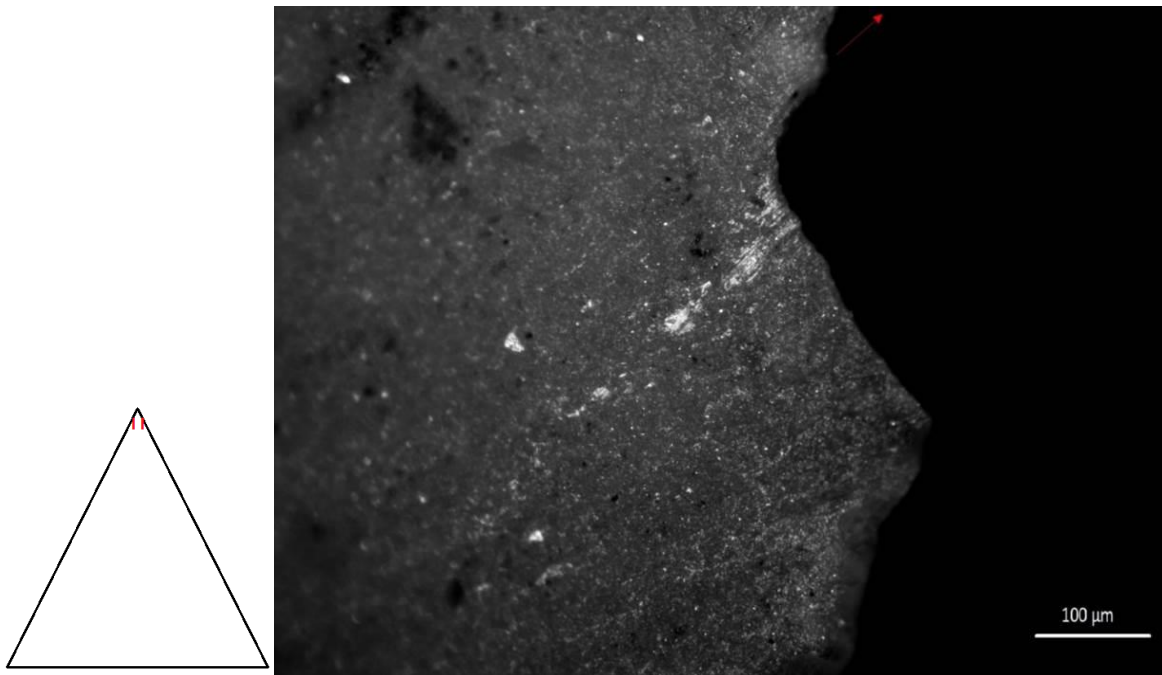


Figure 6.24. MLITs located on the ventral distal tip (Locus D1v). Picture: OLMil, OM 100x, (experiment code: TH-84). The red arrow indicates the location or direction of the distal tip.

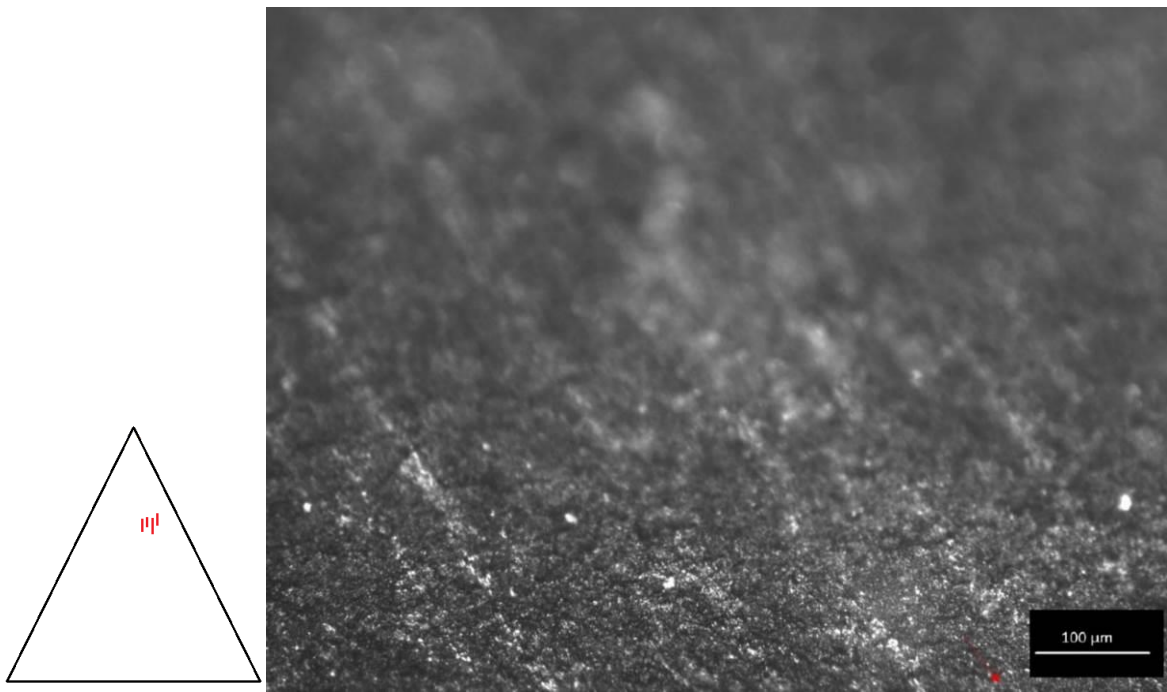


Figure 6.25. MLITs resulting from impact against the ground. They are located on the ventral mesial face (Locus M2v). Picture: OLMil, OM 100x (experiment code: TH-71). The red arrow indicates the location or direction of the distal tip.

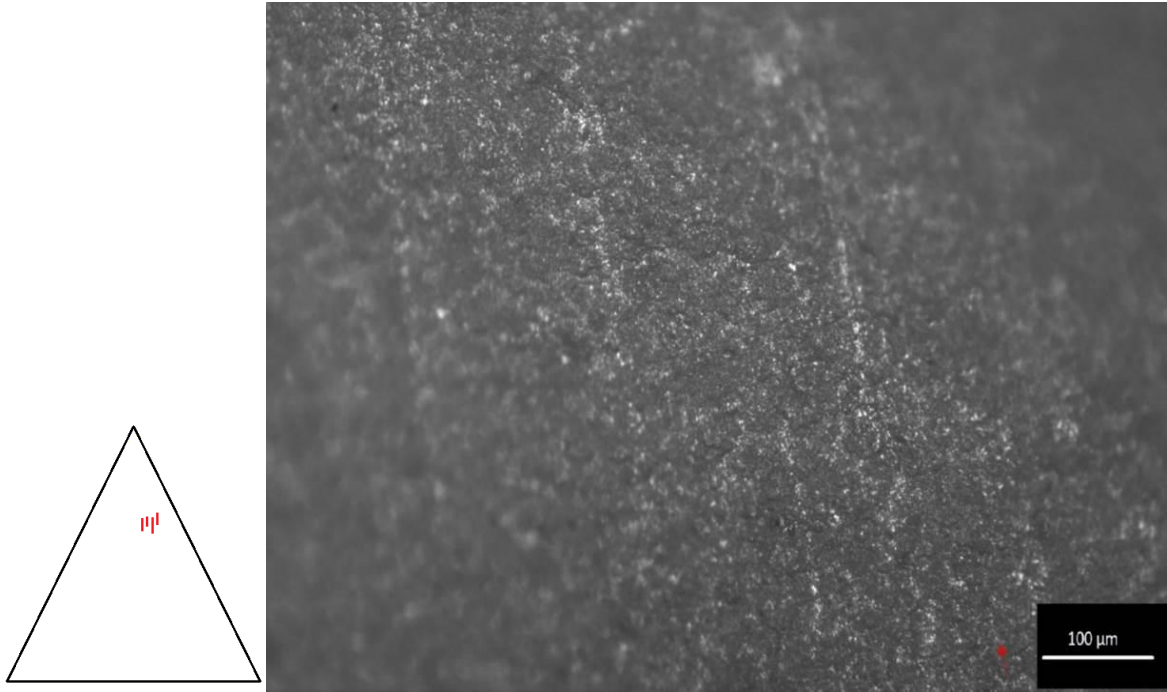


Figure 6.26. MLITs resulting from impact against the ground. They are located on the ventral mesial face (Locus M2v). Picture: OLMil, OM 100x (experiment code: TH-81). The red arrow indicates the location or direction of the distal tip.

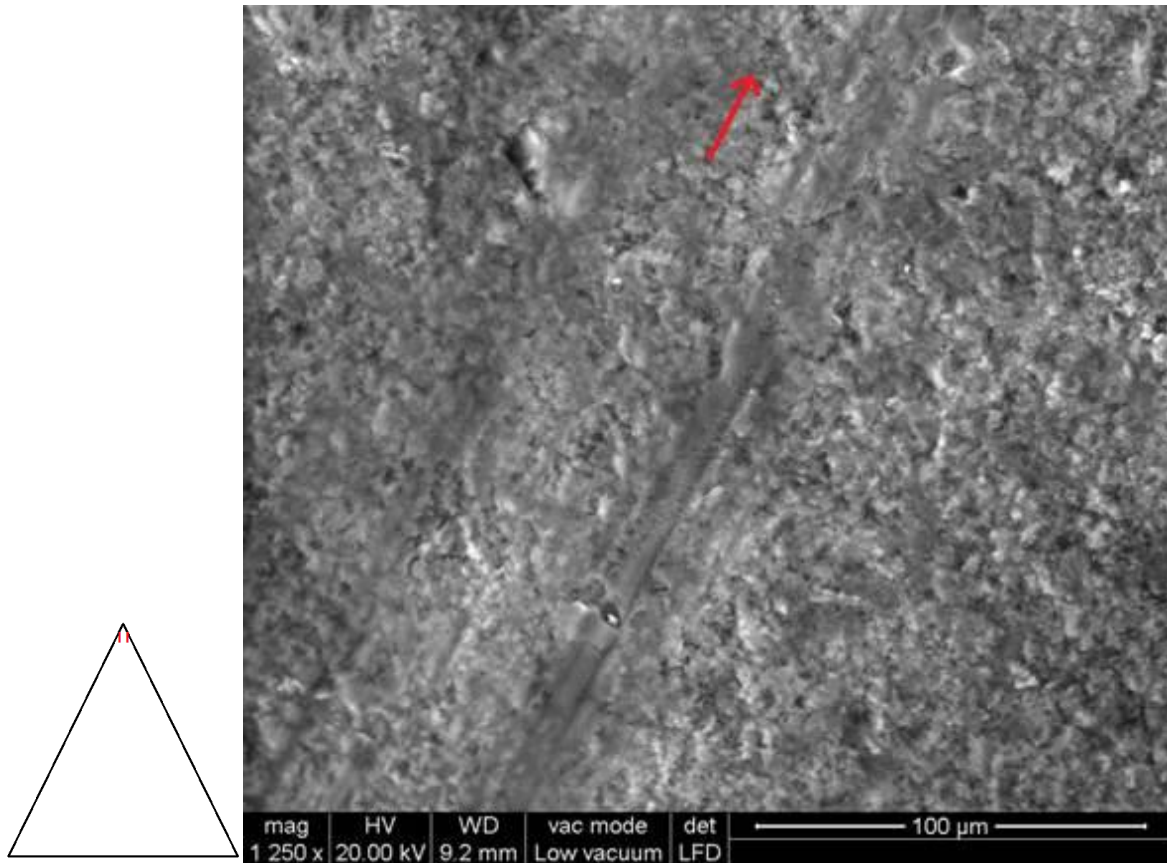


Figure 6.27. MLITs observed with the ESEM, OM 1250x. Plastic deformation of the flint surface in form of channels. The red arrow indicates the location or direction of the distal tip (experiment code: TH-31).

6.3.3.2 Striations in throwing points

Striations were more recurrent in throwing than in thrusting experimental Levallois points (46.4% to 12.5% respectively, Table 6-6), and this presented a statistically different pattern between the two delivery systems (p-value=0.000, Table 6-6).

In the throwing experimental Levallois points, striations were often incorporated within the MLITs (Figure 6.21, Figure 6.22) or within polish traces (Figure 6.29 - Figure 6.32). These exhibited regular edges and ranged between shallow and

deep striations (Figure 6.29). Striations generally showed a parallel direction to the morphological axis of the tools, i.e. they were mostly running parallel to the direction of impact (Figure 6.29). Sometimes, oblique striations were observed to be incorporated within polish traces (Figure 6.30, Figure 6.31, and Figure 6.32). These oblique striations were considered to be the result of a twisting motion of the projectile during the impact, i.e. the spin of the throwing spears observed during the ballistic examination (see CHAPTER 5). The spin-rotation that was observed in the trajectory of the experimental hand-delivered stone-tipped throwing spears can, therefore, cause the formation of specific traces in throwing projectiles (see CHAPTER 5). Therefore, it is highly possible that these oblique striations formed when the projectile entered and penetrated inside the animal target while it was still making a rotatory or twisting movement (Figure 6.30, Figure 6.31, and Figure 6.32). These use-wear traces (Figure 6.30, Figure 6.31, and Figure 6.32) could confirm the spinning effect of the hand-delivered throwing spears (observed in the fluctuation of the trajectory of the hand-delivered throwing spears, CHAPTER 5) and may suggest different use-wear patterns between throwing and thrusting stone-tipped spear projectiles.

6.3.3.3 Polish traces

The results of the high-power microscopic use-wear analysis showed fascinating differences in the pattern of polish traces between throwing and thrusting experimental Levallois points used in hand-delivered stone-tipped spear experiments. It was found that polish traces occurred more often in throwing than in thrusting experimental Levallois points (64.2% to 20.8% respectively, Table 6-6 and Figure 6.20), and this difference was statistically significant (p -value=0.000, Table 6-6). Out of $n=24$ thrusting experimental Levallois points, only five points showed the presence of polish traces, among which only two points showed specific polish traces (Table 6-6). Whereas, among $n=28$ throwing experimental Levallois points, eighteen points showed the presence of polish traces (Table 6-6), between which, sixteen points showed a specific type of polish that consistently

appeared in throwing points and on no occasion was observed on thrusting points. This polish was called “impact polish” and, as no other authors have reported this phenomenon, it is described here in detail.

6.3.3.3.1 Impact polish in throwing points

Impact polish appeared on 57.1% (n=16 tools, Table 6-6) of the experimental Levallois points used in throwing hand-delivered stone-tipped spear experiments. It was not observed before utilisation, and it was not present in any of the high-resolution dental casts of the experimental Levallois points created before the experiments (see Section 3.1). Therefore, considering its location and attributes, the formation of the impact polish could only be linked to the impact of the throwing spears.

The impact polish showed an interesting combination of polish attributes, which are described below. Two variations of “impact polish” traces were observed, with the first (i.e. “Impact polish subtype A”) showing a well-developed and flat polish with clear directionality (Figure 6.28 - Figure 6.33), and the second (i.e. “Impact polish subtype B”) having some of the characteristics of polish traces due to contact against bone materials (i.e. similar to bone-like-polish; see Keeley, 1980, p. 43; Vaughan, 1985; Van Gijn, 1989, p.32 ;) (Figure 6.34 - Figure 6.36).

Eight of the throwing experimental Levallois points (28.5%) showed a well-developed type of polish with clear directionality. This was defined as “Impact polish subtype A” (Figure 6.28 - Figure 6.33). This impact polish developed incredibly well, considering that it formed only after one single shot into the animal target. The impact polish appeared as a flat and very reflective polish with multiple striations within it. The striations within the impact polish always ran parallel or slightly oblique to the direction of the impact (and parallel to the morphological axis of the tools) (Figure 6.28 and Figure 6.29). The striations within the polish were a diagnostic aspect of the “Impact polish subtype A”. The polish areas affected by the impact polish sharply contrasted the unaltered areas on the tool (Figure 6.29).

At 200x, this impact polish showed a smooth texture with a domed-into-flat topography (see Section 2.5.2.2), and a very bright appearance (Figure 6.28, Figure 6.29, Figure 6.31 and Figure 6.32). The smooth texture and flat micro-topography were other diagnostic aspects of the “Impact polish subtype A”. At 200x or 500x, impact polish also showed a certain “mineral or crystalline” polish appearance, as if some minerals were still adhering to the polish (even after intensive cleaning, see Section 3.4.2) (Figure 6.31 and Figure 6.33). This impact polish was always located at the very end of the distal tip (Locus D1v, see Section 2.3), and mainly on the ventral face of the tool. It also appeared on the lateral distal edges of the ventral distal tip (Loci D2v and D3v, see Section 2.3). Sporadically, it was also identified on the highest topographic spots of the distal tip ventral surface. For instance, it was located on the proximity of the knapping stress features (such as ripple marks and radial fissures, which were also the highest topographic spots; see also Appendix A, Volume 2). This impact polish was distributed along the edges and on the inner surface of the tool (i.e. areas cover distribution, see Section 2.5.2.2). The boundary of the “Impact polish A” (i.e. the limit between the polished areas and the unaltered areas) was generally irregular (see Section 2.5.2.2) but clearly visible (Figure 6.29 - Figure 6.31). This impact polish was usually quite intrusive (i.e. low-medium extension, see Section 2.5.2.2), extending from the distal tip into the inner ventral surface (from about 50µm to 150µm) (Figure 6.29 and Figure 6.31). When the raw material and surface of the tool was slightly coarse, the same type of polish appeared rougher and less bright (Figure 6.30).

Eight experimental throwing Levallois points (28.5%) showed a different variation of impact polish, which presented a bone-like polish appearance with a scattered distribution (Figure 6.34 - Figure 6.36). It was defined as “Impact polish subtype B”. This impact polish was very spotted, smooth, highly reflective, but with none or sporadic striations within it (Figure 6.34 - Figure 6.36). It formed primarily on the distal edges of the tip, and, from there, it scattered into the inner distal surface on patches of polish (Figure 6.36). It was rather dispersed on the surface (i.e. spotted distribution, see Section 2.5.2.2) (Figure 6.34 and Figure 6.35), and with a limited

degree of linkage (see Section 2.5.2.2). Once again, it was always located on the distal tip, affecting the highest topographic spots of the inner surface (Loci D1v, D2v and D3v, see Section 2.3; Figure 6.35). It looked moderately developed, considering that it had formed after only a single shot into the animal target (Figure 6.36). Unlike a classic bone-like-polish, this polish did not show come-tails, tiny pits, or bevelled aspect (Keeley, 1980, p. 43; Vaughan, 1985; Plisson, 1985; Van Gijn, 1989, p. 32).

These impact polishes (as described above) cannot be confused with adhesive traces because (i) they were always located in the terminal part of the distal tip (an area that was not in contact with adhesives and/or adhesive residues); (ii) they showed different wear attributes than adhesive traces (such as the lack of an oily and dirty aspect of the polish, the presence of clear directional striations, and the conceivable presence of bone micro-residues [i.e. bone apatite]).

The impact polishes described above all formed in the throwing experimental Levallois points that came into contact with hard tissues (i.e. bone materials) but, during their impact against fresh bone materials, the experimental points had also come into contact with the fresh meat, flesh, and fresh skin materials of the animal targets. Therefore, a straight correlation between impact polish and bone materials cannot be established with this experimental dataset (future experimental studies could further investigate its formation and causation, see CHAPTER 11 and CHAPTER 12).

However, the combination of the high-power microscopic analysis and the results of the ballistic parameters of the throwing hand-delivered stone-tipped spears (presented in CHAPTER 5) may suggest impact polish forms when the projectile reach medium to high velocities (mean >10 m/s). One explanation is that the medium to high speed (i.e. 11.59 m/s impact velocity mean, see Table 5-10) of the throwing hand-delivered spears generated extreme stresses on the stone tool surface of the experimental Levallois points. These stresses may have caused abrupt and sudden changes in very circumscribed microscopic areas of the tool

surface (i.e. mainly in the distal tip and distal edges, which were the first surfaces to hit the target). These stresses, much like a sudden but elevated friction and abrasion of the stone surface against medium-hard materials (such as bone, meat, flesh, and possibly dust and flint particles), and/or a rapid change of temperature, pressure, and force produced by the speed of the projectiles, may have caused a plastic deformation of the stone tool surface, creating this distinctive form of impact polish. When considering that, at higher magnification (e.g. 200x and 500x), it was sometimes possible to observe a “mineral or crystalline” quality to the polish, which might be suggested that some minerals particles (such as bone apatite) were embedded or still adhering into the impact polish (even after intensive cleaning, see Section 3.4.2), opening up possible interpretations of the plasticity of some polish formation processes (see also Anderson, 1980, p. 189; and for further discussions CHAPTER 11). Moreover, the formation of the impact polish under specific stresses and loading rates such as medium to high velocities and high release of kinetic energy may explain the formation of this impact polish type in throwing hand-delivered spear projectiles. The much lower impact velocities recorded for thrusting hand-delivered stone-tipped spears (4.86 m/s to 11.59 m/s velocity means, see Table 5-10) and the higher frequencies of fractures (that have often removed the distal tips of the thrusting points where the impact polish was mostly observed) may perhaps explain the absence of impact polish in the thrusting experimental Levallois points used as hand-delivered stone-tipped spears (see Section 6.3.4).

The hypothesis formulated above, although conceivable considering the current knowledge on polish formation process (Anderson, 1980; Anderson-Gerfaud, 1981; Fullagar, 1991), would require, however, further testing in order to be validated.

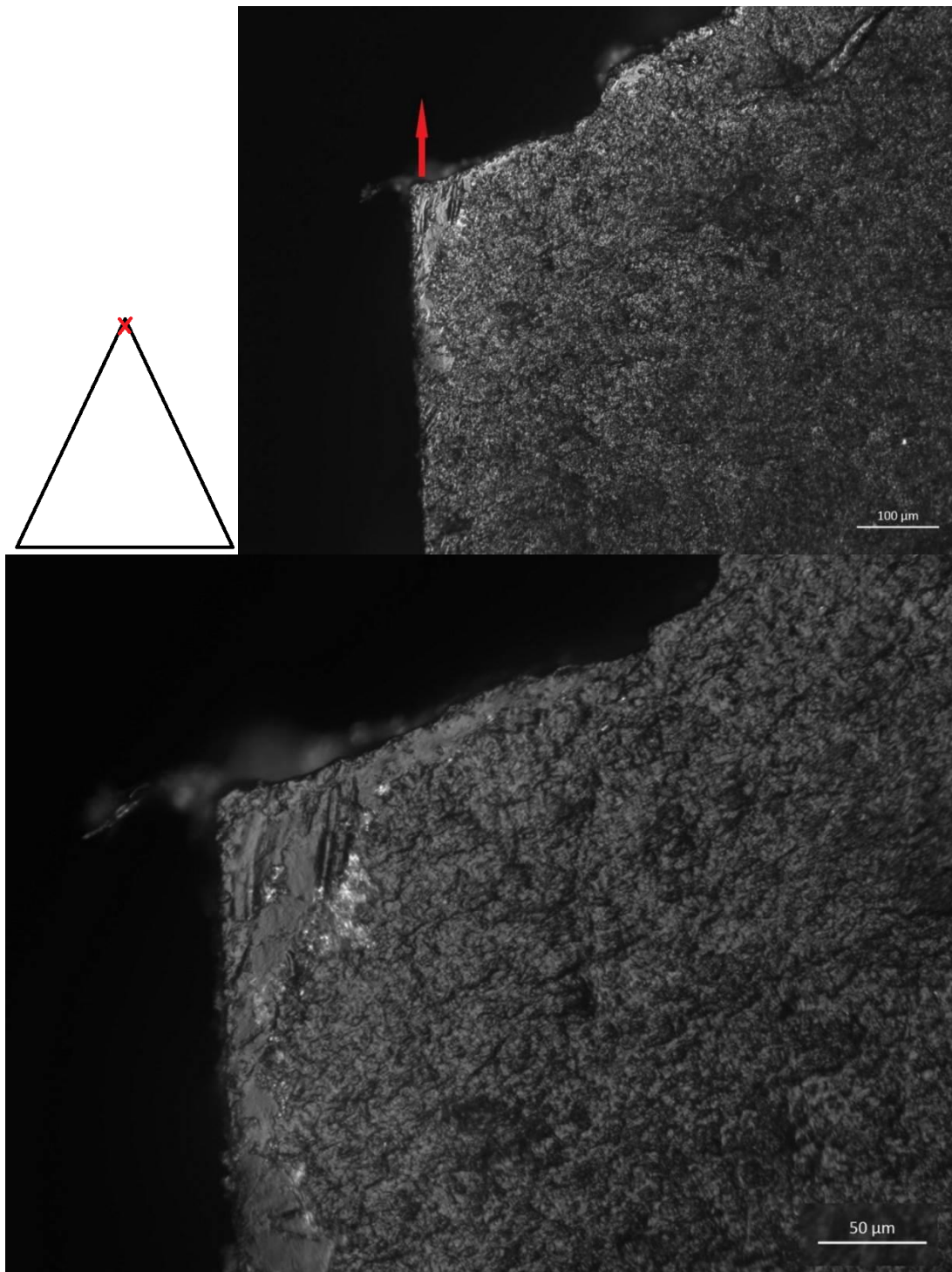


Figure 6.28. Impact polish type A located on the distal tip (Locus D1v). The polish displays a bright and smooth appearance at 100x (above) and a domed-into-flat topography with deep striations at 200x (below). Picture: OLMil, OM 100x (above) and 200x (below), (experiment code: TH-20). The red arrow indicates the location or direction of the distal tip.

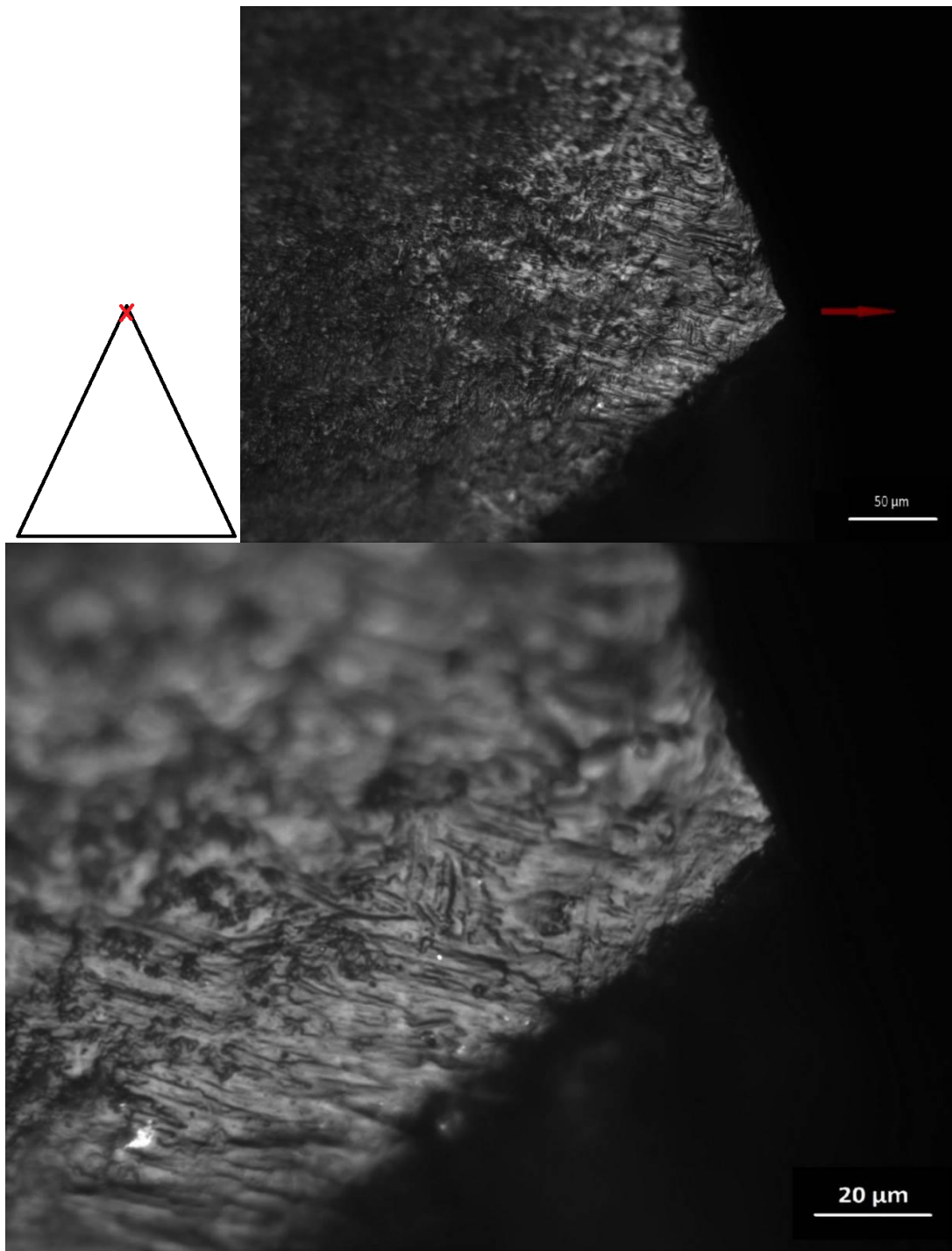


Figure 6.29. Impact polish type A located on the distal tip (Locus D1v). The polish shows a bright aspect at 200x (above) and multiple striations at 500x (below). Picture: OLMil, OM 200x (above) and 500x (below), (experiment code: TH-23). The red arrow indicates the location or direction of the distal tip.

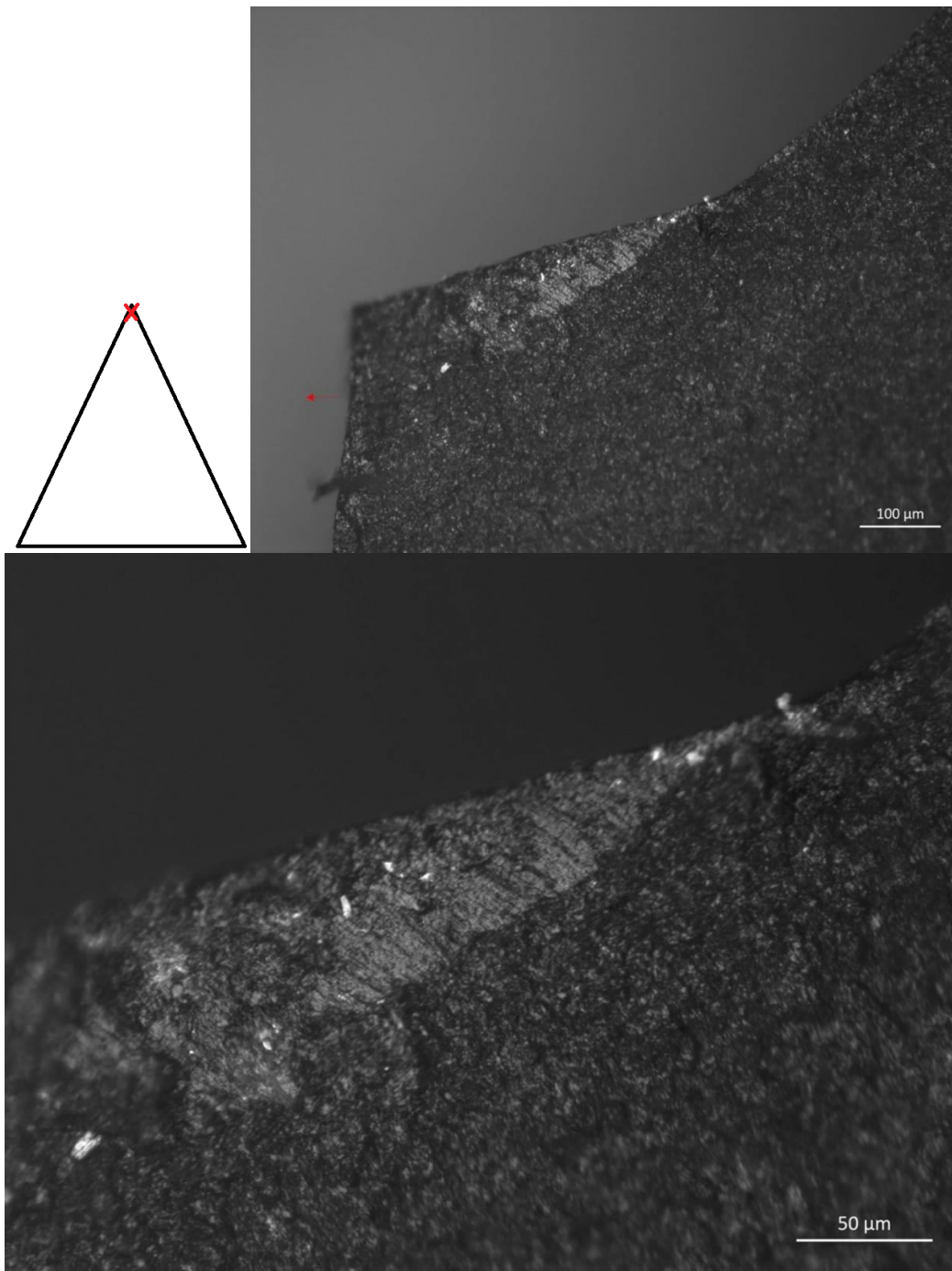


Figure 6.30. Impact polish type A located on the distal tip (Locus D1v). The polish shows a rough texture, a less bright aspect due to the coarse raw material, and small striations. The striations run slightly oblique to the axis of the tool. Picture: OLMil, OM 100x (above) and 200x (below), (experiment code: TH-32). The red arrow indicates the location or direction of the distal tip.

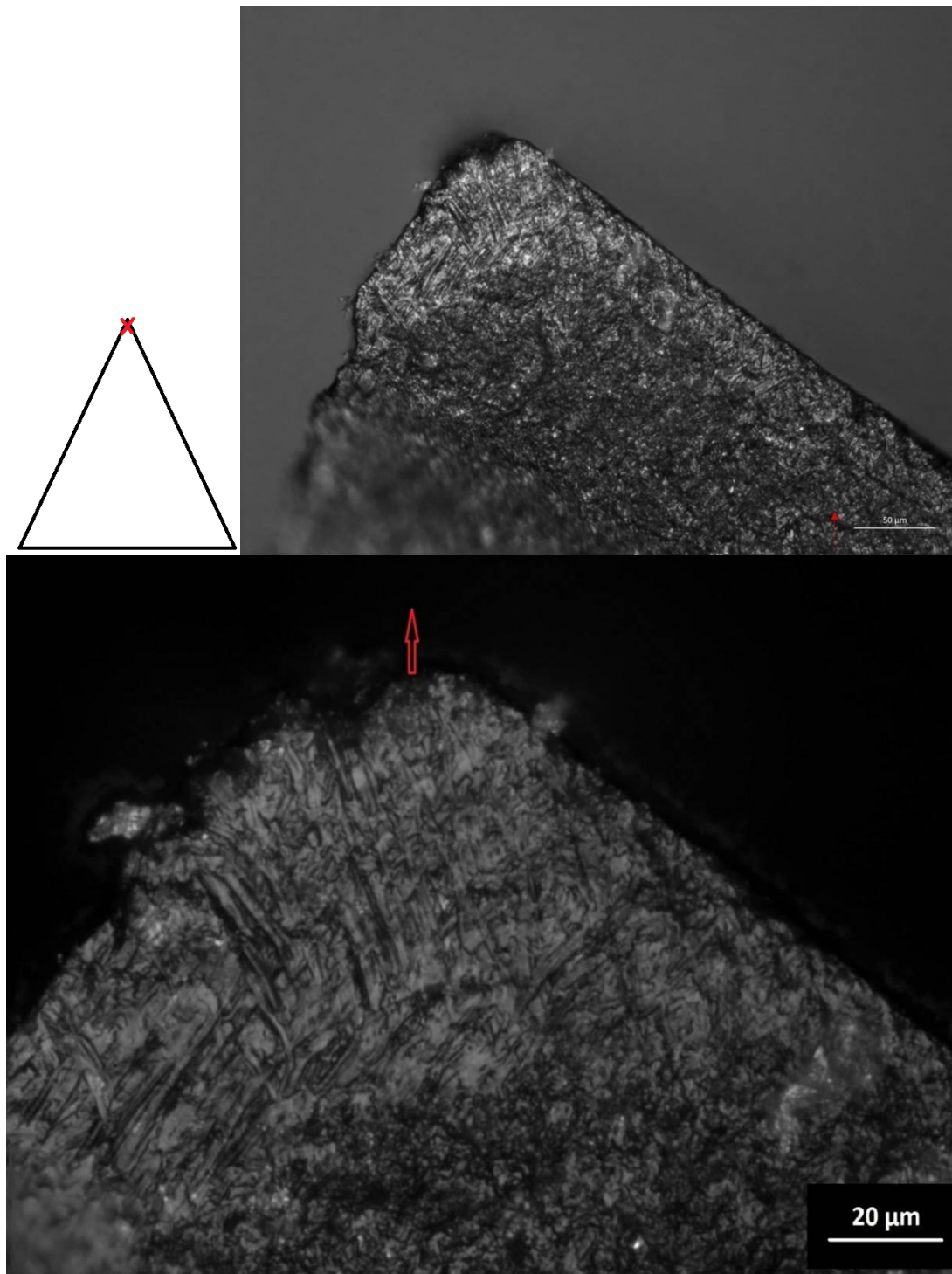


Figure 6.31. Impact polish type A located on the distal tip (Locus D1v). The polish shows a moderately bright aspect at 200x (above) and multiple crossed striations at 500x (below). Picture: OLMil, OM 200x (above) and 500x (below), (experiment code: TH-92). The red arrow indicates the location or direction of the distal tip.

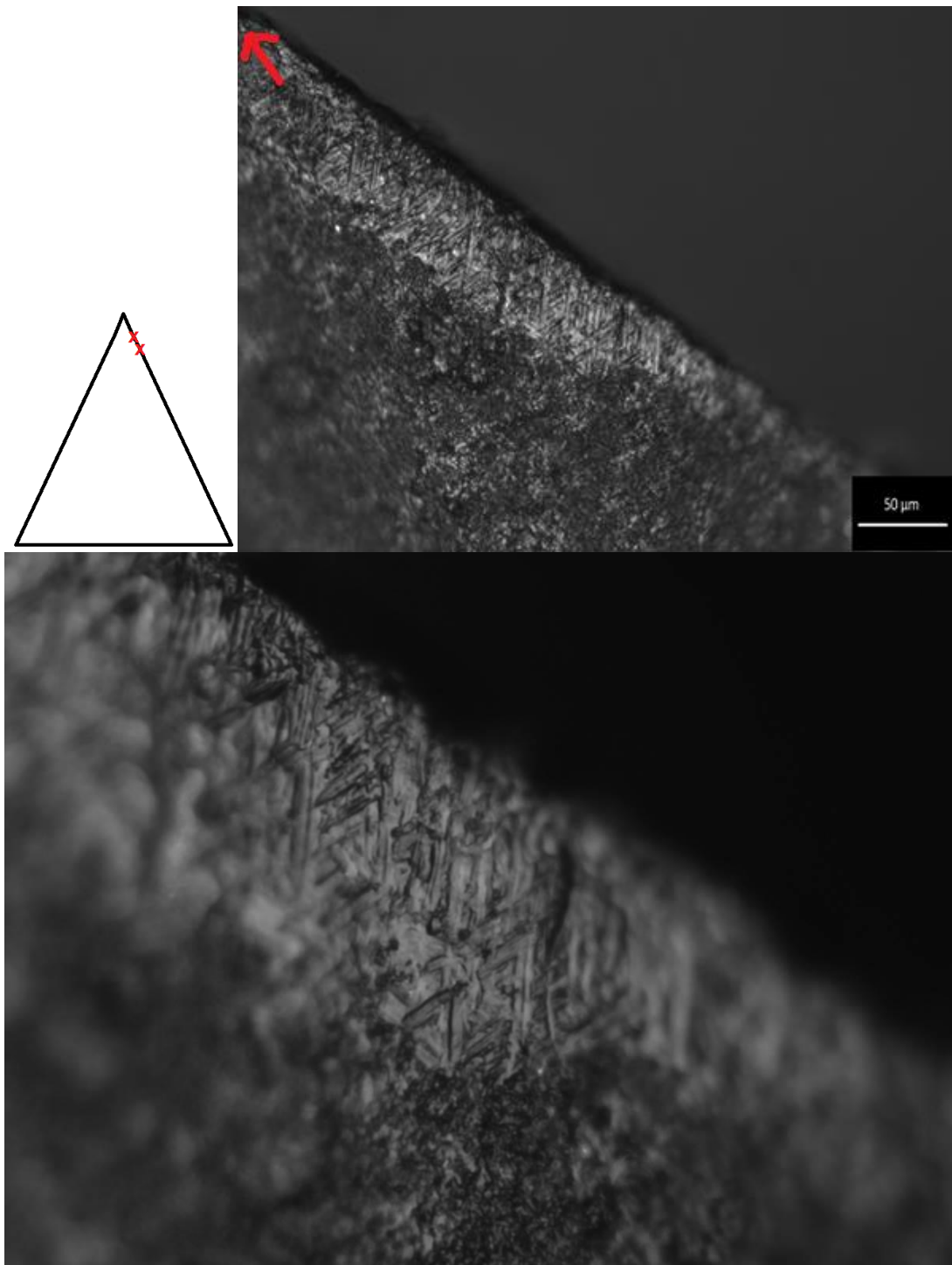


Figure 6.32. Impact polish type A located on the distal lateral edges (Locus D3v). The polish shows a moderately bright aspect at 200x (above) with a flat topography and multiple oblique striations at 500x (below). Picture: OLMil, OM 200x (above) and 500x (below), (experiment code: TH-92). The red arrow indicates the location or direction of the distal tip.

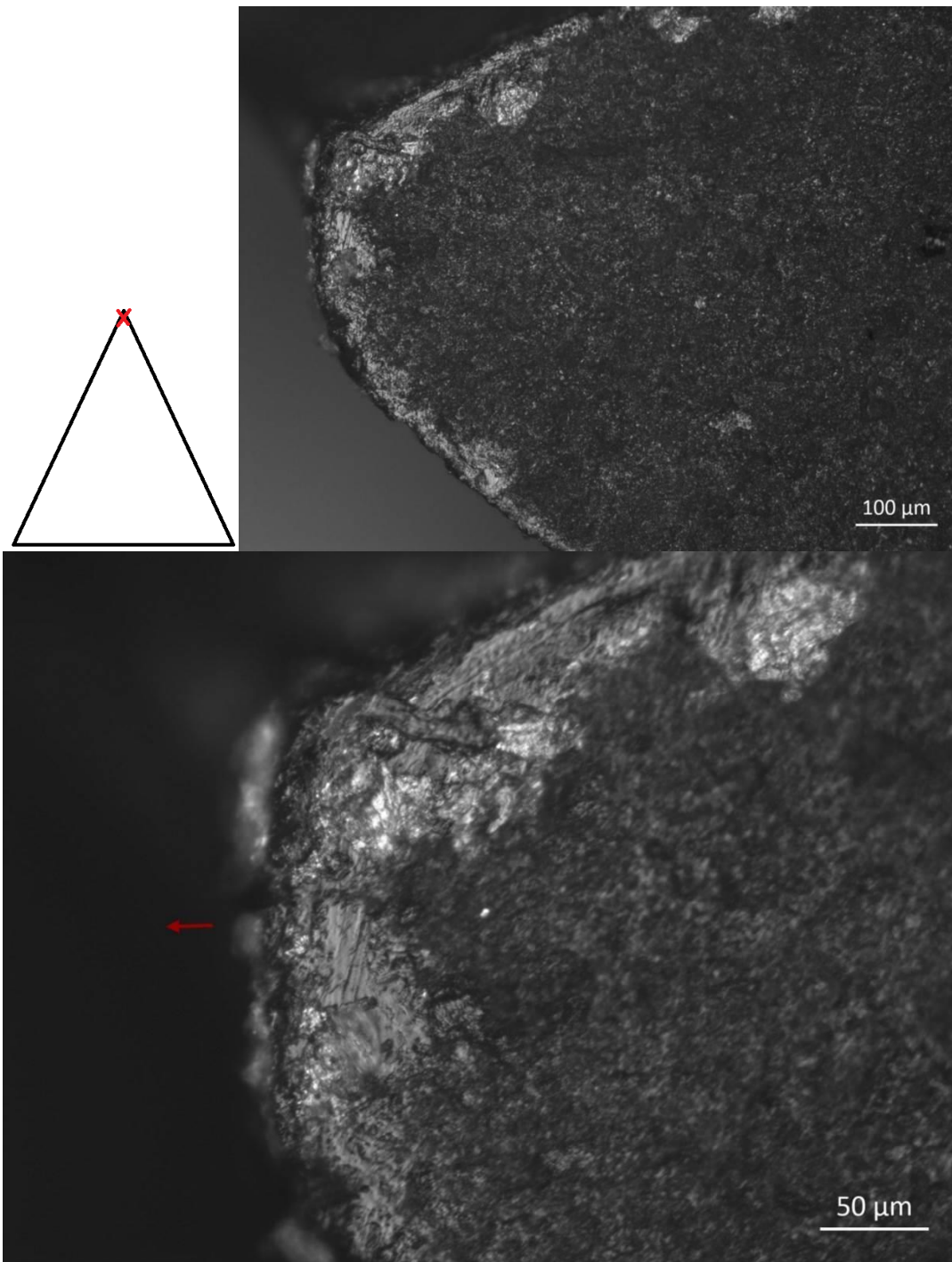


Figure 6.33. Impact polish type A located on the distal tip (Locus D1v). The polish shows a moderately bright aspect at 100x (above) with a domed-into-flat topography and mineral appearance at 200x (below). The roundness of the edge is due to retouch. Picture: OLMil, OM 100x (above) and 200x (below), (experiment code: TH-82). The red arrow indicates the location or direction of the distal tip.

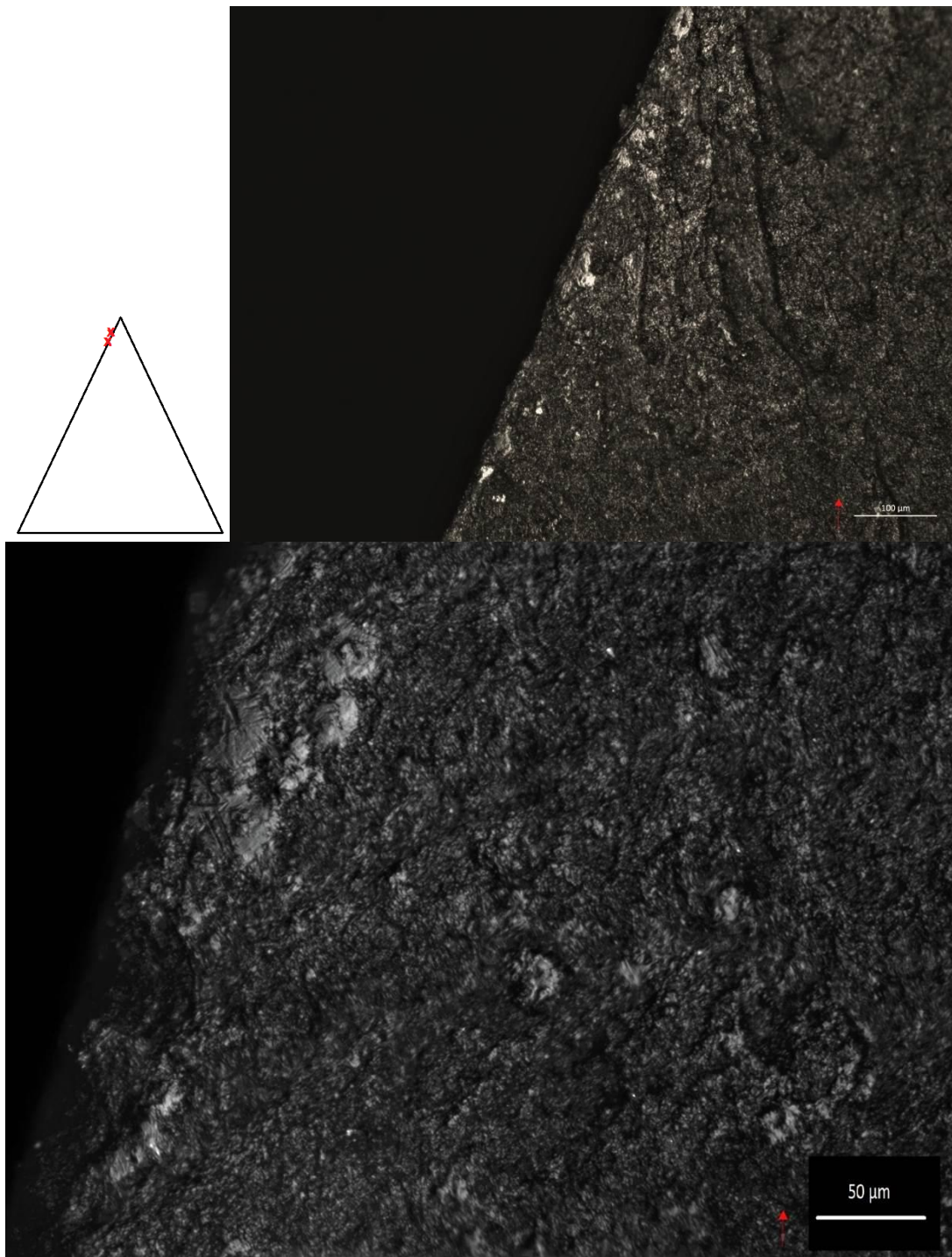


Figure 6.34. Impact polish type B located on the distal lateral edges (Locus D2v). The polish shows a smooth texture, domed topography, and reflective aspect. Only a few striations are present. Picture: OLMil, OM 100x (above) and 200x (below), (experiment code: TH-58). The red arrow indicates the location or direction of the distal tip.

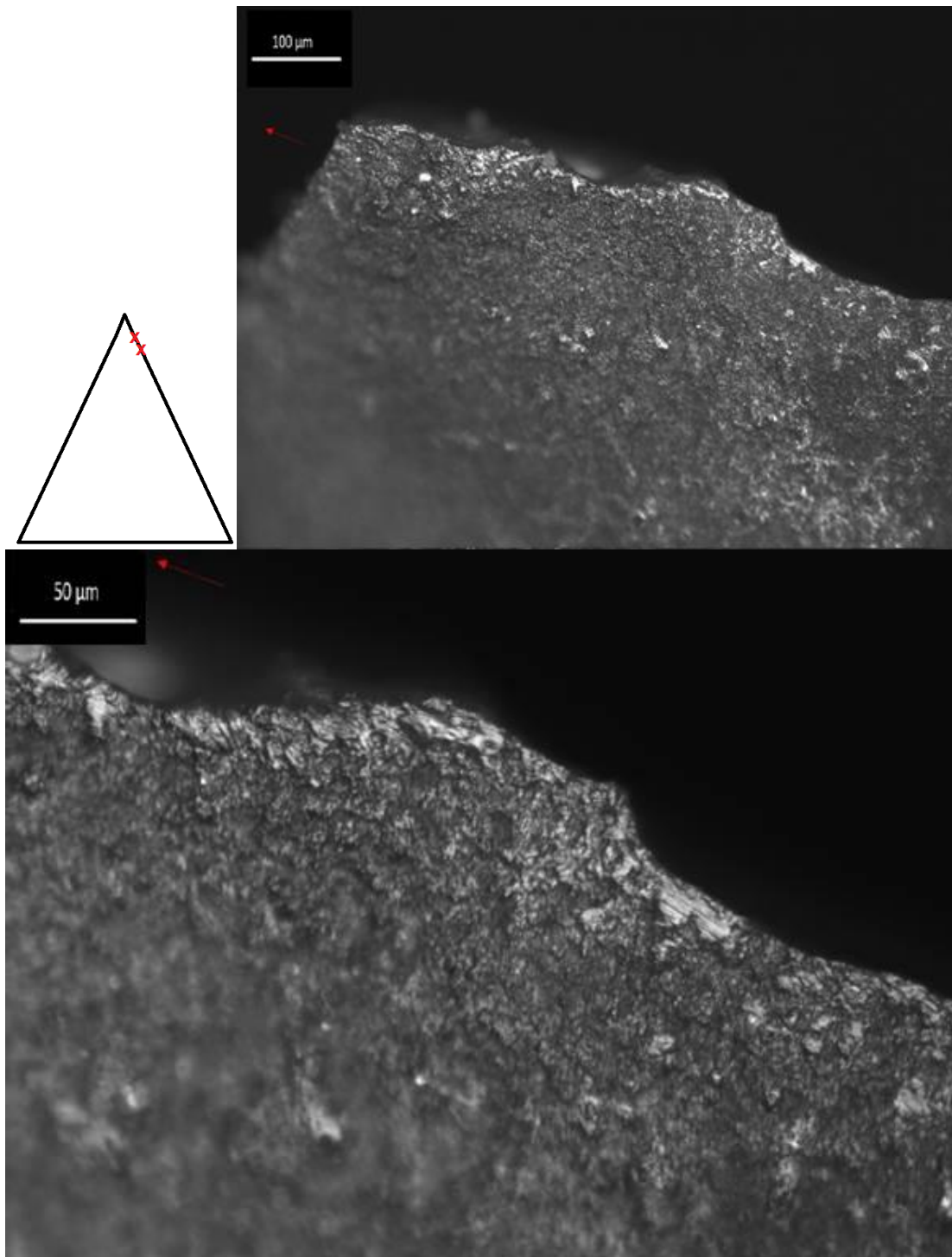


Figure 6.35. Impact polish type B located on the distal lateral edges (Locus D3v). The polish shows a smooth texture, domed topography, and a reflective aspect. Only a few striations are present. Picture: OLMil, OM 100x (above) and 200x (below), (experiment code: TH-68). The red arrow indicates the location or direction of the distal tip.

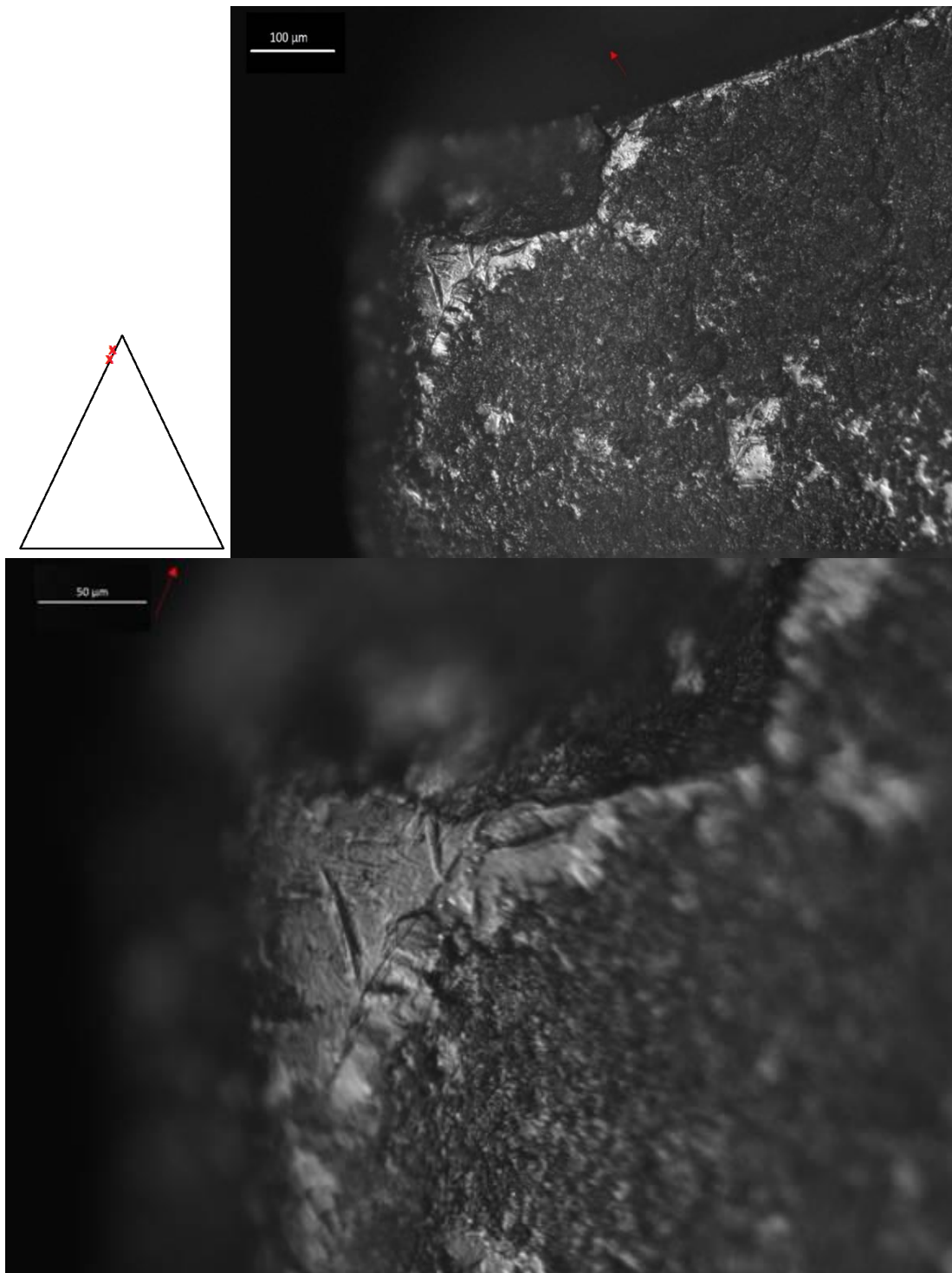


Figure 6.36. Impact polish type B located on the distal lateral edges (Locus D2v). Very reflective polish with domed-into-flat topography and very little striations. Picture: OLMil, OM 100x (above) and 200x (below), (experiment code: TH-68). The red arrow indicates the location or direction of the distal tip.

6.3.3.3.2 Other polish traces in throwing points

Two throwing experimental Levallois points (7.1%) showed a non-specific and not very well-developed polish type (Figure 6.37 and Figure 6.38). The polish had a faint and dull to medium-bright quality. Its development was poor, and it had a scattered distribution (Figure 6.37). It occurred only on the very proximity of the distal ventral tip (Locus D1v, see Section 2.3; Figure 6.37 and Figure 6.38). This polish differed from a meat-like-polish type as it lacked the greasy lustre and the scintillating characteristics typical of a meat-like polish (Keeley, 1980, p. 53; Van Gijn, 1989, p. 41). Moreover, while meat-like polish tends to extend in patches of polish (i.e. speckled aspects), this polish was restricted to the very edges of the tip (affecting only the proximity of the tip; Figure 6.37 and Figure 6.38). Among the two experimental Levallois points that presented non-specific polish traces, one projectile hit the animal target but glanced the spine and land on the ground (tool TH-76), whereas the second projectile passed completely through the rib cage, shattering two ribs (tool TH-62). Therefore, no correspondence can be established between the polish traces and the impact materials.

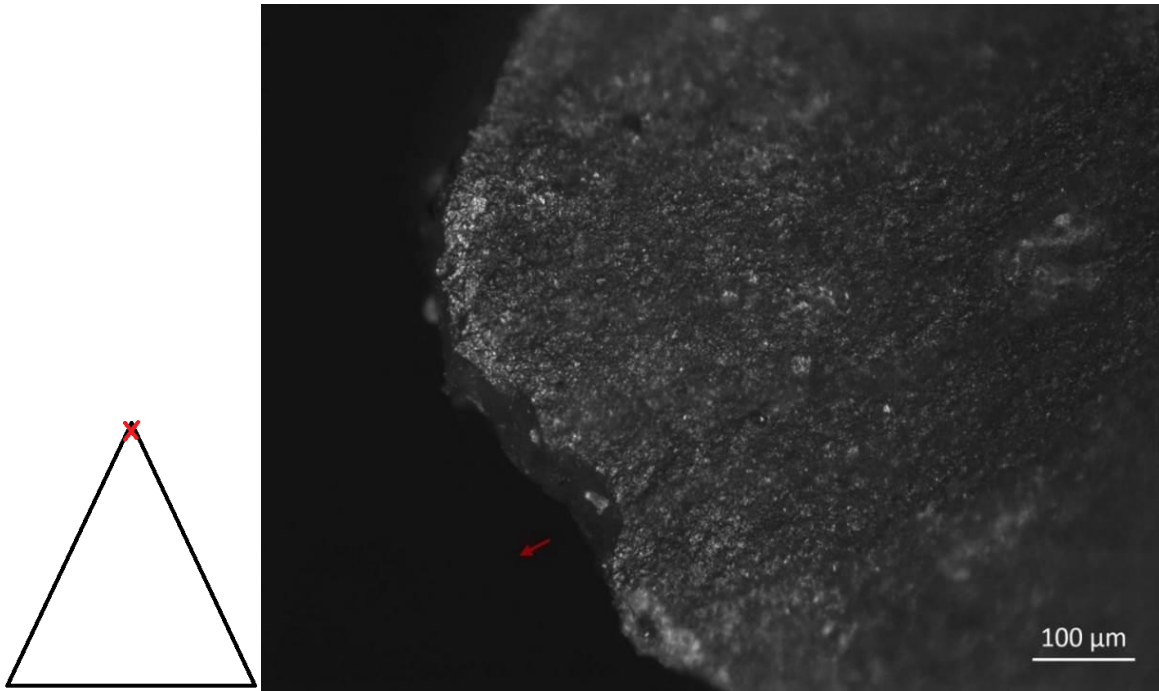


Figure 6.37. Polish located on the distal tip (Locus D1v). The polish shows a poor development and a dull to medium-bright aspect. No striations were observed. Picture: OLMil, OM 100x (experiment code: TH-62). The red arrow indicates the location or direction of the distal tip.

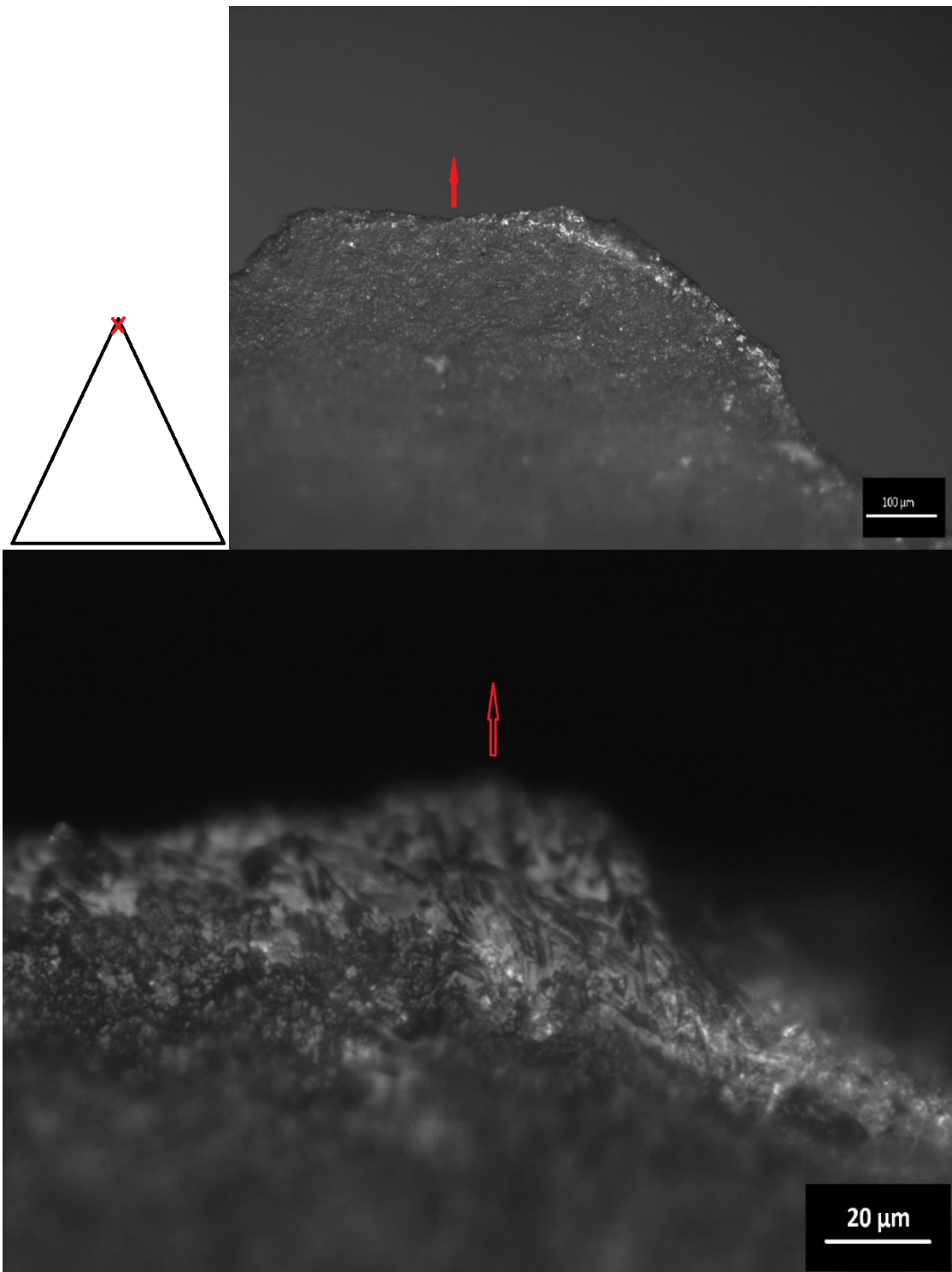


Figure 6.38. Polish located on the distal tip (Locus D1v). The polish shows a poor development and a dull to medium-bright aspect. Few striations were observed. Picture:

OLMil, OM 100x (above), 500x (below), (experiment code: TH-76). The red arrow indicates the location or direction of the distal tip.

6.3.4 Microscopic use-wear traces observed on experimental Levallois points used in thrusting hand-delivered stone-tipped spear experiments

Among the n=24 experimental Levallois points used as hand-delivered thrusting spears, only n=5 points in total developed microscopic use-wear traces, such as MLITs, polish and striations (Table 6-6). No edge-rounding was observed in the thrusting experimental Levallois points (Table 6-6). Microscopic use-wear traces (e.g. adhesive residues and polishes) related to the hafting process were also identified, and these are described in CHAPTER 7.

Three thrusting experimental Levallois points showed a non-specific and not very well-developed polish, while two other thrusting points displayed polish traces (and one tool showed sporadic striations) resultant of contact between the projectile tools and bone materials during the impact (Table 6-6). Only two thrusting points showed MLITs with striations (Table 6-6). None of the remaining thrusting experimental Levallois points showed microscopic use-wear traces (Table 6-6).

MLITs were observed only on two thrusting experimental Levallois points (8.3%, Table 6-6). The first thrusting point showed a single MLIT located on the ventral distal tip (Locus D2v) of the tool (Figure 6.43). The MLIT initiated from a snap fracture. It was already visible at 50x, but, at 100x, it displayed a linear strip of bright polish which incorporated small striations within it (Figure 6.43). The second thrusting point showed a single MLIT, but this was located on the inner surface of the ventral face (M1v) on a high topographic spot of the stone tool's surface (Figure 6.44). At 100x, the microscopic linear impact trace showed a linear band of bright but rough polish, incorporating long striations within it (Figure 6.44).

Striations, when observed, were included in the polish, and they always ran parallel to the direction of the impact.

A not very well-developed polish was observed in two thrusting experimental Levallois points. It appeared as a poorly developed, marginal, and very scattered

rough polish (Figure 6.40). occurring only on the extremity of the distal ventral tip, next to the very edge (Figure 6.40).

Only one thrusting experimental Levallois point had a well-developed and well-defined polish (Figure 6.39). At 200x, the polish was smooth and highly reflective (Figure 6.39). There was a “broken” area in the polish (Van Gijn, 1989, p. 32) and a certain bevelled quality (Plisson, 1985). No striations within the polish were observed. The lack of striations within the polish (which were instead diagnostic of the impact polish observed in throwing points), and the presence of “broken” and bevelled polish, led to the interpretation of this polish as a possible bone-like polish (Figure 6.39). Interestingly, during the thrusting experiments, the experimental Levallois spear-point impacted and perforated the thigh of the animal target, scratching the femur bone (see also Appendix A, Volume 2).

Sporadic and isolated spots of polish were observed in two thrusting experimental Levallois points (Figure 6.41, Figure 6.42). They were generally distinguishable from 200x (Figure 6.42), only sporadically at 100x (Figure 6.41). The polished spots were observed on the ventral face of the tools, mainly located on the highest topographical spots of stone tool’s surface (Figure 6.41, Figure 6.42). The polish forming the isolated spots was poorly developed and not well linked, but it showed a bright appearance with a few longitudinal striations within it (Figure 6.41). The striations ran parallel to the direction of the impact.

“Impact polish”, as described in Section 6.3.3.3.1, was absent.

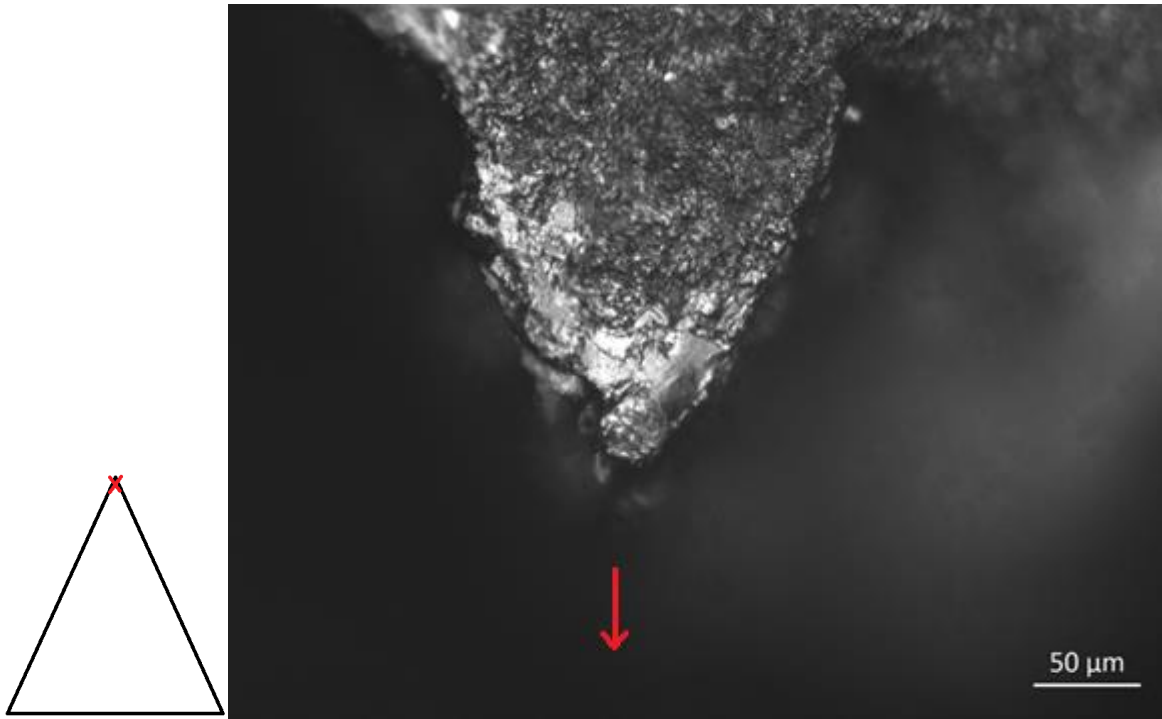


Figure 6.39. Well-developed polish located on the ventral distal tip (Locus D1v) of a thrusting experimental Levallois point. It shows a flat topography and bright aspect, OLMil OM 200x (experiment code: TR-83). The red arrow indicates the location or direction of the distal tip.

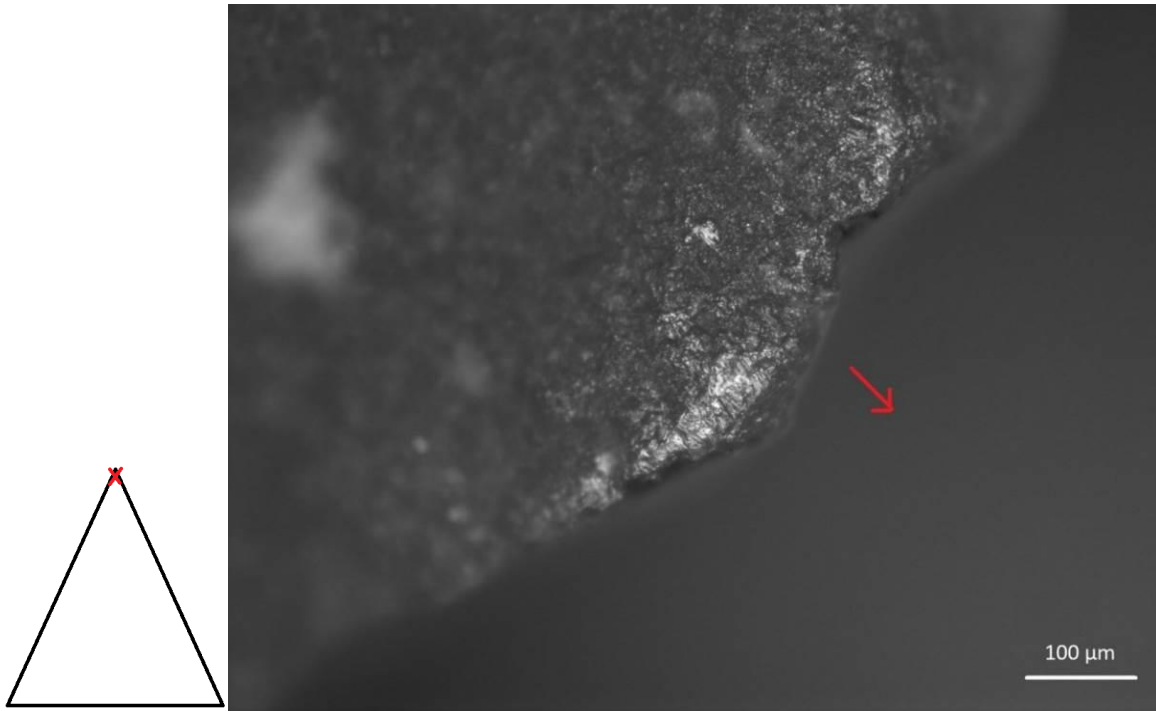


Figure 6.40. Generic and not very well developed polish located on the ventral distal tip (Locus D1v), OLMil OM 100x (experiment code: TR-69). The red arrow indicates the location or direction of the distal tip.

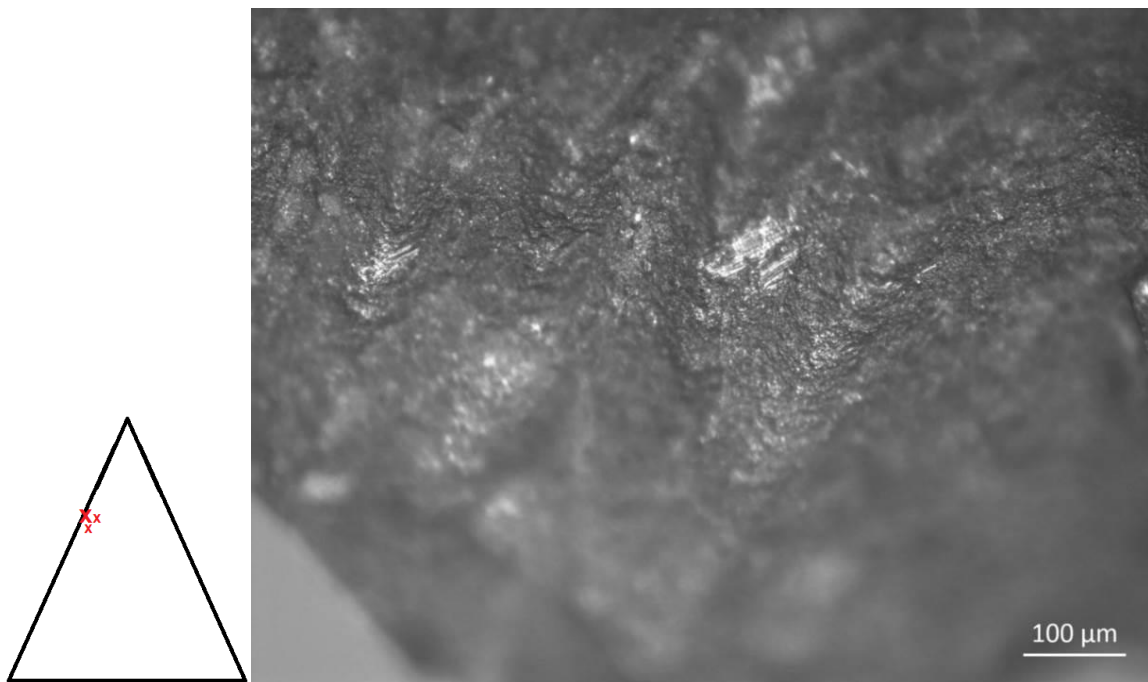


Figure 6.41. Isolated spots of polish located on the ventral mesial part of the tool (Locus M1v), OLMil OM 100x (experiment code: TR-89).

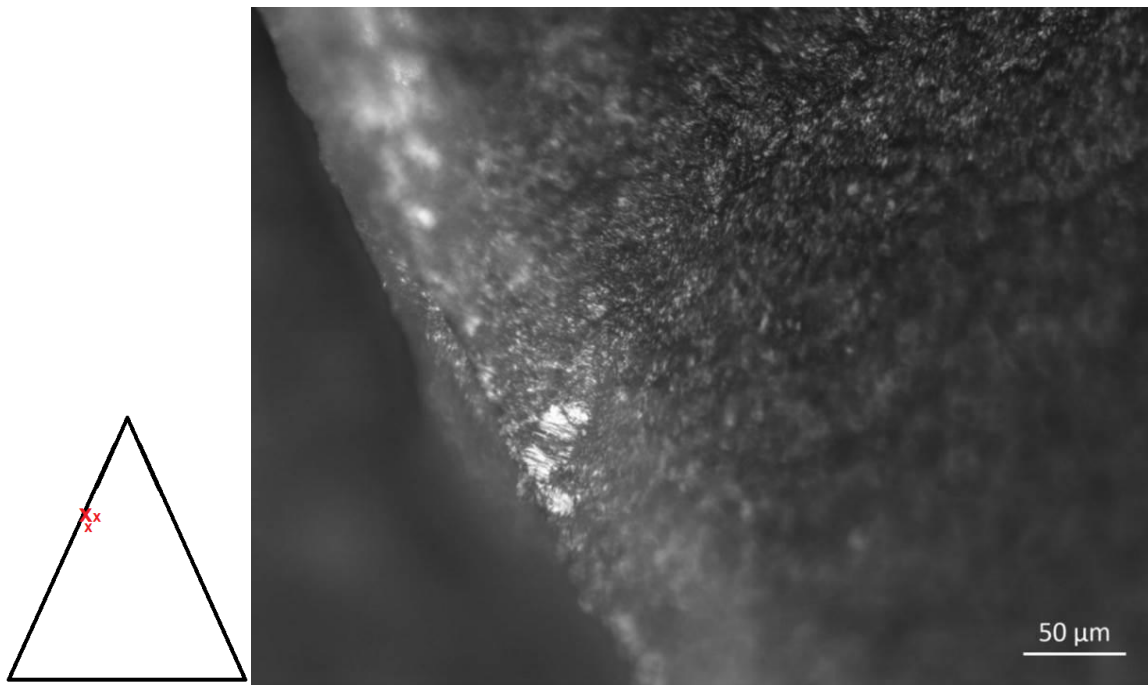


Figure 6.42. Isolated spots of polish located on the ventral mesial part of the tool (Locus M1v), OLMil OM 200x (experiment code: TR-83).

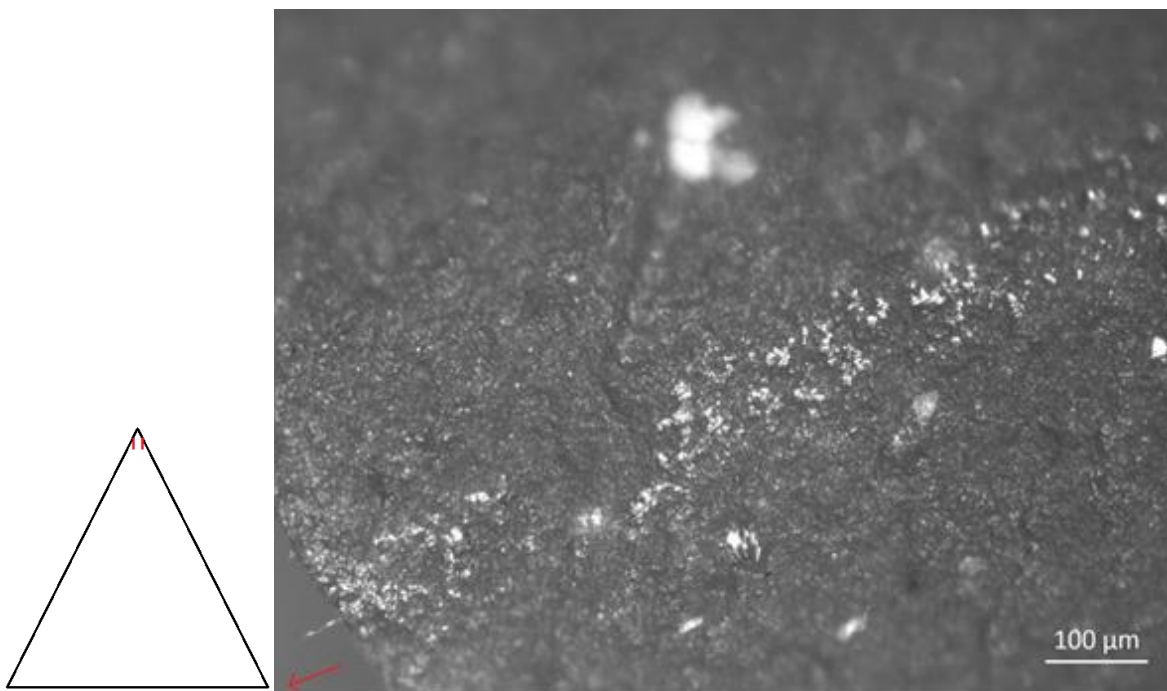


Figure 6.43. MLITs located on the ventral distal tip (Locus D1v). Picture: OLMil, OM 100x, (experiment code: TR-89). The red arrow indicates the location or direction of the distal tip.

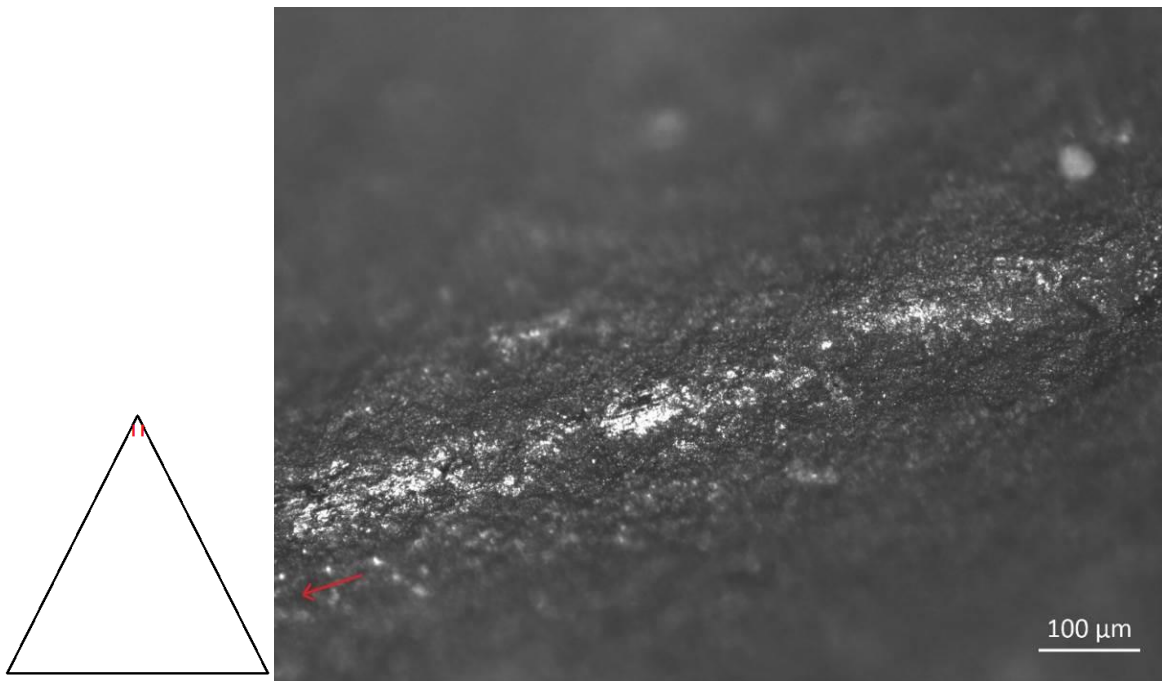


Figure 6.44. MLITs located on the ventral distal tip (Locus D2v inner surface). Picture: OLMil, OM 100x, (experiment code: TR-90). The red arrow indicates the location or direction of the distal tip.

6.3.5 Microscopic use-wear location in throwing and thrusting hand-delivered stone-tipped spear experiments: correlation between delivery systems (i.e. throwing vs thrusting) and use-wear location

To further explore the difference in microscopic use-wear trace patterns between throwing and thrusting hand-delivered spear projectiles, further analysis sought to verify whether or not the location of microscopic use-wear traces (such as MLITs, striations, and polish traces) differed between throwing and thrusting experimental Levallois points.

The location of microscopic use-wear traces on the tool was examined. Traces were plotted against the location they were observed on the tool, i.e. the locus/loci (see Section 2.3) in which the trace was recorded (i.e. distal, mesial, and proximal loci, Table 6-7). If a trace was recorded in multiple loci, all loci were counted. Table 6-7 shows that both throwing and thrusting experimental Levallois points showed similar percentages of distal, mesial, and proximal traces. It appeared that the

location of traces did not differ between the two delivery systems. As a matter of fact, the relationship between the location of microscopic use-wear traces and the delivery systems did not seem to be statistically significant ($\chi^2= 0.648$, $df=2$, p -value= 0.723, Table 6-7). Both throwing and thrusting experimental Levallois points showed a tendency to accumulate microscopic use-wear traces more often on the distal part than on the mesial and proximal parts (Table 6-7), as expected for projectile tools.

Table 6-7. Localisation of microscopic use-wear traces (i.e. MLITs, polish, and striation traces) on the experimental Levallois points (LP), according to the delivery system (i.e. throwing and thrusting). Note: distal loci include traces recorded in D1v, D2v, D3v, D1d, D2d, D3d loci; mesial loci include traces recorded in M1v, M2v, M1d, M2d loci; proximal loci include traces recorded in P1v, P2v, P1d, P2v loci (see Section 2.3).

This thesis 's experiments	Traces in distal loci		Traces in mesial loci		Traces in proximal loci		Total loci with traces
	Count	Percentage	Count	Percentage	Count	Percentage	
Throwing LP	142	86 %	18	10.9%	5	3%	165
Thrusting LP	38	86.3%	5	11.36	1	2.2%	44
Chi ² results	$\chi^2= 0.648$, $df=5$, p -value= 0.723						

6.3.6 Outcomes: can microscopic use-wear types and frequencies be used to distinguish between throwing and thrusting hand-delivered stone-tipped spear projectiles?

In the following results, the frequencies of polish, MLITs, and striation traces are counted considering the number of tools in which they were observed and recorded (Table 6-6).

The microscopic use-wear analysis indicated clear differences between throwing and thrusting experimental Levallois points used in hand-delivered stone-tipped spear experiments. There was an overall tendency for throwing hand-delivered spear projectiles to develop more microscopic use-wear traces than thrusting hand-delivered spear projectiles did. High-power microscopic examination allowed for the distinguishing of the diagnostic microscopic use-wear types that appeared in throwing experimental Levallois points but did not appear in thrusting experimental Levallois points. The most diagnostic microscopic trace types to characterise throwing experimental Levallois points were the “impact polish” and the MLITs, which were both recorded in high-frequencies (i.e. 78.5% of the throwing points, Table 6-6).

The first significant results found that MLITs occurred almost exclusively in throwing experimental Levallois points. MLITs in throwing points appeared on 71% of the throwing experimental Levallois points (n=20 tools), whereas only 8.3% of the thrusting experimental Levallois points (n=2 tools) showed the presence of MLITs (Table 6-6). Moreover, the difference in MLIT frequencies between throwing and thrusting spear experimental projectiles was proven to be a statistically significant pattern ($\chi^2= 169.280$, $df=1$, $p\text{-value}= 0.000$, Table 6-6; Figure 6.20) between the two delivery systems. Furthermore, the MLITs recorded in throwing experimental Levallois points showed typical directional features and a clearly visible polish (under the OLMil) occurring often as double or multiple MLITs. The MLITs in thrusting experimental Levallois points showed a thinner and less bright polish and had less distinctive directional features, occurring as a single MLIT. Therefore, MLITs were here considered to be a diagnostic use-wear trace type with which to distinguish between throwing and

thrusting hand-delivered spear projectiles (see also CHAPTER 11 for discussions).

The second set of results found that there was an overall tendency for throwing spear projectiles to develop more polish traces than thrusting spear projectiles (64.2% to 20.8%, Table 6-6). Polish occurred significantly more often on throwing points than on thrusting points (Table 6-6 and Figure 6.20). Moreover, throwing experimental Levallois points showed a diagnostic type of polish, here defined as "Impact polish". This polish appeared on 57.1% (n=16, Table 6-6) of the experimental Levallois points used in throwing motions, but it was never observed on thrusting experimental Levallois points, and this was a statistically significant difference between throwing and thrusting experimental Levallois points ($\chi^2= 25.920$, $df=1$, $p\text{-value}= 0.000$), (see also CHAPTER 11 for discussions).

Another significant contribution was the observation that striations occurred significantly more often in throwing than in thrusting experimental Levallois points ($\chi^2=81.920$, $df=1$, $p\text{-value}= 0.000$). Many of these striations were incorporated into the MLITs or within the impact polish traces. However, even if striations occurred in higher frequencies on throwing experimental Levallois points (e.g. 46.4% to 12.5%, Table 6-6), this trace alone could not be considered diagnostic of a precise delivery system if not in association with other evidence, such as impact polish, MLITs, or DIFs (see also CHAPTER 11 for discussions).

It is thus suggested that MLITs and polish traces (e.g. impact polish) are diagnostic use-wear traces of throwing hand-delivered spear projectiles. The presence of MLITs and impact polish can, therefore, distinguish throwing experimental Levallois points used in hand-delivered stone-tipped experiments from thrusting experimental Levallois points used in hand-delivered stone-tipped experiments. Although further examination is needed to confirm the nature and the formation process of these microscopic impact traces (see also CHAPTER 11 for discussions).

The observation of statistically significant higher frequencies of MLITs, polish, and striation traces in the experimental Levallois points used in throwing hand-delivered spear experiments has led to the hypothesis that higher impact velocities may result in more microscopic use-wear traces. The results suggest that microscopic use-wear traces (e.g. impact polish, MLITs, and striations) increased when the velocity of the hand-delivered spears increased, i.e. in the experimental Levallois points that were hand-thrown rather than hand-thrust (Figure 6.20). The higher frequencies of microscopic use-wear traces recorded in throwing hand-delivered spear projectiles may signify that at an increase in the velocity of the weapons (e.g. in throwing hand-delivered spears, see Table 5-10) corresponds with an increase in the formation of diagnostic use-wear impact traces, microscopically (with an increase of impact polish, striations, and MLITs traces), but and also macroscopically (with an increase in spin-off fractures, as described in Section 6.2.2, see also CHAPTER 11 for discussions).

The formation process of impact polish(es) and MLTs in throwing points and its absence in thrusting points would warrant further experiments with specific sets of variables. Future experimental studies could, perhaps, focus on the identification of diagnostic polish traces on throwing spear delivery systems and verify the correlation between a single impact material (e.g. bone materials) and the formation of specific polish traces and microscopic linear traces. Similarly, future experimental use-wear analysis on projectile stone tools should correlate with high-power optical analysis with SEM microscopic analysis to further investigate the formation process of polish and microscopic linear traces (see also CHAPTER 11 for discussions).

Considering the outcomes of this high-power microscopic use-wear examination, it is strongly suggested that use-wear analysts attempting to study experimental and archaeological stone projectiles in the future integrate the fracture analysis method (Lombard, 2005) with high-power microscopic use-wear examination, as presented in this study (see also CHAPTER 11 for discussions).

6.4 Use-wear traces experimental Levallois points used as butchering knives (see also Appendix A, Volume 2)

The n=8 experimental Levallois points used as butchering knives (see Section 4.5) were analysed both macroscopically (up to 100x magnifications) and microscopically (with the Olympus BX6, range from 50x to 500x magnifications; see also Section 2.5) after cleaning. The eight experimental tools were used for the performance of eight butchering experiments for different animals (see Section 4.5), for a total of more than 10 hours of work (see Appendix A, Volume 2).

Among the eight experimental Levallois points, only one specimen (used for the butchering of an entire salmon) showed one distal fracture (Table 6-8). This was a bending fracture initiation on the ventral distal tip and terminating with a step-feather termination (Figure 6.45).

Edge-damage was observed in six specimens (Table 6-8). These specimens were the one used for a longer period of time and that came in contact with hard tissues (i.e. bones) during the butchering experiments. Edge-damage appeared in form of cone or bending scars, mostly located on the mesial edges. The scars often presented discontinuous distribution and various morphologies and sizes (Figure 6.46). The two tools that did not present edge-damage were employed for the butchering of a roe deer and a salmon (see also Appendix A, Volume 2).

Polish traces and edge-rounding developed in all specimens (Table 6-8). Depends on the type of butchered animal the polish traces presented different attributes (see also Appendix A, Volume 2).

The specimens that were used for the butchering of roe deer and salmon animals showed polish traces that presented a greasy and faint appearance (Figure 6.47). This polish generally lacked topographic or directional features, such as striations (Figure 6.47). In some cases, spots of bone-like polish traces were observed on the tools due to the sporadic contact with hard tissues (i.e. bone materials) during the butchering. These spots of polish showed a localised domed or flat polish, normally very bright, which included some striations

(Figure 6.48). One specimen used for the butchering of a roe deer carcass it showed fresh-hide-like-polish traces (Van Gijn, 1989, p. 28). The polish was spread in a large band longitudinally distributed along the edge, indicating a longitudinal cutting motion (Figure 6.49). At 100x, the polish, already well-developed, presented a rough and greasy appearance with a less bright aspect (Figure 6.49). It also showed the characteristic “craters” or large micro-pits diagnostic of hide polish traces (Van Gijn 1989, p. 41).

Interestingly, the two other experimental Levallois points used for the butchering of an entire wild boar carcass showed traces of polish similar to the fresh-hide polish described above. The polish located along the mesial edges was well developed (Figure 6.50). It presented a very rough texture and a greasy aspect, incorporating large micro-pits or “craters” characteristic of hide-polish traces (Keeley, 1980, p. 49; Van Gijn 1989, p. 41) (Figure 6.50).

One specimen used for the butchering an entire salmon animal showed some long but very thin streak of polish, that may remind the MLITs formed on the throwing spear projectiles during impact against the ground (Figure 6.51). These traces, however, most likely formed during the de-scaling process of the fish, when the fish scales rubbed against the surface of the tool resulting in long but thin linear polish traces (Figure 6.51). However, they were always in association with a meat-like polish and edge-rounding traces, which were not observed on the experimental projectile points.

In conclusion, all the experimental Levallois points used as butchering knives showed polish traces that were indicative of longitudinal butchering/cutting movements against meat and fresh-hide contact materials, i.e. soft materials. Polish traces (such as meat-like polish and fresh-hide-like polish) according to their attributes, location and patterns were very different than the “impact polish” and MLITs observed on the experimental Levallois points used as hand-delivered throwing spear projectiles. Moreover, the frequencies of fractures observed on the Levallois points used as butchering knives were very low when compared with the experimental Levallois points used in projectile motions (12.5%, see Table 6-8; against 39% or 50%, see Table 6-2). Therefore, it is

possible to conclude that macroscopic and microscopic use-wear traces in butchering experimental Levallois points are different than the macroscopic and microscopic use-wear traces observed on the experimental Levallois points used in hand-delivered spear experiments.

Table 6-8. Trace types and frequencies observed on the experimental Levallois points, used as butchering knives. Note: the number and frequencies refer to the number of tools with traces (more than one fracture can occur on a tool).

Type of trace	Butchering knives with traces (n=6)	% Butchering knives with traces
<u>Bending fractures</u>	1	12.5%
Step-terminating	1	
<u>Edge-damage</u>	6	75%
Polish	8	100%
Specific polish	5	62.5%
Not-specific polish	3	37.5%
Striations like MILTs	1	12.5%
Edge-rounding	8	100%

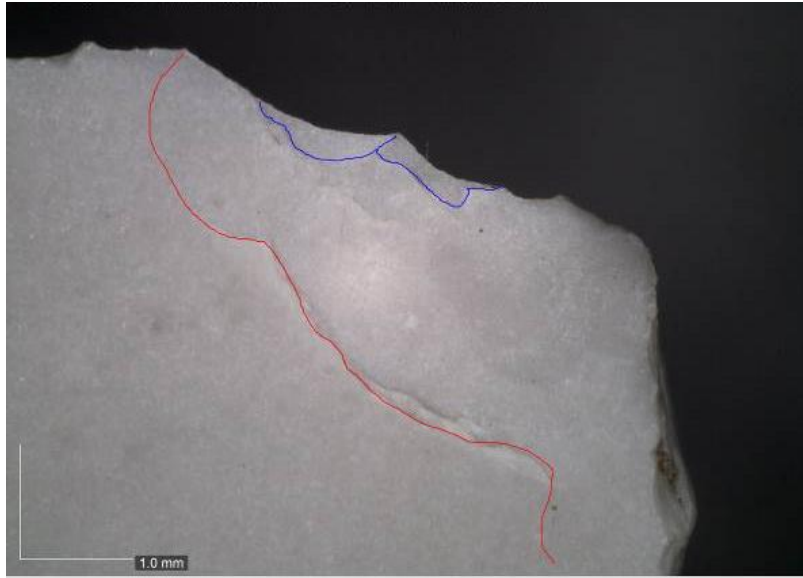
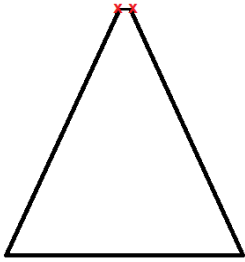


Figure 6.45. Bending fracture with a step-feather termination (in red) plus two cone scars (in blue; experiment code BK-99), DM OM 56x.

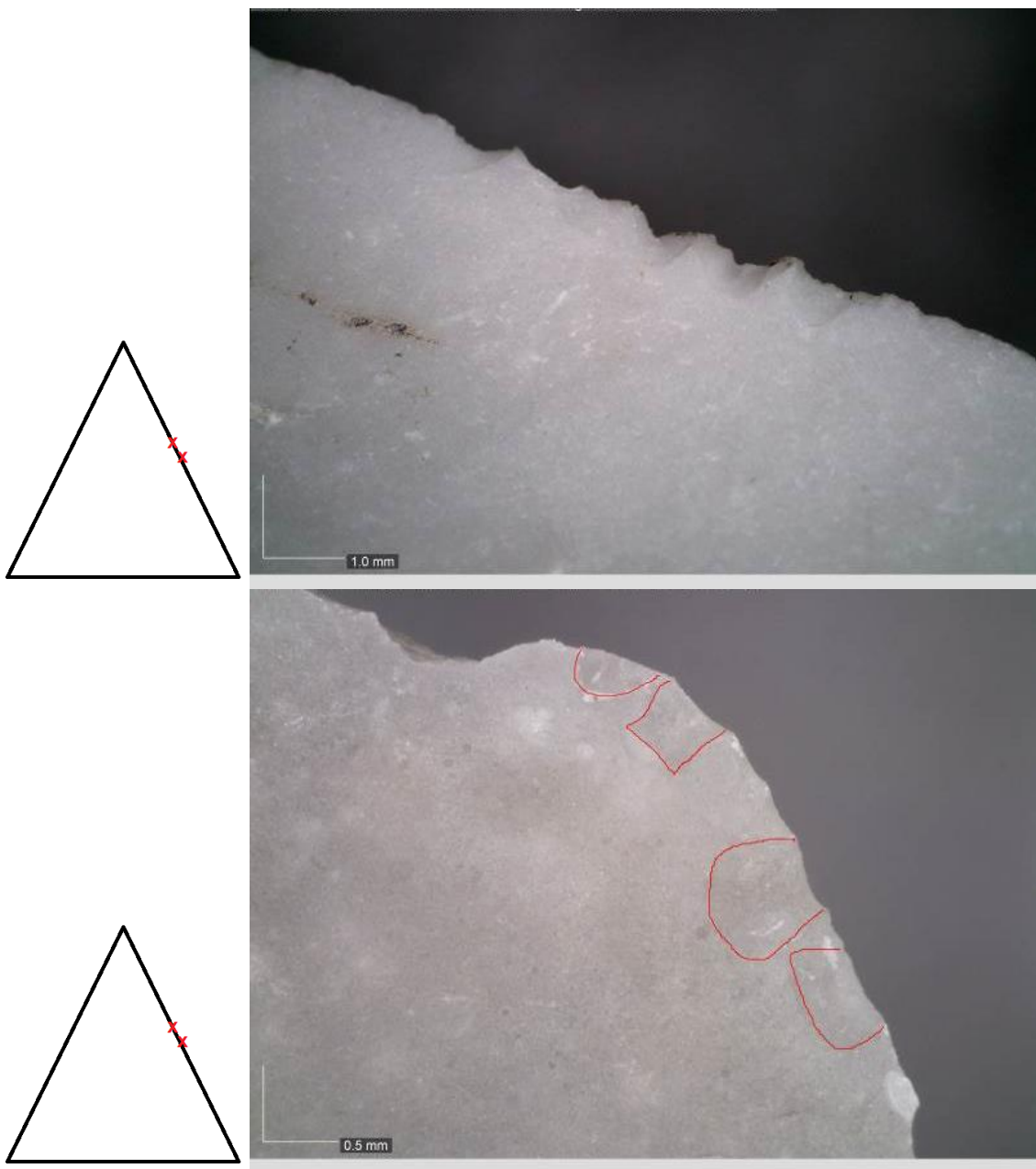


Figure 6.46. Example of edge-damage observed on the experimental Levallois points used as butchering knives. Top picture: medium half-moon scars (DM OM 40x, experiment code BK-96); Bottom picture: large scalar and rectangular scars (DM OM 40x, experiment code BK-99).

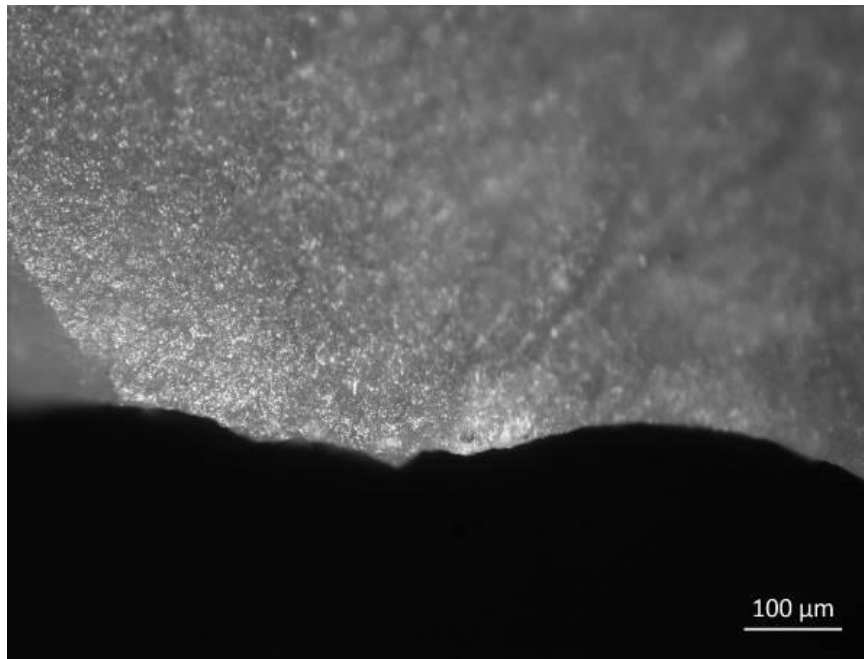
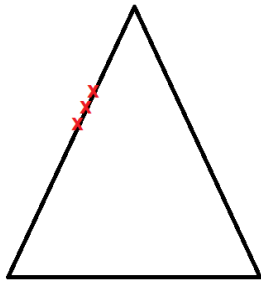
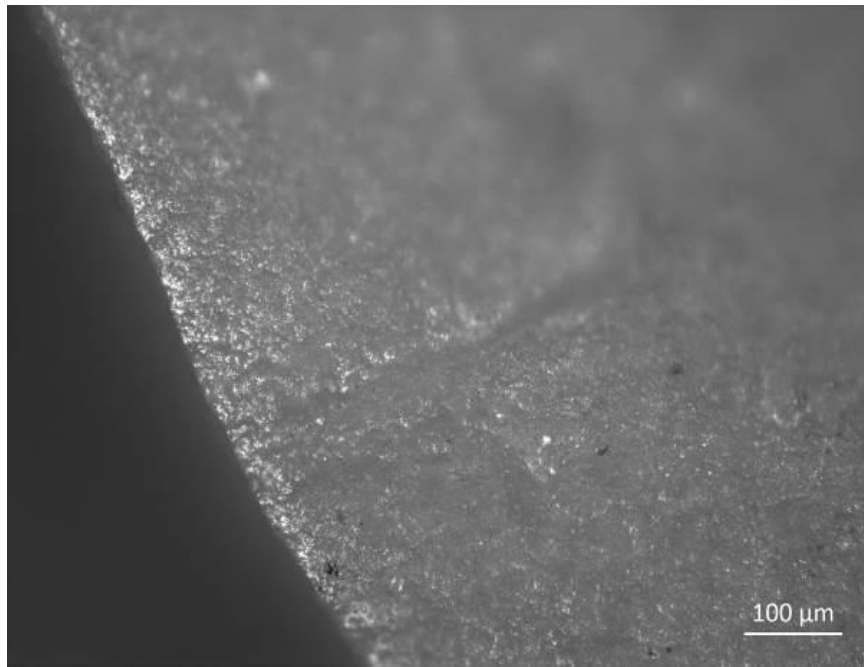
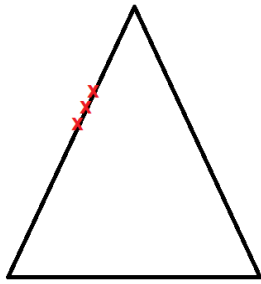


Figure 6.47. Greasy and faint polish observed on the experimental Levallois points used as butchering knives. Top picture: experiment code BK-102, OLMi/OM 100x; Bottom picture experiment code BK-87, OLMi/OM 100x.

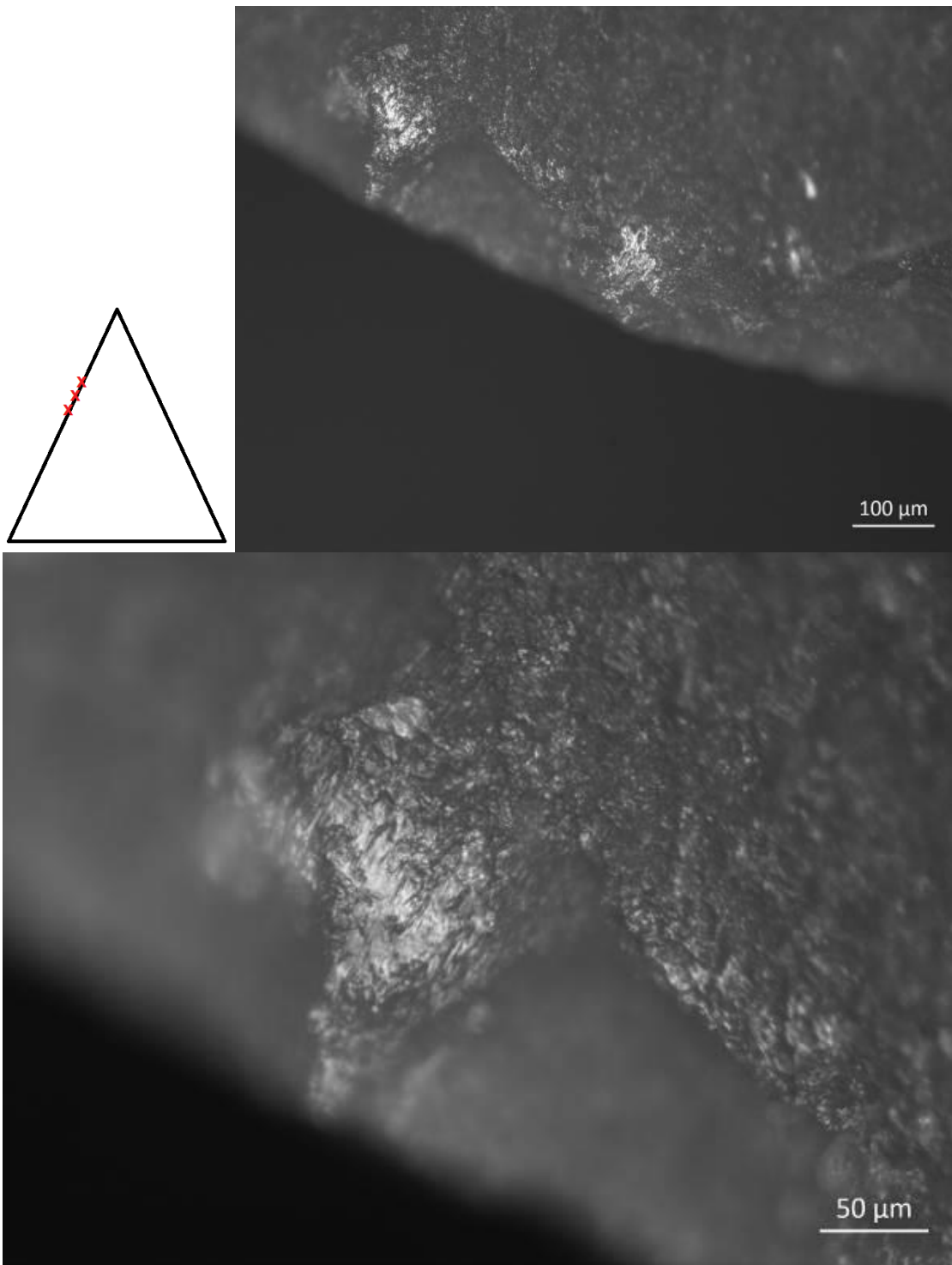


Figure 6.48. Spots of polish due to bone contact. The polish shows flat topography with striations. Picture: OLMil/OM 100x (above) and 200x (below; experiment code BK-59).

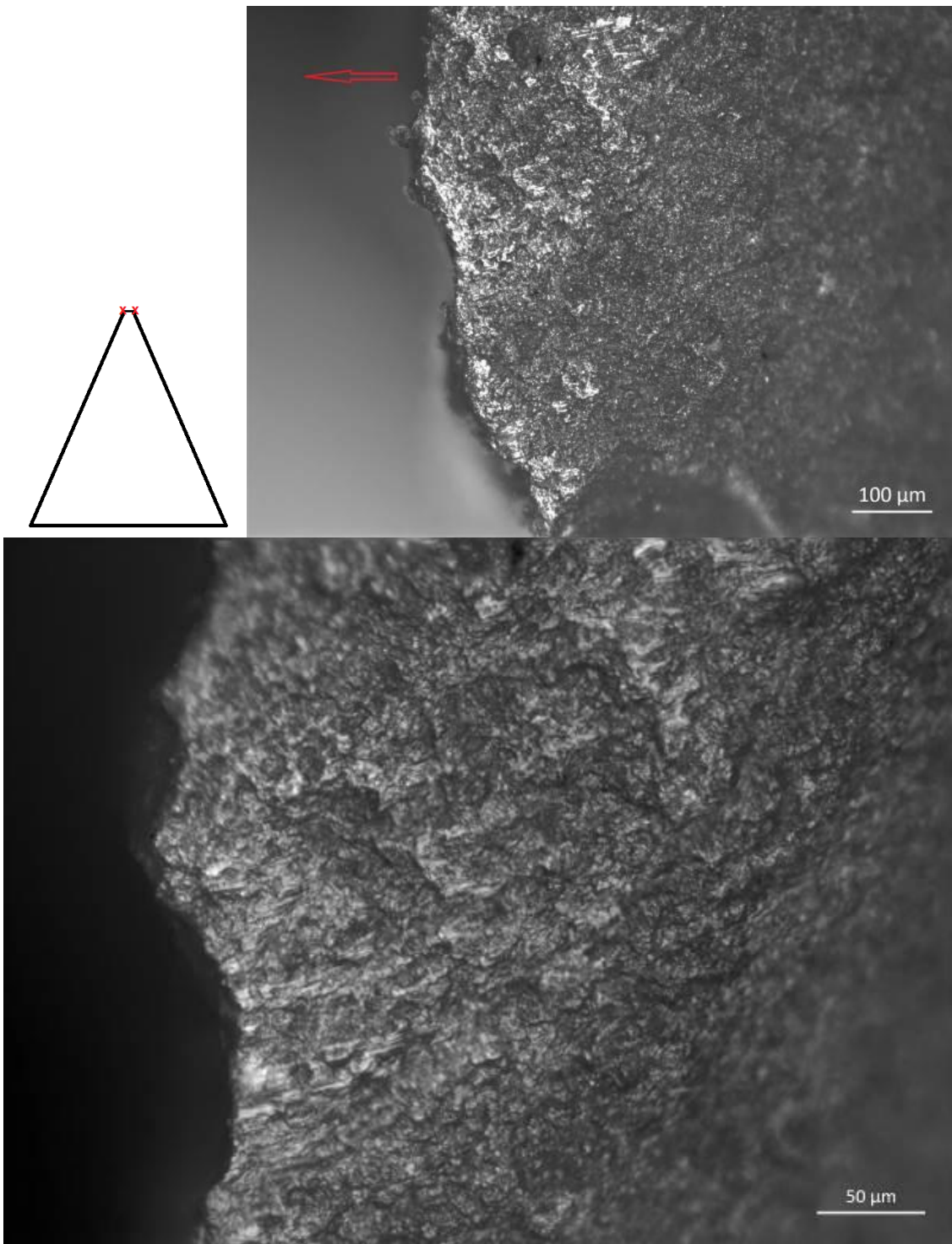


Figure 6.49. Fresh hide-like polish. The polish shows a large band of polish disturbed longitudinally along the edge, At 100x, the polish, already well-developed, presented a rough and greasy appearance (top picture). At 200x, the polish shows characteristic “craters” or large micro-pits traces Picture: OLMil/OM 100x (above) and 200x (below; experiment code BK-97).

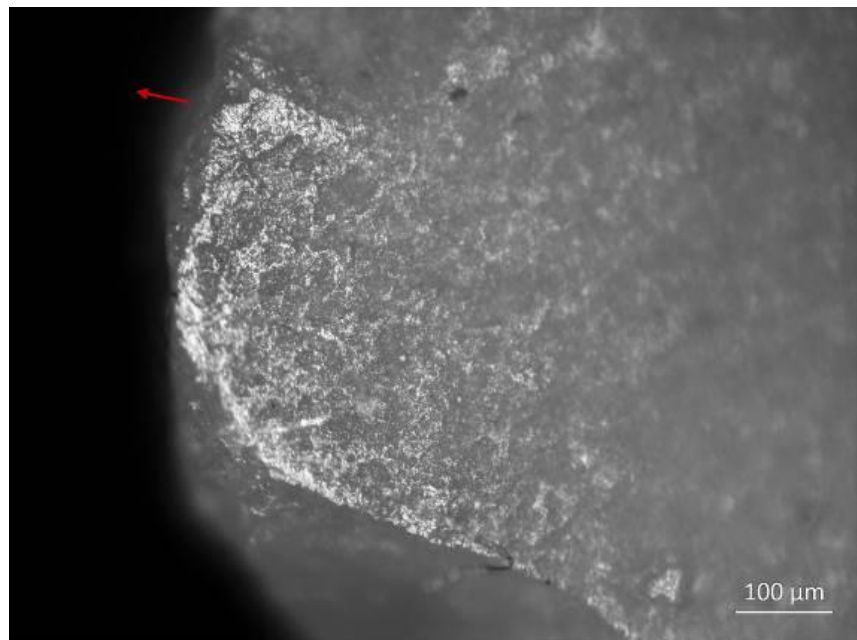
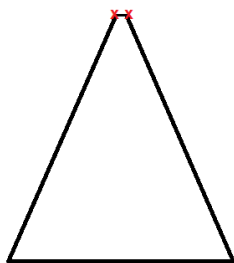
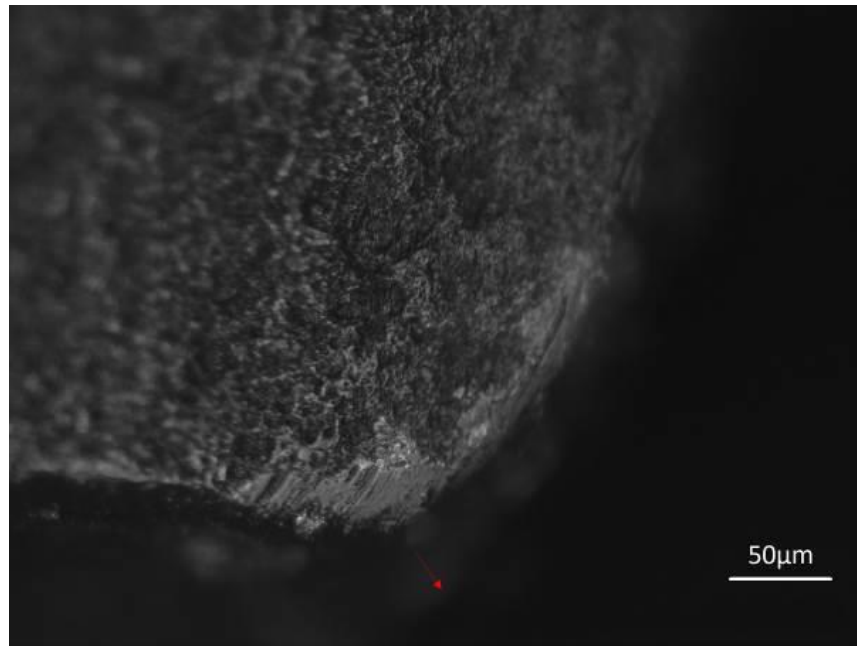
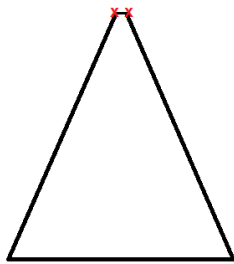


Figure 6.50. Greasy and rough polish due to contact with fresh-hide of the wild boar. Top picture: experiment code BK-101, OLMil/OM 100x; Bottom picture: experiment code BK-100, OLMil/OM 200x.

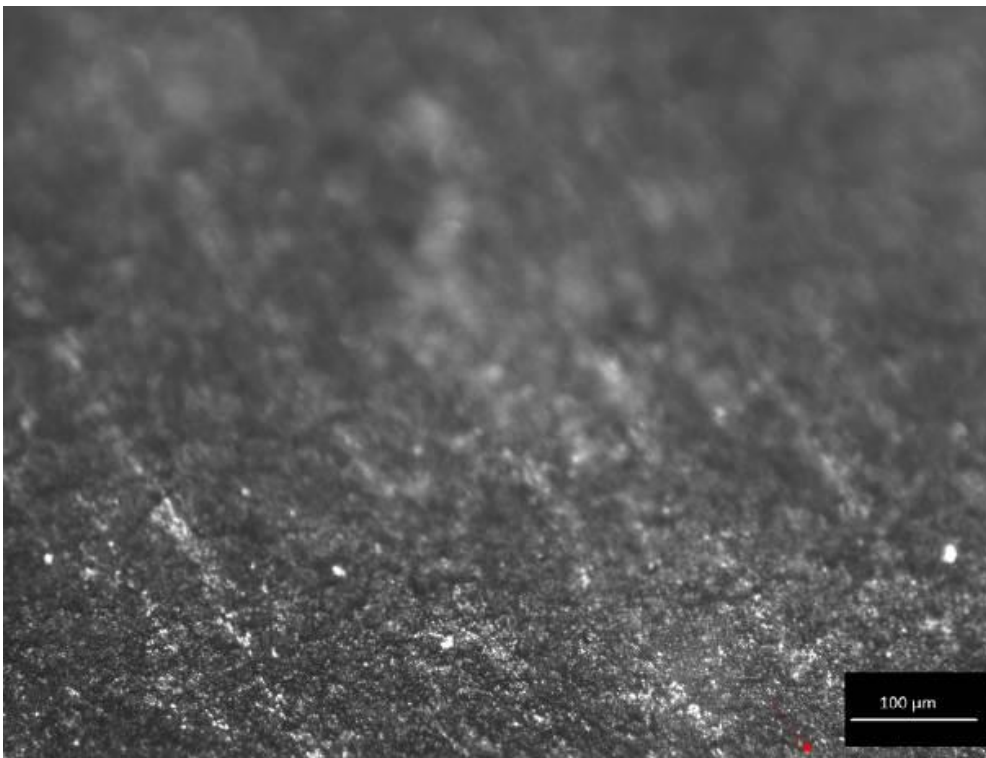
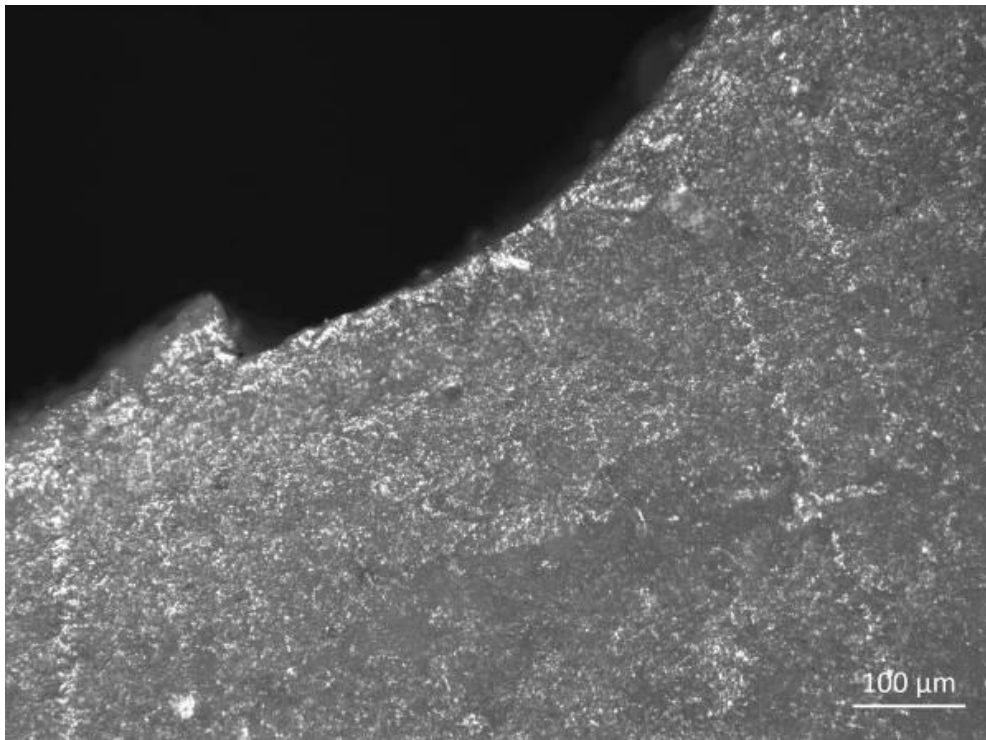


Figure 6.51. Comparison between the streaks of polish observed on the butchering fish knife (top picture, experiment code BK-102, OLMil/OM 100x) and the MLITs formed in a throwing experimental point due to impact against the ground (bottom picture, experiment code TH-71, OLMil/OM 100x).

CHAPTER 7

HAFTING TRACES OF EXPERIMENTAL LEVALLOIS POINTS USED IN THROWING AND THRUSTING HAND-DELIVERED STONE-TIPPED SPEAR EXPERIMENTS

7.1 Introduction and aims

Hafting is a necessary process in the manufacture of projectiles. Stone projectiles cannot be employed as armatures if they are not fixed onto a shaft (Rots, 2016, p. 167). Stone projectiles thus have the potential to demonstrate evidence of both hafting and utilisation processes.

It has been suggested that correct identification of projectile tools should be based on the identification of diagnostic impact traces as well as evidence of hafting traces (Rots, 2009, 2013, 2016; Rots and Van Peer, 2006; Rots and Plisson, 2014). As the experimental Levallois points used in this thesis as hand-delivered throwing and thrusting spear points were all hafted before their utilisation, and de-hafted after the experiments, the primary goal of this chapter was to evaluate the extent to which hand-delivered experimental spear projectiles developed hafting evidence.

The initial aim of this chapter was to determine whether or not experimental Levallois points used as hand-delivered spear projectiles developed hafting traces, and whether these traces could be diagnostic of hafting. This was assessed through a macroscopic and microscopic examination of use-wear traces on a controlled and representative experimental sample. A complementary aim also tested the extent to which hafting traces identified on the experimental Levallois points could be linked to different hafting arrangements, such as those employed during the first sets of experiments (i.e. female, juxtaposed, and flat hafting slot types, see CHAPTER 4). As two types of adhesives were used during the first sets of experiments (i.e. commercial resin and tar, see CHAPTER 4) a further interrogation was undertaken to estimate the extent to which hafting traces showed specific patterns that would assist in the identification of the fixing agents (i.e. adhesives). Lastly, the experiment also assessed the different hafting traces generated by throwing and thrusting hand-delivered spear motions.

7.2 Experimental sample

A total of $n=20$ experimental Levallois points (33.33% of the total experimental dataset) used in hand-delivered stone-tipped spear experiments were analysed to identify types and frequencies of hafting traces (Table 7-1). The sample was deliberately selected considering three main criteria:

- 1) The two different delivery systems used in the experiments (i.e. the selection should be equally distributed between throwing and thrusting experimental Levallois points).
- 2) The types of hafting arrangements used in the experiments (i.e. the selection should be representative of all of the hafting arrangements employed in the experimentation, such as female, flat, and juxtaposed fixed, both with commercial resin and tar, see Section 4.3),
- 3) The time required for the analysis.

As expressed in Section 2.3.2, the removal of the abundant deposits of adhesive left behind following the hafting of the experimental Levallois points was an extremely time-consuming procedure (see Section 2.3.2). The complete removal of the hafting adhesives from all of the experimental Levallois points ($n=60$) was simply not achievable within the timeframe of this study.²³ As such, a macroscopic and microscopic wear analysis of hafting traces was undertaken on a designated tool sample ($n=20$ tools), which were additionally cleaned to completely remove the adhesive deposits (as described in Section 3.4.2). The designated tool sample for the wear analysis of hafting traces counted $n=20$ experimental Levallois points, half of which were used in throwing hand-delivered spear experiments ($n=10$ tools) and half in thrusting hand-delivered spear experiments ($n=10$ tools) (Table 7-1). The designated tool sample was also representative of the different hafting arrangements used during the first and second sets of experiments (Table 7-1). All of the experimental Levallois points employed in the first set of experiments (see Section

²³ The deposits of adhesives resulting from the hafting of the experimental Levallois points were localised only to the proximal part of the tools (loci P1 and P2, see Section 2.3). They therefore represented an impediment to the microscopic wear examination of hafting traces only.

4.3) were selected because they were representative of the three different hafting arrangements: n=4 tools were hafted with a flat hafting slot type (among which n=2 tools were fixed with commercial resin and n=2 tools with commercial tar); n=4 tools were hafted with a juxtaposed slot type (among which n=2 tools were fixed with commercial resin and n=2 tools with commercial tar); and n=4 tools were hafted with a female slot type (among which n=2 tools were fixed with commercial resin and n=2 tools with commercial tar) (Table 7-1). Additionally, n=8 experimental Levallois points, which were all hafted with a female slot type and fixed with commercial tar, were selected from the second set of experiments (see Section 4.4), in order to achieve a tool sample that corresponded with previous use-wear analysis of hafting traces (Table 7-1).

The sample size selected for the use-wear analysis of hafting traces (i.e. n=20 tools corresponding to the 33.33% of the total experimental dataset), was in agreement with previous research that focused on hafting traces. Rots' (2010) research on the differences between hafting arrangements relied on a set of 32 tools, assessing the different traces resulting from male, female, and juxtaposed hafted tools (Rots, 2010, p. 139). Plisson (1982, p. 282) performed hafting experiments with less than 30 end-scrapers, while Moss (1983a, p.. 47) executed 40 experiments with projectile tools but analysed only 30 for hafting traces. The sample presented here, therefore, was broadly comparable with previous hafting experiments and use-wear results, especially considering that the analysis of the hafting traces resulting from throwing and thrusting hand-delivered stone-tipped spear experiments was a complementary research question of this study (see Section 1.5).

Table 7-1. Selected sample of experimental Levallois points (and their experimental variables) for the use-wear analysis of hafting traces.

Experimental set	Type of experiment	Hafting variables			Total
			Commercial tar	Commercial resin (plus beeswax)	
First set of experiments	Throwing	Female	1	1	2
		Juxtaposed	1	1	2
		Flat	1	1	2
	Thrusting	Female	1	1	2
		Juxtaposed	1	1	2
		Flat	1	1	2
Second set of experiments	Throwing	Female	4	-	4
	Thrusting	Female	4	-	4
Total			14	6	20

7.3 Hafting traces: definition and background

Hafting traces are defined here as specific use-wear traces related to the process of hafting and de-hafting stone tools. They are the result of friction between the stone tool, the haft, and the possible fixing materials (adhesives and/or bindings) (Odell, 1980, p. 411).

Hafting traces have been discussed since the early work of Semenov (1964) and Keeley (1978, 1982). Semenov argued that the morphology of tools and the pattern of wear could possibly indicate hafting procedures (Semenov, 1964, p. 19). However, for decades afterwards, hafting and prehension traces were not systematically investigated. The lack of investigation was mainly based upon the concern that hafting and prehension traces could be confused with post-depositional traces (Jensen, 1982; Levi-Sala, 1996, p. 12) and that hafting processes left very little evidence that would not typically survive (Keeley, 1982, p. 807).

The first attempt to recognise precise traces produced by hafting activities was attained independently by a small number of researchers (Odell, 1978, 1994; Plisson, 1982, 1987; Beyries, 1987b). Odell (1978) and Beyries (1987b) recognised that striations that run perpendicular to the central axis of the tool, basal fractures, and localised polish areas on the highest topographic spots were associated with hafting processes, while Plisson (1982) and Moss and Newcomer (1982) found that the use of adhesives prevented the formation of evident hafting traces.

Although these works disclosed the potential to identify hafting traces, only a few use-wear studies included hafting identification afterwards (Moss, 1983a; Anderson-Gerfaud, 1981). Moreover, the interpretation of hafting traces was vaguely made upon the recognition of small traces away from the edge limit and/or patterns in the absence of polish (Anderson-Gerfaud, 1981, p. 41), or was frequently established from the observation of morphological attributes, such as tangs, notches, retouched backs, and resharpening (Keeley, 1982; Owen, 1987; Unger-HaMLITon, 1988; Van Gijn, 1989).

During the 1980s and 1990s, hafting traces progressively started to receive more attention in experiments with projectile tools. Hafting traces were reported for blades

and micro-blades used as arrow-heads (Moss and Newcomer, 1982; Fischer et al., 1984; Anderson-Gerfaud, 1983; Bergman et al., 1988; Dockall, 1997), and for spear-points that had possibly been hafted (Shea, 1988; Shea, 1990; Plisson and Beyries, 1998; Böeda et al., 1999). Although this category of traces progressively gained more interest over this period, it still lacked a systematic investigative methodology.

Only recently have hafting traces been systematically scrutinised through extensive experimental programs (Rots, 2002, 2003, 2010; Wadley et al., 2004; Wadley and Lombard, 2007), and linked to the cognitive skills developed during its acquisition (Barhna, 2013; Lombard and Haidle, 2012; Wadley, 2010; Wadley et al., 2009; Wynn, 2009). Rots (2010) acquired new experimental data from a broad set of experimental tools hafted using different hafting arrangements and materials. The research resulted in a standardised description of macroscopic and microscopic traces and patterns that can occur in different hafting processes. This methodology was later verified through blind tests (Rots et al., 2006) and applied to archaeological collections (Lombard, 2004, 2005b, 2006a, 2006b, 2007, 2011; Rots, 2009, 2013; Rots and Van Peer, 2006; Lombard and Phillipson, 2010; Rots et al., 2011, 2015, 2017). Furthermore, residue analysis has provided evidence concerning the hafting materials and techniques used at different Paleolithic sites (Hardy et al., 2001; Lombard, 2005, 2006, 2008; Wadley et al., 2004; Hardy and Moncel, 2011; Hardy et al., 2013; Lemorini et al., 2014; Rots et al., 2015).

The types of specific traces and attributes diagnostic of hafting and prehension activities are presented below.²⁴

7.3.1 Features of prehension traces

The presence of polish resultant of the contact between bare hands and the stone tool was first recognised by Moss and Newcomer (1982, p. 292), and Jensen (1982). However, Rots (2010) provided an interpretation of its formation.

Prehension polish develops, after a long utilisation, from the friction between bare hands, the worked material particles, and the stone tool. When the worked material

²⁴ Illustrations of previous studies could not be included in this study because for copyright issues.

produces extensive “dust” (i.e. particles detached from the worked material during use), the abrasion caused by bare hands on the tool’s surface may form a distinctive polish, defined as prehension polish (Jensen, 1982; Rots, 2003, 2010). It has been proposed that prehension polish displays the same polish attributes as the contact material (Rots, 2015, p. 86), but lacks a precise directionality. It can be found in association with striations resultant of the scratching of particles under bare hands (Rots, 2010, p. 76), and it can also appear similar to a meat-like-polish (Rots, 2010, 2015; Owen and Unrath, 1989).

Prehension polish has mainly been recognised on experimental tools and in blind tests (Rots, 2003, 2010; Rots et al., 2006). However, the identification of prehension polish on archaeological tools is far more difficult (Jensen, 1982), as weak or underdeveloped polish types may be unrecognised (Beyries, 1988, 1990) or post-depositional alterations may affect and consequently remove prehension wear traces (Levi-Sala, 1996, p. 19).

Stone tools can also be used along with hand-protection surrounding the prehensile part (e.g. leather wrap). In experimental tools, such wrapping materials have been identified by precise patterns of polish or abrasion wear (Rots, 2010; Plisson, 1982).

7.3.2 Features of hafting traces

7.3.2.1 Haft limit or boundary

A good indicator of a haft presence is the so-called “haft boundary” (Rots, 2010, figure 2.9; Rots, 2015, p. 84). The haft boundary or limit is the area of the tool where the haft system ends (Figure 7.1a). The boundary or limit is characterised by an abrupt change of wear traces between the hafted surface and the surface of the stone tool which is not covered by the haft. The un-hafted side of the boundary can display different polish traces, such as the commencement of edge-damage, and/or an overlap of cone fractures (Rots, 2005, 2015, 2016).

7.3.2.2 Macroscopic hafting traces

Intensive edge-damage can be frequent in hafted tools. Edge-damage due to hafting occurs on the edges of the tool which are in contact with the haft system.

Edge-damage is intense when the tool is inserted into a groove and/or when the tool is not tightly fitted inside the haft (Odell, 1978; Moss and Newcomer, 1982). This leaves enough space for the tool to move inside the handle during utilisation, and this movement scars the edges of the tool that are inserted into the haft (Figure 1c). The resultant edge-damage is often located on the proximal edges of the tool, and it results in cone fractures that present multiple terminations or an overlapping distribution (Figure 7.1c; Rots, 2003).

If the tool is well fitted into the handle and no movement is allowed inside the hafting slot (Figure 7.1b), the hafted portion of the tool will lack the presence of edge-damage or scars (Odell, 1978, p. 44; Plisson, 1982, 1987; Moss and Newcomer, 1982). If edge-damage is present on such a tool, it will commonly start above the “haft limit” on the part of the tool that is not covered by the hafting casing, and this is caused by the use of the tool in general activities (Figure 7.1b).

When the hafting arrangement does not cover the edges of a stone tool, edge-damage (from usage activities) can be observed along the tool edges (Figure 7.1d). This can be the case for a projectile hafted with a flat hafting slot (see Figure 4.19) where the hafting arrangement does not protect the edges of the tool (Figure 7.1d). It can also be sporadically observed on female hafting slots if the edges of the tool are not completely inserted into the haft.

In conclusion, when a tool is hafted, the presence/absence of edge-damage, its location, and its distribution depend on several variables (e.g. hafting arrangements, the presence of bindings, and hafting materials). The association of these different trace attributes can lead to an interpretation of the possible hafting arrangement. Although, while the distribution and location of edge-damage over the surface of a stone tool can assist in the identification of the hafting arrangement, edge-damage and scars alone cannot be considered diagnostic of hafting processes if they are not associated with other evidence, as edge-damage can be caused by different usage activities.

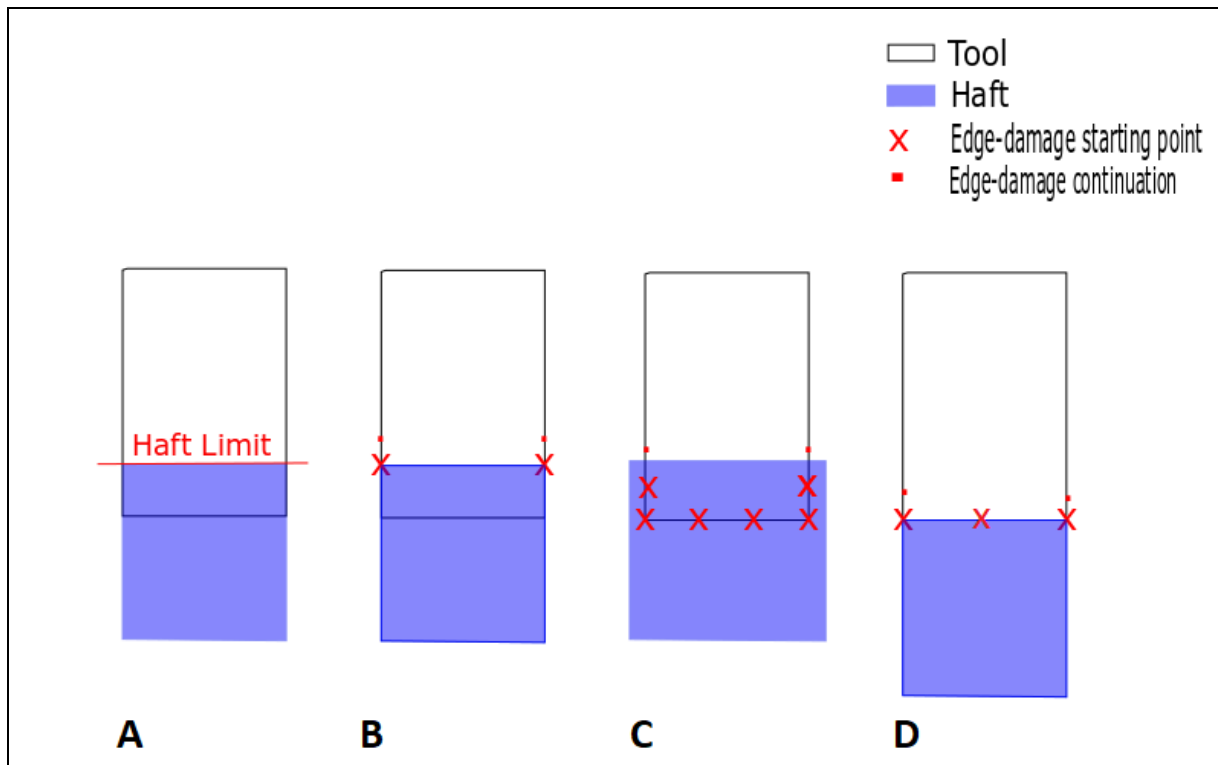


Figure 7.1. Schematic drawing to show possible hafting arrangements and consequent trace distribution. A. Representation of the hafting limit; B. The tool is firmly fixed inside the shaft (e.g. tight hafting), edge-damage starts above the haft limit; C. The tool is loose inside the shaft (e.g. loose hafting), edge-damage starts below the haft limit; D. The tool is not inserted into the shaft, but it lays on top of it (e.g. flat hafting type; or sporadically in female hafting type), the edge-damage starts on the haft limit (Image La Porta).

7.3.2.3 Microscopic hafting traces

It has been proven that the friction between the haft and the stone tool surface leaves microscopic diagnostic traces, such as polish, striations (Odell, 1978; Moss and Newcomer, 1982; Moss, 1983; Rots, 2010), and frictional or bright spots (Rots 2002, 2010). Polish and bright spots have been observed to be the most diagnostic wear trace when recognising hafting systems (Rots, 2010). Conversely, striations and edge-rounding can be supportive evidence of hafting processes, but alone they cannot be diagnostic of hafting.

7.3.2.4 Hafting Polishes

Hafting polishes can be generated in different ways, depending on the contact material, type of movement, and the potential use of fixing agents (Rots, 2010).

These polishes are mainly located on the ridges of the tool or the inner surface (Rots 2015, p. 93). They are only visible in the area covered by the haft, and clearly contrast with unaltered surfaces or other polish types (Rots, 2010).

Hafting polish formation is directly related to the type of movement undertaken with the hafted stone tool (Rots, 2010). If a hafted tool is used in scraping motions, hafting polishes tend to be more frequent in the area around the haft limit (Rots 2015, p. 89). In contrast, percussive motions (e.g. axing, chipping movements) result in a random distribution of hafting traces, whereas perforating motions leave more visible hafting polishes on the dorsal ridges or lateral edges (Rots, 2015, p. 89; Rots, 2010).

Hafting polish can show similar attributes to the polish type of the contact material (e.g. wood-like-polish for wood materials, bone-like-polish for bone materials, and so on). However, if no other evidence of hafting is preserved, this polish type could be easily mistaken for a “use polish” or an “active area” of the tool.

Hafting polishes can also form when the haft abrades the stone surface directly (Rots, 2010). The friction between the haft and the tool forms a distinctive polish that has the same features as the polish of the haft material. The creation of this polish can happen only when there are no other mediums between the haft and the stone tool (Rots, 2003, 2010). When mediums (like adhesives or wrappings) are employed, they represent a barrier between the haft and the stone tool. In this case, the tools will not present traces associated with the haft material. When adhesives are employed, hafting traces can only be deduced by the traces left from the resinous or oily adhesives (Moss and Newcomer, 1982; Rots, 2010), as demonstrated below.

7.3.2.4.1.1 Polish distribution for different hafting arrangements

The location and distribution of hafting polish can give clear indications concerning the hafting arrangements employed.

For instance, a female hafting slot (Figure 4.17) might display different wear patterns on the surface that was in contact with the haft (often the central part of the tool) than on the surface or edges which were not affected by the haft (Rots, 2010; Rots, 2015,

p. 92; Figure 7.1b). Likewise, a juxtaposed hafting slot type (Figure 4.18), would theoretically result in different wear patterns on the ventral and dorsal faces (Rots, 2010), depending on which one was in contact with the haft, whereas a flat hafting slot type (Figure 4.19) would display traces of contact only on the proximal part of the tool (Figure 7.1c). However, these expectations may vary depending on the morphology of the stone tool, on the overall shape of the haft, and whether or not adhesives or other mediums were employed.

7.3.2.4.2 Hafting bright spots

Although bright spots have been linked mainly to post-depositional processes (Vaughan, 1985, p. 185-186; Levi-Sala, 1986, 1996;), they have also been associated with hafting activities (Odell, 1978; Moss, 1983a, p. 101; Rots and Vermeersch, 2000; Rots, 2002, 2003, 2010;).

They have been described as the result of the friction between the haft and the stone tool (Rots, 2002; Rots, 2010, p. 34). Experimentally, Rots (2002) distinguished three different types of bright spots due to the contact between different materials, such as adhesive, antler, and flint-on-flint bright spots. The distribution of bright spots gives an indication of the presence and type of the haft. If they display an organised distribution on the surface, they are more likely to be the result of hafting activities whereas, if they present a random distribution, it could be the result of post-depositional processes (Odell, 1978; Levi-Sala, 1996; Rots, 2002).

7.3.2.5 Binding traces

It has been proposed that the use of animal or vegetal bindings can leave distinctive cone fractures on the lateral edges of a stone tool adjacent to the haft border (Rots, 2010). These scars are defined as sliced scars (Rots, 2010, p. 135) or half-moon scars (Keeley, 1980), and they are mainly associated with vegetal bindings (e.g. cordage). In contrast, animal binding (e.g. sinew) appears to be linked to sporadic edge crushing (Rots, 2010, p. 135). Polish, resultant of the contact between the ligature and the stone tool, can also form, however it is rare, and it depends on the type of ligature used and on its freshness (Plisson, 1982; Moss and Newcomer, 1982; Rots, 2010).

In this thesis' experimental programme, however, no bindings were employed. Thus, for a more detailed description of binding traces, see Rots (2010).

7.3.3 Final remarks on hafting traces

Previous observations have confirmed that hafting traces can be distinguished from use-wear traces (Rots, 2010). Hafting traces have been observed on experimental tools (Rots, 2002, 2003, 2010), in blind tests (Rots et al., 2006), and also on archaeological tools (Rots and Van Peer, 2006, 2011; Rots, 2009, 2013; Lombard and Phillipson, 2010; Wilkins et al., 2012; Pawlik and Thissen, 2011; Rots et al., 2017).

However, for archaeological tools, the identification of hafting traces and the interpretation of the precise hafting arrangements must be undertaken cautiously. Archaeological tools are often affected by patination, weathering, trampling, and chemical modifications that may alter the original stone surface and thus obliterate remaining traces. Moreover, hafting arrangements in the past have been very diverse and highly variable, and no comprehensive or systematic experimental program can hope to completely replicate the full range of hafting techniques that were used, and the related hafting-traces that may be observable in the archaeological record. This is significant because the interpretation of archaeological hafting traces is mainly based on analogy with experimental reference collections. Caution must, therefore, be advised when directly comparing experimental hafting traces with archaeological indications of hafting, as the formation processes, and the appearance of these traces under the microscope can be completely different.

7.4 Results of hafting traces (see also Appendix A, Volume 2)

Hafting traces herein refers to traces caused by the presence of the hafting system as a whole. This thus refers to both the traces caused by the hafting process itself (i.e. insertion of the experimental tool into the fore-shaft and its fixation with adhesives) and also the de-hafting process (i.e. the removal of the experimental tool from the fore-shaft).

The following results document the hafting traces observed on the selected sample of experimental Levallois points (n=20) used in throwing and thrusting hand-delivered spear experiments (see Section 7.2). The most recurrent traces related to hafting systems were (Table 7-2): the presence of a haft boundary, presence of edge-damage located on the proximal part of the experimental tools, and polishes (or polished layers) located on the proximal part of the experimental tools due to contact with adhesives. None of the reported traces associated with hafting were recorded on the high-resolution dental casts (see Section 3.1) of the observed experimental Levallois points, therefore, their formation could only be linked to the utilisation (including hafting) activities.

Table 7-2. Hafting traces recorded on the selected sample of experimental Levallois points, according to the delivery systems and hafting arrangements. Note: trace number refers to the number of tools with the observed trace (more than one trace can occur on a tool). LP stands for experimental Levallois points.

Type of trace	Throwing			Thrusting			Total tools with traces
	Female (n=6 LP)	Juxtaposed (n=2 LP)	Flat (n=2 LP)	Female (n=6 LP)	Juxtaposed (n=2 LP)	Flat (n=2 LP)	
Haft boundary	4	2	2	5	-	-	13 (out of 20)
Proximal edge-damage	4	2	2	4	2	2	16 (out of 20)
Not well-developed polish	1	2		1		1	5 (out of 20)
Adhesive polishes (or polished layers)	6	2	2	5		2	15 (out of 20)
Adhesive residues	4		1	3	1	1	10 (out of 20)
Bright spots				1			1 (out of 20)

7.4.1 Presence of haft boundary

The occurrence of a haft boundary (see Section 7.3.1) was observed on n=13 of the selected sample of experimental Levallois points (Table 7-2). The haft limit was marked by a change of wear traces between the hafted portion of the experimental tool and the remaining part that was free of the haft.

On three experimental Levallois points (out of 20 tools in the selected sample) the haft limit was deduced from the distribution and the location of edge-damage alone. Other nine experimental Levallois points (out of 20 tools in the selected sample), the haft boundary was inferred by the presence and distribution of microscopic use-wear traces, such as the presence of adhesive polishes or polished layers (presented in

Section 7.4.3). The remaining eight experimental Levallois points (out of 20 in the selected sample) displayed no evidence of haft boundaries.

For instance, Tool TH-32, which deeply penetrated the target (45 cm; see Appendix C, Volume 2), displayed edge-damage on both lateral mesial edges (due to projectile impact) only above the haft limit. The proximal part of the tool covered by the resin did not exhibit edge-damage (Figure 7.2). The same observation was valid for experiments TR-36 (Figure 7.3) and TH-39 (Figure 7.4), both of which displayed edge-damage only above the haft limit of one lateral mesial edge, which was the part not protected by the adhesives. The type of scars showed different morphologies (e.g. trapezoidal, half-moon, and scalar; see Section 2.4.2.2), and occasionally they overlapped (Figure 7.4). These three tools were hafted with female slot (n=1, with commercial resin) and flat slot hafting arrangements (n=2, with commercial resin). All displayed a haft boundary located on the mesial parts of the tools (even the two tools hafted with a flat hafting slot). This means that the adhesive that was covering the proximal and mesial part of the tools protected the lateral edges (during projectile impact) both in the female and flat hafting arrangements. Therefore, the observed haft boundaries did not refer to the limit of the wooden shafts, but to the limit of the resin coverages. A fact that can lead to an incorrect interpretation of the hafting type (when the hafting arrangement is unknown, e.g. in archaeological tools).

Haft boundaries were experimentally observed regardless of the type of hafting arrangements and/or the delivery systems (Table 7-2).

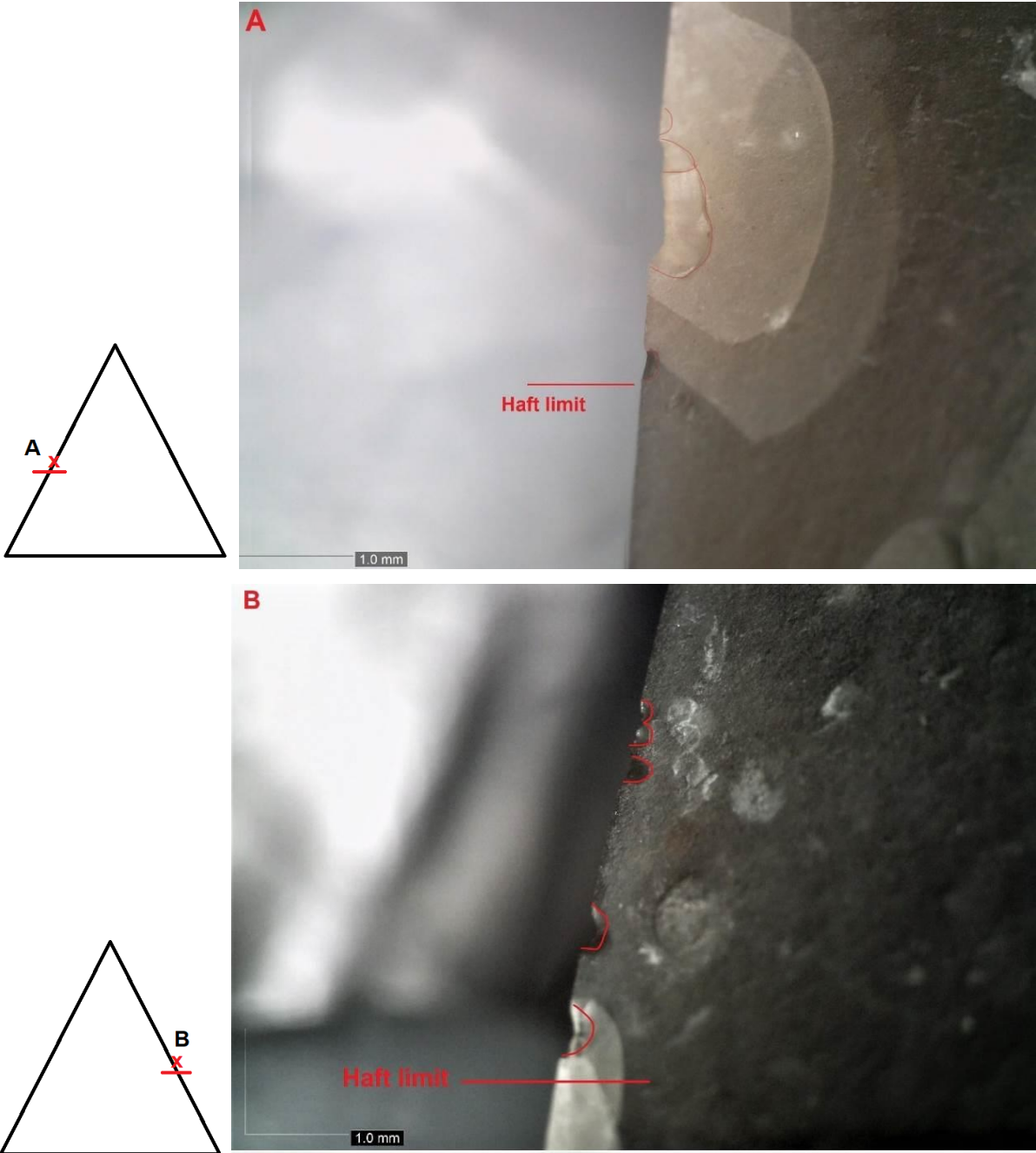


Figure 7.2. Edge-damage due to projectile impact starting above the haft limit (red line). Trapezoidal and triangular scars (in red). A: ventral left side of the tool; B: dorsal left side of the tool. DM OM DM 51x (experiment code: TH-32).

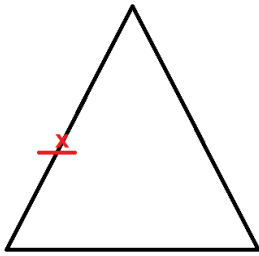


Figure 7.3. Edge-damage due to projectile impact starting above the haft limit (red line). Scalar and half-moon scars (in red). DM OM DM 67x (experiment code: TR-36).

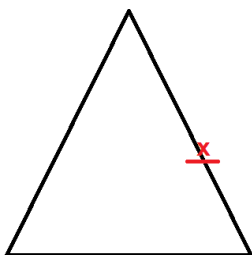


Figure 7.4. Edge-damage due to projectile impact starting above the haft limit (red line). Half-moon scars (in red). OM DM 40x (experiment code: TH-39).

7.4.2 Presence of proximal edge-damage

The analysis of edge-damage was conducted on a macroscopic level only (up to 100x).

Assumption

The difficulty in distinguishing between the edge-damage caused by the presence of the hafting system and the edge-damage caused during projectile impact in the experimental Levallois points was low. This is because the macroscopic and microscopic traces associated with hafting could be located only in association with the limit of the hafting system (which was known since the haft limit and its location was visually recorded for each experimental tool, for instance as in Figure 7.5). The traces located outside the limit of the haft system could, therefore, be caused only by impact activities, as the parts of the tool in which they were recorded were not in contact with the hafting system. As a result, edge-damage caused by the presence of a hafting arrangement was recorded on the proximal edges and proximal parts of the tools only, which were covered by the hafting system. Edge-damage caused by impact activities was instead recorded on the distal part or along the mesial edges of the tools that were not covered by the hafting system (Figure 7.5).

This assumption (and type of analysis) is feasible on experimental projectiles where the haft limit and hafting arrangement is known. In the case of archaeological tools, edge-damage caused by impact/utilisation activities or by hafting is more difficult to distinguish, as the haft limit and hafting arrangement is not always known.

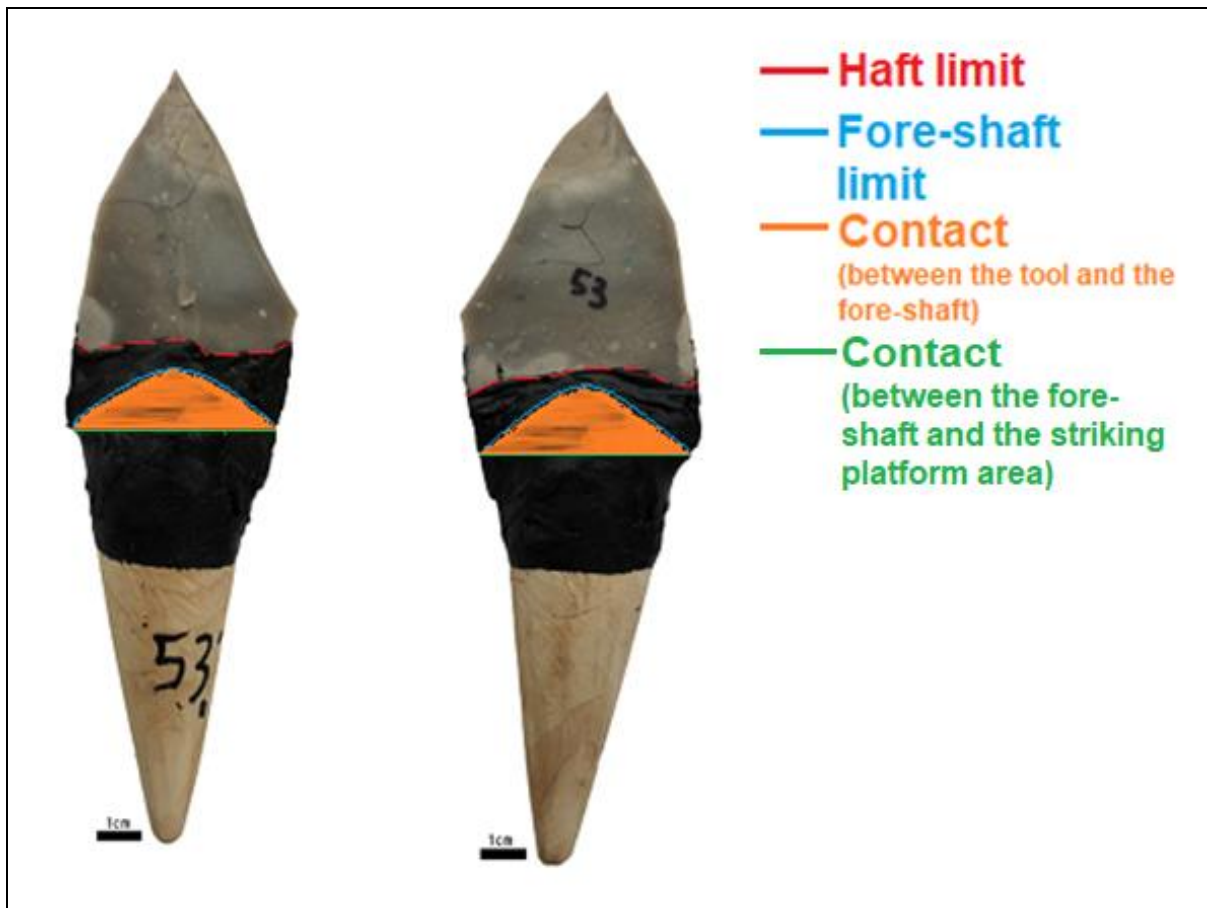


Figure 7.5. An example of hafted Levallois points for hand-delivered stone-tipped spear experiments. The red line represents the line of separation between the area covered by the hafting system and the area not covered by the hafting system (i.e. haft limit). The blue line represents the limit of a fore-shaft slot under the tar adhesive (e.g. in a female slot). The orange area represents the area of contact between the proximal part of tool and the fore-shaft, with the adhesive as a medium, while the green line represents the area of contact between the striking platform of the tool and the fore-shaft, with the adhesive as a medium.

Results

The experimental Levallois points employed as throwing and thrusting hand-delivered stone-tipped spears showed macroscopic traces related to hafting on the proximal parts of the tools only (Loci P1 and P2, see Section 2.3).

Sixteen experimental Levallois points (out of the 20 tools in the selected sample) showed edge-damage related to hafting systems (Table 7-2). The proximal edge-damage was observed on the juncture between the proximal edges of the tools and their striking platform surfaces (Figure 7.7 - Figure 7.14). These were indeed the

areas of contact between the tool surface covered by adhesive and the fore-shaft (green line in Figure 7.5). The morphology of the scars forming the edge-damage was varied (see Section 2.4.2). Half-moon, triangular, and narrow-into-wider scars of different sizes were observed (Figure 7.7 - Figure 7.9). Occasionally, the edge-damage appeared as a complete crushing of the proximal edges (i.e. edge crushing; Figure 7.10).

Edge-damage on the proximal edges was observed regardless of the type of hafting slot being used (i.e. female, juxtaposed, or flat haft slots). However, when the distribution and location of the edge-damage were considered in the analysis, it revealed some patterning associated with the three different hafting types (Figure 7.6). Juxtaposed and flat hafted experimental Levallois points showed that the majority of the scars related to hafting originated from the striking platform surface and the basal proximal parts of the tools (Figure 7.6). In contrast, the hafted female experimental Levallois points showed more scars on the proximal lateral edges, and sporadically also on the dorsal ridges of the tools (Figure 7.6). This set of data is consistent with the type of fore-shaft being used. With regards to the delivery systems (i.e. throwing vs thrusting spear motions), thrusting experimental Levallois points showed a more recurrent presence of proximal edge-damage than throwing experimental Levallois points (Table 7-2), in line with previous studies where thrusting points developed more edge-damage than throwing points (Rots, 2016). However, due to the small sample size, no statistical analyses were performed.

Edge-damage observed in the proximal edges of the experimental Levallois projectile points, although caused by the friction with the fore-shaft and the tool, cannot be considered diagnostic of hafting alone. Edge-damage can also occur as a result of utilisation, trampling, post-depositional activities, retouch, re-sharpening, impact, and other factors. However, it is proposed that, if proximal edge-damage is observed in association with other diagnostic projectile impact traces (such as MLITs, DIFs, and/or impact polish, see CHAPTER 6), it may indicate the presence of

a hafting system (but not the type of arrangement), and that its development is reliant on the tool being used as a projectile ²⁵.

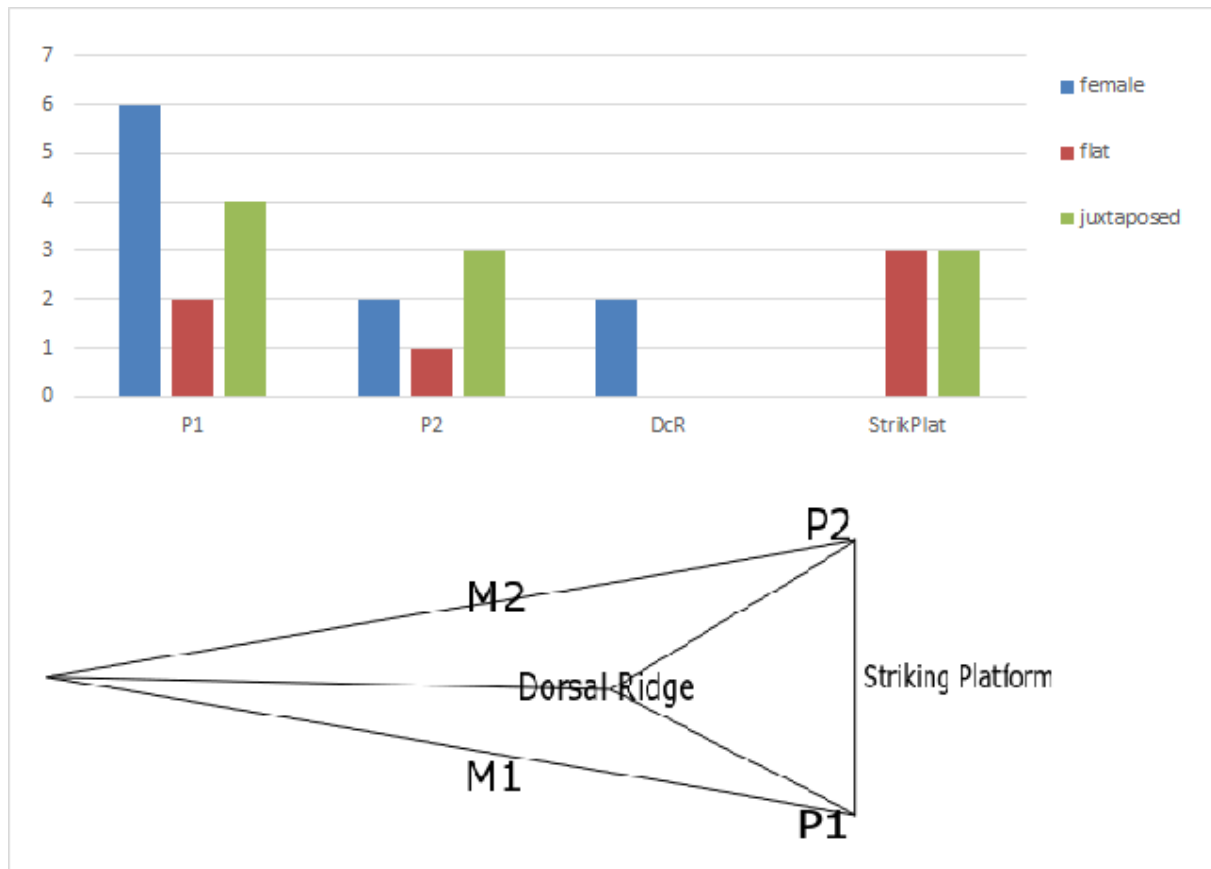


Figure 7.6. Distribution of macroscopic hafting traces according to their location on the selected experimental Levallois points (according to the recording location system, Section 2.3).

²⁵ In this thesis, the term projectile and projectile tool refers to all stone tools mounted in a shaft, regardless of the type of weapon and delivery system (see Glossary).

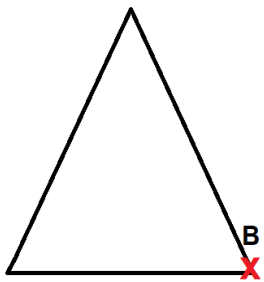
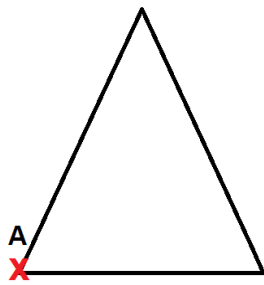


Figure 7.7. Edge-damage due to the presence of a hafting system. Scalar and triangular scars. A: dorsal right proximal side of the tool; B: ventral right proximal side of the tool. DM OM 40x (experiment code: TR-87).



Figure 7.8. Edge-damage due to the presence of a hafting system. Scalar cone scar (with feather termination). DM OM 40x (experiment code: TR-22).



Figure 7.9. Edge-damage due to the presence of a hafting system. Trapezoidal scar (in red). DM OM 60x (experiment code: TR-33).



Figure 7.10. Edge-damage (i.e. edge-crushing) due to the presence of a hafting system. DM OM 60x (experiment code: TH-23).

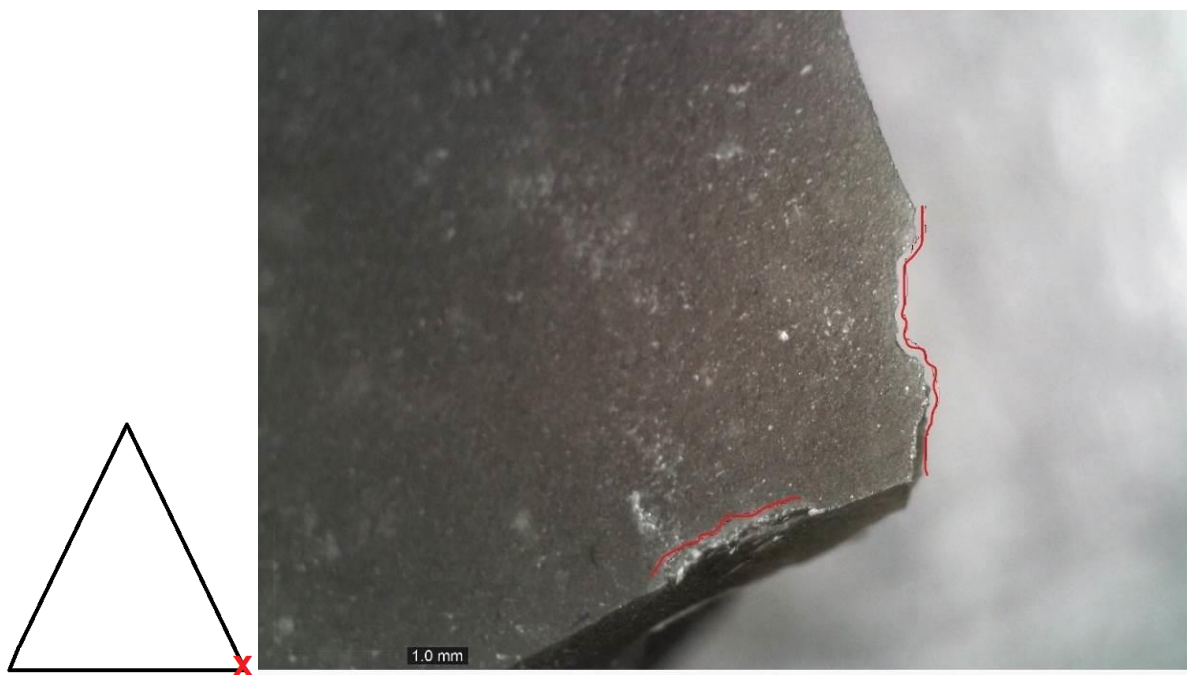


Figure 7.11. Edge-damage due to the presence of a hafting system. DM OM 55x (experiment code: TH-92).



Figure 7.12. Edge-damage due to the presence of a hafting system. Scalar plus small half-moon scars (in red). DM OM DM 80x (experiment code: TH-79).

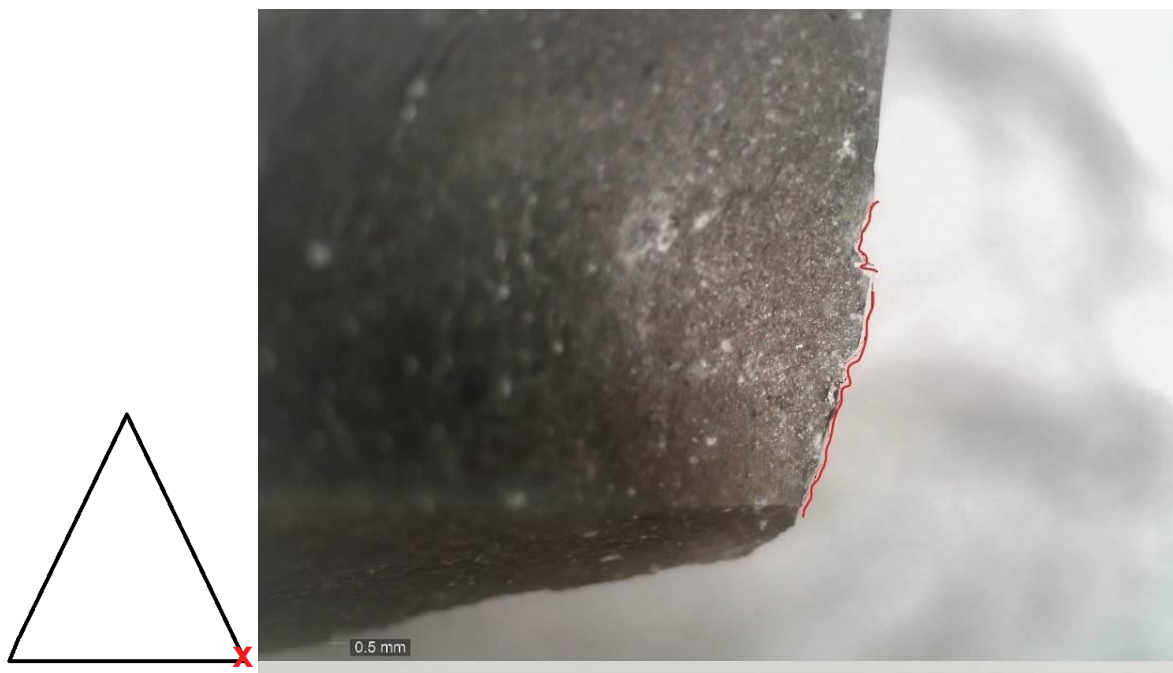


Figure 7.13. Edge-damage due to the presence of a hafting system. DM OM DM 65x (experiment code: TR-34).

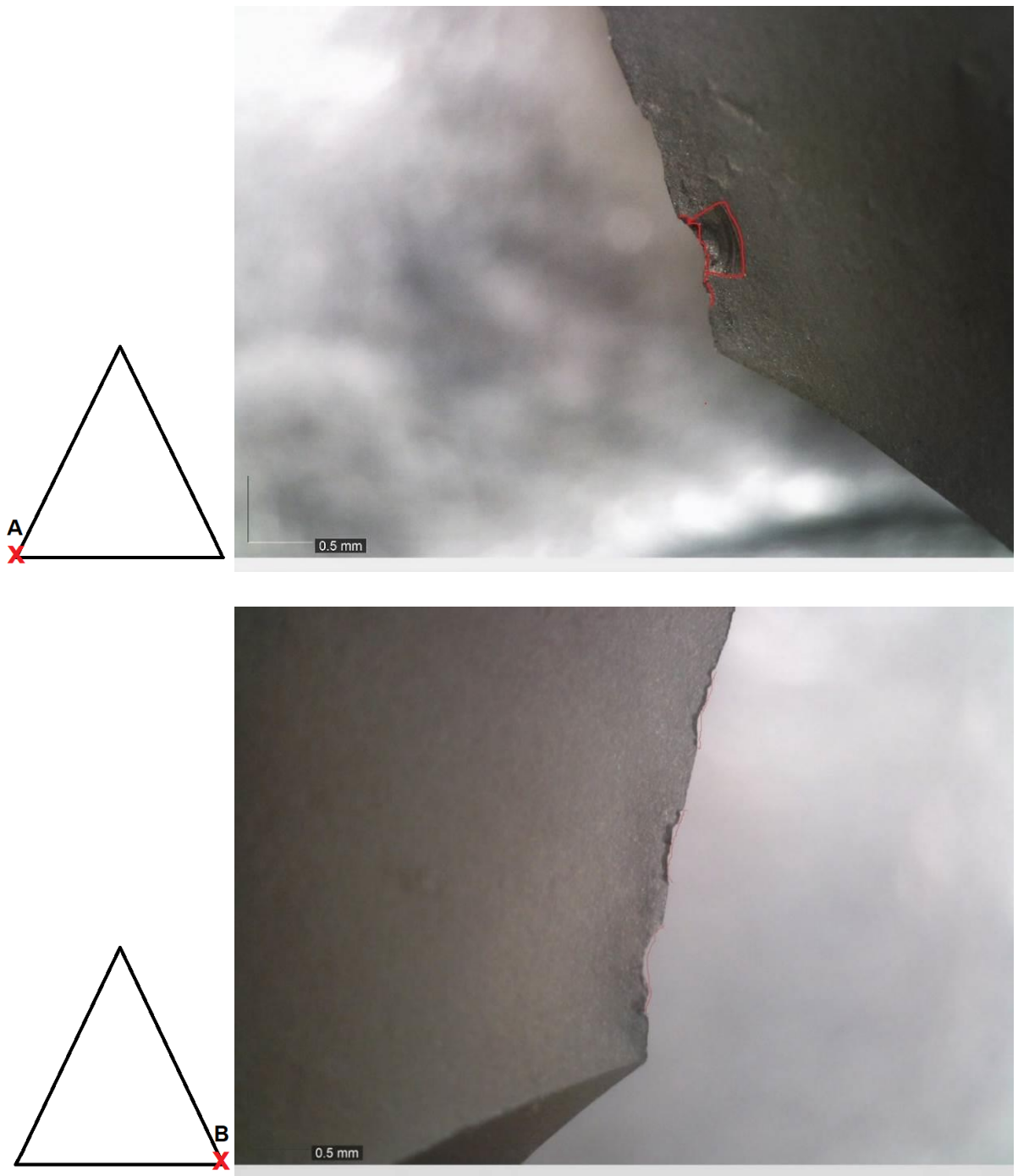


Figure 7.14. Edge-damage due to the presence of a hafting system. A: ventral left proximal side of the tool (trapezoidal plus small half-moon scars, in red); B: ventral right proximal side of the tool (small half-moon scars). DM OM 65x (experiment code: TR-36).

7.4.3 Presence of adhesive polishes (or polished layers) and adhesive residues

The analysis was conducted on a macroscopic level (up to 100x) first, and on a microscopic level (from 100x to 500x magnifications) later. The results presented below were all recorded after intense and repeated cleaning protocols (as described in Section 3.4).

Microscopic traces (such as polish or residues) resulting from tar and resin adhesive particles demonstrated the most recurrent evidence of hafting among the selected sample of experimental Levallois points (Table 7-2). Striations due to hafting presence were rare. No other specific polish types (e.g. wood-like polish from the fore-shaft) were observed. In fact, as previously observed by Rots (2010), indirect hafting arrangements (i.e. the presence of tar or resin adhesives as mediums between the shaft and the stone tool) prevented the formation of wood-like polishes from the fore-shafts. However, although the use of resin and tar significantly limited the formation of traces related to the wooden shaft materials, the tar and resin adhesive itself formed very distinctive microscopic traces, here defined as “adhesive polishes” or “adhesive polished layers”, since their formations process and resistance to chemical cleaning warrants further and future investigation (see below).

Not well-developed polish traces

Five experimental Levallois points (out of the 20 tools in the selected sample) displayed a not well-developed type of polish (Table 7-2; Figure 7.15 and Figure 7.16). At 100x, this polish had a faint and dull-to-medium-bright aspect (Figure 7.15 and Figure 7.16). It showed a poor development, and it presented a very scattered degree of linkage (Figure 7.15 and Figure 7.16). If the location was not taken into account, this polish could resemble a meat-like polish type (Van Gijn, 1990, p. 41). However, when the location was taken into account, the polish was identified as located right on the ventral proximal basal edges (Locus P1v and Bulb; Figure 7.15 and Figure 7.16), which was the area of contact between the adhesive-covered tool and the fore-shaft (Figure 7.5). Therefore, it is possible that this polish could be

related to sporicidal contact between the tool and the wooden fore-shaft, in a small area of the tool that was possibly not covered by the tar ²⁶.

²⁶ The “small spots” of tar were possibly not covered by the adhesive, or the adhesive was possibly rubbed away by the friction of the fore-shaft against the stone tool, either during the hafting and de-hafting processes or during the projectile impact.

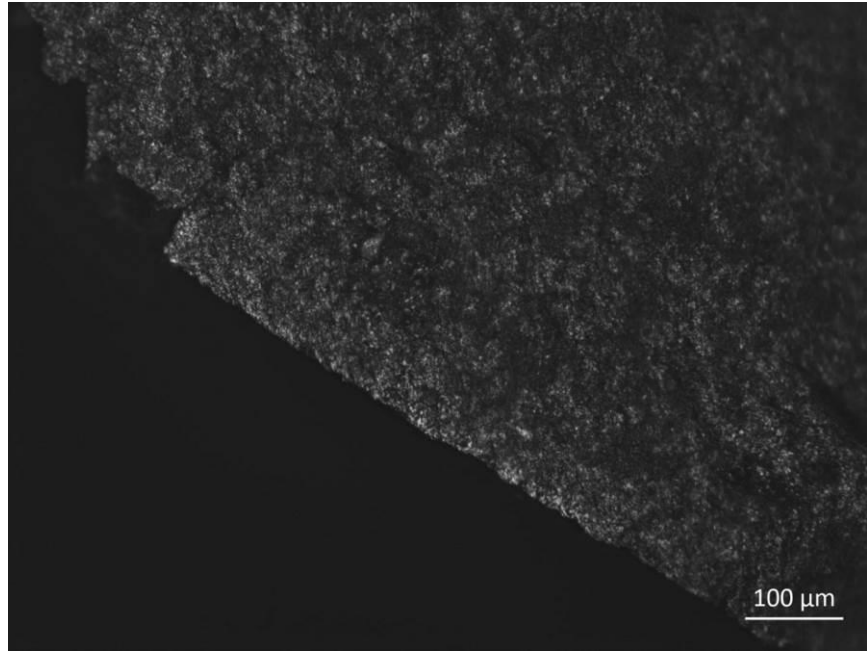
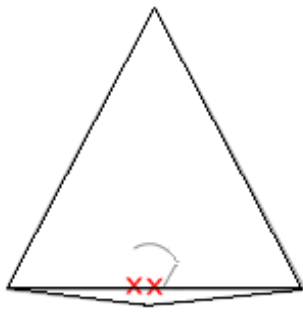


Figure 7.15. Polish located on the proximal basal edge (Locus P1v). The polish shows a poor development with a dull-to-medium-bright aspect. Picture: OLMil 100x (experiment code: TH-24).

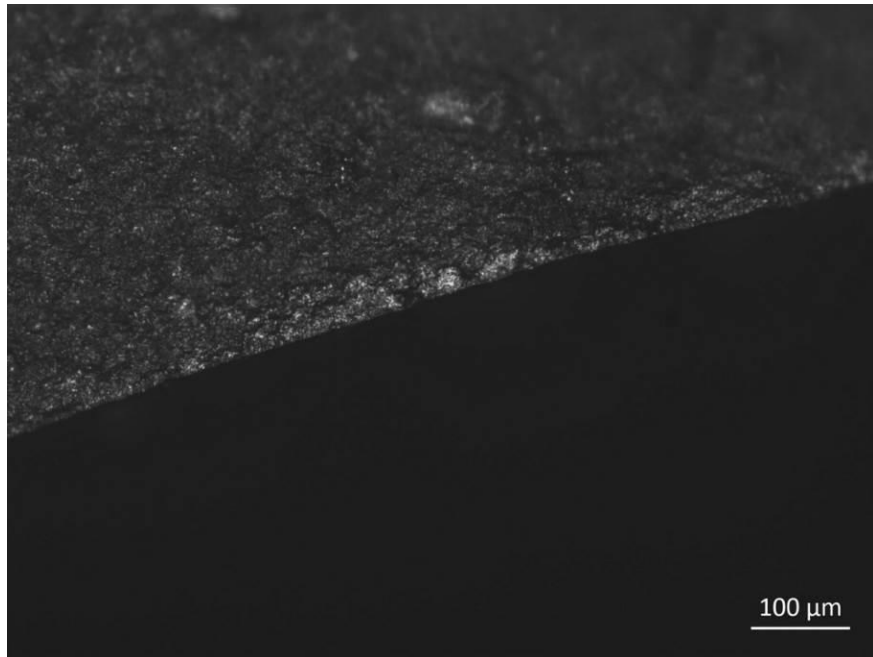
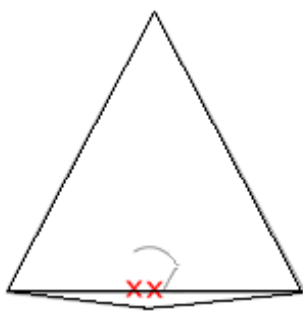


Figure 7.16. Polish located on the proximal basal edges (Locus P1v). The polish shows a poor development with a dull-to-medium-bright aspect. Picture: OLMil 100x (experiment code: TR-39).

Macroscopic tar residues

On the other hand, 15 experimental Levallois points (of the selected tool sample) displayed traces of adhesive polishes (or polished layers) and/or adhesive residues, even after intensive and repeated cleaning protocols (as described in Section 3.4.2).

Ten experimental Levallois points (out of the 20 tools in the selected sample) hafted with commercial tar presented macroscopic tar residues that were still visible under lower-power magnification (up to 100x, and also with the naked eye; Figure 7.17 and Figure 7.18). In one case (Tool TR-83), the tar residues clearly indicated the haft limit (Figure 7.18). The tar residue, located on the mesial ventral face, showed a semi-circular silhouette that outlined the negative profile on the wooden fore-shaft (Figure 7.18). The presence of these macroscopic tar residues suggests that tar adhesives have strong adhering properties that resist intense chemical cleaning, and possibly time, as testified by their survival in the Palaeolithic archaeological record (Boëda et al., 1996; Mazza et al., 2005; see also CHAPTER 11).

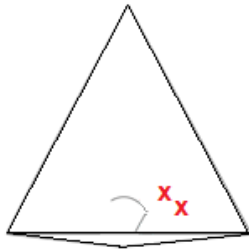


Figure 7.17. Tar residue located on the proximal basal edges (Locus P1v). The residue has a granular and sticky texture. Picture: DM OM 50x (experiment code: TR-87).

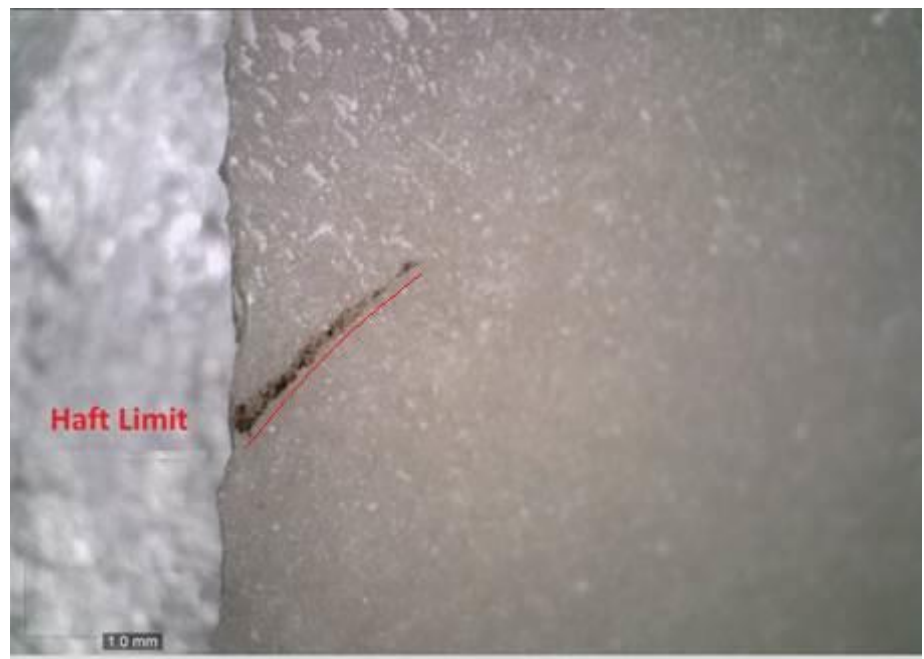
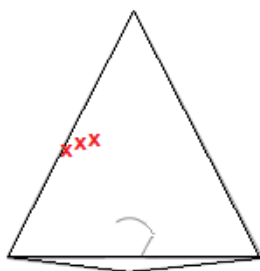


Figure 7.18. Tar residue located on the mesial part of the tool (Locus M2v), clearly indicates the haft boundary. Picture: DM OM 30x (experiment code: TR-83).

Adhesive polishes (or polished layers)

15 experimental Levallois points (out of the 20 tools in the selected sample) displayed adhesive polishes (or polished layers), after intensive and repeated cleaning protocols (as described in Section 3.4.2), which could only be observed microscopically (i.e. with high-power magnification, 100x-500x) (Table 7-2). These polishes or polished layers were visible both in the experimental Levallois points hafted with commercial tar and those with commercial resin (plus beeswax).

Two possible variations of adhesive polishes (or polished layers) have been observed, with the first variation showing a residue-like appearance (i.e. looking like a greasy and oily microscopic layer had been deposited onto the tool surface), and the second variation showing a polish-like appearance (i.e. looking as if it were embedded into the tool surface). Further investigation is required to clarify their nature, formation process, and resistance to further chemical cleaning.

The first variation of adhesive polish (or polished layer) had a greasy and oily quality with numerous pits, resembling micro-bubbles (Figure 7.19 and Figure 7.22). It looked almost like a liquid or a smooth film that covered the tool surface (Figure 7.19). At 100x and 200x, it had a very bright aspect (Figure 7.20 and Figure 7.21). It was seen to adhere to the tool's surface in random lines, patches, or spots (Figure 7.19 - Figure 7.21). It was always located on proximal parts of the tools covered by the hafting arrangements (Loci P1 and P2, see Section 2.3), mostly at the highest micro-topographic areas, such as the bulbar areas, the mesial and proximal lateral edges, and dorsal ridges, or in the depressions of the tool's surface. The overall distribution appeared over the surface randomly, and no clear spatial patterns were recognised.

These adhesive polishes (or polished layers) could be microscopic residues of adhesives adhering onto the tool's surface, that had resisted the chemical cleaning process.

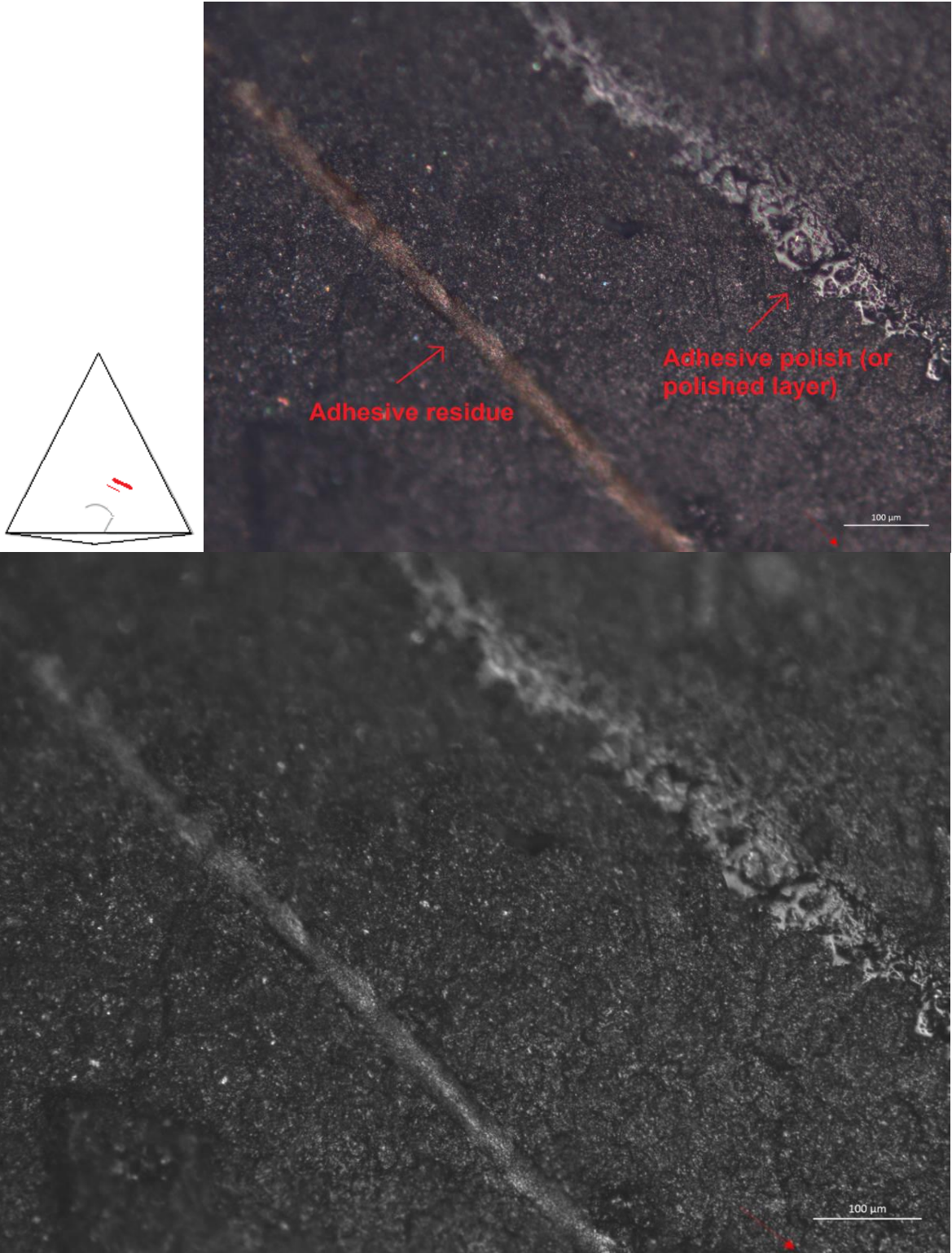


Figure 7.19. An example of adhesive residues and adhesive polish (or polished layer), located on the proximal ventral face (Locus P1v). At 100x, the adhesive polish (or polished layer) looks oily and greasy. Picture: OLMil 100x (experiment code: TH-66).

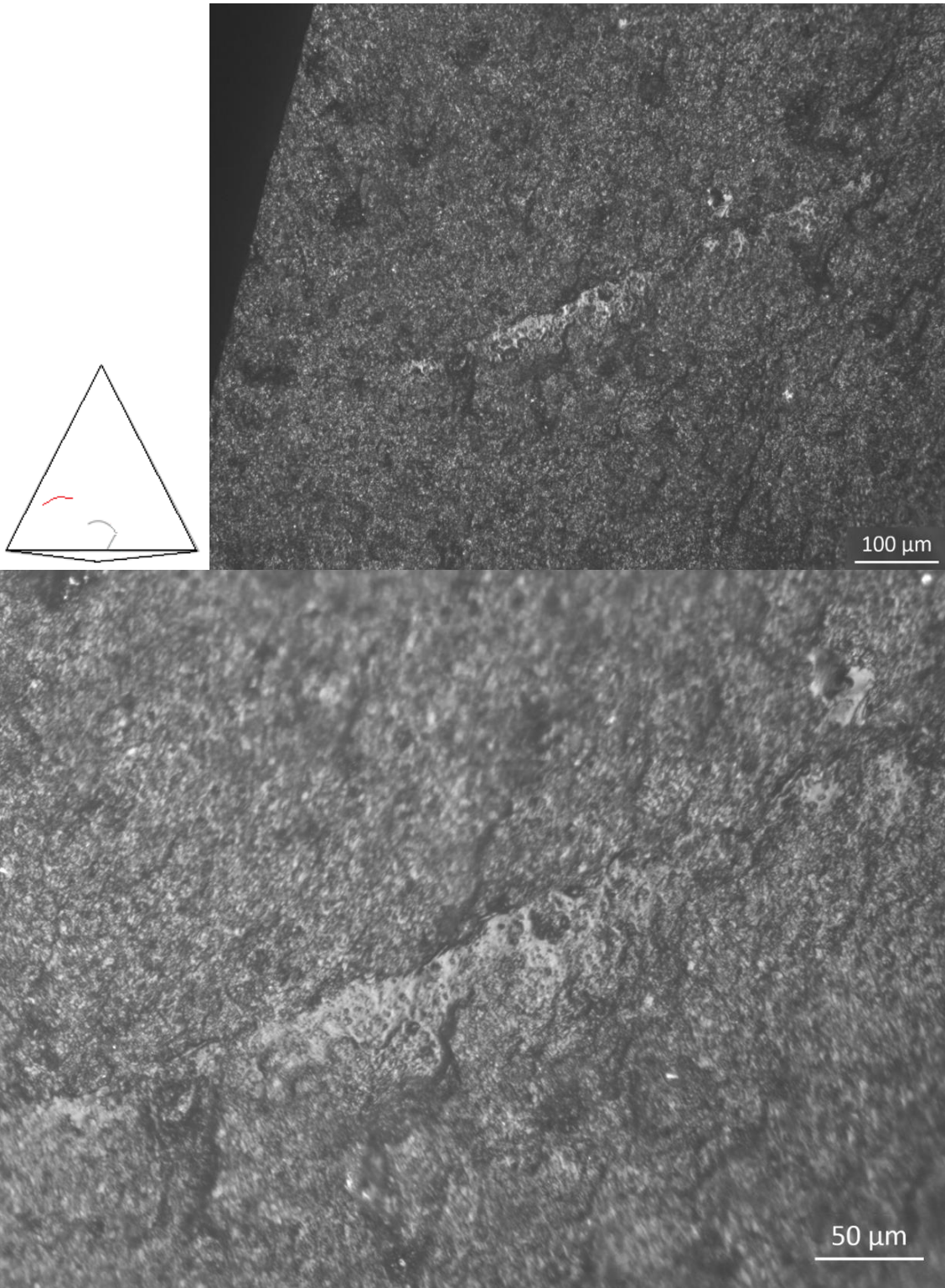


Figure 7.20. Adhesive polish (or polished layer), located on the proximal ventral face (Locus P2v). At 100x, the adhesive polish (or polished layer) looks oily and greasy, at 200x it shows numerous pits and a possible deposition above the surface. Picture: OLMil 100x (above), 200x (below) (experiment code: TH-20).

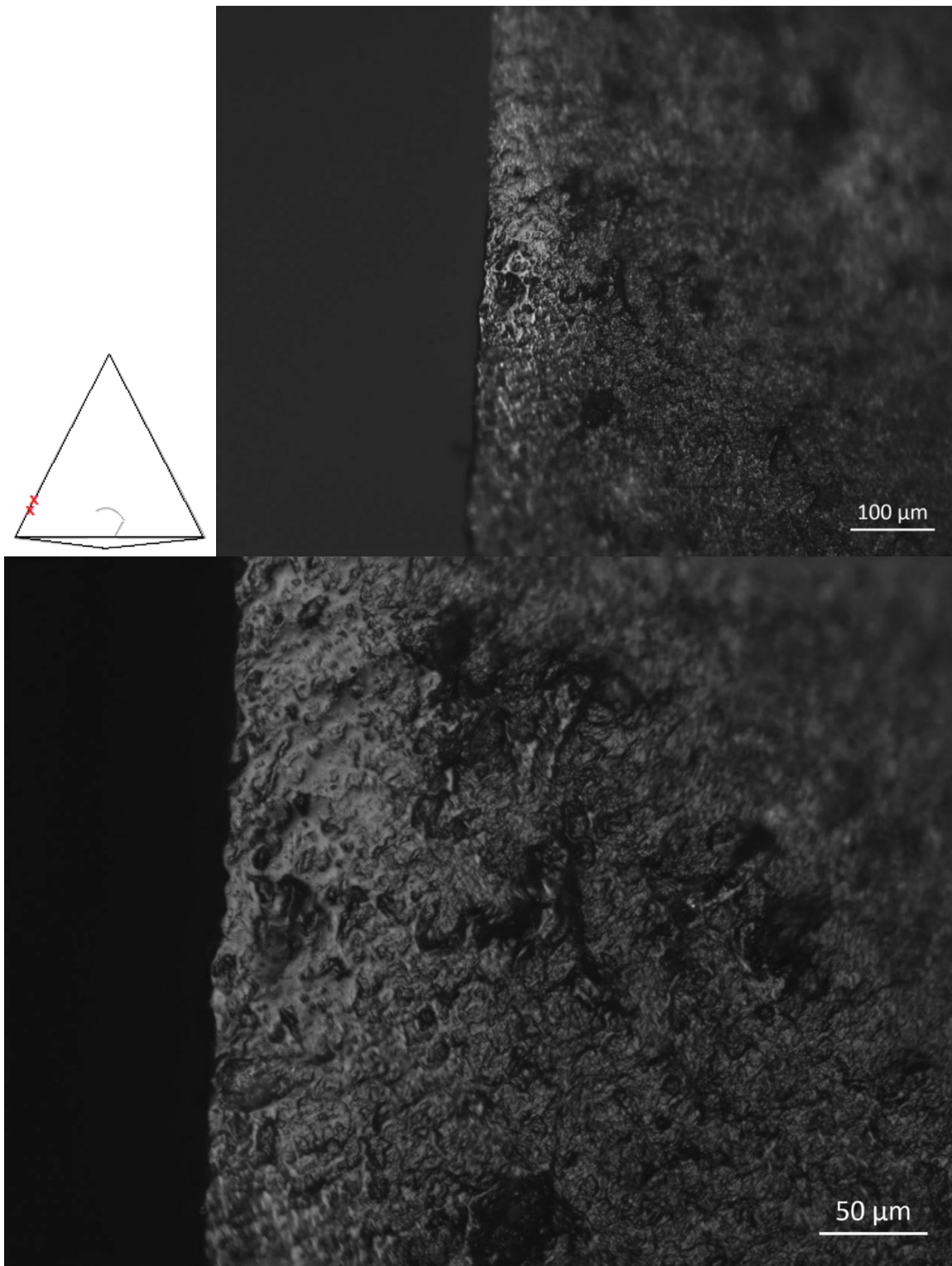


Figure 7.21. Adhesive polish (or polished layer), located on the proximal ventral edge (Locus P2v). At 100x, the adhesive polish (or polished layer) looks oily and greasy, at 200x it shows numerous pits and a covering aspect. Picture: OLMil 100x (above), 200x (below) (experiment code: TR-34).

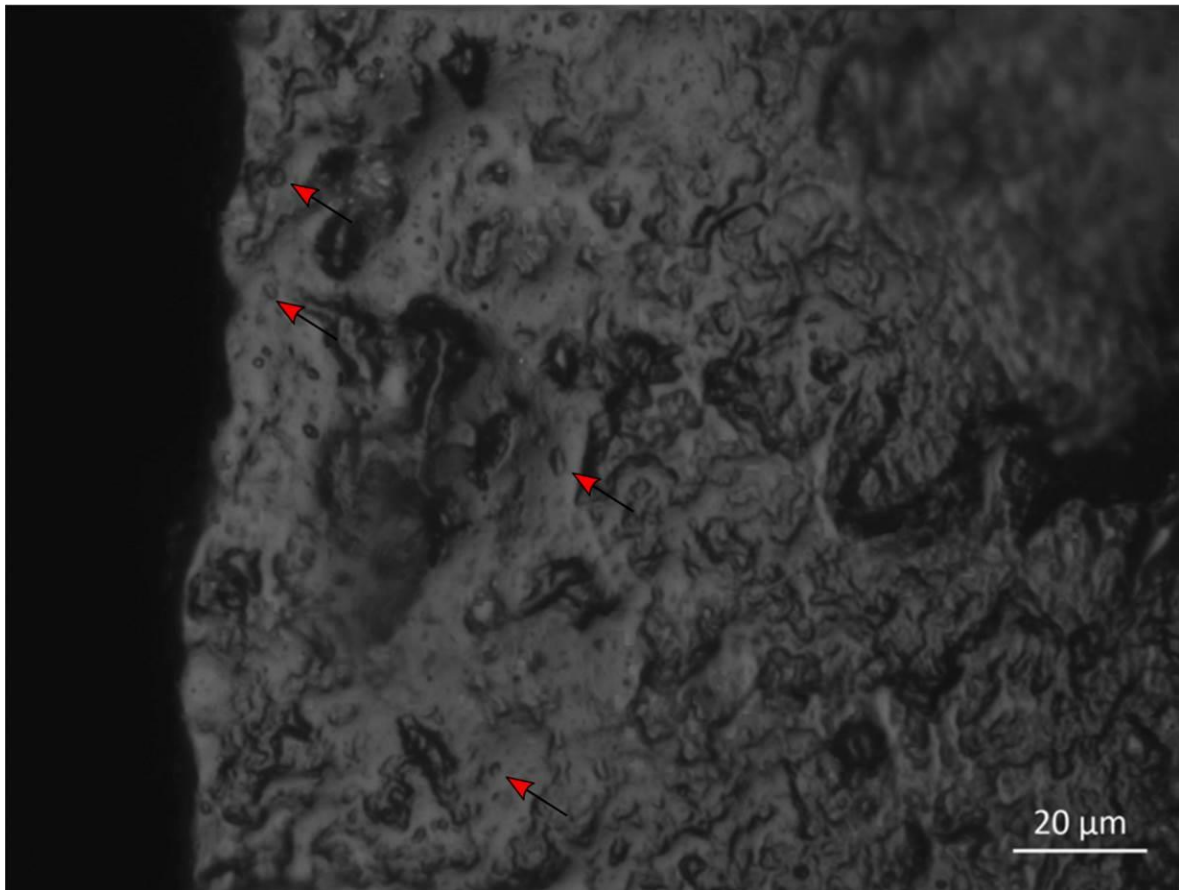


Figure 7.22. Adhesive polish (or polished layer) at 500x. The polish shows an oily aspect and numerous pits, resembling micro-bubbles (red arrows). Picture: OLMil 500x (experiment code: TR-34).

A second variation of the adhesive polish (or polished layer) showed a rough and scattered distribution but a very brilliant aspect (Figure 7.23 and Figure 7.26). It sporadically displayed striations and areas of more intense polish formation (or layer deposition) (Figure 7.23). It spread over broad surfaces, occurring in patches, spots, or lines (Figure 7.23 - Figure 7.26), and its distribution was ubiquitous over the hafted surface. The polish occurred on the bulbar areas (i.e. in the highest micro-topographic spots) and also on the inner parts of the ventral proximal and mesial faces (Figure 7.23 - Figure 7.26). This polish (or layer), once it was found and described, became very distinctive to the eye. It clearly contrasted with the unaltered surface of the tool (Figure 7.23, Figure 7.25, and Figure 7.26). When located on the ventral mesial part of the tool, it was often a good indicator of the haft limit (Figure 7.25 and Figure 7.26).

These adhesive polishes (or polished layers) could have possibly formed as a result of the friction between the adhesive particles and the wooden shaft (or fore-shaft) when, during the impact motions, the fore-shaft rubbed against the tar or resin adhesives that covered the tool surface. Conversely, they could be microscopic residues of adhesives adhering to the tool's surface that had resisted repeated chemical cleaning.

Additional research would be required to further investigate the formation or deposition process of these adhesive microscopic traces and their endurance to chemical cleaning agents (see also CHAPTER 11).

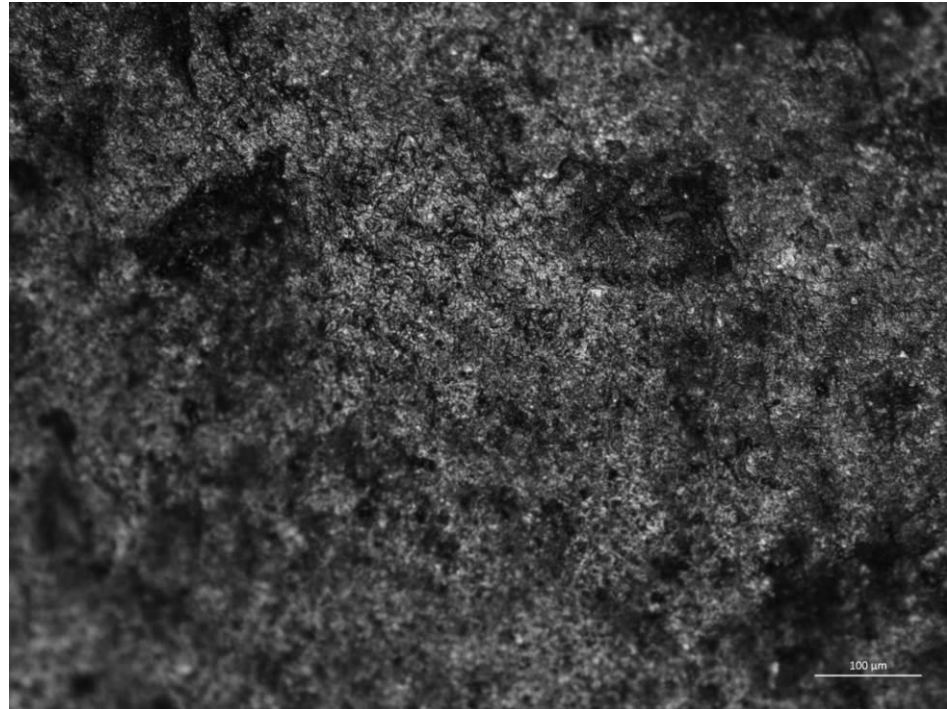
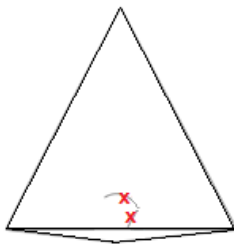


Figure 7.23. Adhesive polish (or polished layer). Rough and very brilliant polish located on the bulbar area of the tool (Locus P1v). Picture: OLMil 100x (experiment code: TH-23).

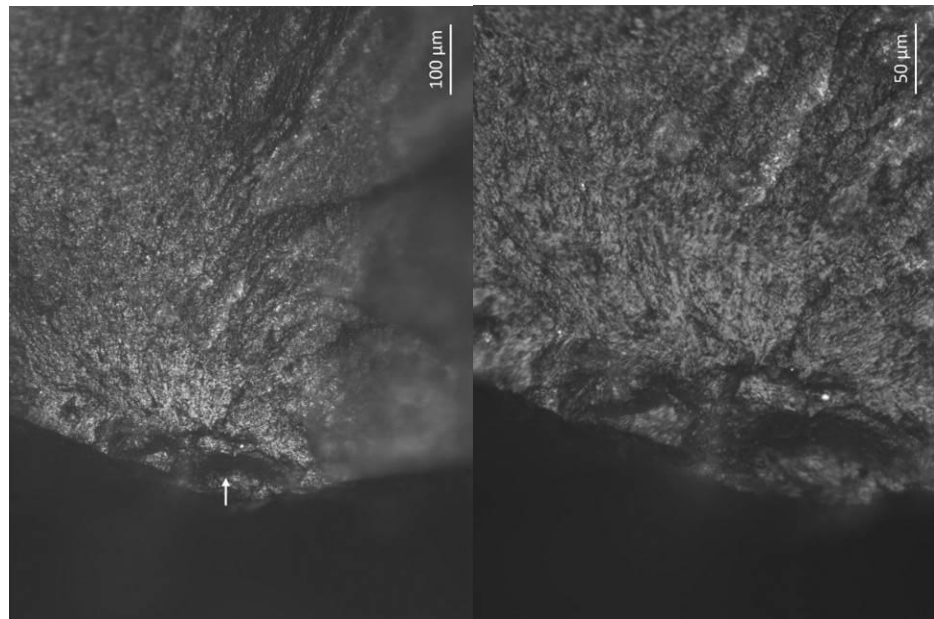
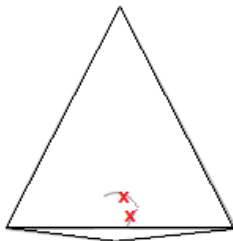


Figure 7.24. Adhesive polish (or polished layer). Rough and very brilliant polish located on the bulbar area of the tool (Locus P1v). Picture: OLMil 100x (left), 200x (right), (experiment code: TH-20).

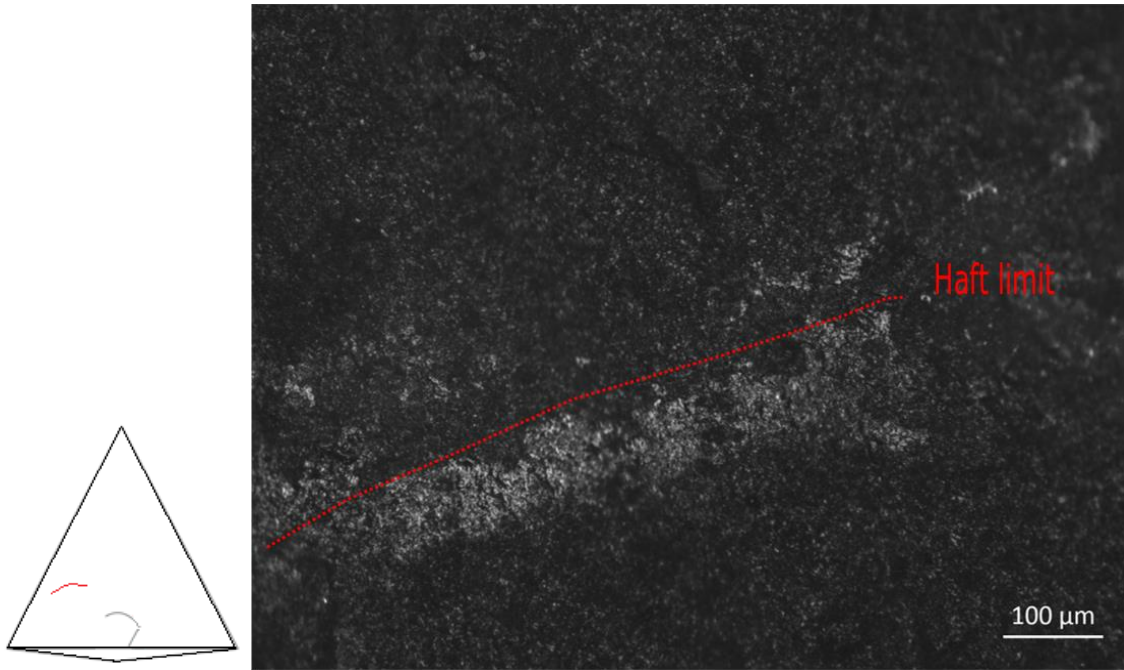


Figure 7.25. Adhesive polish (or polished layer). Rough and very brilliant polish located on the inner proximal ventral face (Locus P2v). It clearly indicates the haft boundary (below the red line). Picture: OLMil 100x (experiment code: TH-32).

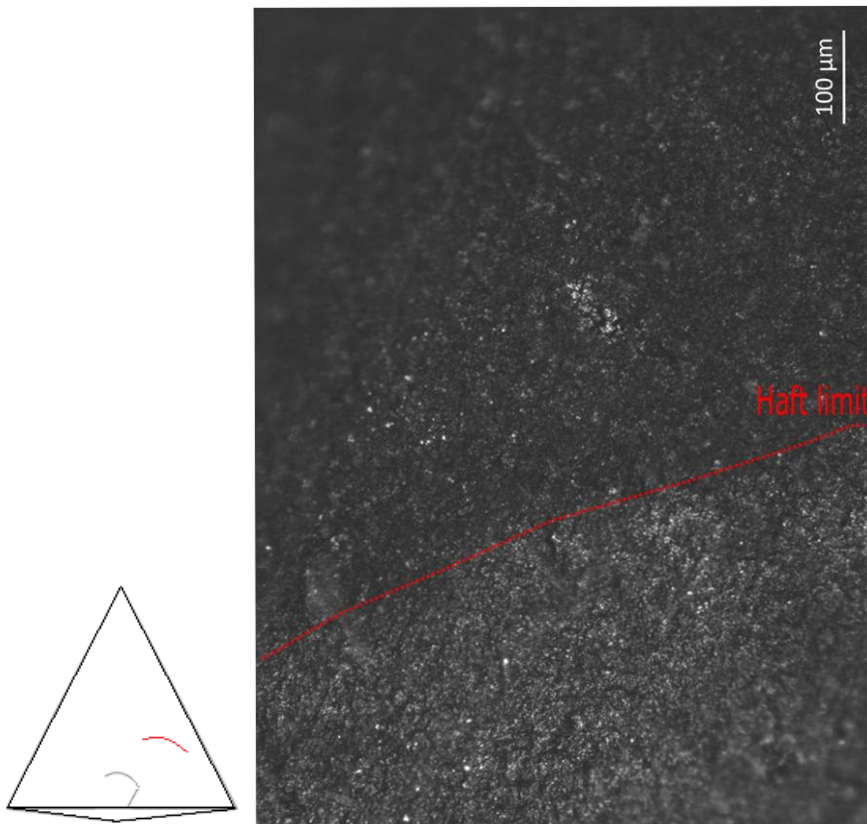


Figure 7.26. Adhesive polish (or polished layer). Rough and very brilliant polish located on the inner proximal ventral face (Locus P1v). It clearly indicates the haft boundary (below the red line). Picture: OLMil 100x (experiment code: TR-93).

7.4.3.1 Polishes (or polished layers) as attributes with which to distinguish hafting arrangements

The distribution and location of the microscopic adhesive polish (or polished layers) supplied sufficient evidence for the recognition of a haft presence and the hafting arrangements used for the hafting system of the selected experimental Levallois points (Figure 7.27).

Hafted female Levallois points fixed with tar or resin were the only tools that showed frequencies of adhesive polish on the mesial ventral and/or dorsal parts of the tool (Loci M1 and M2, see Section 2.3). In contrast, both hafted flat and juxtaposed Levallois points fixed with tar or resin did not show adhesive polish on their mesial ventral and/or dorsal parts (Figure 7.27). Hafted flat and juxtaposed Levallois points instead showed higher frequencies of adhesive polishes on their basal proximal ventral and/or dorsal edges and striking platform surfaces (Loci P1 and P2; Figure 7.27). These were the areas of the tools that had the most contact with the fore-shaft. Lastly, hafted female Levallois points showed more recurrent frequencies of adhesive polish on the dorsal ridges of the points, which were also the parts of the tool that were in contact with the fore-shaft, indicating that the friction between the shaft (or fore-shaft) system could play a role on the formation of adhesive traces. No statistical analyses were performed due to the sample size.

In conclusion, although the utilisation of adhesives inhibited the formation of hafting traces that could specify the shaft material used (in agreement with Rots, 2010), the distribution of the adhesive polishes provided patterns for the recognition of the hafting arrangement employed in the experimental Levallois points. However, the identification of the hafting arrangements was not always correct, as even flat or juxtaposed hafted Levallois points sporadically displayed adhesive polishes (or polished layers) and adhesive residues, both on their dorsal and ventral faces. When this happened, these artefacts were confused with female hafted tools. Moreover, it is worth noting that the presence of these adhesive polishes (or polished layers)

observed on the experimental Levallois points, as well as needing further investigation, might not have survived in archaeological tools, or might disappear once more destructive chemical cleaning agents are employed in experimental tools (see also CHAPTER 11). Therefore, if archaeological or experimental projectiles have been hafted using tar, resin, or other adhesives, the hafting arrangement can be challenging to interpret, and caution must be advised when interpreting the hafting traces.

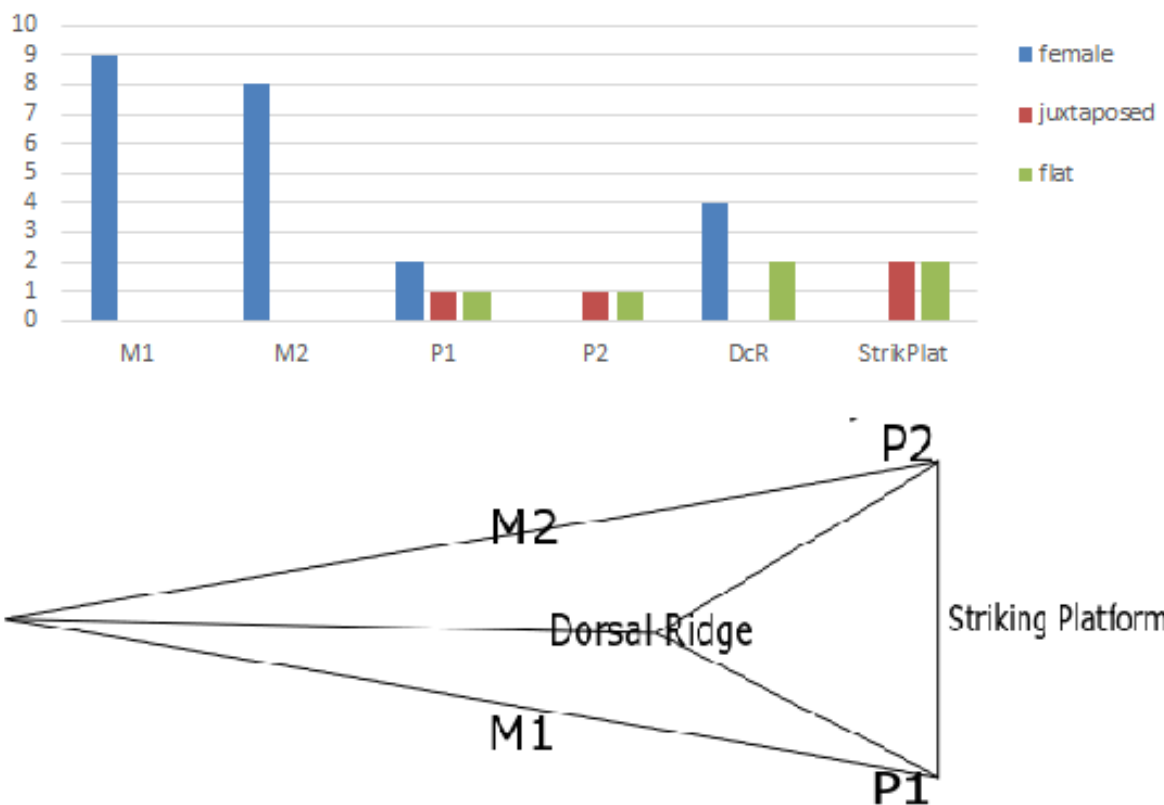


Figure 7.27. Distribution of microscopic hafting traces according to their location in the selected experimental Levallois points (according to the recording location system, Section 2.3).

7.4.4 Presence of hafting bright spots

Hafting bright spots have been considered as diagnostic of hafting when they appear in association with other hafting evidence (Rots, 2002, 2003, 2010).

In the selected sample of Levallois points used as hand-delivered spearheads, hafting bright spots were sporadic (Table 2). Only one tool from the selected sample showed bright spots related to the hafting process. It was an experimental Levallois point used in thrusting hand-delivered spear experiments, hafted with a female hafting slot and fixed with tar.

The bright spots were located under the hafting system (and the tar acted as a medium between the wooden fore-shaft and the tool surface). At 100x, they looked very bright and almost metallic, from 200x they had a smooth texture with a domed-into-flat polish topography (Figure 7.28). They were located on the bulbar area of the tools (i.e. in the highest micro-topographic zones). Because of this, they have been interpreted as the result of friction between the wooden fore-shaft and the tar particles covering the tool surface.

Hafting bright spots were only observed on one of the experimental Levallois points used as thrusting spear points. This may be linked to the fact that thrusting motions resulted in higher degrees of loading forces than throwing motions (see 5.3). It is thus possible that, during the thrusting impact, the higher degree of friction between the stone tool and the wooden shaft produced the observed bright spots (examination of previous literature has shown that bright spots linked only to thrusting spear motions have not been observed before).

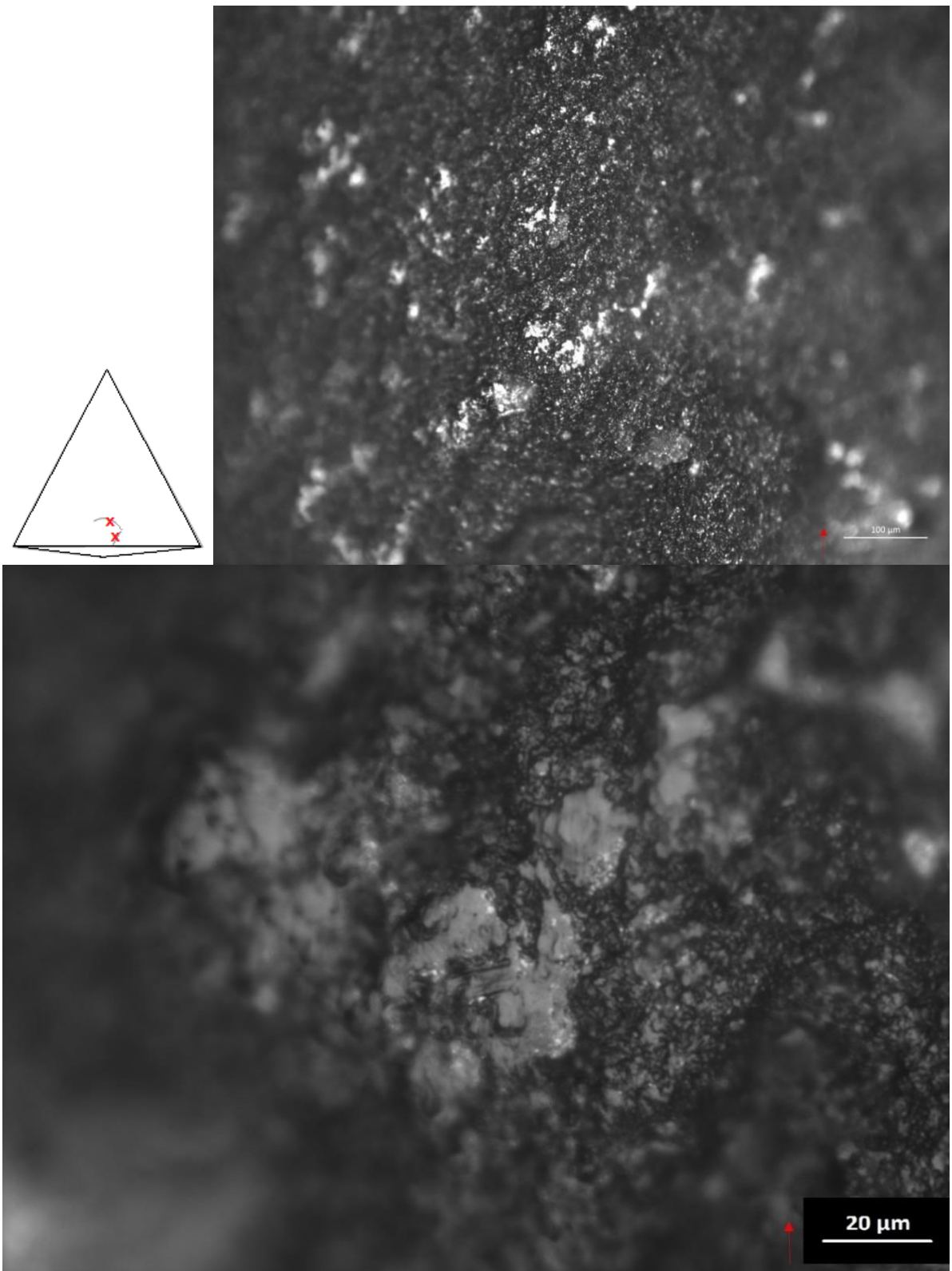


Figure 7.28. Very bright, almost metallic, spots of polish, i.e. bright spots. They were located on the bulbar area of the tool (Locus P1v). Picture: OLMil 100x (above), 200x (below), (experiment code: TR-33).

7.5 Overview

Can macroscopic and microscopic traces be diagnostic of hafting systems on the experimental Levallois points used in hand-delivered stone-tipped spear experiments? Can macroscopic and microscopic hafting traces allow for distinguishing between different hafting arrangements? Do throwing and thrusting experimental Levallois points display different hafting traces?

The experimental Levallois points used as stone-tipped spear projectiles developed a limited presence of edge-damage associated with the presence of hafting systems (see also Table 7-3). When present, edge-damage was only located on the proximal lateral edges and/or on the striking platform surfaces (Table 7-3). It was never observed on the mesial lateral edges, most likely because bindings were not employed. Although proximal edge-damage was a recurrent trace pattern in the hafted experimental Levallois points used as spear projectiles, it was not considered diagnostic of hafting alone (as it could also be caused by activities other than projectile impacts).

Another contribution was the observations that, when experimental projectiles are hafted using adhesives (mainly as a medium between the tool surface and the shaft), the mostly visible macroscopic and microscopic wear traces could be linked to the presence of adhesives only (in agreement with Rots, 2010). The most diagnostic evidence of hafting came from the microscopic examination of wear traces related to adhesive utilisation. The distribution of these adhesive polishes (or polished layers) provided some patterns for distinguishing between different hafting arrangements (i.e. female, juxtaposed, and flat types) (Table 7-3). However, the presence of microscopic adhesive traces on both faces of the experimental tools highlighted the potential for erroneous interpretations of the hafting type, confirming that the use of adhesives reduces the chances of a correct interpretation of the hafting system in both experimental and archaeological tools.

The presence of these adhesive polishes or polished layers has been observed and proposed to be a type of wear trace that warrants further investigation. It has been proposed that adhesive polishes, or polished layers, can be resultant of friction

between the shaft (or fore-shaft) and the tar/resin particles that covered the tool's surface. Alternatively, they could also be microscopic residues of adhesives adhering onto the tool's surface which had resisted the chemical cleaning process. However, microscopic and chemical analyses with SEM microscopes, and possibly with Raman spectroscopy, would be required in the future to further investigate the nature of these microscopic adhesive traces, possibly in conjunction with specific experimentation aiming to investigate the process of chemical degradation (and resistance to chemical cleaning) of tar-based or resin-based adhesives (see also CHAPTER 11).

Therefore, considering the above results (see also Table 7-3), it is proposed that:

- Experimental Levallois points used as hand-delivered stone-tipped spear projectiles, when hafted with adhesives, developed limited hafting traces,
- Macroscopic and microscopic hafting traces were easily distinguished from diagnostic macroscopic and microscopic projectile impact traces (such as "impact polish", MLITs, and DIFs).
- With regards to the hafting arrangements employed in this thesis's experimentation (i.e. female, juxtaposed, and flat hafting slots, see Section 4.3.2.2), hafting patterns could be seen and, to a certain extent, indicate the type of arrangements. However, the presence of adhesive polishes and/or adhesive microscopic traces on both faces of the tool could result in an erroneous interpretation of the hafting arrangements.
- Excluding the presence of friction bright spots in only one thrusting experimental Levallois point, no difference in hafting traces have been observed between throwing and thrusting experimental Levallois points used in hand-delivered spear experiments.

In conclusion, when experimental or archaeological projectiles are hafted with adhesive glues, one should expect a reduction of visible hafting traces, especially those linked to the shaft materials (in agreement with Rots 2016, p. 161). In this case, the available microscopic evidence that could be used to infer hafting presence is then limited to the identification of adhesive traces, which are unlikely to easily preserve in the archaeological record.

Table 7-3. A summary of the observed hafting traces according to the hafting arrangements used in this thesis's experiments.

Type of traces	Trace attributes	Female (plus adhesive)	Juxtaposed (plus adhesive)	Flat (plus adhesive)
Macroscopic traces	Edge-damage	Present (mainly on the lateral proximal edges)	Present (mainly on the proximal basal edge and on the striking platform)	Present (mainly on the striking platform)
	Macroscopic adhesive deposits (after cleaning)	Present in a high number	Present in a medium number	Present in a medium number
	Haft boundary visible by edge-damage	Poor and indicating a mesial boundary (observed only in 1 case)	Absent	Poor and indicating mesial boundary (observed only in 2 cases). It could be confused with a female type
Microscopic traces	Generic polish	Present but very sporadic	Present but very sporadic	Present but very sporadic
	Adhesive polishes (or polished layers)	Abundant and distributed in patches or randomly	Abundant and distributed in patches or randomly	Abundant and distributed in patches or randomly
	Bright spots	Only on thrusting points		
	Haft boundary visible by change in polishes	Present and located in a mesial position. It was often recognised on both faces (dorsal and ventral) It was sporadically observed only on one face (which could be confused with a juxtaposed hafting type)	When present, it was located only on one face (either dorsal or ventral)	Present but it was always located in a mesial position (which could be confused with a female hafting type). Also, it was located either on one face (confusing it with a juxtaposed hafting type) or on both faces (confusing it with a female hafting type)

CHAPTER 8

ARCHAEOLOGICAL SAMPLE TOOLS: SELECTION OF AND INTRODUCTION TO THE ARCHAEOLOGICAL SITES

8.1 Archaeological sites: selection and rationale

One of the main goals of this research was to investigate whether Neanderthals produced and employed stone-tipped spears during the Middle Palaeolithic in Europe and whether these spears were used in hand-delivered throwing and/or thrusting spear activities (see CHAPTER 1). Therefore, key Middle Palaeolithic sites were analysed and selected to compare use-wear traces on experimental Levallois points created using used hand-delivered throwing and thrusting stone-tipped spear experiments, with use-wear traces of archaeological assemblages of Levallois points (or more broadly convergent tools,). A review of several western European Middle Palaeolithic sites with tools displaying Levallois reduction sequences was undertaken. The rationale behind the selection of the archaeological sites was to identify Middle Palaeolithic archaeological assemblages that provided:

- well-excavated stratigraphy with secure dating of the discrete archaeological levels and corresponding stone tools,
- a sufficient number of Levallois points that present no or a low/medium degree of post-depositional alterations in order to secure the preservation of use-wear traces,
- availability and accessibility to the researcher.

The available literature indicated that several Western European Middle Palaeolithic sites preserved middle to high frequencies (between 2% to 5%) of Levallois points or convergent tools (Villa and Lenoir, 2006; Villa et al., 2009a; Rots, 2013, 2016; Goyal et al., 2015) (Table 8-2). Of these, three Middle Palaeolithic archaeological sites were available for research, including Abri du Maras (Ardèche, France), Arma Delle Manie (Liguria, Italy), and Abric Romaní (Capellades, Spain).

The Abri du Maras site was a suitable assemblage for analysis due to the presence of Levallois points (n=51) that presented a low to medium degree of post-depositional alterations and which were all discovered from a recently excavated archaeological unit, i.e. Maras Level 4 dated between MIS4 and MIS3 (Moncel and Michel, 2000; Richard et al., 2015). (In addition, other convergent tools that presented possible impact fractures visible macroscopically n=19 were also preserved at the site). Thus, the archaeological assemblage of Abri du Maras Level 4 was selected for archaeological use-wear examination (Table 8-1).

Arma Delle Manie was another suitable assemblage for study because the Mousterian Levels (Levels VII and II), dated between MIS4 – MIS3 (Karatsori, 2003; Psathi, 2004; Mehidi, 2005), yielded the presence of Levallois points (n=40) which were available for analysis and which showed a low to medium degree of post-depositional alteration. (In addition, n=7 convergent tools that presented possible impact fractures visible macroscopically were also available for analysis) Thus, the archaeological assemblage of Arma Delle Manie Levels VI-II was selected for archaeological use-wear examination (Table 8-1).

Abric Romaní was initially considered for the archaeological use-wear examination because Level O, dated at MIS4 (Bischoff et al., 1988; Burjachs and Julia, 1994; Burjachs et al., 2012), preserved Levallois points (n=18) which were available for analysis. However, an initial data acquisition and microscopic examination of the Levallois points of the Abric Romaní Level O (realised at the Catalan Institute of Human Paleoecology and Social Evolution [IPHES], Spain) revealed the presence of extensive post-depositional alterations (e.g. white patina, glossy patina, and trampling) affecting the selected archaeological tools. Thus, Abric Romaní assemblage was not included as a case study.

Consequently, the Levallois points (and a few selected convergent tools that presented possible impact fractures by naked eye) of Abri du Maras (Level 4) and Arma Delle Manie (Levels VII and II) both dated between MIS 4 and MIS 3, were finally selected as cases of study (Table 8-1 and Figure 8.1).

Table 8-1. Selected archaeological assemblages with the number of Levallois Points (LP) and Convergent Tools (CT) selected for use-wear analysis in this thesis.

Middle Palaeolithic site	Selected archaeological Levels	Relative dating	N. of selected LP and CT
Abri du Maras (Ardèche, France)	Level 4	MIS 4 – MIS 3	LP=51 CT=19
Arma Delle Manie (Liguria, Italy)	Levels II and VII	MIS 4 – MIS 3	LP=40 CT=7

8.1.1 Objectives

The primary objectives during the use-wear examination of the selected archaeological tools of Abri du Maras and Arma Delle Manie were:

- (i) assessing the use-wear traces to interpret the function(s) of the Levallois points (and convergent tools),
- (ii) assessing the presence/absence of stone projectile tools,
- (iii) verifying whether technological tool types may correspond to functional tool types.

A complementary aim was to compare the two selected Middle Palaeolithic sites to provide scope to:

- 1) Compare different environmental regions and geographical zones. Abri du Maras is a valley floor site located in the middle Rhône valley, while Arma Delle Manie is located on a coastal plateau area. These differences offered the possibility of integrating the use-wear results with different paleo-environments, faunal and/or vegetation spectrums, in order to address possible differences in hunting and subsistence strategies among Neanderthals living in different environments.
- 2) Compare subsistence and hunting behaviours across different Middle Palaeolithic sites, e.g. different environment conditions, and various site functions.

- 3) Finally, compare a chronological range of Middle Palaeolithic sites, from end of MIS 5 to MIS 3, to address possible hunting strategies and economic activities.

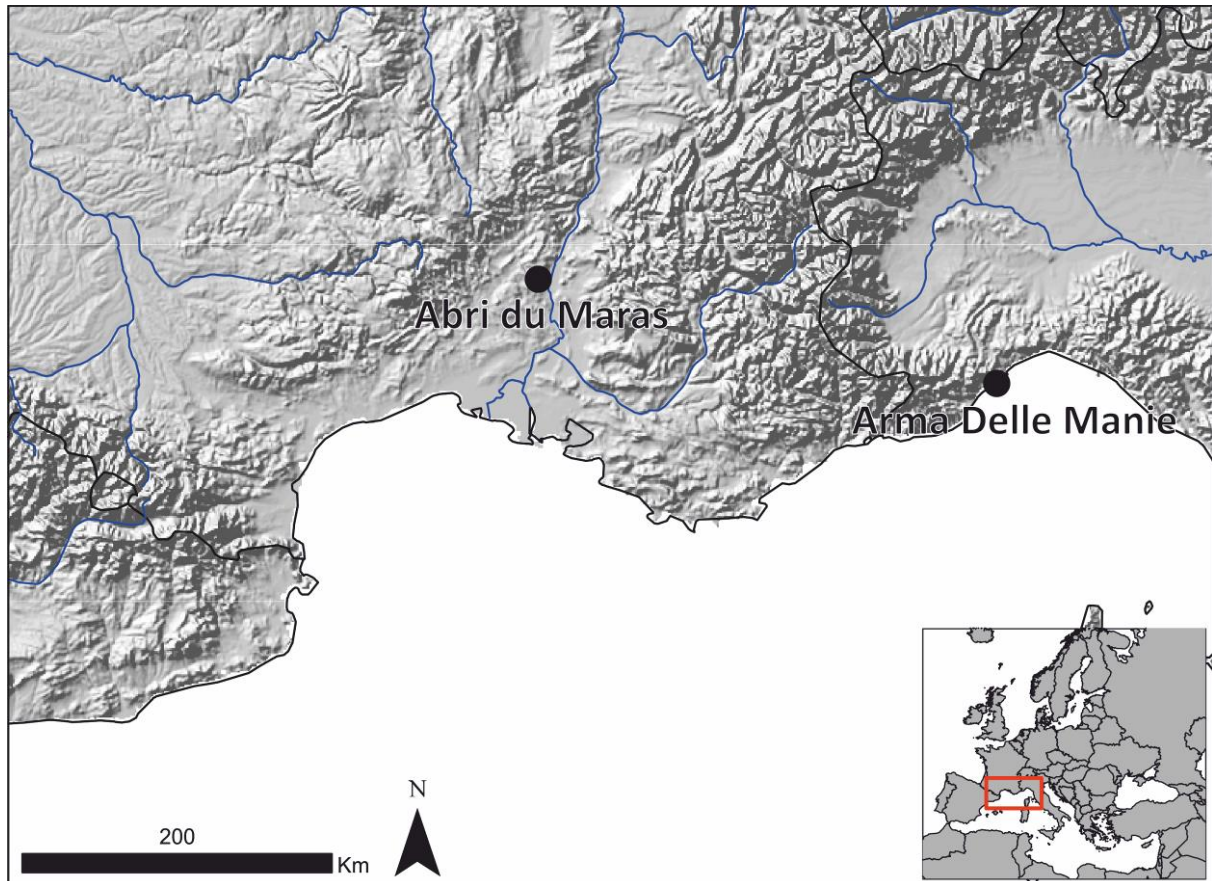


Figure 8.1. Geographic localisation of the selected Middle Palaeolithic archaeological sites, (Map: La Porta and Oyaneder-Rodriguez).

Table 8-2. European Middle Palaeolithic assemblages with significant number of Levallois points (LP), including the archaeological sites selected in this study (in green).

Archaeological site	Total number of LP (% within the site assemblage)	Total number of LP microscopically analysed	Source
Riencourt-les-Bapaume	3 (ND)	-	Goval et al., 2015
Bettencourt-Saint-Ouen	124 (5%)	121	Locht et al., 2003; Goval et al., 2015
Bettencourt-Saint-Ouen (N3)	57 (<2%)	Altered – no analysis	Goval et al., 2015
Therdonne	138 (3%)	119	Coudenneau, 2013
Biache-Saint-Vast (IIa)	5 (ND)	5	Rots, 2013
Fresnoyau-Val (N2)	1 (ND)	1	Goval et al., 2015
Fresnoyau-Val (N1)	13 (ND)	2	Coudenneau, 2013; Goval et al., 2015
Maastricht-Belvédère	137 (including Mousterian points), (2%)	52	Rots, 2016
Sesselfelsgrötte	15 (Mousterian points) (ND)	15	Rots, 2009
Abri Romani	18 (ND)	5 (Gauvrit, 2012)	Gauvrit, 2012; This thesis' data
Abri du Maras	51 (2.4%)	5 (La Porta, 2013); 4 (Hardy et al., 2013)	This thesis' data
Arma Delle Manie	40 (1.72%)	-	This thesis' data

8.2 Arma Delle Manie (Italy)

8.2.1 Introduction to the site

Arma Delle Manie is a Middle Palaeolithic site situated in the Liguria region of northern Italy (Figure 8.2). The region belongs to the northern Mediterranean area. It is surrounded by the Alps to the North and connected to the French Provençal area to the west.

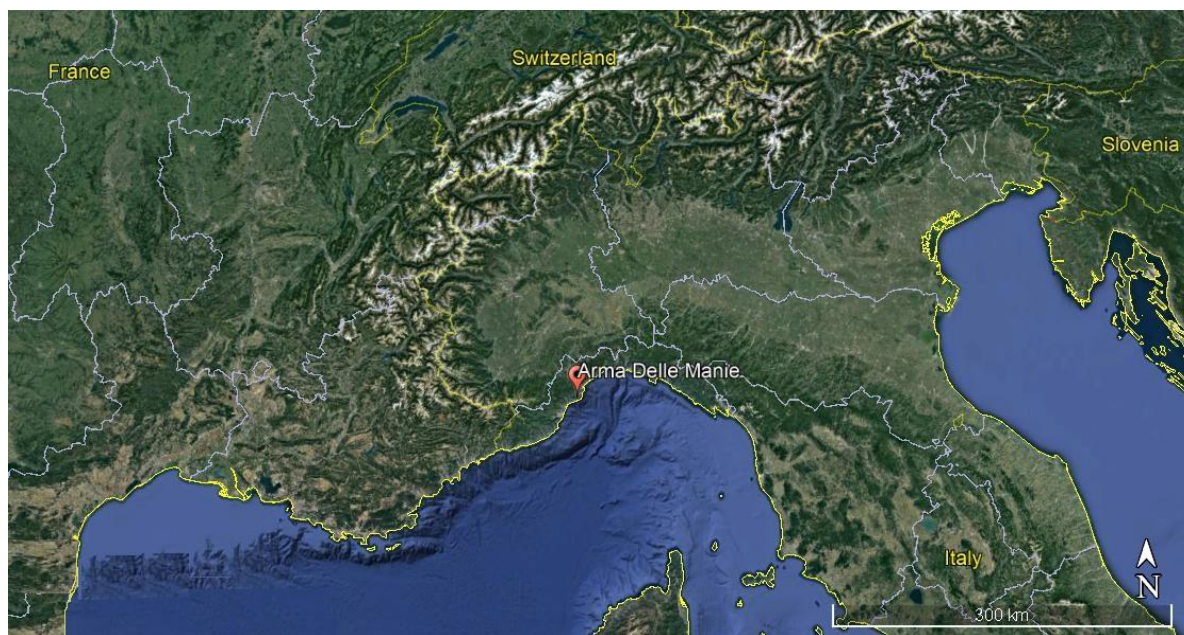


Figure 8.2. Location of Arma Delle Manie site (Italy, Image Google Earth 02-05-2018).

The Arma Delle Manie cave is located on the Manie plateau at 285 m above sea level, near the city of Finale Ligure (Savona; Figure 8.3). The plateau is formed by a geological formation called “Pietra del Finale” or “Finale’s stone” (formed during the Miocene, 20-5 Ma; Comune di Finale report, 2015), which consists of sedimentary carbonate rock, of marine origin, mainly formed from bioclastic limestones, with the limestone showing fragments of fossil remains. The “Pietra del Finale” outcrop forms part of a bigger lithological unit called “Monte Cucco”, which alone represents 90% of the outcrops of the local limestone.

The Arma Delle Manie cave consists of the “Pietra del Finale” formation, which forms the vault of the cave (Figure 8.4), and a Permian schist formation located at the bottom of the cave. The cave is approximately 2 km away from the

present day coastline, and it is situated between two seasonal streams: the Landrassa stream (located hundreds of meters northwest of the cave), and the Manie stream (situated a few hundred meters south of the cave), which both flow in a south-west direction into the Ponci river (Figure 8.3).

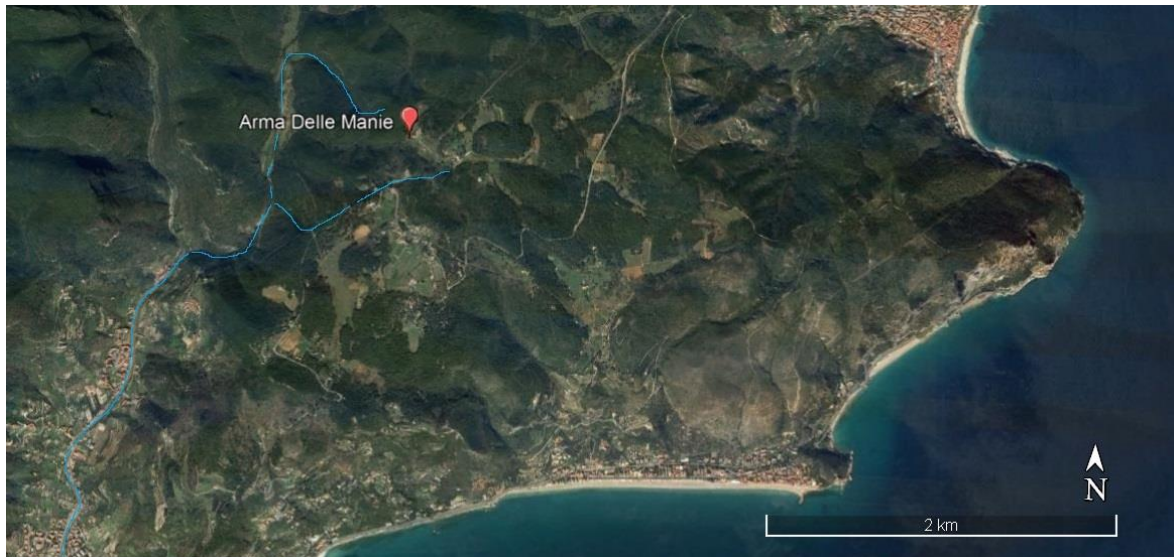


Figure 8.3. The setting of the Arma Delle Manie cave (the location of the waterways is indicated with light blue lines, Image Google Earth 02-05-2018).

The cave is formed of a single large chamber (around 200 m²) surmounted by a large entrance dome facing south, as in prehistoric periods (Leger, 2012) (Figure 8.4). Because of its easy detection within the surrounding landscape, the cave was frequented from Palaeolithic times until the XIX century (during which period it was used as a stable).



Figure 8.4. Arma Delle Manie cave, front-on view from the plateau (Picture La Porta).

The site cave was first noted by G Isetti in 1962 and surveyed by Prof H de Lumley between 1962 and 1965 (Isetti and de Lumley, 1962). From 1968 to 1987 it was systematically excavated by O Giuggiola (Giuggiola and Vicino, 1996). The excavation exposed a complex stratigraphy composed of seven archaeological units (I-VII layers), today dated between MIS 4 and MIS 3/2 (Abbassi, 1999). Since the 1990s, thanks to collaboration between the Soprintendenza Archeologica Della Liguria, the Museo Archeologico del Finale, the Institut de Paléontologie Humaine in Paris, and the Institut de Préhistoire du Lazaret in Nice, there has been an examination of the archaeological assemblages and a programme of accurate radiometric dating (Cauche, 2002; Abbassi, 1999; Mehidi, 2005; Karatsori, 2003). Since 2010, the University of Genova (with Prof F Negrino) and the University of Ferrara (with Prof F Peresani) have undertaken a revised analysis of the archaeological assemblages (Peresani, 2003; Negrino and Starnini, 2010; Santaniello, 2010; Leger, 2012).

8.2.2 Stratigraphy and Chronology

8.2.2.1 Stratigraphy

The cave was used as a shelter and barn in historical times, which caused disturbance of the stratigraphy in the upper levels (Neolithic Levels not included in the actual stratigraphy, and Level I). The main deposits that were recognised belong to three main chronological periods (Figure 8.5; Giuggiola, 1974; Arobba et al., 1976):

- 1) The Neolithic deposits. They have been partially removed due to historical digging, although, traces are still visible from the profile (Figure 8.5). They consisted of pottery and faunal remains incorporated in calcareous sediments, alternating with levels of stalagmites, and the detritus of the roof of the cave that collapsed during Neolithic times.
- 2) The Palaeolithic deposits (Levels II to VII). They were extensively excavated between 1968-1987. They were formed mainly of sand and clay sediments, with abundant stone artefacts and faunal remains (level VII included a large hearth structure; Figure 8.6).
- 3) The sterile bottom of the deposits. It consisted of a stalagmite base, formed by the flowstone and boulders that had collapsed from the vault of the cave.

This image has been removed by the author of this thesis/dissertation for copyright reasons.

Figure 8.5. Arma Delle Manie stratigraphic profile (adapted from Cauche, 2007, figure 10).

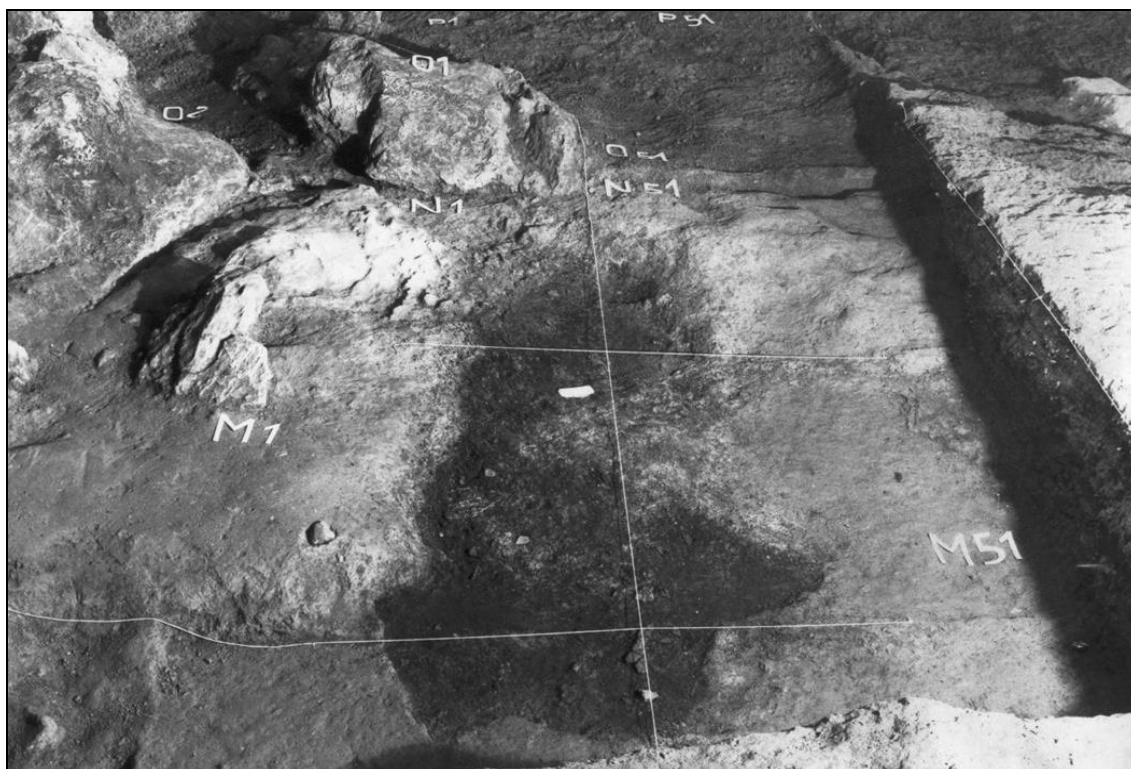


Figure 8.6. Hearth at Arma Delle Manie (Level VII; image reproduced with permission of the Museo Archeologico del Finale).

The archaeological levels, identified during the stratigraphic excavation, were divided into several archaeological units (Giuggiola, 1974; Leger, 2012), as follows (see also Figure 8.5):

- Level I: reddish-brown sandy clay sediment with gravel and clasts. It was reported to contain mixed materials due to trampling activities and to historical use (Giuggiola and Vicino, 1996).
- Level II: reddish-brown sand-less clay sediment rich in gravel.
- Level III: a sandy light-clay with sporadic presence of stones.
- Level IV: hearth level indicated by a burnt clay surface rich in carbon.
- Level V: sandy reddish-brown clay with a few stones and some charcoal sediment.
- Level VI: reddish-brown clay sediment with a sporadic presence of stones.
- Level VII: light red clay sediment with stones, with an increasing presence of blocks at the bottom of the layer.

The entire stratigraphic sequences were deposited on a sterile stalagmite rock base.

8.2.2.2 Chronology

The chronology of Arma Delle Manie site is still under examination (Karatsori, 2003; Mehidi, 2005). Two radiometric methods, U/Th and ESR, have been used to date the stalagmite deposits and the ungulates' enamel teeth (Mehidi, 2005). However, some of the obtained dates were inconsistent with previous paleo-environmental studies and with the general chronology of the site (Negrino, personal communication 2014). Therefore, further analysis will be needed to clarify the precise chronology of the upper levels (Levels IV-II).

U/Th dates on a stalagmite flowstone, located at the very bottom of the shelter (Level VII), gave an age of 82 ± 5.6 BP, corresponding to MIS 5a (Mehidi, 2005). From the bottom of the sequence upwards, combining radiometric and paleo-

environmental dating, a chronological sequence has been proposed as follows (Arobba et al., 1976; Abbassi, 1999; Karatsori, 2003; Mehidi, 2005;), (Table 8-3):

- 4) Level VII is the first layer on top of the stalagmite flow. It started to accumulate around 60 Ka and terminates around 46 Ka (Mehidi, 2005). It was marked by a cool and wet climate, possibly coinciding with the MIS 3-4 transition (Abbassi, 1999; Arobba et al., 1976).
- 5) Levels VI and V were deposited during the MIS 3-4 transition (Mehidi, 2005), in a cold but dry climate (Abbassi, 1999).
- 6) Layer IV is dated to 39 Ka (Mehidi, 2005), during a warmer climatic period within MIS 3 (Abbassi, 1999; Arobba et al., 1976; Karatsori, 2003).
- 7) Level III is dated between 37 and 32 Ka (Mehidi, 2005). It is associated with a cold but moist climate, during MIS 3 (Abbassi, 1999; Arobba et al., 1976; Karatsori, 2003).
- 8) Level II is dated between around 31.5 Ka and 30 Ka, corresponding to MIS 3 (Mehidi, 2005). It is associated with a warm climate (Abbassi, 1999; Arobba et al., 1976; Karatsori, 2003).
- 9) Level I has not been dated due to trampling activities.

Table 8-3. Results of the radiometric and paleo-environmental dating of Arma Delle Manie' archaeological levels (data from Arobba et al., 1976; Abassi, 1999; Karatsori, 2003; Mehidi, 2005).

Archaeological Units	U-Th and ESR/U-Th dating (Mehidi, 2005)	MIS	Paleoenvironmental analysis (Arobba et al., 1976; Abassi, 1999; Karatsori, 2003)	Sub-stage events
Sterile rock: stalagmite base	82±5.6 BP	MIS 5a		
Level VII	60±9 BP	MIS 4-3		
Levels VI-V		MIS 4 – MIS 3?	Presence of <i>Arvicola lacepede</i>	Henrich 5 event around 45 ka (MIS 3)

Level IV		39 Ka MIS 3	Presence of <i>Sicista</i> <i>sp.</i>	Dansgaard-Oeschger 10 and 9 intervals around 40-39 ka (MIS 3)
Level III		37-32 Ka MIS 3		Heinrich 4 event around 38 ka (MIS 3)
Level II		31-30 Ka MIS 3		Dansgaard-Oeschger 5 interval around 30 ka (MIS 3)
Level I	-		-	

8.2.3 Landscape occupation and geological context

During the Pleistocene, the Liguria region was free from the continental ice sheets that periodically covered northern Europe (Del Lucchese et al., 1985), and its calcareous coastline, interspersed with narrow valleys, was densely occupied by human groups. As a result, from the early Middle Palaeolithic onwards, the area was intensively occupied by human groups, both in the caves and on outdoor sites (Negrino and Starnini, 2006, 2010).

Regarding the Middle Palaeolithic, important sites (some with a continuous stratigraphy that goes into the Upper Palaeolithic) are present in the area, such as (from east to west) Grotta Delle Fate (Psathi, 2003), Arene Candide cave (Negrino and Tozzi, 2008), Santa Lucia Superiore cave (Cauche, 2002), Madonna dell'Arma cave (Cauche, 2002), and the Balzi Rossi complex (which includes Barma Grande, Riparo Mocchi, and Grotta del Principe sites, Yamada, 1993; Riel-Salvatore et al., 2013; Figure 8.7).



Figure 8.7. The location of Arma Delle Manie and other key Middle Palaeolithic sites in Liguria (Italy, Image Google Earth 02-05-2018).

The chronologies of these sites, although under revision (Douka et al., 2012; Higham et al., 2009), testify to the presence of Neanderthal groups in the region from MIS 5 to MIS 3 (Negrino and Tozzi, 2008). At Balzi Rossi the lower levels have been dated at MIS 5 (Negrino and Tozzi, 2008; Cremaschi et al., 1991; Isetti et al., 1962). MIS 4 occupation is attested at Grotta del Principe (for example the two hearth structures D and E; de Lumley, 1969), Barma Grande, Madonna dell'Arma (Isetti et al., 1962). MIS 3 occupations are confirmed at Riparo Mochi (Kuhn and Stiner, 1998; Douka et al., 2012) and Riparo Bombrini (Holt et al., 2018). The presence of early or proto-Aurignacian assemblages has been found at Riparo Mocchi and Riparo Bombrini between 39 and 35 BP (Douka et al., 2012; Higham et al., 2014; Benazzi et al., 2015; Holt et al., 2018). The presence of Aurignacian levels (possibly in Levels I and II) at Arma Delle Manie has not been confirmed (Cauche, 2002; Cauche, 2007).

8.2.4 Paleo-environmental data: palynological, sedimentological, and micro-faunal analyses.

Three key fields of research have contributed to reconstructing the paleo-environment and landscape around Arma Delle Manie (Arobba et al., 1976; Abbassi, 1999; Karatsori, 2003; Table 8-4).

Pollen analyses have indicated that the lowest level (Level VII) formed during a cool and humid period featuring a wooded landscape with a deciduous woodland cover, characterised by pine (*Pinus*) and hazel (*Corylus*; Karatsori, 2003; Arobba et al., 1976). Levels VI and V were instead marked by climate cooling, an abrupt decrease of forest taxa and the appearance of a steppe landscape, as suggested by the presence of herbal xenophile taxa (*Artemisia*; Karatsori, 2003). Level IV recorded the coldest phase of the stratigraphy (interpretable as a possible glacial stadial). The landscape around the site in this period was characterised by an open steppe environment in which thermophilic and Mediterranean species retreated in favour of xenophile herbaceous species (Karatsori, 2003). Level III is associated with a climatic improvement, with an increase in the Mediterranean species (*Cistaceae* and *Oleaceae*). This phase was followed by a rapid cooling trend in the upper levels (Level II-I; Arobba et al., 1976).

The woodland species were mainly pine, hazel, cypress associated with oak (in Levels VII-VI), hornbeam and lime trees (in Levels III) (Arobba et al., 1976). Elm, birch and chestnut trees were generally rare (Arobba et al., 1976). *Poaceae* and *Asteraceae* were the main herbal taxa during the cooling periods (Levels V-IV).

The results of micro-faunal assemblage analyses are in accordance with the palynological analysis (Table 8-4), providing more information on the paleoclimate and landscape surrounding Arma Delle Manie (Abbassi, 1999). The presence of *Arvicola*, *Sicista* and *Microtus* species (voles) in the middle layers of stratigraphy (Levels VI-IV) suggests a cold climate period and a possible correlation to MIS 4 (Abbassi and Desclaux, 1996, p. 36), thus

confirming the results of the palynological analysis (Arobba et al., 1976; Karatsori, 2003).

Table 8-4. The main faunal and vegetation taxa in the Arma Delle Manie' archaeological levels.

Arma delle Manie archaeological units	Main faunal taxa	Main vegetation taxa	Climate condition	Source(s)
Level VII-VI	Red deer (<i>Cervus elaphus</i>) – midmountain and forest cover	Pine (<i>Pinus</i>) and hazel (<i>Corylus</i>) – woodland environment	Cold and wet	Arobba et al., 1976; Karatsori, 2003
Level V	Horse (<i>Equus caballus</i>) – grassland	Herbal xenophile taxa (<i>Artemisia</i>) - steppe environment	Cold and dry	Arobba et al., 1976; Karatsori, 2003
Level IV	Aurochs (<i>Bos primigenius</i>) – steppe and open vegetation	Herbal taxa (<i>Artemisia</i>) - open steppe	Cold and dry	Arobba et al., 1976;
Level III	Marmot (<i>Marmota sp.</i>) – warming trend	Mediterranean species (<i>Cistaceae</i> and <i>Asteraceae</i>) – Mediterranean ecotone	Temperate climate	Arobba et al., 1976; Abbassi and Desclaux, 1996;
Level II-I			Cooling trend	Arobba et al., 1976

8.2.5 Faunal assemblage and Taphonomy

Faunal analyses identified the presence of artiodactyls red deer (*Cervus elaphus*), wild boar (*Sus scrofa*), fallow deer (*Dama dama*), roe deer (*Capreolus capreolus*), aurochs (*Bos primigenius*), ibex (*Capra ibex*), carnivores (*Ursus speleaus*, *Ursus arctos*, *Pantera [Leo] spelea*, *Crocuta spelea*, *Canis lupus*, *Vulpes vulpes*, *Mustela nivalis*, and *Meles meles*), perissodactyls (*Stephanorhinus sp.*, *Equus caballus*) and Proboscidea (*Elephantidae indeterminate*; Psathi, 2003; Psathi and Vicino, 2003).

Taphonomic analyses have also emphasised that the archaeological assemblage accumulated mainly due to anthropogenic action, indicated by the limited evidence for carnivore activities. Clear traces of human activities on

carnivore bones (such as cone fractures and cut marks) attest to specific activities such as marrow extraction and de-skinning processes (Valensi and Psathi, 2004; Psathi, 2003), possibly for pelt extraction or opportunistic scavenging.

Red deer are the dominant species in the faunal assemblage of entire sites, followed by roe deer, ibex, horses and wild boar (Psathi and Vicino, 2003). The analysis of the mortality profiles of the herbivores showed a predominance of young adults, especially for red deer (Valensi and Psathi, 2004). Neanderthals at Arma Delle Manie may have followed a specific pattern of red deer transport from kill sites. They transported only the meaty parts (such as upper parts and limb bones) or the entire carcasses without the head (based on the absence of cranial bones) (Valensi and Psathi, 2004). The tooth-eruption and tooth-wear analysis revealed that red deer were mainly killed during later summer and early winter suggesting a seasonal occupation of the cave (Psathi, 2003; Valensi and Psathi, 2004).

Despite the high presence of red deer remains and the selective transportation of animal parts at Arma Delle Manie, Valensi and Psathi (2004, p. 267) interpreted the accumulation of the red deer faunal remains as a living herd profile, excluding exploitation of specific ages or individuals.

The discovery of 8 bone retouchers indicates a bone tool industry at Arma Delle Manie, and the widespread exploitation of available animal resources (Psathi, 2003).

8.2.6 Human remains

A paleo-anthropological analysis conducted on the faunal material in 1998 found four fragmentary cranial remains of Neanderthal: three of these belong to layers I and II, and the last was found in layer IV in the inner part of the cave (Cauche, 2007). A Neanderthal molar was also recovered (Santaniello, 2010, p. 32).

8.2.7 Raw material and Lithic assemblage

The lithic assemblage of Arma Delle Manie was the focus of a previous PhD thesis (Cauche, 2002; Cauche, 2012) and two previous Masters' dissertations (Santaniello, 2010; Leger, 2012). Cauche (2002) performed a comprehensive techno-typological and raw material analysis of the entire stone tool assemblage (Levels I-VII). Santaniello (2011) carried out a technological analysis of the two largest lithic assemblages of the sequence, levels VI-VII; Leger (2002) performed an accurate characterisation and provenance analysis of the lithic outcrops used at Arma Delle Manie, during the occupations of levels V-II.

Comparative studies on the use of raw materials in the Liguria region suggest that Neanderthals used mainly local or regional outcrops, except for jasper outcrops coming from an allochthonous area (Porraz and Negrino, 2008; Negrino and Starnini, 2006). At Arma Delle Manie, the most commonly used lithic raw materials were carbonate rocks. Limestones, dolomites, or mudstones were the main materials in almost all the archaeological levels (Cauche, 2007, figure 20; Leger 2012, figure 3). These were followed in order of decreasing frequency by quartzite (with various different grain sizes), quartz, chert, schist, and rarely jasper (Cauche, 2002; Leger, 2012). Limestones, dolomites, and chert were gathered from local sources less than 5 km from the site, in primary or secondary marine and fluvial deposits (Leger, 2012, p. 55; Figure 8.8). In contrast the micro-quartzite (fine grain quartzite) and silicate limestone pebbles were gathered in specific spots along the western coast (from marine secondary deposits), about 30 km from the site (medium distance; Vicino and D'Errico, 1985; Porraz and Negrino, 2008; Leger, 2012) (Figure 8.8). Jasper tools, occurring mostly in the lower archaeological levels (Level VII mainly) in the form of finished tools, represent less than the 3% of the total raw material (Cauche, 2002, 2007) (Figure 8.8). However, they represent long-range provision, possibly from the Ligurian or Emilian Apennines area, about 100 km away from the site (Porraz and Negrino, 2008) (Figure 8.8). The procurement of the various raw materials at Arma Delle Manie reflects the geomorphological configuration of the region; Neanderthals were experts in the local environment,

and they probably utilised the coastline and the river valleys along an east to west axis, for the sourcing of local and regional rock outcrops (Porraz and Negrino, 2008).

This image has been removed by the author of this thesis/dissertation for copyright reasons.

Figure 8.8. Raw material provenances in the Middle Palaeolithic region of Liguria (from Negrino and Porraz, 2008, figure 1).

8.2.8 Lithic reduction sequences

The upper levels of the site (Levels I, II) are characterised by the presence of laminar products, associated with high frequencies of Discoid and Levallois reduction sequences (Cauche, 2002, 2007; Leger, 2012). These levels were firstly referred to as a possible early Aurignacian techno-complex by G. Vicino (Cauche, 2007, p. 278), but the following technological analyses confirmed the “Mousterian” aspect of the industries (Cauche, 2002; Leger, 2012). The middle levels of the stratigraphy (Levels III-V) show instead high frequencies of centripetal reduction sequences, exploited using mostly Discoid and Levallois methods (Peresani, 2003; Cauche, 2002, 2007; Leger, 2012). The lowest levels (Levels V-VII) have been referred to as “classic Mousterian” (Cauche, 2002), and contain high frequencies of Levallois reduction sequences (Cauche, 2002, 2007; Santaniello, 2010).

Stone tools were generally knapped on the site, as suggested by the presence of the entire “chaîne opératoire” for almost all the different raw materials

(Cauche, 2002; Leger, 2012). Only jasper tools were probably imported as finished products or as small de-cortical cores (Cauche, 2007, p. 276). The index of retouched tools varies between levels, but an increase in the proportion of retouched tools is observed in the lower levels (Levels V-VII; Cauche, 2007, figure 11). The most abundant retouched tools are scrapers and notch tools, while retouched points are rare (Cauche 2002, p. 154). The following is a brief description of the lithic production chains for the various levels (Cauche, 2002, 2007):

- Level VII, VI, V: are very homogeneous and characteristic of the Typical Mousterian. Levels VI and VII show higher frequencies of Levallois reduction sequences compared to the other levels, with centripetal and unidirectional operational schemes, and a tendency to produce larger blanks.
- Level IV: widely used reduction sequences are Discoid with centripetal operational schemes, followed by Levallois reduction sequences (Leger, 2012).
- Level III: characterised by centripetal reduction sequences, mostly Levallois, among which Discoid tools are scarcely recognisable (Cauche, 2002; Leger, 2012).
- Level II: interpreted as in its original stratigraphic position. There is evidence of “opportunistic” blades production, in addition to the presence of centripetal reduction sequences definable as Discoid (Leger, 2012). A sporadic presence of Levallois methods was also observed (Cauche, 2002; Leger, 2012).
- Level I: interpreted as a disturbed level characterised by a mix of laminar tools, associated with Discoid and Levallois tools.

8.2.8.1 Levallois points production at Arma Delle Manie

This section draws on the author’s observations during new field-work (carried out in April 2015) at the Museo Archeologico del Finale (and not available in previous publications).

At Arma delle Manie the previous technological analysis stressed how Levallois points, although spread across all the Mousterian levels, had a higher prevalence in the lower levels of the stratigraphy (Table 8-5). Level VII preserved the highest number of Levallois points and convergent tools recovered (Table 8-5).

Table 8-5. Tools selected for functional analysis according to techno-morphological categories and archaeological level (the frequencies of tool for each level were calculated from the tool totals presented in Leger [2012] and Santaniello [2011]).

Type	Effectives	Archaeological level
Levallois points	16	Level VII
	2	Level VI
	1	Level V
	3	Level IV
	1	Level III
	1	Level II
	2	Level I
	7	Shuffled deposits
Total	33	-

The Levallois points are represented by a small number of tools (n=33). They cover a range of different sizes (e.g. from 30 to 80 mm length, see Appendix F, Volume 2 for techno-morphological attributes) but all have a general convergent morphology (Figure 8.9).

The points were classified following the method presented in Section 8.3.7.1. Two thirds of the Levallois points at Arma Delle Manie were produced by using unidirectional convergent reduction sequences (n=21), which resulted in three-blows point types (Boëda, 1982) with a triangular morphology. Eight points were produced by employing unidirectional longitudinal reduction sequences, which resulted in points with an elongated convergent morphology (Figure 8.9). Only two points were knapped using centripetal sequences, resulting in quite small points (<4 cm length; Figure 8.9). The final two points consisted of proximal fragments for which the reduction sequence was indeterminate (Figure 8.9).

The analysis of the striking platform (butt) of the Levallois points revealed that most of the points (n=20) had a faceted butt, testifying to the preparation of the striking platform. The others displayed either a linear, flat or cortical butt (n=7), indicating that the striking platform was not prepared. For the rest of the points, the striking platform was missing or not determinable.

Levallois points at Arma Delle Manie were sometimes retouched with a short and discontinuous retouch (n=7 tools retouched), among which 3 Mousterian points present a semi-abrupt scalar retouch identifiable as "Quina" retouch (Bordes, 1961, p. 9-10).



Figure 8.9. Example of Levallois points selected at Arma Delle Manie (Image La Porta with permission of Museo Archeologico del Finale).

The dimensions of the Levallois points (length/width ratio, excluding distal or proximal fragments) revealed a linear trend, indicating that the length of the point is generally two thirds of the width.

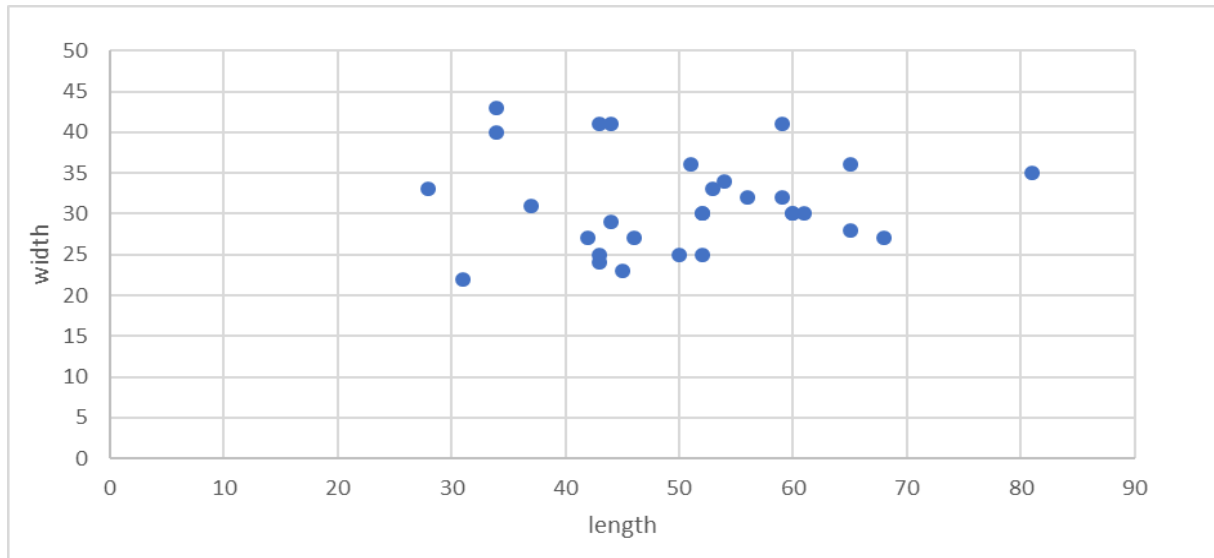


Figure 8.10. Length/width ratio of the selected Levallois points (excluding fragments; n=27) at Abri du Maras.

The Levallois points at Arma Delle Manie were primarily made on fine grain silicified limestone (e.g. limestone and dolomite; n=29), followed by fine grain quartzite (n=11). The raw materials used for the production of the Levallois points reflect the general distribution of the raw materials as observed in the archaeological levels (Cauche, 2002; Leger, 2012). This means that Neanderthals did not select specific raw materials for the production of this specific techno-morphological type of tool (which is believed to be a difficult task, as many professional flint-knappers affirm). Instead, the Neanderthals at Arma Delle Manie adapted their technological savoir-faire to various types of raw materials.

8.2.8.2 TCSA, TCSP, and tip angle values

The analysis of the TCSA and TCSP values (Shea, 2006; Sisk and Shea, 2009; see also Section 8.3.7.1.1) of the Levallois points from Arma Delle Manie (excluding fragments) revealed low values when compared with the archaeological and ethnographic thrusting spear as indicated by Shea (2006, table 1) (Table 8-6). Levallois points' TCSA value at Arma Delle Manie is much lower than the expected

TCSA values of archaeological and ethnographic thrusting spears as indicated by Shea (2006, table 1) (Table 8-6), but it falls between the expected TCSA values of spears tips and the expected TCSA of dart tips, as given by Shea (2006, table 1) (Table 8-6).

Table 8-6. TCSA and TCSP values of the Levallois points from Arma Delle Manie (excluding fragments) compared with TCSA values of ethnographic and experimental projectiles (data from Shea (2006, table 1).

Samples	Mean	SD	Min	Max	n
Manie TCSA	118.45	55	28	231	33
Manie TCSP	92.17	16	66	129	
*All dart tips TCSA (Shea, 2006)	58	18	20	94	40
*Thrusting spear tips TCSA (Shea, 2006)	168	89	50	392	28

The tip angle was calculated for the Levallois points (see Section 8.3.7.1.1). However, the majority of the points (n=25) presented fractures on the distal part of that removed the tip of the tools, and, they were, therefore, excluded from the analysis. As a result, n=6 Levallois points presented tip angles lower than 45°, while n= 9 points presented tip angles larger than 45°.

8.2.9 Type of site and mobility

The regional context of the Ligurian region shows a complex mosaic of Middle and Upper Palaeolithic sites located along the coastal area or in the interior upland valleys (Figure 8.7). During the Middle Paleolithic, these sites show in terms of the production of lithic tools (Bietti and Negrino, 2007; Del Lucchese et al., 2004; Negrino, 2005), and the exploitation of the raw materials (Negrino and Starnini, 2006; Negrino and Tozzi, 2008; Porraz and Negrino, 2008). Moreover, the western Ligurian area appears to be related with the Provencal area (for instance with a connection to the Lazaret and Prince caves), suggested by the presence of a “typical Mousterian” techno-complex (de Lumley, 1976; Cauche, 2002; Porraz and Negrino, 2008). However, there has not yet been a systematic study investigating the mobility strategies of the Neanderthal groups around this geographical area during the

Middle Palaeolithic (but see Porraz and Negrino, 2008; Negrino and Starnini, 2006, 2010).

At Arma Delle Manie the taphonomic analysis shows that the duration of human presence in the cave varied from one layer to another (Psathi and Vicino, 2003, p. 156). Levels VII and II showed repeated occupations but during short seasonal visits. The Neanderthals' occupations in these phases occurred at the end of summer and the beginning of autumn (Valensi and Psathi, 2004, p. 270). It is possible that the site functioned as a seasonal occupation site for the exploitation of animal resources (Psathi and Vicino, 2003, p. 156), and/or as interception point for animal migrations (i.e. hunting stop-camp; see CHAPTER 11). The location of the cave, in the Manie' plateau and near waterways, may have been an optimal observation and sighting point to intercept herds of animals during seasonal migrations. It is also interesting to note that Neanderthal groups at Arma Delle Manie may have systematically exploited red deer, importing only selected animal parts into the cave (Psathi, 2003). However, this has not been interpreted as a monospecific exploitation of red deer species but as unselective killing of mixed herd of red deer (cf. Valensi and Psathi, 2004, p. 259).

8.3 Abri du Maras (Ardèche, France)

The Abri du Maras rock-shelter is located on the right bank of the middle Rhône valley, in a small valley adjacent to the Ardèche river, a tributary of the Rhône River (Figure 8.11 and Figure 8.12). The Rhône Valley is a strategic corridor that connected the Massif Central area (in the West) to the Alps region (in the East), linking the Mediterranean regions with the North of Europe (Figure 8.12). The area is renowned for the presence of several Palaeolithic sites, including the Chauvet Cave, located 32 km from the site and the *Gorges D'Ardèche* National Park.

The Abri du Maras rock-shelter was first identified and excavated by R Gilles and J Combier in the 1950s and 1960s, eight archaeological units described (Combier, 1967). Since 2006, new excavations carried out by Prof MH Moncel have better clarified the stratigraphy and excavated extensive areas of the site.



Figure 8.11. The location of the Maras rock-shelter in the valley. The arrows indicate the directions from the site to the Ardèche River and to the plateau (Image Google Earth 18-03-2018).

This image has been removed by the author of this thesis/dissertation for copyright reasons.

Figure 8.12. The location of Abri du Maras site and the main Middle Palaeolithic sites along the Middle Rhône Valley (south-eastern France). The extension of the Massif Central and Alps areas are shown in grey (from Daujeard et al., 2012, figure 1).

8.3.1 Stratigraphy

The new archaeological excavations, commenced in 2006 and still ongoing, have identified a total of six stratigraphic units (Levels 1-6; Moncel et al., 2017), ().

The excavation extends over a surface of 60 m² (Moncel et al., 2017). In 2006 a trench of 6 m² was opened on the east side of the site to identify the general stratigraphy and context (Figure 8.13). In 2010, it was extended by 34 m² to identify the upper limit of Unit 4 (Level 4.1; Figure 8.13), (Moncel et al., 2010). The excavation continued on the eastern part of the site (24 m²) to depict the lower limit of Unit 4 (Level 4.2) and to expose Unit 5 (Moncel et al., 2017), (Figure 8.13; years 2011-2013). The excavations are focusing on Units 4 and 5 which are two well-preserved occupation levels (Figure 8.13; years 2013-2016).

This image has been removed by the author of this thesis/dissertation for copyright reasons.

Figure 8.13. Extension and progression of the Abri du Maras' excavation from 2006 to 2016 (from Moncel et al., 2017, figure 7).

Six stratigraphic units have been found and defined as follows (Moncel et al., 2012; Moncel et al., 2017), (Figure 8.14):

- Level 1 shows a dark-brown clay matrix with numerous gravel clasts, and some limestone slabs (level thickness 30 cm);
- Level 2 shows a light clay matrix with many pebbles and abundant stones, as a result of the collapse of the ceiling (level thickness 50 - 100 cm);

-
- Level 3 shows small pebbles in a brown sand-silty matrix (level thickness 25 cm),
 - Level 4 is a silty and sandy-silty sedimentary thick accumulation, which is divided into two sub-levels: Level 4.1 and Level 4.2 separated by sterile loess layers. Both sub-levels 4.1 and 4.2 correspond to two preserved human occupation levels. The sedimentary analysis shows that the Level 4 was affected by moderate pedological actions, mostly earthworm and biogenic redistribution of calcium carbonate (Daujeard et al., 2017, p. 4). Sub-level 4.1 is a homogeneous level with aeolian deposits of loess (from the wind erosion of the fluvial terraces of the middle Rhône valley; Nowak, 2013), and presence of coarse fragments due to the frost shattering of the rock-shelter walls. It contains abundant archaeological artefacts, fragments of charcoal, and ashy lens from hearth structures (Moncel et al., 2017, p. 35). The level thickness at the present moment ranges between 50 – 100 cm, covering an excavated area of 50 m² (Moncel et al., 2017, p. 32). Sub-level 4.2, sealed on the top by sterile loess deposits, is a second preserved silty and sandy level rich in archaeological remains.
 - Level 5 preserves red silty sediment thicker than 1.50 m. It is divided into two sub-levels: 5 and 5bis (still under excavation), both preserving evidence of human occupation.
 - Level 6 lies at the bottom of the stratigraphic profile, and preserves mostly sterile red silty sediments (still under excavation). During the last excavation (season 2017) a new stratigraphic unit (Level 7) was detected at the bottom part of the sequence (Moncel et al., 2017). This new discovery is not included in the stratigraphic sequence (Figure 8.14).

**This image has been removed by the author of
this thesis/dissertation for copyright reasons.**

Figure 8.14. The stratigraphic sequences of Maras shelter (modified from Richard et al. 2015, figure 2; and Moncel et al., 2012, figure 5).

8.3.2 Chronology

The human occupation layers at the Abri du Maras site were dated using various methods (TL, ESR, 14C, U-Th; Moncel and Michel, 2000; Richard et al., 2015). U-Th dating of faunal bones indicated ages of 89 ± 4 and 91 ± 4 BP (MIS 5) for Level 5, and 72 ± 3 , 87 ± 5 (MIS 4) for Level 4 (Moncel and Michel, 2000) (see also Table 8-7). However, new ESR/U-Th series dating on ungulate teeth confirmed the age of Level 5 at 90 ± 9 BP but provided more recent dates for Level 4 (Richard et al., 2015), (see Table 8-7). Level 4.1 is now dated between 40 ± 3 and 46 ± 3 BP (MIS

3), while samples from level 4.2 provided ages ranging from 42 ± 3 to 55 ± 2 BP (also MIS 3), (Richard et al., 2015), see Table 8-7.

The new chrono-stratigraphic range of the Abri du Maras site provides evidence of Neanderthal occupation from the end of MIS 5 until the beginning of the last glaciation at MIS 3.

Table 8-7. Results of the radiometric dating of Level 4 and Level 5 of Abri du Maras site (data from Richard et al., 2015; Moncel and Michel, 2000).

Archaeological Unit	U-Th dating (Moncel and Michel, 2000)	MIS	ESR/U-Th dating (Richard et al., 2015)	MIS
Level 4.1	72 ± 3 BP	MIS 4	40 ± 3 BP 46 ± 3 BP	MIS 3
Level 4.2	87 ± 5 BP	MIS 5 (b)	42 ± 3 BP 55 ± 2 BP	MIS 3
Level 5	89 ± 4 BP 91 ± 4 BP	MIS 5 (c-b)	90 ± 9 BP	MIS 5 (c-b)

8.3.3 Landscape setting & raw material sources

The middle Rhône valley played an important role in the peopling processes of the region. The favourable climatic and environmental conditions, with different ecotones, refuge areas and the presence of rivers, gorges and plateaus, favoured human occupation during the Middle and Upper Pleistocene.

Along the Rhône valley and its tributaries, several Middle Palaeolithic sites were identified as follows (Moncel, 2005, 2008; Moncel et al., 2010; Daujeard and Moncel, 2010; Moncel and Daujeard, 2012), (Figure 8.12):

- From North to South: Abri Moula, Payre, Pêcheurs, Figuier, and Maras rock-shelters,
- At East: Orgnac 3 open-air site and Baume Flandin cave.

The sites are located along the Rhône corridor (near the river banks), and on the Massif Central area (Figure 8.12). Most of the sites are rock-shelters or cave sites and only a few open-air sites are known (Bernard-Guelle et al., 2006). Regionally,

the chronology of the Rhône Valley sites indicates a Neanderthal occupation from MIS 8/7 (for example unit F of Payre; Moncel et al., 2008) until MIS 3 (Moncel and Michel, 2000; Moncel et al., 2008; Valladas et al., 2008; Daujeard and Moncel, 2010; Richard et al., 2015).

8.3.4 Paleo-environmental data: faunal, charcoal and isotopic analyses.

Recent multi-stranded archaeological research (palaeontological, charcoal, ecological and isotopic analyses) has provided a precise picture of the regional paleo-environment and landscape framework of the Abri du Maras site (Daujeard, 2008; Daujeard and Moncel, 2010; Moncel and Daujeard, 2012; Daujeard et al., 2012; Daujeard et al., 2017).

The presence of a sterile layer of loess between sub-level 4.1 and 4.2 indicates that the site was not occupied during cooler periods (Daujeard et al., 2017, p. 4; Nowak, 2013; Puaud et al., 2015). The micro-fauna, although poorly preserved, is represented by voles (*Microtus sp.* and *Arvalis agrestis*) which indicates an open environment and dry climate condition, at least for Level 4 (Daujeard et al., 2017, p. 17). Pollen is rarely preserved.

In Level 5 the presence of species such as red deer (*Cervus elaphus*), roe deer (*Capreolus capreolus*) and wild boar (*Sus scrofa*) indicate a temperate and humid climate condition and a forested environment (Daujeard, 2008; Daujeard and Moncel, 2010; Daujeard et al., 2017), (Figure 8.15 and Table 8-8). The presence of taxa such as reindeer (*Rangifer tarandus*), horse (*Equus sp.*), and bison (*Bison sp.*) indicate a cooling trend and the emergence of an open steppe vegetation for Level 4 (Figure 8.15 and Table 8-8). Isotopic results from animal bone collagen of the ungulates species of Level 4 confirm the lack of extensive woodland cover and a grass-dominated environment (Daujeard et al., 2017, p. 11). Charcoal analyses have found the presence of three different taxa in Level 4: birch (*Betula*), pine (*Pinus sylvestris*), and legume family (*Fabaceae*) species. These taxa grow under cold and dry conditions confirming the cooling trend of Level 4 (Daujeard et al., 2017, p. 17).

Table 8-8. The main herbivores and vegetation species presented at Abri du Maras Level 4 and 5.

Abri du Maras Level	Main faunal taxa	Main vegetation taxa	Climate condition
Level 4 *MIS 3	reindeer, horse, bison	birch, pine, Fabaceae	cold and dry with open steppe environment
Level 5 *MIS 5	red deer, roe deer, wild boar	under analysis	temperate and humid condition with forested environment



Figure 8.15. Primary herbivores taxa present in Level 4 and 5 of Abri du Maras (pictures from reindeer <https://www.pbs.org/newshour/science/7-things-didnt-know-reindeer> [last accessed 08-10-2018]; horse <https://en.wikipedia.org/wiki/Horse> [last accessed 08-10-2018]; bison <http://www.ambisonsociety.org/> [last accessed 08-10-2018]; roe deer <https://www.woodlandtrust.org.uk/visiting-woods/trees-woods-and-wildlife/animals/mammals/roe-deer/> [last accessed 08-10-2018]; wild boar <https://blogs.fco.gov.uk/leighturner/2017/05/15/an-encounter-with-a-viennese-wild-boar-wildschwein/> [last accessed 08-10-2018]; red deer <http://www.yorkshirecoastnature.co.uk/blog/290/a-royal-occasion> [last accessed 08-10-2018]).

8.3.5 Faunal assemblage at Abri du Maras

Recent analysis shows a sophisticated pattern of subsistence strategies and land use among the Neanderthals occupying the Abri du Maras rock-shelter and the surrounding region (Moncel, 2005; Raynal et al., 2005; Daujeard and Moncel, 2010; Moncel et al., 2010; Daujeard et al., 2012; Daujeard et al., 2017).

At Abri du Maras several faunal taxa are present. For instance: horses (*Equus cf. germanicus* and *Equus hyndruntinus*), wild boars (*Sus scrofa*), red deer (*Cervus elaphus*), roe deer (*Capreolus capreolus*), reindeer (*Rangifer tarandus*), steppe bison (*Bison priscus*), ibex and (*Capra ibex*), (Daujeard and Moncel, 2010, table 4). The cervids are the most abundant species (around 67% of total identifiable faunal assemblage). Horses (*Equus cf. germanicus* and *Equus hyndruntinus*) are the second most dominant class of fauna identified.

Carnivore tooth marks are low (less than 2% of the total remains), and there are no carnivore remains, which suggests that faunal accumulation is due mainly to hominin activities (Daujeard and Moncel, 2010, p. 376; Daujeard et al., 2017, p.21).

At Abri du Maras the animal carcasses were processed outside the site, and only the best anatomical parts (upper and lower limbs) were selected and imported into the site (selective transport), as is confirmed by the total absence of animal skulls and phalanges (see also Daujeard, 2008; Daujeard and Moncel, 2010; Daujeard et al., 2017). However, butchering cut marks and fracture analyses indicate that animal carcasses or significant anatomical portions have been skinned, filleted, and dismembered *in situ* (Vettesse et al., 2017). Long bones, once transported to the site, were broken and possibly boiled to extract the marrow or used as fuel (Vettesse et al., 2017, p. 160).

Thirteen bone retouchers were identified at the site (Daujeard et al., 2014, figure 6-8).

8.3.5.1 Faunal analysis of Level 4

Recent studies suggest that the accumulation of herbivores at Abri du Maras level 4 is due to hominid exploitation and hunting activities (Daujeard, 2008; Daujeard and Moncel, 2010; Daujeard et al., 2017).

At Abri du Maras Level 4 the most abundant species is reindeer (88%), followed by horse (8%), giant deer (1.5%), bison (0.7%), red deer (0.5%), ibex (0.3%), and lagomorphs (1%), (Daujeard et al., 2017, table 3). The identification of a few teeth of bison (*Bison priscus*) indicates the presence of this animal on the site. Fish bones and fish scales were recovered during the excavation of Level 4 (Moncel et al., 2017). Chub (*Squalius cephalus*) and perch remains (*Perca sp.*) (both common fish species of the Ardèche river) may indicate fishing activity (Daujeard et al., 2017, p. 10).

The recovery of high number of reindeer remains (88% NISP 1033, and 16 MNI; Daujeard et al., 2017, table 3) from Maras Level 4 have been interpreted as monospecific exploitation of reindeer by Neanderthals (Daujeard et al., 2017). The age distribution analysis of the reindeer individuals showed a predominance of young adult reindeer. Taking into account the period of death (estimated based on an analysis of tooth eruption period) and the results from cementum-chronology, it appears that the majority of reindeer (and also horses) died during late summer or early autumn. This period corresponds to the seasonal reindeer fall migration when animals have accumulated fat reserves after summer feeding (Daujeard et al., 2017, p. 14). Furthermore, the analysis of butchering traces and skeletal portions indicate that only the upper and lower limbs were introduced into the site, suggesting selective butchering activities and selective transport strategies (Daujeard et al. 2017, p. 14).

In conclusion, the combination of the zooarchaeological remains and tooth microwear analyses indicate that at Abri du Maras Level 4 Neanderthals were explicitly exploiting reindeer in short-term hunting activities focusing on the migratory season of the reindeer herds, and possibly practising cooperative hunting strategies (Daujeard et al., 2017).

8.3.6 Raw material and lithic assemblage

Petrographic analysis (Fernandes et al., 2008) of the flint artefacts of Abri du Maras shows a great variety of knappable raw materials with local or regional outcrop origins.

At the Abri du Maras shelter, the primary raw material used for the production of stone tools was flint (90% total lithics). It was exploited as tabular fragments, nodules and pebbles (60-90mm length). The flint was collected either from local sources up to the Gorges plateau (less than 5 km away from the site) or from the small watercourses surrounding the site (Moncel et al., 2014, p. 192). Flint sourced from outcrops located a medium distance away (around 20 to 35 km away) was also identified (Figure 8.16), (Moncel, 2003; Moncel et al., 2014, p. 192). Blanks or big flakes from (>6 cm) allochthonous flint types (probably from Alpine outcrops) were also found, but they are generally rare (Moncel and Combier, 1990). Quartz, quartzite and basalt are also represented in the assemblage (<10%). These materials were imported into the site in the form of nodules collected from the Ardèche River or on the Gorges plateau (Moncel and Combier, 1990; Moncel et al., 2014, p. 193).

Neanderthals at Abri du Maras were collecting what they found on their surrounding landscape following an opportunistic but also flexible gathering strategy. In fact, they were able to take advantage of the different raw materials (not only rocks but also organic materials, see Hardy et al., 2013) that were available in multiple local and regional outcrops, without the need to seek specific types of high-quality knappable rocks (Moncel et al., 2014, p. 202).

**This image has been removed by the author of
this thesis/dissertation for copyright reasons.**

Figure 8.16. The localisation of the different flint types found at Abri du Maras within the local and regional context (from Moncel et al., 2014, figure 21).

8.3.7 Lithic reduction sequences

Lithic production at Abri du Maras has been the focus of intensive research (Moncel, 1996, 2005; Hardy et al., 2013; La Porta, 2013; Moncel et al., 2014).

High levels of elongated stone tools characterise the upper units (Levels 1-3). The elongated supports are produced employing either Levallois methods (with unidirectional and bidirectional schemes) or longitudinal volumetric reductions (Moncel, 1996, 2005).

Level 4 is dominated by Levallois reduction sequences (including both sub-levels 4.1 and 4.2). The most abundant tools are: elongated Levallois flakes (Levallois blades), Levallois points, Levallois predeterminant and preferential flakes. Generic flakes and debris (<5 mm, which indicate *in situ* retouching activities) are also produced (Moncel et al., 2014), (Figure 8.17). The presence of complementary reduction sequences is confirmed by Kombewa and Discoid (also defined as pseudo-Levallois) flakes (Moncel et al., 2014, p. 184). At Level 4, blades were produced with Levallois or unidirectional core reduction sequences (Moncel et al., 2014). Levallois points were produced using a wide range of reduction sequences (mainly unidirectional

convergent) and operational schemes (La Porta, 2013; La Porta et al., 2015; see also Section 8.3.7.1), (Figure 8.17). Stone tools are mostly not retouched; only 4% have marginal retouch (Moncel et al., 2014, p. 188). The absence of big cores (>10 cm) and the analysis of refitting show that not all the stages of the “*chaines opératoires*” were present on the site. Two main types of “*chaines opératoires*” were undertaken by Neanderthals at Abri du Maras (Moncel et al., 2014, p. 192):

- *intra-site* reduction sequences which provided small-medium (<6 cm) tools such as Levallois points, blades, flakes, Kombewa and Discoid flakes,
- *extra-site* reduction sequences which provided large blades, large Levallois points (>6 cm), and some cortical flakes.

Level 5 (still under examination so that lithics were not available for analyses) shows the persistence of Levallois reduction sequences, but with the intensification of Quina methods and higher percentages of Quina retouched tools (Raynal et al., 2012; Moncel and Daujeard, 2012, p. 112).

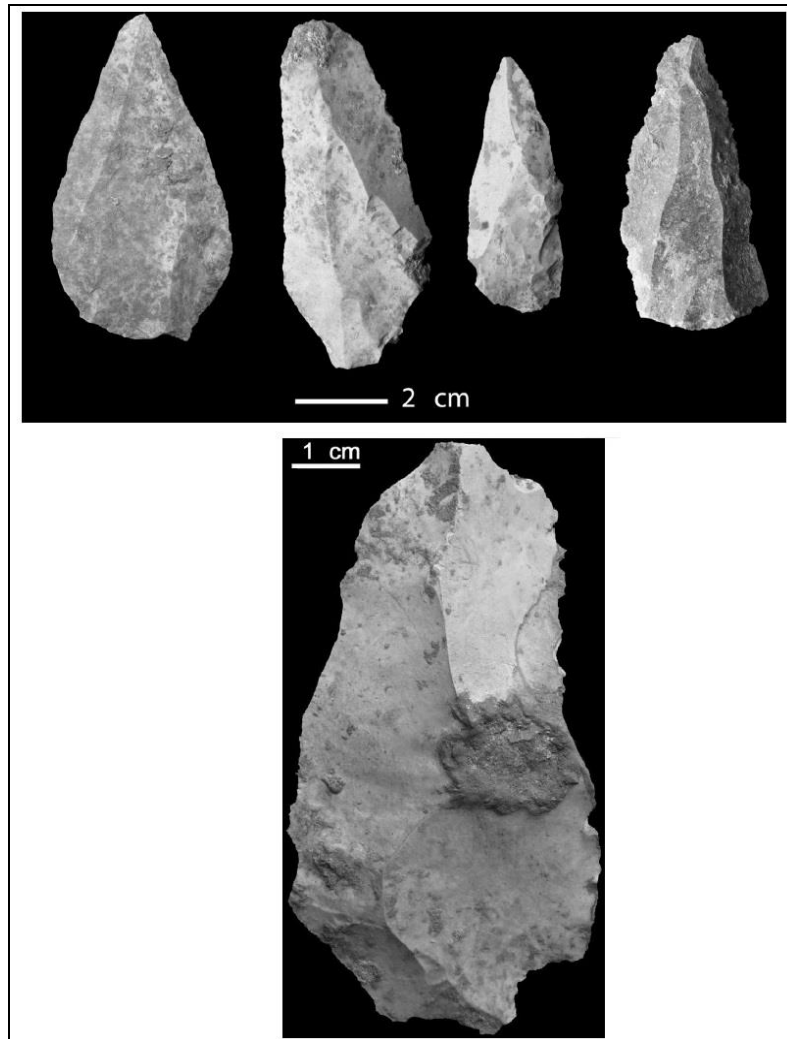


Figure 8.17. Levallois points and Levallois preferential flakes (from Moncel et al., 2017, figure 29).

8.3.7.1 Levallois points at Abri du Maras Level 4 (sublevels 4.1 and 4.2)

The techno-morphological analysis of the Levallois points of Abri du Maras Level 4 was the focus of the author's MA dissertation (La Porta, 2013; see also Moncel et al., 2014; La Porta et al., 2015), of which the following section presents a summary updated with work undertaken during this study.

Levallois points represent a small proportion of the entire assemblage of Level 4 (2.3%; see Table 10-1). Various morphology, size, elongation and cross-sectional profiles were preserved (see Appendix G, Volume 2 for techno-morphological attributes).

The Levallois points were classified into three groups depending on the direction of the removals (La Porta, 2013; Moncel et al., 2014):

- (i) unidirectional, when negative removals follow the direction of the technological axis of the tool,
- (ii) bidirectional, when the negatives are opposite the striking platforms,
- (iii) orthogonal-peripheral, when the negative removals come from the edges of the core or are perpendicular to each other.

They were obtained by employing five main operational schemes, such as Levallois unidirectional convergent, Levallois unidirectional longitudinal, Levallois bidirectional, Levallois peripheral and Levallois orthogonal-peripheral operational schemes (La Porta, 2013; Moncel et al., 2014; La Porta et al., 2015). The main reduction sequences used to produce the Levallois points were Levallois unidirectional sequences (67%), followed by peripheral (13%), centripetal (5%) and bidirectional (5%) sequences. Eleven different techno-morphological types of Levallois points were described (Figure 8.18; La Porta, 2013). The most recurrent type was a Levallois point formed by a base triangle and two convergent lateral negatives, defined as a “three-blows” point (Boëda, 1982, table 4; see also Figure 8.18.a).

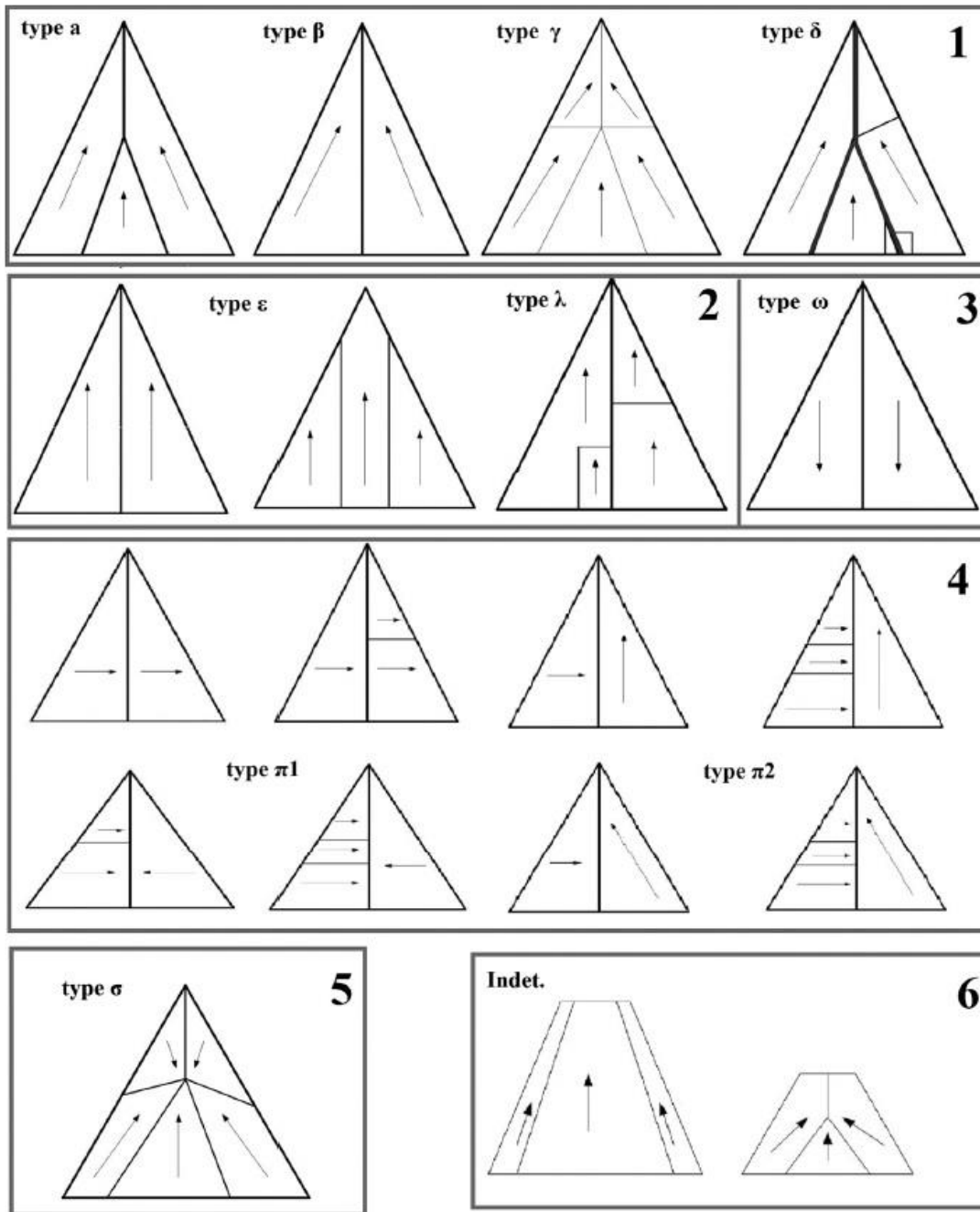


Figure 8.18. The eleven techno-morphological types of Levallois points recognised at Abri du Maras (from La Porta, 2013, figure 11).

The Levallois points presented non-standardised shapes (La Porta, 2013), ranging from triangular to lanceolate silhouettes (La Porta, 2013; Figure 8.19).

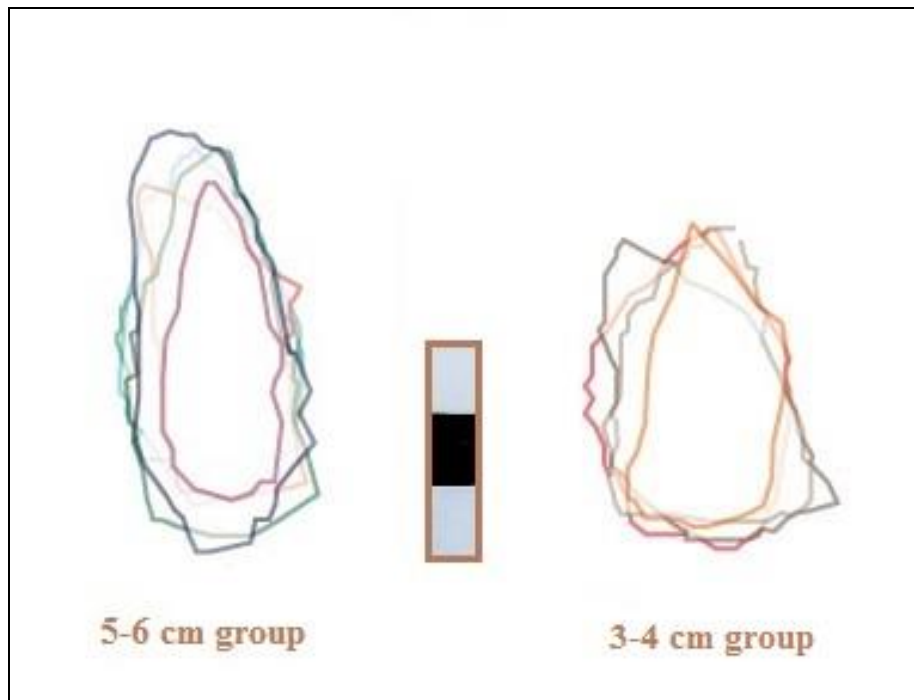


Figure 8.19. Overlaps of the silhouettes of two dimensional groups of Levallois points (from La Porta, 2013, figure 15).

The analysis of the striking platform (butt) of the Levallois points revealed that most of the points (n=36 points) had a faceted butt, indicating the preparation of the striking platform. The other points displayed linear or flat butts (n=15) for which the striking platform was not prepared (La Porta, 2013).

Almost all Levallois points at Abri du Maras level 4 were unretouched. Only 5 points present a lateral semi-abrupt marginal retouch which did not modify the original shape of the point.

The dimensional analysis of the Levallois points (length/width ratio, excluding distal or proximal fragments) revealed a curvilinear trend with two dimensional classes of Levallois points (Figure 8.20):

- small-medium Levallois points (40-60mm),
- large and elongated Levallois points (superior to 60 mm), which were longer but not significantly wider.

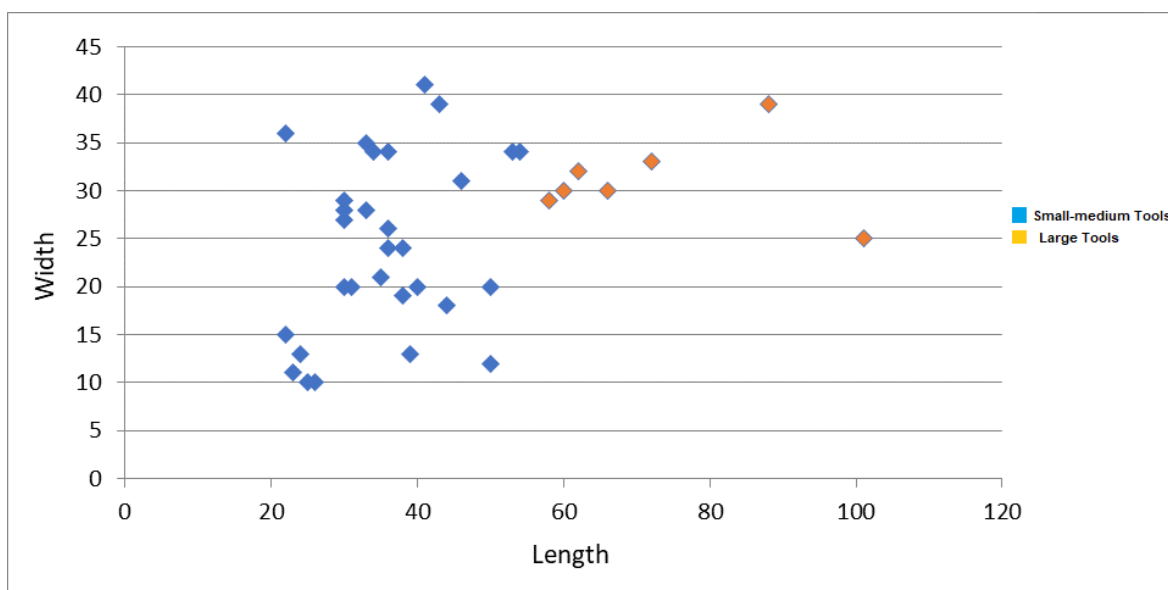


Figure 8.20. Length/width ratio (mm) of the Levallois points at Abri du Maras.

The analysis of the raw materials revealed that all Levallois points were made of flint. The flint came from a local-regional context and was gathered within a 30 km radius from the site (see Section 8.3.6). The weight of the points was not recorded due to a desilicification processes that may have altered the original weight of the tools.

8.3.7.1.1 TCSA, TCSP, and tip angle values

TCSA and TCSP (Shea, 2006; Sisk and Shea, 2009) were calculated as expressed in Section 3.3

At Abri du Maras, the Levallois points (n=51) exhibited a TCSA mean value of 124.20 mm (Table 8-9), which is lower than the expected TCSA values for archaeological and ethnographic thrusting spears as indicated by Shea (2006, table 1) (Table 8-9). It ranges between the expected TCSA values of spears tips and the expected TCSA of dart tips, as given by Shea (2006, table 1), (Table 8-9).

Table 8-9. TCSA values of the Levallois points from Abri du Maras (excluding fragments) compared with TCSA values of ethnographic and experimental projectiles (data from Shea, 2006, table 1).

Samples	Mean	SD	Min	Max	No.
Maras TCSA	124.20	82.54	13	370	51
*All dart tips (Shea, 2006)	58	18	20	94	40
*Thrusting spear tips (Shea, 2006)	168	89	50	392	28

The tip angle was also calculated for all the Levallois points. The tip angle was here defined as the angle of the distal intersection between the two convergent edges of the point (Figure 8.21). The angle was measured with a goniometer (each measurement was repeated three times to ensure the protocol). N=30 Levallois points presented tip angles lower than 45°, while n=21 Levallois points presented tip angles larger than 45°, confirming that the majority of points have a tip angle that tends to be acute (Figure 8.21).

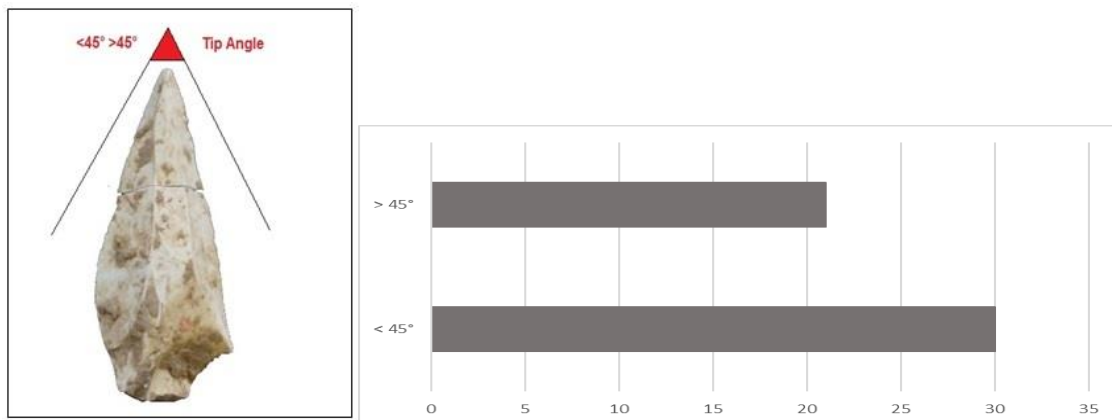


Figure 8.21. Tip angle measurement of the selected convergent stone tools.

8.3.7.1.2 In situ or extra situ production

The techno-morphometric analysis of the Levallois points was also oriented on identifying the “*chaines opératoires*” employed for the production of the Levallois points and describing the origin and position of the points within them (La Porta, 2013). The analysis of cores revealed that Levallois cores are rare at Abri du Maras Level 4 (Moncel et al., 2014). Most of the Levallois cores were of small-medium

dimensions (between 20- and 60-mm in diameter). Only some nodules and plaquettes presented dimensions superior to 60 mm, but they were rare (La Porta, 2013; Moncel et al., 2014).

The majority of the Levallois cores were made on large, cortical flakes (flake-cores). Two types of Levallois cores were identified (Moncel et al., 2014):

- Levallois preferential flake cores (exploited using unidirectional longitudinal, centripetal and bidirectional schemes), to produce small-medium (20-60 mm length) Levallois supports,
- Levallois points cores (using mainly unidirectional convergent schemes), to produce small-medium (20-60 mm length) Levallois points.

All the cores are only minimally scarcely exploited before being discarded. In fact, lateral and central core convexities were not re-installed, and the core platforms were poorly prepared. This suggests that Levallois sequences were not recurrent (Böeda 1996), but were oriented to the obtainment of preferential Levallois flakes and points (La Porta, 2013; Moncel et al., 2014). However, for large cores (> 60 mm diameter), it was not possible to determine whether the negative removals corresponded to a single phase of extraction or if it was anticipated by other phases of extraction and re-preparation of the core convexities (La Porta, 2013; Moncel et al., 2014).

The analyses of the entire core assemblage and refitting (carried out by Dr ME Chacòn) revealed the presence of other reduction sequences (or débitage methods) such as Discoid and Kombewa methods (Moncel et al., 2014). This also indicated that two types of cores were found *in situ* (Moncel et al., 2014):

- small cores and cortical core-flakes (not > 60 mm) used for the extraction of Levallois supports and Kombewa flakes,
- and fragments of thin slabs or nodules (not > 60 mm) for the extraction of Discoid flakes or occasionally Levallois supports.

These data confirm that the Levallois points superior to 60 mm were not produced *in situ*, but were imported from outside the site (Moncel et al., 2014; see also Böeda,

1994). This implies that some of the Levallois points were transported to the site by Neanderthals. The transport of the Levallois points from outside the site indicates that these tools were curated and maintained by Neanderthal as part of their mobile toolkit. Thus, a functional analysis of these tools was essential to understand the function of the Levallois points within the Neanderthal toolkit and to investigate the relationship between the shape of these artefacts and their function.

8.3.8 Type of site and mobility strategies

The regional context of the middle Rhône valley and the Massif Central region shows a multifaceted pattern of Neanderthal mobility strategies, characterised by long-term campsites, short-term hunting campsites and stopover occupations (Moncel, 2003; Raynal et al., 2005; Moncel et al., 2010; Daujeard and Moncel, 2010; Moncel and Daujeard, 2012; Daujeard et al., 2012; Daujeard et al., 2017). This type of logistic organisation of the territory for the middle Rhône Valley has been described as a far-sighted circulating model (Daujeard and Moncel, 2010, p. 385). Here, stopover campsites were located in-between long-term residential sites, while short-term hunting camps were present in refuges or ecotone boundaries (Daujeard and Moncel, 2010; Moncel et al., 2010). Moreover, it has been proposed that Neanderthals might have organised circular, seasonal movements between the long-term residential campsites located on the valley floor of the Rhône river and the mid-mountain sites of the Massif Central area (Daujeard et al., 2012), occupied during the most favourable period of the year for short periods of time (Daujeard et al., 2012; Moncel et al., 2010; Raynal et al., 2005).

Occupation at Abri du Maras Level 4 indicated regular short-term hunting episodes for the exploitation of reindeer herds, during seasonal fall migration (Daujeard et al., 2017, p. 21). This scenario might suggest that Neanderthals at Abri du Maras during MIS 4-3 were practising collective, planned and regular hunting activities for which the use of hunting weapons (such as wooden and stone-tipped spears) would have been an aid both for confrontational and pursuit hunting strategies (see also CHAPTER 11).

Therefore, the type of occupation and strategies undertaken by Neanderthal at Abri du Maras Level 4 (and the taphonomic conditions of the archaeological site) validates the selection of this archaeological site as one of the primary case studies to fulfil the objectives of this thesis.

CHAPTER 9

ARMA DELLE MANIE (LIGURIA, ITALY): USE-WEAR RESULTS OF LEVALLOIS POINTS AND CONVERGENT TOOLS.

The Arma Delle Manie' assemblage has been selected for the use-wear examination of the archaeological Levallois points since it furnished a relatively high number (n=40) of Levallois points. The Levallois points at Arma Delle Manie (plus a few selected Mousterian points, see Table 9-1) represented the 1.73% of the entire stone tool assemblage (Table 9-1). This is a percentage in line with other western European Middle Palaeolithic sites that, between MIS 5 and MIS 3, showed percentages of Levallois points between 2% and 3% of the assemblages (see for instance, Goval et al., 2016, p. 15). Moreover, previous technological studies at Arma Delle Manie had reported the presence of possible diagnostic impact fractures on the Levallois pointed tools (Peresani personal communication, 2013). However, since no use-wear investigation was previously effectuated, this study aimed to undertake the first use-wear analysis of the Levallois points of Arma Delle Manie in the attempt (i) to assess the functionality of this techno-morphological type, (ii) to verify the possible presence of projectile tools within the Levallois point assemblage, (iii) to assess a possible relationship between shape and function.

9.1 Archaeological dataset

The Arma Delle Manie collection is stored at the Museo Archeologico del Finale in the medieval town of Final Borgo (Savona, Italy). The archaeological collection could not be transported outside of the museum or to any other Italian research institution due to the regulations of the Soprintendenza Archeologia, Belle Arti e Paesaggio per la città Metropolitana di Genova e le province di Imperia, La Spezia e Savona²⁷. All the analyses were thus carried out by the

²⁷ The author's permission to access the archaeological stone tool collection of Arma Delle Manie is attached in the USB Stick.

author at the Museo Archeologico del Finale²⁸ during two fieldwork seasons (4 weeks in total, funded by the AHRC SWW DTP). A Dino-lite Edge AM7915MZT portable digital microscope (10x ~ 220x) was purchased (funded by the Department of Archaeology, University of Exeter) and was used for microscopic examinations (see also Section 2.2.5.3).

The aims of the first fieldwork season (April 2015) were:

- Confirm the number of Levallois points within the assemblage of Arma Delle Manie.
- Verify the potential of the Levallois point assemblage for use-wear analysis (e.g. the degree of post-depositional alterations, museum curation practices, and the variety of, and differences in, the raw materials).
- Perform a technological analysis of the convergent tools.

The aim of the second fieldwork season (April 2017) was to undertake and complete the use-wear examination of the Levallois points (and selected convergent tools, see below) selected during the first fieldwork season.

9.1.1 Sampling and procedure of analysis

At the Museo Archeologico del Finale, the stone tools of Arma Delle Manie were stored in wooden drawers, either in separate plastic bags or collectively in cardboard containers. In order to detect and select the Levallois points (see Annex B for definitions), the entire stone tool assemblage was reviewed (more than 10,000 artefacts). A total of n=33 Levallois points and n=7 fragments of Levallois points, retrieved from different archaeological levels, were finally found and sampled for technological and functional analyses (Figure 9.1, Table 9-1 and Annex B). However, during the selection, other types of convergent tools were observed, i.e. n=7 Mousterian points (see Annex B for definitions) present

²⁸ The Museo Archeologico del Finale kindly provided the facilities for the study of the stone tool collection and an ultrasonic tank for the enactment of cleaning protocols. The collection was accessible from 10am to 12am and from 2pm to 4pm, Tuesday to Saturday.

in the assemblage also showed macroscopic fractures visible to the naked eye. A decision was therefore made to include these nominated tools in the sample selected for functional analysis (Figure 9.1 and Table 9-1).

The final selection thus included n=33 Levallois points (see Annex B, Volume 2 for definitions), n=7 proximal fragments of Levallois points, and n=7 Mousterian points (see Annex B, Volume 2 for definitions),): a total of 47 convergent tools coming from different archaeological levels (Figure 9.1 and Table 9-1).

For simplicity, the selected tools have been defined below as “convergent tools”.



Figure 9.1. Example of the selected convergent tools. A: Levallois point. B: proximal fragment of Levallois points. C: Mousterian point (see Annex B for definitions).

Table 9-1. Types and frequencies of convergent tools selected at Arma Delle Manie for techno-functional analyses. The tools were divided by their archaeological levels (stone tools' number per level were calculated from Cauche, 2007, table 4).

Techno-morphological types	Selected tools	No. of tools per Level (debris flakes and cores not included)	Frequencies 0.00%
Levallois points	33		/
Level VII	16	819	1.95%
Level VI	2	109	1.83%
Level V	1	216	0.46%
Level IV	3	367	0.81%
Level III	1	74	0.27%
Level II	3	1124	0.26%
Tools with no indication of the stratigraphic position	7	/	/
Mousterian points	7		
Level VII	4	819	0.48%
Level VI	2	109	1.83%
Level V	1	216	0.46%
Fragment of Levallois points	7		
Level VII	3	819	0.36%
Level VI	1	109	0.91%
Level IV	1	367	2.07%
Level II	2	1124	0.17%
Total	47	2709	1.73%

After the selection, the convergent tools were examined in order to record their techno-morphological attributes into a database and to describe their position in the chaîne opératoire (see Appendix F, Volume 2). They were also checked for post-depositional alterations (e.g. chemical and mechanical alterations; see Section 9.1.2). The convergent tools were then photographed, cleaned, and inspected for functional analysis.

The tools were cleaned for 10 minutes in an ultrasonic bath containing demineralised water and 5% *Derquim* detergent (phosphate free; see Section 3.2), rinsed with fresh water and air-dried. Alcohol or acetone was used locally if a specific trace included bright or dirty spots that scattered the LED light of the portable microscope and prevented a precise observation. Only two specimens were ultrasonically cleaned with a 10-minute bath in pure acetone, to remove the traces of the marking lacquer. No chemical cleaning (such as HCl or NaOH acids) was applied.

The functional analysis was performed using a Dino-lite Edge AM7915MZT portable digital microscope (10x ~ 220x) mounted on a manual stand (Dino-lite RK-10 stand). The stand allowed the user to adjust the final focus and improved the positioning of the tool during the analysis (Figure 2.5). However, it must be noted that the maximum magnification allowed by the Dino-lite Edge AM7915MZT portable microscope was 220x²⁹, which did not always permit the identification of the different polish types and/or attributes. Pictures were taken with the Dino-lite microscope at different magnifications (from 10x to ~220x). Pictures with different depths of field were merged using the Extended Depth of Field automatic setting on the Dino-lite Edge microscope.

The interpretation of the tools' functions was based on multiple lines of evidence. The observed wear traces were compared with the experimental collection of Levallois points presented in this thesis (see CHAPTER 6), a more extensive experimental use-wear collection based at the Department of Archaeology at the University of Exeter, and previously published functional studies (Keeley, 1980; Anderson-Gerfaud, 1981, 1990; Moss, 1983a; Fischer et al., 1984; Plisson, 1985; Vaughan, 1985; Mansur-Francomme, 1986; Beyries, 1987a; Van Gijn, 1989, 2010; Geneste and Plisson, 1989, 1990; Levi-Sala, 1996; Lombard, 2005a; Lombard and Pargeter, 2008; Rots, 2010, 2016; Pargeter, 2013; Pargeter et al., 2016; Sano et al., 2016).

²⁹ The 220x magnification of the Dino-lite Edge AM7915MZT portable microscope corresponded to the 85x magnification of the Olympus BX60 metallographic microscope located at the University of Exeter – Department of Archaeology.

9.1.2 State of preservation of the selected convergent stone tools

Archaeological stone tools can be affected by post-depositional alterations (e.g. chemical or mechanical alterations), excavation practices, or erroneous curation processes (e.g. storage, marking, incorrect cleaning) that can cause evident alterations on the stone tool's surfaces (Keeley and Toth, 1981; Van Gijn, 1989, p. 50-56; Beyries, 1990; Lemorini et al., 2006; Venditti et al., 2016). The risk is, of course, to misinterpret the traces left by post-depositional processes as traces of utilisation (see also Section 2.6). However, this possibility can be reduced by surveying the surfaces of the stone tools for post-depositional alterations, prior to performing a functional analysis (Van Gijn, 1989; Burroni et al., 2002; Lemorini et al., 2006).

Because of this, before conducting the use-wear examinations, the entire sample of convergent tools was examined under the naked eye and at low magnifications (up to 80x with the Dino-lite Edge AM7915MZT microscope) to assess the state of preservation of the stone tool sample. This included the assessment of the degree of intensity of any chemical and mechanical alterations of the selected convergent tools (Table 9-2).

Post-depositional alterations were divided into chemical, mechanical, and discovery modifications (see below). Each alteration found on the tools was described and recorded into a database. Tools affected by post-depositional alterations were divided into three categories: preserved, low-altered, and mostly-altered (as presented in Table 9-2). Only tools that were unaffected (i.e. 'preserved') or subject to low post-depositional modifications (i.e. 'low-altered') were finally selected for use-wear examinations (see below).

9.1.2.1 Chemical alterations

Patination

The main chemical post-depositional alteration detected on the selected sample of tools was the presence of a white patination layer which covered the surface of some of the stone tools (Figure 9.3). The patina layer consisted of minute bright crystals that scattered the light creating an almost white coloured

appearance (Figure 9.4). The silica crystals that composed the white patina (Schmalz, 1960; Rottländer, 1975) presented a granular, coarse, and reflective quality under the Dino-lite microscope (Figure 9.4). This reflective effect was moderated, however, using a built-in adjustable polariser included in the Dino-lite Edge AM7915MZT microscope model. This reduced the reflection of the patina and created a better contrast. The white patina formation occurred in various degrees which were classified into three categories: non-patinated tools (none or sporadic presence of patination), lightly patinated tools (<50% of the tools' surface), and mostly patinated tools (>50% of the tools' surface) (Figure 9.2 and Table 9-2). Among the selected sample (n=47 tools), 11 convergent tools (23.40% of the sample) showed a lack of white patina, 19 convergent tools (40.42% of the sample) showed a low degree of white patina, and 17 convergent tools (36.17% of the sample) showed a high degree of white patina (Figure 9.2). Tools affected by high patination levels (i.e. 'mostly patinated' n=17 tools; Figure 9.2) were not included in the functional analysis or alternatively functional analysis focused mainly on macroscopic use-wear observation (Table 9-2 and Table 9-3).

Acid holes

The stereoscopic observation of the sample also led to the identification of what have since been defined as "acid holes" (Figure 9.5). In the past, previous researchers examining the assemblage had in fact employed a HCl solution for distinguishing limestone from dolomite raw materials (5% in Leger, 2012, p. 49; Santaniello, 2010, but % not reported; and other scholars during post-excavation activities but % unknown, Arroba, 2014, personal communication). This HCl solution was generally dropped onto the central ventral face of the tool, away from the edges (Leger, 2014, personal communication). However, as the stone artefacts were not cleaned after the drop of HCl solution was applied, the acid solution penetrated the rock and, over time, slightly corroded the stone surface, creating small microscopic hollows or depressions (Figure 9.5). The microscopic depressions or "acid holes" were observed only on n=2 tools of the selected sample (4.24%), and they were generally located on the internal ventral surface, away from the edges (Figure 9.2).

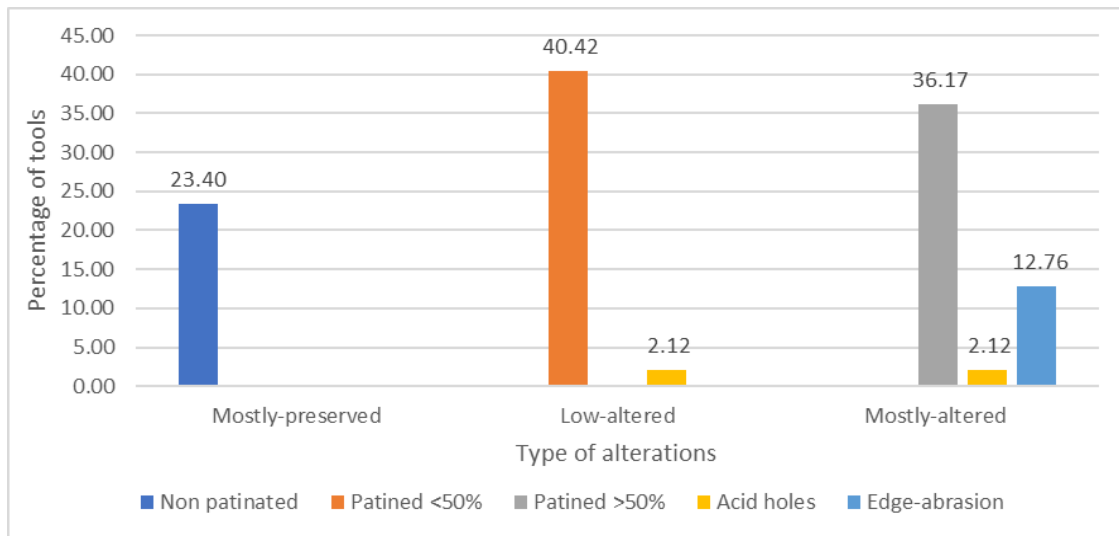


Figure 9.2. Degree of preservation of the selected convergent tools of Arma Delle Manie (n=47).

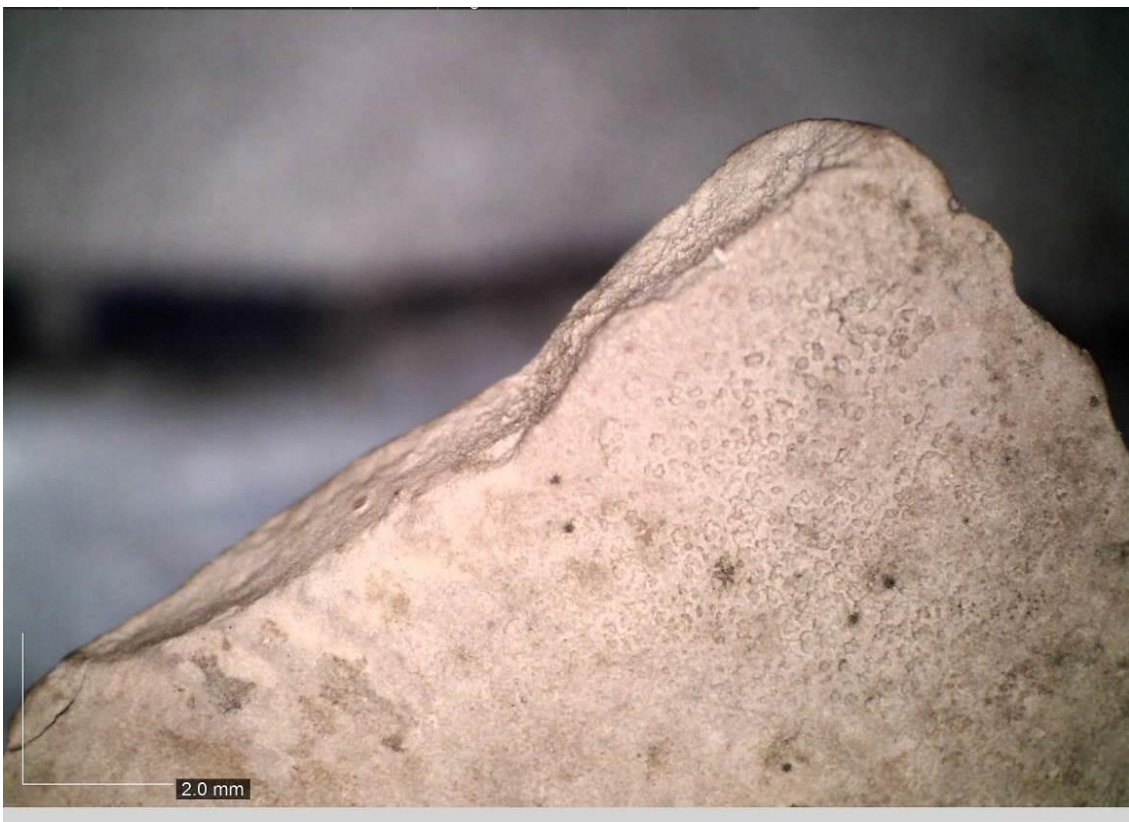


Figure 9.3. White patina and abrasion of the edges. Example of “mostly patinated” tool, DM OM 25x (Tool ID #12 A 23-1967).

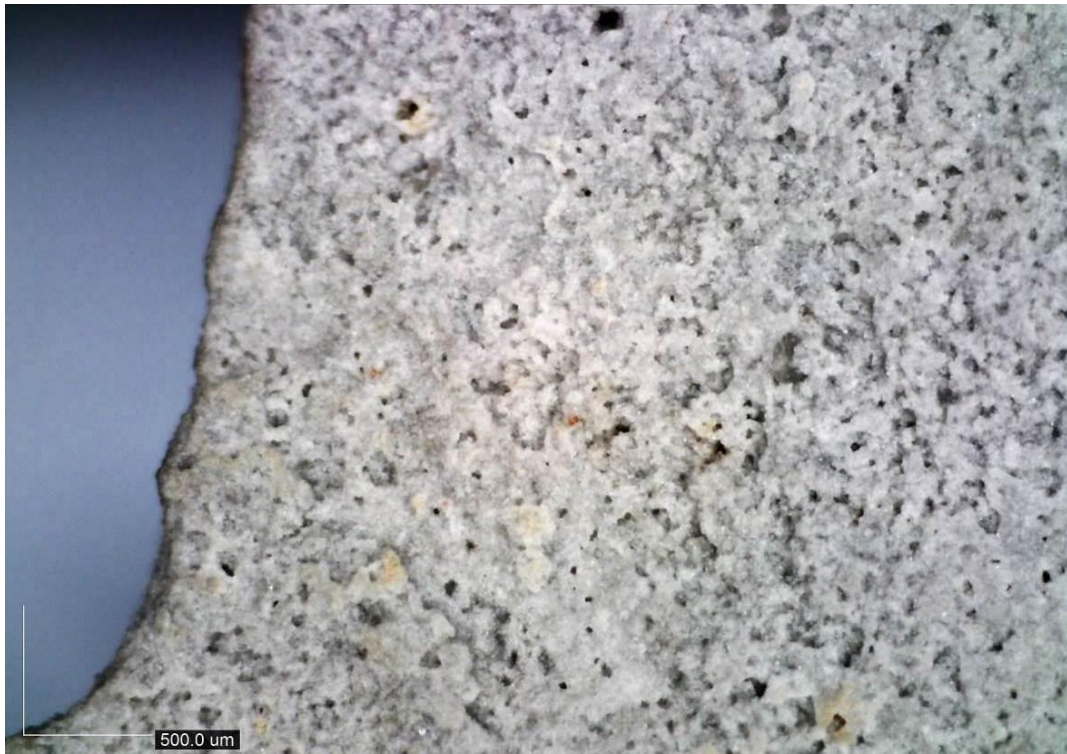


Figure 9.4. The granular and coarse aspect of the white patina at 100x, DM OM 100x (Tool ID #12 A 23-1967).



Figure 9.5. Acid hole created by the corrosion of the stone surface, DM OM 135x (Tool ID #VII 1880).

9.1.2.2 Mechanical alterations

Mechanical post-depositional alterations, such as trampling, scratches, cracks, rounding, and edge abrasion, are often randomly distributed over the lithic surface and located on the prominent topographic areas of the artefact (Shea and Klenck, 1993).

Edge abrasion

At Arma Delle Manie, the majority of the selected tools showed an absence of the mechanical alterations outlined above. Only a few stone tools (n=6, 12.76% of the sample) demonstrated both a high degree of patination and edge abrasion (as, for instance, in Figure 9.2 and Figure 9.6). The patination, edge abrasion, and surfaces of limestone and dolomite tools were most likely caused by weathering processes (i.e. chemical dissolution due to acid water percolating into the sediment). Therefore, the tools affected by this type of mechanical alteration, also highly patinated (Figure 9.2), they were not included in the final sample for functional analysis (Table 9-2).

Trampling

Trampling traces (in the form of edge-damage or fractures) were not observed on the selected convergent tools of Arma Delle Manie. The sample of archaeological tools did not suffer mechanical alterations that could have produced fractures or edge-damage traces that mimicked diagnostic impact traces or could have removed diagnostic traces from the artefacts.



Figure 9.6. Encrustations, edge abrasions, and patination phenomena, DM OM 95x (Tool ID #I2 A 23-1967).

9.1.2.3 Curation traces

Very few tools (n=2) displayed traces of ink and lacquer from the previous marking of the tools (Figure 9.7). The ink and lacquer, when present, was removed with 5 minutes of treatment in an ultrasonic bath of pure acetone. A few of the other tools (n=3) displayed traces of graphite from drawings, which was removed either in an ultrasonic bath of water and 5% *Derquim* detergent or localised acetone dropping.



Figure 9.7. Traces of lacquer and sticker, DM OM 13x (Tool ID #rem C 51-70).

9.1.2.4 Final considerations

The initially selected sample of convergent tools (n=47 in total) showed varying degrees of preservation. N=11 tools of the selected sample were well preserved and did not show any traces of post-depositional alterations. They were classified as mostly-preserved (Table 9-2). N=19 tools presented a low degree of alteration, in the form of a slight presence of white patina. However, this did not affect the preservation of the edges. They were classified as low-altered (Table 9-2). N=17 tools showed a high degree of post-depositional alterations, consisting of white patina, sporadic encrustations, and traces of mechanical alteration (such as ancient trampling or edge abrasion; Table 9-2). They were classified as mostly-altered (Table 9-2). The high degree of alteration on these artefacts limited the possibility of undertaking a detailed microscopic examination, as possible utilisation traces (such as polishes, striations, bright spots, and edge-rounding) could have been completely obliterated by the alterations. Therefore, the n=17 tools, affected by high degrees of post-

depositional alterations (i.e. mostly-altered, Table 9-2), were excluded from further use-wear examination (Table 9-3).

The remaining sample of convergent tools (n=30, Figure 9.2 and Table 9-2) was well preserved or only slightly altered (i.e. low-altered). Therefore, given the general absence of post-depositional alterations, macroscopic and microscopic use-wear analyses were undertaken. The use-wear analysis initially focused on the identification of macroscopic use traces (such as fractures, DIFs, edge-rounding, and macroscopic hafting traces), which are less affected by chemical alterations. Subsequently, for those artefacts without post-depositional alterations (i.e. n=18 out of a total of 30; Table 9-3), the functional examination also focused on the identification of microscopic traces, such as polish, striations, and bright spots (Table 9-3).

Table 9-2. Degree of post-depositional alterations affecting the convergent tools of Arma Delle Manie (n=47).

Intensity of post-depositional alterations		
Mostly-preserved	Low-altered	Mostly-altered
Non-patinated - No presence of white (or glossy) patina. No mechanical abrasion or trampling.	Lightly patinated - Some areas of the tool were sporadically patinated, while the other areas appeared "fresh" (not patinated). No mechanical abrasion or trampling.	Mostly patinated - Patination covered most areas of the tool. Encrustations were sporadically observed. Mechanical abrasion and trampling were detected.
N=11 tools (23.40%)	N=19 tools (40.42%)	N=17 tools (36.17%)

9.1.3 Final sample

All of the selected convergent tools (n=47) were scrutinised for technomorphological attributes (Table 9-3). Among the selected sample (n=47), n=17 tools featured intense post-depositional alterations (e.g. total patination, encrustations, edge abrasion, and/or weathering) which prevented the observation of any possible use-wear traces (i.e. tools "mostly-altered" in Table 9-2). These tools were discarded from the functional analysis and analysed only technologically. Therefore, only the remaining 30 tools were examined both

under low-power (10x ~ 80x) and high-power (100 ~ 220x) magnifications (Table 9-3). Among the n=30 tools, high-power analyses (80x ~ 220x magnification) were successful on n=18 tools, which displayed preserved microscopic traces of utilisation.

Table 9-3. The total number of selected convergent tools examined divided by the analytical approaches used.

Arma Delle Manie	Technological analysis only	Detailed macroscopic use-wear analysis (low-power 10x ~ 80x)	Detailed microscopic use-wear analysis (high-power 80x ~ 220x)
No. of convergent tools analysed	47	30	30 (18 positively analysed)

The functional results presented below are based on the observation and interpretation of macroscopic traces (such as edge-damage, fractures, DIFs, and macro edge-rounding; see Section 2.4) in association with microscopic traces (such as polishes, MLITs, striations, edge-rounding, and bright spots; see Section 2.5), where these were still preserved on the artefacts, of n=30 convergent tools.

9.2 Functional results

Seeing as the archaeological collection of Arma Delle Manie could not be transported elsewhere, all microscopic pictures presented in this chapter were taken with the Dino-lite Edge AM7915MZT portable digital microscope (10x ~ 220x). It is therefore important to note that the microscopic pictures taken sought to maximise the settings and the functionalities of the portable piece of microscopic equipment. However, given the limit of the Dino-lite Edge AM7915MZT portable digital microscope (e.g. the resolution of 5 megapixels - 2592x1944 pixels, the maximum magnification of 220x30, and the built-in LED lights; see also Section 2.2) the pictures had to balance the information given by the use-wear trace (through the choice of balanced magnifications) with the best possible image quality.

9.2.1 Macroscopic analysis

The post-depositional alterations on the sample examined for use-wear (n=30) did not limit the identification of macroscopic use-wear traces. Given the absence of mechanical alterations along the edges (of the selected sample tool), edge-damage, fractures, DIFs, and macro edge-rounding were well preserved.

9.2.1.1 Type and frequencies of fractures

The selected convergent tools showed a high frequency of fractures. N=21 tools (70% of the selected sample) showed the presence of fractures (Table 9-4). Among these, diagnostic impact fractures (DIFs) were observed on 18 tools (among the 30 selected, 60%; Table 9-4).

³⁰ The 220x magnification of the Dino-lite Edge AM7915MZT portable microscope corresponded to around 95x magnification of the Olympus BX60 metallographic microscope located at the University of Exeter – Department of Archaeology.

Table 9-4. Type and frequencies of fractures observed on the selected convergent tools of Arma Delle Manie (n=30). Note: the fracture numbers and frequencies refer to fracture counts, not tools with fractures (more than one fracture can occur on a tool).

Type of fractures	Arma Delle Manie	
	No. of fractures (%)	No. of tool with traces (% out of n=30)
Bending fractures	44 (61.97%)	13 (43.33%)
Step	14 (19.71%)	11 (36.6%)
Hinge	7 (9.85%)	4 (13.3%)
Feather	10 (14.08%)	7 (23.3%)
Snap	13 (18.30%)	13 (43.3%)
Primary Burination fractures	2 (2.81%)	2 (6.66%)
Spin-off fractures	27 (38.02%)	
Unifacial/bifacial Spin-off	16 (22.53%)	13 (43.3%)
Burination Spin-off	11 (12.67%)	7 (23.3%)
Total Fractures	71 (100%)	
Total DIFs (step-terminating bending, unifacial/bifacial spin-off, burination spin-off, and primary burination fractures)	43 (60.56%)	
Total tools with fractures		21 (70%)
Total tools with DIFs (step-terminating bending, unifacial/bifacial spin-off, burination spin-off, and primary burination fractures)		18 (60%)
*Microscopic impact linear traces (MLITs)	6	5
*edge-damage (scars)	76	19 (63.3%)

The majority of the DIFs were unifacial or bifacial spin-off fractures which departed from previous fracture lines (Table 9-4 and Figure 9.9). Spin-off fractures are secondary fractures, considered highly diagnostic of projectile impact (Fischer et al., 1984; Dockall, 1997; Lombard, 2005a; Lombard and Pargeter, 2008; Sano, 2009; Villa et al., 2009a; Iovita et al., 2014; see Section 2.4.1 for definition). A length marker of 6mm was originally considered diagnostic of the difference between spin-off fractures resulting from trampling

(<6mm) and hunting (>6mm; Fischer et al., 1984; Lombard, 2005a). However, recent experiments have shown that the length of the fracture depends on the morphology and size of the tool (Pargeter et al., 2016), and that spin-off fractures <6 mm can also be generated in hunting experiments (Pargeter, 2013), as also observed on the experimental Levallois points used in throwing and thrusting activities which have been presented in this thesis (see Section 6.2.2). Therefore, the analysis of the archaeological convergent tools selected at Arma Delle Manie included all spin-off fractures, regardless their fracture length. As a result, unifacial or bifacial spin-off fractures (of different lengths) were observed on 13 tools (among the 30 selected, 43.3%; Table 9-4, Figure 9.8, and Figure 9.9).

Burination bending fractures, which are fractures departing from an edge or surface but terminating always at an edge, are also considered diagnostic of projectile impact (Fischer et al., 1984; Odell and Cowan, 1986; Caspar and De Bie, 1996; Dockall, 1997; Crombé et al., 2001; Lombard, 2005a). In this thesis, primary burination fractures have been differentiated from secondary burination fractures, which are defined as spin-off burination fractures (see Section 2.4.1.3; Coppe and Rots, 2017). Both types of fractures were observed on the selected convergent tools of Arma Delle Manie (Table 9-4, Figure 9.8, and Figure 9.9). Primary burination fractures were observed on 2 tools (among the 30 selected, 6.6%; Table 9-4, Figure 9.8, and Figure 9.9), whereas, secondary spin-off burination fractures were observed on 13 tools (among the 30 selected, 43.3%; Table 9-4, Figure 9.8, and Figure 9.9).

The selected convergent tools at Arma Delle Manie also showed high frequencies of bending fractures (Table 9-4 and Figure 9.8). In the category of bending fractures, step-terminating bending fractures are considered diagnostic of projectile impacts (Fischer et al., 1984; O'Farrell, 2004; Lombard, 2005a; Lombard and Pargeter, 2008; Lazuén et al., 2012; but see Iovita et al., 2014). Step-terminating bending fractures were the most recurrent type of bending fractures on the selected tools of Arma Delle Manie (Table 9-4, Figure 9.8, and Figure 9.9). They were identified on 11 tools (among the 30 selected, 36.6%; Table 9-4 and Figure 9.8).

Edge-damage due to utilisation³¹ was observed on 19 of the selected tools (56.6%; Table 9-4 and Figure 9.8). It was often located on the distal part of the tools (i.e. distal tip and/or distal edges). It frequently showed an overlapping of several multiple scars perpendicular to the edge that gives the impression of a “crushed edge or tip” (similar to what was observed in the experimental Levallois points used in throwing and thrusting motions; see Section 6.2.3).

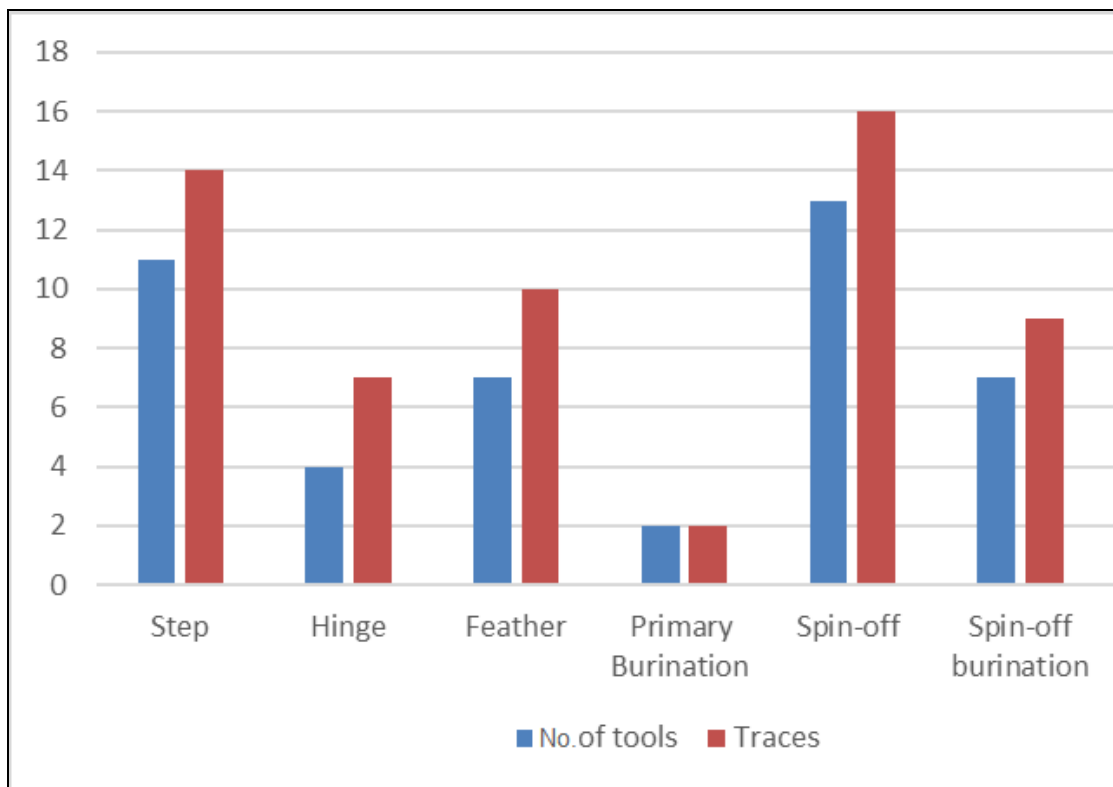


Figure 9.8. Frequencies of traces (in blue) and no. of convergent tools (in red) with fracture (Arma Delle Manie, n=30).

³¹ Edge-damage caused by trampling or by post-depositional processes was differentiated from utilisation edge-damage as the former produced abrupt and random scars not always perpendicular to the edge of the tool (McBrearty et al., 1998; Villa and Soressi, 2000).



Figure 9.9. Example of DIFs observed on the selected convergent tools of Arma Delle Manie. A: Spin-off burination fractures (indicated by the red line); B: Step-terminating bending fractures (in red); C: unifacial spin-off fractures (in red line).

9.2.1.1.1 Location of macroscopic traces

The diagnostic impact fractures (DIFs) observed on the selected convergent tools were mostly located on the distal part of the tools (i.e. distal tip and edges), and only sporadically on the mesial lateral edges of the tools (Table 9-5), similar to what was observed in the experimental Levallois points used in throwing and thrusting motions (see Section 6.2.2).

Edge-damage (i.e. scars) on the selected tools was mostly located on the lateral mesial edges, and on the distal lateral edges (Table 9-5), similar to what was observed in the experimental Levallois points used in throwing and thrusting motions (see Section 6.2.3).

In conclusion, the distribution and location of DIFs on the selected convergent tools of Arma Delle Manie are very similar to what has been observed on the experimental Levallois points used as throwing and thrusting stone-tipped spear projectiles, (see also Table 6-4).

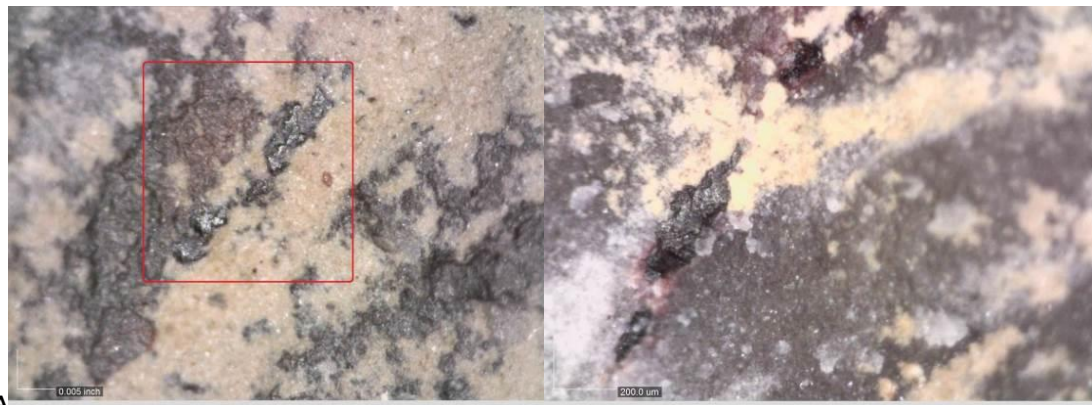
Table 9-5. Frequencies of traces according to their location on the tools (F: fractures; DIFs: diagnostic impact fractures; MLITs: microscopic linear impact traces; ED: edge-damage).

Trace location	No. of fractures	No. of tools with fractures	No. of DIFs	No. of tools with DIFs	No. of MLITs	N. of tools with MLITs	Edge-damage	No. of tools with ED
Distal	61	21	35	18	6	5	24	6
Mesial	9	6	8	6	-		46	17
Proximal	1	2			-		6	3
Total	71		43		6		76	

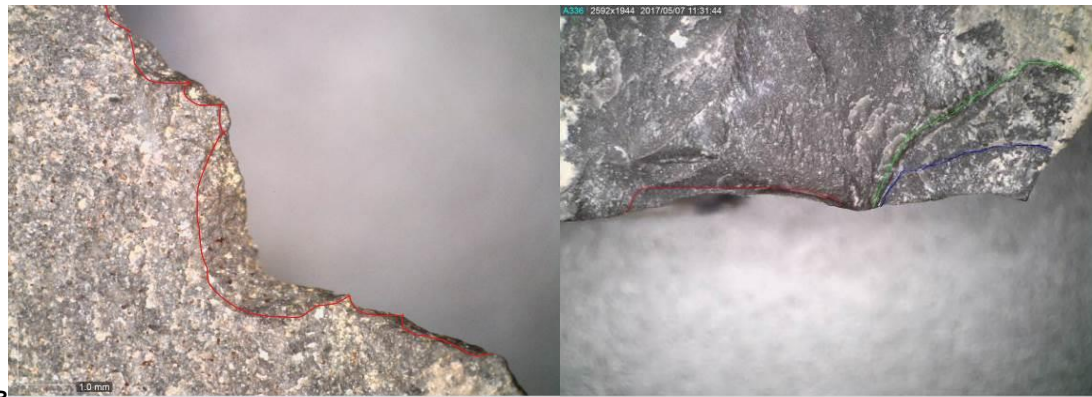
9.2.1.1.2 Macroscopic hafting traces

Two possible residues of adhesives were identified on two Levallois points (Figure 9.10; see Specimen #rem L51 1). These were classified according to their dominant colour as “reddish” or “brownish” (Figure 9.10). Residues were located on the proximal/mesial parts of the tools in a position that, according to the technological tool axis and its relationship with relevant use-wear traces, could be associated with hafting processes (Figure 9.10). A chemical characterisation of the residues was not achievable because the archaeological collection could not be transported outside the museum (and portable equipment such as XRF was not available).

Modification related to hafting was identified on two other Levallois points. These were sliced scars (Rots, 2010; or half-moon scars, Keeley, 1980) located on the proximal edges of the tool, which resulted in the creation of large notches (Figure 9.10). These notches were associated with transversal or perpendicular small striations located on the same proximal part of the tools (e.g. specimen #rem Ind 77/3, below). They were interpreted as the result of possible bindings or ligatures used during hafting processes (see also Rots, 2010).



A



B

Figure 9.10. Example of possible hafting traces observed on the selected convergent tools of Arma Delle Manie. A: black-brown residues (indicated by the red square), DM OM 180x (left) and 220x (right); B: (left) edge-damage, in form of a large sliced scar located on the mesial part of the tool, DM OM 50x; (right) bending scars located on the proximal part of the tool, DM OM 35x.

9.2.2 Microscopic analysis

Microscopic analysis (with a maximum magnification of 220x) focused on the identification of micro-polish, striations, micro edge-rounding, and MLITs. The high-power analysis was undertaken only on those artefacts that showed no or a low degree of post-depositional alteration (i.e. on n=18 tools out of the 30 selected tools; Table 9-3).

The sections presented below aim to exemplify functional categories of tools in which use-wear results are presented.

9.2.2.1 Projectile tools: use-wear evidence

The identification of projectile³² elements was never based on the presence of only one diagnostic trace. DIFs (such as step-terminating bending fractures, primary burination fractures, and secondary spin-off fractures) were always associated with microscopic linear traces (such as MLITs and linear striations), “impact polish”, and hafting traces, in order to achieve a functional interpretation. The location, distribution, and patterning of these traces were also important attributes for the identification of projectile wear. When diagnostic traces were not sufficient to reach a functional interpretation, or not completely preserved, the piece was tentatively marked as “possible projectile” (Table 9-7).

The archaeological tools presented below are exemplifications of the “projectile motion” category.

³² In this thesis, the terms ‘projectile’ and ‘projectile tool’ refer to all stone tools mounted on a shaft, regardless of the type of weapon or delivery system (see Glossary).

Specimen #IV O5 416:

- Technological description: the point is made of black siliceous limestone, this was extracted from the central part of the core using longitudinal convergent reduction sequences (Boëda, 1982, 1986). The original core, presumably of large dimensions (>10 cm), was possibly prepared to define the central and distal convexities that assisted the extraction of the predetermined point (Figure 9.11). No retouch was applied.
- Use-wear: the Levallois point showed a pattern of multiple DIFs. A very large spin-off burination fracture (>5mm) departed from a distal snap fracture (Figure 9.12a). Two bifacial spin-off fractures started from the snap fracture (Figure 9.12c). Next to the burination fracture, there was a long MLIT starting from the fracture line (Figure 9.12b). Edge-damage was observed on the lateral distal edges (Locus D2 and D3).
- Hafting traces: the Levallois point also exhibited two large sliced notch scars (Rots, 2010) on the lateral proximal edges (Figure 9.12d,e). Due to the location, morphology of the scars, and the patterning, this could be interpreted as resultant of a binding process.
- Interpretation: the pattern of multiple DIFs in association with the presence of a MLIT and distal edge-damage suggests the utilisation of this Levallois point as a projectile (in agreement with the results of Lombard and Pargeter, 2008; Rots, 2013, 2016; Sano and Oba, 2015; Sano et al., 2016; Pargeter et al., 2016; Rots et al., 2017). The presence of a MLIT suggests a possible utilisation in a throwing motion, since MLITs are statistically diagnostic traces of hand-delivered throwing spear projectiles (see Section 6.3.3.1). Moreover, the presence of two large sliced notches in the proximal part of the point (right above the “debordant” part of the flake) could be indicative of hafting processes.

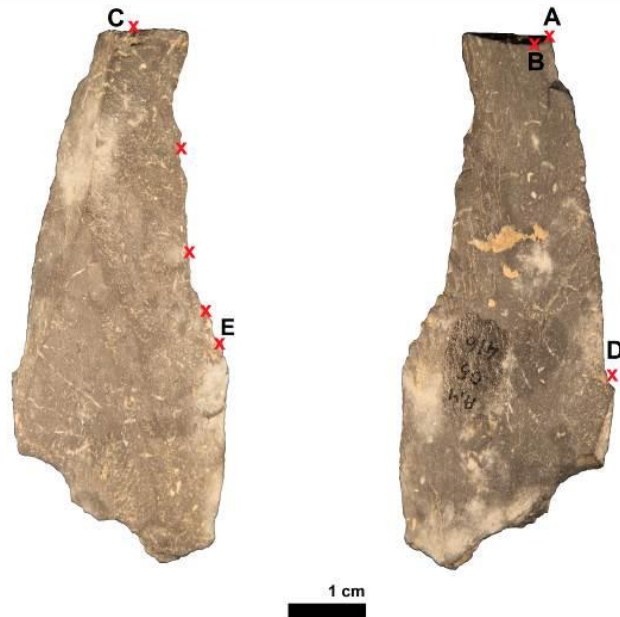
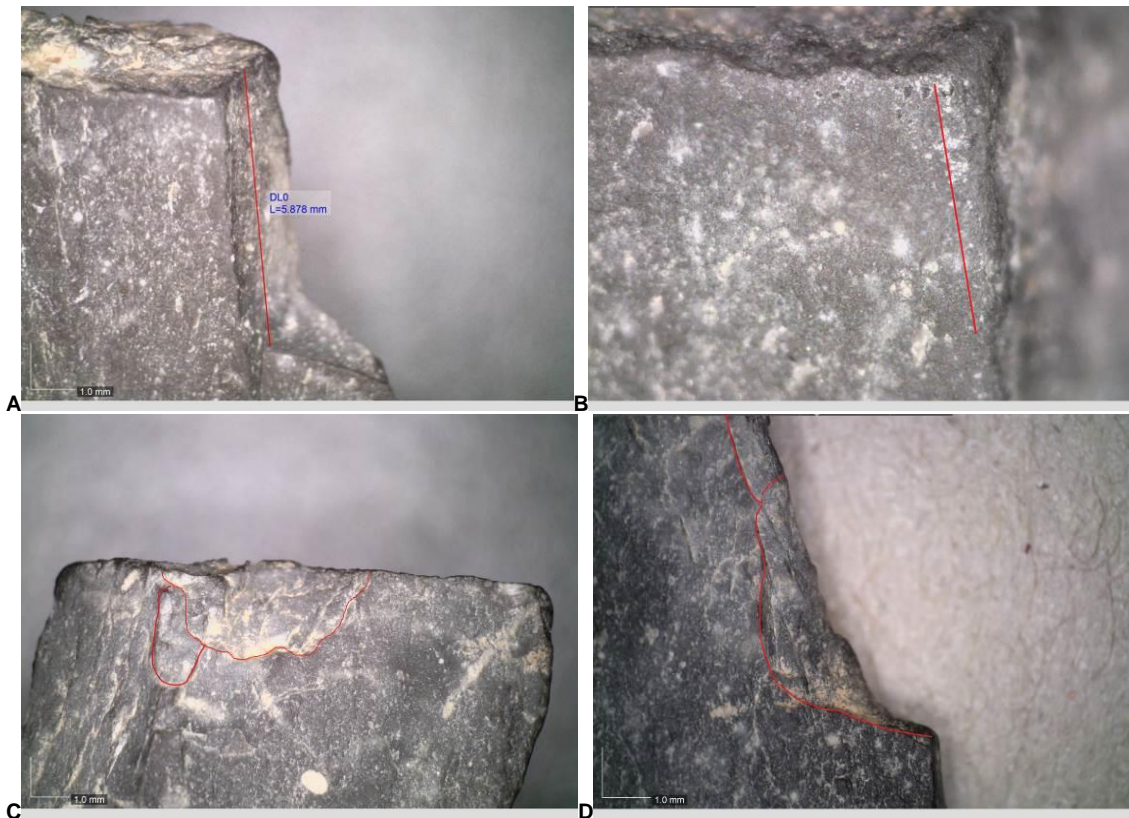


Figure 9.11. Projectile motion: Specimen #IV O5 416 with indications of trace locations (red x indicates the location of individual traces and letters show the location in which microscopic pictures were taken: Figure 9.12).





E
Figure 9.12. Specimen #IV O5 416. Location A: Spin-off burination fracture (>5mm), DM OM 35x. Location B: MLIT departing from a previous fracture, DM OM 200x. Location C: double spin-off fractures (ventral face view), DM OM 30x. Location D: proximal notches (dorsal face view), DM OM 38x. Location E: proximal notches, DM OM 38x.

Specimen #rem Ind 77/3:

- Technological description: the point was made of black micro-quartzite, and this was extracted from the central part of the core using the convexity created by the central ridge of the core, belonging to a Levallois volumetric conception (Boëda, 1982, 1986, 1995). It testified to the employment of a unidirectional longitudinal reduction sequence, with poor preparation of the striking platform (Figure 9.13). No retouch was applied.
- Use-wear: a spin-off burination fracture (>1mm) departed from a distal snap and terminated in a distal lateral edge (Figure 9.14a). This spin-off burination fracture was also associated with another diagnostic unifacial spin-off fracture, departing from the distal snap fracture (Figure 9.14a). The distal portion of the pointed tool showed several longitudinal linear microscopic traces, parallel to the main morphological axis of the tool (Figure 9.14b). The microscopic linear traces departed right from the spin-off burination fracture (Figure 9.14b). The Levallois point also showed a high degree of edge-damage, observed mainly on the distal-mesial lateral left edge (dorsal view; Figure 9.14b), which created a concavity on the edge (Figure 9.13). This type of intense edge-damage (i.e. edge-crushing) has been observed on the experimental Levallois points used in handed-delivered thrusting spear motions, when the projectile hit and perforated hard surfaces such as bones or joints (see Section 6.2.3).
- Hafting traces: a few transversal striations were observed on the proximal lateral edge running perpendicularly to the morphological axis of the tool (Figure 9.14b; Beyries, 1987b). Edge-damage started only from the mesial part of the tools and no edge-damage was observed on the proximal part of the tool (i.e. possible evidence of hafting limit; see CHAPTER 7). The Levallois point also showed also a techno-morphological thinning on the proximal area (i.e. pseudo-tang; Figure 9.13) that could have facilitated the hafting process.

-
- Interpretation: the association of multiple DIFs with linear traces and longitudinal striations support the functional interpretation of this artefact as a projectile tool (in agreement with the results of Lombard and Pargeter, 2008; Rots, 2013, 2016; Sano and Oba, 2015; Sano et al., 2016; Rots et al., 2017). The presence of linear traces (MLITs observed experimentally in throwing points, see Section 6.3.3.1) and abundant edge-damage (observed in higher frequencies in thrusting points, see Section 6.2.3) may suggest the multiple utilisation of this projectile tool, both in throwing and thrusting spear motions.



Figure 9.13. Projectile motion: Specimen #rem Ind 77/3 with indications of trace locations (red x indicates the location of individual traces and letters show the location in which microscopic pictures were taken: Figure 9.14).

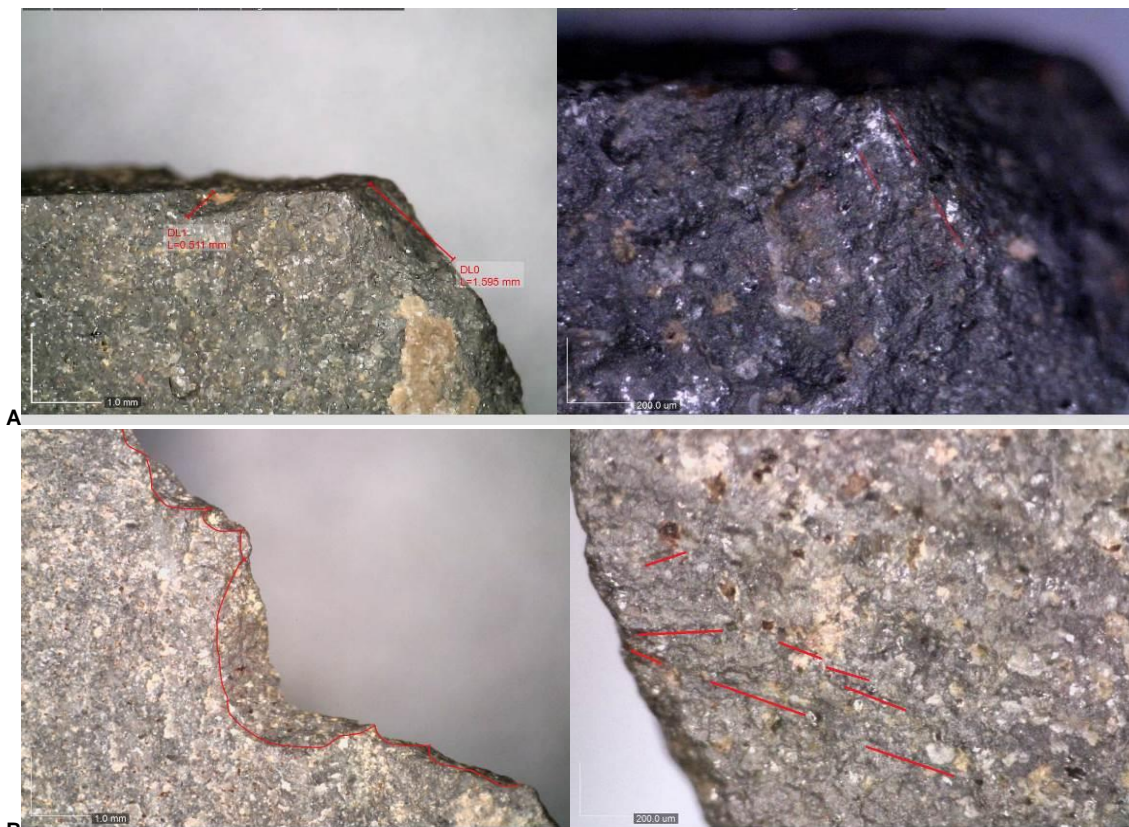


Figure 9.14. Specimen #rem Ind 77/3. Location A: (left) uniface spin-off (0.5 mm) and spin-off burination fracture (1.55mm), DM OM 50x; (right) MLIT departing from the spin-off burination fracture, DM OM 200x. Location B: (left) edge-damage departing only from mesial part of the tool, DM OM 50x; (right) perpendicular and oblique striations located on the proximal part of the tool, DM OM 150x.

Specimen #rem L1 68mi:

- Technological description: the point is made of black micro-quartzite, and this was extracted from the central part of the core using a unidirectional convergent reduction sequence (Figure 9.15), which followed a Levallois volumetric conception (Boëda, 1986). The Levallois point was later retouched on the distal and proximal right part (dorsal view), using a semi-abrupt type of retouch (Figure 9.15).
- Use-wear: the Levallois point showed a pattern of multiple DIFs on the distal tip. The pattern is composed of (i) a unifacial spin-off fracture which departed from a snap fracture and terminated in the distal dorsal face of the tool (Figure 9.16a); (ii) spin-off burination fractures (Figure 9.16a). Edge-damage was observed on the lateral left side (Figure 9.15).
- Hafting traces: no traces were observed or preserved. However, the morphology of the proximal part of the tool becomes narrower, creating a thinner base (i.e. pseudo-tang; Figure 9.15), which could have facilitated a hafting process.
- Interpretation: the presence of multiple patterns of bending fractures (amongst which was a spin-off fracture - highly diagnostic of projectile breakage) indicates that this Levallois point was used in projectile motions (in agreement with the results of Lombard and Pargeter, 2008; Rots, 2013, 2016; Sano and Oba, 2015; Sano et al., 2016; Pargeter et al., 2016; Rots et al., 2017).

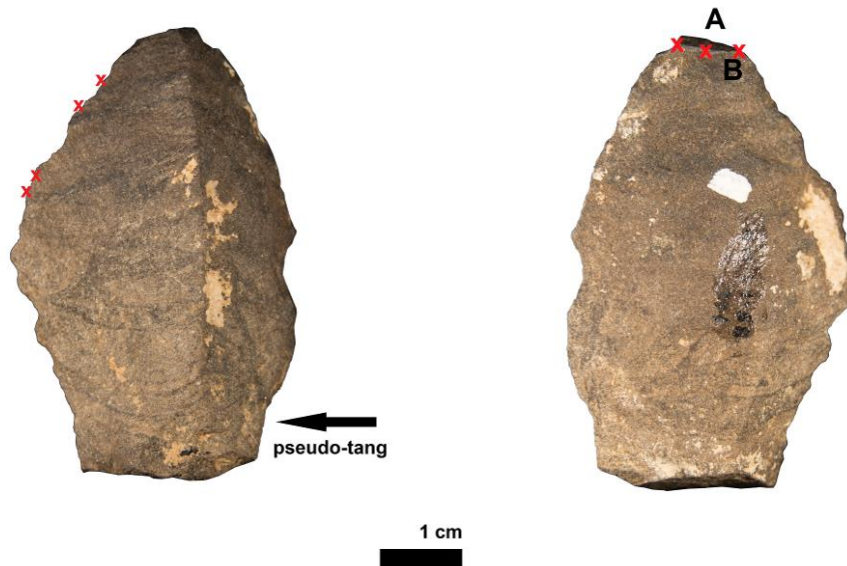


Figure 9.15. Projectile motion: specimen #rem L1 68mi with indications of trace locations (red x indicates the location of individual traces, letters the location where microscopic pictures were taken; Figure 9.16).

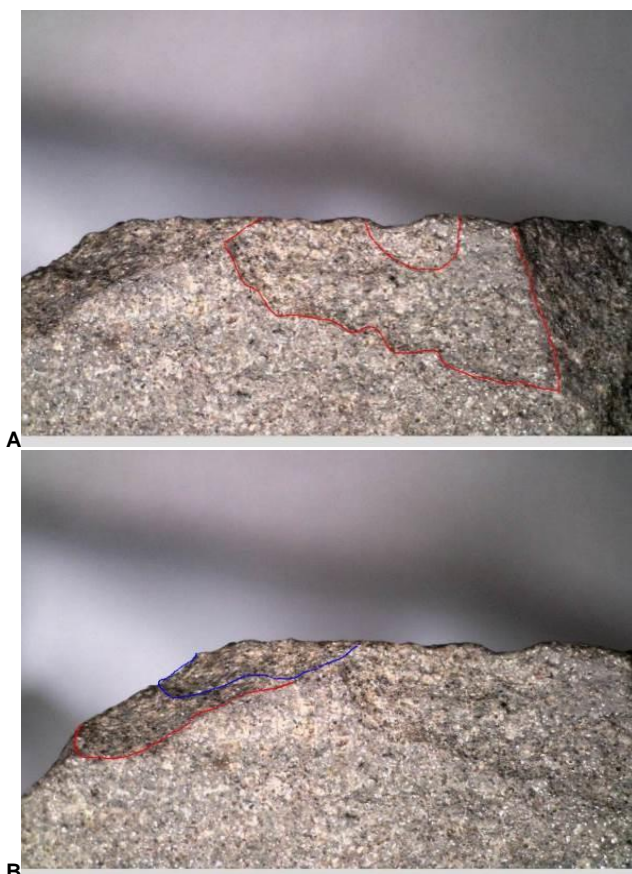


Figure 9.16. Specimen #rem L1 68mi. Location A: unifacial spin-off fractures DM OM 35x. Location B: spin-off burination fractures starting from a snap fracture, DM OM 35x.

Specimen #rem L51 1:

- Technological description: the point showed partial patination on the dorsal face and lateral edges. However, the edges were not affected by mechanical alterations. The Levallois point was extracted from the central part of the core, which was previously prepared with unidirectional convergent negatives that created the central and distal convexities used to obtain the Levallois point (Figure 9.17). The platform was prepared (faceted butt) and the point was not retouched.
- Use-wear: the distal tip showed multiple patterns of DIFs (Figure 9.17). Two bending fractures with feather-hinge terminations were observed on the distal ventral tip (Locus D1v) in association with multiple small cone fractures (Figure 9.18a). The dorsal distal tip showed three large bending fractures, all with step terminations (Figure 9.18a). These fractures could potentially be associated with badly preserved microscopic linear traces (Figure 9.18b). The possible linear traces run longitudinally to the morphological axis of the tool (indicating a longitudinal perforation). Abundant edge-damage (with triangular and trapezoidal scar morphologies; Figure 9.18c) ran discontinuously along the lateral left edge (ventral view) but only above the possible haft limit (Figure 9.18c).
- Hafting traces: “black and reddish” residues were located on the mesial dorsal and ventral faces of the tool (Figure 9.17 and Figure 9.18d). The residue presented a brown-black colour and it had a granular texture. It demonstrated a similar distribution and texture to the experimental adhesive residues observed on the experimental Levallois points (see Figure 7.17). Moreover, this Levallois point also showed a morphological thinning of the proximal area, which could have facilitated the hafting process (Figure 9.17).
- Interpretation: the association of multiple patterns of DIFs linked with the presence of possible linear traces, running longitudinal to the direction of impact attest to the utilisation of this Levallois point as a projectile tool (in agreement with the results of Lombard and Pargeter, 2008; Yaroshevich

et al., 2010; Rots, 2013, 2016; Sano and Oba, 2015; Sano et al., 2016; Pargeter et al., 2016; Rots et al., 2017). Moreover, the presence of black residues, very similar to experimental pitch residues, might suggest a hafting process, although the chemical characterisation of the possible residue is warranted.

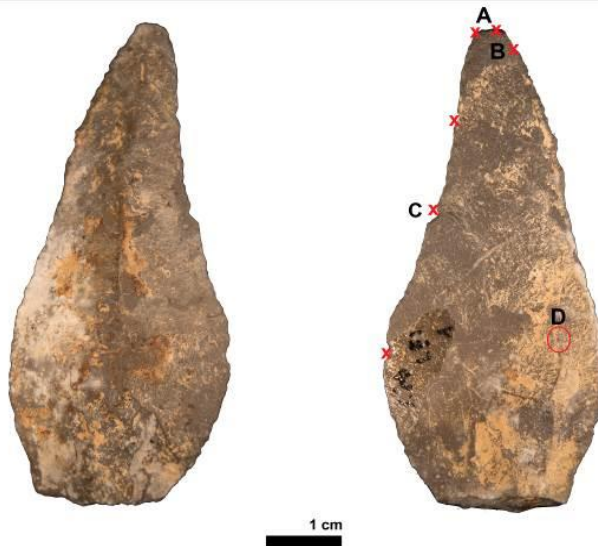
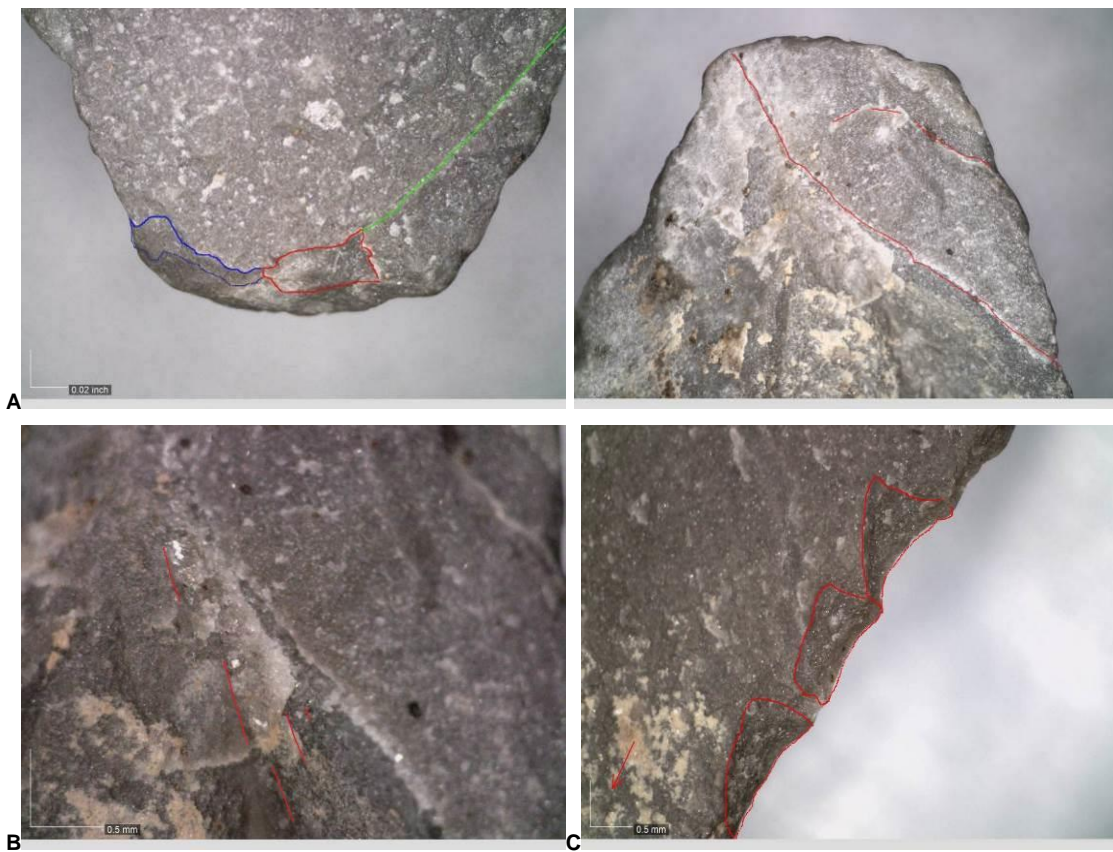


Figure 9.17. Projectile motion: Specimen #rem L51 1 with indications of trace locations (red x indicates the location of individual traces and letters show the location in which microscopic pictures were taken: Figure 9.18).



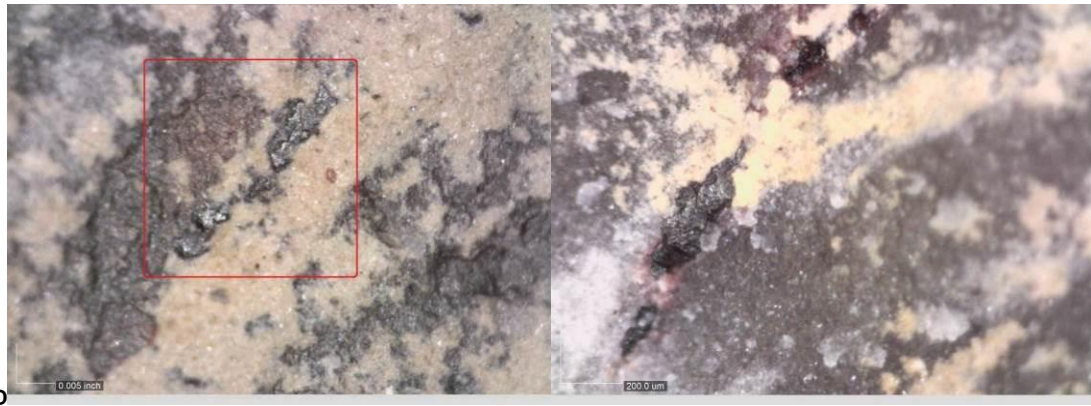


Figure 9.18. Specimen #rem L51 1. Location A: multiple bending fractures, DM OM 55x. Location B: a possible MLIT (not-well-preserved), DM OM 110x. Location C: edge-damage, DM OM 50x. Location D: black-brown residues, DM OM 180x (left) and 220x (right).

Specimen #III P6 92:

- Technological analysis: the fragment is a proximal fragment of a unidirectional convergent Levallois point, as testified by the faceted butt (striking platform prepared) and the convergence of the negative removals visible on the dorsal face of the fragment (Figure 9.19). The fragment showed direct, abrupt, and continuous retouch on the right edge (dorsal view; Figure 9.19).
- Use-wear: the breakage of the tool created a mesial bending fracture with a step termination (Figure 9.20). Several spin-off fractures started from this bending fracture (Figure 9.20). The breakage of the point (hence the multiple fracture patterns) cut off the retouch (which has been interpreted as a diagnostic trace of projectile tools, Sano, 2009; Figure 9.19). Microscopic traces and hafting traces were not observed, possibly due to preservation issues (i.e. post-depositional alterations).
- Interpretation: the mesial step bending fracture associated with spin-off, and the spin-off burination fractures, are indicators of a breakage resultant of projectile motions (Fischer et al., 1984; Lombard, 2005a; Sano, 2009, 2012). Moreover, these fractures cut off the retouch, which is a trait considered diagnostic of impact as the breakage happened only after production (Sano, 2009, 2012). It is, therefore, possible to suggest that the Levallois point broke during projectile impact activities, creating the proximal fragment. It was then probably transported into the archaeological site either inside the animal prey (refitting not found) or still inserted into the weapon (as proximal fragments are likely to remain inserted in the shaft after breakage).

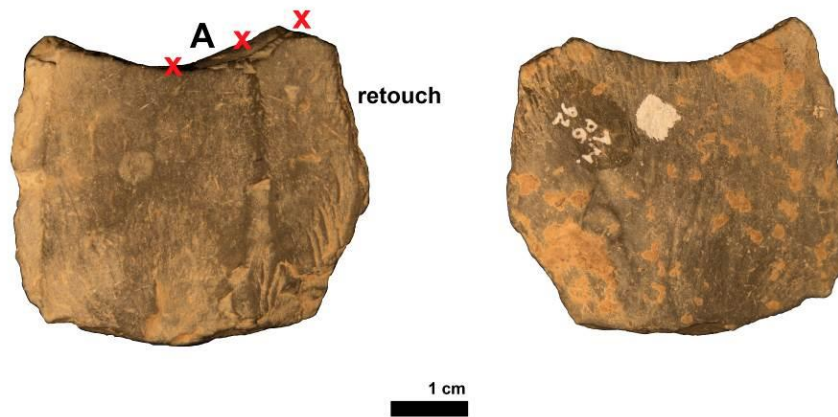
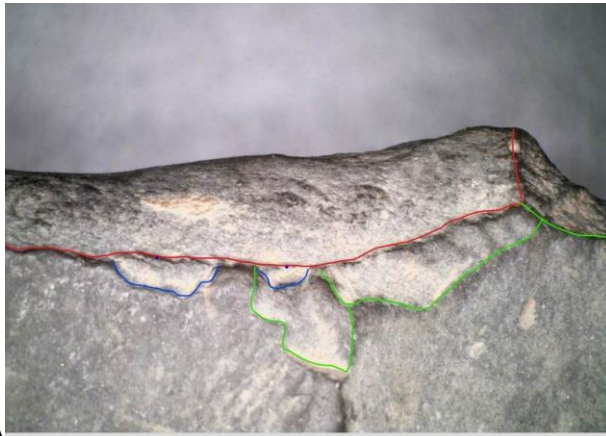


Figure 9.19. Projectile motion: Specimen #III P6 92 with indications of trace locations (red **x** indicates the location of individual traces and letters show the location in which microscopic pictures were taken: Figure 9.20).



A
Figure 9.20. Specimen #III P6 92. Location A: multiple pattern of DIFs, bending step (in red), spin-off (in blue), fractures with bending-missing initiation and step termination (in green), DM OM 35x.

Specimen #VII M1 897:

- Technological description: the point was made of black siliceous limestone and still exhibited the original cortex of the core. The tool was extracted from the right lateral side of the core, exploiting the central and distal convexities created by two longitudinal convergent removals (Figure 9.21). It is, therefore, possible to observe a Levallois conception of the core (Böeda, 1986).
- Use-wear: on the distal part, the fragment showed multiple fracture patterns. A bending fracture departed from the dorsal face and terminated on the ventral face with a step termination (Figure 9.22). From this bending fracture, a spin-off fracture started (Figure 9.22a), and another fracture which was conceivable as a burination fracture (Figure 9.22a). From the fracture line, some patches of linear and longitudinally distributed polish were observed (Figure 9.22b). They showed signs of directionality with small striations that ran obliquely to the main morphological axis of the point (Figure 9.22b).
- Hafting traces: the proximal part of the point, near the striking platform, showed a pattern of bending-missing fractures with step and hinge terminations (Figure 9.22c; similar to the proximal edge-damage observed on the experimental Levallois points used in hand-delivered spear experiments; see Section 7.3.2.2). It is unlikely that these bending fractures would be the result of the percussion of the hammer against the tool, as a hard-hammer generally causes fractures or scars next to the percussion points (i.e. bulb). Therefore, they could be interpreted as resultant of the compression between the shaft and the tool during possible impact (as observed for the experimental Levallois points used in hand-delivered spear experiments, see Section 7.3.2.2).
- Interpretation: the lateral Levallois point showed sufficient evidence of projectile use. The distal tip snapped off, leaving multiple patterns of DIFs in association with a faint polish, with striations that ran longitudinally to the impact motion (Figure 9.22b; in agreement with the

results of Sano, 2012; Sano and Oba, 2015; Sano et al., 2016). The bending fractures observed on the proximal lateral part of the tool could be due to the compression between the shaft and the point, as the result of an impact (as observed in the experimental Levallois points used in hand-delivered spear experiments, see Section 7.3.2.2).

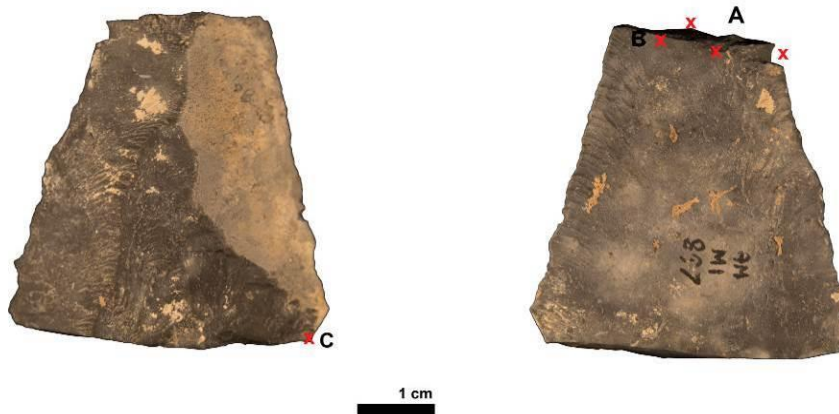


Figure 9.21. Projectile motion: Specimen #VII M1 897 with indications of trace locations (red x indicates the location of individual traces and letters show the location in which microscopic pictures were taken: Figure 9.22).

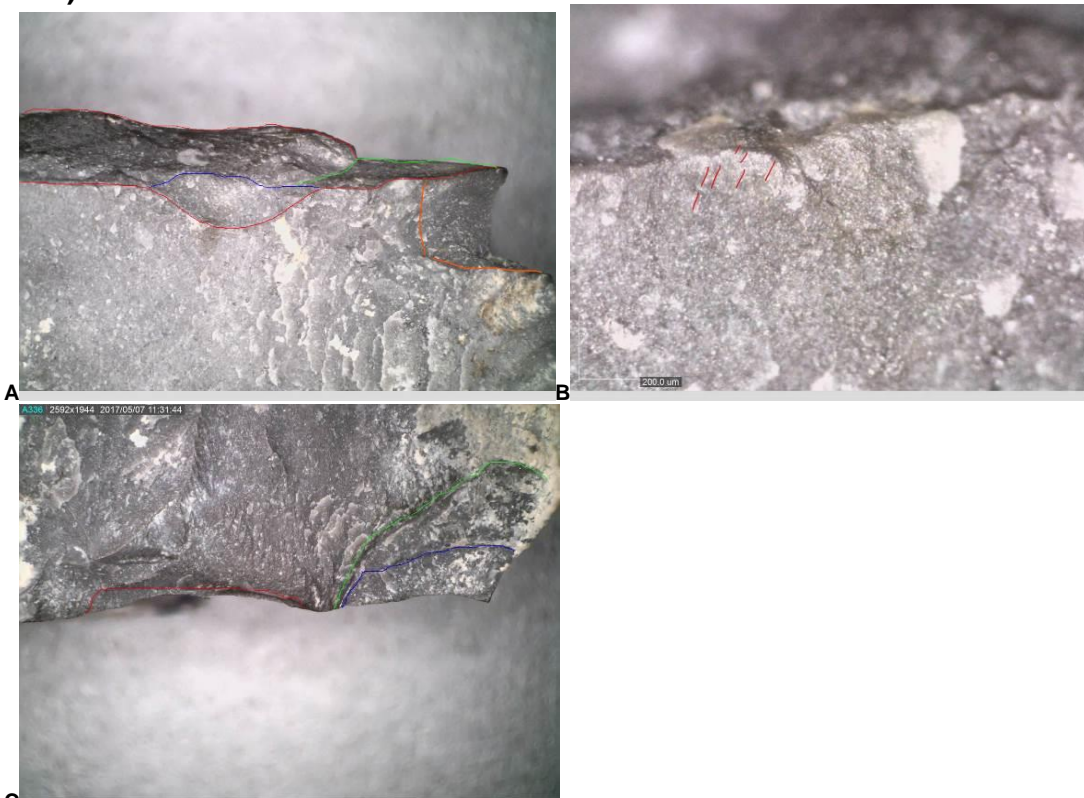


Figure 9.22. Specimen #VII M1 897. Location A: multiple patterns of DIF, bending step (in red), spin-off (in blue-red), burination fractures (in orange), DM OM 30x. Location B: faint and linear polish with longitudinal striations, DM OM 220x. Location C: bending scars (step in green and red, feather in blue) on the proximal part of the tool, DM OM 35x.

Specimen #VII G 2014:

- Technological description: the Levallois point was made of black limestone and it was extracted from the central part of the core, prepared with unidirectional longitudinal removals, still visible on the dorsal face of the tool (Figure 9.23).
- Use-wear: the distal part of the point completely snapped off with a transversal snap fracture (Figure 9.24). From this fracture line departed a spin-off fracture which terminated in the dorsal face (Figure 9.24a). Another DIF, a spin-off burination fracture, terminated on the distal left edge (dorsal view; Figure 9.24b).
- Hafting traces: small scalar notches have been observed on the proximal part of the Levallois tool. However, they were not clearly linked to possible hafting process.
- Interpretation: the presence of two different DIFs, such as a primary burination and a spin-off fractures, starting from a previous snap fracture suggest that the tool was possibly used in impact motions (in agreement with the results of Fischer et al., 1984; Lombard, 2005a; Lombard and Pargeter, 2008; Villa et al. 2009a) and, as a result, it was classified as a “possible projectile” tool (see Table 9-7).

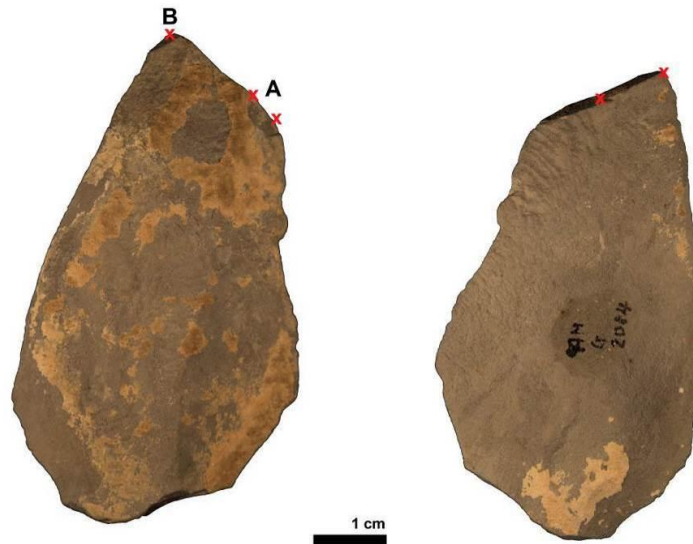


Figure 9.23. Possible projectile motion: Specimen #VII G 2014 VII M1 897 with indications of trace locations (red x indicates the location of individual traces and letters show the location in which microscopic pictures were taken: Figure 9.24).



Figure 9.24. Specimen #VII G 2014. Location A: large (<5mm) spin-off fracture (in red), DM OM 32x. Location B: spin-off burination fracture, DM OM 32x.

9.2.2.2 Tools used in longitudinal motions: use-wear

Two tools (6.6% of the selected sample) showed traces of longitudinal motions, such as cutting or sawing (Table 9-7). The two “cutting” tools were both Levallois points of relatively small dimensions (with lengths of between 4 cm and 5 cm). They presented abundant edge-damage, polish and striations only on the left lateral edge (e.g. as in Figure 9.25).

Specimen #VII G 2067 is here presented as an exemplification of the “longitudinal motion” category.

Specimen #VII G 2067:

- Technological description: the point is made of siliceous brown limestone, and this was extracted from the central part of the core using a unidirectional convergent reduction sequence with the three-blows operational scheme (La Porta, 2013), therefore, definable as a “three-blows” or classic Levallois point (Boëda, 1982, 1986; Figure 9.25).
- Use-wear: abundant edge-damage was observed along the entire lateral left edge, including large scars (1-2mm) terminating in steps and hinges (Figure 9.26b). The degree of edge-damage suggested a contact material of medium-hardness. These scars were associated with edge-rounding, polishes and striations on the ventral face of the tool. Edge-rounding was well-developed, resulting in rounded and smooth edges (Figure 9.26a and Figure 9.26c), suggesting a contact material of medium hardness (Tringham et al., 1974, table 2; Keeley, 1980). A faint polish was also observed on the inner edge of the distal edge (Figure 9.26a). Striations were observed running parallel to the used edge (and to the main axis of the tool), suggesting a longitudinal motion (Figure 9.26c).
- Interpretation: on the lateral left edge, the presence of abundant edge-damage associated with high degree of edge-rounding suggests contact with a medium-hard material, whereas the presence of longitudinal striations (parallel to the edge) indicates a longitudinal type of motion,

possibly as a cutting tool. However, due to the limits of the maximum magnification of the microscope (220x), the microscopic polish attributes, and thus the type of polishes, were difficult to interpret.

Both Levallois points that had possibly been used in longitudinal actions also displayed bending fractures (with feather or hinge terminations) on the distal tip (Figure 9.25). This could suggest that the tip was also employed during the phase of utilisation, and perhaps that the medium hardness of the material worked during the cutting motion caused the breakage of the distal end of the tool.

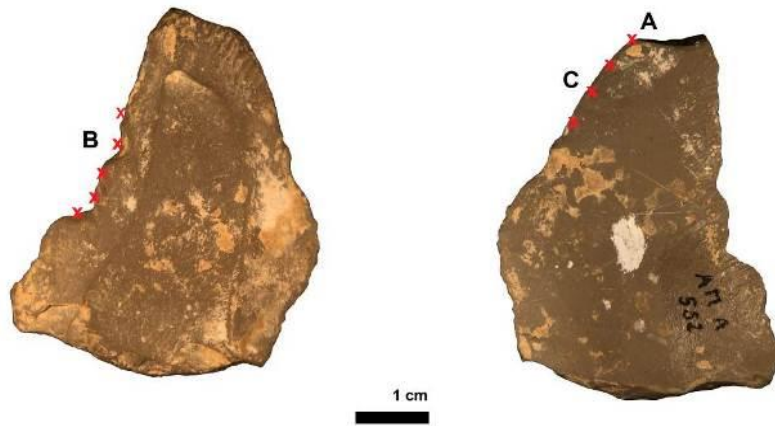


Figure 9.25. Longitudinal motion: Specimen #VII G 2067 with indications of trace locations (red x indicates the location of individual traces and letters show the location in which microscopic pictures where taken: Figure 9.26).

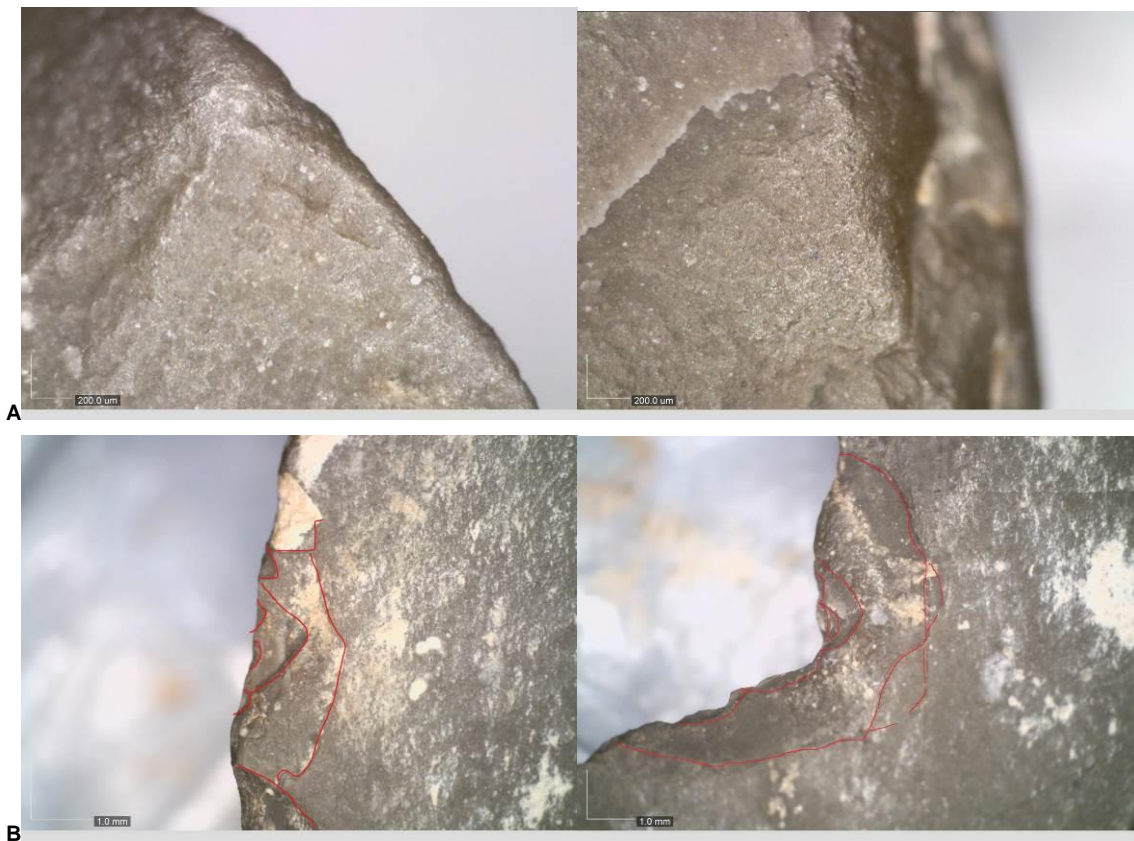




Figure 9.26. Specimen #VII G 2067. Location A: Faint polish located on the distal tip, DM OM 155x. Location B: Edge-damage, DM OM 40x. Location C: striations parallel to the edge, DM OM 180x (left) 200x (right).

9.2.2.3 Tools used in transversal motions: use-wear evidence

Four tools (13% of the selected sample) showed traces of transversal motions, possibly used in scraping and/or whittling movements (Table 9-7). The tools interpreted as scrapers were three Mousterian points and one Levallois point (Table 9-7).

Interestingly, the only three Mousterian points which were selected for the functional analysis all presented traces of utilisation suggestive of their usage as scrapers. Moreover, all three points (for example Figure 9.27 and Figure 9.29) showed a bilateral stepped-scalar retouch, also known as a Quina retouch (Dibble, 1984, p. 433). This suggests a possible analogy between a typological tool type and a specific function.

The three Mousterian points displayed traces of utilisation on both lateral edges and on the striking platform areas of the tools (e.g. Figure 9.27 and Figure 9.29). The proximal and striking platform parts were the areas of the tools that presented the most distinctive traces of utilisation, suggesting that these were the active zones of the tools (i.e. zones of utilisation).

The three Mousterian points exhibited very small-scale edge-damage (scalar scars <0.5mm) with feather terminations (Figure 9.30a), which may be suggestive of the relative softness of the contact material (Tringham et al., 1974, table 2; Keeley, 1980). Well-developed polishes appeared on the proximal lateral edges and on the bulb and striking platform areas of the Mousterian points (Loci M2, M1, P1, and P2), (Figure 9.28a,b and Figure 9.30b). The polishes were well-developed and they extended into the inner surface, with a good degree of polish-linkage (Figure 9.28a,b and Figure 9.30b). The polish development followed a perpendicular or oblique direction in relation to the edge (Figure 9.28a), suggesting transversal utilisations (Keeley, 1980; Van Gijn, 1989). Transversal striations within the polish were also observed (Figure 9.28a,b and Figure 9.30a,c). However, due to the maximum magnification of the portable microscope (220x) the microscopic polish attributes, and thus the type of polish, was difficult to interpret.

Specimen #rem 600r, #VII 1880 G (two Mousterian points) and #VII G 2067 (a Levallois point) are here presented as exemplifications of the “transversal motion” category, as both are good examples of Mousterian points used as scrapers (Figure 9.27 and Figure 9.29).

Specimens #rem 600r and #VII 1880 G:

- Technological description: both specimens are Mousterian points that present bilateral continuous stepped-scalar retouches. Specimen #rem 600r testifies the presence of unidirectional longitudinal negative of removals (Figure 9.27), whereas specimen #VII 1880 G present centripetal negative of removals (Figure 9.29).
- Use-wear: at 100x (magnifications with Dino-lite Edge AM7915MZT), both tools showed the presence of well-developed polishes on the lateral proximal edges and striking platform areas (Figure 9.28 and Figure 9.30). The polish showed a transversal development with oblique striations included within it (Figure 9.28a,b and Figure 9.30a,c). Specimen #rem 600r showed also a solid edge-rounding located on the dorsal central ridge, which presented bright polished edges (Figure 9.31). This evidence has been interpreted as potentially indicative of a hafting system that was rubbing against the dorsal central ridge.
- Interpretation: the presence of a well-developed type of polish with a transversal distribution and oblique striations included within it, suggests that the lateral edges and striking platform surfaces of both tools were used in transversal motions, possibly as scraper tools, whereas the presence of a low degree of edge-rounding could indicate a contact against soft contact materials (e.g. fresh skins; Tringham et al., 1974, table 2). However, due to the limits of the maximum magnification of the microscope (220x), the microscopic polish attributes, and thus the type of polishes, were difficult to interpret.

For specimen #rem 600r, the presence of a possible hafting system has been theorised due to the occurrence of strong abrasion of the central dorsal ridge (Figure 9.31).

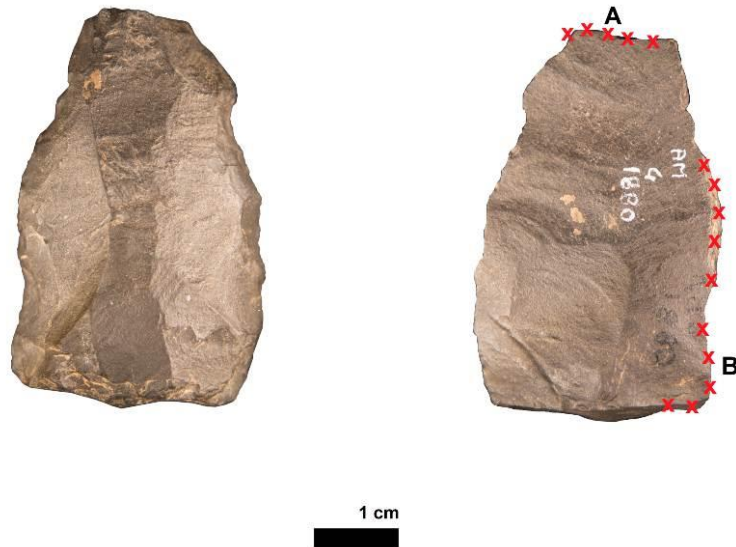


Figure 9.27. Transversal motion: Specimen #VII 1880 G with indications of trace locations (red x indicates the location of individual traces and letters show the location in which microscopic pictures were taken: Figure 9.28).



Figure 9.28. Specimen #VII 1880 G. Location A: (left) polish with a transversal development, DM OM 41x, (right) polish with oblique striations, DM OM 150x. Location B: polish with oblique striations, DM OM 150x (left) 180x (right).

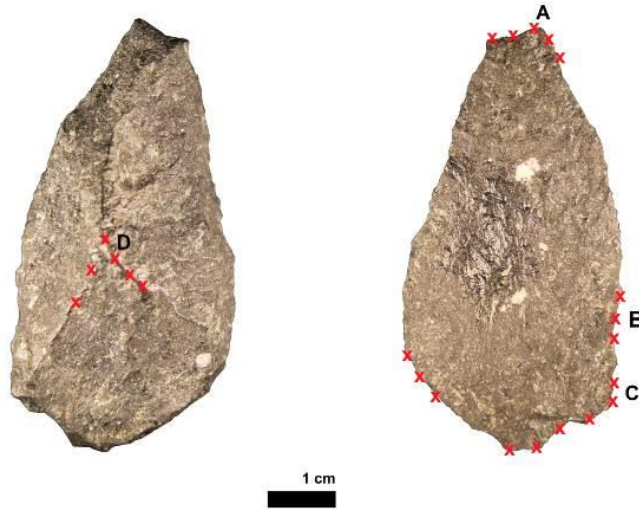
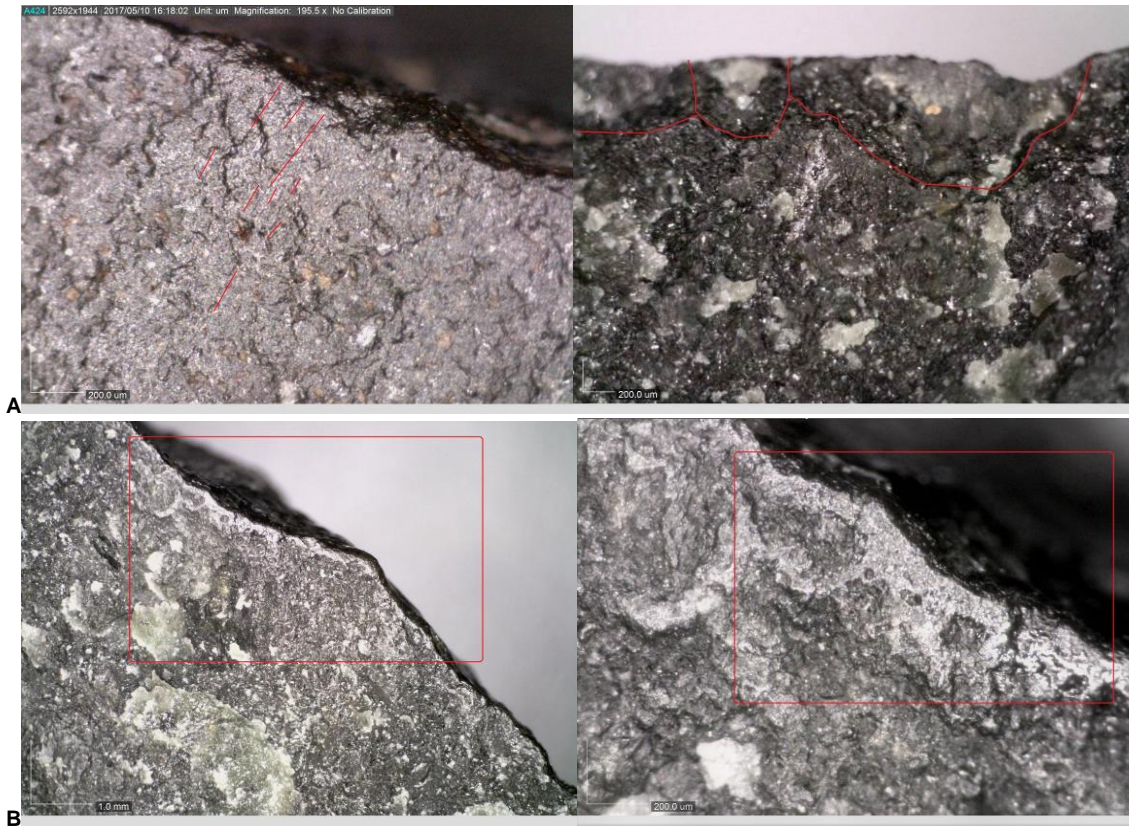
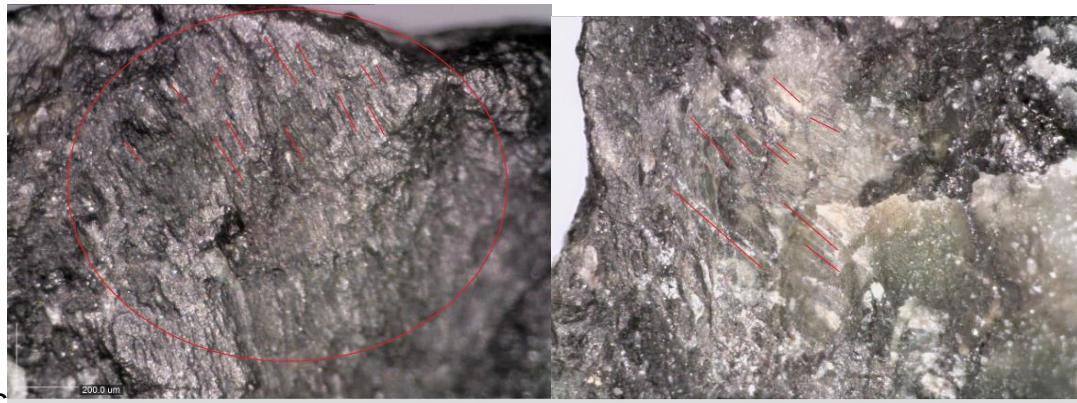
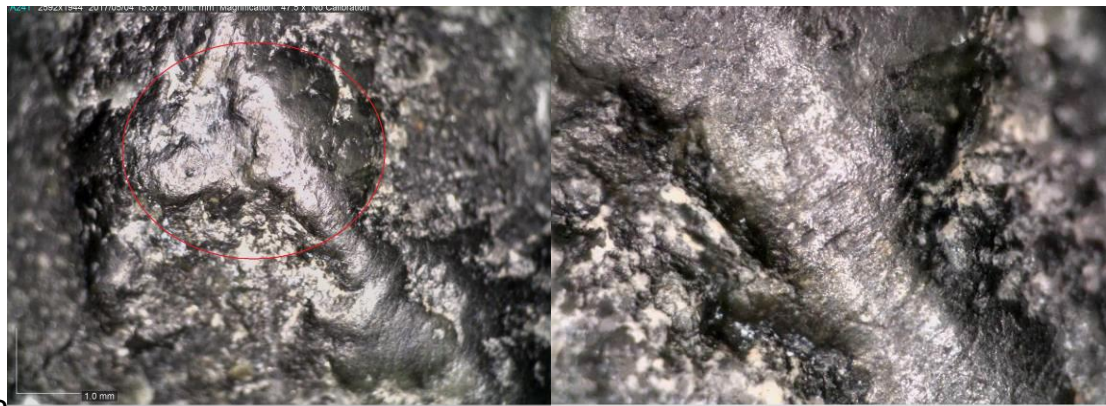


Figure 9.29. Transversal motion: specimen #rem 600r with indications of trace locations (red x indicates the location of individual traces and letters show the locations in which microscopic pictures were taken: Figure 9.30).





C
Figure 9.30. Specimen #rem 600r. Location A: (left) polish with oblique striations, DM OM 195x, (right) edge-damage, DM OM115x. Location B: well-developed polish and edge-rounding, DM OM 45x (left), 220x (right). Location C: polish with oblique striations, DM OM 220x.



D
Figure 9.31. Specimen #rem 600r. Location D: extensive edge-rounding, with striations and polish on the dorsal central ridge (interpreted as resultant of a hafting system), DM OM 50x (left), 150x (right).

Specimen #VII G 2067:

- Technological description: the cortical point was made of siliceous limestone, and this was extracted from the lateral part of the core (left side in plan view; Figure 9.32) using the convexity created by the longitudinal negative of removals of the core (Figure 9.32), therefore belonging to a Levallois volumetric conception (Boëda, 1986).
- Use-wear: the distal part of the tool showed the most distinctive traces of utilisation, suggesting that the distal tip could have been the active zone of the tool (i.e. the zone of utilisation). Indeed, the distal tip had a trapezoidal and quite rounded cross-section (Figure 9.32), a shape that could have assisted the whittling motion of the distal tip. In the distal part, the point also showed a high degree of edge-rounding (Figure 9.33a2) with the presence of a faint and speckled polish (at 220x; Figure 9.33a1). The same polish yielded a few striations which ran obliquely to the distal edge, suggesting a transversal action of the distal tip (Figure 9.33a2; Keeley, 1980; Van Gijn, 1989).
- Interpretation: the presence of abundant edge-rounding on the distal tip associated with the presence of a polish with transversal striations within it, suggests that the distal tip could have been used in a transversal motion, possibly with a low-angle of movement (i.e. whittling motion; Keeley, 1980, p. 171). Due to the maximum magnification of the portable microscope (220x), the microscopic polish attributes, and thus the type of polish, could not be clearly identified or interpreted. However, the relative softness of the contact material can be inferred by the absence of extensive edge-damage.



Figure 9.32. Transversal motion: Specimen #VII G 2067 with indications of trace locations (red x indicates the location of individual traces and letters show the location in which microscopic pictures where taken: Figure 9.33).



Figure 9.33. Specimen #VII G 2067. Location A1: faint polish and edge-rounding on the dorsal tip, DM OM 26x (left), DM OM 60x (right). Location A2: polish with oblique striations, DM OM 150x (left), DM OM 200x (right).

9.2.2.4 Tools used in multiple motions: use-wear evidence

None of the sampled tools displayed or preserved traces that could indicate two different actions or more than one utilisation (i.e. there was no use-wear evidence or preserved traces to suggest that they were used in multiple tasks or as multifunctional tools).

9.3 Outcomes: functional interpretations

Use-wear analyses on the selected tools of Arma Delle Manie found that, out of 30 Levallois points and convergent tools, eighteen (also analysed under a high-power approach, see Table 9-3) showed positively microscopic traces of utilisation which allowed the tools to be considered “used tools” (Table 9-6). Five other tools were interpreted as “possibly used tools” due to the presence of moderate post-depositional alterations (Table 9-6). Four convergent tools showed no visible traces of utilisation and were classified in the “no traces” category³³ (Table 9-6). Three more tools showed substantial post-depositional alterations that did not allow for a reliable interpretation and were classified as “non-interpretable” (Table 9-6).

Table 9-6. Functional interpretation of the selected convergent tools (n=30).

Use interpretation	Analysed tools
Used	18
Possibly used	5
No traces	4
Non-interpretable	3
Total	30

Among the 18 selected tools (also analysed under high magnification; Table 9-3) that showed positive traces of utilisation (“used” tools; Table 9-6), 11 tools were positively identified as projectiles; four tools were recognised as having been used in activities with transversal motions (scraping, planing); and three tools were recognised to have been used with longitudinal motions (cutting, sawing; Table 9-7).

³³ The “no traces” category is preferred to the “not used” category. Short periods of utilisation and/or utilisation against soft contact materials (e.g. meat) can leave very few traces on stone tool surfaces. Therefore, the “no wear” category has the scope to contain under-represented tools that may have been used for short periods in the Middle Palaeolithic without leaving clear traces of utilisation.

Among the five tools interpreted as “possibly used” (Table 9-6) due to the moderate presence of post-depositional alterations, four tools were interpreted to be possible projectiles and one was thought to potentially be a knife (i.e. longitudinal motion), (Table 9-7).

The remaining seven tools that either showed “no traces” or were too altered to allow a precise functional interpretation to be made (Table 9-6 and Table 9-7) were not presented in this chapter because of the lack of interpretable traces.

Table 9-7. Functional interpretations of the convergent tools (n=30) according to the types of motion.

Techno-morphological tool type	Used tools			Possibly used		No traces	Altered	Total
	Projectile motions	Transversal motions	Longitudinal motions	Possible longitudinal motions	Possible projectile motions			
Unretouched Levallois points (n=15)	6	1	1	1	2	2	2	15
Levallois points fragments (n=5)	3				1	1		5
Retouched Levallois points (n=4)	2		1				1	4
Convergent Levallois flakes (n= 3)			1		1	1		3
Mousterian points (n=3)		3						3
Total	11 (36.6)	4 (13.3 %)	3 (10 %)	1 (3.3%)	4 (13.3%)	4 (13.3%)	3 (10%)	30

CHAPTER 10

ABRI DU MARAS (ARDÈCHE, FRANCE): USE-WEAR RESULTS OF LEVALLOIS POINTS AND CONVERGENT TOOLS.

Abri du Maras Level 4 (sublevels 4.1 and 4.2) has been selected for the use-wear examinations of the Levallois points and convergent tools since it furnished the highest percentage of Levallois points of the entire sequence (Table 10-1). The archaeological unit Abri du Maras Level 4 (sublevels 4.1 and 4.2) has yielded n=51 Levallois points (Table 10-1). Although they characterised only 2.31% of the unit (Table 10-1), this percentage is in line with other other Middle Palaeolithic sites (see Table 8-2). At Abri du Maras, the presence of a high number of Levallois points, which are known for being predetermined and standardised pointed tools (Boëda, 1994), produced with controlled reduction sequences (La Porta, 2013), has raised the central question of what Neanderthals were doing with those points. Therefore, this study aimed to asses whether the Levallois points were produced for specific functional purposes, e.g. as projectile tools, and if it was possible to observe a relationship between shape and function.

Table 10-1. Distribution of the stone tools of Abri du Maras (until 2016) divided by technological categories (data from Moncel et al., 2017; Moncel et al., 2014; La Porta, 2013).

Type of tool	Level 3	Level 4.1	Level 4.2	Level 5	Level 6
Flakes	42	789	183	221	12
Backed flakes		51	24		
Flakes with a back		29	22		
Levallois flakes		76	26		
Kombewa flakes		1	6		
Cortical flakes		12	7		
Small (<10mm) and micro (<5mm) flakes		411	163		
Blades		84	32		2
Bladelets	11	101	27	16	
Points	2	39	16	16	2
Levallois points		35 (1.58%)	16 (0.72%)	2	
Cortical points or backed points		4	-	14	2
Fragments		368	70		
Pebbles	3	30	17	9	9
Bifacial		1	1		
Cores	1	41	28	11	1
*Others		168	211	2	
Total	59	1620	585	277	26

10.1 Archaeological dataset

The Abri du Maras' collection is stored at the "Institut de Paléontologie Humaine" (IPH), a division of the Muséum National d'Histoire Naturelle (MNHN) in Paris. The archaeological collection, due to national regulations, cannot be transported abroad. Therefore, all the analyses were carried out at the MNHN in Paris (through a collaboration with Prof MH Moncel), during a fieldwork season (4 weeks in total, funded by the AHRC SWW DTP).

The fieldwork season (February 2017) aimed to select the Levallois points present in the assemblage. This involved verification of the potential of the Levallois point assemblage for use-wear analysis (e.g. scrutinising the degree of post-depositional alterations, and the variety of, and differences in, the raw materials), and use-wear examination of the selected sample of Levallois points (and convergent tools, see below).

The technological analysis of the Levallois points of Abri du Maras Level 4 was undertaken by the author in 2012 during her Master dissertation' work (presented at the MNHN, Paris; La Porta, 2013; Moncel et al., 2014; La Porta et al., 2015; see Section 8.3.7.1), and, therefore, during the fieldwork season (February 2017) the technological analysis was not repeated. However, techno-morphological attributes were recorded for all the selected sample tools (as described in Section 3.3).

10.1.1 Sampling and procedure of analysis

All stone tools of Abri du Maras Level 4 were sealed in separate plastic bags immediately after their discovery on the excavation, stored in plastic boxes (protected with foam to prevent possible movements), and arranged according to their archaeological levels, upon arriving at the IPH. This facilitated the review and selection of all Levallois points series from the entire Level 4 stone tool assemblage. A total of $n=1706$ tools from Level 4 (sublevels 4.1 and 4.2) were reviewed (excluding flakes $< 2\text{mm}$), from which $n=51$ Levallois points were selected (Table 10-2; see Annex B for definitions). However, during the selection, it was noticed that other types of convergent tools (such as triangular Levallois flakes and convergent tools, see Annex B for definitions) also showed macroscopic fractures visible to the

naked eye. Therefore, it was decided to include these tools in the sample selected for functional analysis (Table 10-2). As a result, a total of n=70 convergent tools were selected for functional analysis (Figure 10.1 and Table 10-2). According to their techno-morphometric attributes, the 70 convergent stone tools were divided into the following techno-morphological tool categories (Figure 10.1 and Table 10-2; each techno-morphological category is described in Annex B):

- A. N=51 retouched and unretouched Levallois points from Level 4 (sub-levels 4.1 and 4.2; Figure 10.1) (see Annex B, Volume 2 for definitions).
- B. N=10 Levallois triangular flakes, which were all unretouched, from Level 4 (sub-levels 4.1 and 4.2; Figure 10.1), (see Annex B, Volume 2 for definitions).
- C. N=6 retouched convergent tools from Level from Level 4 (sub-levels 4.1 and 4.2; Figure 10.1), (see Annex B, Volume 2 for definitions),
- D. N= 3 generic cortical points (sub-levels 4.1 and 4.2; Figure 10.1).

For simplicity, the selected tools have been defined below as “convergent tools”.

Table 10-2. Tools selected for functional analysis according to techno-morphological categories.

Typological tool type	Level 4.1	Level 4.2
Levallois points	35	16
Unretouched Levallois points	30	16
Retouched Levallois points	3	-
Elongated Levallois point	2	-
Triangular Levallois flakes	8	2
Retouched convergent tools	5	1
Mousterian points	2	-
Side scraper	2	1
Convergent scraper	1	-
Cortical points	2	1
Sub-total	50	20
Total	70	

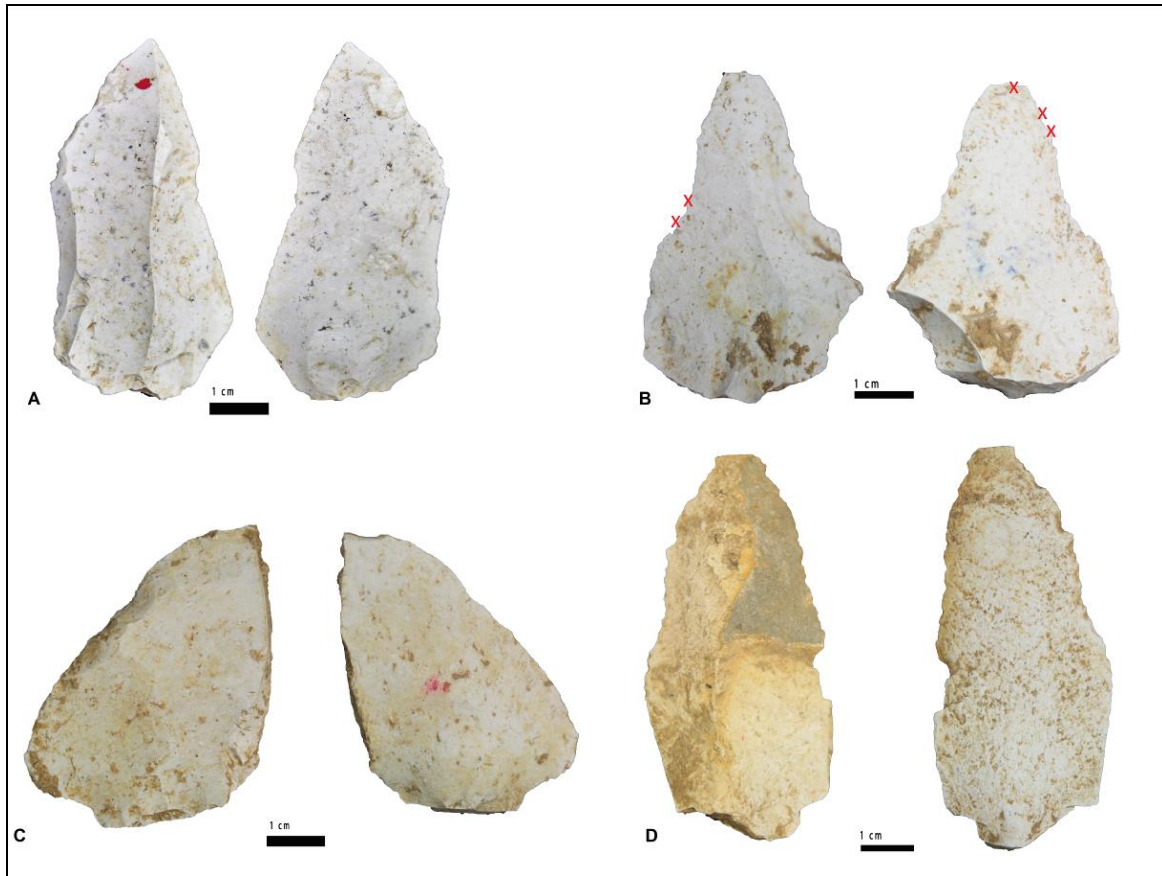


Figure 10.1. Example of the selected convergent tools. A: unretouched Levallois point. B: Triangular Levallois flake. C: convergent déjeté scraper. D: cortical point (see Annex B for definitions).

The 70 selected convergent tools (Table 10-2) were first examined to record their techno-morphological features (see Appendix G, Volume 2). After the techno-morphological analysis of the resulting artefact database, the selected convergent tools were inspected for post-depositional alterations (see below) and subsequently for functional analysis.

The functional analysis took place at the MNHN. Here, the low-magnification analysis was performed with a free-access binocular microscope Leica S8 APO (10x-80). The high-power analysis was performed with the digital microscope Hirox KH-8700 DM (35x-2500x; see also Section 2.2.3 and 2.2.5.2). However, due to museum regulations, access to the digital microscope Hirox KH-8700 DM was possible only via fee payment (which was kindly covered by prof MH Moncel). This allowed access to the Hirox KH-8700 DM for a total of six hours.

The functional analysis was performed following a step-by-step procedure. Stone tools were first analysed under a low-power microscope (10x-80x; binocular microscope). The low-power analysis (10x-80x) focused on the identification of use-wear that could be diagnostic of functional utilisation such as fractures, diagnostic impact fractures (DIFs), edge-damage and edge-rounding. The stone tools that showed diagnostic wear-traces attributable to use and/or hafting were selected for a detailed high-power analysis with the Hirox KH-8700 digital microscope. The high-power analysis focused instead on the identification of microscopic wear traces such as polish, MLITS, striations, bright spots, and edge-rounding that could be related to utilisation, hafting, or projectile impact activities.

For low-power analysis, the archaeological tools were only rinsed with demineralised water, since residue analysis is still ongoing on the Abri du Maras collection (Hardy and Moncel, 2011; Hardy et al., 2013). During high-power analysis, alcohol or occasionally acetone was used locally if a specific trace included bright or dirty spots scattered the light of the microscope and prevented a precise observation.

The interpretation of the tools' functions was based on multiple lines of evidence. The observed wear traces were compared with the experimental collection of Levallois points presented in this thesis (see CHAPTER 6), a more extensive experimental use-wear collection based at the Department of Archaeology at the University of Exeter, and previously published functional studies (Keeley, 1980; Anderson-Gerfaud, 1981, 1990; Moss, 1983a; Fischer et al., 1984; Plisson, 1985; Vaughan, 1985; Mansur-Francomme, 1986; Beyries, 1987a; Van Gijn, 1989, 2010; Geneste and Plisson, 1989, 1990; Lombard, 2005a; Lombard and Pargeter, 2008; Rots, 2010, 2013, 2016; Pargeter, 2013; Pargeter et al., 2016; Sano et al., 2016).

10.1.2 State of preservation of the selected tools

Palaeolithic stone tool assemblages may present more post-depositional alterations than more recent assemblages (Rots, 2014; Anderson-Gerfaud, 1990; Beyries, 1988). However, to mitigate the effect of post-depositional alterations, these can be assessed by surveying the surface of stone tools with low-power or naked eye

before the performance of use-wear analysis (Van Gijn, 1989; Burrioni et al., 2002; Lemorini et al., 2006).

Thus, before conducting use-wear examinations, the selected sample of convergent tools of Abri du Maras Level 4 was examined under the naked eye and at low magnifications (up to 80x with the binocular microscope Leica S8 APO) to assess the state of preservation of the stone tool sample, including the degree of intensity of any chemical and mechanical alterations of the selected sample (Figure 10.3 and Table 10-3). Post-depositional alterations were divided into chemical, mechanical, and discovery modifications (if observed).

10.1.2.1 Chemical alterations

Patination

At the Abri du Maras Level 4 (sublevels 4.1 and 4.2), most of the flint tools (n=55; Figure 10.4 and Table 10-3) presented a post-depositional microscopic layer of chalcedony composed of silica crystals (Fernandes, 2012), also definable as white patina (Schmalz, 1960; Rottländer, 1975). This crystalline layer partly covered the surfaces of the tools making microscopic use-wear traces (e.g. polish, striations, MLITs) sometimes difficult to identify. Under the microscope, the silica crystals that composed the patina presented a very granular aspect, almost “sugary” (Van Gijn, 1989, p. 5; Figure 10.2). Under the Hirox KH-8700 digital microscope, the patina caused optical effects of breaking up or scattering the light (Figure 10.2). This dazzling effect was mitigated using polariser filters, which allowed a better microscopic examination (35x-2000x).



Figure 10.2. The granular and shiny aspect of the patination phenomena. Example of “lightly patinated tool”, DM OM 600x. (Tool ID #J6 4.1 45).

At Abri du Maras, the white patina or chalcedony layer occurred in various degrees of alterations. These were classified into three categories: non-patinated tools (none or sporadic presence of patination), lightly patinated tools (<50% of the tools' surface), and mostly patinated tools (>50% of the tools' surface) (Table 10-3). Among the selected sample (n=70 tools), 15 convergent tools (21.42%) showed a lack of white patina, 25 convergent tools (35.71%) showed a low coverage of white patina, and 30 convergent tools (42.85%) showed a high degree of white patina (Figure 10.3). When tools were affected by complete patination, they were not selected for functional analysis or the functional analysis focused mainly on macroscopic use-wear observation (up to 80x; see Table 10-4).

Other alterations

A few of the “mostly-altered” tools (n=2) also exhibited traces of rubefaction due to ancient contact with fire (Figure 10.3 and Table 10-3).

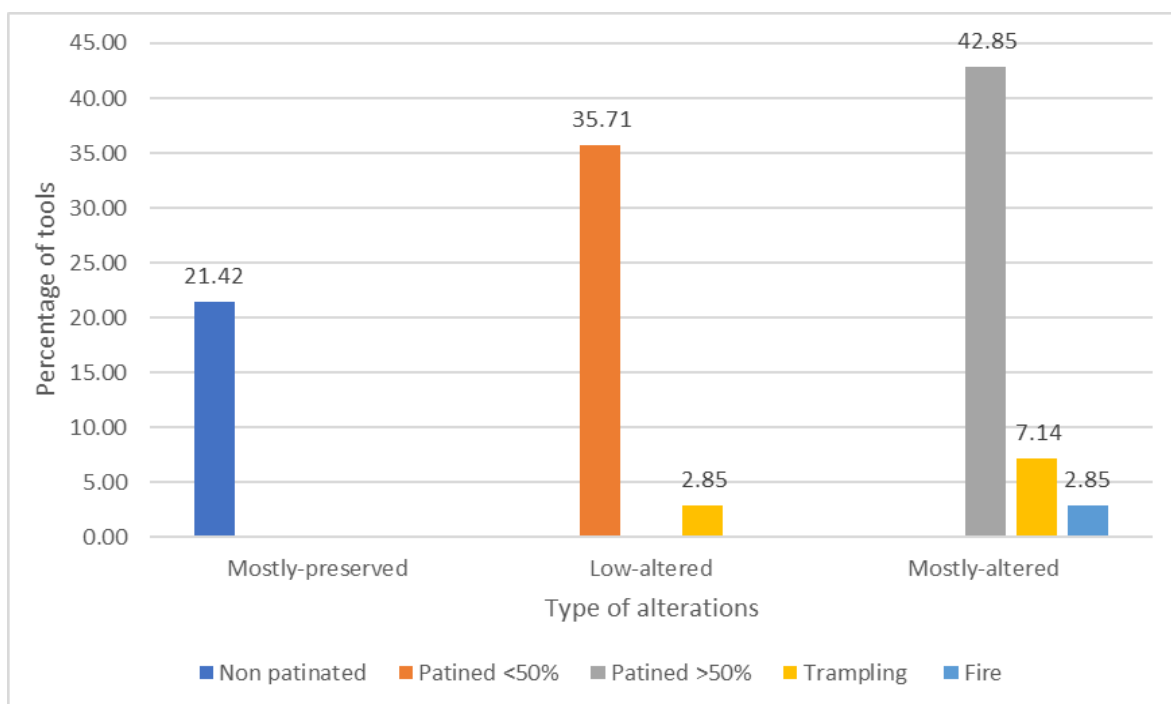


Figure 10.3. Post-depositional alterations affecting the selected tools (n=70) for functional analysis at Abri du Maras Level 4.

10.1.2.2 Mechanical alterations

Mechanical post-depositional alterations such as trampling, scratches, cracks, and abrasion of the edges are often randomly distributed over the lithic surface and located on the prominent topographic areas of the artefacts (Shea and Klenck, 1993).

Trampling

At Abri du Maras Level 4, the majority of the selected convergent tools showed a low occurrence of the mechanical alterations outlined above. Only nine tools (Figure 10.3 and Table 10-3) were affected by modern or ancient trampling. Modern trampling was identifiable on two tools (Figure 10.3) because of the absence of the patina layer on the scars, which appeared like modern crushing (Figure 10.4). Ancient trampling was inferred, when possible, by the random distribution of small scars along the lateral edges of the convergent tools (Tringham et al., 1974, p. 192; Shea and Klenck, 1993). Since stone tools at Abri du Maras were rarely retouched, it was unlikely that ancient trampling could be confused with retouch. Ancient trampling was detected on seven archaeological convergent tools (7.14% of the sample, Figure

10.3). However, these tools were all excluded from functional analysis in order to avoid the risk of confusing post-depositional traces with traces that could mimic impact or utilisation activities.

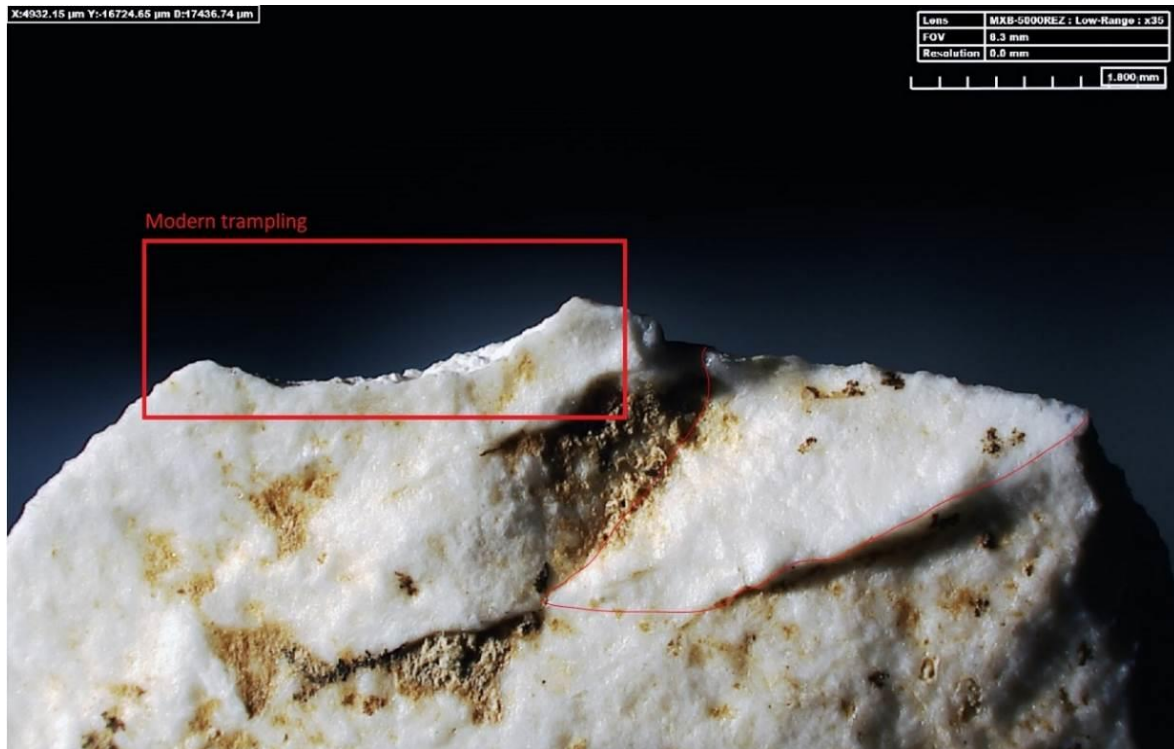


Figure 10.4. Modern trampling (i.e. crushed edge) visible due to the lack of patination, DM OM 35x (Tool ID #J6 4.1 45).

10.1.2.3 Final considerations

The entire panoply of post-depositional alterations was taken into account during the macroscopic (low-power) and microscopic (high-power) examination. Each alteration found on the tools was described and recorded in a database (see also Section 2.6). Tools affected by post-depositional alterations were divided into three categories (Figure 10.5, Figure 10.3 and Table 10-3):

- Mostly preserved tools (none or sporadic alterations observed, Figure 10.5),
- Lightly altered tools (<50% of the tool surface covered by patina or other alterations, Figure 10.5),
- Mostly altered tools (>50% of the tool surface covered by patina or other alterations, Figure 10.5).

Only tools that were unaffected (i.e. 'preserved') or subject to low to medium post-depositional modifications (i.e. 'low-altered') were finally selected for use-wear examinations.

The initially selected sample of convergent tools (n=70 in total) showed varying degrees of preservation. N=15 of the selected tools were mostly preserved and show sporadic or none post-depositional alterations (Figure 10.3 and Table 10-3). N=25 tools presented a low to medium degree of alteration, in the form of a moderate presence of white patina (<50% of the tool surface) and/or encrustations, which did not affect the preservation of the edges (Table 10-3). N=30 tools showed a high degree of post-depositional alterations, consisting of intense white patina (>50% of the tool surface), abundant encrustations, and traces of mechanical alterations (such as trampling; Figure 10.4 and Table 10-3). The high degree of alterations on these artefacts limited the possibility of undertaking a detailed microscopic examination, since possible utilisation traces such as polishes, striations, bright spots, and edge-rounding, but also edge-damage, could have been obliterated by the alterations. Therefore, the n=30 convergent tools (of the sample), affected by high degrees of post-depositional alterations, were excluded from further use-wear examination (Table 10-3, see also next Section). The remaining tools were instead examined with low-power and high-power magnifications for use-wear analysis.

Table 10-3. Degree of post-depositional alterations affecting the convergent tools of Abri du Maras Level 4 (n=70).

Intensity of post-depositional alterations		
Mostly-preserved	Low-altered	Mostly-altered
Not or sporadically patinated – None or sporadic presence of white (or glossy) patina, or encrustations No mechanical alteration.	Lightly patinated - Some areas of the tool were sporadically patinated, while the rest of the areas appeared "fresh" (not patinated). None or light mechanical alteration.	Mostly patinated - Patination covered most of the areas of the tool. Encrustations and mechanical alterations were observed. Mechanical abrasion and trampling were detected.
N=15 tools (21.42%)	N=25 tools (35.71%)	N=30 tools (42.85%)

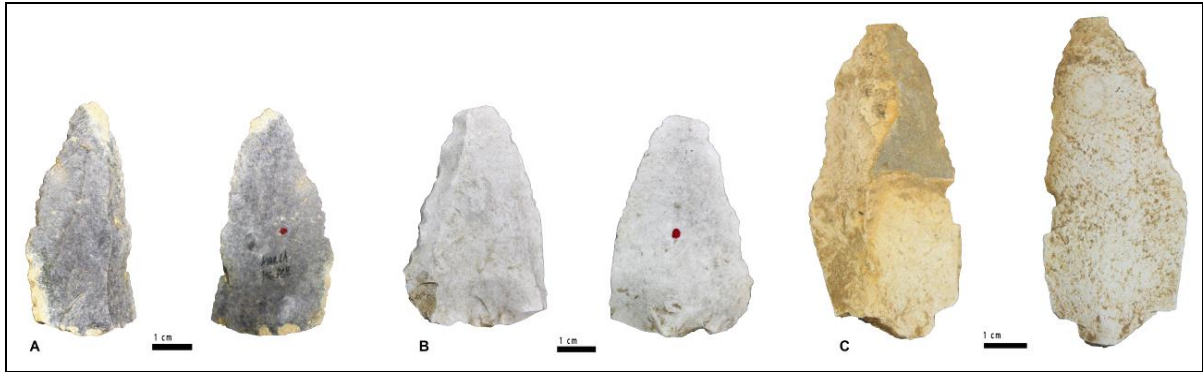


Figure 10.5. Example of degree of post-depositional alterations affecting the convergent tools of Abri du Maras Level 4. A: Mostly-preserved tool. B: low-altered tool. C: Mostly-altered tool.

10.1.3 Final sample

All selected convergent tools (n=70) were examined for techno-morphological analysis (Table 10-4), and post-depositional alterations. Among these, n=38 tools were considered not relevant for detailed use-wear examination because: (i) they did not show macroscopic wear that could be recognised as diagnostic of use (n=8 tools), and/or (ii) they were affected by intense post-depositional alteration (n=30 tools, “mostly altered” tools in Table 10-3). Therefore, n=32 convergent stone tools were finally analysed for the detailed low and high-power microscope examination (Table 8). Among these, a total of n=19 convergent tools were positively examined for high-power analysis (Table 10-4).

Table 10-4. The total number of selected convergent tools examined per analytical approaches used.

Abri du Maras (Level 4)	Technological analysis only	Detailed macroscopic use-wear analysis (low-power 10x ~ 80x)	Detailed microscopic use-wear analysis (high-power ~ 1000x)
No. of convergent tools analysed	70	32	32 (19 positively examined)

10.2 Functional results

It should be acknowledged that at Abri du Maras Level 4 the medium degree of post-depositional alterations affecting the n=32 selected convergent tools often prevented a detailed high-power analysis since patination phenomena annihilated the presence of preserved use-wear traces. Therefore, when this was the case, the functional interpretations of the convergent tools were not identified. However, when a final functional interpretation was achieved (see “used” category in Table 10-6), it was based on the association between macroscopic use-wear traces and the preserved microscopic use-wear traces. The main approach was to apply a degree of caution in the interpretation of each tool due to the presence of low to moderate post-depositional patination phenomena.

The selected convergent tool of Abri du Maras Level 4 did not show overall high frequencies of fractures or diagnostic impact fractures (DIFs), as the Arma Delle Manie’ convergent tools (see Section 9.2.1), therefore, the macroscopic and microscopic use-wear results are presented together for each tool or category of tools (see Sections below).

The sections presented below aim to exemplify functional categories of tools in which use-wear results are presented.

10.2.1.1 Projectile tools: use-wear evidence

The identification of projectile³⁴ tools was never based on the presence of only one diagnostic trace. DIFs (such as step-terminating bending fractures, primary burination fractures, and secondary spin-off fractures) were associated with microscopic linear traces (such as MLITs and linear striations), when preserved, and/or hafting traces to achieve a functional interpretation. The location, distribution and patterning of the observed use-wear traces were also important attributes for the identification of projectile tools. When diagnostic traces were not sufficient to reach a

³⁴ In this thesis, the terms ‘projectile’ and ‘projectile tool’ refer to all stone tools mounted on a shaft, regardless of the type of weapon or delivery system (see Glossary).

functional interpretation, or not completely preserved, the piece was tentatively marked as “possible projectile” (Table 10-7).

Eight convergent tools (out of the 32 analysed convergent tools, 25%) showed diagnostic traces of projectile. Four tools were interpreted as projectiles, whereas four tools were interpreted as “possible projectiles” (Table 10-7). The tools interpreted as projectiles were all Levallois points (three points and one proximal fragment, Table 10-7). The tools interpreted as “possible projectiles” were one Levallois point, two Levallois convergent flake, and one déjeté scraper (Table 10-7; see also Appendix B, Volume 2 for definitions).

The analysed convergent tools showed all multiple patterns of DIFs (Table 10-5). The more recurrent types of fractures were bending fractures with step termination (29%), followed by feather (20.8%), hinge and snap types (16.6% respectively; Table 10-5). Other DIFs, i.e. primary burination fractures and spin-off fractures, were equally present in the sample (8.3% respectively, Table 10-5). Linear traces (in form of microscopic striations or MLITs; Figure 10.7 and Figure 10.11), located on the distal portion of the tools, were also observed on two tools (6.2%, Table 10-5), although this low frequency could be related to issues of preservation of traces. Linear traces, when observed or preserved, normally departed from the fracture line of previous breakages, running parallel or slightly oblique to the longitudinal axis of the point (Figure 10.7b and Figure 10.11a). The superimposition of DIFs, microscopic linear traces and abundant distal edge-damage on the same tool was considered as diagnostic of projectile utilisation (in agreement with Fischer et al., 1984; Lombard, 2005a, 2005b; Lombard and Pargeter, 2008; Rots, 2009, 2013, 2016; Pargeter, 2013; Sano and Oba, 2015; Pargeter et al., 2016; and the experimental use-wear results presented in CHAPTER 6).

The tools presented below have been interpreted within the “projectile motion” category (Table 10-7).

Table 10-5. Type and frequencies of fractures observed on the convergent tools of Abri du Maras (n=32). Note: the fracture numbers and frequencies refer to fracture counts, not tools with fractures (more than one fracture can occur on a tool).

Type of fractures	Abri du Maras	
	No. of fractures (%)	No. of tool with traces (%)
Bending fractures	20 (83.3%)	10 (31.2%)
Step	7 (29%)	5 (15.6%)
Hinge	4 (16.6%)	2 (6.2%)
Feather	5 (20.8%)	3 (9.3%)
Snap	4 (16.6%)	4 (12.5%)
Primary Burination fractures	2 (8.3%)	2 (6.2%)
Spin-off fractures	2 (8.3%)	2 (6.2%)
Unifacial/bifacial Spin-off	1 (4.1%)	1 (3.1%)
Burination Spin-off	1 (4.1%)	1 (3.1%)
Total Fractures	24 (100%)	
Total DIFs (step-terminating bending, unifacial/bifacial spin-off, burination spin-off, and primary burination fractures)	11 (45.8%)	
Total tools with fractures		10 (31.2%)
Total tools with DIFs (step-terminating bending, unifacial/bifacial spin-off, burination spin-off, and primary burination fractures)		8 (25%)
*Microscopic impact linear traces (MLITs)	2	2 (6.2%)

Specimen #J7 111 4.1:

- Technological description: the Levallois point was extracted from the central part of a Levallois core using a unidirectional convergent c (Figure 10.6; Boëda, 1982, 1986; La Porta, 2013).
- Use-wear: the distal tip showed a primary burination fracture longer than 15mm, ending on the right ventral edge (which has been considered a diagnostic trace and measurement of projectile impact, Fischer et al., 1984; Lombard, 2005a; Lombard and Pargeter, 2008; Vila et al. 2009a; Sano, 2009, 2012; Pargeter, 2013; Figure 10.7). It was associated with a bending fracture terminating with a double termination (feather-step) on the ventral face (Figure 10.7). Below the bending fracture, abundant edge-damage started on the lateral ventral tip, in form of cone scars (Figure 10.7). A possible microscopic linear impact trace (MLIT), poorly preserved, was visible on the lateral ventral tip (Figure 10.7), associated with other longitudinal striations (Figure 10.7). Lateral scars were identified on the ventral proximal edges (Figure 10.7), and edge-damage started only above these (interpreted as an indication of the presence of a possible hafting systems, see Section 7.4.1 and Rots, 2010).
- Interpretation: the presence of multiple diagnostic impact fractures (DIFs) such as a primary burination fracture and a step-terminating bending fracture, associated with edge-damage located and microscopic linear traces on the distal part of the tool (Figure 10.7), suggests the utilisation of this Levallois point as a projectile (in agreement with the results of Lombard, 2005a; Lombard and Pargeter, 2008; Yaroshevich et al., 2010; Rots, 2009, 2013, 2016; Sano, 2012b; Sano and Oba, 2015; Sano et al., 2016; Pargeter et al., 2016; Rots et al., 2017). Whereas, the presence of a possible, even if poorly preserved, MLIT, which has appeared as a statistically diagnostic trace of hand-delivered throwing spears on the experimental Levallois points presented in this study (see Section 6.3.3.1), could suggest the utilisation of this point in possible throwing motions. Moreover, the presence of lateral scars, below which edge-damage was absent, may suggest the presence of a possible hafting system (Rots, 2010; Rots, 2016).

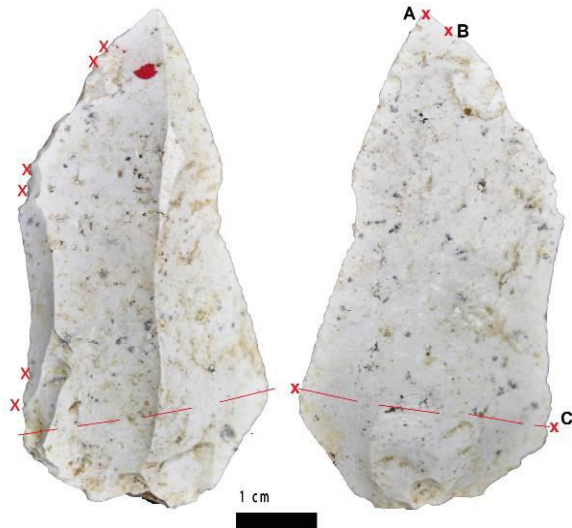


Figure 10.6. Projectile motion: Specimen #J7 111 4.1 with indications of trace locations (red x indicates the location of individual traces and letters show the location in which microscopic pictures were taken [Figure 10.7], the red line indicates the possible haft limit).

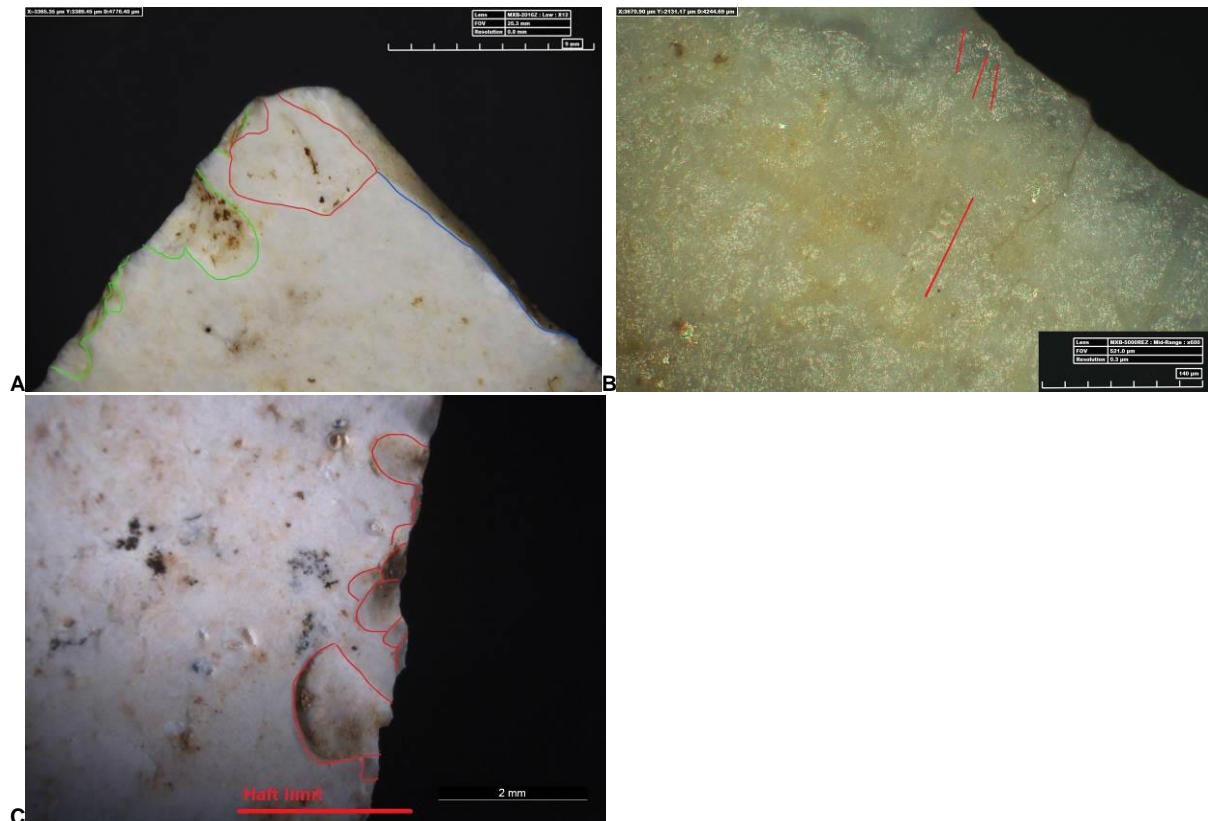


Figure 10.7. Specimen #IJ7 111 4.1. Location A: primary burination fracture (in blue), bending fracture terminating in a feather/step (in red) and abundant edge-damage on the left ventral tip (in green), DM OM 12x. Location B: poorly preserved MLIT departing from the previous burination fracture, DM OM 600x. Location C: proximal edge-damage (with possible indication of the haft limit), SM OM 50x;

Specimen #M6 894 4.2:

- Technological description: the tool is a large (42mm) proximal fragment of a retouched Levallois point cut in half by a mesial snap fracture (Figure 10.8).
- Use-wear: the mesial snap fracture transversally cut the point (Figure 10.9). From the ventral fracture line of the snap fracture, a large spin-off fracture (> 5mm) developed, which has been observed to be a diagnostic traces in the experimental Levallois points used as hand-delivered spear projectiles (see Section 6.2) and in agreement with previous projectile studies (Fischer et al., 1984; Lombard, 2005a; Lombard and Pargeter, 2008; Sano, 2009, 2012) (Figure 10.9). The mesial fragment also showed a step terminating fracture (with a bending-missing initiation) on the dorsal face (Figure 10.9). Moreover, the mesial snap fracture interrupted the retouch of the point (Figure 10.9), which suggested that the fracture was posterior to the retouch and production of the tool. A criterion that has been recognised as a diagnostic trace of projectile impact (Sano, 2009, 2012). The point showed also a micro-polish located on the mesial transversal fracture which displayed a flat-into-domed topography and a very localised distribution (Figure 10.9). This polish displayed similar attributes with the impact polish identified on the experimental Levallois points used as throwing spear-points (see Section 6.3.3.3.1), suggesting that polish due to projectile impact activities may also be identified in the archaeological tools. No evident traces of hafting were observed or preserved, except for some edge-damage, in form of crushing of the dorsal proximal area and a notch scar on the proximal right edge (Figure 10.8).
- Interpretation: the association of multiple diagnostic impact fractures and traces suggest that the fragment broke due to projectile impact motions. The presence of a mesial snap fracture from which departed a large spin-off fracture (> 5mm), is indicative of projectile utilisation (Fischer et al., 1984; Lombard, 2005a;). Moreover, the fact that the mesial snap fracture snapped the point in two halves cutting off the retouch, add evidence to suggests that the break was posterior the technological production of the tool, considered by

some as diagnostic of projectile motions (Sano, 2009, 2012; Sano and Oba, 2015). The lack of evident hafting traces can be due to preservation issues or to the employment of particular hafting arrangements that left minimal traces. Although the projectile utilisation of this tool can be inferred by the association of multiple DIFs and traces, the same cannot suggest the type of delivery motions used for the projectile.

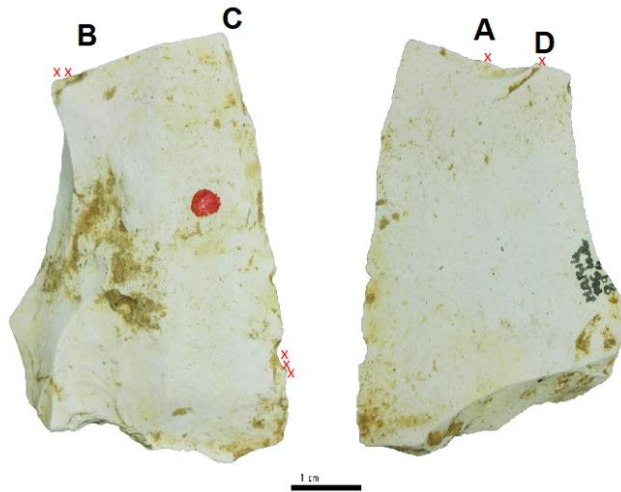


Figure 10.8. Projectile motion: Specimen #M6 894 4.2 with indications of trace locations (red x indicates the location of individual traces and letters show the location in which microscopic pictures were taken [Figure 10.9]).

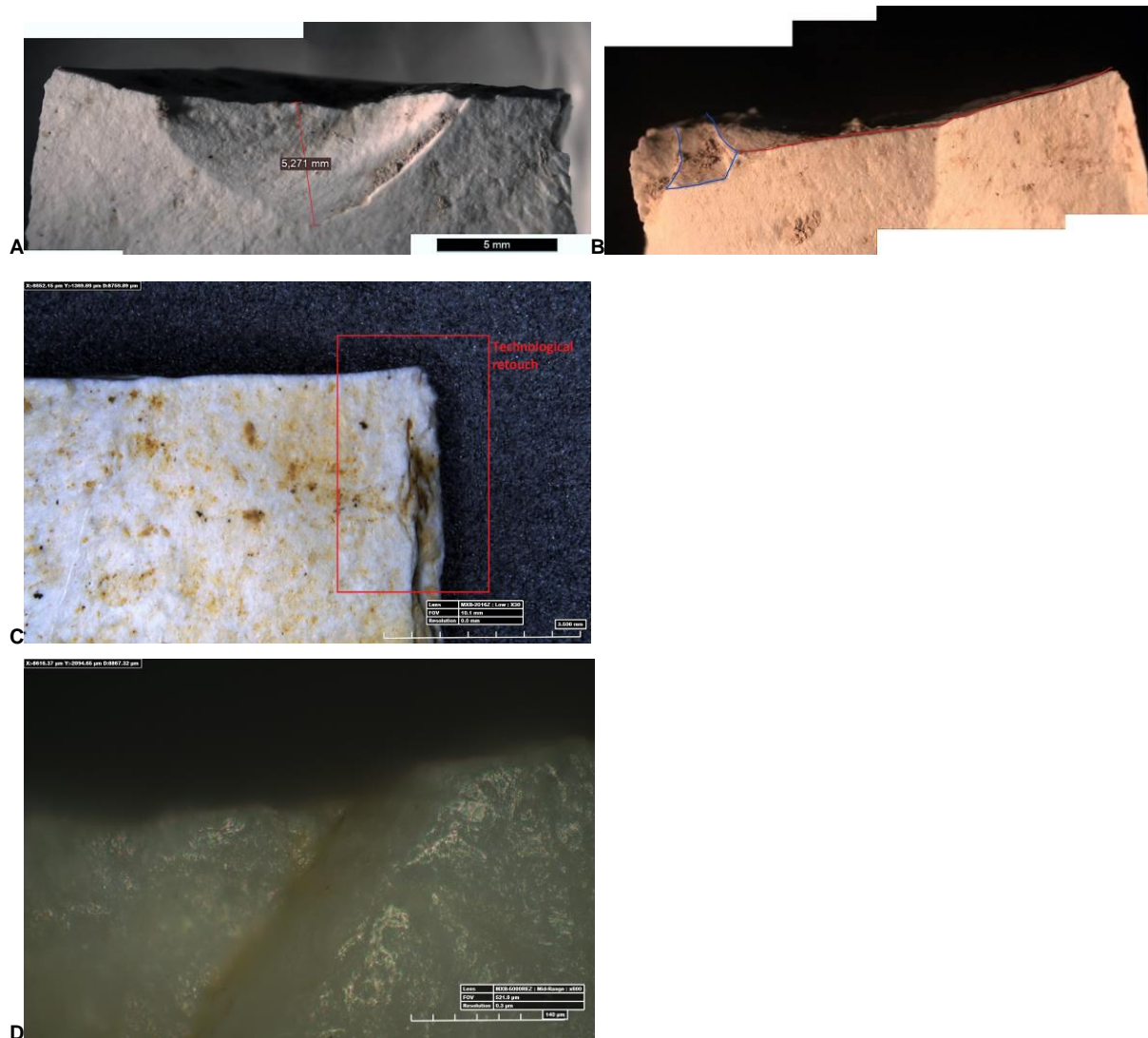
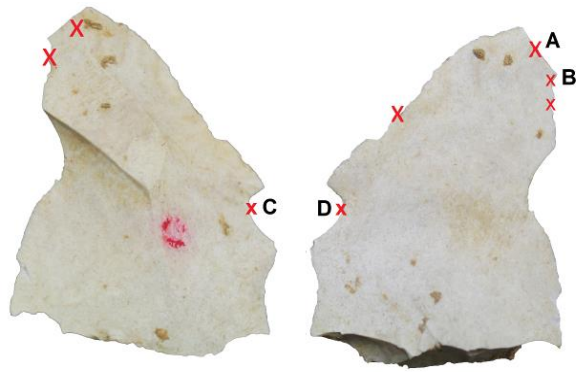


Figure 10.9. Specimen #M6 894 4.2. Location A: mesial snap fracture from which departed a large spin-off fracture (>5mm), SM OM 10x. Location B: the mesial snap fracture (in red) plus a step-terminating fracture (in blue) on the dorsal face, SM OM 10x. Location C: the mesial snap fracture cut the retouch on the dorsal distal face, SM OM 30x. Location D: polish located right on the fracture line. It shows a bright aspect with a domed-into flat topography and few longitudinal striations within it (showing analogues attributes to the observed experimental “impact polish”, see Section 6.3.3.3.1), DM OM 400x.

Specimen #M6 1033 4.2:

- Technological description: the convergent flake showed a prepared striking platform surface and a management of the lateral convexities that followed Levallois unidirectional longitudinal reduction sequences (Figure 10.10; Boëda, 1986).
- Use-wear: a transversal snap fracture was observed on the distal tip. This fracture, although not being diagnostic, was associated with abundant edge-damage (in form of crushed edges) of the right ventral distal edge (Locus D3v; Figure 10.11). The microscopic examination revealed the presence of polish on the distal ventral tip (Figure 10.11). This polish showed a flat topography with longitudinal striations within it (Figure 10.11), showing similar attributes with the “impact polish” observed on the experimental Levallois points used as throwing spears (see Section 6.3.3.3.1). Two functional notches were observed on both proximal edges of the tool (Figure 10.10). The notches were sliced scars located on the right and left proximal edge (Locus P2d; Figure 10.11). Right next to the mesial left ventral notch (Locus M1v), a rough and dull polish was also observed (possibly related to binding agents; Figure 10.11).
- Interpretation: the distal tip of the tool showed intense damage, testified by the association between the distal snap fracture and the crushing of both distal lateral edges, which it has been observed experimentally on the experimental Levallois points used in hand-delivered thrusting spear experiments (Figure 10.11). The combination of these traces plus the observation of a polish on the distal tip which presented similar attributes to the “impact polish” observed on the experimental Levallois points used in hand-delivered throwing spear experiments (see Section 6.3.3.3.1) suggests the utilisation of this tool as a projectile tool, possibly in throwing motions. The presence of two sliced notched and the rough, dull polish (Figure 10.11) may be interpreted as traces resulting from the utilisation of soft bindings, forming part of a possible hafting system.



1 cm

Figure 10.10. Projectile motion: Specimen #M6 1033 4.2 with indications of trace locations (red **x** indicates the location of individual traces and letters show the location in which microscopic pictures were taken [Figure 10.11]).

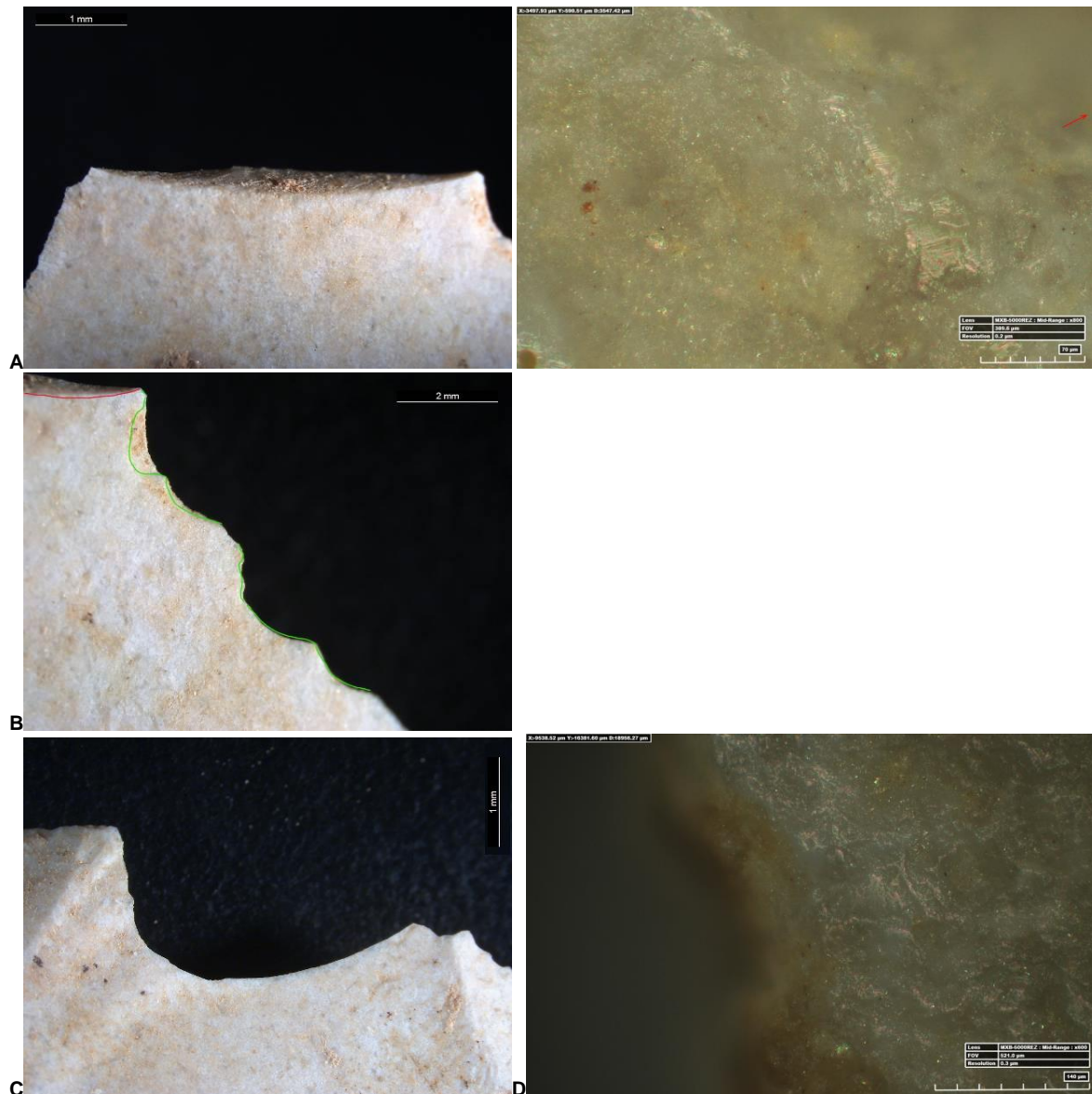


Figure 10.11. Specimen #M6 894 4.2. Location A: (left) snap fracture of the distal tip, SM OM25x; (right) polish located on the fracture line of the snap fracture. It shows a flat topography with longitudinal striations, DM OM 400x. Location B: snap fracture (in red) plus edge-damage (crushing of right lateral edge, in green), SM OM. Location C: sliced notch on the right dorsal edge, SM OM 25x. Location D: rough and dull polish located on the right dorsal notch, DM OM 600x.

Specimen #16 336 4.1:

- Technological description: the Levallois point has been extracted from the central part of the core using longitudinal convergent Levallois reduction sequences (La Porta, 2013; Boëda, 1982). The original core, presumably of large dimensions (>10 cm), was prepared to define the central and distal convexities that help the extraction of the predetermined point, as testified by the presence of a pronounced central ridge (Figure 10.12).
- Use-wear: a primary burination fracture (>5 mm) associated with intense edge-damage (in form of crushing of the lateral distal edges) was visible also to the naked eye (Figure 10.12 and Figure 10.13). Isolated lateral sliced scars were observed on the lateral mesial-proximal edges (Figure 10.12), possibly relating to hafting processes.
- Interpretation: although distal edge-damage alone is not diagnostic of projectile impact utilisation (even if this patterning has been observed on the experimental Levallois points used as thrusting spear-points; see Section 6.2.3), its association with a primary burination fracture with a bending initiation (which is considered diagnostic of projectile impact, Geneste and Plisson, 1989, 1990; Lombard, 2005a; Lombard and Pargeter, 2008; Yaroshevich et al., 2010, 2016; Pargeter, 2013) suggest the utilisation of this Levallois point as a projectile point, although the type of delivery motion could not be identified.

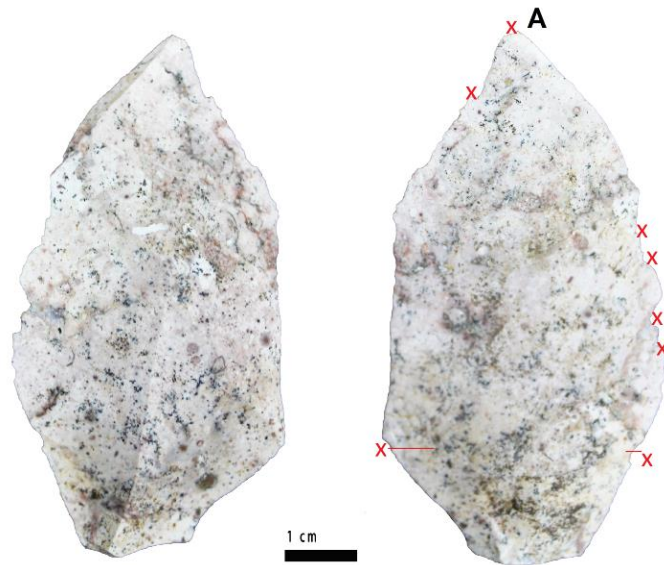


Figure 10.12. Projectile motion: specimen #I6 336 4.1 with indications of trace locations (red x indicates the location of individual traces and letters show the location in which microscopic pictures were taken [Figure 10.13], the red line indicates the possible haft limit).



A
Figure 10.13. Specimen # I6 336 4.1. Location A: primary burination fracture starting on the distal tip, associated with edge-damage on the lateral dorsal edges, SM OM 45x.

Four other convergent tools were interpreted as conceivable projectiles (Table 10-7). However, since use-wear traces were not completely preserved as a result of moderate post-depositional alterations, the functional interpretation was marked as “possible” (Table 10-7).

Specimen #M8 54 4.1:

- Technological description: the Levallois point was produced by employing Levallois unidirectional convergent reduction sequences, with a three-blow technique (La Porta, 2013; Boëda, 1982; Figure 10.14).
- Use-wear: the tool presented a step-hinge bending fracture terminating on the dorsal distal tip (Locus D1d; Figure 10.15). The bending fracture was associated with edge-damage on both distal edges (Locus D2d, D3d; Figure 10.15). No microscopic wear traces were observed (or preserved).
- Interpretation: the association between the step-hinge terminating bending fracture and the distal edge-damage may suggest the utilisation of this Levallois point as a possible projectile tool, however, no further traces were observed. Hafting was not explicitly recognised, although, the dorsal central ridge presented a high-degree of abrasion (Figure 10.15). This abrasion could be associated with a hafting presence (resulting from the pressure of the haft against the tool) or conversely could have also been produced also by post-depositional alteration (by the rubbing of the tool against the depositional soil). Therefore, hafted was not inferred.

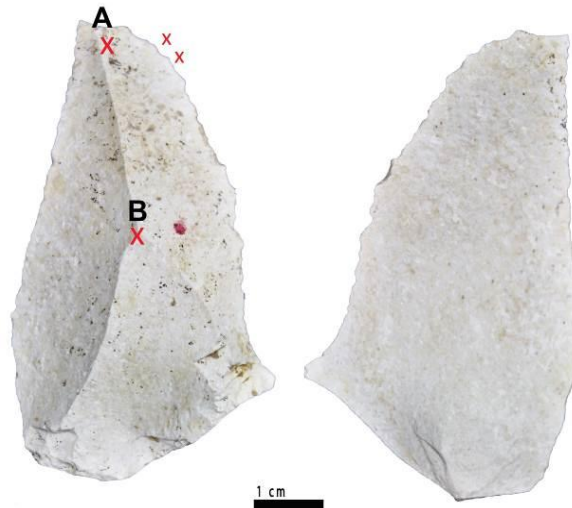


Figure 10.14. Projectile motion: specimen #M8 54 4.1 with indications of trace locations (red **x** indicates the location of individual traces and letters show the location in which microscopic pictures where taken [Figure 10.15].



Figure 10.15. Specimen # M8 54 4.1. Location A: bending fracture terminating in a step-hinge on the dorsal distal tip and distal edge-damage (D1d), SM OM 15x, and DM OM 6x. Location B: abrasion of the dorsal central ridge, DM OM 600x (left picture) and 1000x (right picture).

Specimen #J7 35 4.1:

- Technological description: the Levallois convergent flakes was extracted employing unidirectional convergent reduction sequences (Figure 10.16).
- Use-wear: it showed a bending fracture terminating in a hinge-step, associated with abundant edge-damage located only on the distal-mesial part of the tool, also visible to the naked eye (Figure 10.17 and Figure 10.16). No evident hafting traces were observed (due to preservation or low-development in the past).
- Interpretation: the association between the diagnostic bending fracture and edge-damage located only on the distal portion of the tool may suggest that the tool was used as a possible projectile.

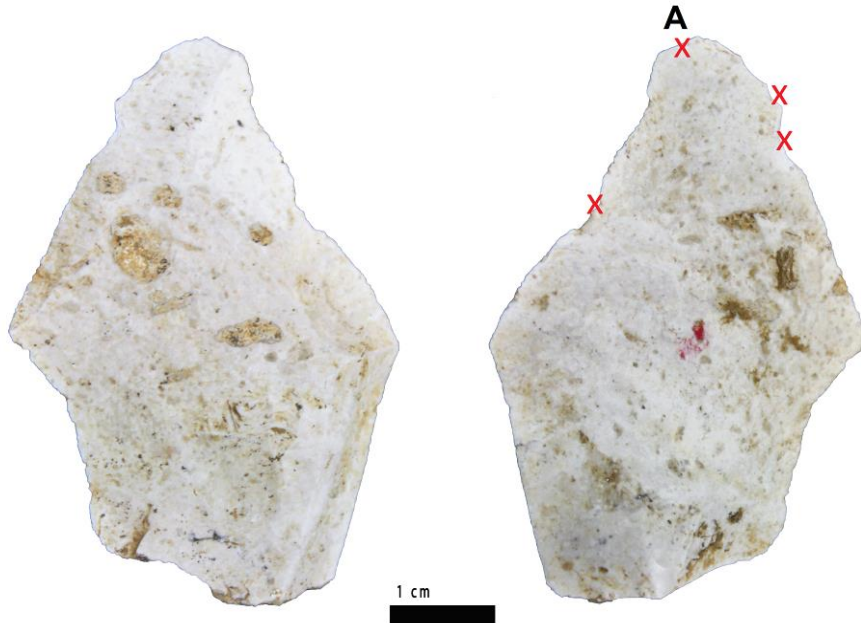
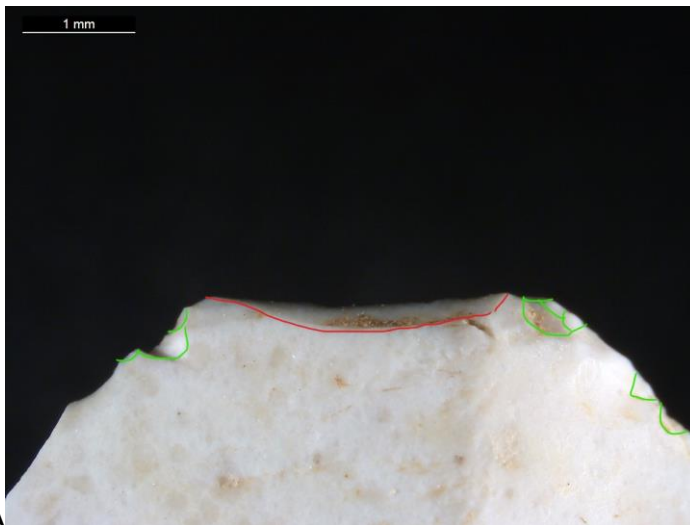


Figure 10.16. Projectile motion: specimen # J7 35 4.1. with indications of trace locations (red x indicates the location of individual traces and letters show the location in which microscopic pictures were taken [Figure 10.17].



A
Figure 10.17. Specimen #J7 35 4.1. Location A: bending fracture terminating in a step/hinge on the dorsal tip (in red), plus distal edge-damage (in green), SM OM 25x.

Specimen #M7 192 4.2:

- Technological description: the tool is a convergent déjeté scraper obtained by continuous retouch on both lateral edges. The blank was produced by exploiting the lateral convexity of a unidirectional core, possibly Levallois (Figure 10.18).
- Use-wear: on the distal tip, the tool displayed a large bending fracture terminating in a hinge (Figure 10.19). This was associated with abundant edge-damage on the distal area. Two isolated lateral sliced scars were observed on the lateral mesial-proximal edges (Figure 10.19), and the retouch starts only above these.
- Interpretation: the association of the large bending fracture and distal edge-damage may suggest the utilisation of this tool as a possible projectile. The tool, moreover, showed a specific technological expedient, which may suggest the presence of a hafting system. The retouch started only above the proximal part of the tool (Figure 10.18), and this part presented sliced scars that can be associated to the presence of a hafting system (Figure 10.19). This expedient may indicate that the tool was retouched, and/or re-sharpened when it was already inserted into a hafting system (Figure 10.18). This technological behaviour had been defined as retooling, and it can be indicative of hafting process (Keeley, 1982). A possible (but not unique) interpretation is that the possible projectile was retooled when it was already inserted into the haft system (or conversely, it was re-tooled and used for different activities). However, the lower preservation of microscopic traces did not allow further functional results.

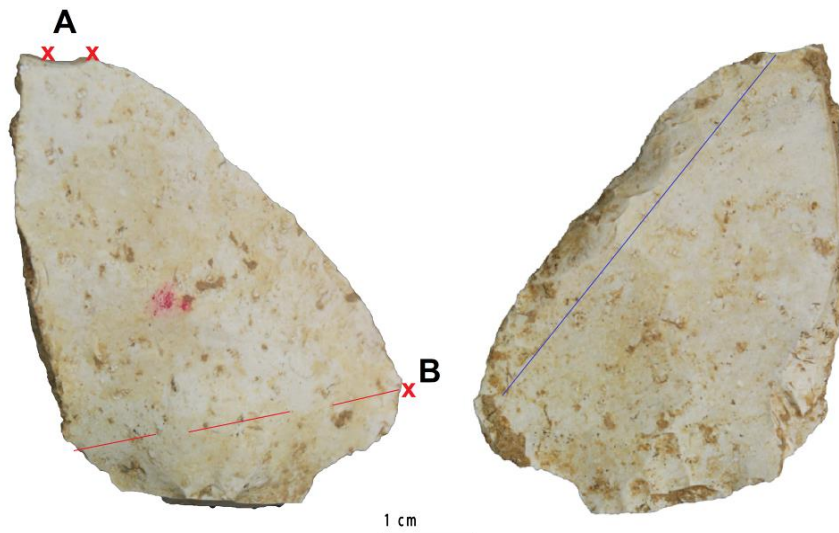


Figure 10.18. Projectile motion: specimen #M7 192 4.2 with indications of trace locations (red **x** indicates the location of individual traces and letters show the location in which microscopic pictures were taken [Figure 10.19]), the blue line indicates the retouch, and red line the possible haft limit).

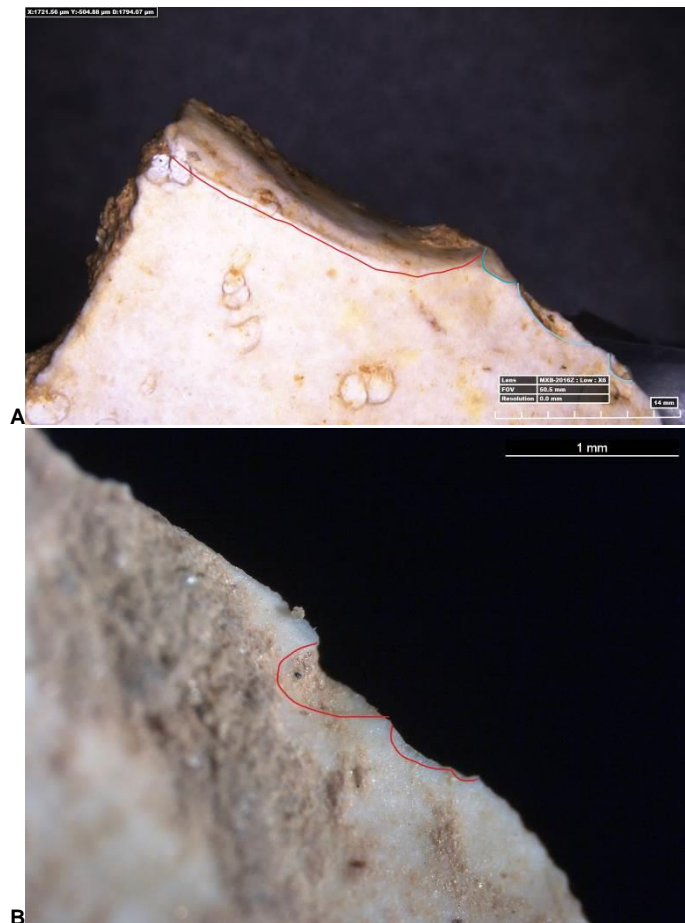


Figure 10.19. Specimen # M7 192 4.2. Location A: bending fracture terminating in a hinge on the distal ventral tip (in red) plus small cone scars (in blue), DM OM 6x. Location B: notch characterises by sliced scars (in red) on the dorsal right edge, SM OM 25x.

Specimen #F6 39 4.2:

- Technological description: the Levallois convergent flake was extracted using centripetal schemes from the lateral part of a Levallois core (Figure 10.20).
- Use-wear: on the ventral distal tip, the tool displayed a bending fracture with an undetermined termination (Figure 10.21). The fracture was associated with isolated edge-damage on the lateral mesial edges (locus M1v, M2v), which started only from the proximal part of the tool.
- Interpretation: the sharply defined limit of the edge-damage only above the proximal part of the tools, may indicate the presence of a hafting system. The association of this evidence with bending fractures located on the distal tip of the tool may suggest the utilisation of this tool as a “possible projectile”. However, no further traces were observable due to the presence of post-depositional alterations.

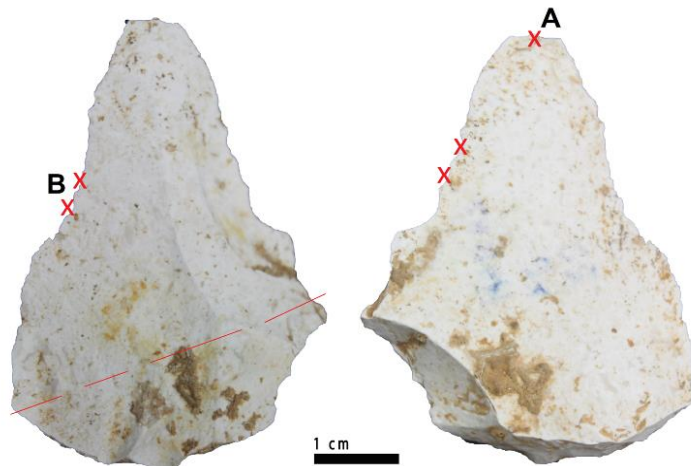


Figure 10.20. Projectile motion: specimen # F6 39 4. with indications of trace locations (red **x** indicates the location of individual traces and letters show the location in which microscopic pictures were taken [Figure 10.21], and red line the possible haft limit).

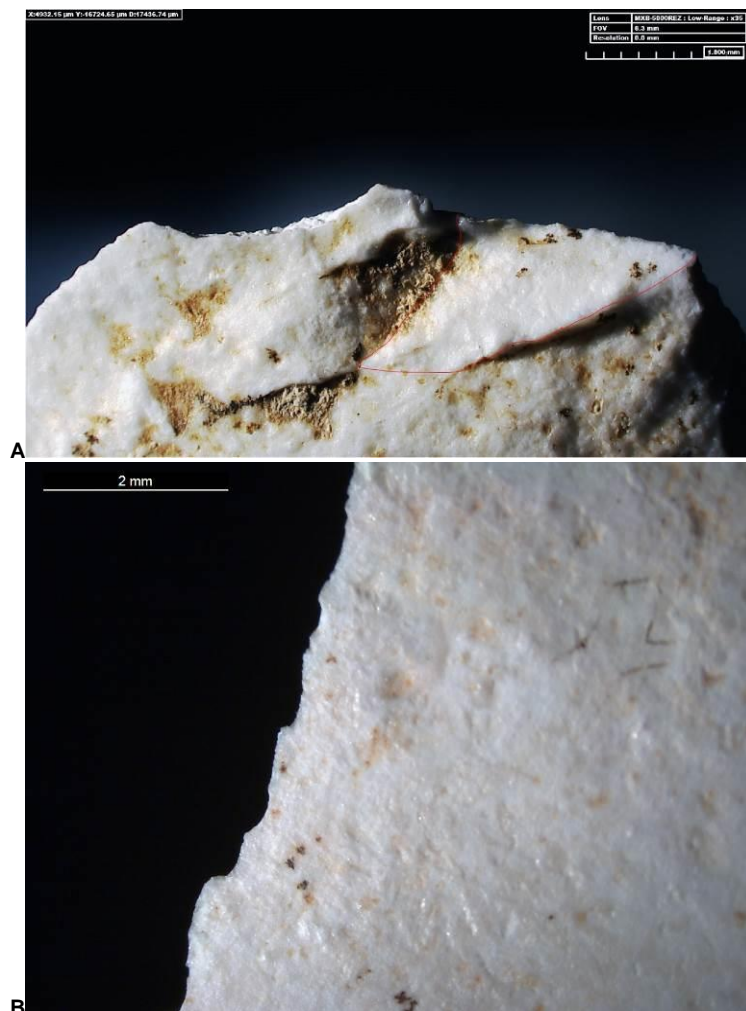


Figure 10.21. Specimen #F6 39 4.2. Location A: bending fracture with undetermined termination on the distal tip (in red), and modern trampling, DM OM 35x. Location B: edge-damage, on the left dorsal edges, SM OM 35x.

10.2.1.2 Tools used in longitudinal motions: use-wear evidence

On tool showed traces of longitudinal motions (such as cutting or sawing movements; Table 10-7).

Specimen #K6 379 4.1:

- Technological description: the Levallois point was produced by employing Levallois unidirectional convergent reduction sequences, with the three-blow technique (Figure 10.22; see Section 8.3.7.1). It showed a méplat on the left lateral edge and a rounded tip (75° angle), (Figure 10.22).
- Use-wear: the point showed traces of utilisation on the right mesial edge and rounded tip (interpreted as active areas of utilisation). On the distal tip, a fluid polish was identified (Jensen, 1994, p. 38; Figure 10.23). It showed a smooth texture, a flat topography, and a reasonable degree of linkage (Figure 10.23). It has been interpreted as a plant-like polish. This polish was located all along the tip and it presented small longitudinal striations within it (Figure 10.23). On the proximal surface, the tool displayed a strip of globular black residue located on the proximal dorsal right part of the ventral face (Figure 41). This residue showed optical resemblance (in term of texture and granulometry) with the experimental residues of tar adhesives observed on the experimental Levallois points used in hand-delivered stone-tipped spears (see Figure 7.17). However, chemical analysis (spectroscopy analysis in progress) is needed to confirm the nature of this residue. On the proximal right edge, the tool displayed intense fracturing (with multiple bending fractures) especially on the proximal right corner (Figure 10.23).
- Interpretation: the presence of a plant-like polish³⁵ (Jensen, 1994) on the distal tip and distal edges which showed small longitudinal striations indicates

³⁵ Roots polishes (caused by the presence of roots in an archaeological depositional soil) have been sometimes misinterpreted as plant polish (Van Gijn, 1989, p. 48). However, in this case, the location and distribution of the plant polish covers the entire tip edge, which makes it difficult to suppose that this polish is due to roots presence, since root polishes have a random location and a localised distribution (Van Gijn, 1989, p. 48).

that the Levallois point was used against plant materials (e.g. reed or harder siliceous plants), in longitudinal motions (Keeley, 1980; Van Gijn, 1989, p. 40). On the proximal right edge, the presence of intense fracturing especially on the proximal right corner associated with a possible adhesive residue (e.g. tar-like residue) suggests that the tool was inserted into a hafting system and possibly fixed with glues. The haft contact material was not possible to be interpreted as wear traces were poorly preserved, or they did not develop in the past. However, by the proximal location of the hafting traces, it is likely that the tool was inserted longitudinally into the haft system with the main convergent edges free for the most part.

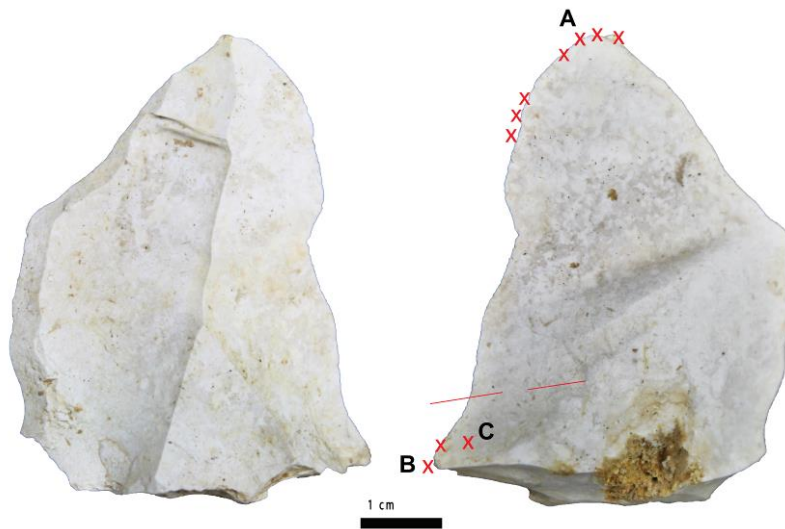
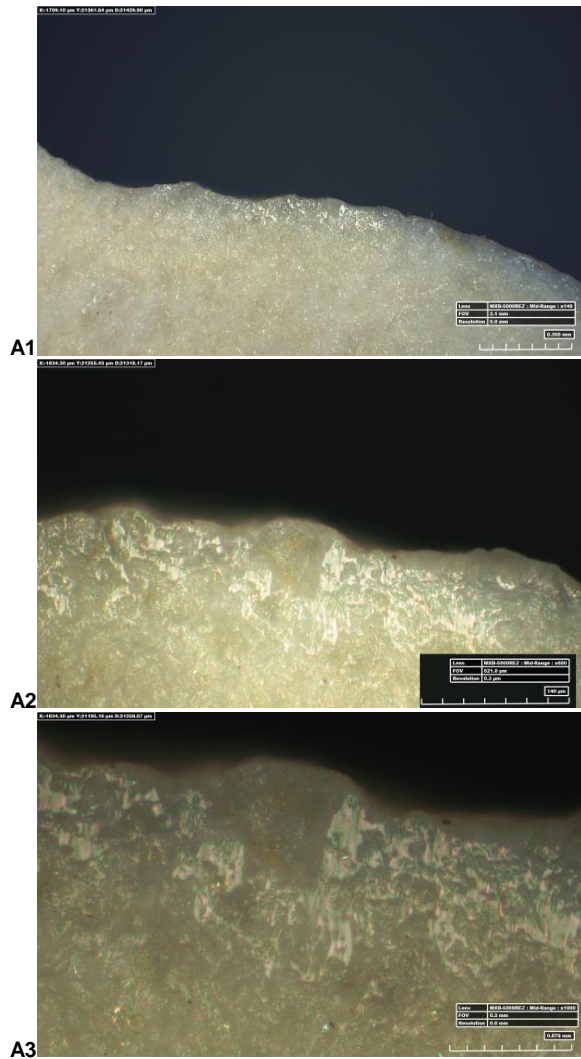


Figure 10.22. Longitudinal motion: specimen #K6 379 4.1 1 with indications of trace locations (red x indicates the location of individual traces and letters show the location in which microscopic pictures were taken [Figure 10.23], the red line indicates the possible haft limit).



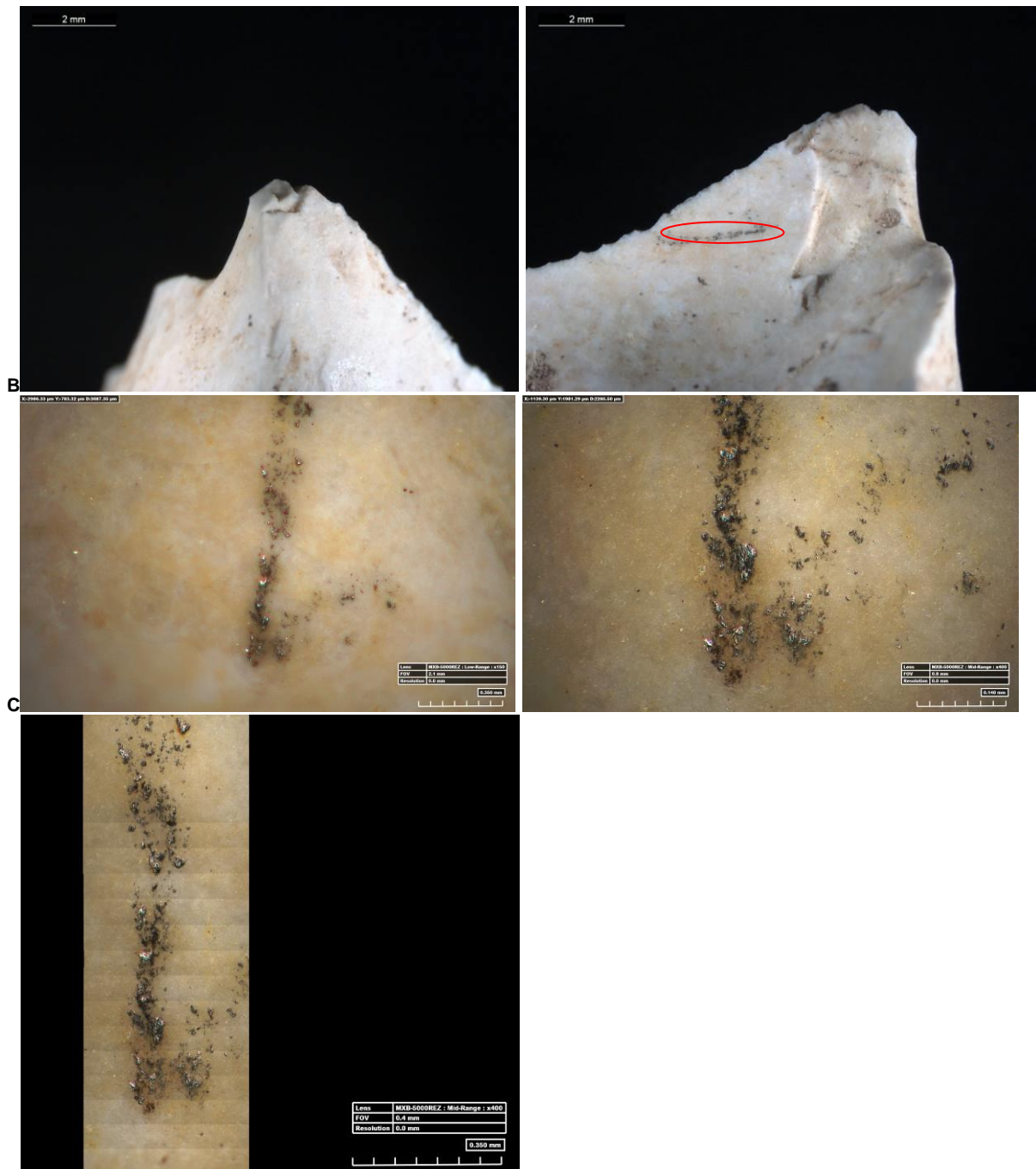


Figure 10.23. Specimen # K6 379 4.1. Location A: polish located on the distal ventral tip. At 140x (A1) it shows a very bright aspect (DM OM 140x); at 400x (A2), the polish shows a linked degree and a domed-flat topography (DM OM 400x); at 600x (A3) the polish shows edge-rounding and longitudinal striations embedded in the polish (DM OM 600x). Location B: edge-damage and bending-step fractures on the proximal right edge (interpreted as a result of insertion in the haft) the red circle indicates the position of the black globular residue, SM OM 50x. Location C: black strip of globular residue (similar to the experimental tar adhesives, see Figure 7.17) DM OM 100x and 400x.

10.2.1.3 Tools used in transversal motions: use-wear evidence

One tool showed traces of transversal motions (such as scraping movements; Table 10-7).

Specimen #H6 26 4.1:

- Technological description: the tool is a convergent Levallois preferential flake with a rounded distal edge and a tip angle of 85° (Figure 10.24).
- Use-wear: the tool presented a high degree of edge-damage all around the distal edge. The edge-damage, in form of triangular and scalar cone scars with a subparallel direction, presented very angular damage, suggesting a high degree of contact-angle between the tool and the contact material (Figure 10.25). On the distal edge, microscopic analysis revealed the presence of a functional polish. The polish showed an intrusive distribution, a domed topography with an almost pitted aspect (Van Gjin, 1989; Figure 10.25). It presented clear transversal striations embedded into the polish (Figure 10.25). Intense edge-rounding of the distal edge was visible (Figure 10.25).
- Interpretation: the association of intense edge-damage with an angular inclination and the presence of transversal striations embedded into the polish indicates that the tool was used in transversal motions (possibly as a scraper; Tringhman, 1974, table 2). Whereas, the intensity of edge-damage suggests a medium-hardness of the contact material (Tringhman, 1974, table 2; Van Gjin, 1989). Due to visible patination on the ventral face and post-depositional shine, the interpretation of the type of polish was not defined.

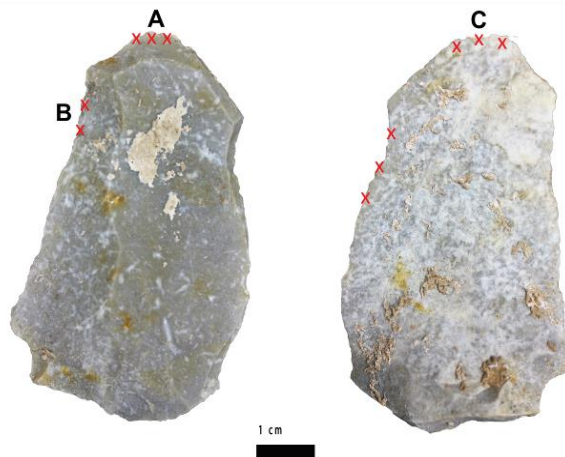


Figure 10.24. Transversal motion: specimen #H6 26 4.1 with indications of trace locations (red x indicates the location of individual traces and letters show the location in which microscopic pictures were taken [Figure 10.25]).

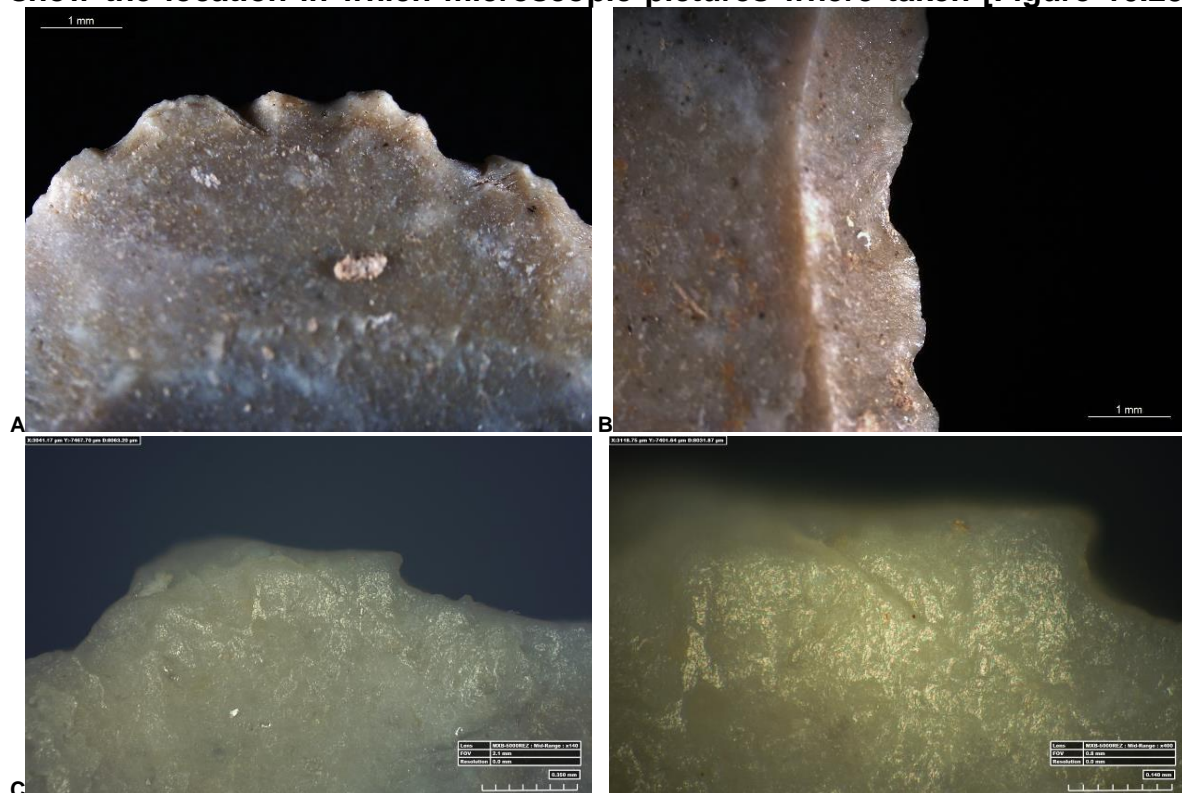


Figure 10.25. Specimen #H6 26 4.1. Location A: edge-damage (triangular and scalar scars) on the distal ventral end of tool, SM OM 10x. Location B: edge-damage (scalar scars) on the lateral dorsal edge, SM OM 20x. Location C: edge-rounding and polish located on the ventral distal edge (left) DM OM 140x, (right) the polish presents a pitted aspect and an intrusive distribution (the shiny lustre is possibly due to post-depositional alteration), DM OM 400x.

10.2.1.4 Tools used in multiple motions: use-wear evidence

One tool showed traces of utilisation in different motions (i.e. multifunctional tool; Table 10-7).

Specimen #K6 371 4.1:

- Technological description: the Levallois point was extracted from the central part of the core using the two lateral convexities of a prepared Levallois core, employing unidirectional convergent reduction sequences (Figure 10.26; Boëda, 1982, 1986; La Porta, 2013).
- Use-wear: the tool exhibited three active parts (i) the distal tip, and (ii) both lateral edges. The distal tip showed intense and pronounced edge-rounding, associated with the presence of three bending fractures (a step and two hinge fractures) terminating on the distal ventral tip. The ventral distal tip presented also a bright and well-distributed polish (Figure 10.27). The polish exhibited a fluid-aspect, a smooth texture and good-degree of linkage (Figure 10.27). The two lateral mesial showed intense edge-damage in form of large cone scars (with scalar morphology; Figure 10.27).
- Interpretation: the intense degree of edge-rounding of the distal tip associated with intense fracturing (three bending fractures) may suggest the utilisation of the distal tip in rotatory motions (e.g. drilling, boring movements; Van Gijn, 1989), whereas the presence of a fluid, plant-like polish may indicate a utilisation against plant contact materials (e.g. reed/harder siliceous plants; Jensen, 1994). Therefore, the distal tip of the Levallois point could have been used as a piercer or borer against plant materials. Whereas, the intense degree of scarring of the lateral edges (with large cone scalar scars) cannot be related to utilisation against soft materials (since soft contact materials would produce a gentler edge-damage; Keely, 1980; Van Gijn, 1989; Jensen, 1994), indicating instead a possible contact against medium-hard materials (Tringham, 1974, table 2), as confirmed by the presence of abundant edge-damage running along both edges (Figure 10.27). In conclusion, the tool presented three functional parts: the distal tip employed in a rotatory motion

against a soft material (i.e. plant-like materials), and the two lateral edges employed possibly in cutting/sawing motion against a medium-hard material (although its lanceolate morphology, impeccable for a projectile tip!). The combination of these data indicated the versatility of the tool, which was used in multiple actions and possibly against different materials. No traces of hafting were identified.

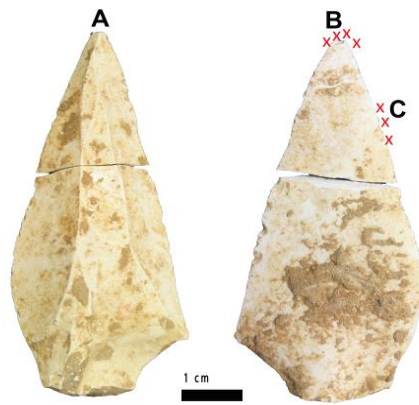
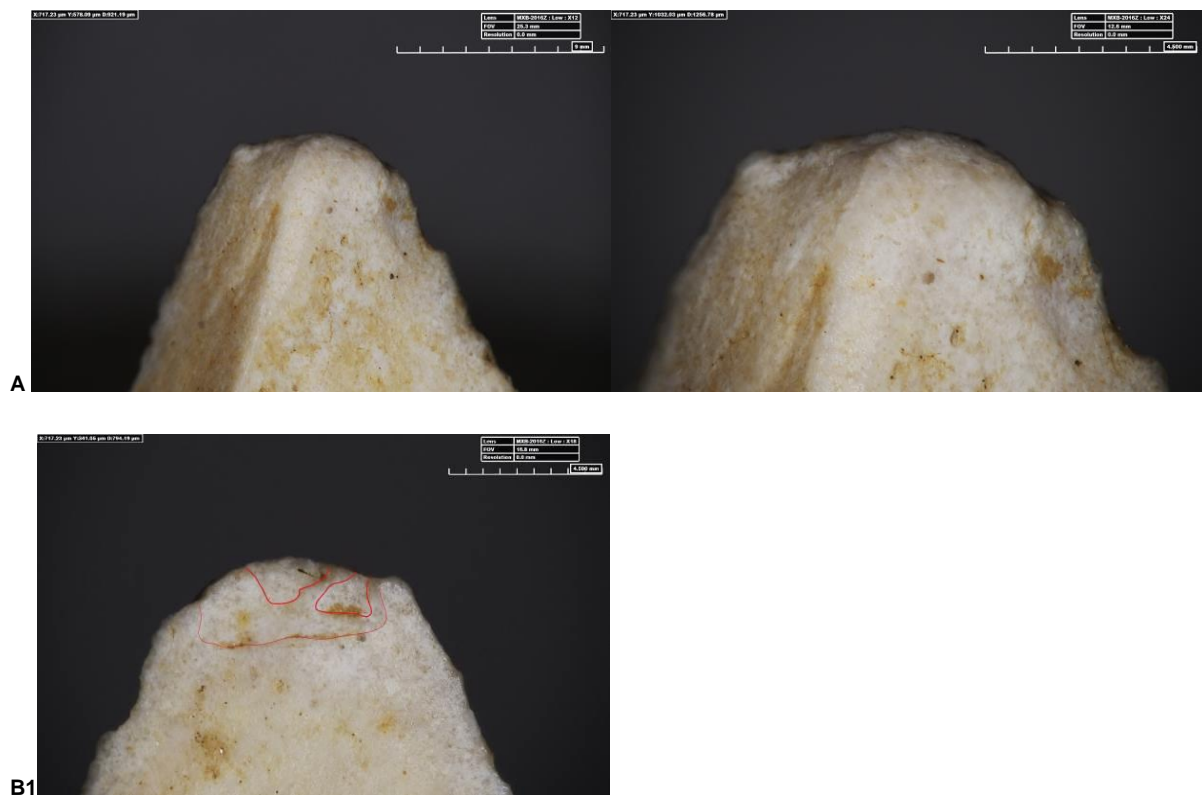
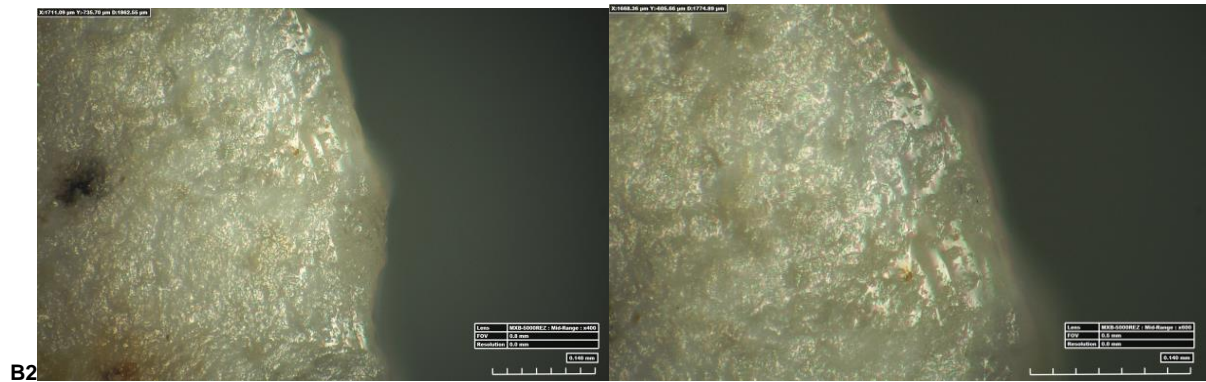
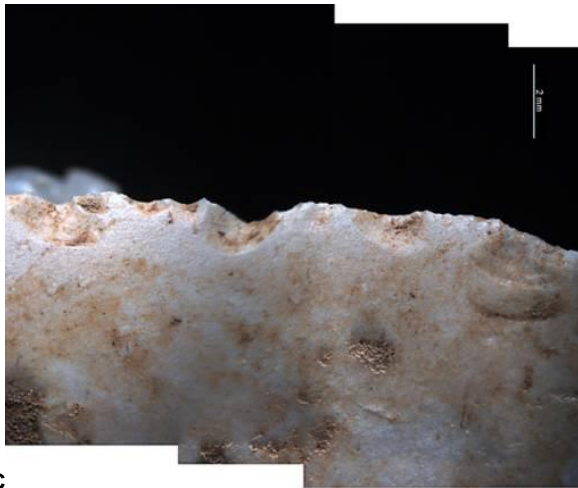


Figure 10.26. Multiple motions: specimen # K6 371 4.1 with indications of trace locations (red x indicates the location of individual traces and letters show the location in which microscopic pictures where taken [Figure 10.27]).





B2



C

Figure 10.27. Specimen #K6 371 4.1. Location A: intense edge-rounding on the distal dorsal tip, DM OM at 12x and 24 x. Location B1: three bending fractures with step and hinge terminations (in red), on the distal ventral tip, DM OM 18x. Location B2: (left) polish located on the distal tip (D1v). It shows an invasive distribution along the edge, DM OM 400x; (right) the same polish presents a fluid aspect, a smooth texture, and a flat topography, DM OM 600x. Location C: edge-damage on the lateral edge that present large scalar scars, SM OM 10x.

10.2.1.5 Used tools but unknown function: use-wear evidence

A total of seven Levallois points and three convergent tools were recognised as used tools (Table 10-7). However, due to intense post-depositional alteration or low preservation of traces the function, motion and contact materials could not be inferred.

Specimens #N6 186 4.1 and #M6 368 4.1 are here presented as an exemplification of the.

Specimen #N6 186 4.1:

- Technological description: the small point (40 mm length) was produced by employing unidirectional convergent reduction sequences, exploiting the lateral convexities of a prepared core (Figure 10.28).
- Use-wear: the tool was characterised by the presence of edge-damage on both lateral edges (Figure 10.29). Two notches in form of sliced scars (Rots, 2010), one on the proximal/mesial left and right edges, were also observed (Figure 10.29; perhaps indicating a sort of half limit).
- Interpretation: due to the poor preservation of the use-wear traces the interpretation of the movement and contact material was not possible. However, the degree and location of edge-damage indicated that two lateral edges were used (i.e. active parts). The small dimension of the Levallois point tool, and the fact that it was used possibly against soft-medium materials, as suggested by the light degree of edge-damage, might suggest that the small tool was used for completing light tasks.

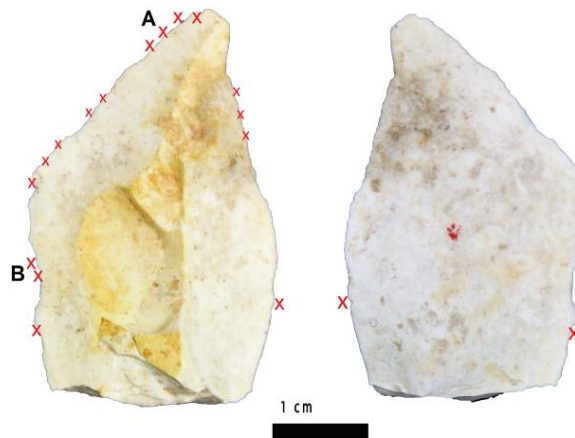


Figure 10.28. Unknown motion: specimen #N6 186 4.1 with indications of trace locations (red **x** indicates the location of individual traces, letters the location where microscopic pictures where taken [Figure 10.29]).

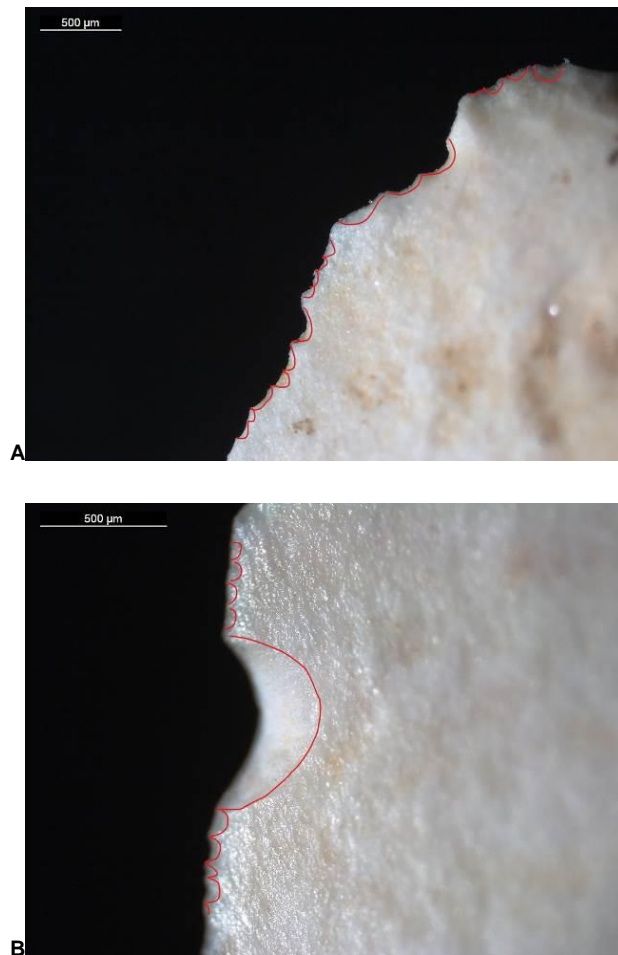


Figure 10.29. Specimen #N6 186 4.1. Location A: edge-damage (scalar and half-moon scars) located on the distal portion of the tool, SM OM 35x; Location B: edge-damage (sliced and half-moon scars) located on the mesial portion of the tool, SM OM 50x.

Specimen #M6 368 4.1:

- Technological description: the tool was an elongated Mousterian point (64 mm length) with semi-abrupt, invasive bilateral retouch. The blank was produced by employing a Levallois unidirectional longitudinal reduction sequence (Figure 10.30).
- Use-wear: edge-damage was present only on the left side (in ventral view). The scars with a discontinuous extension had mostly a rectangular and trapezoidal morphology (Figure 10.31).
- Interpretation: due to patination and encrustations, motion and worked material was difficult to identify. However, the presence of edge-damage indicates that the left side part of the tool was used (i.e. active part).

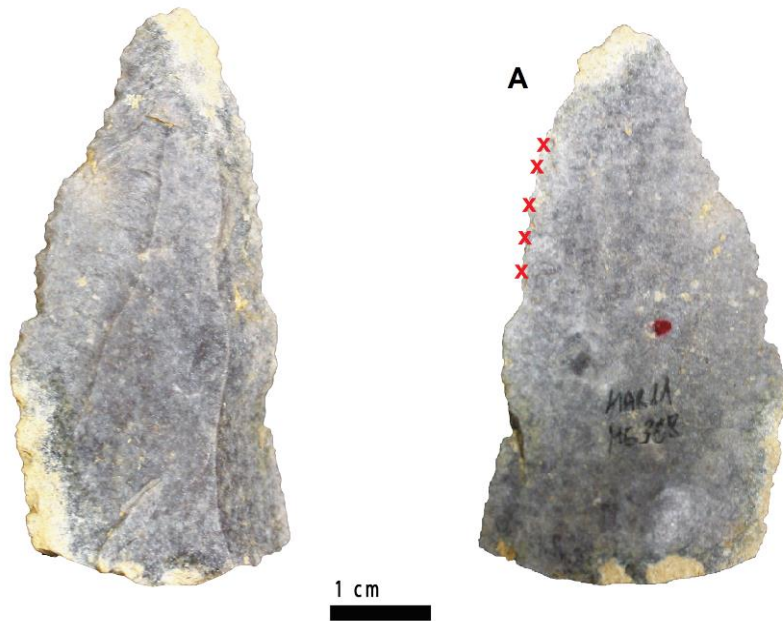


Figure 10.30. Unknown use: specimen # M6 368 4.1 with indications of trace locations (red x indicates the location of individual traces, letters the location where microscopic pictures where taken [Figure 10.31]).



Figure 10.31. Specimen # M6 368 4. 1. Location A: Edge-damage (rectangular and trapezoidal scars) on the left ventral edge of the tool, SM OM 30x.

10.3 Outcomes: functional interpretations

Use-wear analyses on the selected convergent tools of Abri du Maras found that out of n=32 tools, fourteen (also analysed with high-power approach, see Table 10-4) showed evident traces of utilisation that allowed a functional interpretation as “used tools” (Table 10-6). Eight other tools have been interpreted as “possibly used tools” because use-wear traces were not completely preserved due to the presence of moderate post-depositional alterations (Table 10-6). Six tools presented no visible traces of utilisation and were classified as “no traces” category³⁶ (Table 10-6). Four more tools showed substantial post-depositional alterations that did not allow a reliable interpretation and were classified as “not interpretable” (Table 10-6).

Table 10-6. Functional interpretation of the analysed convergent tools (n=32).

Use interpretation	Level 4 (n=32)
Used	14
known	7
unknown	7
Possibly used	8
No traces	6
Not interpretable	4
Total	32

Among the 14 convergent tools (analysed also with higher magnifications) that showed positive traces of utilisation (i.e. “used” tools, Table 10-6), four tools were identified as projectiles (Table 10-7 and Section 10.2.1.1); one to be used in activities with transversal motions (Table 10-7 and Section 10.2.1.3); one in longitudinal motions (Table 10-7 and Section 10.2.1.1); and one to be used as a

³⁶ “No traces” category is here preferred to the “not used” category. In fact, short periods of utilisation and/or utilisation against soft contact materials (e.g. meat) can leave very few traces on stone tool surfaces. Therefore, the “no wear” category has the scope to contain under-represented tools that might have been used for short periods in the Middle Palaeolithic without leaving clear traces of utilisation.

multifunctional tool, i.e. used for more than one motion (Table 10-7 and Section 10.2.1.4). The other seven tools that presented traces of utilisation (i.e. “used tools”, Table 10-6), the movement and/or contact material was not interpretable due to lack of clear preserved traces. They were, therefore, classified as “used but unknown” (Table 10-7 and Section 10.2.1.5).

Among the eight tools interpreted as “possibly used” (Table 10-6), due to a moderate presence of post-depositional alterations, four tools have been interpreted as “possible projectiles” (Table 10-7 and Section 10.2.1.1), and four tools as generic “possibly used” tools (Table 10-7). This because traces were not completely preserved and caution was applied in the final interpretation, defining them as “possible used” tools (Table 10-7).

The remaining ten tools that showed “no traces” or were too altered (i.e. “not interpretable”, Table 10-6) to allow a precise functional interpretation to be made, are not presented in this chapter because of the lack of interpretable traces.

Regarding the contact materials, two convergent tools presented evidence of plant working (specimens #K6 371 4.1 and #K6 379 4.1), suggesting that plant working activities took place in the site (as also proposed by Hardy and Moncel, 2011; Hardy et al., 2013). Whereas, the use-wear examination of the Levallois points and convergent tools evidenced a lack of butchering or meat processing tools. However, this trend can be flawed by the presence of patination and post-depositional phenomena that may have entirely obliterated possible butchering and animal processing use-traces³⁷, or short contact utilisation.

On the other hand, the use-wear analysis has also shown that at least n=5 Levallois points and other n=3 convergent tools (out of the 32 analysed convergent tools) were employed in projectile motions, which represented 25% of the analysed convergent tool of Abri du Maras Level 4 (Table 10-7). This evidence indicates that at Abri du

³⁷ Residues (Hardy and Moncel, 2011) and zooarchaeological analyses (Daujeard et al., 2017; Vetesse et al., 2017) have revealed the presence of cut-marks on bones and animal residues on stone tools, testifying that butchering activities were undertaken at Abri du Maras Level 4 (see also Section 8.3.5).

Maras Level 4, a part of the Levallois points and convergent tools were employed for activities concern projectile utilisations, most likely related to animal hunting (see also CHAPTER 11). The interpretation of the projectiles tools was based on multiple lines of evidence. Multiple impact-fractures such as burination, bending initiating fractures, and spin-off were presented in all the eight interpreted projectile tools (Section 10.2.1.1). Microscopic linear impact traces (MLITs) were observed in at least one case (specimen #IJ7 111 4.1; Section 10.2.1.1), although they were not well preserved due to patination phenomena. The presence of polish traces similar to the “impact polish” observed in the experimental Levallois points used in hand-delivered spear experiments, may suggest that “impact polis” can also be visible in archaeological projectile tools. These results indicate under multiple lines of evidence that at least a part of convergent tools at Abri du Maras Level 4 were employed as projectile tools (Table 10-7). However, due to the low preservation of microscopic wear traces, the type of delivery system of these projectile tools was not possible to infer. Nevertheless, the presence of polish traces possibly due to impact activities (i.e. “impact polish”) and linear traces (such as MLITs and longitudinal striations) which this study have proved to be statistically significant of hand-delivered throwing stone-tipped spears, may suggest that at least two projectile tools (specimens #M6 894 4.2 and #J7 111 4.1) may have been used in throwing motions (see also CHAPTER 11).

To conclude, the results of the functional analysis indicate that Levallois points and convergent tools at Abri du Maras Level 4 were used in a different panoply of motions such as projectile, longitudinal, transversal and rotatory motions (Table 10-7), and, therefore, a univocal correspondence between a function and a shape cannot be established. However, the presence of 25% of projectile tools within the analysed sample of Levallois points may suggest a preferential utilisation of this techno-morphological tool type as a weapon tool (see also CHAPTER 11).

Table 10-7. Functional interpretations of the convergent tools (n=30) of Abri du Maras, according to their techno-morphological class.

Techno-morphological tool type	Used tools					Possibly used		No traces	Altered	Total
	Projectile motions	Transversal motions	Longitudinal motions	Multiple motions	Unknown	Possible projectile motions	Possible used			
Levallois points (n=17)	3		1	1	4	1	3	3	1	17
Levallois points fragments (n=2)	1							1		2
Levallois triangular flakes (n=7)		1			1	2	1	1	1	7
Others (retouched and cortical convergent tools, n=6)					2	1		1	2	6
Total	4	1	1	1	7	4	4	6	4	32

CHAPTER 11

DISCUSSION

11.1 Research approaches

The primary aim of this thesis was to investigate the use of stone-tipped spear technology in the European Middle Palaeolithic, in order to explore *Homo neanderthalensis*'s capability of producing and using throwing and/or thrusting stone-tipped spears. The overarching research questions of this study, as outlined in CHAPTER 1, were:

- (i) to test the performance and effectiveness (expressed through penetration depth) of throwing and thrusting stone-tipped spear replicas when hand-delivered by trained human participants into animal targets (using realistic but controlled experimental variables).
- (ii) to test whether diagnostic projectile use-wear traces, patterns, and/or frequencies could assist in distinguishing between hand-delivered throwing and hand-delivered thrusting spear projectiles (using Levallois points as a control techno-morphological tool type).
- (iii) to test whether diagnostic projectile use-wear traces were still visible and preserved in stone tools from the archaeological record, in order to test the presence/absence of projectile tools and corroborate or reject the hypothesis that Neanderthals produced and employed stone-tipped spears, and that these spears were used either in thrusting or throwing activities respectively, or in both.

This was done by applying a multi-disciplinary approach which combined quantitative and qualitative experimental data with the use-wear analysis of experimental and archaeological stone tools (i.e. Levallois points and nominated convergent tools).

11.1.1 Experimental approach

The first approach consisted of the implementation of a systematic, comprehensive, and multi-set experimental programme, which utilised realistic but controlled sets of

variables in order to investigate hand-delivered stone-tipped spear technology. The precise choice of this experimental methodology, which integrated realistic but controlled variables with a meticulous experimental protocol and recording system (i.e. accelerometer and high-speed cameras), allowed this research to capture high-resolution data both on diagnostic macroscopic and microscopic use-wear traces (see CHAPTER 5). Furthermore, for the first time in the field of experimental archaeology, it allowed the realistic ballistic measurements of hand-delivered stone-tipped spears delivered by a trained and skilled human participant to be recorded, reaching a statistically effective sample.

As expressed in detail in CHAPTER 4 and CHAPTER 5, the use of trained human participants who had previous experience with hand-delivered spears in real hunting scenarios with the Ju/'hoansi bushmen group (at the Nyae Nyae Conservancy, Namibia; see Section 4.3.4) for the execution of these experiments, as opposed to calibrated firing-machines, allowed for the correct replication of both throwing and thrusting spear motions. This resulted in kinematic spear motions which fully replicated the trajectory of the throwing and thrusting spears, including rotatory spin in throwing motions and the accurate changes in momentum for thrusting motions (see CHAPTER 5). The replication of the entire kinematic motions of the experimental throwing and thrusting spears allowed for the formation of “real” and accurate use-wear traces on the experimental Levallois points used as spear projectiles. It has been suggested (Milks, 2016; Rots and Plisson, 2014; CHAPTER 5 of this thesis) that variations between different weapon types and delivery systems (e.g. throwing and thrusting systems) cannot only be expressed simply by replicating impact velocities or draw weights (as, for instance, in Shea et al., 2001; Iovita et al., 2014; Sano and Oba, 2015; Sano et al., 2016; Iovita et al., 2016), as the complete replication of spear throwing and spear thrusting motions is a complex phenomenon that must consider the entire trajectory of the spears, the degree of rotatory spinning motions (for throwing spears), and changes in momentum (for thrusting spears). With details summarised in CHAPTER 5, analysis of the spear acceleration profiles of hand-delivered throwing spears showed that spears start to accumulate acceleration (and therefore momentum) when the human thrower releases the

spear. This acceleration remains steady during the entire “flying time” of the spear³⁸ (during which, in experiments, light rotatory oscillations were recorded) and, upon impact against the target, when the spear loses acceleration (and therefore momentum), it relies on the accumulated kinetic energy to penetrate the target. In contrast to this, it has been shown, through the analysis of hand-delivered thrusting spear acceleration profiles (for instance that of the two-push profiles, see Section 5.3.4.2) that, in thrusting spear motions, the human thruster can generate further acceleration (and therefore a change in momentum) upon and after the impact, as the person’s body reacts to the resistance of the target (as also found by Milks et al., 2016). Therefore, proper replication of throwing and thrusting spear motions is essential in order to replicate “correct” use-wear on spear projectiles because motion invariably affects the type and degree of impact damage generated.

Similarly, the use of realistic but controlled variables, such as equivalent animal targets for each set of experiments (rather than ballistic gel targets), permitted a comparability between use-wear traces of experimental tools, and use-wear traces of archaeological tools (as suggested by Rots and Plisson, 2014). Moreover, because this study also focused on the analysis of microscopic use-wear traces, animal targets were more favourable, as microscopic use-wear traces (such as polish, striations, and MLITs) depend entirely on the characteristics of the contact material used (e.g. meat and bone; Hayden, 1979; Del Bene, 1979; Anderson, 1980; Anderson-Gerfaud, 1981; Levi-Sala, 1988; Fullagar, 1991; Ollé and Vergès, 2008), and therefore, the ballistic gel, although mimicking the behaviour of the muscle tissues, cannot present the same diversity of chemical composition and texture of animal tissues. Furthermore, as shown in Section 5.4, seeing as a strong correlation exists between the deceleration of the spears and their impact location (soft vs. hard tissues), if ballistic gel targets are employed in experimental settings it is highly recommended that they should incorporate bone tissues (in support of Rots and Plisson, 2014).

³⁸ In this study, the short distance of only 5 metres from the target did not allow for deceleration over time.

Likewise, the replication of realistic but standard spear-shafts (i.e. shafts with uniform shapes and controlled morphologies) that were accurate replicas of existing Middle Pleistocene archaeological spear shafts (i.e. Schöningen spear II, Schoch et al., 2015; see CHAPTER 4) meant that the experimental spear shafts had comparable values of spear mass with the selected archaeological spear shafts and, once again, this allowed for accurate replication.

11.1.2 Ballistic approach

On the other hand, the analysis of the performance and the recording of the ballistic measurements of the experimental hand-delivered stone-tipped spears (as expressed in detail in CHAPTER 5) allowed for the evaluation of the effectiveness of these weapon types and facilitated a better understanding of the kinematics of hand-delivered stone-tipped spears (which is still a new discipline in the field of projectile technology, see Milks et al., 2016, 2019; Gaudzinski-Windheuser et al., 2018). This resulted in the first calculation of representative ballistic parameters (e.g. impact velocities, kinetic energy, momentum, trajectories, deceleration at impact, and maximum penetration) both for throwing and thrusting experimental stone-tipped spears when hand-delivered by trained and skilled human participants into animal targets (but see also Milks et al., 2016, 2019; Gaudzinski-Windheuser et al., 2018 for thrusting spear experiments). The representative ballistic parameters calculated in this study can, in the future, be used to develop experimental protocols that aim to replicate and control precise kinematic values in spear experiments. Ultimately, the capturing of ballistic parameters has allowed for cross-comparisons to be made between the experimental use-wear traces formed on the Levallois points used in throwing and thrusting spear experiments and the condition (e.g. impact velocities and kinetic energy values) under which those traces formed, and this allowed for better investigation and explanation of the formation of diagnostic use-wear traces (discussed in Section 11.2).

11.1.3 Use-wear approach

The use-wear analysis of the experimental Levallois points used in throwing and thrusting stone-tipped spear experiments meant it was possible to differentiate

between diagnostic impact trace types and frequencies that can form both in throwing and in thrusting spear projectiles, which was one of the main research questions of this study. Moreover, the quantification of types, patterns, and frequencies of diagnostic impact traces that occurred for throwing points, but did not occur for thrusting points, allowed for the identification of diagnostic traces that enabled experimental distinction between throwing spear projectiles and thrusting spear projectiles. Furthermore, the creation of an experimental collection of projectile tools and tools used in activities other than projectiles (which represented a statistically significant dataset) for use-wear analysis enabled better comparisons to be made between experimental and archaeological use-wear traces.

In conclusion, the large amount of quantitative and qualitative data emerging from the experimental data-set meant that it was possible to create a robust methodological protocol for the use-wear analysis of projectile tools, and provided comparative data to support the interpretation of the archaeological stone tools.

11.1.4 Archaeological approach

Finally, the last approach of this study consisted of the archaeological examination of use-wear traces on the selected Levallois points and convergent tools of two Middle Palaeolithic stone tool assemblages: Arma delle Manie (Italy) and Abri du Maras (France) (see CHAPTER 8). This archaeological investigation sought to identify the presence/absence of stone projectiles in the archaeological assemblages and, if possible (considering issues of preservation of the use-wear traces), to reconstruct the delivery system employed for the launching of the recognised stone projectiles. The latter approach meant it was possible to enlarge the field of investigation in order to assess the main research question of this study, i.e. whether Neanderthal populations in the selected European Middle Palaeolithic sites produced and used throwing and/or thrusting stone-tipped spears and, if so, what evolutionary implications of this technology could be deduced.

The most significant results of this thesis are outlined below and are analysed in relation to their own importance, while also compared with previous studies in the field of Middle Palaeolithic spear technology and use-wear analysis.

11.2 Assessing the performance and effectiveness of Middle Palaeolithic hand-delivered stone tipped spear replicas

Data recorded with regards to the variables, performance, and ballistic parameters of hand-delivered throwing and thrusting stone-tipped spear experiments have been presented and largely discussed in CHAPTER 5. The results of this thesis have demonstrated, through the analysis of ballistic parameters, penetration depth, and acceleration profiles, that stone-tipped spear systems (when hand-delivered by skilled and experienced participants) were effective weapons, both in throwing and thrusting motions (see Section 5.6). This discussion now focuses on the comparison of the major findings of this thesis in terms of the performance of hand-delivered spear replicas mounted with experimental flint Levallois points, and their implication in the evolutionary context of Neanderthals using throwing and thrusting stone-tipped spears.

As addressed in CHAPTER 1, according to multiple authors (Shea, 2006; Churchill and Rhodes, 2009; Shea and Sisk, 2010) wooden spears (for instance, Schöningen spears) mounted with Middle Palaeolithic points “were too large, heavy, and slow-moving [for throwing]”, and that they should have been used as heavy thrusting weapons in short-range confrontation only (Shea and Sisk, 2010, p. 102; Schmitt et al., 2003). This hypothesis was mainly based on ethnographic analogies of morphometric values and the effective distance of throwing spears for modern hunter-gatherers’ groups (Churchill, 1993, but see Villa and Soriano, 2010; Shea, 2006). However, it has never been challenged experimentally. No experimental research has previously investigated the performance of hand-delivered Middle Palaeolithic stone-tipped spear replicas in order to verify their effectiveness in real scenarios; i.e. whether or not stone-tipped spears could effectively penetrate animal targets when delivered by hand. Moreover, no previous research has systematically tested the difference in performance between hand-delivered throwing and hand-delivered thrusting stone-tipped spear systems to evaluate possible differences or analogies. Consequently, the most important implications of this thesis lie in having tested and compared hand-delivered throwing and thrusting stone-tipped spear systems in a realistic scenario, i.e. with animal targets, demonstrating that replicas of

Middle Palaeolithic wooden spears mounted with flint Levallois points not only are effective thrusting spears (as also suggested by Shea et al., 2001; and Iovita et al., 2014), but are also highly effective throwing spears (with a constant distance of 5 m, kept as a controlled variable), as shown in Sections 5.4 and 5.6 .

The kinematic analysis of the experimental hand-delivered stone-tipped spears showed that both throwing and thrusting hand-delivered spears reached values of impact velocities, kinetic energies, and momentum in line with the estimated values of ethnographic throwing spears (Hughes, 1998; Table 1) (data presented in Table 5-10 and Table 5-11). Moreover, this study has shown that ballistic parameters of hand-delivered spears (velocity means of between 11.59 and 4.86 m/s; *KE* means of 43.50 and 16.90 J, see Section 5.3 and Table 5-11; and a momentum mean between 7.49 and 6.52 kgm/s, see Section 5.3 and Table 5-11) were sufficient not only to hit and cut through the skin of the animal, but to reach full penetration of the animal target, with peaks of 90 cm penetration depth for throwing spears and 122 cm for thrusting spears. The fact that hand-delivered throwing spears recorded a penetration mean of 30.9 cm into a real animal target (well beyond the theoretical lethality threshold), despite their heavy mass (646 g and 642 g mean), demonstrates that Middle Palaeolithic replicas of stone-tipped spears, when hand-thrown by expert users, can achieve enough kinetic energy and momentum values to be able to lethally penetrate the target. This confirms that the higher mass of a stone-tipped spear, when used by a skilled participant, is not a limiting factor when computing throwing motions.

The analysis of penetration depth showed that both throwing and thrusting spears had recorded much higher penetration values than the threshold of lethality (considered at 20 cm; Hughes, 1998); with slightly higher, but not statistically significant, values for thrusting (37.92 cm) than for throwing spears (30.90 cm; see 5.3.3). The means and ranges of penetration depths recorded for stone-tipped hand-delivered spears were much higher than in any previous experiments (either untipped spears, Milks et al., 2016; or tipped spears, Wilkins et al., 2014), possibly suggesting that stone-tipped spears can reach higher values of penetration depth

than untipped spears (contra Wilkins et al., 2014). Although, further and larger experimental samples would be needed to corroborate this hypothesis.

This study has also shown that, when used by trained and skilled participants, experimental spears mounted with replicas of flint Levallois points performed superbly well, both as throwing and thrusting spears (see Sections 5.3.3, 5.3.5., 5.6, and accompanying files, comments and videos on the USB). For throwing spears, excluding the spears that missed and went into the ground (n=6, Table 5-16), all spears penetrated the animal targets. The majority of the hand-delivered throwing spears not only reached a penetration depth greater than 20 cm (see Table 5-12), but they broke through the entire carcass, penetrating the target from side to side, causing large gaping wounds and crushing multiple ribs (see Section 5.3.5, and accompanying files, comments and videos on the USB). These data may support Wilkins's et al. (2014) hypothesis that stone-tipped spears create larger inner wound cavities and more damage than untipped spears. Even those throwing spears that achieved partial penetration (between 10 and 20 cm) created large wounds (a mean of 27 cm² area, see Table 5-10). On the other hand, all of the throwing stone-tipped spears that had a low penetration, <5 cm (see Table 5-16), impacted against the hardest part of the animal target, i.e. either the spine, scapula, or pelvis bone and, although they hit and cut through the skin, they bounced off. This was reflected in a significant negative correlation between impact location with hard tissues and lower penetration depth ($r_2=-.639$ $p=0.034$, see Section 5.4). On the other hand, except for one case (specimen TH-78), no catastrophic breaks of the experimental Levallois points were observed, and only n=5 tools (9.6% of the total sample) dehafted during their impact with the animal target, which suggests that all remaining tools (90.3%) could have been used multiple times (contra Shea et al., 2001, who recorded high levels of broken Levallois points during their experiments³⁹, however this difference could be due to their use of firing-machines and multiple numbers of shots).

³⁹ Shea et al., 2001 reported that 20.37% of Levallois points broke during utilisation. However, the definition of "broken point" is not clearly specified in the study and, therefore, a comparison could not be made.

It has also been shown that the penetration depth of the hand-delivered spears did not correlate with morphometric parameters, such as TCSA and TCSP (Shea, 2006; Sisk and Shea, 2009), or impact velocities (see Section 5.4). Partial correlation results showed that TCSA, TCSP and impact velocities were not significant predictors of penetration depth when multiple variables were taken into account, and, therefore, an important outcome of this research is that the use of TCSA and TCSP as ballistic proxies for distinguishing projectile delivery systems has been rejected (see Section 5.4; contra Shea, 2006; Sisk and Shea, 2009; Shea and Sisk, 2010; in agreement with Newman and Moore, 2013; and Clarkson, 2016).

In conclusion, the kinematic analysis of the hand-delivered stone-tipped spears provided by this study represent the first attempt in the field of experimental archaeology to record realistic ballistic parameters on hand-delivered throwing and thrusting stone-tipped spears, providing data for future replicative studies. The data presented in CHAPTER 5 validates the hypothesis that Middle Palaeolithic stone-tipped spears mounted with flint Levallois points were very effective weapons, not only as hand-delivered thrusting spears but also as hand-delivered throwing spears, and, despite their dense mass (mean of 646 g for throwing and 642 g for thrusting), reached sufficient levels of kinetic energy and momentum as to reach high means of penetration depth, which caused large and deep wounds and the breakage of multiple bones in the real animal target. Moreover, as they regularly caused gaping wounds, broke multiple bones, and deep penetration values on middle size animal targets (i.e. roe deer species), it is possible to suggest that they would have also been effective throwing hunting weapons against medium to large size mammals. The comprehensive data of this study therefore reject the hypothesis of Shea and colleagues (Shea, 2006; Churchill and Rhodes, 2009; Shea and Sisk, 2010) that Middle Palaeolithic stone-tipped spears, because of their heavy mass, were mostly used as confrontational thrusting weapons, opening new possibilities of interpretation concerning Middle Palaeolithic stone-tipped throwing systems.

The aptitude of Middle Palaeolithic stone-tipped spears to be used as effective throwing weapons, although within certain range limits (see Section **Error! Reference source not found.**), may have offered Neanderthals the possibility of

adopting more diverse hunting strategies that were not limited to face-to-face confrontation with the prey only, but also included a certain degree of flexibility thanks to the acquired distance (see Section **Error! Reference source not found.**).

The next section discusses the difference in use-wear traces between throwing and thrusting stone-tipped spear projectiles.

11.3 Assessing diagnostic use-wear traces of experimental hand-delivered throwing and thrusting spear projectiles

11.3.1 Macroscopic diagnostic traces

The experimental Levallois points, when used as hand-delivered stone-tipped spears for two different delivery systems (i.e. throwing and thrusting), showed that, when only macroscopic traces are analysed, a relationship between projectile diagnostic impact fractures (DIFs) and delivery systems cannot be easily established (see CHAPTER 6), and that the differences in DIF frequencies observed between throwing and thrusting Levallois points was not statistically different ($\chi^2=3.265$, $df=7$, $p\text{-value}=0.352$, see Table 6-2). However, the presence and absence of some types of diagnostic impact fractures (DIFs) observed in the experimental throwing and thrusting Levallois points raised interesting arguments that may assist in distinguishing between low-speed and high-speed projectile weapons, as discussed below.

The macroscopic use-wear examination of the experimental sample of this thesis showed that Levallois points when used as spear projectiles for thrusting spears (with mean velocity of 4.86 m/s and a *KE* mean of 16.90 J; see Table 5-11) suffer more damage than Levallois points used as spear projectiles for throwing spears (with mean velocity of 11.59 m/s and a *KE* mean of 43.50 J; see Table 5-11). Thrusting spear points recorded 50% of fracture frequencies, whereas throwing spear points recorded 39.28% of fracture frequencies (Table 11-1). These data suggest that, although throwing spear points reported a higher velocity mean than thrusting points (11.59 m/s vs 4.86 m/s, see Table 5-11), thrusting spear points were subjected to more damage during projectile impact possibly because of the higher values of force involved in the thrusting motions. This is comparable with what has

been observed concerning acceleration profiles where, in thrusting motions the human thruster applied additional mass, and therefore force to the spear, which are transferred onto the weapon tip causing major damage (in the form of edge-damage and breaks).

This hypothesis agrees with previous experiments, which have reported higher frequencies of damage in low-speed projectiles (e.g. spear tips) than in high-speed projectiles (e.g. arrow tips) (Pargeter et al., 2016; Iovita et al., 2016; Fischer et al., 1984; Lombard et al., 2004; Table 11-1). For instance, Pargeter et al. (2016, p. 150) have noted that spear projectiles (i.e. lower-speed weapons, thrown at a velocity mean of 9 m/s and with a mass mean of 512 g) showed higher frequencies of damage (73% vs 45%) than arrowheads (i.e. high-speed weapons, shoot at a velocity mean of 28 m/s with a mass mean of 30 g; Table 11-1). This is because throwing or thrusting spears, although low-speed weapons, are generally heavier than high-speed weapons (e.g. arrows and darts), as shown by the records of the mass of ethnographic spear and arrow shafts in Hughes (1998, table 1) and Thomas (1978, table 1). Therefore, this difference in weight results in higher kinetic energy and momentum values for the spear weapons and, therefore, more damage for the stone tips. This observation is important for two reasons. Firstly, because it suggests, once again, that not only impact velocities but also *KE* values are correlated to the formation of impact fractures, and, therefore, need to be evaluated in an experimental protocol. Secondly, although the degree of damage cannot be considered diagnostic of a specific delivery system alone, if stone tool assemblages present diagnostic projectile impact traces (such as presence of multiple DIFs, MLITs, and/or impact polish) the presence of abundant damage or higher fracture frequencies may suggest that the projectile was used in thrusting spear activities or in low-speed delivery systems (i.e. hand-delivered spear weapons).

When DIFs (i.e. step-terminating bending fractures, primary burination bending fractures, unifacial/bifacial spin-off fractures, and burination spin-off fractures) were taken into consideration alone, the experimental sample of this thesis showed that higher impact velocities generated higher frequencies of DIFs (Figure 11.1 and Table 11-1). This means that, when velocity increases, there is an increase of DIFs.

Indeed, DIFs became slightly more frequent in throwing experimental Levallois points (when the velocity mean was higher, 11.59 m/s) than in thrusting Levallois points (when the velocity mean was lower, 4.86 m/s, see Table 5-11 and Table 11-1). This result agrees with previous experiments that have also observed an increase of DIFs when the velocity of the experimental projectiles increased (Sano et al., 2016; Sano and Oba, 2015; Iovita et al., 2014). This means that, although the difference in DIFs between throwing and thrusting experimental Levallois points was not statistically significant to differentiate between the two delivery systems (see Section 6.2.6), the presence or absence of certain types of DIFs can provide indicators to distinguish low-speed projectiles from high-speed projectiles, as discussed below.

This study has found that step-terminating bending fractures, considered to be diagnostic projectile impact fractures (e.g. Fischer et al., 1984; Lombard, 2005a), although appearing slightly more often in the experimental Levallois points used in throwing motions than in thrusting motions (with an insignificant difference, $\chi^2=0.109$, $df=4$, $p\text{-value}=0.741$, see Table 6-2), appeared generally with low frequencies both in the throwing and in the thrusting sample (5.7% in throwing and 4.8% in thrusting, see Table 6-2 and Figure 11.1). Seeing as step-terminating bending fractures appeared with higher percentages in some of the previous projectile experiments (Table 11-1), the low frequencies of step-terminating bending fractures recorded in this study raise interesting questions about the mechanics of the formation of this particular type of bending fracture. It has been experimentally observed that step-terminating bending fractures occur more often in high-speed projectiles (i.e. arrow tips) than in low-speed projectiles (i.e. spear tips; Coppe and Rots, 2017; Pargeter et al., 2016; Sano and Oba, 2015; Iovita et al., 2014; Lombard et al., 2004; Fischer et al., 1984). Therefore, the low frequencies of step-terminating bending fractures recorded in this thesis's experimental sample may suggest that step-terminating bending fractures appeared with low frequencies in hand-delivered stone-tipped spear projectiles, because they are low-speed projectiles. The infrequent appearance of step-terminating bending fractures can therefore be an important criterion for the distinction between low-speed projectiles (i.e. hand-delivered weapons) and high-speed projectiles (i.e. mechanically delivery weapons).

For instance, when in a stone tool assemblage, where evidence of projectile use is readily available (such as the presence of multiple DIFs, MLITs, and/or impact polish), low frequencies of step-terminating bending fractures (<10%) might suggest a correlation with low-speed projectiles, whereas higher frequencies of step-terminating bending fractures (10%-30%) might suggest a correlation with high-speed projectiles. However, although these data may provide a potential means of distinguishing low-speed projectiles from high-speed projectiles, further investigation is warranted to better investigate the threshold of step-terminating bending fractures in experimental tools, and its applicability in archaeological assemblages (see below).

Similarly, this study has found that primary burination bending fractures, although appearing slightly more often in the experimental Levallois points used in throwing motions than in thrusting motions (with an insignificant difference, $\chi^2=3.046$, $df=1$, $p\text{-value}=0.081$, see Table 6-2), generally occurred with low frequencies in both the throwing and the thrusting sample (5.7% in throwing and 2.4% in thrusting points, see Table 6-2 and Figure 11.1). These frequencies were interestingly low, especially when compared with some of the previous projectile experiments (Table 11-1; Fischer et al., 1984; Odell and Cowan, 1986; De Bie and Caspar, 1996; Lombard et al., 2004; Pargeter et al., 2016). Pargeter et al. (2016) reported 13% of impact burination fractures in experimental hand-delivered spear projectiles, while Lombard and Pargeter (2008) reported 26% of impact burination fractures in mechanically delivered experimental projectiles (Table 11-1). Whereas, Iovita et al. (2014) observed that primary burination bending fractures (called longitudinal fractures in their study) became more frequent when the velocity increased. The discrepancies of burination fracture frequency between this study and previous studies may be due to two main factors. Firstly, a difference in tool morphologies and raw materials between the experimental tools employed in this study and the ones employed in previous studies (Iovita et al., 2016; Pargeter et al., 2016; Lombard and Pargeter, 2008); secondly, the fact that, in previous studies, all experimental tools were fired with higher impact velocities (e.g. 15.5 m/s and 28 m/s, Iovita et al., 2014) than the ones recorded in this study (11.59 m/s, see Table 5-11). Thus, it is plausible that the velocity of the spears affected the formation of primary burination bending fractures,

and that low-speed projectiles (i.e. hand-delivered weapons) develop lower frequencies of primary burination bending fractures than high-speed projectiles (i.e. mechanically delivered weapons), confirming the hypotheses of Iovita et al. (2014), who proposed that primary burination fractures appear more frequently on high-speed projectiles. Consequently, the presence/absence of primary burination bending fractures and their frequencies can be seen as another discriminating factor in distinguishing between hand-delivered and mechanically delivered projectile tools. However, further investigation would be needed to verify the applicability of these findings for archaeological tools (see below).

On the other hand, the high presence of spin-off fractures, both in throwing and in thrusting experimental Levallois points observed in this study (62.8% in throwing points and 51.2% in thrusting points, see Table 6-2), confirms that this category of fractures is highly diagnostic of projectile impact activities. However, seeing as spin-off fractures have also been observed in high frequencies in previous experiments employing high-speed and low-speed projectiles (i.e. experimental arrow and dart tips; Coppe and Rots, 2017; Clarkson, 2016; Sano and Oba, 2015; Iovita et al., 2014; Lombard and Pargeter, 2008; Fischer et al., 1984; Table 11-1), it is proposed here that spin-off fractures should be considered diagnostic of projectile impact activities but cannot be considered diagnostic of one type of delivery system or another (contra Sano and Oba, 2015, who suggested spin-off fractures were more indicative of high-speed projectiles).

It has also been noted that the overall number of DIFs recorded in the experimental Levallois points was generally low (with a total of 35 fractures observed in 28 experimental throwing points and 41 fractures observed in 24 experimental thrusting points; see Table 6-2). Moreover, during the execution of the experiments, it was noticed that the experimental Levallois points (used only for one shot, in line with protocol) were still usable, as the fractures, although more recurrent on the distal tip, did not prevent the possible reutilisation of the points for the same purpose. This could suggest that flint Levallois points were not only effective spear projectiles (as discussed in Section 11.2 and CHAPTER 5), but they also resisted projectile impact

well, enhancing the potential of this techno-morphological type to be used as a projectile tool requiring low levels of maintenance.

In conclusion, experimental Levallois points used in throwing spear motions developed more DIFs than experimental Levallois points used in thrusting motions, although these frequency levels were not sufficiently different to distinguish between the two delivery systems. Therefore, a correlation between DIF type and frequencies and delivery systems could not be confirmed. Nevertheless, the overall tendency for thrown Levallois points to develop higher frequencies of step-terminating bending fractures, primary burination bending fractures, and spin-off fractures has been related to an increase in impact velocities of this category of projectile. However, so far there is not a universal proxy for distinguishing between different delivery systems based on the frequencies of DIFs alone (as also suggested by Rots and Plisson, 2014; Sano and Oba, 2015; Sano et al., 2016). This is because DIF frequencies can be subjected to different parameters, such as raw material, the morphology of the stone tool, the type of target, the angle of impact, impact velocities, and *KE* values (as, for instance, in Table 11-1). Moreover, seeing as archaeological tools are further subjected to variability due to the presence of unused tools within the assemblage, potentially extended periods of utilisation (with multiple and repeated shots), different types of targets, differences in the distance from the targets, and post-depositional processes, the frequencies of DIFs observed in experimental assemblages should be compared with the archaeological assemblages only with caution, and when multiple diagnostic traces of projectile utilisation are present in the assemblages.

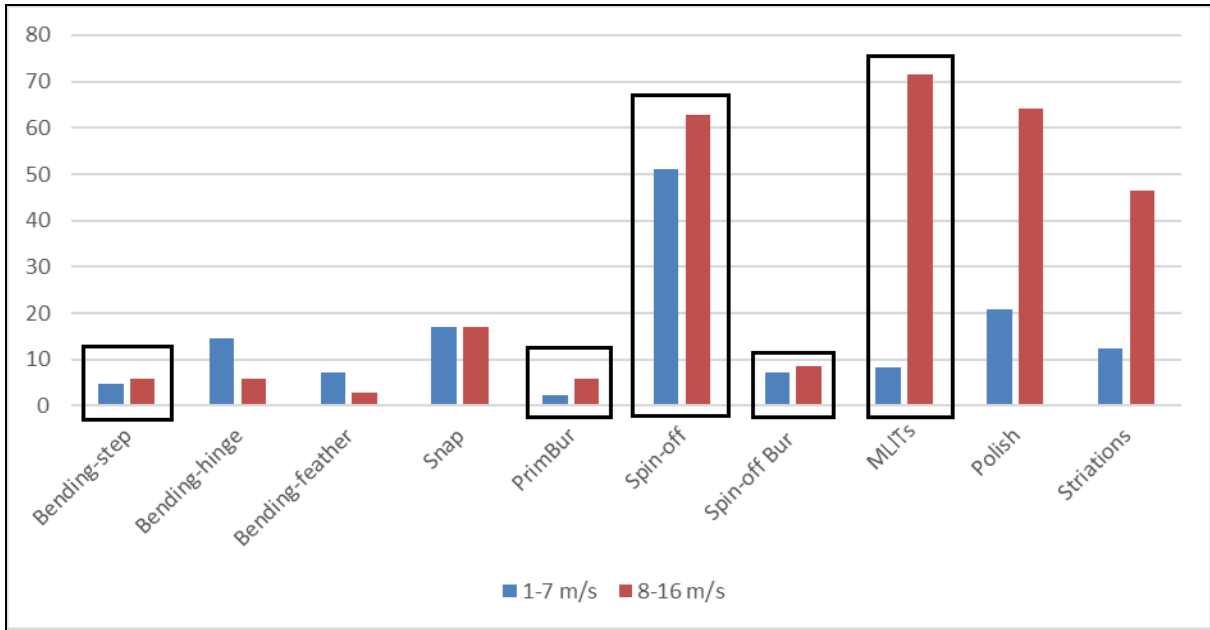


Figure 11.1. Types and frequencies of fractures according to the recorded impact velocities of the same projectiles (DIFs and MLITs are within black squares).

Table 11-1. DIF frequencies recorded in this study (in green) and DIF frequencies recorded in previous projectile experiments.

Tool sample	Number of tools	Tools with DIFs	% of tools with DIFs	% Step bending fractures	% Primary Burination fractures	% Spin-off fractures	% MLITs	Delivery system
La Porta, in this thesis Throwing LP Thrusting LP	28 24	13 12	46.2% 50%	5.7% 4.8%	5.7% 2.4%	62.8% 51.2%	71.4% 8.3%	Hand-delivered by trained human participants
Fischer et al., 1984 Arrows Spears	137 11	54 6	39% 55%	--	--	--	66% 60%	Bow Hand-delivered (ND)
Lombard and Pargeter, 2008 Generic weapon	30	12	40%	3%	36%	10%	--	Firing-machine (cross-bow)
Lombard et al. 2004 Spears	35	20	57%	--	--	--	--	Firing-machine (cross-bow)
Pargeter et al., 2016 Throwing spears (quartz tools) Arrows (quartz tools)	75 75	55 34	73.3% 45.3%	22.17% 40.66%	13.7% 6.6%	13% 11%	--	Hand-delivered by the author Bow
Sano and Oba, 2015 Thrusting spears Throwing spears Darts Arrows	--	--	--	3% 10%	13% 32%	--	20% 40% 80% 80%	Hand-delivered by the author Firing-machine (cross-bow) Firing-machine (cross-bow) Firing-machine (cross-bow)
Coppe and Rots, 2017 Darts Arrows	30 30	--	--	16% 10%	13% 32%	33% 29%	--	Hand-delivered by the author Bow

11.3.2 Discussion on microscopic diagnostic traces

The experimental Levallois points, when used as hand-delivered stone-tipped spears in two different delivery systems (i.e. throwing and thrusting), showed that when microscopic use-wear traces are analysed a significant relationship between diagnostic projectile microscopic use-wear traces and delivery systems can be established (see CHAPTER 6). The microscopic use-wear examination of the experimental sample of this thesis showed two substantial results:

- Firstly, it proved that microscopic linear impact traces (MLITs) are diagnostic use-wear traces of throwing experimental Levallois points. 71% of the experimental Levallois points used (n=18 tools) in throwing spear motions exhibited multiple, long and clear linear streaks of polish (i.e. MLITs), whereas only 8.3% of the thrusting experimental Levallois points (n=2 tools) showed the presence of a single linear streak of polish (i.e. MLITs, Table 11-1). As a result, the difference in MLIT frequencies between throwing and thrusting spear experimental projectiles was proven to be a statistically significant pattern ($\chi^2= 169.280$, $df=1$, $p\text{-value}= 0.000$, Table 6-6).
- Secondly, a new type of microscopic trace was evidenced. This specific type of polish consistently appeared on throwing points and on no occasion was observed on thrusting points, it was termed “impact polish” (see Section 6.3.3.3). 57.1% of the experimental Levallois points used in throwing spear motions (n=16 tools) exhibited clear and diagnostic “impact polish” traces, whereas none of the thrusting experimental Levallois points showed evidence of this (see Table 6-6). As a result, this was a statistically significant pattern between throwing and thrusting experimental Levallois points ($\chi^2= 25.920$, $df=1$, $p\text{-value}= 0.000$, Table 6-6).

These results are discussed below to examine whether or not these traces can be used as indicators for identifying delivery systems on experimental and archaeological stone tools.

11.3.2.1 Presence and frequencies of microscopic linear impact traces (MLITs)

In this study, the ratio of the experimental Levallois points with MLITs (Moss, 1983a; Fischer et al., 1984) rose according to the delivery systems and impact velocities (Figure 11.2). Thrown experimental Levallois points showed significantly higher frequencies of MLITs than thrusting experimental Levallois points ($\chi^2= 169.280$, $df=1$, $p\text{-value}= 0.000$; Table 6-6), which suggests that, at higher impact velocities (i.e. in throwing points), the frequencies of MLITs increased (Figure 11.2). These data correlate with previous experiments that have observed a positive link between impact velocities and frequencies of MLITs (Fischer et al., 1984; Sano and Oba, 2015; Sano et al., 2016). For instance, Fischer and colleagues (1984, p. 35) have reported frequencies of MLITs of 61% for experimental throwing spears and 66% for experimental arrows, whereas Sano and Oba (2015, table 2) reported a 0% presence of MLITs for experimental thrusting points, 40% for experimental throwing spears, 70% for experimental darts, and 90% for experimental arrows (with a tool sample of 10 specimens for each category). This thesis, which offered a larger sample size than previous experiments (Fischer et al., 1984; Sano and Oba, 2015; Sano et al., 2016), has instead observed clear and long MLITs in 71.4% of the experimental throwing points ($n=20$ tools out of 28), which were clearly diagnostic of the directionality of the projectile impact, and often occurred in multiple patches, with only two single MLIT in two experimental thrusting points (out of 24 tools, 8.2%), presenting a less bright aspect, a shorter length, and a less definable appearance (see Section 6.3.3.1 and 6.3.4). What emerged from this comparison (Table 11-1) is that MLITs form significantly more frequently on stone projectile tools that have been “launched” (i.e. weapons that have left the hand of the thrower), such as throwing spears, darts, and arrow stone projectiles, whereas they are very rare and almost absent in thrusting projectiles.

However, due to the lack of a single and absolute experimental threshold at which MLITs can be considered diagnostic of one or another projectile delivery system (as frequencies of MLITs differ also among experiments that have employed a similar delivery system, possibly due to differences in the raw materials and/or morphology

of the tools), the experimental frequencies of MLITs cannot be directly compared with archaeological frequencies of MLITs. Moreover, in archaeological assemblages, MLITs are not always preserved because of post-depositional processes, absence of traces in the past (i.e. traces did not form during utilisation or tools were not used), and/or possible overlapping with other traces (e.g. MLITs were covered by other traces, eliminated by subsequent breakages, or retouch occurred on the same tool).

However, other possibilities related to the presence of MLITs for the interpretation of the delivery system in archaeological tools are possible. For instance, if archaeological tools presented diagnostic projectile impact traces, such as multiple DIFs, “impact polish”, and/or hafting traces, the presence of MLITs could suggest a higher probability that the implements were used as “launched” projectiles (i.e. weapons that have left the hand of the thrower, such as throwing spears, darts, or arrows), as MLITs have been shown to be very rare in thrusting spears. Therefore, the presence of MLITs would likely exclude the utilisation of the archaeological tools as thrusting spear projectiles.

With reference to Middle Palaeolithic archaeological assemblages, there is yet another observation related to the presence of MLITs that can assist in the recognition of the delivery system of the archaeological tools. At the present moment, there is a lack of evidence showing that Neanderthals used mechanically-delivered weapons (i.e. dart or arrow weapons; Shea, 2006; Shea and Sisk, 2010), which develop comparable MLITs frequencies to throwing spears. The presence of MLITs in archaeological tools that presented diagnostic projectile impact traces (such as multiple DIFs, “impact polish”, and/or hafting traces) could indicate a more likely, or almost exclusive, utilisation of those implements as throwing spear projectiles, as MLITs are very rare in thrusting spears (and, if present, are often shorter, less bright, and less visible). Therefore, in Middle Palaeolithic stone tools, the observation of MLITs associated with other diagnostic projectile traces may suggest a utilisation of these implements as throwing spear projectiles.

In summary, the evidence presented above about the formation process and frequencies of MLITs in experimental projectiles demonstrates the necessity of future research to better investigate the mechanics of the formation of these microscopic

diagnostic projectile impact traces, and their frequencies. As proposed in more detail in CHAPTER 6, MLITs can be the result of plastic deformation of the flint surface due to the action of different “scratching agents” (as originally proposed by Fischer et al., 1984, but see also Section 6.3.3.1) However, considering the above discussions, the velocity of the projectile under which the MLITs form should also play an essential role in the formation of these diagnostic traces (see Section 6.3.3.1). Future research should isolate variables, such as tool morphology, raw material, impact velocities and contact material, to better understand the conditions under which MLITs form and the precise frequencies reached by different delivery systems. This is because MLITs, together with impact polish traces, may represent good indicators for distinguishing between different projectile delivery systems.

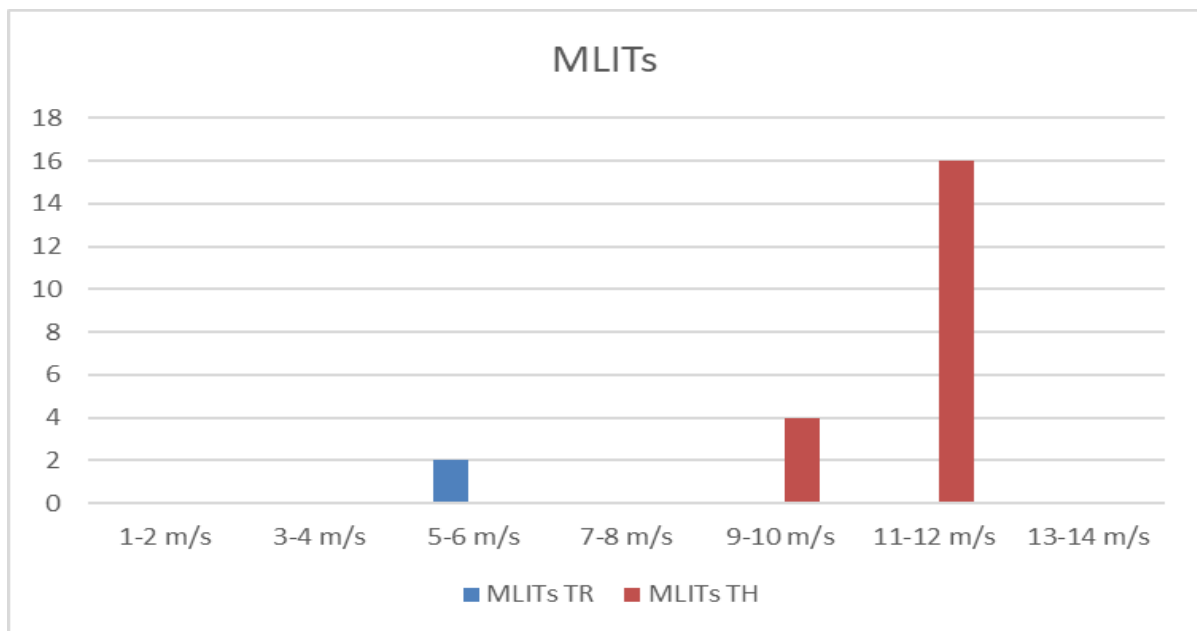


Figure 11.2. Number of recorded MLITs according to the impact velocities of the same projectiles.

11.3.2.2 Presence and frequencies of “impact polish”

Another important contribution of this study was the identification of a new specific type of polish trace, termed “impact polish”. Impact polish, extensively described in Section 6.3.3.3, generally appears as a well-developed, flat, and very reflective polish, with characteristic striations running parallel or slightly oblique to the direction of the impact (description at 200x; Figure 11.3). It was observed on 57.1% of the experimental Levallois points used in throwing spear motions (n=16 tools out of 28) and was never observed on the experimental Levallois points used in thrusting spear motions, resulting therefore in a highly diagnostic and statistically significant pattern ($\chi^2= 25.920$, $df=1$, $p\text{-value}= 0.000$, Table 6-6).

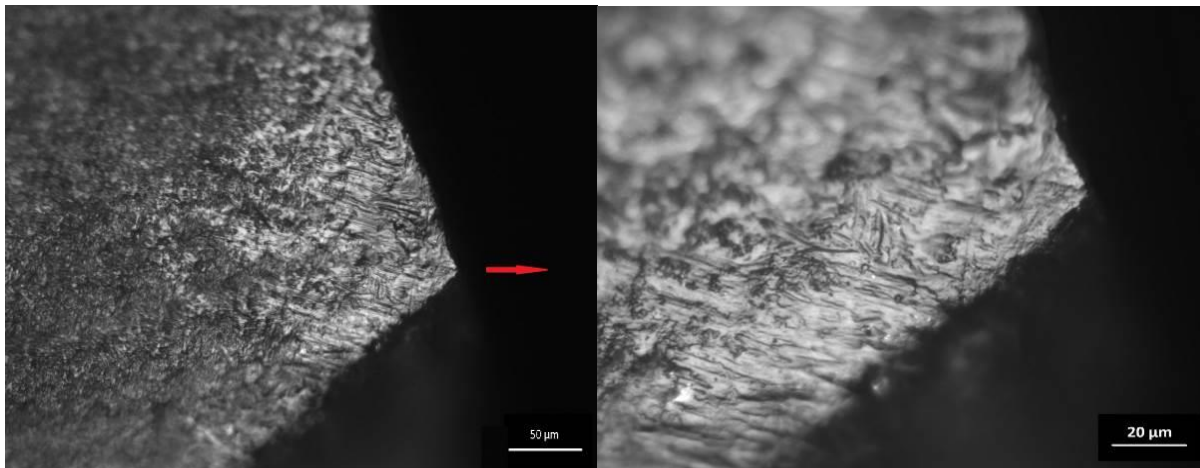


Figure 11.3. Example of impact polish observed on experimental Levallois points used in throwing motions (left picture: OLMil/OM 50x; right picture: OLMil/OM 200x, experiment code TH-23).

A detailed review of previous literature has showed that “impact polish” has never been extensively described, quantified, and/or proposed as a diagnostic trace for projectile tools. However, a few studies have mentioned the presence of a similar type of polish that had developed on experimental projectile tools and archaeological tools. For instance, Lammers-Keijers and colleagues (2015, p. 460 and p. 463) have acknowledged the presence of “a relatively flat but reflective polish with striations, resulting from contact with animal material” on the distal tip of experimental flint barbed points and triangular points used as arrowheads. From the image included in the publication, the description, and the appearance of the trace, is highly comparable with the proposed “impact polish” of this study (Figure 11.4; this

comparability was also confirmed by one of the authors of the study during an exchange of information with this thesis's author; Verbaas, 2018, personal communication). Another study (Hays and Surmely, 2005) has reported the observation of a "*poli atypique* (atypical polish trace)" termed "*poli d'impact* (impact polish)" on a distal fragment of a flint microgravette point from the site of Le Sire (Auvergne, France) (Hays and Surmely, 2005, p. 6 and Figure 3.b). Moreover, Moss (1983a, p. 95) has stated that experimental barb points used as arrowheads showed "a distinct meat polish" that presented "characteristic striations" within the polish, which is a definition that correlates with the impact polish observed in this study (see also Section 6.3.3.3.1), but unfortunately, the poor quality of the 1980s black and white pictures (Moss 1983, p. 97, plate 6.5 c and d) does not permit a further comparison. However, in Moss and Newcomer (1982, p. 296), Moss reiterated the observation of a distinct type of "well-developed, meat polish with characteristic fine striations" both on experimental barb points (specimen MNH-44 B3) and in one archaeological tool from the Upper Palaeolithic levels of Pincevent (France). Therefore, it appears that, in earlier literature, the presence of an "impact polish" or an "atypical meat polish", both on experimental projectile tools and archaeological tools, was noticed but, unfortunately, was not further explored.

The reasons for the divergence of the identification of impact polish between this study and other works (Fischer et al., 1984; Geneste and Plisson, 1989; Lombard, 2005a; Lombard and Pargeter, 2008; Rots, 2016; Sano et al., 2016) are many. For instance, the over-emphasis on fracture analysis for projectile tools has contributed towards a shortage of information and focused research on microscopic use-wear traces diagnostic of projectile activities (as also suggested by Barton and Bergman, 1982; Moss, 1983a; Rots and Plisson, 2014). Differences in the raw materials and morphology of the tools can also contribute to different use-wear results amongst different experimental projectile assemblages. Similarly, different frequencies of breakage among experimental assemblages (Table 11-1) may have contributed to the loss of the distal tip of the experimental projectiles, and therefore the removal of the part where the most diagnostic microscopic traces, including impact polish, are generally observed. These divergences, however, open up fascinating questions

concerning the formation of impact polish traces in projectile tools, as discussed below.

With regards to the results of this study, it has been noticed that the ratio of the experimental Levallois points and the presence of impact polish rose according to the delivery systems. It has been observed that throwing experimental Levallois points showed significantly higher frequencies of impact polish than thrusting experimental Levallois points ($\chi^2= 25.920$, $df=1$, $p\text{-value}= 0.000$; Table 6-6), which suggests that, at higher impact velocities (i.e. in throwing points, 11.59 m/s), the frequencies of impact polish increased (as also shown for MLITS). In addition to this, it has been observed that impact polish forms only on those throwing experimental Levallois points that impact against hard tissues (i.e. bone materials, see Section 6.3.3.3.1), although a direct correlation could not be proven as the projectiles that impacted against bone also came into contact with the fresh meat, flesh, and skin tissues of the animal targets.

The fact that the frequencies of impact polish increase with the increasing speed of the projectiles may justify its absence from the experimental Levallois points used in thrusting motions. Thanks to the measurements of the maximum deceleration of the experimental stone-tipped spears, it was possible to observe that hand-delivered throwing stone-tipped spears had much higher deceleration values than thrusting spears (45 m/s² mean for throwing vs 16 m/s² mean for thrusting spears, Table 5-11). This means that, upon impact, throwing spears decelerated, i.e. lost their velocity, much quicker than thrusting spears. As suggested in CHAPTER 6, this sudden change of velocity upon impact with the target (recorded only for throwing motions), could have generated high levels of stress (in the form of abrasion and/or friction) in very circumscribed areas of the tool surface (i.e. the distal tip, which was the first surface to hit the target). This may have caused abrupt changes in temperature, pressure, and force which could have caused a plastic deformation of the stone tool surface, creating this distinctive form of impact polish. Impact velocities for hand-delivered thrusting stone-tipped spears were lower (mean of 4.86 m/s) and, therefore, had lower levels of deceleration, which could have prevented

the formation of impact polish on the experimental Levallois points used in thrusting motions.

This hypothesis concerning the formation of impact polish traces (as well as MLITs), would possibly explain why, in this study, hand-delivered thrusting spear projectiles did not develop impact polish traces (and not MLITs). It would also correlate with the fact that other authors have reported similar polish traces on experimental and archaeological arrowheads (as indicated by Lammers-Keijers et al., 2015; Hays and Surmely, 2005, p. 6; Moss, 1983, p. 95; Moss and Newcomer, 1982, p. 296) which, being high-speed projectiles, may have developed impact polish traces.

It is therefore essential to continue the investigation on microscopic use-wear traces formed in projectile tools, in order to better understand the formation process and conditions (i.e. velocity, kinetic energy, momentum, and deceleration values) under which impact polish traces may form. This is because impact polish, together with MLITs, may represent good indicators for distinguishing between different projectile delivery systems, and have been proven diagnostic of hand-delivered throwing spear projectiles.

This image has been removed by the author of this thesis/dissertation for copyright reasons.

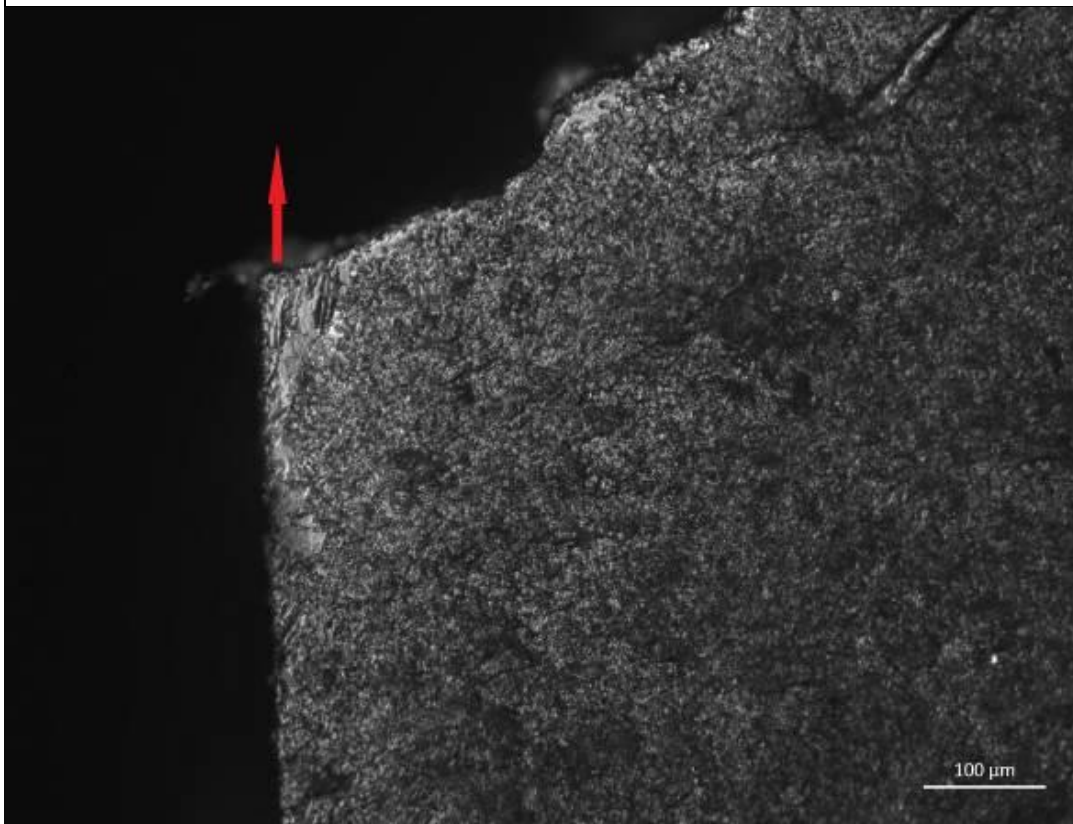


Figure 11.4. Comparison between the “flat and reflective” polish described by Lammers-Keijers (et al., 2015, Figure 3.d; above) located on the distal tip of experimental arrowheads, and the “impact polish” described in this thesis, located on a throwing spearheads (below, TH-20).

11.3.2.3 A hint on hafting traces

The analysis of hafting traces (on a selected sample of experimental projectile tools), described in detail in CHAPTER 7, showed that, when the experimental Levallois points were hafted with abundant adhesives (such as commercial tar or resin, as in

this study), they developed limited to zero presence of diagnostic traces associated with the hafting systems (see CHAPTER 7; in agreement with Rots, 2010). Therefore, if archaeological projectiles were hafted with adhesives, one should expect a reduction of visible hafting traces and/or a lack of diagnostic hafting traces. In this case, the over-emphasis of hafting traces as a “must-see” required for the correct identification of projectile tools (see for instance Rots, 2010; Rots et al., 2011; Rots, 2009, 2013, 2016) is not supported by the experimental results of this thesis, as used projectiles may not develop diagnostic hafting traces. Future investigation is therefore warranted to further explore the formation of hafting traces in projectile activities, and the resulting microscopic traces of adhesives (see also CHAPTER 7).

11.3.2.4 Overview

The presented data are the first results of a systematic and large-scale experimental program focusing on the understanding of different use-wear traces between throwing and thrusting hand-delivered spear projectiles, linked with the kinematics and ballistic parameters of the same weapons.

The discussion has shown that projectile use-wear traces are strongly influenced by the motions, impact velocities, and *KE* values of the weapon and its delivery system. Differences in impact velocities have resulted in different macroscopic and microscopic diagnostic traces of projectile activities, with a positive relationship between higher velocities and number of diagnostic traces. DIFs, such as step-terminating bending fractures, impact burination bending fractures, and spin-off fractures, have been discussed as their frequencies can indicate the presence of different projectile delivery systems. Similarly, the presence of MLITs and impact polish has been discussed as diagnostic of throwing hand-delivered projectiles, as these trace types both increased with higher impact velocities. However, it has also been emphasised that, in analysing macroscopic traces and DIFs alone, it was not possible to distinguish between throwing and thrusting hand-delivered spear projectiles, and that the combination of low-power and high-power analyses is essential for projectile use-wear analysis.

Lastly, the general scope for comparison between experimental assemblages and archaeological assemblages has been discussed. These hypotheses need to be applied with caution, as archaeological samples are highly variable and, therefore, the frequencies of DIFs and microscopic diagnostic projectile use-wear traces should be analysed in accordance with their archaeological context.

Below, the results from the archaeological use-wear analysis are discussed considering the results of these experimental data within the framework of stone-tipped spear technology in the European Middle Palaeolithic.

11.4 Assessing the presence of projectile tools within archaeological assemblages: implication for Neanderthals' hunting behaviour

11.4.1 Comparison of archaeological results

The techno-morphological and macroscopic and microscopic use-wear analysis of the selected sample of Levallois points and convergent tools from Arma Delle Manie (Italy) and Abri du Maras (France), presented in detail in CHAPTER 9 and CHAPTER 10, has shown the following results:

- At Arma Delle Manie, among n=47 selected convergent tools (i.e. Levallois points and Mousterian points), n=30 tools were finally selected for use-wear analysis due to the presence of a low-degree of post-depositional alterations (see Section 9.1). Whereas, at Abri du Maras, due to more intense post-depositional alterations, out of n=70 selected convergent tools (i.e. Levallois points, Levallois convergent flakes, retouched convergent tools, and cortical points), n=32 tools were examined for use-wear analysis. These different sampling ratios are due to different degrees of post-depositional alterations between the sites (possibly due to differences in the geological deposition of the layers and taphonomy) (see Section 10.1).
- Arma Delle Manie showed a larger variety of raw materials employed for the production of convergent tools, such as fine grain quartzite, dolomite, and siliceous limestone (mainly from local sources). Whereas, at Abri du Maras

the unique raw material used to produce the convergent tools was flint (from local and medium distance outcrops).

- In both sites, the Levallois points (n=40 at Arma delle Manie; and n=51 at Abri du Maras) were all produced by Levallois methods (or volumetric conception; Boëda, 1994, 1995) mainly employing unidirectional convergent reduction sequences or periodical three-blow techniques (Boëda, 1982; La Porta, 2013; see CHAPTER 8). However, while at Abri du Maras the selected convergent tools were mostly unretouched (90.1% unretouched), at Arma Delle Manie the selected convergent tools showed a higher percentage of retouching (33.3% retouched).
- The macroscopic use-wear analysis results showed different frequencies of DIFs between the two sites. At Arma Delle Manie, out of n=30 selected convergent tools, n=18 showed DIFs, resulting in a total of 60% of convergent tools with DIFs (see CHAPTER 9). Whereas, at Abri du Maras, out of n=32 convergent tools, n=10 exhibited DIFs, giving a total of 31.2% of convergent tools (CHAPTER 10).
- The microscopic use-wear analysis of the selected convergent tools at Arma Delle Manie revealed the presence of n=11 positive and n=4 possible projectiles, giving a total of n=15 tools interpreted as projectiles, i.e. 50% of the sample (Table 9-7). Whereas, at Abri du Maras, n=8 tools were interpreted as projectiles (n=4 positive and n=4 possible projectiles), giving a total of 25% of the sample (Table 10-7).
- In both assemblages, some other convergent tools were also employed for different utilisations, such as transversal, longitudinal, rotatory, or multiple motions against soft and medium-hard materials (see Table 9-7 and Table 10-7) and, therefore, an univocal relationship between shape and function cannot be addressed.

These results are now compared and discussed against the experimental dataset of this thesis and previous experimental and archaeological use-wear studies.

11.4.2 Diagnostic impact fractures (DIFs) observed on the archaeological tools

Archaeological tools commonly show lower frequencies of DIFs than experimental tools (Fischer et al., 1984; Lombard and Pargeter, 2008; Villa and Soriano, 2010; Sano and Oba, 2015). This is because, in experimental assemblages, all of the tools are employed during the execution of the projectile experiments, whereas the archaeological assemblages may present unused tools, fragmented tools, and tools that were used for other tasks (Fischer et al., 1984; Lombard, 2007; Lombard and Pargeter, 2008; Villa and Soriano, 2010). Previous experimental tools employed as projectiles have shown frequencies of DIFs of between 40% to 75% (Table 11-1), depending on the type of tools, delivery systems, and/or raw materials. This study has shown that Levallois points, when used as throwing or thrusting stone-tipped spear projectiles, develop between 46% to 50% of DIFs (Table 11-2). Similarly, Fischer et al. (1984) showed that experimental Upper Palaeolithic points, when used as experimental spearheads or arrowheads, developed between 39% to 55% of DIFs (Table 11-2), whereas Lombard and Pargeter (2004, 2008) reported frequencies of DIFs on experimental tools between 40% to 57% (Table 11-1). On the other hand, archaeological assemblages, when investigated for the use-wear analysis of projectile tools, show a diverse range of DIFs (Table 11-3). Middle Palaeolithic and MSA assemblages of Levallois points, Mousterian points, or unifacial points investigated for the use-wear analysis of projectile tools show frequencies of DIFs generally between 5.3% to 13.4% (Table 11-3; Lombard, 2004; Villa and Lenoir, 2006, 2009; Lombard and Pargeter, 2008; Villa et al., 2009; Villa and Soriano, 2010). Upper Palaeolithic sites show frequencies of DIFs between 6.4% and 43% (Table 11-3; Fischer et al., 1984; Crombé et al., 2001), depending on the type of site and its occupation. Only Mesolithic or Paleoindian sites interpreted as killing sites have shown frequencies of DIFs superior to 40% on the archaeological tools (Table 11-3; Frison, 1974; Bratlund, 1996), and these are generally the highest frequencies of DIFs observed in the archaeological record.

The analysis of fractures of the convergent tools from Arma Delle Manie (Mousterian levels) and Abri du Maras (Level 4), however, indicated an indisputable and extremely high frequency of DIFs in both assemblages. Arma Delle Manie showed a

frequency of 60% of convergent tools with DIFs, whereas Arma Delle Manie had 31.2% of convergent tools with DIFs, which is not only comparable to previous experiments' frequencies of DIFs (Table 11-2), but also with frequencies of DIFs from Upper Palaeolithic killing sites (Table 11-3). One can argue that the high frequencies of DIFs recorded on the convergent tools of both sites could perhaps be the result of taphonomic disturbance (at least in part). However, seeing as a detailed examination of post-depositional alterations was undertaken for both assemblages, and all the tools affected by post-depositional alterations were excluded from the analysis, this is a possibility that can be excluded (see Sections 9.1 and 10.1). Moreover, as expressed by Sano (2009, p. 82) DIFs are strictly established as diagnostic damage, resulting only from projectile impact activities as they hardly occur during other activities, included trampling (and, if they do, they show low frequencies, <3%; see also Lombard, 2005a; Pargeter and Bradfield, 2011; Pargeter, 2013). Thus, the presence of high frequencies of diagnostic impact fractures at Arma Delle Manie (Mousterian levels) and Abri du Maras (Level 4) indicate that the analysed convergent tools at these sites were mostly used as stone-tipped projectiles, and this suggests that Neanderthals at both sites were practising weaponry activities with stone-tipped weapons.

Moreover, Table 11-3 shows that only in Late Palaeolithic or Paleoindian killing sites, i.e. archaeological sites specialised in the slaughtering and butchering of a large number of animals, where frequencies of DIFs in convergent or pointed tools very high (around 40%; comparable with what is observed in experimental projectiles). Whereas, in other sites associated with residential or manufacturing activities, the frequencies of DIFs are much lower (<20%) because convergent and pointed tools in these sites were likely employed for carrying out different activities and were not exclusively used as projectile weapons (Villa and Soriano, 2010; Plisson and Beyries, 1998). Therefore, the fact that, at Arma Delle Manie, convergent tools displayed 60% of diagnostic impact fractures, could indicate a specific specialisation of the site, perhaps as a hunting site (Binford, 1980) or a site where hunting activities were the major focus (see Section 11.4.3). Whereas, at Abri du Maras, 31.2% of DIFs out of the analysed convergent tools (which emerged from a single Unit, Level 4) is still higher than any recorded DIFs from other Middle Palaeolithic or MSA

archaeological assemblages (Lombard, 2004; Lombard and Pargeter, 2008; Villa et al., 2009; Villa and Lenoir, 2006, 2009; Lazuén, 2012; Table 11-3), and this could also justify an interpretation of this site as a site in which hunting was specifically carried out.

Below, the results of the microscopic use-wear analysis are compared with possible interpretations of the function of the two archaeological assemblages.

Table 11-2. Frequencies of DIFs recorded at Arma Delle Manie and Abris du Maras (in green) compared with experimental frequencies of DIFs.

Tool sample	Number of tools examined	Tools with DIFs	Percentage of tools with DIFs	Delivery system
Arma Delle Manie	30	18	60%	-
Abris du Maras	32	10	31.2%	-
La Porta, in this thesis				
Throwing LP	30	13	46.2%	Hand-delivered by trained human participants
Thrusting LP	26	12	50%	
Fischer et al. 1984				
Arrows	137	54	39%	Bow
Spears	11	6	55%	Hand-delivered
Lombard and Pargeter 2008				
Generic weapon	30	12	40%	Mechanically
Lombard et al. 2004				
Spears	35	20	57%	Mechanically

Table 11-3. Frequencies of DIFs recorded at Arma Delle Manie and Abris du Maras (in green) compared with Middle Palaeolithic, MSA, Upper Palaeolithic, Palaeoindian and Bronze Age sites.

Site and samples	Type of site	No. of analysed	No. of tools with impact	% of impact	Age	Sources
------------------	--------------	-----------------	--------------------------	-------------	-----	---------

		points	scars	scars		
Abri du Maras Level 4 (Levallois points)	Multiple occupations (with a main phase of occupation during Level 4)	32	10	31.2%	MIS 4	This thesis's analysis; Daujeard et al., 2017
Arma Delle Manie - Mousterian Levels (Levallois points)	Multiple seasonal occupations	30	18	60%	MIS 4-3	This thesis's analysis; Psathi and Vicino, 2003
Bouheben (Mousterian points)	--	113	6	5.3%	MIS 6	Villa and Soriano, 2010, Table 2
Biache-Saint-Vast IIa (Levallois points)	Long term occupation	5	--	--	MIS 6	Rots, 2013
Abric del Pastor (Mousterian points)	Multiple occupation episodes	64	7 ±	10.9%	MIS 3	Villa and Soriano, 2010, Table 2
Oscurusciuto Unit 1 (Mousterian points)	Multiple occupation episodes	19	1	5.3%	MIS 3	Villa and Soriano, 2010, Table 2
Oscurusciuto Unit 2 (Mousterian points)	Multiple occupation episodes	38	3	7.9%	MIS 3	Villa et al., 2009a
Sibudu, post-HP layers (Unifacial points)	Residential	101	9	8.9%	46.0 ± 1.9 (OSL)	Villa and Soriano, 2010, Table 2
Blombos, Still Bay (Bifacial points)	Residential	82	11	13.4%	77-70 ka	Villa and Soriano, 2010, Table 2
Bromme (Tanged points)	Residential	47	3	6.4%	End of Last Glacial	Fischer et al., 1984
Ommelshoved (Tanged points)	Residential	88	11	12.5%	End of Last Glacial	Villa and Soriano, 2010, Table 2
Stellmoor, upper level (Tanged points)	Reindeer kill site (MNI=302)	45	19	42.2%	End of Last Glacial	Villa and Soriano, 2010, Table 2

Casper site (Bifacial points)	Bison kill site (MNI=74)	60	26	43%	10.0 ± 170 14C BP,	Frison, 1974
Muldbjerg (Transversal arrowheads)	Residential	30	9	30%	2800 BC	Villa and Soriano, 2010, Table 2
Præstelyng (Transversal arrowheads)	Residential	56	8	14.3	3200 BC	Villa and Soriano, 2010, Table 2
Vejlebro, level 8 (transversal arrowheads)	Residential	24	5	20.8	3500 BC	Villa and Soriano, 2010, Table 2

11.4.3 Differences between the two assemblages: the support of microscopic use-wear analysis

The sample sizes of Middle Paleolithic convergent tools are rarely large (2-3%; Table 11-4) as it is related to the number of Levallois points (and/or convergent tools) presented within the archaeological assemblages. Table 11-4 shows that the size of this thesis' archaeological samples is comparable with previous use-wear studies of Middle Palaeolithic convergent tools. Nevertheless, it is acknowledged that the following interpretation refers only to the analysed sample of convergent tools and not to the entire tool assemblage.

Table 11-4. European Middle Paleolithic site with presence of Levallois points and/or convergent tools analysed for use-wear analysis.

European Middle Paleolithic sites	Total number of convergent tools	Number of analysed convergent tools for use-wear analysis
Arma Delle Manie	47	30 (the others were affected by post-depositional alterations)
Abri du Maras	70	32 (the others were affected by post-depositional alterations)
Villa et al. 2009a		
Oscurusciuto Unit 1	Not stated	19
Oscurusciuto Unit 2	Not stated	38
Lazuén, 2012		
Cueva Morin	Not stated	5
El Castillo	7	7
Goval et al., 2015		
Fresnoy-au-Val	32	2 (the others were affected by post-depositional alterations)
		9
Bettencourt-Saint-Ouen N2b2	9	
Bettencourt-Saint-Ouen N2b3	117 ⁴⁰	Not stated (7 with traces)

11.4.3.1 Occupation at Arma Delle Manie

At Arma delle Manie, microscopic use-wear analysis of the selected convergent tools has allowed the identification of a total of n=15 tools interpreted as projectile tools (Table 9-7). All of them were Levallois points or Levallois convergent flakes (Table 9-7). These data suggest a double trend, on the one hand, it indicates that 50% of the analysed convergent tools were used entirely as projectile tools in stone-tipped weapons (mostly likely spears, see below) and, on the other hand, it suggests, to a

⁴⁰ Bettencourt-Saint-Ouen N2b3 is the only European Middle Palaeolithic site to present a high number of convergent tools (5% of the entire assemblage) dominated by Levallois points (see also Goval et al., 2015).

certain extent, a homology between a techno-morphological type and a specific function. Although, this homology cannot be completely supported as some parts of the convergent tools were also used for activities such as cutting and scraping (26.6%; Table 9-7).

In terms of the type of weapons and/or the delivery systems of the identified projectiles, at Arma Delle Manie at least three specimens (#rem L1 68mi, #rem Ind 77/3, and #VII M1 897, see Section 9.2.2.1) showed the presence of MLITs or longitudinal striations departing from distal bending fractures, which are traces that have been proven to be diagnostic of hand-delivered throwing spears or “launched” weapons only (i.e. throwing spear, dart or arrow tips; see Section 11.3). As the presence of mechanically-delivered weapons (i.e. arrows and spear-thrower darts) in the Middle Palaeolithic has been rejected (Shea, 2006; Sisk and Shea, 2009; Shea and Sisks, 2010; Iovita and Sano, 2016), the presence of MLITs and longitudinal striations in the nominated specimens suggests that at least three projectiles could have been used as hand-delivered throwing stone-tipped spears, opening interesting discussions concerning the capability of Neanderthals in manufacturing composite tools and using them as throwing weapons (see Section **Error! Reference source not found.**).

The association of the use-wear results on the convergent tools with previous faunal and environmental data from Arma Delle Manie may support the interpretation of this site as a hunting site, or a site in which hunting activities were the primary focus. At Arma Delle Manie, the faunal assemblage (of the Mousterian levels) have indeed shown that the dominant species was red deer (MNI=49; Valensi and Psathi, 2004, Table 1), followed by roe deer, ibex, horses, and wild boar (Psathi and Vicino, 2003; see Section 8.2.5). The analysis of the mortality profiles of the herbivores also showed a predominance of young adults, especially for red deer (Valensi and Psathi, 2004), whereas tooth-eruption analysis revealed that red deer were mainly killed during late summer and early winter, suggesting a seasonal occupation of the cave (Psathi, 2003; Valensi and Psathi, 2004). As red deer is a species often associated with mixed vegetation and a territorial behaviour (Clutton-Brock et al., 1982), this provides knowledge pertaining to the territory and animal behaviour patterns of this

species linked to its capture. Therefore, considering the presence of an elevated number of projectile tools (50% of the convergent tool sample), the presence of high frequencies of DIFs (i.e. 60%, only comparable to the frequencies recorded in Upper Palaeolithic hunting sites), the presence of at least three possible throwing stone-tipped spear projectiles, and the predominance of red deer species with a young adult mortality profile, it is possible to suggest that Neanderthals, during late summer and the beginning of winter at Arma Delle Manie, were primarily hunting red deer species (but not exclusively, see Section 8.2.5) with stone-tipped spears and, sometimes (at least in three cases), these spears were used as throwing weapons. Red deer species could have been frequenters of the surrounding area of the cave, intercepted perhaps nearby at the Val Ponci (a post-Miocene valley) and the Rio Ponci water stream, located less than 2 km away from the cave (see Section 8.2.1). Here, the animals could have been exploited during the late Summer-autumn aggregation, when both males and females tend to be in good condition in terms of body weight and fat percentage.

Moreover, stone-tipped spears, when used as throwing weapons, may have aided the interception of specific individuals - in this case young adult red deer - and therefore, the utilisation of (at least three) throwing stone-tipped spear projectiles at Arma Delle Manie possibly indicates the development of specific and more diverse hunting strategies related to “killing at distance” and/or “targeted” hunting, adapted to the local environment and to the behaviour of the animals during the hunting season (see also Section **Error! Reference source not found.**). Moreover, the use of composite stone-tipped spears for hunting purposes would have required planning and forecasting skills in order to manufacture the weapon first and use it later (see also Section **Error! Reference source not found.**).

11.4.3.2 Occupation at Abri du Maras

At Abri du Maras, microscopic use-wear analysis has shown that n=8 convergent tools (among which five were Levallois points and three were convergent flakes) were likely used as projectiles (Table 10-7), indicating that the 25% of the analysed convergent tools (all from the same archaeological unit, Level 4) were used exclusively as projectile tools. However, microscopic analysis has also shown that

some parts of the convergent tools (9.3%) were used in other activities, such as cutting, scraping, or rotatory movements against soft or medium materials (Table 10-7). Therefore, at Abri du Maras, a direct correspondence between shape and function cannot be found.

In terms of the type of weapons and/or the delivery systems of the identified projectiles, at Abri du Maras the identification of the delivery system of the identified projectile tools has been difficult. This is because the most diagnostic traces for distinguishing between throwing and/or thrusting projectile activities are microscopic traces such as MLITs and/or impact polish. However, due to a low preservation of microscopic use-traces, MLITs and impact polish traces were difficult to identify and, therefore, it was harder to put forth a confident interpretation concerning delivery systems. Nevertheless, considering the hypothesis that mechanically delivered weapons, such as darts or arrows, were not in use during the Middle Palaeolithic (Shea, 2006; Sisk and Shea, 2011), the identified projectiles can be conceived both as throwing and/or thrusting stone-tipped spears (see also Section **Error! Reference source not found.**).

The faunal assemblage of Abri du Maras Level 4 has recently been interpreted as an example of planned, collective, and selective Middle Palaeolithic reindeer hunting (Daujerd et al., 2017). At Abri du Maras, reindeer are the most abundant species (88% of the NISP, Daujerd et al., 2017, table 3), as attested by 1170 bone remains and 16 MNI which all present abundant cutmarks, green bone fracturing, and periosteum removal for marrow extraction. Comparison with other Middle Palaeolithic monospecific faunal assemblages within a similar spectrum, has shown an abundance of young adult individuals slaughtered during summer or early autumn (Daujerd et al., 2017). It is therefore possible to suggest that monospecific reindeer hunting activities at Abri du Maras Level 4 are linked with the presence of the projectile tools identified among the convergent tools (25% of the analysed sample). Here Neanderthals may have planned organised hunting episodes with the aid of stone-tipped spears to intercept reindeer herds during seasonal fall migrations (see also Section **Error! Reference source not found.**). Reindeer, which can be either migratory or sedentary species (Daujerd et al., 2017), could have been intercepted

in the surroundings of the site near the Ardèche gorges area or at some of the possible water sources located along the Rhône valley. This interpretation is supported by the high frequencies of DIFs among the analysed convergent tools (32.3%; Table 11-3) and by the presence of stone-tipped projectiles (at least 25% of the analysed sample of convergent tools).

11.5 Revisiting Neanderthal hunting strategies

In the last few decades, a mosaic of new archaeological discoveries has drastically shifted the debate around European Middle Palaeolithic subsistence activities and hunting behaviours.

During the 1980s and early 1990s the existence and nature of hominin hunting practises during the Middle Palaeolithic was fiercely debated (Binford, 1984; Stiner, 1991, 1994; contra Marean, 1998; see also Section 1.4). Since then, new archaeozoological analyses of Middle Palaeolithic faunal assemblages (Jaubert et al., 1990; Patou-Mathis, 1999; Burke, 2000; Gaudzinski, 1996; Airvaux, 1999; Conard and Prindiville, 2000; Gaudzinski and Roebroeks, 2000; Moncel et al., 2012; Discamps and Faivre, 2017; Daujeard et al., 2017; see also Section 1.4), combined with isotopic analysis of Neanderthal remains (Bocherens et al., 2005; Richards and Trinkaus, 2009; see also Section 1.4) and the identification of diagnostic impact traces on Middle Palaeolithic stone tools (Villa and Lenoir, 2006, 2009; Villa et al., 2009; Lazuèn, 2012; Rots, 2013; La Porta et al., 2015; see also Section 1.4.3.2.2) have strongly suggested that Neanderthals were efficient hunters of large mammals. Site-specific examples also suggest that Neanderthals could flexibly adapt their strategies in response to seasonal and local environmental variations (see also Section 1.4). Therefore, today the main question (and a key area of focus for this thesis) is not “whether Middle Palaeolithic people could hunt, but how they chose to hunt” (Burke, 2000, p. 281).

A central debate concerns whether Neanderthals only employed hand-delivered weapons for close-range, confrontational and, therefore, dangerous and probably unselective hunting activities (as originally proposed by Churchill and colleagues [Churchill, 1996; Shea, 2006; Churchill and Rhodes, 2009; Rhodes and Churchill,

2009]), or whether they developed hand-thrown weapons, most likely tipped and untipped spears, that acted as effective hunting weapons, aided in self-defence against predators and/or for interpersonal violence, and contributed to the development of selective hunting and behaviour strategies (Villa and Soriano, 2010; Milks et al., 2019).

Once the anatomical capability of Neanderthals to practise thrown movements (Churchill et al., 1996; Schmitt et al., 2003; Rhodes and Churchill, 2009; Churchill and Rhodes, 2009) has been challenged (Shaw et al., 2012; Maki, 2012) and, in light of new discoveries, dismissed (Roach et al., 2012, 2013; Faivre et al., 2014; Roach and Richmond, 2015a, 2015b) (see also Section 1.3), it is possible to fully address issues concerned hunting behaviours in the Middle Palaeolithic. Although this can be considered speculative, it has also been argued that “a return to a more holistic perspective to develop a comprehensive overall perspective of Neandertal social behaviour” is a practise missing in modern archaeological research (Gaudzinski-Windheuser and Kindler, 2012, p. 1). This call for new approaches is particularly important as there is currently a remarkably low number of publications specifically addressing hunting strategies in the Middle Palaeolithic (but see White et al., 2016), beyond those interpreting faunal assemblages or mortality profiles (e.g. see Burke, 2000; Gaudzinski, 2000; Conard and Prindiville, 2000; Yeshurun et al., 2007). Therefore, the experimental data and archaeological evidence gathered in this thesis (and discussed in the above Sections, 11.2 and 11.4) are compared below with existing literature to recreate possible hunting scenarios, using a holistic approach of the sort proposed by Gaudzinski-Windheuser and Kindler (2012). On the basis of these comparisons a new proposal will be made as to whether or not a wider, more diverse array of Middle Palaeolithic hunting strategies are required by the available evidence.

In a recent paper, White and colleagues (White et al., 2016) proposed that a series of open-air Middle Palaeolithic killing sites (e.g. Mauran, La Borde, Taubach, Zwolèn, and Salzgitter), previously interpreted as examples of the selective hunting activities of Neanderthals (in terms of species and age profiles; Bratlund, 1999; Gaudzinski, 1996; Gaudzinski and Roebroeks, 2000; Gaudzinski, 2000; Gaudzinski, 2006),

represented instead unselective hunting episodes. They proposed that the main strategy employed by Neanderthals was to drive the animal herds into natural topographic traps (e.g. karstic depressions, narrow valleys, and over cliffs), and then use unselective ambushing or stalking the prey with short-range confrontational spears to make their kills (White et al., 2016). They suggested that during the killing stage “the Neanderthal hunts were marked by chaos” and that “within the effective ranges of their weapons” the selection of prey and decision-making were unfeasible behaviours (White et al., 2016, p. 17). The selection was instead occurring during the butchery stage, when the Neanderthal groups decided which carcasses to process (in terms of species and age; White et al., 2016).

In contrast to White et al. (2016) and others (Shea, 2006; Churchill and Rhodes, 2009), the archaeological evidence of the two study cases combined with the experimental dataset presented in this thesis points towards an additional interpretation: that distance killing and selective hunting were also possible strategies that could have been accomplished with Middle Palaeolithic hand-delivered stone-tipped spears (such as the ones designed and used in this thesis' experiments, see CHAPTER 4). As discussed in CHAPTER 5 and Sections 11.2, this study has corroborated, using multiple lines of evidence, that Middle Palaeolithic stone-tipped spear replicas were very effective hunting weapons when used in throwing activities, both in term of penetration depth and ranges of impact velocities and kinetic energy reached. Moreover, although this thesis has only tested the effectiveness of hand-delivered throwing spears at specific ranges (i.e. over a 5 m range in order to control multiple variables, see CHAPTER 4), other recent experiments testing the performance of similar morphological weapons (in terms of spear shaft length, diameter, and weight; i.e. replicas of the Schöningen wooden spears) support effective use over longer distances (Milks et al., 2019). Milks et al. (2019) have demonstrated that early Middle Palaeolithic untipped spears, despite being heavy and thick weapons, can reach at least twice as far as the previously proposed distance when hand-thrown by skilled throwers (Milks et al., 2019; contra Churchill, 1993). These data shift the current threshold of distance range for hand-delivered throwing spears from 6-8 m (Churchill, 1993) to 20 m (Milks et al., 2019), especially when the targeted preys are medium to large size mammals (e.g. horses,

bison, or mammoths). The results of this thesis, combined with other research, therefore suggest that Middle Palaeolithic hand-delivered spears (both tipped and untipped) could have been used as distance weapons and may have enabled more “selective” and “distance killing” adaptive hunting strategies.

For example, within a maximum distance range of 20 m (Milks et al., 2019), tipped and untipped Middle Palaeolithic spears, as well as being used for confrontational short-range, ambushing, disadvantaging, and physically dangerous hunting strategies (as originally proposed by Shea, 2006; and Churchill and Rhodes, 2009), could have also been used to practice “selective” hunting strategies, with throws aimed at specific individuals within a herd. With powerful hand-delivered throwing spears (as suggested by the parameters presented in Table 5-11), and possibly with longer distance ranges (Milks et al., 2019), once a Middle Palaeolithic hunter approaches the group of animals, he/she could target selected individuals within the group. It is important to recognise that targeted individuals, e.g. animals of specific ages or sex, need not be prime age individuals. For example, immature individuals may have been the most vulnerable elements and an easier target due to their inexperience and/or slowness. Moreover, young individuals of red deer, horse, and some cattle species, commonly stand next to the mothers and, when in mixed herds, tend to stand on the lateral sides of the herd/drove (Frison, 2014; White et al., 2016). In this context, with a herd in a resting position possibly nearby to water sources (as for example in the case of the Ardèche or Ponci rivers near the two archaeological sites presented in this thesis), a group of Neanderthals could have first quietly hidden themselves downwind so as not to frighten the herd, and then quickly could have struck all at the same time with their powerful throwing tipped spears targeted towards the most disadvantaged individuals of the herd, which possibly would have stood in more favourable positions and were unaware of the danger. Such strategies might generate the selective hunting profiles previously proposed at sites such as Salzgitter-Lebenstedt (Gaudzinski, 1996; Gaudzinski and Roebroeks, 2000), but at the hunting stage rather than the butchery stage (contra White et al. 2016). Moreover, the new proposed threshold of c. 20 m for the effective distance range for hand-delivered throwing spears (Milks et al., 2019) would have allowed the hunters

to remain at a safer distance, at least until the herd scattered, giving them the possibility of relative safety and/or escape (against dangerous and large prey).

On the other hand, the selection of specific individuals would have been more difficult with only thrusting spears, as confrontational hunting has a certain element of unpredictability and hazard (as remarked by White et al., 2016). However, this does not mean that spears were always or only used as thrown weapons, even within single hunting events. Neanderthals would have probably taken full advantage of their weaponry technologies (i.e. both tipped and untipped spears) by using them in multiple hunting strategies, dictated by an array of variables, both more and less predictable. These may have included the terrain and vegetation cover, the degree and/or sense of threat/danger, the position and size of the target, the prey's behaviour, and the skill and/or experience of the hunter. Moreover, during any hunting scenario there might have been rapid and multiple transitions from 'safe distance' encounters (e.g. during the initial stages of the kill) to 'close-quarter' encounters (e.g. as the herd scattered). When Middle Palaeolithic hunter(s) were surrounded by aggressive (e.g. kicking, biting) prey it seems likely that there was an instinctive response to the nearest source of threat (see also White et al., 2016), resulting in a spear thrust or throw depending on the specific distance between hunter and prey at that particular moment.

This proposed hunting scenario, based around the use of effective hand-delivered throwing spears to select specific species and individuals (i.e. ages and sexes) within a herd during planned hunting episodes, fits extremely well with the archaeological evidence of the two study cases analysed in this thesis. As discussed in Section 11.4, at the Arma Delle Manie and Abri du Maras sites are characterised by the presence of (i) high frequencies of DIFs among the convergent tool assemblages (only comparable with Upper Palaeolithic killing sites, see Section 11.4.2), (ii) the identification of projectile elements with examples of use-wear evidence for throwing (see CHAPTER 9 and 10), and (iii) the presence of monospecific faunal assemblages suggesting the selective hunting of sub-adult and prime age reindeer (at Abri du Maras; Daujerdard et al., 2017) and red deer (at Arma Delle Manie; Valensi and Psthi, 2004; Psathi and Vicino, 2003). In combination this

evidence supports the interpretation of hunting strategies using effective (and possibly long-range) throwing spears. This would also support the original interpretation of Gaudzinski and colleagues that saw the Neanderthals as the main active hunting agents for the accumulation of the selective monospecific faunal assemblages (Gaudzinski, 2000; Patou-Mathis, 2000; Gaudzinski and Roebroeks, 2000; Daujeard et al., 2017), with principal selection at the kill stage rather than the butchery stage.

Such strategies also have implications for the physical and skeletal trauma observed in Neanderthal remains that have been alternatively interpreted as a possible result of close-range confrontational hunting activities (Berger and Trinkaus, 1995) and, subsequently (Trinkaus, 2012), with reference to different and non-mutual explanations (e.g. inter-personal violence and Pleistocene mobility). Recent evidence of body injuries on Upper Palaeolithic human remains indicate no statistically significant difference between Neanderthals' traumatic body lesions and AMH' traumatic body lesions (Trinkaus, 2012, p.3692; Wu et al., 2011), suggesting that either the hunting strategies among the two species analysed were similar (and thus creating similar patterns of injuries), or that the body injuries observed on the two samples are due to causes other than hunting activities. Since there is widespread evidence for more distance hunting in the Upper Palaeolithic (Cattelain, 1997; Knecht, 1997; Bar-Yosef, 2002; Shea, 2006), the latter interpretation for the differences seems more likely, and Trinkaus (2012) concluded that interpersonal violence and Pleistocene mobility issues should be considered the main factors that contributed to the presence of traumatic lesions in the upper body of Neanderthals. Trinkaus, therefore, also suggested that the Middle Palaeolithic close-range weaponry hypothesis should be abandoned as the only explanation of Neanderthal body injuries (Trinkaus, 2012). The issue is further complicated by the small samples sizes (Berger and Trinkaus, 1995), which could also have affected the proportions of upper versus lower limb body injuries (as remarked by Trinkaus, 2012, p. 3692), but the results of this thesis, supporting Neanderthals use of throwing weapons, is therefore in-keeping with Trinkaus (2012) revised interpretation of the trauma data.

However, and as also remarked by White et al. (2016, p. 18), the author of this thesis is not suggesting that hunting with effective and targeted hand-delivered throwing spears was the only hunting strategy of Neanderthals. However, the possibility that Neanderthals also hunted their prey with effective throwing weapons at longer killing ranges is an innovative and viable working hypothesis, supported by the experimental dataset of this thesis (along with others, see Milks et al, 2016, 2019; Coppe et al., 2019) and by the archaeological use-wear evidence acquired at Abri du Maras and Arma Delle Manie. This may open further research avenues in terms of experimental trials (e.g. testing maximum distance ranges of hand-delivered stone-tipped spears), cognitive and social learning processes (i.e. acquisition of hunting and throwing skills among ethnographic groups), and archaeological investigations (i.e. seeking for additional use-wear evidence of throwing projectiles in Middle Palaeolithic assemblages, by applying the experimental use-wear methodology proposed in this thesis).

In conclusion, it has previously been argued that the selective hunting strategies of Neanderthals may have involved the development of planning and decision-making skills with regard to the specific individuals targeted (White et al., 2016; Gaudzinski and Roebroeks, 2000). Here it is proposed that monospecific faunal assemblages, which intensified from MIS 6 onward, in combination with diagnostic impact wear on Middle Palaeolithic tools, which also intensified from MIS 6, may also attest to a change in the hunting strategies and/or weapons employed by Neanderthals, i.e. the development of hand-delivered throwing spears for killing at distance.

Finally, the development of throwing weapons has been previously proposed to be a technological innovation and cognitive behaviour that was exclusive to AMH (Mellars, 1973, 1995, 1999; Stringer and Gamble, 1993; Bar-Yosef, 1998; Stringer, 2002; Shea, 2006; Shea and Sisk, 2010; see also INTRODUCTION), developed in Africa during the Middle Stone Age (around 300-100 Ka) and subsequently brought into Europe through different corridors (McBrearty and Brooks, 2000; Shea, 2006; Lombard and Parsons, 2011; Shea and Sisk, 2010; Sisk and Shea, 2011). However, what emerges from the experimental and archaeological evidence presented in this thesis (along with other research; Villa and Soriano, 2010; Milks et al., 2019) is that

throwing weapons, i.e. stone-tipped spears, were likely in use among Neanderthal populations and widespread in the European Middle Palaeolithic at least from the end of MIS 5/beginning of MIS 4 (considering the dating of the archaeological sites presented in this thesis), or possibly earlier (Villa and Lenoir, 2006, 2009; Rots, 2013). Therefore, it is possible that throwing weapons, specifically stone-tipped throwing spears, emerged broadly in parallel, and perhaps independently, both in the African Middle Stone Age where they were associated with AMH (Brooks et al., 2006; Lombard and Parsons, 2011) or pre-AMH (Wilkins et al., 2012; Sahle et al., 2013), and in the European Middle Palaeolithic in association with Neanderthals (d'Errico et al., 2003; Zilhão, 2011). This may correspond to an emergence of more sophisticated behaviours and social hunting practises that occurred around 200-100 Ka both in Eurasia and Africa (McBrearty and Brooks, 2000; d'Errico, 2003; Peresani et al., 2011; Villa and Roebroeks, 2014; Jaubert et al., 2016; Hoffmann et al., 2018b). After all, if hunting was a major component of food procurement strategies, it should not be surprising that both AMH and Neanderthals may have developed effective throwing weapons without necessarily have been in contact. Future research on weaponry technologies among Neanderthals and early AMH will undoubtedly contribute to better understanding of the origins of modern 'human' complexity in the later Middle and Late Pleistocene.

CHAPTER 12

CONCLUSIONS

Middle Palaeolithic hand-delivered stone-tipped spears such as a wooden spear shaft (similar to those found at Schöningen, Schoch et al., 2015) mounted with a Middle Palaeolithic stone point (e.g. Levallois points, or retouched and unretouched convergent tools) would have enabled Neanderthals to develop innovative and effective hunting strategies, and therefore, advance subsistence and technological behaviour.

This research has contributed to the systematic investigation of stone-tipped spear technology in both throwing and thrusting motions, combining experimental and archaeological approaches. This includes the kinematic analysis of experimental stone-tipped throwing and thrusting motions, the investigation of the resulting macroscopic and microscopic use-wear traces, and the applicability of these methodologies to the Middle Palaeolithic archaeological record, to answer the question of how Neanderthals were employing stone-tipped spears.

12.1 Research outcomes: experimental data

In this study, the performance of stone-tipped spears was explored by employing controlled but realistic variables assisted with high-resolution recording protocols. These experiments demonstrated that experimental Middle Palaeolithic stone-tipped spears are effective hunting weapons not only when used as thrusting spears, but also when used as throwing spears. Despite high mass values, the replicas of stone-tipped spears reached a high lethal threshold of penetration depth under simulations, recording ranges and means of penetration depths that were considerably higher than in previous tipped and untipped spear experiments (Milks et al., 2016; Wilkins et al., 2014a).

This study has also demonstrated the negative correlation between penetration depth of both throwing and thrusting spears with the impact location (i.e. impact against hard tissues resulted significantly often in lower penetration depths), and a non-significant correlation with the morphometric indexes of tip cross-sectional area

(TCSA; Shea, 2006) and tip cross-sectional perimeter (TCSP; Sisk and Shea, 2009) or impact velocities. The fact that TCSA and TCSP are poor predictors of penetration depth, puts into doubt the validity of using TCSA and TCSP as ballistic proxies to infer weapon lethality or difference in delivery systems (contra Shea, 2006; and Sisk and Shea, 2009).

As a first study linking stone-tipped spear performance with the recording of ballistics parameters (see Milks et al. [2016, 2019] for untipped spears), it demonstrated the complexity of reconstructing hand-delivered spear motions and the large variability included in the spear trajectory (due to the response of the weapons and/or the human thruster against the target upon impacts; but see also Milks et al., 2016). While hand-delivered stone-tipped spear throwing motions resulted in higher impact velocities than thrusting motions, the latter also recorded different values of kinetic energy and momentum due to the external force and response of the human thruster. Changes in impact velocities, kinetic energy and momentum values, together with spear deceleration upon impact are, therefore, all ballistic parameters that influence the outcomes of hand-delivered stone-tipped spear motions, and as such they must all be considered in experimental protocols. The experimental dataset and ballistic measurements generated by this thesis provide representative proxies for future experiments, favouring the development of new and more realistic experimental protocols in order to better understand stone-tipped technology and the resulting diagnostic use-wear traces. For instance, implementing experiments with trained and skilled human participants (instead of firing-machines) and realistic animal targets allows for the replication of “real and correct” use-wear traces, for subsequent comparison with archaeological specimens.

The use-wear results of this study suggest that the reconstruction of the delivery systems of stone-tipped spears is easier for experimental tools than for archaeological tools. This thesis has shown that if experimental stone tool projectiles are analysed employing a combined macro-and microscopic use-wear approach, the differentiation of the two hand-delivered spear systems is possible. The analysis of microscopic use-wear traces resulting from the hand-delivered spear experiments provided a much better method for distinguishing between hand-thrown and hand-

trust spear projectiles, indicating clear and significant differences on the use-wear traces of the two delivery systems (which were also different to those on experimental butchering knife tools). Macroscopic fracture analysis, although providing relevant information concerning which types of fractures and frequencies could be observed in both throwing and thrusting spear projectiles, demonstrated no significant difference in fracture types, patterns and frequencies between the two different delivery systems. As macroscopic fractures are not absolute proxies and the presence of different fracture types and higher or lower frequencies can change according to the morphology and/or raw materials of the stone tools, it is essential that the use-wear examination of experimental stone projectiles in future incorporates microscopic use-wear analysis (i.e. a high-power approach).

The microscopic use-wear results of this study found that throwing points develop much more abundant and diagnostic polish, linear traces and striations than thrusting points, and these patterns were all statistically significant and distinguished between the two delivery systems. The first important results found that microscopic linear impact traces (MLITs) occurred significantly more often in the throwing experimental Levallois points than in thrusting experimental Levallois points, with clear directionality and bright aspect in throwing and a scarce presence and a less diagnostic aspect in the thrusting points. The second set of results found that throwing spear projectiles develop more polish traces than thrusting spear projectiles, possibly due to the higher impact velocities of the weapons. A new type of well-developed, flat and reflective polish with clear directionality specified by the abundant striations, called “impact polish”, was recognised as diagnostic of throwing spear projectiles, since it was never observed in thrusting spear projectiles. These different patterns of microscopic use-wear traces allowed the distinction between experimental hand-delivered throwing spear projectiles and hand-delivered thrusting spear projectiles, as the formation of diagnostic polish traces can be possibly linked to differences in impact velocities and kinetic energy values of the two delivery systems. Therefore, this study represents a first step towards a distinction between hand-delivered stone-tipped spear technologies and it testifies the importance of reproducing representative variables in the conceptualisation of experimental protocols that aim to investigate use-wear traces.

The use-wear analysis for the experimental Levallois points employed in stone-tipped spear experiments also showed that non-adhesive hafting traces (such as fractures, edge-damage, polish or striations traces) were limited, due to the usage of adhesives as a medium between the stone tool and the shaft/fore-shaft of the weapons, and no difference of hafting traces was observed between throwing or thrusting spear projectiles. Although a small sample size was used, no major differences in hafting traces and/or patterns were observed among the three different hafting arrangements employed during the experiments (i.e. female, juxtaposed, or flat slots). This is because the most diagnostic traces left on the stone tool surface were adhesive traces in the form of polish or additive layers, whose nature and formation deserve future investigation.

Considering the outcomes of the experimental analyses, it is possible to support the following findings:

- Middle Palaeolithic stone-tipped spear replicas (mounted with experimental Levallois points) were effective hunting weapons when used both in hand-delivered throwing and thrusting spear motions.
- That the experimental Levallois points delivered in hand-throwing spear motions developed diagnostic and significantly different wear traces to those delivered in a hand-thrusting spear motions. This is because diagnostic projectile use-wear traces form under different impact velocities and kinetic energy values, and therefore a certain relationship between the energy yielded by the spear (i.e. impact velocity and *KE*) and the attributes of macroscopic and microscopic use-wear could be recognised.
- That the wear traces formed on the experimental Levallois points used as spear projectiles were different than the wear traces formed on equivalent experimental tools that were deployed in other experimental activities, i.e. as handheld or hafted butchering tools.
- That macroscopic and microscopic use-wear traces did not distinguish between different hafting arrangements (i.e. female, juxtaposed, and flat

hafting slot types), possibly due to the presence of adhesives as a medium between the stone tools and the shaft/fore-shaft system.

12.2 Research outcomes: archaeological data

The experimental results of this thesis when assessed against two selected Middle Palaeolithic assemblages provided interesting results, suggesting that stone-tipped spear projectiles, such as throwing and thrusting hand-delivered spears, were in use by Neanderthals in the European Middle Palaeolithic.

The preliminary assessment of the Levallois points and convergent tools of Arma Delle Manie (Italy) and Abri du Maras (France), dated between MIS 4 and MIS 3 (see CHAPTER 8), indicated the presence of projectile tools within these assemblages. Levallois points and convergent tools in the two archaeological sites were primarily used as stone-tipped projectiles (although with different percentages among the assemblages). Utilisation in longitudinal or scraping motions were also identified, confirming the multifunctional nature of the Levallois points and Middle Palaeolithic convergent tools.

The presence of post-depositional alterations, however, made the recognition of the delivery system of the identified archaeological stone projectiles more difficult to interpret. Diagnostic polish traces and linear traces (such as MLITs and impact polish) appeared rarely in the archaeological tools, either because they did not preserve or because they did not form in the past. Among the two assemblages, only a few specimens showed linear traces interpretable as MLITs, and only two tools showed a type of polish that can be comparable with the identified experimental impact polish (see CHAPTER 6). Therefore, additional investigation is essential to further verify the presence, formation, and preservation of diagnostic projectile impact traces (such as MLITs and impact polish) in the archaeological tools, by enlarging the sample of analysed artefacts and including assemblages that present minimum or no post-depositional alterations. Nevertheless, a limited number of specimens (both at Arma Delle Manie and Abri du Maras) yielded enough traces to support an interpretation as stone-tipped throwing spear projectiles.

Therefore, the identification of stone projectiles within two environmentally and geographically different sites dated at the end of MIS 4/beginning of MIS 3 suggests regular use of stone-tipped weapons among different Neanderthal groups, and shows that hunting techniques employing stone-tipped spears spread during the European Middle Palaeolithic. The presence of throwing projectiles (although in limited identifiable numbers) linked to the presence of monospecific faunal assemblages and young individual mortality profiles in both selected archaeological sites may indicate that specific hunting strategies were utilised. A “selective aiming hunting” towards specific classes of animals, could have been carried out with hand-thrown stone-tipped spears which would be deliverable over longer distances than hand-thrust stone-tipped spears.

The use of stone-tipped spears, i.e. composite technology, attested in the two selected archaeological sites may also suggest the enhancement of certain skills (see Section 1.4.2.2). Long-term memory, planning and anticipation of future needs, as well as the enhancement of technical behaviour are all skills required for the manufacture of the different components of a composite weapon, such as a stone-tipped spear (Ambrose, 2001, 2010; Wynn, 2009; Wadley et al., 2009; Wadley, 2009, 2010; Haidle, 2009, 2010; Lombard and Haidle, 2012; Barham, 2013). The manufacture and use of composite weapons would have also enhanced social relations in terms of cooperation and communication for the supplying and production of the large set of constituent parts.

The hypothesis that Neanderthals may have used stone projectiles in Europe is not new (see Villa and Soriano, 2010 for a synthesis), but this study provides more empirical evidence to distinguish between stone-tipped spear technologies, and suggests that thrown stone-tipped spears were in use among Neanderthals in the European Middle Palaeolithic from at least MIS 4. This evidence is important in evolutionary terms, since the development of throwing weapons may signal a step towards more advanced hunting strategies and enhanced cognitive processes. Ultimately, this raises the question of how much of ‘human’ complex behaviour can be assigned exclusively to Anatomical Modern Humans in the Palaeolithic.

12.3 Future directions

As with all extended research projects, this research has opened up the ground for future research that warrants consideration:

- Microscopic projectile use-wear traces. This thesis has shown that several diagnostic microscopic use-wear traces form in hand-delivered throwing spear projectiles. These traces, such as MLITs and impact polish, deserve future investigation in order to understand the process of formation, and investigation as to under which variables and ballistic parameters they may occur. It would be essential to focus on a specific morphotype and raw material, as the morphology and/or raw materials may influence the formation of these microscopic traces. Experiments should focus upon isolating the effect that specific variables (such as impact velocity and kinetic energy) may have on the formation of these microscopic traces. However, it is this author's opinion that the use of animal targets is essential for the replication of "correct and comparable" microscope use-wear traces on projectile tools. It would also be interesting to test if ballistic gel may originate similar traces. Similarly, the investigation of microscopic use-wear traces on projectile tools would benefit from the combination of optical microscopic use with scanning electron microscopy, allowing for a better interpretation of the microtopography of the traces and a possible chemical characterisation.
- Microscopic Adhesive traces. This thesis has identified characteristic polish or additive layers resulting from the deposition or location of adhesive traces onto the stone tool surface. Future research is warranted to answer the question if those traces are simply microscopic residue that strongly adhere to the surface of the stone tools, or alternately if they are bound onto the surface. Therefore, testing specific cleaning protocols and the chemical characterisation of the residues would aid the interpretation of this characteristic type of hafting traces.
- Tipped and untipped spear technologies. Future experiments should focus upon the differences in performance between stone-tipped and untipped spear weapons, in order to better investigate the evolutionary advantage of

employing composite weapons, and the reasons for choosing one or the other technology. However, investigation should involve a multiple experimental programme focusing first on the performance of these different weapon systems employing realistic variables and only later executing controlled laboratory experiments.

- Archaeological analysis of Middle Palaeolithic stone tools. It is essential to apply the experimental results of this thesis to larger and more numerous archaeological assemblages in order to investigate if the microscopic use-wear traces diagnostic of throwing spear motions, MLITS and impact polish traces, can be better preserved in the archaeological record. If this is the case, an investigation of European Middle Palaeolithic sites with different chronologies may shed light on the timing of the emergence, and subsequent spread, of throwing stone-tipped spear technology among Neanderthal populations.

Hunting techniques are crucial for understanding subsistence strategies and human evolution. The multidisciplinary approach employed in this thesis by the combination archaeological analysis, systematic experiments and ballistic investigation has shown the value of this methodology for investigating prehistoric hunting technology. As a result, I envisage my future research as an ongoing dialogue between the study of archaeological stone tools, the contributions of experimental archaeology (working alongside skilled craftsmen) and the possibility of undertaking ethnoarchaeological investigations. This methodological approach will increase our understanding of the development of ancient weaponry technologies among different hunter-gatherers across prehistory.

BIBLIOGRAPHY

Abbassi, M. (1999) *Les rongeurs du Sud-Est de la France et de Ligurie: implications systématiques, biostratigraphiques et paléoenvironnementales*, PhD thesis, Paris, Muséum national d'histoire naturelle.

Abbassi, M. and Desclaux, E. (1996) "Arvicola Lacépède, 1799 (Rodentia, Mammalia) de quatre séquences du Sud-Est de la France et de Ligurie datant de la fin du Pléistocène moyen et du début du Pléistocène supérieur", *Quaternaire*, vol. 7, no. 7-1, pp. 29-35.

Aboitiz, F. and Garcia, R. (1997) "The evolutionary origin of the language areas in the human brain. A neuroanatomical perspective", *Brain Research Reviews*, vol. 25, no. 3, pp. 381-396.

Adler, D. S., Wilkinson, K. N., Blockley, S., Mark, D. F., Pinhasi, R., Schmidt-Magee, B. A., Nahapetyan, S., Mallol, C., Berna, F., Glauberman, P. J. and Raczynski-Henk, Y. (2014) "Early Levallois technology and the Lower to Middle Paleolithic transition in the Southern Caucasus", *Science*, vol. 345, no. 6204, pp.1609-1613.

Ahler, S. A. and McMillan, R. B. (1976) "Material culture at Rodgers Shelter: a reflection of past human activities", in Wood, W. R. and McMillan, R. B. (eds) *Prehistoric man and his environments: a case study in the Ozark Highland*, Amsterdam, Academic Press, pp.163-199.

Airvaux, J. (1999) "Le site paléolithique de chez-Pinaud à Jonzac (Charente-Maritime)", *Bulletin de la Société préhistorique française*, vol. 96, no. 4, pp. 636-638.

Akoshima, K. (1987) "Micro-flaking quantification", in Sieveking, G. D. G. and Newcomer M. H. (eds) *The human uses of flint and chert: Papers from the Fourth International Flint Symposium*, Cambridge, Cambridge University Press, pp. 71–79.

Allué E., Cabanes D., Solé A., and Sala R. (2012) "Hearth Functioning and Forest Resource Exploitation Based on the Archeobotanical Assemblage from Level J", in Roura, E. (eds) *High Resolution Archaeology and Neanderthal Behavior: Time and Space in Level J of Abric Romaní (Capellades, Spain)*, Springer, pp. 373–385.

Ambrose, S. H. (2010) "Coevolution of composite-tool technology, constructive memory, and language: implications for the evolution of modern human behaviour", *Current Anthropology*, vol. 51, no. S1, pp. 135-147.

Anderson, P. C. (1980) "A testimony of prehistoric tasks: diagnostic residues on stone tool working edges", *World Archaeology*, vol. 12, no. 2, pp.181-194.

Anderson, P. C., Beyries, S., Otte, M., and Plisson, H. (1993) *Traces et fonction: les gestes retrouvés*, Liege, Service de Préhistoire, Université de Liege.

Anderson, P. C., Georges, J. M., Vargiolu, R., and Zahouani, H. (2006) "Insights from a tribological analysis of the tribulum", *Journal of Archaeological Science*, vol. 33, no. 11, pp.1559-1568.

Anderson-Gerfaud, P. (1981) *Contribution méthodologique à l'analyse des microtraces d'utilisation sur les outils préhistoriques*, PhD thesis, Talence, Université de Bordeaux I.

Anderson-Gerfaud, P. (1982) "Comment préciser l'utilisation agricole des outils préhistoriques? in Travaux de laboratoire", *Cahiers de l'Euphrate St-André-de-Cruzières*, vol. 3, pp. 149-164.

Anderson-Gerfaud, P. (1983) "A consideration of the uses of certain backed and «lusted» stone tools from late Mesolithic and Natufian levels of Abu Hureyra and Mureybet (Syria)", *Travaux de la Maison de l'Orient*, vol. 5, no. 1, pp. 77-105.

Anderson-Gerfaud, P. (1990) "Aspects of behaviour in the Middle Palaeolithic: functional analysis of stone tools from southwest France", in Mellars, P. (eds) *The emergence of modern humans: an archaeological perspective*, Ithaca, NY, Cornell University Press, pp. 389-418.

Andrefsky, W. (1998) *Lithics*, Cambridge, Cambridge University Press.

Aranguren B., Revedin A., Amico N., Cavulli F., Giachi G., Grimaldi S., Macchioni, N., and Santaniello, F. (2018) "Wooden tools and fire technology in the early Neanderthal site of Poggetti Vecchi (Italy)", *Proceedings of the National Academy of Sciences*, vol. 115, no. 9, pp. 2054–2059.

Aranguren, B., Longo, L., Mariotti Lippi, M., and Revedin, A. (2012) "Evidence of edible plant exploitation", in Svoboda, J. (eds) *Pavlov Excavations 2007-2011*, Brno, The Dolní Věstonice Studies, pp.170-179.

Arndt, S. and Newcomer, M. (1986) "Breakage Patterns on Prehistoric Bone Points: An Experimental Study" in Roe, D. A. (eds) *Studies in the Upper Palaeolithic of Britain and Northwest Europe*, Oxford, BAR International Series, vol. 296, pp. 165-173.

Arobba D., Giuggiola O., Imperiale G., Lamberti A., Oxilia M., and Vicino G. (1976) "Le Mànie. Il giacimento musteriano dell'Arma (Finale Ligure-SV)", in Soprintendenza Archeologica della Liguria (eds) *Archeologia in Liguria, scavi e scoperte 1967-75*, Genova, Soprintendenza Archeologica della Liguria, pp. 113-144.

Arroba, D. (2014) Personal communication to La Porta, A., Finalpia, 7th April.

Arsuaga, J. L., Lorenzo, C., Carretero, J. M., Gracia, A., Martínez, I., García, N., de Castro, J. M. B., and Carbonell, E. (1999) "A complete human pelvis from the Middle Pleistocene of Spain", *Nature*, vol. 399, no. 6733, pp. 255-258.

-
- Ashton, N. (2017) "Landscapes of habit and persistent places during MIS 11 in Europe: a return journey from Britain", in Pope, M., McNabb, J., and Gamble, C. (eds) *Crossing the human threshold, dynamic transformation and persistent places during the Middle Pleistocene*, Routledge, pp. 164-186.
- Ashton, N., Lewis, S. G., Parfitt, S. A., Penkman, K. E., and Coope, G. R. (2008) "New evidence for complex climate change in MIS 11 from Hoxne, Suffolk, UK", *Quaternary Science Reviews*, vol. 27, no.7-8, pp.652-668.
- Asryan, L., Ollé, A., and Moloney, N. (2014) "Reality and confusion in the recognition of post-depositional alterations and use-wear: an experimental approach on basalt tools", *Journal of Lithic Studies*, vol.1, no. 1, pp. 9-32.
- Auguste, P. (2003) "La chasse à l'ours au Paléolithique moyen: Mythes, réalités et état de la question", in Pathou-Mathis, M., and Bocherens, H. (eds) *Le rôle de l'environnement dans le comportement de chasseurs-cueilleurs préhistoriques*, Oxford, BAR International Series, vol. 1105, pp. 135-142.
- Backwell, L., d'Errico, F., and Wadley, L., (2008) "Middle stone age bone tools from the Howiesons Poort layers, Sibudu Cave, South Africa", *Journal of Archaeological Science*, vol. 35, no. 6, pp. 1566-1580.
- Bamforth, D. B. (1988) "Investigating microwear polishes with blind tests: the institute results in context", *Journal of Archaeological Science*, vol. 15, no. 1, pp. 11-23.
- Bamforth, D. B. (2010) "Conducting Experimental Research as a Basis for Microwear Analysis", in Ferguson, J. R. (eds) *Designing experimental research in archaeology: examining technology through production and use*, University Press of Colorado, pp. 93– 109.
- Barham, L. (1998) "Possible early pigment use in south-central Africa", *Current Anthropology*, vol. 39, no. 5, pp. 703-710.
- Barham, L. (2002) "Backed tools in Middle Pleistocene central Africa and their evolutionary significance", *Journal of Human Evolution*, vol. 43, no. 5, pp. 585-603.
- Barham, L. (2013) *From hand to handle: the first industrial revolution*, Oxford, Oxford University Press.
- Barton, H. (1990) *Raw Material and Tool Function: a residue and use-wear analysis of artefacts from a Melanesian rock shelter*, PhD thesis, Sydney, Sydney University.
- Barton, R. N. E. and Bergman, C. A. (1982) "Hunters at Hengistbury: some evidence from experimental archaeology", *World archaeology*, vol. 14, p. 2, pp. 237-248.

-
- Bar-Yosef, O. (1987) "Direct and indirect evidence for hafting in the Epi-Palaeolithic and Neolithic of the Southern Levant", *Travaux de la Maison de l'Orient*, vol. 15, no. 1, pp. 155-164.
- Bar-Yosef, O. (1998) "On the nature of transitions: the Middle to Upper Palaeolithic and the Neolithic Revolution", *Cambridge Archaeological Journal*, vol. 8, no. 2, pp. 141-163.
- Bar-Yosef, O. (2002) "The upper paleolithic revolution", *Annual review of anthropology*, vol. 31, no. 1, pp. 363-393.
- Baugh, R. A. (2003) "Dynamics of spear throwing", *American Journal of Physics*, vol. 71, no. 4, pp. 345-350.
- Becker, C. J. (1945) *En 8000-aaig Stenalderplads i Holmegaard Mose*, Copenhagen, Nationalmuseets Arbejdsmark, pp. 61-72.
- Benazzi, S., Douka, K., Fornai, C., Bauer, C.C., Kullmer, O., Svoboda, J., Pap, I., Mallegni, F., Bayle, P., Coquerelle, M., and Condemi, S. (2011) "Early dispersal of modern humans in Europe and implications for Neanderthal behaviour", *Nature*, vol. 479, no. 7374, pp. 525-528.
- Benazzi, S., Slon, V., Talamo, S., Negrino, F., Peresani, M., Bailey, S. E., Sawyer, S., Panetta, D., Vicino, G., Starnini, E., and Mannino, M. A. (2015) "The makers of the Protoaurignacian and implications for Neandertal extinction", *Science*, vol. 348, no. 6236, pp. 793-796.
- Berger, T. D. and Trinkaus, E. (1995) "Patterns of trauma among the Neandertals", *Journal of Archaeological Science*, vol. 22, no. 6, pp. 841-852.
- Bergman, C. A. (1993) "The development of the bow in Western Europe: a technological and functional perspective", *Archeological Papers of the American Anthropological Association*, vol. 4, no. 1, pp. 95-105.
- Bergman, C. A. and Newcomer, M. H. (1983) "Flint arrowhead breakage: examples from Ksar Akil, Lebanon", *Journal of Field Archaeology*, vol. 10, no. 2, pp. 238-243.
- Bergman, C. A., McEwen, E., and Miller, R. (1988) "Experimental archery: projectile velocities and comparison of bow performances", *Antiquity*, vol. 62, no. 237, pp. 658-670.
- Bernard-Guelle, S., Bernard, C., and Bressy, C. (2006) "Le site moustérien de plein air de Maumuye (Saint-Roman, Drôme): premiers résultats", *Bulletin de la Société préhistorique française*, vol. 103, no. 1, pp. 9-15.
- Best, R. J., Bartlett, R. M., and Morriss, C. J. (1993) "A three-dimensional analysis of javelin throwing technique", *Journal of sports sciences*, vol. 11, no. 4, pp. 315-328.

Beyries, S. (1987a) *Variabilité de l'industrie lithique au Moustérien: approche fonctionnelle sur quelques gisements français*, Oxford, BAR International Series, vol. 328.

Beyries, S. (1987b) "Quelques exemples de stigmates d'emmanchements observés sur des outils du Paléolithique moyen", *Travaux de la Maison de l'Orient*, vol. 15, no. 1, pp. 55-62.

Beyries, S. (1988) "Functional variability of lithic sets in the Middle Paleolithic" in Dibble, H. L. (eds) *Upper Pleistocene prehistory of western Eurasia*, University of Pennsylvania Press, pp. 213-223.

Beyries, S. (1990) "Problems of interpreting the functional results for ancient periods", in Gräslund, B. and Knutsson, H. (eds) *The Interpretative Possibilities of Microwear Studies*, Uppsala, Societas Archaeologica Upsaliensis, pp. 71-76.

Beyries, S. (1993) "Are we able to determine the function of the earliest Palaeolithic tools", in Berthelet, A. and Chavaillon J. (eds) *Use of Tools by Human and Non-human Primates*, Oxford, Clarendon Press, pp. 225-236.

Beyries, S. (1995) "Expérimentation archéologique et savoir-faire traditionnel: l'exemple de la découpe d'un cervidé", *Techniques & Culture. Revue semestrielle d'anthropologie des techniques*, vol. 22, pp. 53-79.

Béyries, S. (1997) "Ethnoarchéologie: un mode d'expérimentation" *Préhistoire anthropologie méditerranéennes*, vol. 6, pp. 185-196.

Beyries, S., Delamare, F., and Quantin, J. C. (1988) "Tracéologie et rugosimétrie tridimensionnelle", in Beyries, S. (eds) *Industries lithiques: traceologie et technologie*, Oxford, BAR International Series, vol. 411, no. 2, pp. 115-132.

Bicho, N. and Haws, J. (2008) "At the land's end: marine resources and the importance of fluctuations in the coastline in the prehistoric hunter-gatherer economy of Portugal", *Quaternary Science Reviews*, vol. 27, no. 23-24, pp. 2166-2175.

Bicho, N., Marreiros, J., and Gibaja, J. F. (2015) "Use-Wear and Residue Analysis in Archeology", in Marreiros, J., Gibaja, J. F., and Bicho, N. (eds) *Use-wear and residue analysis in archaeology*, Cham, Springer, pp. 1-4.

Bietti, A. and Negrino, F. (2007) "Transitional" Industries from Neandertals to Anatomically Modern Humans in Continental Italy: Present State of Knowledge", in Riel-Salvatore, J. and Clark A. G. (eds) *New Approaches to the Study of Early Upper Paleolithic "Transitional" Industries in Western Eurasia. Transitions Great and Small*, Oxford, BAR International Series, vol. 1620, pp. 41-60.

-
- Binford, L. R. (1973) "Interassemblage variability: The Mousterian and the functional argument", in Renfrew, C. (eds) *The explanation of culture change: models in prehistory*, London, Gerald Duckworth, pp. 27-254.
- Binford, L. R. (1979) "Organization and formation processes: looking at curated technologies", *Journal of anthropological research*, vol. 35, no. 3, pp. 255-273.
- Binford, L. R. (1980) "Willow smoke and dogs' tails: hunter-gatherer settlement systems and archaeological site formation", *American antiquity*, vol. 45, no. 1, pp. 4-20.
- Binford, L. R. (1981) *Bones: Ancient Men and Modern Myths*, New York, New York Academic Press.
- Binford, L. R. (1983) *In Pursuit of the Past*, London, Thames and Hudson.
- Binford, L. R. (1984) "Butchering, sharing, and the archaeological record", *Journal of Anthropological Archaeology*, vol. 3, no. 3, pp. 235-257.
- Binford, L. R. (1985) "Human ancestors: changing views of their behaviour", *Journal of Anthropological Archaeology*, vol. 4, pp. 292–327.
- Binford, L. R. (1987) "Searching for camps and missing the evidence? Another look at the Lower Paleolithic", in Soffer, O. (eds) *The Pleistocene Old World: Regional Perspectives*, Springer, pp. 17–31.
- Bischoff, J. L., Julià, R., and Mora, R. (1988) "Uranium-series dating of the Mousterian occupation at Abric Romani, Spain", *Nature*, vol. 332, no. 6159, pp. 68.
- Bischoff, J. L., Williams, R. W., Rosenbauer, R. J., Aramburu, A., Arsuaga, J. L., García, N., and Cuenca-Bescós, G. (2007) "High-resolution U-series dates from the Sima de los Huesos hominids yields 600 – 66+ ∞ kyrs: implications for the evolution of the early Neanderthal lineage", *Journal of Archaeological Science*, vol. 34, no. 5, pp. 763-770.
- Blasco, R. and Peris, J. F. (2012) "Small and large game: human use of diverse faunal resources at Level IV of Bolomor Cave (Valencia, Spain)", *Comptes Rendus Palevol*, vol. 11, no. 4, pp. 265-282.
- Blumenschine, R. J., Cavallo, J. A., and Capaldo, S. D. (1994) "Competition for carcasses and early hominid behavioral ecology: A case study and a conceptual framework", *Journal of Human Evolution*, vol. 27, pp. 197–213.
- Bocherens, H., (2009) "Neanderthal dietary habits: review of the isotopic evidence", in Richards P. M. and Hublin, J. J. (eds) *The evolution of Hominin diets*, Netherlands, Springer, pp. 241-250.

-
- Bocherens, H., Drucker, D. G., Billiou, D., Patou-Mathis, M., and Vandermeersch, B. (2005) "Isotopic evidence for diet and subsistence pattern of the Saint-Césaire I Neanderthal: review and use of a multi-source mixing model", *Journal of human evolution*, vol. 49, no. 1, pp. 71-87.
- Bocherens, H., Drucker, D.G., Billiou, D., Patou-Mathis, M. and Vandermeersch, B. (2005) "Isotopic evidence for diet and subsistence pattern of the Saint-Césaire I Neanderthal: review and use of a multi-source mixing model", *Journal of human evolution*, vol. 49, no. 1, pp. 71-87.
- Boëda, E. (1982) "Etude expérimentale de la technologie des pointes Levallois", in Cahen, D. (eds) *Tailler! Pourquoi faire? Préhistoire et technologie lithique II, Recent Progress in Microwear Studies*, Leuven, Studia Praehistorica Belgica, vol. 2, pp. 23-56.
- Boëda, E. (1986) *Approche technologique du concept Levallois et évaluation de son champ d'application: étude de trois gisements saaliens et weichseliens de la France septentrionale*, PhD thesis, Paris, Université de Paris 10.
- Boëda, E. (1994) *Le concept Levallois: variabilité des méthodes*, Paris, CNRS.
- Boëda, E. (1995) "Levallois: a volumetric construction, methods, a technique", in Dibble, H. L. and Bar-Yosef, O. (eds) *The definition and interpretation of Levallois technology*, Prehistory Press, vol. 23, pp. 41-65.
- Boëda, E., Bonilauri, S., Connan, J., Jarvie, D., Mercier, N., Tobey, M., Valladas, H., Al Sakhel, H., and Muhesen, S. (2008) "Middle Palaeolithic bitumen use at Umm el Tlel around 70 000 BP", *Antiquity*, vol. 82, n. 318, pp. 853-861.
- Boëda, E., Connan, J., and Muhesen, S. (2002) "Bitumen as hafting material on Middle Paleolithic artifacts from the El Kowm Basin, Syria", in Akazawa, T., Aoki, K., and Bar-Yosef, O. (eds) *Neandertals and modern humans in Western Asia*, US, Springer, pp. 181-204.
- Boëda, E., Connan, J., Dessort, D., Muhesen, S., Mercier, N., Valladas, H., and Tisnérat, N. (1996) "Bitumen as a hafting material on Middle Palaeolithic artefacts", *Nature*, vol. 380, no. 6572, pp. 336.
- Boëda, E., Geneste, J. M., and Meignen, L. (1990) "Identification de chaînes opératoires lithiques du Paléolithique ancien et moyen", *Paléo, Revue d'Archéologie Préhistorique*, vol. 2, no. 1, pp. 43-80.
- Boëda, E., Geneste, J. M., Griggo, C., Mercier, N., Muhesen, S., Reyss, J. L., Taha, A., and Valladas, H. (1999) "A Levallois point embedded in the vertebra of a wild ass (*Equus africanus*): hafting, projectiles and Mousterian hunting weapons", *Antiquity*, vol. 73, no. 280, pp. 394-402.
- Bonneau, A., Pearce, D. G., and Pollard, A. M. (2012) "A multi-technique characterization and provenance study of the pigments used in San rock art, South Africa", *Journal of Archaeological Science*, vol. 39, no. 2, pp. 287-294.

-
- Bordes, F. (1947) "Etude comparative des differetes techniques de taille du silex et des roches dures", *l'Anthropologie*, pp.1-29.
- Bordes, F. (1953) "Essai de classification des industries moustériennes", *Bulletin de la Société préhistorique de France*, vol. 50, no. 7-8, pp. 457-466.
- Bordes, F. (1954) "Racloirs convergents et déjetés, limaces", *Bulletin de la Société préhistorique de France*, vol. 51, no. 7, pp. 336–338.
- Bordes, F. (1961) *Typologie du paléolithique ancien et moyen*, Bordeaux, Imprimeries Delmas.
- Bordes, F. (1971) "Physical evolution and technological evolution in man: a parallelism", *World Archaeology*, vol. 3, pp. 1–5.
- Borel, A. (2010). *Formes et fonctions au sein des industries lithiques de la fin du Pléistocène et du début de l'Holocène en Asie du Sud-Est: un nouvel apport à la compréhension des comportements humains*, PhD thesis, Paris, Muséum national d'histoire naturelle.
- Borel, A., Ollé, A., Vergés, J. M., and Sala, R. (2014) "Scanning electron and optical light microscopy: two complementary approaches for the understanding and interpretation of usewear and residues on stone tools", *Journal of Archaeological Science*, vol. 48, pp. 46-59.
- Boschin, F. and Crezzini, J. (2012) "Morphometrical analysis on cut marks using a 3D digital microscope", *International Journal of Osteoarchaeology*, vol. 22, no. 5, pp. 549-562.
- Bourlon, M. (1906) "L'Industrie Mousterienne au Moustier", *XIII Congres International d'Anthropologie et d'Archeologie Prehistoriques: Compte Rendu de la Triezieme Session*, Monaco 1906. Monaco, Imprimerie Monaco, pp. 287- 322.
- Bradfield, J. and Lombard, M. (2011) "A macrofracture study of bone points used in experimental hunting with reference to the South African Middle Stone Age", *South African Archaeological Bulletin*, vol. 66, no. 193, pp.67.
- Bratlund, B. (1996) "Hunting strategies in the Late Glacial of Northern Europe: a survey of the faunal evidence", *Journal of World Prehistory*, vol. 10, no. 1, pp. 1-48.
- Bratlund, B. (1999) "Anthropogenic factors in the thanatocoenose of the Last Interglacial travertines at Taubach (Germany)", in Gaudzinski, S. and Turner, E. (eds.) *The role of early humans in the accumulation of European Lower and Middle Palaeolithic bone assemblages*, pp. 255-263.
- Bridgland, D. R., Field, M. H., Holmes, J. A., McNabb, J., Preece, R. C., Selby, I., Wymer, J. J., Boreham, S., Irving, B. G., Parfitt, S. A., and Stuart, A. J. (1999) "Middle Pleistocene interglacial Thames–Medway deposits at Clacton-on-Sea, England: reconsideration of the biostratigraphical and

environmental context of the type Clactonian Palaeolithic industry”, *Quaternary Science Reviews*, vol. 18, no. 1, pp. 109-146.

Brooks, A. S., Nevell, L., Yellen, J. E., and Hartman, G. (2006) “Projectile technologies of the African MSA”, in Hovers, E. and Kuhn, S. (eds) *Transitions before the transition*, US, Springer, pp. 233-255.

Brown, K. S., Marean, C. W., Jacobs, Z., Schoville, B. J., Oestmo, S., Fisher, E. C., Bernatchez, J., Karkanas, P., and Matthews, T. (2012) “An early and enduring advanced technology originating 71,000 years ago in South Africa”, *Nature*, vol. 491, no. 7425, pp. 590.

Brown, K., Fa, D. A., Finlayson, G., and Finlayson, C. (2011) “Small game and marine resource exploitation by Neanderthals: the evidence from Gibraltar”, in Bicho, N. F., Haws, J. A., and Davis, L. G. (eds) *Trekking the shore: Changing coastlines and the antiquity of coastal settlement*, US, Springer, pp. 247-272.

Bunn, H. T. (1981) “Archaeological evidence for meat-eating by Plio-Pleistocene hominids from Koobi Fora and Olduvai Gorge”, *Nature*, vol. 291, no. 5816, pp. 574.

Bunn, H. T. (1986) “Patterns of skeletal representation and hominid subsistence activities at Olduvai Gorge, Tanzania, and Koobi Fora, Kenya”, *Journal of Human Evolution*, vol. 15, no. 8, pp. 673-690.

Burjachs, F. and Julià, R. (1994) “Abrupt climatic changes during the last glaciation based on pollen analysis of the Abric Romani, Catalonia, Spain”, *Quaternary Research*, vol. 42, no. 3, pp. 308-315.

Burjachs, F., López-García, J. M., Allué, E., Blain, H. A., Rivals, F., Bennàsar, M., and Expósito, I. (2012) “Palaeoecology of Neanderthals during Dansgaard–Oeschger cycles in northeastern Iberia (Abric Romani): from regional to global scale”, *Quaternary International*, vol. 247, pp. 26-37.

Burke, A. (2000) “The view from Starosele: faunal exploitation at a Middle Palaeolithic site in western Crimea”, *International Journal of Osteoarchaeology*, vol. 10, no. 5, pp. 325-335.

Burroni, D., Donahue, R. E., Pollard, A. M., and Mussi, M. (2002) “The surface alteration features of flint artefacts as a record of environmental processes”, *Journal of Archaeological Science*, vol. 29, no. 11, pp. 1277-1287.

Butler, W. B. (1975) “The atlatl: the physics of function and performance”, *Plains Anthropologist*, vol. 20, no. 68, pp. 105-110.

Callow, P. (1986) “The flint tools”, in Callow, P. and Cornford, J. (eds) *La Cotte de St. Brelade*, Norwich, Geo Books, pp. 251–314.

Carbonell E. and Castro-Curel Z. (1992) “Palaeolithic Wooden Artifacts from The Abric Romani (Capellades, Barcelona, Spain)”, *Journal of Archaeological Science*, vol. 19, pp. 707–719.

Carrère, P. (1990) "Contribution de la balistique au perfectionnement des études technofonctionnelles des pointes de projectiles préhistoriques", *Paléo*, vol. 2, no. 1, pp. 167-176.

Carrère, P. and Lepetz, S. (1988) *Etude de la dynamique des pointes de projectiles: élaboration d'une méthode*, Mphil thesis, Paris, Université de Paris I-Panthéon Sorbonne.

Caspar, J. P. and De Bie, M. (1996) "Preparing for the hunt in the Late Paleolithic camp at Rekem, Belgium", *Journal of Field Archaeology*, vol. 23, no. 4, pp. 437-460.

Cattelain, P. (1989) "Un crochet de propulseur solutréen de la grotte de Combe-Saunière 1 (Dordogne)", *Bulletin de la Société préhistorique française*, vol. 86, no. 86, pp. 213-216.

Cattelain, P. (1997) "Hunting during the Upper Paleolithic: bow, spearthrower, or both?", in Knecht, H. (eds) *Projectile technology*, US, Springer, pp. 213-240.

Cauche, D. (2002) *Les cultures moustériennes en Ligurie italienne: études des industries lithiques des grottes de la Madonna dell'Arma, d'Arma delle Manie et de Santa Lucia Superiore*, PhD thesis, Marseille, Université de la Méditerranée-Aix-Marseille II.

Cauche, D. (2007) "Les cultures moustériennes en Ligurie italienne: analyse du matériel lithique de trois sites en grotte", *L'anthropologie*, vol. 111, no. 3, pp. 254-289.

Cauche, D. (2012) "Productions lithiques et comportements techno-économiques de groupes humains acheuléens et moustériens en région liguro-provençale", *Comptes Rendus Palevol*, vol. 11, no. 7, pp. 519-527.

Chadwick, E. K., Nicol, A.C., Lane, J. V., and Gray, T. G. (1999) "Biomechanics of knife stab attacks", *Forensic Science International*, vol. 105, pp. 35-44.

Chevalier-Skolnikoff, S., Galdikas, B. M., and Skolnikoff, A. Z. (1982) "The adaptive significance of higher intelligence in wild orang-utans: a preliminary report", *Journal of Human Evolution*, vol. 11, no. 7, pp. 639-652.

Christensen, M., Calligaro, T., Consigny, S., Dran, J.C., Salomon, J., and Walter, P. (1998) "Insight into the usewear mechanism of archaeological flints by implantation of a marker ion and PIXE analysis of experimental tools", *Nuclear Instruments and Methods in Physics Research Section B: Beam Interactions with Materials and Atoms*, vol. 136, pp. 869-874.

Christenson, A. L. (1986) "Projectile point size and projectile aerodynamics: an exploratory study", *Plains Anthropologist*, vol. 31, no. 112, pp. 109-128.

Churchill, S. E. (1993) "Weapon technology, prey size selection, and hunting methods in modern hunter-gatherers: implications for hunting in the Palaeolithic and Mesolithic", *Archeological Papers of the American Anthropological Association*, vol. 4, no. 1, pp. 11-24.

Churchill, S. E. and Rhodes, J. A. (2009) "The evolution of the human capacity for "killing at a distance": the human fossil evidence for the evolution of projectile weaponry", in Richards P. M. and Hublin, J. J. (eds) *The evolution of Hominin diets*, Netherlands, Springer, pp. 201-210.

Churchill, S. E. and Schmitt, D. (2003) "Biomechanics in paleoanthropology: engineering and experimental approaches to the investigation of behavioral evolution in the genus Homo", in Harcourt, C. and Crompton, R. (eds) *New Perspectives in Primate Evolution and Behavior*, Otley, Westbury Academic and Scientific Publishing, pp. 59-90.

Churchill, S. E., Franciscus, R. G., McKean-Peraza, H. A., Daniel, J. A., and Warren, B. R. (2009) "Shanidar 3 Neandertal rib puncture wound and paleolithic weaponry", *Journal of human evolution*, vol. 57, no. 2, pp. 163-178.

Churchill, S. E., Weaver, A. H., and Niewoehner, W. A. (1996) "Late Pleistocene human technological and subsistence behavior: functional interpretations of upper limb morphology", *Quaternaria Nova*, vol. 6, pp. 413-447.

Clark, G. (1969) *World Prehistory: A New Outline*, Cambridge, Cambridge University Press.

Clark, J. D. (1970) *The prehistory of Africa*, New York, Praeger.

Clarkson, C. (2016) "Testing archaeological approaches to determining past projectile delivery systems using ethnographic and experimental data", in Iovita, R. and Sano, K. (eds) *Multidisciplinary approaches to the study of Stone Age weaponry*, Dordrecht., Springer, pp. 189-201.

Clarkson, C., Shipton, C., and Weisler, M. (2015) "Front, back and sides: experimental replication and archaeological analysis of H awaiian adzes and associated debitage", *Archaeology in Oceania*, vol. 50, no. 2, pp. 71-84.

Claud, E. (2015) "The use of biface manufacturing flakes: Functional analysis of three Middle Palaeolithic assemblages from southwestern and northern France", *Quaternary International*, vol. 361, pp. 131-141.

Clutton-Brock, T. H., Guinness, F. E. and Albon, S. D. (1982) *Red deer: behavior and ecology of two sexes*, Chicago, University of Chicago press.

Coffey, B. P. (1994) "The chemical alteration of microwear polishes: an evaluation of the Plisson and Mauger findings through replicative experimentation", *Lithic Technology*, vol. 19, no. 2, pp. 88-92.

Coles, J. (1973) *Archaeology by experiment*, London, Hutchinson.

Comble, J. (1967) *Le Paléolithique de l'Ardèche dans son cadre paléoclimatique*, Bordeaux, Imprimeries Delmas.

-
- Conard, N. J. and Prindiville, T. J. (2000) "Middle Palaeolithic hunting economies in the Rhineland", *International Journal of Osteoarchaeology*, vol. 10, no. 5, pp. 286-309.
- Conard, N. J., Serangeli, J., Böhner, U., Starkovich, B. M., Miller, C.E., Urban, B., and Van Kolfshoten, T. (2015) "Excavations at Schöningen and paradigm shifts in human evolution", *Journal of human evolution*, vol. 89, pp. 1-17.
- Conard, N.J. and Prindiville, T.J. (2000) "Middle Palaeolithic hunting economies in the Rhineland", *International Journal of Osteoarchaeology*, vol. 10, no. 5, pp. 286-309.
- Connolly, P., Sim, D., and Watson, C. (2001) "An evaluation of the effectiveness of three methods of spear grip used in antiquity", *Journal of Battlefield Technology*, vol. 4, pp. 49-54.
- Conte, I. C., Fernández, T. L., Astruc, L., and Rodríguez, A. R. (2015) "Use-wear analysis of nonflint lithic raw materials: the cases of quartz/quartzite and obsidian", in Marreiros, J., Gibaja, J. F., and Bicho, N. (eds) *Use-wear and residue analysis in archaeology*, Springer, pp. 59-81.
- Coolidge, F. L. and Wynn, T. (2005) "Working memory, its executive functions, and the emergence of modern thinking", *Cambridge Archaeological Journal*, vol. 15, no. 1, pp. 5-26.
- Coppe, J. and Rots, V. (2017) "Focus on the target. The importance of a transparent fracture terminology for understanding projectile points and projecting modes", *Journal of Archaeological Science: Reports*, vol. 12, pp. 109-123.
- Coppe, J., Lepers, C., Clarenne, V., Delaunois, E., Pirlot, M. and Rots, V. (2019) "Ballistic Study Tackles Kinetic Energy Values of Palaeolithic Weaponry", *Archaeometry*, pp. 1-24. [Online]. Available at <https://onlinelibrary.wiley.com/doi/epdf/10.1111/arc.12452>
- Cortés-Sánchez, M., Morales-Muñiz, A., Simón-Vallejo, M.D., Lozano-Francisco, M.C., Vera-Peláez, J.L., Finlayson, C., Rodríguez-Vidal, J., Delgado-Huertas, A., Jiménez-Espejo, F.J., Martínez-Ruiz, F., and Martínez-Aguirre, M.A. (2011) "Earliest known use of marine resources by Neanderthals", *PLoS one*, vol. 6, no. 9, pp. e24026.
- Costamagno, S., Liliane, M., Cédric, B., Bernard, V., and Bruno, M. (2006) "Les Pradelles (Marillac-le-Franc, France): A mousterian reindeer hunting camp?", *Journal of Anthropological Archaeology*, vol. 25, no. 4, pp. 466-484.
- Cotterell, B. and Kamminga, J. (1977) *The mechanics of flaking*, Sydney, Department of Mechanical Engineering, University of Sydney.
- Cotterell, B. and Kamminga, J. (1986) "Finials on stone flakes", *Journal of Archaeological Science*, vol. 13, no. 5, pp. 451-461.

Cotterell, B. and Kamminga, J. (1987) "The formation of flakes", *American Antiquity*, vol. 52, no. 4, pp. 675-708.

Cotterell, B. and Kamminga, J. (1990) *Mechanics of pre-industrial technology: an introduction to the mechanics of ancient and traditional materials culture*, Cambridge, Cambridge University Press.

Cotterell, B., Kamminga, J., and Dickson, F. P. (1985) "The essential mechanics of conchoidal flaking", *International Journal of Fracture*, vol. 29, no. 4, pp. 205-221.

Coudenneau, A. (2013) *Éléments triangulaires et armes de chasse au Paléolithique moyen: Constats et réflexions à travers l'étude techno-morpho-fonctionnelle de quatre séries d'Europe occidentale*, PhD thesis, Mareille, Université de Aix-Marseille.

Crabtree, D. E. (1972) *An introduction to flintworking. Part 1. An introduction to the technology of stone tools*, Pocatello, Idaho State University Museum.

Crevaschi, M., De Lucchese, A., Negrino, F., Ottomano, C., and Wilkens, B. (1993) "Ventimiglia (Imperia). Località Balzi Rossi. Nuovi dati sulla successione stratigrafica del ciclo interglaciale-glaciale-postglaciale. Scavi 1990", *Bollettino di Archeologia*, vol. 8, pp. 47-50.

Crezzini, J. and Boschin, F. (2016) "3D digital microscopy and taphonomy: two examples from Palaeolithic sites (Grotta dei Santi–Grosseto and Grotta Paglicci-Foggia)", *Atti del 7° Convegno Nazionale di Archeologia*. Ferrara, 22-23 November. Ferrara, *Annali dell'Università degli Studi di Ferrara Museologia Scientifica e Naturalistica*, vol. 12, pp. 3-10.

Croft, S., Chatzipanagis, K., Kröger, R., and Milner, N. (2018) "Misleading residues on lithics from Star Carr: Identification with Raman microspectroscopy", *Journal of Archaeological Science: Reports*, vol. 19, pp. 430-438.

Crombé, P., Perdaen, Y., Sergeant, J., and Caspar, J.P. (2001) "Wear analysis on early Mesolithic microliths from the Verrebroek site, East Flanders, Belgium", *Journal of Field Archaeology*, vol. 28, no. 3-4, pp. 253-269.

Daujeard, C. (2008) *Exploitation du milieu animal par les Néanderthaliens dans le Sud-Est de la France*, PhD thesis, Lyon, Université de Lyon 2.

Daujeard, C. and Moncel, M.H. (2010) "On Neanderthal subsistence strategies and land use: a regional focus on the Rhone Valley area in southeastern France", *Journal of Anthropological Archaeology*, vol. 29, no. 3, pp. 368-391.

Daujeard, C., Fernandes, P., Guadelli, J. L., Moncel, M. H., Santagata, C., and Raynal, J. P. (2012) "Neanderthal subsistence strategies in Southeastern France between the plains of the Rhone Valley

and the mid-mountains of the Massif Central (MIS 7 to MIS 3)", *Quaternary International*, vol. 252, pp. 32-47.

Daujeard, C., Moncel, M. H., Fiore, I., Tagliacozzo, A., Bindon, P., and Raynal, J. P. (2014) "Middle Paleolithic bone retouchers in Southeastern France: Variability and functionality", *Quaternary International*, vol. 326, pp. 492-518.

Daujeard, C., Vettese, D., Britton, K., Béarez, P., Boulbes, N., Crégut-Bonnoure, E., Desclaux, E., Lateur, N., Pike-Tay, A., Rivals, F., and Allué, E. (2017) "Neanderthal selective hunting of reindeer? The case study of Abri du Maras (south-eastern France)", *Archaeological and Anthropological Sciences*, pp. 1-27.

De la Peña, P., Taipale, N., Wadley, L., and Rots, V. (2018) "A techno-functional perspective on quartz micro-notches in Sibudu's Howiesons Poort indicates the use of barbs in hunting technology", *Journal of Archaeological Science*, vol. 93, pp. 166-195.

De Lumley, H. (1969) *Le Paléolithique inférieur et moyen du Midi méditerranéen dans son cadre géologique*, Paris, CNRS.

Del Bene, T. A. (1979) "Once upon a striation: current models of striation and polish formation", in Hayden, B (eds) *Lithic use-wear analysis*, New York, Academic press, pp.167-177.

Del Lucchese, A., Formicola, V., Holt, B., Negrino, F., and Vicino, G. (2004) "Riparo Bombrini, Balzi Rossi (Ventimiglia, Imperia). Notizie preliminari degli scavi 2002-2004", *Ligures*, vol. 2, pp. 287-289.

Del Lucchese, A., Giacobini, G., Vicino, G. (1985) *L'uomo di Neandertal in Liguria*, Genova, Quaderni della Soprintendenza archeologica della Liguria, vol. 2, p. 111.

d'Errico, F. (2003) "The invisible frontier. A multiple species model for the origin of behavioral modernity", *Evolutionary Anthropology: Issues, News, and Reviews*, vol. 12, no. 4, pp. 188-202.

d'Errico, F. and Stringer, C. B. (2011) "Evolution, revolution or saltation scenario for the emergence of modern cultures?", *Philosophical Transactions of the Royal Society of London B: Biological Sciences*, vol. 366, no. 1567, pp. 1060-1069.

d'Errico, F., Henshilwood, C., Lawson, G., Vanhaeren, M., Tillier, A. M., Soressi, M., Bresson, F., Maureille, B., Nowell, A., Lakarra, J., and Backwell, L. (2003) "Archaeological evidence for the emergence of language, symbolism, and music—an alternative multidisciplinary perspective", *Journal of World Prehistory*, vol. 17, no. 1, pp. 1-70.

d'Errico, F., Henshilwood, C., Vanhaeren, M., and Van Niekerk, K. (2005) "Nassarius kraussianus shell beads from Blombos Cave: evidence for symbolic behaviour in the Middle Stone Age", *Journal of Human Evolution*, vol. 48, no. 1, pp. 3-24.

d'Errico, F., Zilhão, J., Julien, M., Baffier, D., and Pelegrin, J. (1998) "Neanderthal acculturation in Western Europe? A critical review of the evidence and its interpretation", *Current Anthropology*, vol. 39, no. S1, pp. S1-S44.

Dibble, H. L. (1984) "Interpreting typological variation of Middle Paleolithic scrapers: function, style, or sequence of reduction?", *Journal of Field Archaeology*, vol. 11, pp. 431–436.

Dibble, H. L. (1987) "The interpretation of Middle Paleolithic scraper morphology", *American Antiquity*, vol. 52, no. 1, pp. 109-117.

Dibble, H. L. (1995) "Middle Paleolithic scraper reduction: background, clarification, and review of evidence to data", *Journal of Archaeological Method and Theory*, vol. 2, no. 4, pp. 299–368.

Dibble, H. L. and Bar-Yosef, O. (1995) *The definition and interpretation of Levallois technology*, Madison, Prehistory Press, vol. 23.

Discamps, E. and Faivre, J. P. (2017) "Substantial biases affecting Combe-Grenal faunal record cast doubts on previous models of Neanderthal subsistence and environmental context", *Journal of Archaeological Science*, vol. 81, pp. 128-132.

Dockall, J. E. (1997) "Wear traces and projectile impact: a review of the experimental and archaeological evidence", *Journal of Field Archaeology*, vol. 24, no. 3, pp. 321-331.

Domínguez-Rodrigo, M. (1999) "Flesh availability and bone modifications in carcasses consumed by lions: palaeoecological relevance in hominid foraging patterns", *Palaeogeography Palaeoclimatology Palaeoecology*, vol. 149, pp. 373-388.

Domínguez-Rodrigo, M. (2002) "Hunting and scavenging by early humans: the state of the debate", *Journal of World Prehistory*, vol. 16, no. 1, pp. 1-54.

Domínguez-Rodrigo, M. and Barba, R. (2007) "Five more arguments to invalidate the passive scavenging version of the carnivore-hominid-carnivore model: a reply to Blumenshine et al. (2007a)", *Journal of Human Evolution*, vol. 53, no. 4, pp. 427-433.

Domínguez-Rodrigo, M., Bunn, H.T., Mabulla, A.Z., Baquedano, E., Uribelarrea, D., Pérez-González, A., Gidna, A., Yravedra, J., Díez-Martín, F., Egeland, C. P., and Barba, R. (2014) "On meat eating and human evolution: a taphonomic analysis of BK4b (Upper Bed II, Olduvai Gorge, Tanzania), and its bearing on hominin megafaunal consumption", *Quaternary International*, vol. 322, pp.129-152.

Douka, K., Grimaldi, S., Boschian, G., del Lucchese, A., and Higham, T. F. (2012) "A new chronostratigraphic framework for the Upper Palaeolithic of Riparo Mochi (Italy)", *Journal of Human Evolution*, vol. 62, no. 2, pp. 286-299.

-
- Douze, K. and Delagnes, A. (2016) "The pattern of emergence of a Middle Stone Age tradition at Gademotta and Kulkuletti (Ethiopia) through convergent tool and point technologies", *Journal of Human Evolution*, vol. 91, pp. 93-121.
- Dumont, J. (1982) "The quantification of microwear traces: a new use for interferometry", *World Archaeology*, vol. 14, no. 2, pp. 206-217.
- Ellis, C. J., 1997. Factors influencing the use of stone projectile tips. In Knecht, H. (eds) *Projectile technology*, US, Springer, pp. 37-74.
- Endicott, P., Ho, S. Y., and Stringer, C. (2010) "Using genetic evidence to evaluate four palaeoanthropological hypotheses for the timing of Neanderthal and modern human origins", *Journal of Human Evolution*, vol. 59, no. 1, pp. 87-95.
- Eren, M. I., Lycett, S. J., Patten, R. J., Buchanan, B., Pargeter, J., and O'Brien, M. J. (2016) "Test, model, and method validation: the role of experimental stone artifact replication in hypothesis-driven archaeology", *Ethnoarchaeology*, vol. 8, no. 2, pp. 103-136.
- Erlandson, J. M., Rick, T. C., Braje, T. J., Casperson, M., Culleton, B., Fulfrost, B., Garcia, T., Guthrie, D. A., Jew, N., Kennett, D. J., and Moss, M. L. (2011) "Paleoindian seafaring, maritime technologies, and coastal foraging on California's Channel Islands", *Science*, vol. 331, no. 6021, pp.1181-1185.
- Evans, A. A. (2014) "On the importance of blind testing in archaeological science: the example from lithic functional studies", *Journal of Archaeological Science*, vol. 48, pp. 5-14.
- Evans, A. A. and Donahue, R. E. (2008) "Laser scanning confocal microscopy: a potential technique for the study of lithic microwear", *Journal of Archaeological Science*, vol. 35, no. 8, pp. 2223-2230.
- Evans, A. A. and Macdonald, D. (2011) "Using metrology in early prehistoric stone tool research: further work and a brief instrument comparison", *Scanning*, vol. 33, no. 5, pp. 294-303.
- Faivre, J. P., Maureille, B., Bayle, P., Crevecoeur, I., Duval, M., Grün, R., Bemilli, C., Bonilauri, S., Coutard, S., Bessou, M. and Limondin-Lozouet, N. (2014) "Middle Pleistocene human remains from Tourville-la-Rivière (Normandy, France) and their archaeological context", *PloS one*, vol. 9, no. 10, pp. e104111.
- Farizy, C., David, F., Jaubert, J., and Eisenmann, V. (1994) *Hommes et bisons du Paléolithique moyen à Mauran (Haute-Garonne)*, Paris, CNRS.
- Fernandes, P. (2012) *Itinéraires et transformations du silex: une pétroarchéologie refondée, application au Paléolithique moyen*, PhD thesis, Bordeaux, Université de Bordeaux 1.

-
- Fernandes, P., Raynal, J. P., and Moncel, M. H. (2008) "Middle Palaeolithic raw material gathering territories and human mobility in the southern Massif Central, France: first results from a petro-archaeological study on flint", *Journal of Archaeological Science*, vol. 35, no. 8, pp. 2357-2370.
- Finlayson, C., Brown, K., Blasco, R., Rosell, J., Negro, J. J., Bortolotti, G. R., Finlayson, G., Marco, A. S., Pacheco, F. G., Vidal, J. R., and Carrión, J. S. (2012) "Birds of a feather: Neanderthal exploitation of raptors and corvids", *PloS one*, vol. 7, no. 9, p. e45927.
- Finlayson, C., Pacheco, F. G., Rodríguez-Vidal, J., Fa, D. A., López, J. M. G., Pérez, A. S., Finlayson, G., Allue, E., Preysler, J. B., Cáceres, I., and Carrión, J. S. (2006) "Late survival of Neanderthals at the southernmost extreme of Europe", *Nature*, vol. 443, no. 7113, pp. 850-853.
- Fiore, I., Gala, M., and Tagliacozzo, A. (2004) "Ecology and subsistence strategies in the Eastern Italian Alps during the Middle Palaeolithic", *International Journal of Osteoarchaeology*, vol. 14, no. 3-4, pp. 273-286.
- Fischer, A., Hansen, P.V., and Rasmussen, P. (1984) "Macro and micro wear traces on lithic projectile points: experimental results and prehistoric examples", *Journal of Danish Archaeology*, vol. 3, no. 1, pp. 19-46.
- Flenniken, J. J. and Raymond, A. W. (1986) "Morphological projectile point typology: replication experimentation and technological analysis", *American Antiquity*, vol. 51, no. 3, pp. 603-614.
- Flenniken, J. J. and Wilke, P. J. (1989) "Typology, technology, and chronology of Great Basin dart points", *American Anthropologist*, vol. 91, no. 1, pp. 149-158.
- Foley, R. and Lahr, M. M. (1997) "Mode 3 technologies and the evolution of modern humans", *Cambridge Archaeological Journal*, vol. 7, no. 1, pp. 3-36.
- Franklin, A. D. (1981) "What makes a 'good' experiment?", *The British Journal for the Philosophy of Science*, vol. 32, no. 4, pp. 367-374.
- Frison, G. C. (1974) *Casper Site: a Hell Gap Bison Kill On the High Plains*, New York, Academic Press.
- Frison, G. C. (1989) "Experimental use of Clovis weaponry and tools on African elephants", *American Antiquity*, vol. 54, no. 4, pp. 766-784.
- Frison, G. C. (2004) *Survival by hunting: prehistoric human predators and animal prey*, Berkeley, University of California Press.
- Fullagar, R. (1991) "The role of silica in polish formation", *Journal of Archaeological Science*, vol. 18, no. 1, pp. 1-24.

Fullagar, R. (2006) "Residues and use-wear", in Balme, J. and Paterson, A. (eds) *Archaeology in practice: a student guide to archaeological analyses*, Hong Kong, Blackwell Publishing, pp. 207-234.

Fullagar, R. (2016) "Uncertain evidence for weapons and craft tools: Functional investigations of Australian microliths", in Iovita, R. and Sano, K. (eds) *Multidisciplinary approaches to the study of Stone Age weaponry*, Dordrecht, Springer, pp. 159-166.

Fullagar, R., Furby, J., and Hardy, B. (1996) "Residues on stone artefacts: state of a scientific art", *Antiquity*, vol. 70, no. 270, pp. 740-745.

Fullagar, R., McDonald, J., Field, J., and Donlon, D. (2009) "Deadly weapons: backed microliths from Narrabeen, New South Wales", in Haslam, M., Robertson, G., Crowther, A., Nugent, S., and Kirkwood, L. (eds) *Archaeological science under a microscope: Studies in residue and ancient DNA analysis in honour of Thomas H. Loy*, Canberra, ANU E Press, pp. 258-270.

Gamble, C. (1987) "Man the shoveler: alternative models for middle Pleistocene colonization and occupation in northern latitudes", in Soffer, O. (eds) *The Pleistocene Old World. Regional Perspectives*, New York, Springer, pp. 81-98.

Gaspari, A., Erič, M., and Odar, B. (2011) "A Palaeolithic wooden point from Ljubljansko barje, Slovenia", *Submerged Prehistory*, pp.186-192.

Gassin, B. (1996) *Évolution socio-économique dans le Chasséen de la grotte de l'Église supérieure (Var.) Apport de l'analyse fonctionnelle des industries lithiques*, Paris, CNRS.

Gaudzinski, S. (1996) "On bovid assemblages and their consequences for the knowledge of subsistence patterns in the Middle Palaeolithic", *Proceedings of the prehistoric society*, vol. 62, pp. 19-39.

Gaudzinski, S. (1999) "The faunal record of the Lower and Middle Palaeolithic of Europe: remarks on human interference", in Roebroeks, W. and Gamble, C (eds) *The Middle Palaeolithic Occupation of Europe*, Leiden, Leiden University press, pp. 215–233.

Gaudzinski, S. (2006) "Monospecific or species-dominated faunal assemblages during the Middle Paleolithic in Europe", in Hovers, E. and Kuhn, S. (eds) *Transitions before the transition*, Boston, Springer, pp. 137-147.

Gaudzinski, S. and Roebroeks, W. (2000) "Adults only. Reindeer hunting at the middle palaeolithic site Salzgitter Lebenstedt, northern Germany", *Journal of Human Evolution*, vol. 38, no. 4, pp. 497-521.

Gaudzinski-Windheuser, S. and Kindler, L. (2012) "Research perspectives for the study of Neandertal subsistence strategies based on the analysis of archaeozoological assemblages", *Quaternary International*, vol 247, pp. 59-68.

Gaudzinski-Windheuser, S., Jöris, O., Sensburg, M., Street, M., and Turner, E. (2006) "Come in... and find out. Opening a New Door into the Analysis of Hunter-Gatherer Social Organisation and Behaviour", paper presented at *15th IUPPS Conference*, 4-9 September 2006, Lisbon.

Gaudzinski-Windheuser, S., Noack, E.S., Pop, E., Herbst, C., Pfleging, J., Buchli, J., Jacob, A., Enzmann, F., Kindler, L., Iovita, R., and Street, M. (2018) "Evidence for close-range hunting by last interglacial Neanderthals", *Nature*, vol. 2, no. 7, p. 1087.

Geneste, J. M. and Plisson, H. (1989) "Analyse technologique des pointes à cran solutréennes du Placard (Charente), du Fourneau du Diable, du Pech de la Boissière et de Combe-Saunière (Dordogne)", *Paléo*, vol. 1, no. 1, pp. 65-106.

Geneste, J. M. and Plisson, H. (1990) "Technologie fonctionnelle des pointes à cran solutréennes: l'apport des nouvelles données de la grotte de Combe Saunière (Dordogne)", in Kozłowski, J. K. (eds) *Feuilles de pierre: les industries à pointes foliacées du Paléolithique supérieur européen*, Liège, Université de Liège, vol. 42, pp. 293-320.

Geneste, J. M. and Plisson, H. (1993) "Hunting technologies and human behavior: Lithic analysis of Solutrean shouldered points", in White, R., Knecht, H., and Pike-Tay, A. (eds) *Before Lascaux: The Complex Record of the Early Upper Paleolithic*, Boca Raton, CRC Press, pp. 117-135.

Geyh, M. A. and Müller, H. (2005) "Numerical ²³⁰Th/U dating and a palynological review of the Holsteinian/Hoxnian Interglacial", *Quaternary Science Reviews*, vol. 24, no. 16-17, pp. 1861-1872.

Gibson, N. E., Wadley, L., and Williamson, B. S. (2004) "Microscopic residues as evidence of hafting on backed tools from the 60 000 to 68 000-year-old Howiesons Poort layers of Rose Cottage Cave, South Africa", *Southern African Humanities*, vol. 16, no. 1, pp. 1-11.

Giuggiola, O. (1974) "Lo scavo a « Le Mànie » (Finale Ligure)", *Atti XVI^o Riunione Scientifica dell'Istituto Italiano di Preistoria e Protostoria*, Liguria, 1973, Istituto Italiano di Preistoria e Protostoria, p. 91.

Giuggiola, O. and Vicino, G. (1996) "Arma delle Manie (Finale Ligure, Savona)", *Atti XIII^o Congresso internazionale delle Scienze Preistoriche e Protostoriche*, Forlì, 8-14 settembre 1996, Forlì, Abaco, vol. 6, pp. 191-197.

Gómez-Olivencia, A., Sala, N., Núñez-Lahuerta, C., Sanchis, A., Arlegi, M., and Rios-Garaizar, J. (2018) "First data of Neandertal bird and carnivore exploitation in the Cantabrian Region (Axlor);

Barandiaran excavations; Dima, Biscay, Northern Iberian Peninsula)", *Scientific reports*, vol. 8, no. 1, pp.10551.

González-Urquijo, J. E. and Ibáñez-Estévez, J. J. (1994) "Metodología de análisis funcional de instrumentos tallados en sílex. 14. Universidad de Deusto", *Cuadernos de Arqueología*, pp. 301.

González-Urquijo, J. E. and Ibáñez-Estévez, J. J. (2003) "The quantification of use-wear polish using image analysis. First results", *Journal of Archaeological Science*, vol. 30, no. 4, pp. 481-489.

Goodall, J. (1964) "Tool-using and aimed throwing in a community of free-living chimpanzees", *Nature*, vol. 201, no. 4926, pp. 1264.

Goodall, J. (1986) *The chimpanzees of Gombe: Patterns of behaviour*, Cambridge, The Belknap Press of Harvard University Press.

Goval, E., Hérisson, D., Loch, J. L., and Coudenneau, A. (2015) "Levallois points and triangular flakes during the Middle Palaeolithic in northwestern Europe: Considerations on the status of these pieces in the Neanderthal hunting toolkit in northern France", *Quaternary International*, vol. 411, pp. 216-232.

Gowlett, J. A. (1984) "Mental abilities of early man: a look at some hard evidence", *Higher Education Quarterly*, vol. 38, no. 3, pp.199-220.

Grace, R. (1990) "The limitations and applications of use wear analysis", in Gräslund, B., Knutsson, H., Knutsson, K., and Taffinder, J. (eds.) *The Interpretive Possibilities of Microwear Studies: proceedings of the International Conference on Lithic Use-Wear Analysis*, Uppsala, Societas Archaeologica Upsaliensis, pp. 9-14.

Grace, R., Graham, I.D.G., and Newcomer, M.H. (1985) "The quantification of microwear polishes", *World Archaeology*, vol. 17, no. 1, pp. 112-120.

Gräslund, B., Knutsson, H., Knutsson, K., and Taffinder, J. (1990) *The Interpretive Possibilities of Microwear Studies: proceedings of the International Conference on Lithic Use-Wear Analysis*, Uppsala, Societas Archaeologica Upsaliensis.

Grayson, D. K. and Delpech, F. (2002) "Specialized early Upper Palaeolithic hunters in southwestern France?", *Journal of Archaeological Science*, vol. 29, no. 12, pp. 1439-1449.

Gregor, R. J. and Pink, M. (1985) "Biomechanical analysis of a world record javelin throw: A case study", *International Journal of Sport Biomechanics*, vol. 1, no. 1, pp. 73-77.

Greiser, S. T. and Sheets, P. D. (1979) "Raw material as a functional variable in use-wear studies", in Hayden, B. (eds) *Lithic use-wear analysis*, New York, Academic press, pp. 289-296.

Gripp, K. R., Schütrumpf, Kollau, W., Krause, W., and Rust, A. (1943) *Die alt-und mittelsteinzeitlichen Funde von Stellmoor*, Neumünster in Holstein, K. Wachholtz.

Groom, P., Schenck, T. and Pedersen, G. M. (2015) "Experimental explorations into the aceramic dry distillation of *Betula pubescens* (downy birch) bark tar", *Archaeological and Anthropological Sciences*, vol. 7, no. 1, pp. 47-58.

Grünberg, J. M. (2002) "Middle Palaeolithic birch-bark pitch", *Antiquity*, vol. 76, no. 291, pp. 15-16.

Haidle, M. N. (2009) "How to think a simple spear", in de Beaune, S. A., Coolidge, L. F., and Wynn, T. (eds) *Cognitive archaeology and human evolution*, New York, Cambridge University Press, pp. 57-73.

Haidle, M. N. (2010) "Working-memory capacity and the evolution of modern cognitive potential: implications from animal and early human tool use", *Current Anthropology*, vol. 51, no. S1, pp. S149-S166.

Haidle, M. N. (2012) *How to Think Tools? A Comparison of Cognitive Aspects in Tool Behavior of Animals and During Human Evolution*, PhD thesis, Tübingen, Universitäts Tübingen.

Hamon, C. and Plisson, H. (2008) "Functional analysis of grinding stones: the blind-test contribution", *Prehistoric technology*, vol. 40, pp. 29-38.

Hardy, B. L. and Garufi, G. T. (1998) "Identification of woodworking on stone tools through residue and use-wear analyses: experimental results", *Journal of Archaeological Science*, vol. 25, no. 2, pp. 177-184.

Hardy, B. L. and Moncel, M. H. (2011) "Neanderthal use of fish, mammals, birds, starchy plants and wood 125-250,000 years ago", *PloS one*, vol. 6, no. 8, pp. e23768.

Hardy, B. L., Kay, M., Marks, A. E., and Monigal, K. (2001) "Stone tool function at the paleolithic sites of Starosele and Buran Kaya III, Crimea: behavioral implications", *Proceedings of the National Academy of Sciences*, vol. 98, no. 19, pp. 10972-10977.

Hardy, B. L., Moncel, M. H., Daujeard, C., Fernandes, P., Béarez, P., Desclaux, E., Navarro, M.G.C., Puaud, S., and Gallotti, R. (2013) "Impossible Neanderthals? Making string, throwing projectiles and catching small game during Marine Isotope Stage 4 (Abri du Maras, France)", *Quaternary Science Reviews*, vol. 82, pp. 23-40.

Hardy, K., Buckley, S., Collins, M. J., Estalrich, A., Brothwell, D., Copeland, L., García-Tabernero, A., García-Vargas, S., de la Rasilla, M., Lalueza-Fox, C., and Huguet, R. (2012) "Neanderthal medics? Evidence for food, cooking, and medicinal plants entrapped in dental calculus", *Naturwissenschaften*, vol. 99, no. 8, pp. 617-626.

Hayden, B. (1979) *Lithic use-wear analysis*, New York, Academic press.

Hays, M. and Surmely, F. (2005) "Réflexions sur la fonction des microgravettes et la question de l'utilisation de l'arc au Gravettien ancien", *Paléo, Revue d'archéologie préhistorique*, vol. 17, pp. 145-156.

Heizer, R. F. and Hester, T. R. (1978) *Great Basin projectile points: forms and chronology*, Socorro, Ballena Press, vol. 10.

Henry, A. G., Brooks, A. S., and Piperno, D. R. (2011) "Microfossils in calculus demonstrate consumption of plants and cooked foods in Neanderthal diets (Shanidar III, Iraq; Spy I and II, Belgium)" *Proceedings of the National Academy of Sciences*, vol. 108, no. 2, pp. 486-491.

Henshilwood, C. S., D'errico, F., Marean, C. W., Milo, R. G., Yates, R. (2001) "An early bone tool industry from the Middle Stone Age at Blombos Cave, South Africa: implications for the origins of modern human behaviour, symbolism and language", *Journal of Human Evolution*, vol. 41, no. 6, pp. 631-678.

Henshilwood, C. S., Marean, C. W., Chase, P., Davidson, I., Gamble, C., Holliday, T. W., Klein, R. G., Mc Brearty, S., Zilhão, J., Henshilwood, C. S., and Marean, C. W. (2003) "The origin of modern human behavior: critique of the models and their test implications" *Current Anthropology*, vol. 44, no. 5, pp. 627-651.

Higham, T., Brock, F., Peresani, M., Broglio, A., Wood, R., and Douka, K. (2009) "Problems with radiocarbon dating the Middle to Upper Palaeolithic transition in Italy", *Quaternary Science Reviews*, vol. 28, no. 13-14, pp. 1257-1267.

Higham, T., Douka, K., Wood, R., Ramsey, C.B., Brock, F., Basell, L., Camps, M., Arrizabalaga, A., Baena, J., Barroso-Ruíz, C., and Bergman, C. (2014) "The timing and spatiotemporal patterning of Neanderthal disappearance", *Nature*, vol. 512, no. 7514, pp. 306-309.

Hitchcock, R. and Bleed, P. (1997) "Each according to need and fashion", in Knecht, H. (eds) *Projectile technology*, US, Springer, pp. 345-368.

Ho Ho Committee (1979) "The Ho Ho classification and nomenclature committee report", in Hayden, B. (eds) *Lithic Use-Wear Analysis*, New York, Academic Press, pp.134-158.

Hoffecker, J. F. and Cleghorn, N. (2000) "Mousterian hunting patterns in the northwestern Caucasus and the ecology of the Neanderthals", *International Journal of Osteoarchaeology*, vol. 10, no. 5, pp. 368-378.

Hoffmann, D. L., Angelucci, D. E., Villaverde, V., Zapata, J., and Zilhão, J. (2018a) "Symbolic use of marine shells and mineral pigments by Iberian Neandertals 115,000 years ago", *Science Advances*, vol. 4, no. 2, pp. eaar5255.

Hoffmann, D. L., Standish, C. D., García-Diez, M., Pettitt, P. B., MLITon, J. A., Zilhão, J., Alcolea-González, J.J., Cantalejo-Duarte, P., Collado, H., De Balbín, R., and Lorblanchet, M. (2018b) "U-Th dating of carbonate crusts reveals Neandertal origin of Iberian cave art", *Science*, vol. 359, no. 6378, pp. 912-915.

Hoffmann, D. L., Standish, C. D., Pike, A. W., García-Diez, M., Pettitt, P. B., Angelucci, D. E., Villaverde, V., Zapata, J., Milton, J. A., Alcolea-González, J., Cand antalejo-Duarte, P. (2018) "Dates for Neanderthal art and symbolic behaviour are reliable", *Nature Ecology & Evolution*, vol. 2, no. 7, pp.1044.

Holdaway, S. (1989) "Were there hafted projectile points in the Mousterian?", *Journal of Field Archaeology*, vol. 16, no. 1, pp. 79-85.

Holt, B., Negrino, F., Riel-Salvatore, J., Formicola, V., Arellano, A., Arobba, D., and Boschian G., (2018 in press) "The Middle-Upper Paleolithic transition in Northwest Italy: new evidence from Riparo Bombrini (Balzi Rossi, Liguria, Italy)", *Quaternary International*.

Hopkins, W. D., Bard, K. A., Jones, A., and Bales, S. L. (1993) "Chimpanzee hand preference in throwing and infant cradling: Implications for the origin of human handedness", *Current Anthropology*, vol. 34, no. 5, pp. 786-790.

Hopkins, W. D., Russell, J. L., and Schaeffer, J. A. (2012) "The neural and cognitive correlates of aimed throwing in chimpanzees: a magnetic resonance image and behavioural study on a unique form of social tool use", *Philosophical Transactions of the Royal Society of London B: Biological Sciences*, vol. 367, no. 1585, pp. 37-47.

Horsfall, I., Prosser, P. D., Watson, C. H., and Champion, S.M. (1999) "An assessment of human performance in stabbing", *Forensic Science International*, vol. 102, pp. 79–89.

Howard, C. D. (2002) "The gloss patination of flint artifacts", *The Plains Anthropologist*, vol. 47, no. 182, pp. 283-287.

Hughes, S. S. (1998) "Getting to the point: evolutionary change in prehistoric weaponry", *Journal of Archaeological Method and Theory*, vol. 5, no. 4, pp. 345-408.

Hurcombe, L. (1988) "Some criticisms and suggestions in response to Newcomer et al. (1986)", *Journal of Archaeological Science*, vol. 15, no. 1, pp. 1-10.

Hurcombe, L. (1992) *Use wear analysis and obsidian: theory, experiments and results*, Sheffield, Sheffield Academic Press.

Hutchings, W. K. (1991) *The nachcharini composite projectile: Design theory and the study of hunting systems technology at Mugharat en-Nachcharini in the Post-Natufian Levant (Lebanon)*, MA Thesis, Toronto, University of Toronto.

Hutchings, W. K. (1999) "Quantification of fracture propagation velocity employing a sample of Clovis channel flakes", *Journal of Archaeological Science*, vol. 26, no. 12, pp. 1437-1447.

Hutchings, W. K. (2011) "Measuring use-related fracture velocity in lithic armatures to identify spears, javelins, darts, and arrows", *Journal of Archaeological Science*, vol. 38, no 7, pp. 1737-1746.

Hutchings, W. K. (2015) "Finding the Paleoindian spearthrower: quantitative evidence for mechanically-assisted propulsion of lithic armatures during the North American Paleoindian Period", *Journal of Archaeological Science*, vol. 55, pp. 34-41.

Hutchings, W. K. (2016) "When is a point a projectile? Morphology, impact fractures, scientific rigor, and the limits of inference", in Iovita, R. and Sano, K. (eds) *Multidisciplinary approaches to the study of Stone Age weaponry*, Dordrecht, Springer, pp. 3-12.

Hutchings, W. K. and Brüchert, L. W. (1997) "Spearthrower performance: ethnographic and experimental research", *Antiquity*, vol. 71, no. 274, pp. 890-897.

Ibáñez, J. J., González-Urquijo, J. E., and Gibaja, J. (2014) "Discriminating wild vs domestic cereal harvesting micropolish through laser confocal microscopy", *Journal of Archaeological Science*, vol. 48, pp. 96-103.

Ibáñez-Estévez, J. J. and González-Urquijo, J. E. (1996) *From tool use to site function: Use-wear analysis in some Final Upper Palaeolithic sites in the Basque country*, Oxford, BAR International Series, vol. 658.

Inizan, M. L., Reduron-Ballinger, M., and Roche, H. (1999) *Technology and terminology of knapped stone: followed by a multilingual vocabulary arabic, english, french, german, greek, italian, portuguese*, Nanterre, Cercle de Recherches et d'Etudes Préhistoriques, vol. 5.

Iovita, R. and Sano, K. (2016) *Multidisciplinary approaches to the study of Stone Age weaponry*, Dordrecht, Springer.

Iovita, R., Schönekeß, H., Gaudzinski-Windheuser, S., and Jäger, F. (2014) "Projectile impact fractures and launching mechanisms: results of a controlled ballistic experiment using replica Levallois points", *Journal of Archaeological Science*, vol. 48, pp. 73-83.

Iovita, R., Schönekeß, H., Gaudzinski-Windheuser, S., and Jäger, F. (2016) "Identifying weapon delivery systems using macrofracture analysis and fracture propagation velocity: A controlled

experiment”, in Iovita, R. and Sano, K. (eds) *Multidisciplinary approaches to the study of Stone Age weaponry*, Dordrecht, Springer, pp. 13-27.

Isaac, B. (1987) “Throwing and human evolution”, *African Archaeological Review*, vol. 5, no. 1, pp. 3-17.

Isaac, G. (1978) “The food-sharing behavior of protohuman hominids”, *Scientific American*, vol. 238, no. 4, pp. 90-109.

Isetti, G. and de Lumley, H. (1962) “Prima segnalazione di un giacimento musteriano nell'arma delle Manie (finale)”, *Rivista Ingauna e Intemelia*, vol. XVI, no. 1-4, pp. 3-8.

Isetti, G., de Lumley, H., Miskovsky, J. C. (1962) « Il giacimento musteriano della grotta della Madonna dell'Arma presso Bussana (Sanremo) », *Rivista di studi liguri*, vol. 28, pp. 5-116.

Jaubert, J. and Brugal, J. P. (1990) “Contribution à l'étude du mode de vie au Paléolithique moyen: Les chasseurs d'aurochs de La Borde”, in Jaubert, J. M., Lorblanchet, H., Laville, R., Slott-Moller, A. Turq, and Brugal, J. P. (eds) *Les chasseurs d'aurochs de La Borde: un site du Paléolithique moyen (Livernon, Lot)*, Paris, Documents d'Archéologie Française, vol. 27, pp. 128-145.

Jaubert, J., Verheyden, S., Genty, D., Soulier, M., Cheng, H., Blamart, D., Burlet, C., Camus, H., Delaby, S., Deldicque, D., and Edwards, R.L. (2016) “Early Neanderthal constructions deep in Bruniquel Cave in southwestern France”, *Nature*, vol. 534, no. 7605, pp.1-11.

Jensen, H. J. (1994) *Flint tools and plant working: hidden traces of stone age technology: a use wear study of some Danish Mesolithic and TRB implements*, Aarhus, Aarhus University Press.

Jensen, J. H. (1982) “A preliminary analysis of blade scrapers from Ringkloster, a Danish Late Mesolithic site”, *Studia Praehistorica Belgica*, vol. 2, pp.323-327.

Kamminga, J. (1979) “The Nature of Use-Polish and Abrasive Smoothing on Stone Tools”, in Hayden, B. (eds) *Lithic use-wear analysis*, New York, Academic press, pp. 143-157.

Kamminga, J. (1982) *Over the edge: functional analysis of Australian stone tools*, St. Lucia, Queensland, University of Queensland.

Karakostis, F. A., Hotz, G., Turloukis, V., and Harvati, K. (2018) “Evidence for precision grasping in Neandertal daily activities”, *Science advances*, vol. 4, no. 9, pp. eaat2369.

Karatsori, E. (2003) Environnement végétal de l'homme fossile et climats en Ligurie pendant le dernier cycle climatique et le postglaciaire: Étude palynologique des sites préhistoriques italiens de Caverna delle Fate, de Arma delle Manie (finale Ligure) et de San Francesco (San Remo), PhD thesis, Paris, Muséum national d'histoire naturelle.

-
- Keeley, L. H. (1974) "The methodology of microwear analysis: a comment on Nance", *American Antiquity*, vol. 39, no. 1, pp. 126-128.
- Keeley, L. H. (1974b) "Technique and methodology in microwear studies: a critical review", *World Archaeology*, vol. 5, no. 3, pp.323-336.
- Keeley, L. H. (1978) "Preliminary microwear analysis of the Meer assemblage", In Van Noten, F. (eds) *Les chasseurs de Meer*, Brugge, De Tempel, vol. 18, pp. 78-86.
- Keeley, L. H. (1980) *Experimental determination of stone tool uses: a microwear analysis*, Chicago, University of Chicago Press.
- Keeley, L. H. (1982) "Hafting and retooling: effects on the archaeological record", *American Antiquity*, vol. 47, no. 4, pp. 798-809.
- Keeley, L. H. and Newcomer, M. H. (1977) "Microwear analysis of experimental flint tools: a test case", *Journal of Archaeological Science*, vol. 4, no. 1, pp. 29-62.
- Keeley, L. H. and Toth, N. (1981) "Microwear polishes on early stone tools from Koobi Fora, Kenya", *Nature*, vol. 293, no. 5832, pp. 464.
- Kelm, R. (2013) "The Stine Age Park Dithmarschen (Steinzeitpark Dithmarschen) – Concept and Development of a visit oriented Educational Center for Sustainable Development", in Kelm, R. and OpenArch (eds) *Archaeology and Crafts: experiences and experiments on traditional skills and handicrafts in archaeological open-air museums in Europe*, Husum, Aoz and Husum Druck.
- Kerkhoff, F. and Müller-Beck, H. (1969) "Zur bruchmechanischen Deutung der Schlagmarken an Steingeräten", *Glastechnische Berichte*, vol. 42, pp. 439-448.
- Knecht, H. (1997) "Projectile points of bone, antler, and stone", In Knecht, H. (eds) *Projectile technology*, Boston, Springer, pp. 191-212.
- Knecht, H. (1997) "The history and development of projectile technology research", In Knecht, H. (eds) *Projectile technology*, Boston, Springer, pp. 3-35.
- Knecht, H. (1997) *Projectile technology*, US, Springer.
- Kneubuehl, B. P. (2011) *Wound ballistics: basics and applications*, Springer.
- Knudson, R. (1979) "Inference and imposition in lithic analysis", in Hayden, B. (eds) *Lithic use-wear analysis*, New York, Academic press, ppp. 269-281.
- Koch, P. L. and Barnosky, A. D. (2006) "Late Quaternary extinctions: state of the debate", *Annual Review of Ecology, Evolution, and Systematics*, vol. 7, pp .215-250.

-
- Koller, J., Baumer, U. and Mania, D. (2001) "High-tech in the Middle Palaeolithic: Neandertal-manufactured pitch identified", *European Journal of Archaeology*, vol. 4, no. 3, pp.385-397.
- Kortlandt, A. (2002) "Neanderthal anatomy and the use of spears", *Evolutionary Anthropology: Issues, News, and Reviews*, vol. 11, no. 5, pp. 183-184.
- Kozowyk, P. R. B., Poulis, J. A., and Langejans, G. H. J. (2017b) "Laboratory strength testing of pine wood and birch bark adhesives: a first study of the material properties of pitch" *Journal of Archaeological Science: Reports*, vol. 13, pp. 49-59.
- Kozowyk, P. R. B., Soressi, M., Pomstra, D., and Langejans, G. H. J. (2017a) "Experimental methods for the Palaeolithic dry distillation of birch bark: implications for the origin and development of Neandertal adhesive technology", *Scientific Reports*, vol. 7, no. 1, pp. 8033.
- Kuhn, S. L. and Stiner, M. C. (1998) "Reports the Earliest Aurignacian of Riparo Mochi (Liguria, Italy)", *Current Anthropology*, vol. 39, no. S1, pp. S175-S189.
- La Porta, A. (2013) *Points and Convergent Tools in the European Middle Palaeolithic Sites: The Regional Context of the South-East of Massif Central (France), Shelters of Maras and Baume-Vallée*, MA Thesis, Paris, Muséum national d'histoire naturelle.
- La Porta, A., Moncel, M. H., and Raynald, J. P., (2015) "Preliminary results of Middle Paleolithic points from the sites of Maras and Baume-vallee shelters (France): technological analysis and some remarks on macro-traces", in Brancato, R., Busacca, G., and Massimino, M. (eds) *Archeologi in progress: il cantiere dell'archeologia di domani*, Catania, Bradypus, pp. 90-100.
- Lammers-Keijsers, Y., Verbaas, A., Van Gijn, A., and Pomstra, D. (2015) "Arrowheads without traces: not used, perfect hit or excessive hafting materials?", in Marreiros, J., Bicho, N., and Gibaja, J. F. (eds) *International Conference on Use-Wear Analysis: Use-Wear 2012*, Newcastle upon Tyne, Cambridge Scholars Publishing, pp. 45-55.
- Langejans, G. H. (2010) "Remains of the day-preservation of organic micro-residues on stone tools", *Journal of Archaeological Science*, vol. 37, no. 5, pp. 971-985.
- Larsson, L. and Sjöström, A. (2011) "Bog sites and wetland settlement during the mesolithic: research from a bog in central Scania, southern Sweden", *Archäologisches korrespondenzblatt*, vol. 41, no. 4, pp. 456-472.
- Larsson, L. and Sjöström, A. (2011) "Early Mesolithic flint-tipped arrows from Sweden", *Antiquity*, vol. 85, no. 330.

Lazuén, T. (2012) "European Neanderthal stone hunting weapons reveal complex behaviour long before the appearance of modern humans", *Journal of Archaeological Science*, vol. 39, no. 7, pp. 2304-2311.

Lazuén, T. (2014) "Please do not shoot the pianist. Criteria for recognizing ancient lithic weapon use", *Journal of Archaeological Science*, vol. 46, pp. 1-5.

Leger, E. (2012) *Interpretazione tecnologica ed economica dell'industria litica di Arma delle Manie (strati V, IV, III, II). I livelli musteriani dello Stadio Isotopico 3*, MA Thesis, Ferrara, Università degli Studi di Ferrara.

Leger, E. (2014) Personal communication to La Porta, A., Finale Ligure, 10th April.

Lemorini, C. and Cocca, E. (2013) "Functional perspectives on the lithic projectile points from Gobero: experimental and use-wear approaches", in Garcea, E. A. A. (eds) *Gobero: The No-Return Frontier Archaeology and Landscape at the Sahara-Sahelian Borderland*, Frankfurt am Main, Africa Magna Verlag, pp. 195-208.

Lemorini, C., Cesaro, S. N., Nucara, A., Maselli, P., Skakun, N., Gopher, A., and Shahal, A. (2014) "The function of prehistoric lithic tools: a combined study of use-wear analysis and FTIR microspectroscopy. Results and open problems", in Lemorini, C. and Cesaro, S. N. (eds) *An integration of the use-wear and residue analysis for the identification of the function of archaeological stone tools. Proceedings of the international workshop, Rome, March 5th-7th, 2012*, BAR International Series, vol. 2649. Pp. 63-76.

Lemorini, C., Peresani, M., Rossetti, P., Malerba, G., and Giacobini, G. (2005) "Techno-morphological and use-wear functional analysis: an integrated approach to the study of Discoid industry", in Peresani, M. (eds) *Discoid lithic technology: advances and implication*, Oxford, Bar International Series, vol. 1120, pp. 257-275

Lemorini, C., Stiner, M. C., Gopher, A., Shimelmitz, R., and Barkai, R. (2006) "Use-wear analysis of an Amudian laminar assemblage from the Acheuleo-Yabrudian of Qesem Cave, Israel.", *Journal of Archaeological Science*, vol. 33, no. 7, pp. 921-934.

Levi Sala, I. (1986) "Use wear and post-depositional surface modification: a word of caution", *Journal of Archaeological Science*, vol. 13, no. 3, pp. 229-244.

Levi-Sala, I. (1996) *A study of microscopic polish on flint implements*, Oxford, BAR International Series, vol. 629.

Levi-Sala, I. (1988) "Processes of polish formation on flint tool surface", in Beyries, S. (eds) *Industries Lithiques: Tracéologie et Technologie*, Oxford, BAR international Series, vol. 411, pp. 83-98.

Liu, H., Leigh, S., and Yu, B. (2010) "Sequences of upper and lower extremity motions in javelin throwing", *Journal of Sports Sciences*, vol. 28, no. 13, pp. 1459-1467.

Locht, J. L., Antoine, P., Bahain, J. J., Dwirila, G., Raymond, P., Limondin-Lozouet, N., Gauthier, A., Debenham, N., Frechen, M., Rousseau, D., and Hatté, C. (2003) "Le gisement paléolithique moyen et les séquences pléistocènes de Villiers-Adam (Val-d'Oise): chronostratigraphie, environnement et implantations humaines". *Gallia préhistoire*, vol. 45, no. 1, pp. 1-111.

Lombard, M. (2004) "Distribution patterns of organic residues on Middle Stone Age points from Sibudu Cave, KwaZulu-Natal, South Africa", *The South African Archaeological Bulletin*, vol. 59, pp.37-44.

Lombard, M. (2005a) "A method for identifying Stone Age hunting tools"; *The South African Archaeological Bulletin*, vol. 60, no. 182, pp. 115-120.

Lombard, M. (2005b) "Evidence of hunting and hafting during the Middle Stone Age at Sibudu Cave, KwaZulu-Natal, South Africa: a multianalytical approach", *Journal of Human Evolution*, vol. 48, no. 3, pp. 279-300.

Lombard, M. (2006a) "Direct evidence for the use of ochre in the hafting technology of Middle Stone Age tools from Sibudu Cave", *Southern African Humanities*, vol. 18, no. 1, pp. 57-67.

Lombard, M. (2006b) "First impressions of the functions and hafting technology of Still Bay pointed artefacts from Sibudu Cave", *Southern African Humanities*, vol. 18, no. 1, pp. 27-41.

Lombard, M. (2007) "The gripping nature of ochre: the association of ochre with Howiesons Poort adhesives and Later Stone Age mastics from South Africa", *Journal of Human Evolution*, vol. 53, no. 4, pp. 406-419.

Lombard, M. (2008) "Finding resolution for the Howiesons Poort through the microscope: micro-residue analysis of segments from Sibudu Cave, South Africa", *Journal of Archaeological Science*, vol. 35, no. 1, pp. 26-41.

Lombard, M. (2011) "Quartz-tipped arrows older than 60 ka: further use-trace evidence from Sibudu, KwaZulu-Natal, South Africa", *Journal of archaeological Science*, vol. 38, no. 8, pp. 1918-1930.

Lombard, M. (2015) "Hunting and hunting technologies as proxy for teaching and learning during the stone age of Southern Africa", *Cambridge Archaeological Journal*, vol. 25, no. 4, pp. 877-887.

Lombard, M. and Haidle, M. N. (2012) "Thinking a bow-and-arrow set: cognitive implications of Middle Stone Age bow and stone-tipped arrow technology"; *Cambridge Archaeological Journal*, vol. 22, no. 2, pp. 237-264.

-
- Lombard, M. and Pargeter, J. (2008) "Hunting with Howiesons Poort segments: pilot experimental study and the functional interpretation of archaeological tools", *Journal of Archaeological Science*, vol. 35, no. 9, pp. 2523-2531.
- Lombard, M. and Parsons, L. (2011) "What happened to the human mind after the Howiesons Poort?", *Antiquity*, vol. 85, no. 330, pp. 1433-1443.
- Lombard, M. and Phillipson, L. (2010) "Indications of bow and stone-tipped arrow use 64 000 years ago in KwaZulu-Natal, South Africa", *Antiquity*, vol. 84, no. 325, pp. 635-648.
- Lombard, M. and Wadley, L. (2007) "The morphological identification of micro-residues on stone tools using light microscopy: progress and difficulties based on blind tests", *Journal of Archaeological Science*, vol. 34, no. 1, pp. 155-165.
- Lombard, M. and Wadley, L. (2016) "Hunting Technologies During the Howiesons Poort at Sibudu Cave: What They Reveal About Human Cognition in KwaZulu-Natal, South Africa, Between~ 65 and 62 ka", *Vertebrate Paleobiology and Paleoanthropology*, pp. 273-286.
- Lombard, M., Parsons, L., and Van der Ryst, M. M. (2004) "Middle Stone Age lithic point experimentation for macro-fracture and residue analyses: the process and preliminary results with reference to Sibudu Cave points: Sibudu Cave", *South African Journal of Science*, vol. 100, no. 3-4, pp.159-166.
- Longo, L., and Skakun, N. N. (2008) *Prehistoric technology" 40 years later: functional studies and the Russian legacy*, Oxford, BAR International Series, vol. 1783.
- Lycett, S. J. and Eren, M. I. (2013) "Levallois economics: an examination of 'waste' production in experimentally produced Levallois reduction sequences", *Journal of Archaeological Science*, vol. 40, no. 5, pp. 2384-2392.
- Macdonald, D. A. (2014) "The application of focus variation microscopy for lithic use-wear quantification", *Journal of Archaeological Science*, vol. 48, pp. 26-33.
- MacDonald, K. (2007) "Cross-cultural comparison of learning in human hunting", *Human Nature*, vol. 18, no. 4, pp. 386-402.
- Maki, J. M. (2013) *The Biomechanics of Spear Throwing: An Analysis of the Effects of Anatomical Variation on Throwing Performance, with Implications for the Fossil Record*, PhD Thesis, St. Louis, Washington University.
- Malmer, M. P. (1966) "Die Microlithen in dem Pfeil-fund von Loshult", *Meddelanden från Lunds universitets historiska museum*, vol. 1966-1968, pp. 249-255.

Mania, D. and Mania, U. (2005) "The natural and socio-cultural environment of Homo erectus at Bilzingsleben, Germany", in Gamble, C. and Porr, M. (eds) *The individual hominid in context: archaeological investigations of lower and middle palaeolithic landscapes, locales and artefacts*, London, Routledge, pp. 98-114.

Mansur, M. E. (1982) "Microwear analysis of natural and use striations: New clues to the mechanism of striation formation", *Studia Prehistorica Belgica*, vol. 2, pp. 213-233.

Mansur-Francomme, M. E. (1983) "Scanning Electron Microscopy of Dry Hide Working Tools: The Role of Abrasives and humidity in microwear polish formation", *Journal of Archaeological Science*, vol. 10, pp. 223-230.

Mansur-Francomme, M. E. (1986) *Microscopie du matériel lithique préhistorique. Traces d'utilisation, altérations naturelles, accidentelles et technologiques: exemples de Patagonia*, Paris, CNRS.

Marean, C. W. (1998) "A critique of the evidence for scavenging by Neandertals and early modern humans: new data from Kobeh Cave (Zagros Mountains, Iran) and Die Kelders Cave 1 Layer 10 (South Africa)", *Journal of human evolution*, vol. 35, pp. 111–136.

Marean, C. W. and Assefa, Z. (1999) "Zooarcheological evidence for the faunal exploitation behavior of Neandertals and early modern humans", *Evolutionary Anthropology: Issues, News, and Reviews*, vol. 8, no. 1, pp. 22-37.

Marean, C. W. and Kim, S. Y. (1998) "Mousterian large-mammal remains from Kobeh Cave behavioral implications for Neanderthals and early modern humans", *Current Anthropology*, vol. 39, no. S1, pp. S79-S114.

Marean, C. W., Bar-Matthews, M., Bernatchez, J., Fisher, E., Goldberg, P., Herries, A.I., Jacobs, Z., Jerardino, A., Karkanas, P., Minichillo, T., and Nilssen, P. J. (2007) "Early human use of marine resources and pigment in South Africa during the Middle Pleistocene", *Nature*, vol. 449, no. 7164, pp. 905.

Mazza, P. P. A., Martini, F., Sala, B., Magi, M., Colombini, M. P., Giachi, G., Landucci, F., Lemorini, C., Modugno, F., and Ribechini, E. (2006) "A new Palaeolithic discovery: tar-hafted stone tools in a European Mid-Pleistocene bone-bearing bed", *Journal of Archaeological Science*, vol. 33, no. 9, pp. 1310-1318.

McBrearty, S. and Brooks, A. S. (2000) "The revolution that wasn't: a new interpretation of the origin of modern human behaviour", *Journal of Human Evolution*, vol. 39, no. 5, pp. 453-563.

McBrearty, S., Bishop, L., Plummer, T., Dewar, R., and Conard, N. (1998) "Tools underfoot: human trampling as an agent of lithic artifact edge modification", *American Antiquity*, vol. 63, no. 1, pp. 108-129.

Mehidi, N. (2005) *Datation de sites moustériens de Ligurie par les méthodes U/Th et RPE: Abri Mochi et Arma delle Manie*, PhD Thesis, Paris, Muséum national d'histoire naturelle.

Mélard, N., Boust, C., Cogné, G., and Maignret, A. (2016) "Comparison of imaging techniques used in the microanalysis of Palaeolithic mobiliary art", *Journal of Archaeological Science: Reports*, vol. 10, pp. 903-909.

Mellars, P. (1973) "The Character of the Middle-up per Paleolithic Transition in south-west France", in Renfrew, C. (eds) *The explanation of culture change: models in prehistory: proceedings of a meeting of the Research Seminar in Archaeology and Related Subjects held at the Univ. of Sheffield*, Pittsburgh, University of Pittsburgh Press, pp. 225-276.

Mellars, P. (1989) "Major issues in the emergence of modern humans", *Current Anthropology*, vol. 30, no. 3, pp. 349-385.

Mellars, P. (1999) "The Neanderthal problem continued", *Current Anthropology*, vol. 40, no. 3, pp. 341-364.

Mellars, P. (2005) "The impossible coincidence. A single-species model for the origins of modern human behavior in Europe", *Evolutionary Anthropology: Issues, News, and Reviews*, vol. 14, no. 1, pp. 12-27.

Mellars, P. (2006) "Archeology and the dispersal of modern humans in Europe: Deconstructing the "Aurignacian"", *Evolutionary Anthropology: Issues, News, and Reviews*, vol. 15, no. 5, pp. 167-182.

Mellars, P. (2006) "Why did modern human populations disperse from Africa ca. 60,000 years ago? A new model", *Proceedings of the National Academy of Sciences*, vol. 103, no. 25, pp. 9381-9386.

Mellars, P. A. (1995) *The Neanderthal legacy: an archaeological perspective from Western Europe*, Princeton, Princeton University Press.

Mercier, N. and Valladas, H. (2003) "Reassessment of TL age estimates of burnt flints from the Paleolithic site of Tabun Cave, Israel", *Journal of Human Evolution*, vol. 45, no. 5, pp. 401-409.

Meyer, M., Arsuaga, J.L., de Filippo, C., Nagel, S., Aximu-Petri, A., Nickel, B., Martínez, I., Gracia, A., de Castro, J.M.B., Carbonell, E., and Viola, B. (2016) "Nuclear DNA sequences from the Middle Pleistocene Sima de los Huesos hominins", *Nature*, vol. 531, no. 759, pp. 504.

Milks, A., Champion, S., Cowper, E., Pope, M., and Carr, D. (2016) "Early spears as thrusting weapons: Isolating force and impact velocities in human performance trials", *Journal of Archaeological Science: Reports*, vol. 10, pp. 191-203.

-
- Milks, A., Parker, D., and Pope, M. (2019) "External ballistics of Pleistocene hand-thrown spears: experimental performance data and implications for human evolution", *Scientific reports*, vol. 9, no. 1, p.820.
- Miller, D. I. and Munro, C. F. (1983) "Javelin position and velocity patterns during final foot plant preceding release", *Journal of Human Movement Studies*, vol. 9, no. 1, pp. 1-20.
- Miller, S. A. and Jones, M. D. (1996) "Kinematics of four methods of stabbing: a preliminary study", *Forensic Science International*, vol. 82, pp. 183–190.
- Milo, R. G. (1998) "Evidence for hominid predation at Klasies River Mouth, South Africa, and its implications for the behaviour of early modern humans", *Journal of Archaeological Science*, vol. 25, no. 2, pp. 99-133.
- Moncel, M. H. (1996) "L'industrie lithique du Paléolithique moyen de l'abri du Maras (Ardèche)", *Gallia Préhistoire*, vol. 38, no. 1, pp. 1-41.
- Moncel, M. H. (2003) *L'exploration de l'espace et la mobilité des groupes humains au travers des assemblages lithiques à la fin du pléistocène moyen et au début du pléistocène supérieur: la moyenne vallée du Rhône entre Drôme et Ardèche, France*, Oxford, BAR International Series, vol. 1184.
- Moncel, M. H. (2005) "Baume Flandin et Abri du Maras: deux exemples de débitage laminaire du début du Pléistocène supérieur dans la Vallée du Rhône (sud-est, France)", *l'Anthropologie*, vol. 109, no. 3, pp. 451-480.
- Moncel, M. H. (2008). *Le site de Payre. Occupations humaines dans la vallée du Rhône à la fin du Pléistocène moyen et au début du Pléistocène supérieur*, Paris, Société préhistorique française.
- Moncel, M. H. and Combier, J. (1990) "L'exploitation de l'espace au Pléistocène moyen: L'approvisionnement en matières premières lithiques: L'exemple du site d'Ornac 3 (Ardèche, France)", *Bulletin de la Société préhistorique française*, vol. 87, no. 10, pp. 299-313.
- Moncel, M. H. and Daujeard, C. (2012) "The variability of the Middle Palaeolithic on the right bank of the Middle Rhône Valley (southeast France): Technical traditions or functional choices?", *Quaternary International*, vol. 247, pp. 103-124.
- Moncel, M. H. and Michel, V. (2000) "Première tentative de datation par U-Th du site paléolithique moyen de l'Abri du Maras (Ardèche, France)", *Bulletin de la Société préhistorique française*, vol. 97, no. 3, pp. 371-375.
- Moncel, M. H., Allue, E., Bearez, N., Chacon Navarro, M. G., Courty, A., Daujeard, C., Desclaux, A., Fernandes, P., Gallotti, R., Hardy, B., Lateur, N., La Porta, A., Limondin-Lozouet, N., Pike-Tay, A.,

Puaud, S., Richard, M., Rivals, F., Roger, T., and Amélie Sarl datations (2012) *Abri du Maras (Saint-Martin d'Ardèche)*, Report of exaction, N° 1378.

Moncel, M. H., Allue, E., Bearez, P., Boulbes, N., Britton, K., Chacon Navarro, M. G., Courty, A., Crégut-Bonnoure, A., Daujeard, C., Desclaux, E., Eixea, A., Fernandes, P., Gallotti, R., Hardy, B., Joannes-Boyau, R., Kerfant, C., Lateur, N., La Porta, A., Limondin-Lozouet, N., Marin Hernando, J., Miras, Y., Pike-Tay, A., Puaud, S., Richard, M., Rivals, F., Roger, T., Sepehr Akhavan, M., Vettese, D., and Amélie Sarl datations (2017), *Abri du Maras (Saint-Martin d'Ardèche)*, Report of exaction, N° 2017/3084.

Moncel, M. H., Chacón, M. G., La Porta, A., Fernandes, P., Hardy, B., and Gallotti, R. (2014) "Fragmented reduction processes: Middle Palaeolithic technical behaviour in the Abri du Maras shelter, southeastern France", *Quaternary International*, vol. 350, pp. 180-204.

Moncel, M. H., Daujeard, C., Crégut-Bonnoure, E., Boulbes, N., Puaud, S., Debard, E., Bailon, S., Desclaux, E., Escudé, E., Roger, T., and Dubar, M. (2010) "Nouvelles données sur les occupations humaines du début du Pléistocène supérieur de la moyenne vallée du Rhône (France). Les sites de l'Abri des Pêcheurs, de la Baume Flandin, de l'Abri du Maras et de la Grotte du Figuier (Ardèche)", *Quaternaire. Revue de l'Association française pour l'étude du Quaternaire*, vol. 21, no. 4, pp. 385-411.

Moncel, M. H., Moigne, A. M., and Combiér, J. (2012) "Towards the Middle Palaeolithic in western Europe: the case of Orgnac 3 (southeastern France)" *Journal of Human Evolution*, vol. 63, no. 5, pp. 653-666.

Moretti, E., Arrighi, S., Boschini, F., Crezzini, J., Aureli, D., and Ronchitelli, A. (2015) "Using 3D microscopy to analyze experimental cut marks on animal bones produced with different stone tools", *Ethnobiology Letters*, vol. 6, no. 2, pp. 267-275.

Moroni, A., Boscato, P., and Ronchitelli, A. (2013) "What roots for the Uluzzian? Modern behaviour in Central-Southern Italy and hypotheses on AMH dispersal routes", *Quaternary International*, vol. 316, pp. 27-44.

Morriss, C. and Bartlett, R. (1996) "Biomechanical factors critical for performance in the men's javelin throw", *Sports Medicine*, vol. 21, no. 6, pp. 438-446.

Moss, E. H. (1983a) *The functional analysis of flint implements: Pincevent and Pont d'Ambon: two case studies from the French final Palaeolithic*, Oxford, BAR International Series, vol. 177.

Moss, E. H. (1983b) "A Microwear Analysis of Burins and Points from Tell Abu Hureyra, Syria in Traces d'utilisation sur les outils néolithiques du Proche-Orient", *Travaux de la Maison de l'Orient Lyon*, vol. 5, pp. 143-162.

-
- Moss, E. H. (1983c) "Some comments on edge damage as a factor in functional analysis of stone artifacts", *Journal of Archaeological Science*, vol. 10, no. 3, pp. 231-242.
- Moss, E. H. (1986) "What microwear analysts look at", in Owen, L. and Unruth, G. (eds) *Technical Aspects of Microwear Studies on Stone Tools*, Tübingen, Archaeologica Venatoria, Institut für Urgeschichte, vol. 9, pp. 91-96.
- Moss, E. H. (1987). A review of "Investigating microwear polishes with blind tests". *Journal of Archaeological Science*, 14(5), 473-481.
- Moss, E. H. and Newcomer, M. H. (1982) "Reconstruction of Tool Use at Pincevent: Microwear and Experiments", in Cahen, D. (eds) *Tailler! Pour quoi faire: préhistoire et technologie lithique I: recent progress in microwear studies*, Leuven, Studia Praehistorica Belgica Leuven, pp. 289-312.
- Movius, H. L. (1950) "A wooden spear of third interglacial age from lower Saxony", *Southwestern Journal of Anthropology*, vol. 6, no. 2, pp. 139-142.
- Mussi, M. (1999) "The Neanderthals in Italy: a tale of many caves", in Roebroeks, W. and Gamble, C. (eds) *The Middle Palaeolithic Occupation of Europe*, Leiden, Leiden University, pp. 49–80.
- Mussi, M. and Roebroeks, W. (1996) "The big mosaic", *Current Anthropology*, vol. 37, no. 4, pp. 697-699.
- Negrino, F. (2005) "Riparo Bombrini, Balzi Rossi (Ventimiglia, IM): La campagna 2005", *Ligures*, vol. 3, pp. 194-196.
- Negrino, F. (2014) Personal communication to La Porta, A., Genova, 21st April.
- Negrino, F. and Starnini, E. (2006) "Modelli di sfruttamento e circolazione delle materie prime per l'industria litica scheggiata tra Paleolitico inferiore ed Età del Rame in Liguria", *Atti della XXXIX Riunione scientifica: materie prime e scambi nella preistoria italiana: nel cinquantenario della fondazione dell'Istituto italiano di preistoria e protostoria*, Firenze 25-27 Novembre 2004, Firenze, Istituto italiano di preistoria e protostoria.
- Negrino, F. and Starnini, E. (2010) "Dinamiche di sfruttamento e circolazione delle materie prime silicee per l'industria litica scheggiata in Liguria tra Paleolitico inferiore ed Età del Rame", *Atti della Tavola Rotonda*, Genova, pp.21-34.
- Negrino, F. and Tozzi, C. (2008) "Il Paleolitico in Liguria", *Bulletin du Musée d'anthropologie préhistorique de Monaco*, vol. 50, pp. 21-28.
- Newcomer, M. H. (1976) "Spontaneous retouch", *Staringia*, vol. 3, no. 1, pp. 62-64.

-
- Newcomer, M., Grace, R., and Unger-Hamilton, R. (1986) "Investigating microwear polishes with blind tests", *Journal of Archaeological Science*, vol. 13, no. 3, pp. 203-217.
- Newman, K. and Moore, M. W. (2013) "Ballistically anomalous stone projectile points in Australia", *Journal of Archaeological Science*, vol. 40, no. 6, pp. 2614-2620.
- Noack, E. and Gaudzinski-Windheuser, (2018) "Ballistic Archaeology: a new agenda for contextualizing the origin and evolution of prehistoric weaponry", paper presented at *XVIII word UISPP Congress*, 4-9 June. Paris.
- Nowak, M. (2013) *Identification de téphras dans le remplissage sédimentaire du site préhistorique de l'Abri du Maras (Saint-Martin-d'Ardèche, Ardèche): essai de caractérisation—physico-chimie, origine et chronologie*, MA Thesis, Paris, Muséum national d'Histoire naturelle.
- O'Farrell, M. (2004) "Les pointes de La Gravette de Corbiac (Dordogne) et considérations sur la chasse au Paléolithique supérieur ancien", in Bodu, P. (eds) *Approches fonctionnelles en préhistoire*. Société préhistorique française, Paris, Société Préhistorique Française, pp. 121-138
- Oakley, K. P., Andrews, P., Keeley, L. H, and Clark, J. D. (1977) "A reappraisal of the Clacton spearpoint", *Proceedings of the Prehistoric Society*, vol. 43, pp. 13-30.
- Odell, G. H. (1975) "Micro-wear in perspective: A sympathetic response to Lawrence H. Keeley", *World Archaeology*, vol. 7, no. 2, pp. 226-240.
- Odell, G. H. (1978) "Préliminaires d'une analyse fonctionnelle des pointes microlithiques de Bergumermeer (Pays-Bas)", *Bulletin de la Société préhistorique française*, pp.37-49.
- Odell, G. H. (1980) "Toward a more behavioral approach to archaeological lithic concentrations", *American Antiquity*, vol. 45, no. 3, pp. 404-431.
- Odell, G. H. (1981) "The mechanics of use-breakage of stone tools: some testable hypotheses", *Journal of Field Archaeology*, vol. 8, no. 2, pp. 197-209.
- Odell, G. H. (1988) "Addressing prehistoric hunting practices through stone tool analysis", *American Anthropologist*, vol. 90, no. 2, pp. 335-356.
- Odell, G. H. (1996) "Economizing behavior and the concept of "curation", in Odel, G. H. (eds) *Stone Tools*, Boston, Springer, pp. 51-80.
- Odell, G. H. (2001) "Stone tool research at the end of the millennium: classification, function, and behaviour", *Journal of Archaeological Research*, vol. 9, no. 1, pp. 45-100.
- Odell, G. H. (1994) "Prehistoric hafting and mobility in the North American Midcontinent: Examples from Illinois", *Journal of Anthropological Archaeology*, vol. 13, no. 1, pp. 51-73.

Odell, G. H. and Cowan, F. (1986) "Experiments with spears and arrows on animal targets", *Journal of Field Archaeology*, vol. 13, no. 2, pp. 195-212.

Odell, G. H. and Odell-Vereecken, F. (1980) "Verifying the reliability of lithic use-wear assessments by 'blind tests': the low-power approach", *Journal of Field Archaeology*, vol. 7, no. 1, pp. 87-120.

Ollé, A. (2003) *Variabilitat i patrons funcionals en els sistemes tècnics de mode 2. Anàlisi de les deformacions d'ús en els conjunts lítics del Riparo Esterno de Grotta Paglicci (Rigano Garganico, Foggia), Aridos (Arganda, Madrid) i Galeria-TN (Atapuerca, Burgos)*. Universitat Rovira i Virgili (Dept. Història i Història de l'Art) Tarragona, PhD Thesis, Tarragona, Institut Català de Paleoecologia Humana i Evolució Social.

Ollé, A. and Vergès, J. M. (2008) "SEM functional analysis and the mechanism of microwear formation", in Longo, L. and Skakun, N. (eds) *Prehistoric technology*, Oxford, BAR International Series, vol. 40, pp. 39-49.

Ollé, A. and Vergès, J. M. (2014) "The use of sequential experiments and SEM in documenting stone tool microwear", *Journal of Archaeological Science*, vol. 48, pp. 60-72.

Ollé, A., Pedergrana, A., Fernández-Marchena, J. L., Martín, S., Borel, A., and Aranda, V. (2016) "Microwear features on vein quartz, rock crystal and quartzite: A study combining Optical Light and Scanning Electron Microscopy", *Quaternary International*, vol. 424, pp. 154-170.

Otte, M. (1995) "The nature of Levallois. The definition and interpretation of Levallois technology", in Dibble, H. L. and BarYosef, O. (eds) *The Definition and Interpretation of Levallois Technology*, Madison, Prehistory Press, pp.117-124.

Outram, A. K. (2008) "Introduction to experimental archaeology"; *World Archaeology*, vol. 40, no. 1, pp. 1-6.

Ovchinnikov, I. V., Götherström, A., Romanova, G. P., Kharitonov, V. M., Liden, K., and Goodwin, W. (2000) "Molecular analysis of Neanderthal DNA from the northern Caucasus", *Nature*, vol. 404, no. 6777, pp. 490-493.

Owen, L. R. (1987) "Hafting microblades: Examples from the Dorset Culture of the North American Arctic", *Travaux de la Maison de l'Orient*, vol. 15, no. 1, pp. 147-150.

Owen, L. R. and Unrath, G. (1989) "Microtraces d'usure dues a la prehension", *l'Anthropologie*, vol. 93, no. 4, pp. 673-688.

Palter, J. L. (1977) "Design and construction of Australian spear-thrower projectiles and hand-thrown spears", *Archaeology in Oceania*, vol. 12, no. 3, pp. 161-172.

-
- Pargeter, J. (2007) "Howiesons Poort segments as hunting weapons: experiments with replicated projectiles", *The South African Archaeological Bulletin*, vol. 62, no. 186, pp. 147-153.
- Pargeter, J. (2011) "Human and cattle trampling experiments in Malawi to understand macrofracture formation on Stone Age hunting weaponry", *Antiquity*, vol. 85, no. 327, pp. 2013.
- Pargeter, J. (2013) "Rock type variability and impact fracture formation: working towards a more robust macrofracture method", *Journal of Archaeological Science*, vol. 40, no. 11, pp. 4056-4065.
- Pargeter, J. and Bradfield, J. (2012) "The effects of Class I and II sized bovids on macrofracture formation and tool displacement: results of a trampling experiment in a southern African Stone Age context", *Journal of Field Archaeology*, vol. 37, no. 3, pp. 238-251.
- Pargeter, J., Shea, J., and Utting, B. (2016) "Quartz backed tools as arrowheads and hand-cast spearheads: Hunting experiments and macro-fracture analysis", *Journal of Archaeological Science*, vol. 73, pp. 145-157.
- Patou-Mathis, M. (2000) "Neanderthal subsistence behaviours in Europe", *International Journal of Osteoarchaeology*, vol. 10, no. 5, pp. 379-395.
- Patou-Mathis, M. (2004) "Subsistence behaviours in a Middle Palaeolithic site in Poland: the Raj Cave", *International Journal of Osteoarchaeology*, vol. 14, no. 3-4, pp. 244-255.
- Patou-Mathis, M. and Chabai, V. (2003) "Kabazi II (Crimée, Ukraine): un site d'abattage et de boucherie du Paléolithique moyen", *l'Anthropologie*, vol. 107, no. 2, pp. 223-253.
- Pawlik, A. F. (2004) "Identification of hafting traces and residues by scanning electron microscopy and energy-dispersive analysis of X-rays", *Lithics in Action. Lithic Studies Society Occasional Paper*, vol. 8, pp. 169-179.
- Pawlik, A. F. (2011) "Have we overlooked something? Hafting traces and indications of modern traits in the Philippine Palaeolithic", *Bulletin of the Indo-Pacific Prehistory Association*, vol. 30, pp. 35-53.
- Pawlik, A. F. and Thissen, J. P. (2011) "Hafted armatures and multi-component tool design at the Micoquian site of Inden-Altdorf, Germany", *Journal of Archaeological Science*, vol. 38, no. 7, pp. 1699-1708.
- Pawlik, A.F. (2001) "Microscopic use-wear analysis: a basic introduction on how to reconstruct the functions of stone tools", *Journal for Archaeological Research in Asia and the Pacific*, vol. 3, no. 1, pp. 1-25.
- Pedergrana, A. and Ollé, A. (2017) "Monitoring and interpreting the use-wear formation processes on quartzite flakes through sequential experiments", *Quaternary International*, vol. 427, pp. 35-65.

Peresani, M. (2003) "An initial overview of the middle Palaeolithic discoid industries in Central-Northern Italy" in Peresani, M. (eds) *Discoid lithic technology, advances and implications*, Oxford, BAR International Series, vol. 1120, pp. 209-223.

Peresani, M. (2013) email to La Porta, A, January.

Peresani, M., Fiore, I., Gala, M., Romandini, M., and Tagliacozzo, A. (2011) "Late Neandertals and the intentional removal of feathers as evidenced from bird bone taphonomy at Fumane Cave 44 ky BP, Italy", *Proceedings of the National Academy of Sciences*, vol. 108, no. 10, pp. 3888-3893.

Pettitt, P. (2011) "The living as symbols, the dead as symbols: problematising the scale and pace of hominin symbolic evolution", in Henshilwood, C. S. and d'Errico, F. (eds) *Homo symbolicus: the dawn of language, imagination and spirituality*, Amsterdam, John Benjamins Publishing Company, pp. 141-162.

Pinhasi, R., Higham, T.F., Golovanova, L.V., and Doronichev, V.B. (2011) "Revised age of late Neanderthal occupation and the end of the Middle Paleolithic in the northern Caucasus", *Proceedings of the National Academy of Sciences*, vol. 108, no. 21, pp. 8611-8616.

Plisson, H. (1982) "Analyse fonctionnelle de 95 micro-grattoirs tourassiens", in Cahen, D. (eds) *Tailler! Pourquoi faire? Préhistoire et technologie lithique II, Recent Progress in Microwear Studies*, Leuven, Studia Praehistorica Belgica, vol. 2, pp. 279-287.

Plisson, H. (1983a) "De la conservation des micro-polis d'utilisation", *Bulletin de la Société Préhistorique Française. Comptes Rendus des Séances Mensuelles Paris*, vol. 80, no. 3, pp. 74-77.

Plisson, H. (1983b) "An application of casting techniques for observing and recording of microwear", *Lithic Technology*, vol. 12, no. 1, pp. 17-21.

Plisson, H. (1985) *Études Fonctionnelles des Outillages Préhistoriques par l'Analyse des Micro-Usures: Recherche Méthodologique et Archéologique*, PhD Thesis, Paris, Université de Paris I, Panthéon-Sorbonne.

Plisson, H. (1987a) "L'emmanchement dans l'habitation n° I de Pincevent", *Travaux de la Maison de l'Orient*, vol. 15, no. 1, pp. 75-88.

Plisson, H. (1987b) "A propos de quelques micro-grattoirs du Paléolithique final", *Publications de la Maison de l'Orient et de la Méditerranée*, vol. 15, no. 1, pp. 129-134.

Plisson, H. (2014) "3D en kit: des solutions pour la tracéologie et au-delà", *Archeologia e Calcolatori*, vol. 5, pp. 102-116.

Plisson, H. and Beyries, S. (1998) "Pointes ou outils triangulaires? Données fonctionnelles dans le Moustérien levanting", *Paléorient*, vol. 24, no. 1, pp. 5-24.

Plisson, H. and Mauger, M. (1988) "Chemical and mechanical alteration of microwear polishes: an experimental approach", *Helinium*, vol. 28, no. 1, pp. 3-16.

Popper, K. (1959) *The Logic of Scientific Discovery*, London, Routledge (this edition 2002).

Porraz, G. and Negrino, F. (2008) "Espaces économiques et approvisionnement minéral au Paléolithique moyen dans l'aire liguro-provençale", *Bulletin du Musée d'anthropologie préhistorique de Monaco*, vol. 1, pp. 29-39.

Potts, R. (1984) "Home bases and early hominids", *Scientific American*, vol. 72, pp. 338-347.

Prinsloo, L. C., Wadley, L., and Lombard, M. (2014) "Infrared reflectance spectroscopy as an analytical technique for the study of residues on stone tools: potential and challenges", *Journal of Archaeological Science*, vol. 41, pp. 732-739.

Psathi, E. (2003) *Les sites moustériens de la Caverna delle Fate et de l'Arma delle Manie (Ligurie, Italie): Étude paléontologique et archéozoologique des faunes des grands mammifères*, PhD Thesis, Paris, Muséum national d'histoire naturelle.

Psathi, E. and Vicino, G. (2003) *Le site moustérien de l'Arma delle Manie (Ligurie, Italie) L'apport de l'étude archéozoologique des grands mammifères*, Oxford, BAR International Series, vol. 1105, pp. 149-158.

Puaud, S., Nowak, M., Pont, S., and Moncel, M. H. (2015) "Minéraux volcaniques et alpins à l'abri du Maras (Ardèche, France): témoins de vents catabatiques dans la vallée du Rhône au Pléistocène supérieur"; *Comptes Rendus Palevol*, vol. 14, no. 4, pp. 331-341.

Radovčić, D., Sršen, A. O., Radovčić, J., and Frayer, D. W. (2015) "Evidence for Neandertal jewelry: Modified white-tailed eagle claws at Krapina", *PLoS One*, vol. 10, no. 3, pp. e0119802.

Raynal, J. P., Le Corre-le-Bueux, M., Santagata, C., Fernandes, P., Guadelli, J. L., Fiore, I., Tagliacozzo, A., Lemorini, C., Rhodes, E., Bertran, P., Kieffer, G., and Vivent, D. (2005) "Paléolithique moyen dans le Sud du Massif central: les données du Velay (Haute-Loire, France)", in Molines, N., Moncel, M. H., and Monnier, J. L. (eds) *Données récentes sur les modalités de peuplement et sur le cadre chronostratigraphique, géologique et paléogéographique des industries du Paléolithique ancien et moyen en Europe (Rennes, 22-25 septembre 2003)*, Oxford, BAR International Series, vol. S1364, pp. 173-201.

Raynal, J. P., Moncel, M. H., Deaujard, C., Fiore, I., Tagliacozzo, A., Fernandes, P., Fiore, I., Lecorre-Le Buex, M., Chacon Navarro, G., and Theodoropoulou, A. (2012) "Neanderthal land-use and related tool-kits at MIS 5/4 boundary on the South-East border of the Massif Central", in Ruebens, K. (eds) *Unravelling the Palaeolithic: ten years of research at the Centre for the Archaeology of Human Origins (CAHO, University of Southampton)*, Oxford, Archaeopress, pp. 53-72.

Rendu, W., Costamagno, S., Meignen, L., and Soulier, M.C. (2012) "Monospecific faunal spectra in Mousterian contexts: Implications for social behaviour", *Quaternary International*, vol. 247, pp.50-58.

Revedin, A., Aranguren, B., Becattini, R., Longo, L., Marconi, E., Lippi, M. M., Skakun, N., Sinitsyn, A., Spiridonova, E., and Svoboda, J. (2010) "Thirty thousand-year-old evidence of plant food processing", *Proceedings of the National Academy of Sciences*, vol. 107, no. 44, pp. 18815-18819.

Reynolds, P. J. (1999) "The nature of experiment in archaeology", in Harding, A. F. (eds) *Experiment and design: archaeological studies in honour of John Coles*, Oxford, Oxbow Books, pp.156-162.

Rhodes, J. A. and Churchill, S. E. (2009) "Throwing in the Middle and Upper Paleolithic: inferences from an analysis of humeral retroversion", *Journal of Human Evolution*, vol. 56, no. 1, pp. 1-10.

Richard, M., Falguères, C., Pons-Branchu, E., Bahain, J. J., Voinchet, P., Lebon, M., Valladas, H., Dolo, J. M., Puaud, S., Rué, M. and Daujeard, C. (2015) "Contribution of ESR/U-series dating to the chronology of late Middle Palaeolithic sites in the middle Rhône valley, southeastern France", *Quaternary Geochronology*, vol. 30, pp. 529-534.

Richards, M. P. and Trinkaus, E. (2009) "Isotopic evidence for the diets of European Neanderthals and early modern humans", *Proceedings of the National Academy of Sciences*, vol. 106, no. 38, pp. 16034-16039.

Richter, D. and Krbetschek, M. (2015) "The age of the Lower Paleolithic occupation at Schöningen", *Journal of Human Evolution*, vol. 89, pp. 46-56.

Richter, D. and Krbetschek, M. (2015) "The age of the Lower Paleolithic occupation at Schöningen", *Journal of Human Evolution*, vol. 89, pp. 46-56.

Rieder, H. (2003) "Der große Wurf der frühen Jäger: nachbau altsteinzeitlicher Speere"; *Biologie in unserer Zeit*, vol. 33, no. 3, pp. 156-160.

Riel-Salvatore, J., Ludeke, I. C., Negrino, F., and Holt, B. M. (2013) "A spatial analysis of the late mousterian levels of Riparo Bombrini (Balzi Rossi, Italy)", *Canadian Journal of Archaeology Journal Canadien d'Archéologie*, vol. 37, no. 1, pp. 70-92.

Rios-Garaizar, J., López-Bultó, O., Iriarte, E., Pérez-Garrido, C., Piqué, R., Aranburu, A., Iriarte-Chiapusso, M. J., Ortega-Cordellat, I., Bourguignon, L., Garate, D., and Libano, I. (2018) "A Middle Palaeolithic wooden digging stick from Aranbaltza III, Spain", *PloS one*, vol. 13, no. 3, pp. e0195044.

Roach, N. T. and Richmond, B. G. (2015a) "Humeral torsion does not dictate shoulder position, but does influence throwing speed"; *Journal of Human Evolution*, vol. 85, pp. 206-211.

Roach, N. T. and Richmond, B. G. (2015b) "Clavicle length, throwing performance and the reconstruction of the Homo erectus shoulder"; *Journal of Human Evolution*, vol. 80, pp. 107-113.

-
- Roach, N. T., Lieberman, D. E., Gill, T. J., Palmer, W. E., and Gill, T. J. (2012) "The effect of humeral torsion on rotational range of motion in the shoulder and throwing performance"; *Journal of Anatomy*, vol. 220, no. 3, pp. 293-301.
- Roach, N. T., Venkadesan, M., Rainbow, M. J., and Lieberman, D. E. (2013) "Elastic energy storage in the shoulder and the evolution of high-speed throwing in Homo"; *Nature*, vol. 498, no. 7455, pp. 483.
- Roberts, M. B. and Parfitt, S. A. (1999) *Boxgrove: A Middle Pleistocene Hominid Site at Eartham Quarry, Boxgrove, West Sussex*, London, English Heritage.
- Rodríguez-Hidalgo, A., Rivals, F., Saladié, P., and Carbonell, E. (2016) "Season of bison mortality in TD10. 2 bone bed at Gran Dolina site (Atapuerca): integrating tooth eruption, wear, and microwear methods", *Journal of Archaeological Science: Reports*, vol. 6, pp. 780-789.
- Rodríguez-Vidal, J., d'Errico, F., Pacheco, F. G., Blasco, R., Rosell, J., Jennings, R. P., Queffelec, A., Finlayson, G., Fa, D. A., López, J. M. G., and Carrión, J. S. (2014) "A rock engraving made by Neanderthals in Gibraltar", *Proceedings of the National Academy of Sciences*, vol. 111, no. 37, pp. 13301-13306.
- Roebroeks, W. (2001) "Hominid behaviour and the earliest occupation of Europe: an exploration", *Journal of Human Evolution*, vol. 41, no. 5, pp. 437-461.
- Roebroeks, W., Sier, M. J., Nielsen, T. K., De Loecker, D., Parés, J. M., Arps, C. E., and Múcher, H. J. (2012) "Use of red ochre by early Neandertals", *Proceedings of the National Academy of Sciences*, vol. 109, no. 6, pp. 1889-1894.
- Romandini, M., Peresani, M., Laroulandie, V., Metz, L., Pastoors, A., Vaquero, M., and Slimak, L. (2014) "Convergent evidence of eagle talons used by late Neanderthals in Europe: a further assessment on symbolism", *PloS one*, vol. 9, no. 7, pp. e101278.
- Romandini, M., Terlato, G., Nannini, N., Tagliacozzo, A., Benazzi, S., and Peresani, M. (2018) "Bears and humans, a Neanderthal tale. Reconstructing uncommon behaviors from zooarchaeological evidence in southern Europe", *Journal of Archaeological Science*, vol. 90, pp. 71-91.
- Rots, V. (2002) "Bright spots and the question of hafting", *Anthropologica et Praehistorica*, vol. 113, pp. 61-71.
- Rots, V. (2003) "Towards an understanding of hafting: the macro-and microscopic evidence", *Antiquity*, vol. 77, no. 298, pp. 805-815.
- Rots, V. (2004) "Prehensile wear on flint tools", *Lithic Technology*, vol. 29, no. 1, pp. 7-32.

Rots, V. (2005) "Wear traces and the interpretation of stone tools", *Journal of Field Archaeology*, vol. 30, no. 1, pp. 61-73.

Rots, V. (2009) "The functional analysis of the Mousterian and Micoquian assemblages of Sesselfelsgrötte, Germany: aspects of tool use and hafting in the European Late Middle Palaeolithic", *Quartär*, vol. 56, pp. 37-66.

Rots, V. (2010) *Prehension and hafting traces on flint tools: a methodology*, Leuven, Leuven University Press.

Rots, V. (2012) "Trace formation, strike-a-lights, and the contribution of functional analyses for understanding Palaeolithic contexts", in Terberger, T., Street, M., Barton, N., Stapert, D., and Niekus, M. J. L. T. (eds) *A mind set on flint: studies in honour of Dick Stapert*, Groningen, Groningen University Library, pp. 149-162.

Rots, V. (2013) "Insights into early Middle Palaeolithic tool use and hafting in Western Europe. The functional analysis of level IIa of the early Middle Palaeolithic site of Biache-Saint-Vaast (France)", *Journal of Archaeological Science*, vol. 40, no. 1, pp. 497-506.

Rots, V. (2015) "Keys to the identification of prehension and hafting traces", in Marreiros, J., Gibaja, J. F., and Bicho, N. (eds) *Use-wear and residue analysis in archaeology*, Cham, Springer, pp. 83-104.

Rots, V. (2016) "Projectiles and hafting technology", in Iovita, R. and Sano, K. (eds) *Multidisciplinary approaches to the study of Stone Age weaponry*, Dordrecht., Springer, pp. 167-185.

Rots, V. and Plisson, H., (2014) "Projectiles and the abuse of the use-wear method in a search for impact"; *Journal of Archaeological Science*, vol. 48, pp. 154-165.

Rots, V. and Van Peer, P. (2006) "Early evidence of complexity in lithic economy: core-axe production, hafting and use at Late Middle Pleistocene site 8-B-11, Sai Island (Sudan)", *Journal of Archaeological Science*, vol. 33, no. 3, pp. 360-371.

Rots, V. and Vermeersch, P. M. (2000) "Experimental characterization of hafting traces and their recognition in archaeological assemblages", in Walker, E.A., Wenban-Smith, F., and Healy, F. (eds) *Lithics in Action*, Oxford, Oxbow, pp. 156-168.

Rots, V. and Williamson, B. S. (2004) "Microwear and residue analyses in perspective: the contribution of ethnoarchaeological evidence", *Journal of Archaeological Science*, vol. 31 no. 9, pp. 1287-1299.

Rots, V., Hardy, B. L., Serangeli, J., and Conard, N. J. (2015) "Residue and microwear analyses of the stone artifacts from Schöningen", *Journal of Human Evolution*, vol. 89, pp. 298-308.

Rots, V., Lentfer, C., Schmid, V. C., Porraz, G., and Conard, N. J. (2017) "Pressure flaking to serrate bifacial points for the hunt during the MIS5 at Sibudu Cave (South Africa)", *PloS one*, vol. 12, no. 4, pp. e0175151.

Rots, V., Pirnay, L., Pirson, P., and Baudoux, O. (2006) "Blind tests shed light on possibilities and limitations for identifying stone tool prehension and hafting", *Journal of Archaeological Science*, vol. 33, no. 7, pp. 935-952.

Rots, V., Van Peer, P., and Vermeersch, P.M. (2011) "Aspects of tool production, use, and hafting in Palaeolithic assemblages from Northeast Africa", *Journal of Human Evolution*, vol. 60, no. 5, pp. 637-664.

Rottalnder, R. (1975) "The formation of patina on flint", *Archaeometry*, vol. 17, no. 1, pp. 106-110.

Sahle, Y., Hutchings, W. K., Braun, D. R., Sealy, J. C., Morgan, L. E., Negash, A., and Atnafu, B. (2013) "Earliest stone-tipped projectiles from the Ethiopian Rift date to >279,000 years ago", *PLoS One*, vol. 8, no. 11, pp. e78092.

Sala, I. L. (1996) *A study of microscopic polish on flint implements*, Oxford, BAR International Series, vol. 629.

Sandgathe, D. M., Dibble, H. L., Goldberg, P., McPherron, S. P., Turq, A., Niven, L., and Hodgkins, J. (2011) "On the role of fire in Neandertal adaptations in Western Europe: evidence from Pech de l'Azé IV and Roc de Marsal, France", *PaleoAnthropology*, pp.216-242.

Sano, K. (2009) "Hunting evidence from stone artefacts from the Magdalenian cave site Bois Laiterie, Belgium: A fracture analysis", *Quartär*, vol. 56, pp. 67-86.

Sano, K. (2012a) *Functional variability in the late upper palaeolithic of north-western Europe: a traceological approach*, Bonn, Habelt.

Sano, K. (2012b) "Functional variability in the Magdalenian of north-western Europe: a lithic microwear analysis of the Gönnersdorf K-II assemblage", *Quaternary International*, vol. 272, pp. 264-274.

Sano, K. and Oba, M. (2012) "Projectile experimentation for identifying hunting methods with replicas of Upper Palaeolithic weaponry from Japan, in in Marreiros, J., Bicho, N., and Gibaja, J. F. (eds) *International Conference on Use-Wear Analysis: Use-Wear 2012*, Newcastle upon Tyne, Cambridge Scholars Publishing, pp. 474-486.

Sano, K. and Oba, M. (2015) "Backed point experiments for identifying mechanically-delivered armatures", *Journal of Archaeological Science*, vol. 63, pp. 13-23.

-
- Sano, K., Denda, Y., and Oba, M. (2016) "Experiments in fracture patterns and impact velocity with replica hunting weapons from Japan", in Iovita, R. and Sano, K. (eds) *Multidisciplinary approaches to the study of Stone Age weaponry*, Dordrecht, Springer, pp. 29-46.
- Santaniello, F. (2011) *Studio dell'industria litica del musteriense finale dell'Arma delle Manie (Liguria): gli strati VI e VII*, MA Thesis, Ferrara, Università degli Studi di Ferrara.
- Schlanger, N. (1996) "Understanding Levallois: lithic technology and cognitive archaeology", *Cambridge Archaeological Journal*, vol. 6, no. 2, pp. 231-254.
- Schmalz, R. F. (1960) "Flint and the patination of flint artifacts", *Proceedings of the Prehistoric Society*, vol. 26, pp. 44-49.
- Schmitt, D., Churchill, S. E., and Hylander, W. L. (2003) "Experimental evidence concerning spear use in Neandertals and early modern humans", *Journal of Archaeological Science*, vol. 30, no. 1, pp. 103-114.
- Schoch, W. H., Bigga, G., Böhner, U., Richter, P., and Terberger, T. (2015) "New insights on the wooden weapons from the Paleolithic site of Schöningen", *Journal of Human Evolution*, vol. 89, pp. 214-225.
- Schoville, B. J. (2010) "Frequency and distribution of edge damage on Middle Stone Age lithic points, Pinnacle Point 13B, South Africa", *Journal of Human Evolution*, vol. 59, no. 3-4, pp. 378-391.
- Schoville, B. J. (2014) "Testing a taphonomic predictive model of edge damage formation with Middle Stone Age points from Pinnacle Point Cave 13B and Die Kelders Cave 1, South Africa", *Journal of Archaeological Science*, vol. 48, pp. 84-95.
- Schreve, D.C. (2006) "The taphonomy of a Middle Devensian (MIS 3) vertebrate assemblage from Lynford, Norfolk, UK, and its implications for Middle Palaeolithic subsistence strategies", *Journal of Quaternary Science: Published for the Quaternary Research Association*, vol. 21, no. 5, pp. 543-556.
- Scourse, J. (2006) "Comment on: Numerical $^{230}\text{Th}/\text{U}$ dating and a palynological review of the Holsteinian/Hoxnian Interglacial by Geyh and Müller", *Quaternary Science Reviews*, vol. 21, no. 25, pp. 3070-3071.
- Sellier, K. G. and Kneubuehl, B. P. (1994) *Wound ballistics and the scientific background*, Amsterdam, London, New York, Elsevier.
- Semenov, S. A. (1964) *Prehistoric technology*, Bath, Adams & Mackay.
- Serangeli, J., Böhner, U., Hassmann, H., and Conard, N.J. (2012) "Die pleistozänen Fundstellen in Schöningen—eine Einführung", in Behre, K.E. and für Vor, R.G.Z.F. (eds) *Die chronologische*

Einordnung der paläolithischen Fundstellen von Schöningen, Verlag des Römisch-Germanischen Zentralmuseums, pp. 1-22.

Shaw, C. N., Hofmann, C. L., Petraglia, M. D., Stock, J. T., and Gottschall, J. S. (2012) "Neandertal humeri may reflect adaptation to scraping tasks, but not spear thrusting" *PloS one*, vol. 7, no. 7, pp. e40349.

Shea, J. J. (1987) "On accuracy and relevance in lithic use-wear analysis", *Lithic Technology*, vol. 16, no. 2-3, pp. 44-50.

Shea, J. J. (1988) "Spear points from the Middle Paleolithic of the Levant", *Journal of Field Archaeology*, vol. 15, no. 4, pp. 441-450.

Shea, J. J. (1997) "Middle Paleolithic spear point technology", in Knecht, H. (eds) *Projectile technology*, Boston, Springer, pp. 79-106.

Shea, J. J. (2006) "The origins of lithic projectile point technology: evidence from Africa, the Levant, and Europe", *Journal of Archaeological Science*, vol. 33, no. 6, pp. 823-846.

Shea, J. J. (2009) "The impact of projectile weaponry on Late Pleistocene hominin evolution", in Richards P. M. and Hublin, J. J. (eds) *The evolution of Hominin diets*, Netherlands, Springer, pp. 189-199.

Shea, J. J. and Sisk, M. L. (2010) "Complex projectile technology and Homo sapiens dispersal into western Eurasia", *PaleoAnthropology*, pp. 100-122.

Shea, J. J., Brown, K. S., and Davis, Z. J. (2002) "Controlled experiments with Middle Palaeolithic spear points: Levallois points", in Mathieu, J. (eds) *Experimental archaeology: replicating past objects, behaviors, and processes*, Oxford, BAR International Series, vol. 1035, pp. 55-72.

Shea, J., Davis, Z., and Brown, K. (2001) "Experimental tests of Middle Palaeolithic spear points using a calibrated crossbow", *Journal of Archaeological Science*, vol. 28, no. 8, pp. 807-816.

Shea, J.J. (1988) "Spear points from the Middle Paleolithic of the Levant", *Journal of Field Archaeology*, vol. 15, no. 4, pp. 441-450.

Shea, J.J. (1990) "A further note on Mousterian spear points", *Journal of Field Archaeology*, vol. 17, no. 1, pp. 111-114.

Shea, J.J. (1992) "Lithic microwear analysis in archeology", *Evolutionary Anthropology: Issues, News, and Reviews*, vol. 1, no. 4, pp. 143-150.

-
- Shea, J.J. (1993) "Lithic Use-Wear Evidence for Hunting by Neandertals and Early Modern Humans from the Levantine Mousterian", *Archeological Papers of the American Anthropological Association*, vol. 4, no, 1, pp. 189-197.
- Shea, J.J. and Klenck, J.D. (1993) "An experimental investigation of the effects of trampling on the results of lithic microwear analysis", *Journal of Archaeological Science*, vol. 20, no. 2, pp. 175-194.
- Shipman, P. (1983) "Early hominid lifestyle: hunting and gathering or foraging and scavenging", *Animals and Archaeology*, vol. 1, pp. 31-49.
- Shipman, P. (2008) "Separating "us" from "them": Neanderthal and modern human behaviour", *Proceedings of the National Academy of Sciences*, vol. 105, no. 38, pp. 14241-14242.
- Shott, M. J. (1997) "Stones and shafts redux: the metric discrimination of chipped-stone dart and arrow points", *American Antiquity*, vol. 62, no. 1, pp. 86-101.
- Sierralta, M., Frechen, M., and Urban, B. (2012) "230Th/U dating results from opencast mine Schöningen", in Behre, K. E. (eds) *Die chronologische Einordnung der paläolithischen Fundstellen von Schöningen*, Mainz, Römisch-Germanisches Zentralmuseum, pp.143-154.
- Sisk, M. L. and Shea, J. J. (2009) "Experimental use and quantitative performance analysis of triangular flakes (Levallois points) used as arrowheads", *Journal of Archaeological Science*, vol. 36, no. 9, pp. 2039-2047.
- Sisk, M. L. and Shea, J. J. (2011) "The African origin of complex projectile technology: an analysis using tip cross-sectional area and perimeter" *International Journal of Evolutionary Biology*, pp. 1-8. [Online]. Available at <http://dx.doi.org/10.4061/2011/968012>.
- Skibo, J. M. (1992) "Ethnoarchaeology and Experimental Archaeology Defined", in Skibo, J. M. (eds) *Pottery Function*, New York, Springer, pp. 9-30.
- Skibo, J. M., Walker, W. H. and Nielsen, A. E. (2002) *Expanding archaeology*, Salt Lake City, University of Utah Press.
- Sorensen, A. C., Claud, E., and Soressi, M. (2018) "Neandertal fire-making technology inferred from microwear analysis", *Scientific Reports*, vol. 8, no. 1, pp. 10065.
- Soressi, M. and D'errico, F. (2007) "Pigments, gravures, parures: les comportements symboliques controversés des Néandertaliens", in Vandermeersch, B., Maureille, B., and Coppens, Y. (eds) *Les Néandertaliens. Biologie et cultures*, Éditions du CTHS, pp.297-309.
- Soressi, M., McPherron, S. P., Lenoir, M., Dogandžić, T., Goldberg, P., Jacobs, Z., Maigrot, Y., Martisius, N.L., Miller, C. E., Rendu, W., and Richards, M. (2013) "Neandertals made the first

specialized bone tools in Europe”, *Proceedings of the National Academy of Sciences*, vol. 110, no. 35, pp. 14186-14190.

Soriano, S. (1998) “Les microgravettes du Périgordien de Rabier à Lanquais (Dordogne): analyse technologique fonctionnelle”, *Gallia Préhistoire*, vol. 40, no. 1, pp. 75-94.

Stemp, W.J. and Stemp, M. (2001) “UBM laser profilometry and lithic use-wear analysis: a variable length scale investigation of surface topography”, *Journal of Archaeological Science*, vol. 28, no. 1, pp. 81-88.

Stemp, W.J. and Stemp, M. (2003) “Documenting stages of polish development on experimental stone tools: surface characterization by fractal geometry using UBM laser profilometry”, *Journal of Archaeological Science*, vol. 30, no. 3, pp. 287-296.

Stevens, N.E., Harro, D.R., and Hicklin, A. (2010) “Practical quantitative lithic use-wear analysis using multiple classifiers”, *Journal of Archaeological Science*, vol. 37, no. 10, pp. 2671-2678.

Stewart, T. D. (1977) “The Neanderthal skeletal remains from Shanidar Cave, Iraq: A summary of findings to date”, *Proceedings of the American Philosophical Society*, vol. 121, no. 2, pp. 121-165.

Stiner, M. C. (1991) “A taphonomic perspective on the origins of the faunal remains of Grotta Guattari (Latium, Italy)”, *Current Anthropology*, vol. 32, pp. 103–117.

Stiner, M. C. (1994) *Honor among Thieves: A Zooarchaeological Study of Neandertal Ecology*, Princeton, Princeton University Press.

Stiner, M. C. (2002) “Carnivory, coevolution, and the geographic spread of the genus *Homo*”, *Journal of Archaeological Research*, vol. 10, no. 1, pp. 1-63.

Stringer, C. (2002) “Modern human origins: progress and prospects”, *Philosophical Transactions of the Royal Society of London B: Biological Sciences*, vol. 357, no. 1420, pp. 563-579.

Stringer, C. (2012) “The status of *Homo heidelbergensis* (Schoetensack 1908)”, *Evolutionary Anthropology: Issues, News, and Reviews*, vol. 21, no. 3, pp. 101-107.

Stringer, C. and Gamble, C. (1993) *In search of the Neanderthals: solving the puzzle of human origins*, New York, Thames and Hudson.

Stringer, C. B., and Buck, L. T. (2014) “Diagnosing *Homo sapiens* in the fossil record”, *Annals of Human Biology*, vol. 41, no. 4, pp. 312-322.

Stringer, C. B., Finlayson, J. C., Barton, R. N. E., Fernández-Jalvo, Y., Cáceres, I., Sabin, R. C., Rhodes, E. J., Currant, A. P., Rodríguez-Vidal, J., Giles-Pacheco, F., and Riquelme-Cantal, J. A.

(2008) "Neanderthal exploitation of marine mammals in Gibraltar", *Proceedings of the National Academy of Sciences*, vol. 105, no. 38, pp. 14319-14324.

Taipale, N. and Rots, V. (2018) "Breakage, scarring, scratches and explosions: understanding impact trace formation on quartz", *Archaeological and Anthropological Sciences*, vol. 11, no. 6, pp. 3013-3039.

Taylor, N. (2011) "The origins of hunting & gathering in the Congo basin: a perspective on the Middle Stone Age Lupemban industry", *Before Farming*, vol. 1, pp. 1-20.

Terauds, J. (1975) "Javelin release characteristics", *Track Technique*, vol. 61, pp. 19-45.

Thieme, H. (1997) "Lower Palaeolithic hunting spears from Germany", *Nature*, vol. 385, no. 6619, pp. 807-810.

Thieme, H. (1999) "Lower Palaeolithic throwing spears and other wooden implements from Schöningen, Germany", In Ullrich, H. (eds) *Hominid evolution: lifestyles and survival strategies*, Gelsenkirchen, Ed. Archaea, pp.383-395.

Thieme, H. and Veil, S. (1985) "Neue Untersuchungen zum eemzeitlichen Elefanten-Jagdplatz Lehringen. Ldkr. Verden", *Die Kunde*, vol. 36, pp. 11-58.

Thomas, D. H. (1978) "Arrowheads and atlatl darts: how the stones got the shaft", *American Antiquity*, vol. 43, no. 3, pp. 461-472.

Thomas, D. H. (1981) "How to classify the projectile points from Monitor Valley, Nevada" *Journal of California and Great Basin Anthropology*, vol. 3, no. 1, pp. 7-43.

Tixier, J. (1967) *Pièces pédonculées atériennes du Maghreb et du Sahara: types 1-30*, Paris, Muséum national d'histoire naturelle, vol. 3.

Tomasso, A., Rots, V., Purdue, L., Beyries, S., Buckley, M., Cheval, C., Cnuts, D., Coppe, J., Julien, M.A., Grenet, M., and Lepers, C. (2018) "Gravettian weaponry: 23,500-year-old evidence of a composite barbed point from Les Prés de Laure (France)", *Journal of Archaeological Science*, vol. 100, pp. 158-175.

Tomasso, S., Rots, V., Perdaen, Y., Crombé, P., and Meylemans, E. (2015) "Hunting with trapezes at Bazel-Sluis: the results of a functional analysis", *Notae Praehistoricae*, vol. 35, pp. 239-251.

Tringham, R. (1978) "Experimentation, ethnoarchaeology, and the leapfrogs in archaeological methodology", in Gould, R. A. (eds) *Explorations in ethnoarchaeology*, Albuquerque, University of New Mexico Press, pp.169-199.

-
- Tringham, R., Cooper, G., Odell, G., Voytek, B., and Whitman, A. (1974) "Experimentation in the formation of edge damage: a new approach to lithic analysis", *Journal of Field Archaeology*, vol. 1, no. 1-2, pp. 171-196.
- Trinkaus, E. (2012) "Neandertals, early modern humans, and rodeo riders", *Journal of Archaeological Science*, vol. 39, no. 12, pp. 3691-3693.
- Trinkaus, E. and Ruff, C. B. (1999) "Diaphyseal cross-sectional geometry of Near Eastern Middle Palaeolithic humans: the tibia", *Journal of Archaeological Science*, vol. 26, no. 10, pp. 1289-1300.
- Trinkaus, E. and Zimmerman, M. R. (1982) "Trauma among the Shanidar Neandertals", *American Journal of Physical Anthropology*, vol. 57, no. 1, pp. 61-76.
- Trinkaus, E., Churchill, S. E., and Ruff, C. B. (1994) "Postcranial robusticity in Homo. II: Humeral bilateral asymmetry and bone plasticity", *American Journal of Physical Anthropology*, vol. 93, no. 1, pp. 1-34.
- Tumung, L., Bazgir, B., and Ollé, A. (2015) "Applying SEM to the study of use-wear on unmodified shell tools: an experimental approach", *Journal of Archaeological Science*, vol. 59, pp. 179-196.
- Unger-Hamilton, R. (1983) "An investigation into the variables affecting the development and the appearance of plant polish on flint blades", *Travaux de la Maison de l'Orient*, vol. 5, no. 1, pp. 243-250.
- Unger-Hamilton, R. (1984) "The formation of use-wear polish on flint: Beyond the "deposit versus abrasion" controversy", *Journal of Archaeological Science*, vol. 11, no. 1, pp. 91-98.
- Unger-Hamilton, R. (1988) *Method in microwear analysis: prehistoric sickles and other stone tools from Arjouna, Syria*, Oxford, BAR International Series. vol. 45.
- Unrath, G., Owen, L., van Gijn, A., Moss, E., Plisson, H., and Vaughan, P. (1986) "An evaluation of microwear studies: a multi-analyst approach", *Early Man News*, vol. 9-11, pp. 117-176.
- Urban, B. and Sierralta, M. (2012) "New palynological evidence and correlation of early Paleolithic sites Schöningen 12B and 13 II, Schöningen open lignite mine", in Behre, K. E. (eds), *Die chronologische Einordnung der paläolithischen Fundstellen von Schöningen. Forschungen zur Urgeschichte aus dem Tagebau von Schöningen 1*, Mainz, Verlag Römisch-Germanisches Zentralmuseum, pp. 77-96.
- Valensi, P. and Psathi, E. (2004) "Faunal Exploitation during the Middle Palaeolithic in south-eastern France and north-western Italy", *International Journal of Osteoarchaeology*, vol. 14, no. 3-4, pp. 256-272.

-
- Valladas, H., Mercier, N., Ayliffe, L.K., Falguères, C., Bahain, J.J., Dolo, J.M., Froget, L., Joron, J.L., Masaoudi, H., Reyss, J.L., and Moncel, M.H. (2008) "Radiometric dates for the middle Palaeolithic sequence of Payre (Ardeche, France)", *Quaternary Geochronology*, vol. 3, no. 4, pp. 377-389.
- Van Buren, G. E. (1974) *Arrowheads and Projectile Points*, Garden Grove, Calif, Arrowhead Pub. Co.
- Van Gijn, A. L. (1989) *The Tear and Wear of Flint*, Leiden, Analecta Praehistorica Leidensia, vol. 22.
- Van Gijn, A. L. (2010) *Flint in focus. Lithic Biographies in the Neolithic and Bronze Age*, Leiden, Sidestone Press.
- Van Gijn, A. L. (2014) "Science and interpretation in microwear studies", *Journal of Archaeological Science*, vol. 48, pp. 166-169.
- Van Peer, P. (1992) *The Levallois reduction strategy*, Madison, Prehistory Press.
- Vaughan, P. (1981) "Microwear analysis of experimental flint and obsidian tools", *Staringia*, vol. 6, no. 1, pp. 90-91.
- Vaughan, P. and Plisson, H. (1986) "Comment presenter les données tracéologiques?", in Owen, L. and Unruth, G. (eds) *Technical Aspects of Microwear Studies on Stone Tools*, Tübingen, Archaeologica Venatoria, Institut für Urgeschichte, pp. 177-182.
- Vaughan, P. C. (1985) *Use-wear analysis of flaked stone tools*, Tucson, University of Arizona Press.
- Venditti, F., Tirillò, J., and Garcea, E. A. (2016) "Identification and evaluation of post-depositional mechanical traces on quartz assemblages: An experimental investigation", *Quaternary International*, vol. 424, pp. 143-153.
- Verbaas, A. (2018) Personal communication to La Porta, A., Nice, Awrana conferece, 28th May.
- Vergès, J. M. and Ollé, A. (2011) "Technical microwear and residues in identifying bipolar knapping on an anvil: experimental data", *Journal of Archaeological Science*, vol. 38, no. 5, pp. 1016-1025.
- Vettese, D., Daujeard, C., Blasco, R., Borel, A., Caceres, I., and Moncel, M. H. (2017) "Neandertal long bone breakage process: standardized or random patterns? The example of Abri du Maras (Southeastern France, MIS 3)", *Journal of Archaeological Science: Reports*, vol. 13, pp. 151-163.
- Vicino, G., and d'Errico, F. (1985) "L'approvvigionamento di materia prima litica", in Del Lucchese, A., Giacobini, G., and Vicino, G. (eds) *L'uomo di Neandertal in Liguria*, Genova, Quaderni della Soprintendenza archeologica della Liguria, vol. 2., pp. 72-74.
- Villa, P. and Lenoir, M. (2006) "Hunting weapons of the Middle Stone Age and the Middle Palaeolithic: spear points from Sibudu, Rose Cottage and Bouheben", *Southern African Humanities*, vol. 18, no. 1, pp. 89-122.

-
- Villa, P. and Lenoir, M. (2009) "Hunting and hunting weapons of the Lower and Middle Paleolithic of Europe", in Richards P. M. and Hublin, J. J. (eds) *The evolution of Hominin diets*, Netherlands, Springer, pp. 59-85.
- Villa, P. and Roebroeks, W. (2014) "Neandertal demise: an archaeological analysis of the modern human superiority complex", *PLoS One*, vol. 9, no. 4, p. e96424.
- Villa, P. and Soriano, S. (2010) "Hunting weapons of Neanderthals and early modern humans in South Africa: similarities and differences", *Journal of Anthropological Research*, vol. 66, no. 1, pp. 5-38.
- Villa, P., Boscato, P., Ranaldo, F., and Ronchitelli, A. (2009a) "Stone tools for the hunt: points with impact scars from a Middle Paleolithic site in southern Italy", *Journal of Archaeological Science*, vol. 36, no. 3, pp. 850-859.
- Villa, P., Delagnes, A., and Wadley, L. (2005) "A late Middle Stone Age artifact assemblage from Sibudu (KwaZulu-Natal): comparisons with the European Middle Paleolithic", *Journal of Archaeological Science*, vol. 32, no. 3, pp. 399-422.
- Villa, P., Soressi, M., Henshilwood, C. S., and Mourre, V. (2009b) "The Still Bay points of Blombos Cave (South Africa)", *Journal of Archaeological Science*, vol. 36, no. 2, pp. 441-460.
- Wadley, L. (2001) "What is cultural modernity? A general view and a South African perspective from Rose Cottage Cave", *Cambridge Archaeological Journal*, vol. 11, no. 2, pp. 201-221.
- Wadley, L. (2003) "How some archaeologists recognize culturally modern behaviour: Reviews of current issues and research findings: human origins research in South Africa", *South African Journal of Science*, vol. 99, no. 5-6, pp. 247-250.
- Wadley, L. (2005) "Putting ochre to the test: replication studies of adhesives that may have been used for hafting tools in the Middle Stone Age", *Journal of Human Evolution*, vol. 49, no. 5, pp. 587-601.
- Wadley, L. (2010) "Compound-adhesive manufacture as a behavioral proxy for complex cognition in the Middle Stone Age", *Current Anthropology*, vol. 51, vol. S1, pp. S111-S119.
- Wadley, L. and Lombard, M. (2007) "Small things in perspective: The contribution of our blind tests to micro-residue studies on archaeological stone tools", *Journal of Archaeological Science*, vol. 34, pp. 1001-1010.
- Wadley, L. and Mohapi, M. (2008) "A segment is not a monolith: evidence from the Howiesons Poort of Sibudu, South Africa", *Journal of Archaeological Science*, vol. 35, no. 9, pp. 2594-2605.

-
- Wadley, L., Hodgskiss, T., and Grant, M. (2009) "Implications for complex cognition from the hafting of tools with compound adhesives in the Middle Stone Age, South Africa", *Proceedings of the National Academy of Sciences*, vol. 106, no. 24, pp. 9590-9594.
- Wadley, L., Lombard, M., Williamson, B. (2004) "The first residue analysis blind tests: results and lessons learnt", *Journal of Archaeological Science*, vol. 31, no. 11, pp. 1491-1501.
- Wadley, L., Trower, G., Backwell, L., and d'Errico, F. (2015) "Traditional glue, adhesive and poison used for composite weapons by Ju/'hoan San in Nyae Nyae, Namibia. Implications for the evolution of hunting equipment in prehistory", *PloS one*, vol. 10, no. 10, pp. e0140269.
- Wadley, L., Williamson, B., and Lombard, M. (2004) "Ochre in hafting in Middle Stone Age southern Africa: a practical role", *Antiquity*, vol. 78, no. 301, pp. 661-675.
- Wagner, E. (1995) *Cannstatt I. Grofiwildjager im Travertingebiet. Forschungen und Berichte zur Vor- und Friihgeschichte in Baden-Wiirttemberg 61*, PhD thesis, Stuttgart, University of Stuttgart.
- Waguespack, N. M., Surovell, T. A., Denoyer, A., Dallow, A., Savage, A., Hyneman, J., and Tapster, D. (2009) "Making a point: wood-versus stone-tipped projectiles", *Antiquity*, vol. 83, no. 321, pp. 786-800.
- Warren, S. H. (1922) "The Mesvinian Industry of Clacton-on-Sea, Essex", *Proceedings of the Prehistoric Society of East Anglia*, vol. 3, no. 4, pp. 597-602.
- Weber, M. J., Grimm, S. B., and Baales, M. (2011) "Between warm and cold: Impact of the Younger Dryas on human behavior in Central Europe", *Quaternary International*, vol. 242, no. 2, pp. 277-301.
- Weyrich, L.S., Duchene, S., Soubrier, J., Arriola, L., Llamas, B., Breen, J., Morris, A.G., Alt, K.W., Caramelli, D., Dresely, V., and Farrell, M. (2017) "Neanderthal behaviour, diet, and disease inferred from ancient DNA in dental calculus", *Nature*, vol. 544, no. 7650, p. 357.
- White, M. and Ashton, N. (2003) "Lower Palaeolithic core technology and the origins of the Levallois method in north-western Europe", *Current Anthropology*, vol. 44, no. 4, pp. 598-609.
- White, M., Ashton, N., and Scott, B. (2011) "The emergence, diversity and significance of Mode 3 (prepared core) technologies", in Ashton, N., Lewis, S., and Stringer, C. (eds) *Developments in Quaternary Sciences*, Elsevier, vol. 14, pp. 53-65.
- White, M., Pettitt, P., and Schreve, D. (2016) "Shoot first, ask questions later: Interpretative narratives of Neanderthal hunting", *Quaternary Science Reviews*, vol. 140, pp. 1-20.
- Wilkins, J., Schoville, B. J., and Brown, K. S. (2014) "An experimental investigation of the functional hypothesis and evolutionary advantage of stone-tipped spears", *PloS one*, vol. 9, no. 8, p. 104514.

Wilkins, J., Schoville, B. J., Brown, K. S., and Chazan, M. (2012) "Evidence for early hafted hunting technology", *Science*, vol. 338, no. 6109, pp. 942-946.

Wilkins, J., Schoville, B. J., Brown, K. S., and Chazan, M. (2015) "Kathu Pan 1 points and the assemblage-scale, probabilistic approach: A response to Rots and Plisson. Projectiles and the abuse of the use-wear method in a search for impact", *Journal of Archaeological Science*, vol. 54, pp. 294-299.

Williams, V. M., Burke, A., and Lombard, M. (2014) "Throwing spears and shooting arrows: preliminary results of a pilot neuroarchaeological study", *The South African Archaeological Bulletin*, vol. 69, no. 200, pp. 199-207.

Witthoft, J. (1967) "Glazed polish on flint tools", *American Antiquity*, vol. 32, no. 3, pp. 383-388.

Witthoft, J. (1968) "Flint arrowpoints from the Eskimo of northwestern Alaska", *Expedition*, vol. 10, no. 2, p. 30-37.

Wu, X.J., Schepartz, L.A., Liu, W. and Trinkaus, E. (2011) "Antemortem trauma and survival in the late Middle Pleistocene human cranium from Maba, South China", *Proceedings of the National Academy of Sciences*, vol. 108, no. 49, pp. 19558-19562.

Wynn, T. (2009) "Hafted spears and the archaeology of mind", *Proceedings of the National Academy of Sciences*, vol. 106, no. 24, pp. 9544-9545.

Wynn, T. and Coolidge, F. L. (2004) "The expert Neandertal mind", *Journal of Human Evolution*, vol. 46, no. 4, pp. 467-487.

Wynn, T. and Coolidge, F. L. (2011) "The implications of the working memory model for the evolution of modern cognition", *International Journal of Evolutionary Biology*, vol. 2011, pp. 1-12. [Online] Available at <https://www.hindawi.com/journals/ijeb/2011/741357/abs/>.

Xhaufclair, H. (2014) *Plant Use in the Subsistence Strategies of Prehistoric Huntergatherers in Palawan Island Assessed from the Lithic Industry. Building up a Reference Collection*, PhD thesis, Paris, Muséum national d'Histoire naturelle.

Xhaufclair, H., Pawlik, A., Gaillard, C., Forestier, H., Viales, T. J., Callado, J. R., Tandang, D., Amano, N., Manipon, D., and Dizon, E. (2016) "Characterisation of the use-wear resulting from bamboo working and its importance to address the hypothesis of the existence of a bamboo industry in prehistoric Southeast Asia", *Quaternary International*, vol. 416, pp. 95-125.

Yamada, M. (1993) *Contribution a l'etude des industries lithiques mousteriennes les sites des balzi rossi, grimaldi (ligurie, italie): grottes du prince et du cavillon et site du casino*, PhD thesis, Paris, Muséum national d'histoire naturelle.

Yaroshevich, A., Kaufman, D., Nuzhnyy, D., Bar-Yosef, O., and Weinstein-Evron, M. (2010) "Design and performance of microlith implemented projectiles during the Middle and the Late Epipaleolithic of the Levant: experimental and archaeological evidence", *Journal of Archaeological Science*, vol. 37, no. 2, pp. 368-388.

Yaroshevich, A., Zaidner, Y., and Weinstein-Evron, M. (2016) "Projectile damage and point morphometry at the early middle paleolithic misliya cave, mount carmel (Israel): preliminary results and interpretations", in Iovita, R. and Sano, K. (eds) *Multidisciplinary approaches to the study of Stone Age weaponry*, Dordrecht., Springer, pp. 119-134.

Young, R. W. (2003) "Evolution of the human hand: the role of throwing and clubbing", *Journal of Anatomy*, vol. 202, no. 1, pp. 165-174.

Zilhão, J. (2011) "The emergence of language, art and symbolic thinking", in Henshilwood, C. S. and d'Errico, F. (eds) *Homo symbolicus: the dawn of language, imagination and spirituality*, Amsterdam, John Benjamins Pub. Co., pp. 111-131.

Zilhao, J. (2012) "Personal ornaments and symbolism among the Neanderthals", *Developments in Quaternary Sciences*, vol. 16, pp. 35-49.

Zilhão, J. (2013) "Neandertal-modern human contact in western Eurasia: issues of dating, taxonomy, and cultural associations", in Akazawa, T., Nishiaki, Y., and Aoki, K. (eds) *Dynamics of Learning in Neanderthals and Modern Humans Cultural Perspectives*, Japan, Springer, pp. 21-57.

Zilhão, J., Angelucci, D.E., Badal-García, E., d'Errico, F., Daniel, F., Dayet, L., Douka, K., Higham, T.F., Martínez-Sánchez, M.J., Montes-Bernárdez, R., and Murcia-Mascarós, S. (2010) "Symbolic use of marine shells and mineral pigments by Iberian Neanderthals", *Proceedings of the National Academy of Sciences*, vol. 107, no. 3, pp. 1023-1028.

Web Resources:

Comune di Finale report (1995) *Comune di Finale Ligure, Inquadramento geologico geomorfologico e idrogeologico*, [Online] Available at

<http://www.comunefinaleligure.it/sites/default/files/allegati/pagina/PUC-A2.pdf>

Microscope features: [http://hirox-](http://hirox-europe.com/products/microscope/index8700.html?PHPSESSID=q5snk93cf61o92gc9q66ahubk4)

[europe.com/products/microscope/index8700.html?PHPSESSID=q5snk93cf61o92gc9q66ahubk4](http://hirox-europe.com/products/microscope/index8700.html?PHPSESSID=q5snk93cf61o92gc9q66ahubk4), [last accessed 05-05-2017].

Picture from: <http://www.ambisonsociety.org>, [last accessed 08-10-2018].

Picture from: <http://www.olympic.org/montreal-1976/athletics/javelin-throw-men>, [last accessed 03-11-2018].

Picture from: <http://www.yorkshirecoastnature.co.uk/blog/290/a-royal-occasion>, [last accessed 08-10-2018].

Picture from: <https://blogs.fco.gov.uk/leighturner/2017/05/15/an-encounter-with-a-viennese-wild-boar-wildschwein>, [last accessed 08-10-2018].

Picture from: <https://en.wikipedia.org/wiki/Horse>, [last accessed 08-10-2018].

Picture from: <https://www.olympus-lifescience.com/en/microscope-resource/primer/anatomy/reflected/>, [last accessed 14-02-2015]

Picture from: <https://www.pbs.org/newshour/science/7-things-didnt-know-reindeer>, [last accessed 08-10-2018].

Picture from: <https://www.woodlandtrust.org.uk/visiting-woods/trees-woods-and-wildlife/animals/mammals/roe-deer/>, [last accessed 08-10-2018].